

# Photocatalytic Generation of Carbanions from Carbonyl Compounds and Ipso-Borylation Inert C<sub>aryl</sub>-Hetero Bonds

**Dissertation**

Zur Erlangung des Doktorgrades der Naturwissenschaften

(Dr. rer. nat.)

an der Fakultät für Chemie und Pharmazie

der Universität Regensburg



vorgelegt von

**Shun Wang**

Aus Huili City, Sichuan Province, P. R. China

2021



The experimental part of this work has been carried out between November 2016 and February 2021 under the supervision of Prof. Dr. Burkhard König at the University of Regensburg, Institute of Organic Chemistry.

Date of submission: 12.04.2021

Date of colloquium: 18.05.2021

Board of examiners:

Prof. Dr. Richard Buchner	(Chair)
Prof. Dr. Burkhard König	(1st Referee)
Prof. Dr. Alexander Breder	(2nd Referee)
Prof. Dr. Patrick Nürnberger	(Examiner)



*Dedicated*  
*To*  
*My family*



## Table of contents

<b>1. Catalytic Generation of Carbanionic Species through Carbonyl Umpolung</b> .....	<b>1</b>
1.1 Introduction .....	1
1.2 Catalytic Wolff-Kishner reaction.....	2
1.2.1 Metal-assisted trapping of carbanions.....	3
1.2.2 Carbanion generation via radical addition to sulfonyl hydrazones .....	5
1.3 Generation of carbanions via catalytic single-electron reduction of imines .....	8
1.4 Generation of carbanions via catalytic sequential single-electron reduction of carbonyl.....	10
1.5 Conclusion and Outlook.....	14
1.6 References .....	16
<b>2. Photoinitiated Carbonyl-Metathesis: Deoxygenative Reductive Olefination of Aromatic Aldehydes via Photoredox Catalysis</b> .....	<b>19</b>
2.1 Introduction .....	20
2.2 Results and discussion .....	21
2.2.1 Optimization of reaction condition .....	21
2.2.2 Synthetic scope.....	22
2.2.3 Mechanistic investigation .....	24
2.3 Conclusions.....	29
2.4 Experimental part.....	30
2.4.1 General information.....	30
2.4.2 Starting materials.....	30
2.4.3 Experimental procedures .....	32
2.4.4 Optimization of reaction conditions .....	33
2.4.5 Mechanistic studies.....	37
2.5 Characterization of products .....	54
2.6 Computational details .....	65
2.7 References.....	68
<b>3. Umpolung Difunctionalization of Carbonyls via Visible-Light Photoredox Catalytic Radical-Carbanion Relay</b> .....	<b>71</b>
3.1 Introduction.....	72
3.2 Results and discussion.....	73

3.2.1 Generation of $\alpha$ -sulfenyl carbanions and their reactions with electrophiles.....	73
3.2.2 Generation of $\alpha$ -CF <sub>3</sub> carbanions and their fragmentation reactions .....	77
3.2.3 Reaction mechanism.....	79
3.3 Conclusion .....	81
3.4 Experimental part.....	82
3.4.1 General information .....	82
3.4.2 Starting materials.....	83
3.4.3 Experimental procedures.....	84
3.4.4 Optimization details for the reaction conditions.....	85
3.4.5 Mechanistic studies .....	90
3.4.6 Characterization of products .....	109
3.5 References.....	131
<b>4. Light-Induced Single-Electron Transfer Processes Involving Sulfur Anions as Catalysts .....</b>	<b>135</b>
4.1 Introduction.....	135
4.2 Light-induced thiolate catalysis mediated by an electron donor–acceptor complex.....	136
4.3 Photo-induced xanthate anion catalysis via in-situ formation of the light-absorbing species.....	138
4.4 Light-induced thiolate catalysis enabled by the excited state of thiolate .....	142
4.5 Conclusion and outlook .....	144
4.6 References.....	145
<b>5. Photo-Induced Thiolate Catalytic Activation of Inert C<sub>aryl</sub>-Hetero Bonds for Radical Borylation.....</b>	<b>147</b>
5.1 Introduction.....	148
5.2 Results and discussion .....	149
5.2.1 Investigation of reaction conditions .....	149
5.2.2 Scope of leaving group for ipso-borylation.....	151
5.2.3 Substrate scope for the borylation of C-X, C-O and C-S bonds.....	152
5.2.4 Mechanistic insights .....	154
5.3 Conclusion .....	156
5.4 Experimental part.....	157



5.4.1 General information.....	157
5.4.2 Starting materials.....	159
5.4.3 Experimental procedures .....	160
5.4.4 Optimization details for the reaction condition .....	161
5.4.5 Side product detection and unsuccessful substrates.....	165
5.4.6 Mechanistic studies.....	169
5.4.7 Characterization of compounds .....	189
5.5 References .....	202
<b>6. Summary.....</b>	<b>205</b>
<b>7. Zusammenfassung.....</b>	<b>206</b>
<b>8. Abbreviations .....</b>	<b>208</b>
<b>9. Acknowledgement.....</b>	<b>211</b>
<b>10. Curriculum Vitae.....</b>	<b>212</b>



# Catalytic Generation of Carbanionic Species through Carbonyl Umpolung

## 1.1 Introduction

The concept of Umpolung, first introduced by Wittig<sup>[1]</sup> and then popularized by Seebach describes the polarity inversion of a particular functional group in organic chemistry.<sup>[2]</sup> Umpolung reactions create new reactivity by inverting the natural polarity of common organic functionalities and consequently enable the development of unconventional bond-forming strategies in organic synthesis. With Umpolung tactics, retrosynthetic disconnections can be performed in an inverted manner, permitting the assembly of a target molecule from synthons with both normal and reversal polarities. Over the past few decades, the successful development of numerous C–C bond-forming Umpolung reactions has greatly expanded the repertoire of organic synthesis.

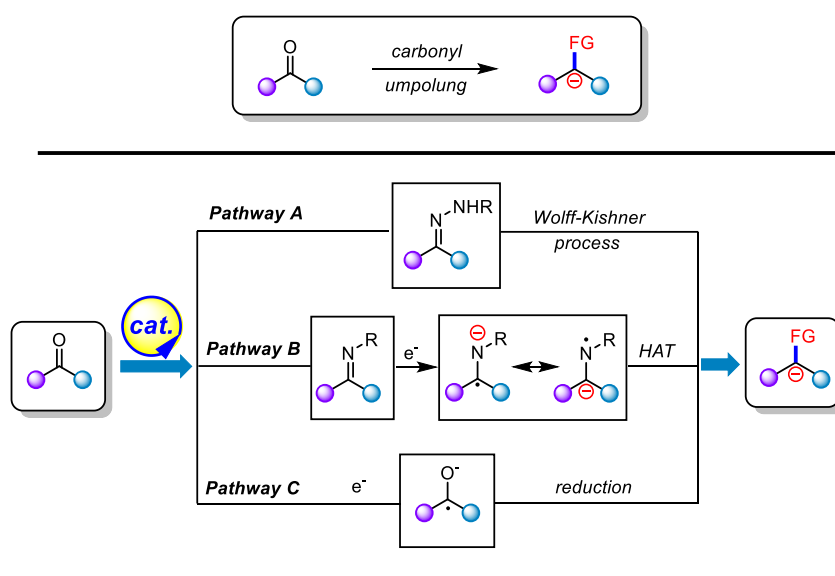
In the case of the carbonyl (C=O) functionality, the strong electronegativity of the oxygen atom renders the carbon atom of the carbonyl group partially positively charged that can be attacked by nucleophilic species. In a typical carbonyl Umpolung, the electronic nature of the carbonyl carbon is inverted from electrophilic to nucleophilic. This allows chemists to construct new chemical bonds by reacting the newly obtained carbon nucleophiles with various electrophiles. Two types of synthetically valuable anionic synthons are obtained through carbonyl Umpolung: acyl anion equivalents and alkyl carbanionic intermediates.

Research interest in the generation of acyl anion synthons by carbonyl Umpolung dates back to the cyanide-catalyzed benzoin reaction reported in 1832.<sup>[3]</sup> However, systematic and more vigorous Umpolung research started with Corey and Seebach, who described the use of dithianes to access acyl anion synthetic equivalents from aldehydes in the 1960s.<sup>[4]</sup> The development of N-heterocyclic carbene (NHCs) catalysis provides another valuable and important addition to the chemistry of acyl anion equivalents with great efforts devoted to the design and synthesis of novel NHC catalysts that catalyze the carbonyl Umpolung reactions.<sup>[5]</sup> The above-mentioned three Umpolung strategies constitute the most widely used approaches to access acyl anion species from carbonyl compounds. These seminal discoveries mark true breakthroughs in synthetic method development of the past decades and they have stimulated significant activity in designing efficient catalysts for carbonyl Umpolung.

On the other hand, Umpolung strategies can be applied for the generation of alkyl carbanionic species from a C=O moiety. In comparison to its well-explored acyl anion counterpart, the generation of alkyl carbanions via carbonyl Umpolung has received considerably less attention. This type of carbonyl Umpolung holds great synthetic potential considering that the generated alkyl carbanion is a versatile intermediate for the construction of C–C bonds by reacting with electrophiles. The earliest example of this Umpolung dates back to the Wolff-Kishner (WK) reduction in which carbonyl functionalities are converted into methylene groups.<sup>[6]</sup> Over one century after its discovery, the WK reaction and related modified reactions remain an important carbonyl deoxygenation tool in modern synthesis. Recent developments have provided new routes for the catalytic generation of carbanionic intermediates through the merger of the WK process and other catalytic reaction systems such as transition metal catalysis and photoredox catalysis. These advances have greatly expanded the application of this century-old reaction and therefore received increasing research interest.

Furthermore, in recent years new techniques for the catalytic generation of carbanionic species through the single-electron reduction of imines and carbonyls have emerged.<sup>[7]</sup> Classically, the reduction of imines or carbonyls requires the use of stoichiometric reactants (e.g., low-valent metals) or electrochemical methods for the reduction. Recent advances have demonstrated that photocatalysis can not only serve as an ideal replacement of the classic reaction system for the C=O/N moiety reduction, but also generate new carbanionic reactivity from carbonyl Umpolung.

We summarize and discuss in the following part the catalytic generation of alkyl carbanionic species from carbonyl Umpolung particularly emphasizing emerging new technologies and trends (Scheme 1). We structure our discussion along the two major reaction pathways for the generation of alkyl carbanions from carbonyl compounds: the catalytic WK process (pathway A) and the catalytic single-electron reduction of imines and carbonyls (pathway B and C).

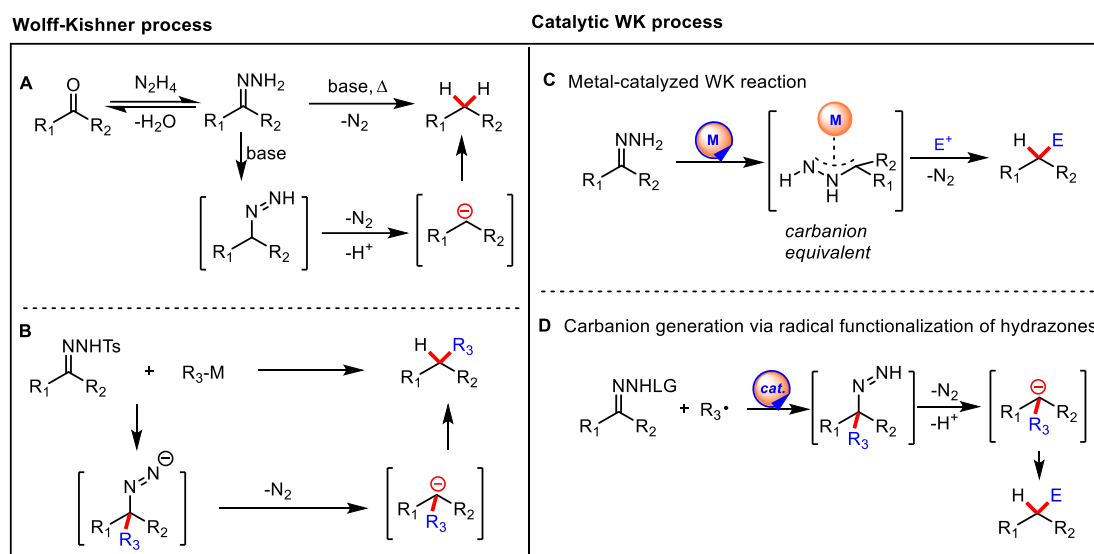


**Scheme 1.** Catalytic generation of carbanions from carbonyl Umpolung

## 1.2 Catalytic Wolff-Kishner reaction - Pathway A

Before the discussion of the catalytic WK process, it is worthwhile to give first an overview of the WK reaction mechanism. In a regular WK process, the reaction proceeds through the formation of hydrazones from carbonyl and hydrazine. Subsequent deprotonation-tautomerization sequence occurs to give the diazene intermediate from hydrazone. After a second deprotonation, this intermediate rapidly loses molecular nitrogen to give the carbanion, which is then protonated to give the alkane product (Scheme 2A).<sup>[6a]</sup> The formation of the two key intermediates, hydrazone and diazene, can considerably influence the course of a WK process. Many elegant modifications including the well-known Huang Minlong,<sup>[8]</sup> Barton,<sup>[9]</sup> Cram,<sup>[10]</sup> and Henbest<sup>[11]</sup> protocols have focused on a more efficient hydrazone formation by removal of water from the reaction medium, whereas Caglioti<sup>[12]</sup> and Meyers<sup>[13]</sup> have utilized substituted hydrazones as alternatives to the classical WK reaction allowing the facile generation of the diazene intermediate. In particular, the use of sulfonyl hydrazone in the Caglioti modification not only allows the WK reduction under mild conditions but also inspired the generation of substituted carbanions by reacting sulfonyl hydrazone with organometallic reagents (e.g., RLi, RMgBr) (Scheme 2B).<sup>[14]</sup> This reaction pathway represents one of the earliest pathways for the utilization of WK process

for C-C bond construction.



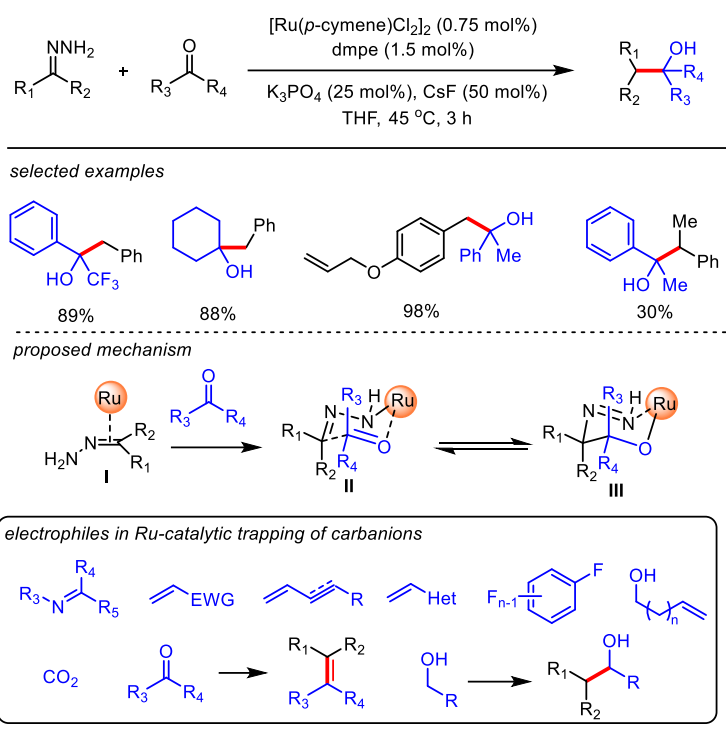
**Scheme 2.** Generation of carbanions via carbonyl Umpolung

Despite being a very effective way of producing carbanions, the synthetic applications of the WK reaction have been mainly limited to carbonyl deoxygenation.<sup>[6a]</sup> Only a few attempts were made over the past years in developing new catalytic systems, i.e., catalytic variants of the WK reaction for the generation and/or trapping of the generated alkyl carbanions thus forging C-C bonds. However, the transformation bears the potential for a plethora of carbanion-based transformations by merging the WK process with other catalytic systems (e.g., transition metal catalysis, photoredox catalysis) (Scheme 2C and 2D) that waits to be discovered.

### 1.2.1 Metal-assisted trapping of carbanions

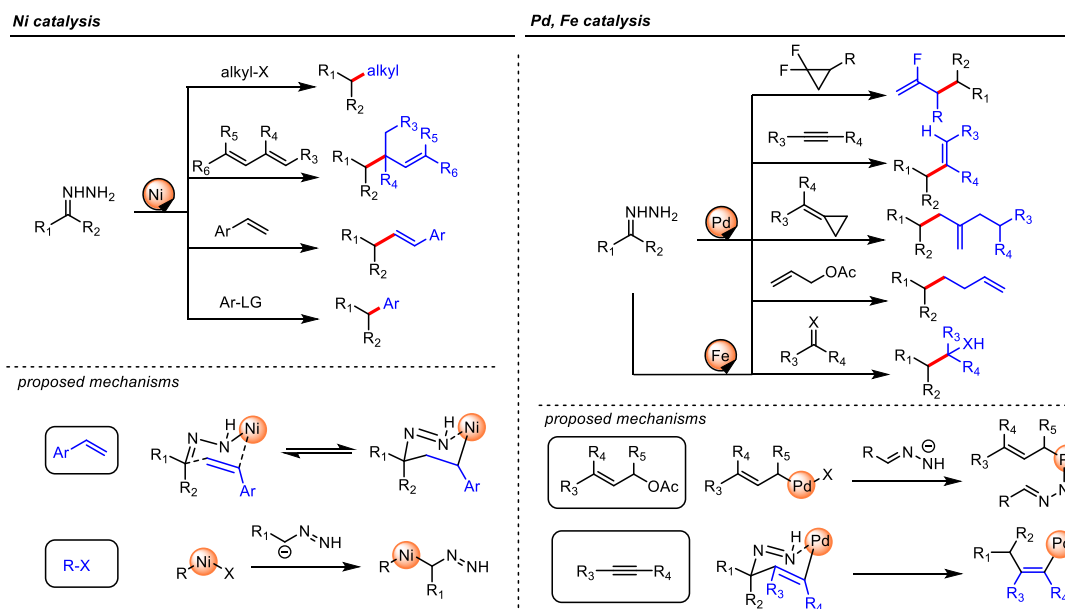
The Li group made significant progress in the catalytic carbanion trapping in a WK process. In 2017, they first described a ruthenium-catalyzed strategy for the facile capture of the carbanionic species generated in a WK process by carbonyl compounds (ketone and aldehydes) to give the desired Grignard-type products.<sup>[15]</sup> The reaction demonstrates broad functional group tolerance for both the hydrazone and carbonyl compounds with different substitution patterns. Notably, the reaction system is compatible with functional groups (including ester, amide, as well as tertiary alcohols), which are normally incompatible with classical Grignard reactions. In their mechanism proposal, ruthenium complex **I** was initially generated from the association of hydrazone to the ruthenium catalyst. The resulting Ru complex **I** interacts with carbonyl compounds via a Zimmerman-Traxler transition state **II** followed by its rearrangement to give intermediate **III**. The Grignard type addition product was released from **III**, concomitant with the regeneration of the Ru catalyst. The coordination of ruthenium complex with substrate is believed to be capable of promoting the decomposition of hydrazine,<sup>[16]</sup> rendering the N<sub>2</sub> extrusion from hydrazone under mild conditions. This new catalysis opens new possibilities by offering an expanded toolbox to harness the carbanions generated from easily available carbonyl compounds in the WK reaction for catalytic C-C bond forming reactions. Following this report, this Ru-catalytic system has been extended and the carbanionic species was reacted with a broad range of electrophiles including imines,<sup>[17]</sup> alkenes,<sup>[18],[19]</sup> CO<sub>2</sub>,<sup>[20]</sup> dienes,<sup>[21]</sup> multi-fluoro arenes,<sup>[22]</sup> carbonyls (for C=C bond

construction)<sup>[23]</sup> and *in-situ* generated carbonyl compounds (Scheme 3).<sup>[24]</sup>



**Scheme 3.** Ru-catalyzed trapping of carbanionic species generated in WK process

In addition, the Li group and others have demonstrated that other transition metal catalysts including Ni, Pd, and Fe<sup>[25]</sup> could efficiently be merged with the WK processes realizing different mechanistic



**Scheme 4.** Ni, Pd, Fe-catalyzed trapping of carbanionic species generated in WK process

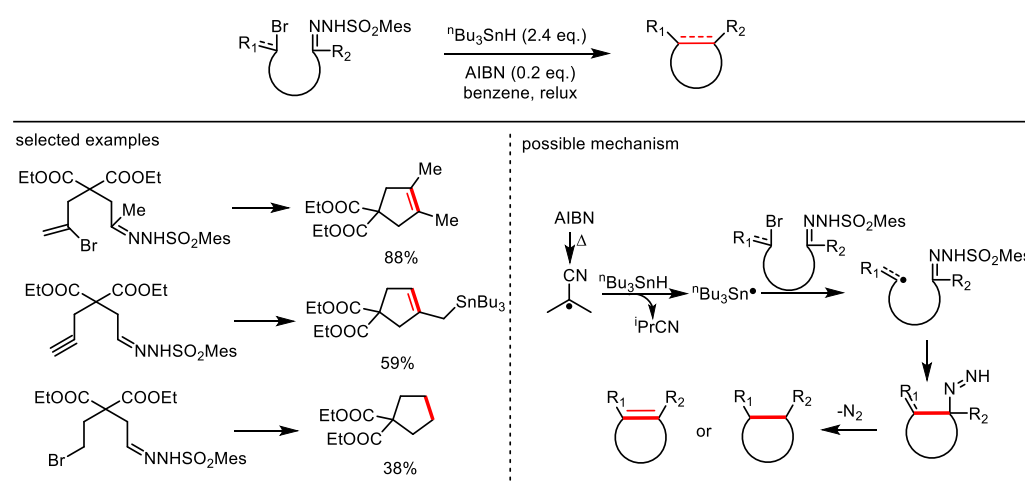
pathways (Scheme 4). This results in a vastly expanded set of accessible coupling partners such as alkyl halides,<sup>[26]</sup> dienes,<sup>[27]</sup> styrenes,<sup>[28]</sup> phenol derivatives,<sup>[29]</sup> aryl halides<sup>[30]</sup> in Ni catalysis and methylenecyclopropanes,<sup>[31]</sup> alkynes<sup>[32]</sup>, allylic acetates<sup>[33]</sup> and *gem*-difluorocyclopropanes<sup>[34]</sup> in Pd

catalysis. Several plausible reaction pathways in the different catalytic systems were postulated, as shown in Scheme 4. When styrenes and alkynes were employed as coupling partners, the authors proposed six-membered intermediates, analogous to the Zimmerman-Traxler transition state proposed for the Ru-catalytic Grignard-type reaction, as the key species for the new bond construction. The ligand exchange between deprotonated hydrazone (C-nucleophile or N-nucleophile) with the metal complex (Ni or Pd) was proposed as the key step in the catalytic cycle in the case of (pseudo) halides as electrophiles. Combining transition metal catalysis with the WK reaction creates unprecedented reactivity for widespread use in organic synthesis.

### 1.2.2 Carbanion generation via radical addition to sulfonyl hydrazones

Nucleophilic addition of organometallic reagents to C=N bonds of sulfonyl hydrazones leads to the generation of substituted carbanions (Scheme 2B). However, this approach has a limited functional group compatibility, and competing side reactions may occur. Moreover, the number of nucleophiles that can be engaged in such a modified WK process is limited. Aiming to overcome these limitations, strategies for the addition of radical species to sulfonyl hydrazone derivatives were developed.

The earliest example which invokes such a radical-initiated WK reaction pathway has been reported by Kim et al. as early as 1992.<sup>[35]</sup> In their report, the intramolecular addition of alkyl or vinyl radicals, generated from alkyl or vinyl bromides using an AIBN/<sup>n</sup>Bu<sub>3</sub>SnH condition, towards a C=N bond affords a cyclized diazene intermediate. The corresponding alkyl diazene decomposes to form a cyclized alkane product likely via a carbanion intermediate, whereas its allylic diazene counterpart undergoes a pericyclic rearrangement to give an endocyclic alkene product after N<sub>2</sub> extrusion (Scheme 5).

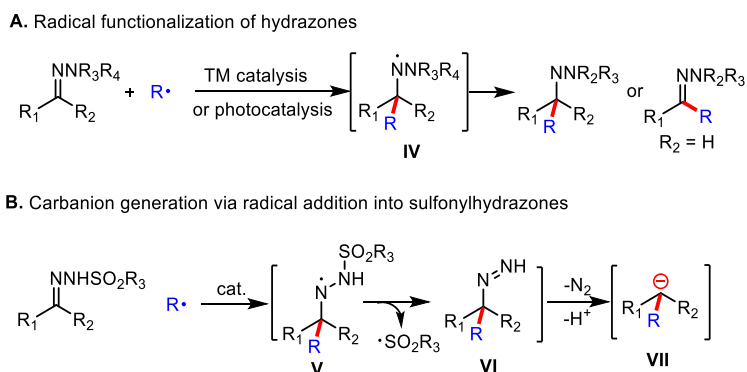


**Scheme 5.** Intramolecular radical functionalization of sulfonylhydrazones

While this protocol could be deemed as a representative radical-initiated WK process for the formation of versatile diazene species, this chemistry has been hardly appreciated over the past few decades with merely scattered examples reported.<sup>[36]</sup> However, this reaction sequence needs to be revisited considering reports of radical addition to other hydrazone acceptors (e.g., N,N-dialkyl hydrazones) using transition metal or photoredox catalysis (Scheme 6A).<sup>[37],[38]</sup>

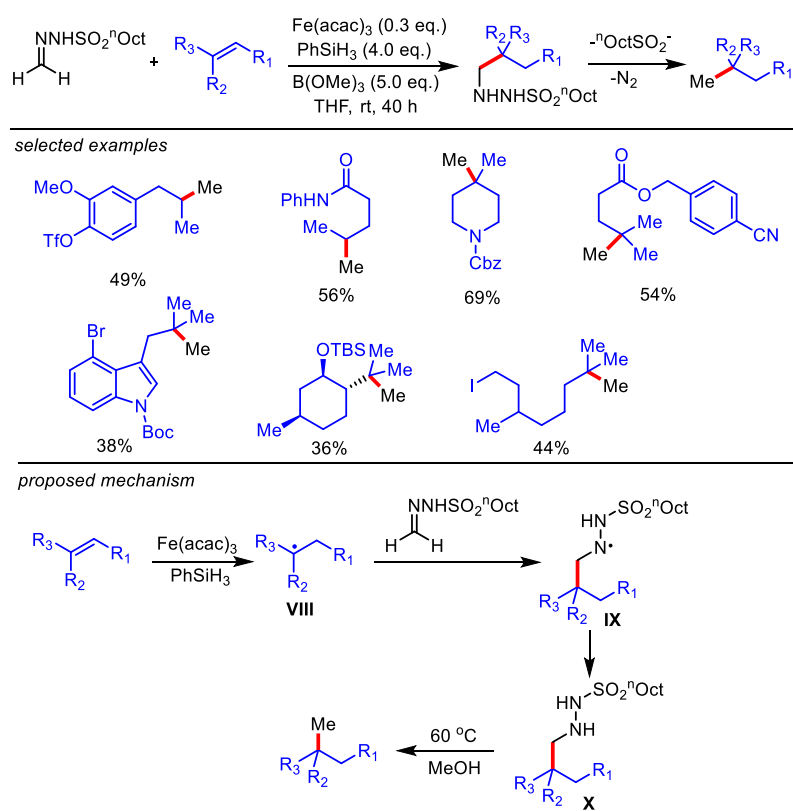
In a catalytic radical functionalization approach, aminyl radical intermediate **V** is first generated from radical addition to the C=N moiety of a N-sulfonyl hydrazone (Scheme 6B). The resulting N-centered radical undergoes  $\beta$ -fragmentation to release a sulfonyl radical affording the diazene intermediate **VI**.<sup>[35]</sup>

This diazene then enters a WK reaction sequence to afford the desired carbanion **VII** after N<sub>2</sub> extrusion. There are several distinct advantages in introducing new catalysis to this reaction sequence: milder reaction conditions to access carbanion equivalents and the facile generation of functionalized carbanions using different radicals.



**Scheme 6.** Catalytic radical functionalization of hydrazones

In this context, Baran and co-workers described that carbon radicals formed in the reaction of an intermediate [Fe–H] species with an alkene partner can couple efficiently with formaldehyde-derived *n*-octylsulfonylhydrazone to give a hydromethylation product (Scheme 7).<sup>[39]</sup> This reaction sequence could



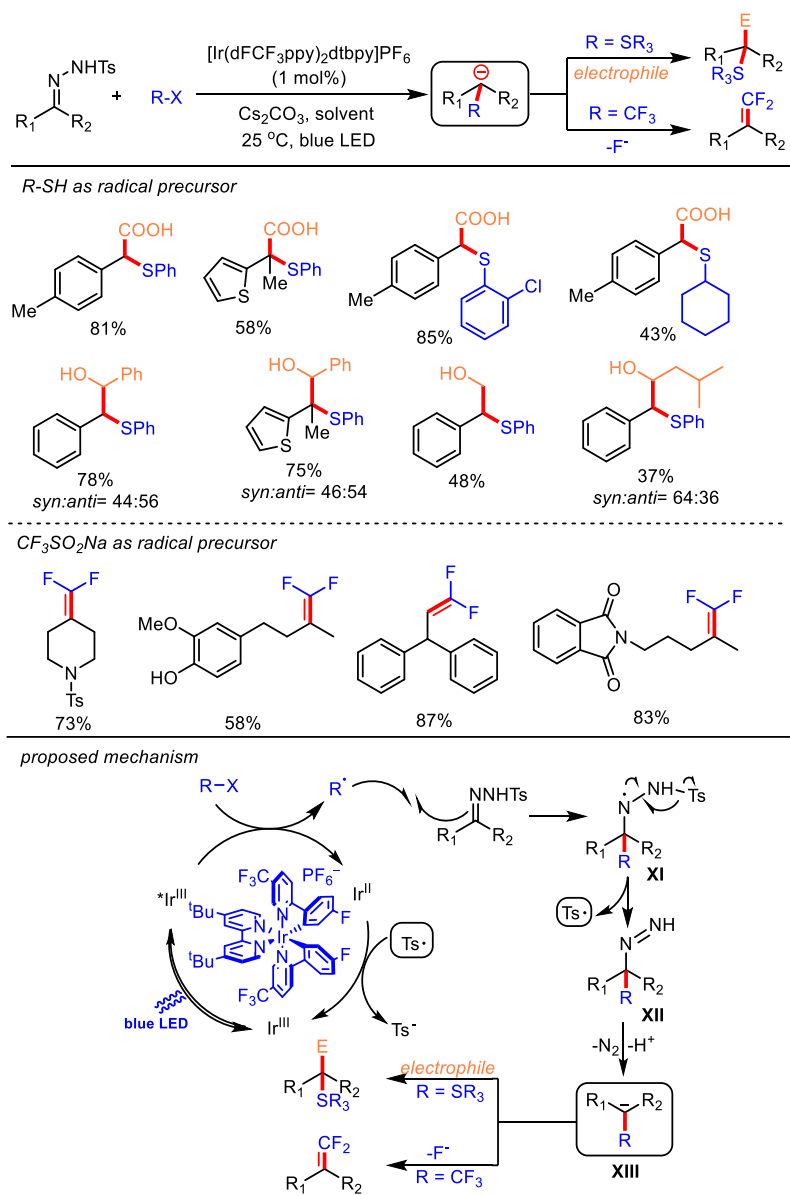
**Scheme 7.** Iron-catalyzed hydromethylation of alkenes

be initiated by using a stoichiometric or catalytic amount of Fe(acac)<sub>3</sub> with excess amounts of B(OMe)<sub>3</sub> being an essential additive in the latter case. Alkyl hydrazide **X** was observed as the key intermediate, which decomposes upon heating to 60 °C in MeOH to eliminate sulfinate and nitrogen to yield the



hydromethylated product presumably via an ionic pathway. Opposite to the organometallic-functionalization method as shown in Scheme 2B, this radical-based reaction tolerates base- and nucleophile-sensitive functional groups such as free alcohols, halides, azides and esters. The iron-catalytic system was further extended by Bradshaw to the alkylation of non-activated alkenes by using N-tosylhydrazones as radical acceptors.<sup>[40]</sup>

Over the last decades, photocatalysis has emerged as a powerful tool to access radicals for use in a broad range of chemical transformations through single-electron transfer between the excited state of a photocatalyst and substrates.<sup>[41]</sup> In the context of our ongoing research developing photoredox catalysis for carbanion generation, we questioned if a photo-Wolff-Kishner process can be realized by adding



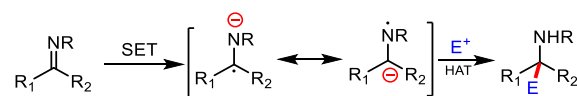
**Scheme 8.** Photo-WK reaction for catalytic difunctionalization of hydrazones

photo-generated radicals to sulfonyl hydrazones.<sup>[42]</sup> The envisioned reaction process was initiated by the SET-oxidation of a suitable substrate by the excited state of a photocatalyst to afford the radical and the reduced photocatalyst. Subsequent radical addition to the N-sulfonylhydrazone produces an aminyl radical species **XI**, which undergoes β-sulfonyl radical fragmentation generating a functionalized

diazene intermediate **XII**. The resulting diazene enters the WK process to give the key carbanion species **XIII**, capable of reacting with various electrophiles in a polar fashion. Finally, electron transfer between the reduced photocatalyst and the sulfonyl radical regenerates the catalyst, rendering the overall transformation redox-neutral. When thiols were used as radical precursors with an Ir-based catalyst, the thus generated  $\alpha$ -sulfenyl carbanions were efficiently produced, then trapped by CO<sub>2</sub> or aldehydes. In the case of a CF<sub>3</sub> radical, gem-difluoroalkenes were produced as the final product after E1cB elimination of a fluoride anion from the resulting  $\alpha$ -CF<sub>3</sub> carbanions (Scheme 8). This protocol shows that the merger of photocatalysis and a classical WK process leads to an efficient carbanion generation and broadens the available electrophiles scope for carbanion trapping.

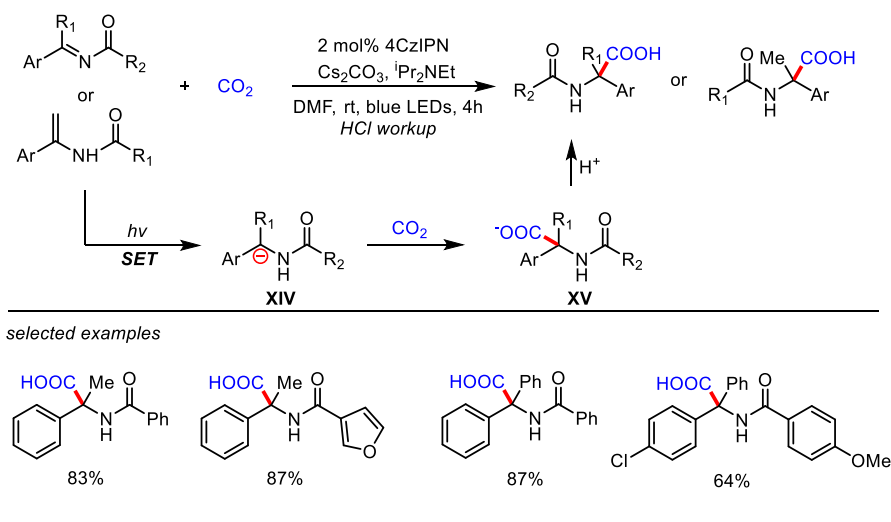
### 1.3 Generation of carbanions via catalytic single-electron reduction of imines - Pathway B

The generation of imine radical anions through single-electron reduction is well-documented and has been employed for many transformations utilizing stoichiometric reductants.<sup>[43]</sup> In recent years, new photocatalytic strategies have been developed as desirable alternatives for the single-electron reduction of imine derivatives.<sup>[7, 44]</sup> Imine radical anions can show C-centered and N-centered radical reactivity depending on the precursor and the reaction conditions. The C-centered radical species have been shown to engage in various radical coupling reactions.<sup>[7, 14, 44]</sup> While the N-centered radical can abstract hydrogen atoms from the reaction medium to give an  $\alpha$ -amino carbanion capable of reacting with various electrophiles in an ionic fashion (Scheme 9).



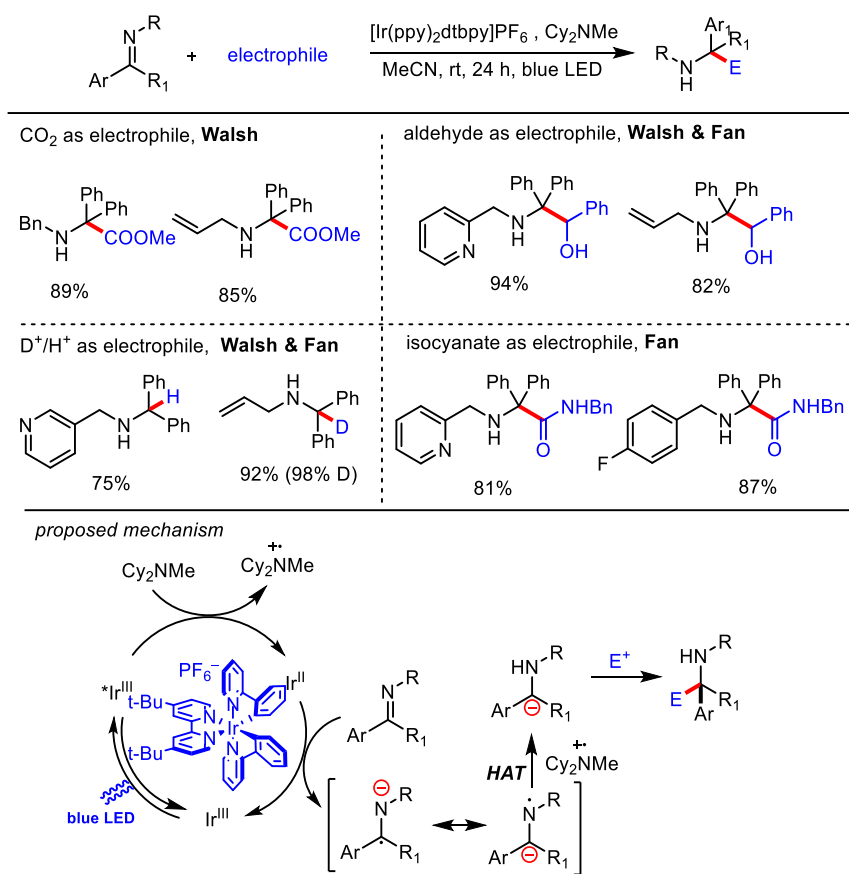
**Scheme 9.** Photoredox catalytic generation of  $\alpha$ -amino carbanions

In 2018, the Yu group reported a photoredox catalytic procedure for the hydrocarboxylation of enamides and aromatic imines with CO<sub>2</sub> (1 atm) yielding  $\alpha, \alpha$ -disubstituted  $\alpha$ -amino acids (Scheme 10).<sup>[45]</sup> The reaction relies on the photochemical reduction of the imine using a tertiary amine (DIPEA) as a sacrificial reductant to generate the  $\alpha$ -amino carbanion **XIV** as the key intermediate for CO<sub>2</sub> trapping. The authors conducted a series of control experiments and deuterium-labelling studies to prove the existence of the intermediate carbanion in the reaction.



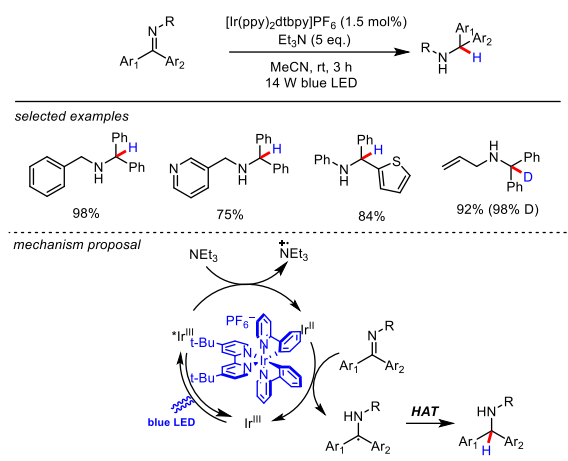
**Scheme 10.** Yu's photoredox catalytic hydrocarboxylation of imines

The same concept was independently developed by Fan, Walsh and co-workers using  $\text{Ir}(\text{ppy})_2(\text{dtbbpy})\text{PF}_6$  as photocatalyst,  $\text{Cy}_2\text{NMe}$  as terminal reductant for the visible-light-induced hydrocarboxylation of *N*-alkyl and *N*-aryl imines with  $\text{CO}_2$ .<sup>[46a]</sup> Their mechanistic proposal commences with the reductive quenching of the photoexcited  $\text{Ir}^{3+}$  species by  $\text{Cy}_2\text{NMe}$ , generating the reducing  $\text{Ir}^{2+}$  species and the amine radical cation. Subsequent single-electron transfer between imine and the  $\text{Ir}^{2+}$  species gives an amine radical cation and regenerates  $\text{Ir}^{3+}$ . The generated *N*-centered radical anion reacts with the amine radical cation in a HAT process providing the key carbanion intermediate, which was then trapped by  $\text{CO}_2$  to afford carboxylic acid as product after protonation. Furthermore, they found that the carbanions generated in the reaction are efficiently trapped by protons,<sup>[46b]</sup> aldehydes<sup>[47]</sup> or isocyanate<sup>[48]</sup> (Scheme 11).



**Scheme 11.** Fan and Walsh's photoredox catalytic system for the generation of carbanions from imines

In the same year, Polyzos and co-workers reported a similar method for the photo-induced hydrogenation of diaryl imines wherein  $\text{Ir}(\text{ppy})_2(\text{dtbbpy})\text{PF}_6$  and  $\text{Et}_3\text{N}$  were used as photocatalyst and terminal reductant.<sup>[49]</sup> It is worth mentioning that an  $\alpha$ -amino carbon-centered radical instead of the  $\alpha$ -amino carbanion (proposed in Fan and Walsh's work) was suggested as the key intermediate in their mechanistic proposal (Scheme 12).

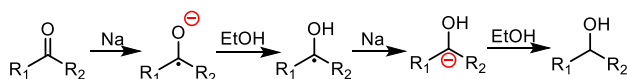


**Scheme 12.** Polyzos's photoredox catalytic system for the hydrogenation of imines

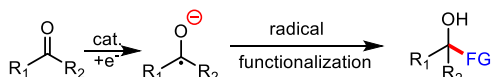
## 1.4 Generation of carbanions via catalytic sequential single-electron reduction of carbonyl - Pathway C

Single-electron reduction of carbonyl groups results in ketyl radical formation, a reactive intermediate which can participate in a wide range of chemical transformations. Although the resonance structure of a ketyl radical comprises carbon radical and carbon anion character, the most explored reactions, such as radical-radical coupling and radical addition to double bonds, arise from its carbon radical nature.<sup>[43c]</sup> In contrast to imine radical anions, carbanion generation from a carbonyl group requires a second single-electron reduction process of the ketyl radical. This pathway dates back to the well-known Bouveault-Blanc reduction, wherein an  $\alpha$ -hydroxy carbanion was produced as a key intermediate through two sequential single-electron reduction steps of esters by sodium metal (Scheme 13A).<sup>[50]</sup> Classic methods to induce the carbonyl reduction rely on strong reductants such as alkali metals,<sup>[51]</sup> vanadium,<sup>[52]</sup> titanium,<sup>[53]</sup> tin,<sup>[54]</sup> zinc<sup>[55]</sup> and samarium diiodide (SmI<sub>2</sub>).<sup>[43c, 56]</sup> In this context, visible-light-induced photocatalysis has been developed as ideal alternatives to access ketyl radicals from carbonyls by leveraging the reduction power of photocatalysis. As a consequence, a wide range of C-C bond-coupling reactions have been discovered by reacting ketyl radicals with C-centered radicals or unsaturated bonds (Scheme 13B). The research advance in exploiting the reactivity of ketyl radicals for C-C bond construction has been summarized in several recent reviews.<sup>[57]</sup> We therefore will focus on the catalytic generation of carbanions from the sequential reduction of carbonyls (Scheme 13C).

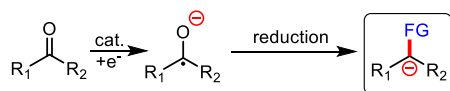
### A. Bouveault-Blanc reduction



### B. Catalytic generation and trapping of ketyl radical (well-explored reactivity)



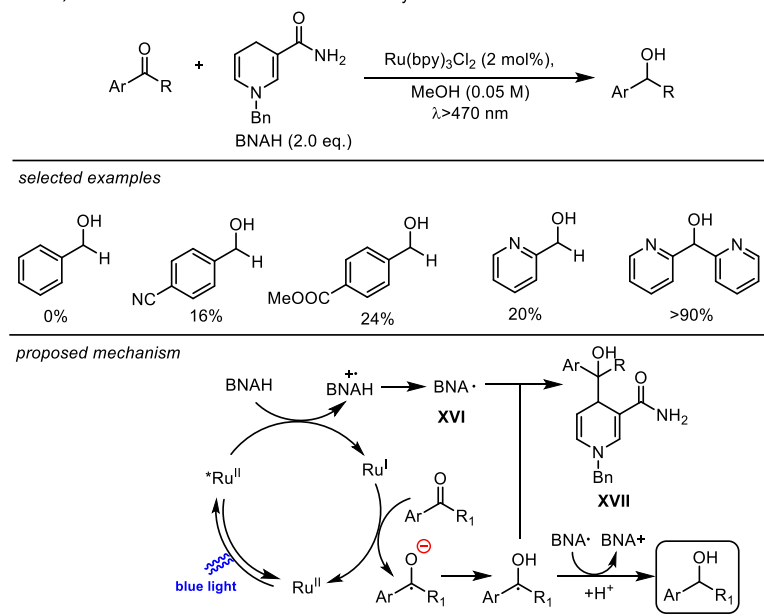
### C. Catalytic generation of carbanions from carbonyls



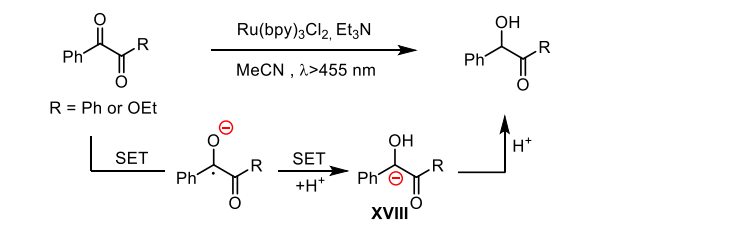
### Scheme 13. Generation of carbanions via sequential reduction of carbonyls

In 1983, Pac et al. reported the first example of a photoredox catalytic reduction of carbonyls in the presence of  $\text{Ru}(\text{bpy})_3\text{Cl}_2$  as the photocatalyst and N-benzyl-1,4-dihydronicotinamide (BNAH) as the reductant (Scheme 14A).<sup>[58]</sup> In the proposed mechanism, the excited state of  $^*\text{Ru}(\text{bpy})_3^{2+}$  was quenched by BNAH to produce  $\text{Ru}(\text{bpy})_3^+$  and  $\text{BNA}\cdot$  (**XVI**) after deprotonation. Single-electron transfer occurred between  $\text{Ru}(\text{bpy})_3^+$  and the carbonyl group yielding a ketyl radical and regenerating the photocatalyst. The resulting ketyl radical can undergo either a single-electron transfer process with  $\text{BNA}\cdot$  to give an

A. Pac, 1983: Photoreduction of ketones and aldehydes



B. Willner, 1990: Photoreduction of benzil and benzoylformate

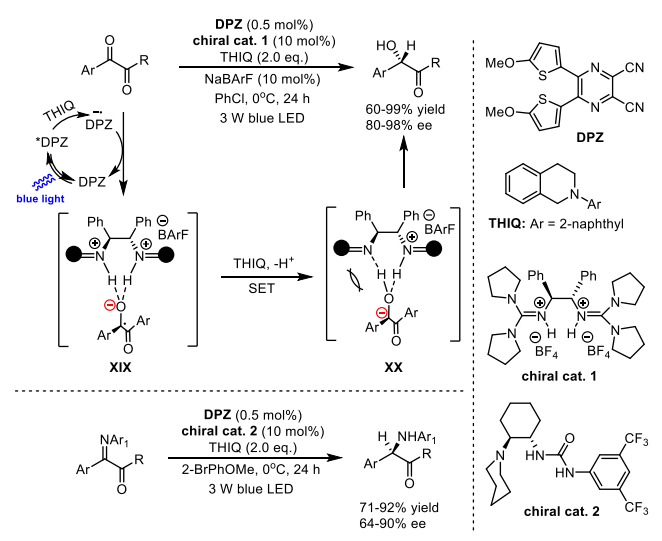


### Scheme 14. Photo-induced Ru-catalytic generation of carbanions via sequential reduction of carbonyls

alcohol or form by radical-radical coupling with  $\text{BNA}\cdot$  compound **XVII**. The interaction between the ketyl radical and **XVI** was dependent on the electronic property and structure of carbonyl compounds, and it was found that the existence of electron-withdrawing substituents and steric hindrance favors the electron transfer process between the two species. Later, a similar photoredox catalytic system for the reduction of activated ketones, including benzil and ethyl benzoylformate, was reported by Willner with  $\text{Ru}(\text{bpy})_3\text{Cl}_2$  as photocatalyst and  $\text{Et}_3\text{N}$  as reductant.<sup>[59]</sup> The reaction involves two successive photo-induced SET processes to generate the  $\alpha$ -hydroxyl carbanion **XVIII**, which was protonated to afford the hydrogenated product (Scheme 14B).

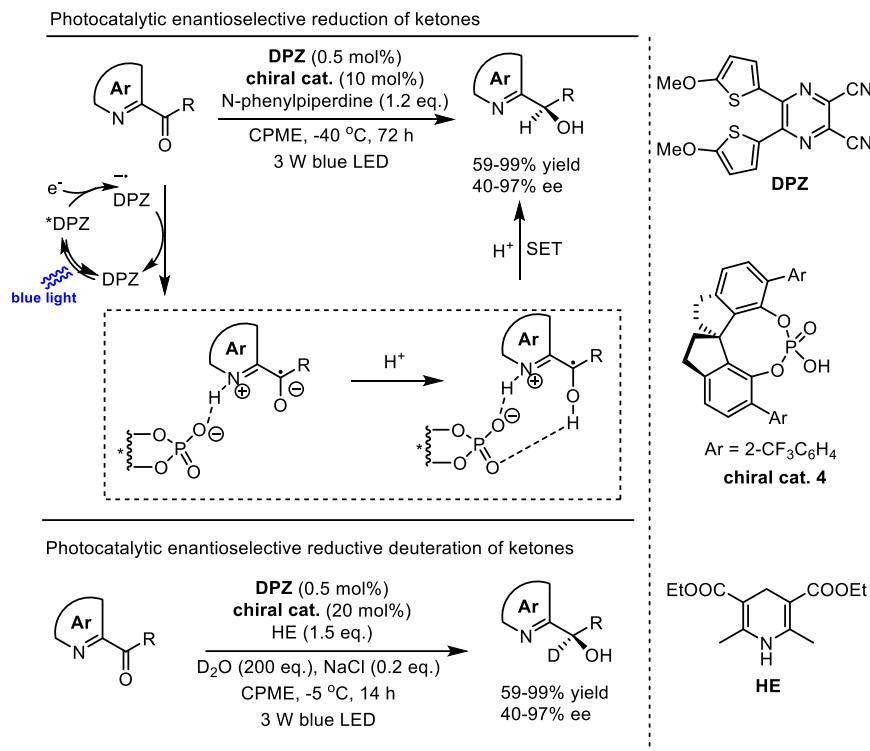
Recently, Jiang et al. demonstrated a unique dual photo/asymmetric Brønsted acid catalysis system for

enantioselective hydrogenations of 1,2-diketones (Scheme 15).<sup>[60]</sup> The catalytic system consists of an organic photocatalyst (DPZ), a chiral guanidinium salt catalyst **1**, a borate additive NaBARf and an electron donor N-2-naphthyl tetrahydroisoquinoline (THIQ). Non-covalent bonding between the Brønsted acid and the ketyl intermediate was found to be crucial for the reaction process. The second reduction of intermediate **XIX** was accomplished by THIQ to afford carbanion **XX** poised for the following enantioselective protonation process. The authors noted that the reaction occurs in the absence of DPZ through an electron-donor-acceptor mechanism, reaching comparable yields and enantioselectivities to those obtained in the photoredox catalytic system. The photocatalytic system was further applied for asymmetric hydrogenations of  $\alpha$ -keto ketimines to produce  $\alpha$ -amino ketones by exchanging the chiral catalyst from guanidinium salt **1** to a chiral 1,2-cyclohexanediamine-based urea-tertiary amine catalyst **2**.



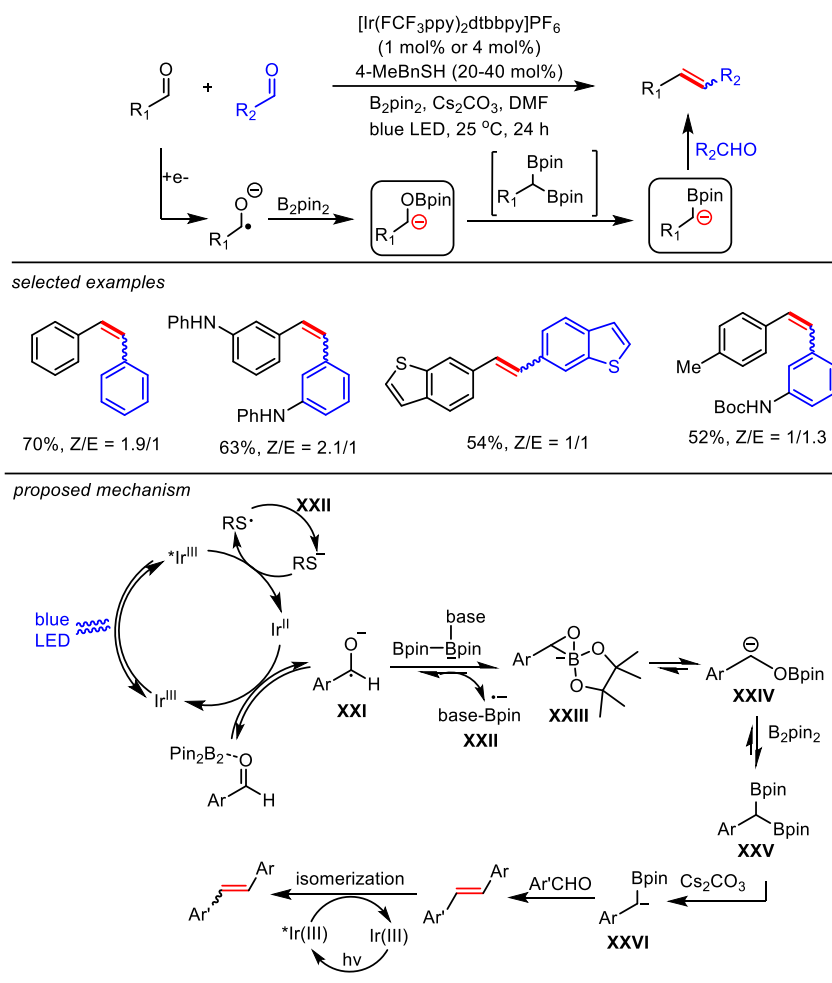
**Scheme 15.** Photocatalytic enantioselective hydrogenation of 1,2-diketones and  $\alpha$ -keto ketimines

Later, the same group extended this dual catalysis strategy to the asymmetric reduction of azaarene-based ketones.<sup>[61]</sup> Similarly, ketones underwent two single-electron reduction processes to give carbanions that participate in enantioselective protonation or deuteration using SPINOL-CPA **4** as chiral catalyst. A wide range of chiral azaarene-based secondary (deuterated) alcohols with diverse substitution patterns could be prepared in high yields with moderate to excellent enantioselectivity using this protocol (Scheme 16).



**Scheme 16.** Photocatalytic enantioselective reduction of ketones

The aforementioned methods relied on the photocatalytic successive single-electron reduction of an activated carbonyl functionality to access  $\alpha$ -hydroxyl carbanions, thus enabling the facile hydrogenation of these ketones. We speculated that the ketyl radical from a photo-induced single-electron reduction process could be further deoxygenated by an external reductant to afford other types of functionalized carbanions. In 2019, we demonstrated that a ketyl radical generated by the photoredox catalytic system from an aromatic aldehyde could be deoxygenated with  $B_2pin_2$  to yield an  $\alpha$ -boryl carbanion (Scheme 17).<sup>[62]</sup> The key to obtaining the desired reactivity was the use of thiol as a co-catalyst for shuttling electrons from  $B_2pin_2$  to the photocatalytic system. The resulting  $\alpha$ -boryl carbanion reacted with another molecule of benzaldehyde to afford the alkene as the final product, thus providing a mild and efficient photocatalytic McMurry reaction. The reaction system was applicable to the synthesis of both symmetrical and unsymmetrical alkenes with broad substrate scope and high level of functional group tolerance. Based on the *in-situ* NMR studies and experimental results, we propose the following reaction mechanism: reductive quenching of the excited  $Ir^{III}$  complex by thiolate affords a thiyl radical and the reduced photocatalyst  $Ir^{II}$ . The single-electron transfer between the  $Ir^{II}$  species and benzaldehyde regenerates the photocatalyst and yields a ketyl radical **XXI**, which participates in a radical borylation-“bora-Brook” rearrangement sequence to give  $\alpha$ -oxyboryl carbanion **XXIV** and a base-bond boryl radical anion **XXII**. Reduction of the thiyl radical by **XXII** regenerates the thiolate. The  $\alpha$ -oxyboryl carbanion **XXIV** reacted with another molecule of  $B_2pin_2$  yielding the 1,1-benzylidiboronate ester **XXV**, which underwent base-assisted deborylation to give  $\alpha$ -boryl carbanion **XXVI**. Subsequent B-O elimination after nucleophilic addition to another aldehyde and an energy-transfer process yielded a mixture of the *E*- and *Z*-alkene.



**Scheme 17.** Photocatalytic catalytic generation of  $\alpha$ -boryl carbanion

## 1.5 Conclusion and outlook

We have summarized recent advances in the generation of carbanionic intermediates by catalytic carbonyl Umpolung strategies. Three reaction pathways yield carbanions starting from carbonyls. First, the merger of the Wolff-Kishner reaction with catalysis provides efficient ways for the generation and/or trapping of carbanionic species, which impressively revitalizes this century-old chemistry. Second,  $\alpha$ -amino carbanions are obtained by exploiting the carbanionic property of an imine radical anion from a catalytic single-electron reduction process. Besides, catalytic strategies have been applied for the production of carbanionic species via successive reduction of carbonyl functionalities. In comparison to catalytic carbonyl Umpolung reactions involving an acyl anion, research addressing the analogous catalytic chemistry of alkyl carbanion equivalents from carbonyls has received considerably less attention. One reason was the absence of suitable catalytic methods. This has changed and the combination of the classic reaction modes with recent transition metal or photocatalysis have demonstrated a great potential for the generation of alkyl carbanions, capable of participating in various C-C bond forging reactions in a mild and controllable manner.

However, despite the impressive advances in this field, further development is still required to address the limitations and challenges. The catalytic radical-initiated WK reaction using a sulfonyl hydrazone



as radical acceptor has merely appeared in a limited number of literature reports (pathway A). We anticipate that synthetic applications of this chemistry can be further explored towards addressing the following aspects: 1) Expanding the scope of radical precursors for the production of carbanions. 2) Exploiting the reactivity of the generated diazene intermediates for more transformations (e.g., pericyclic arrangements to construct unsaturated bonds). 3) Exploring the possibility of combining other catalysis (for the radical generation) with the WK process to produce anionic species. In the case of strategies involving the catalytic single-electron reduction of imines and carbonyls (pathway B and C), related transformations remain in their infancy and suffer from a limited substrate scope as well as the small diversity of trapping electrophiles. Efforts are therefore expected to be devoted to the development of more efficient catalytic systems to address these challenges and limitations.

In our opinion, numerous exciting opportunities in the catalytic carbonyl Umpolung for carbanions generation wait to be discovered, expanding the toolbox of valuable transformations in organic synthesis. We hope this review will stimulate more chemists to exploit new catalytic methods and strategies to address the above-described challenges in the future.

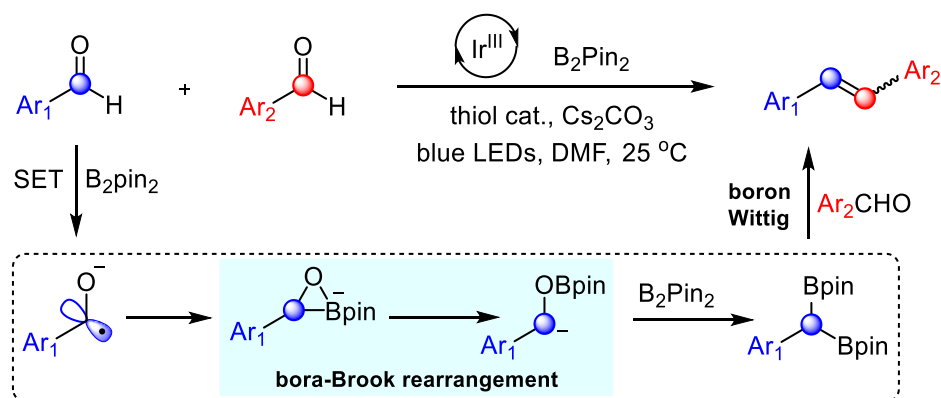
## 1.6 References

- [1] G. Wittig, P. Davis, G. Koenig, *Chem. Ber.* **1951**, *84*, 627-632.
- [2] D. Seebach, *Angew. Chem. Int. Ed.* **1979**, *18*, 239-258.
- [3] Wöhler, Liebig, *Ann. Phar.* **1832**, *3*, 249-282.
- [4] a) E. J. Corey, D. Seebach, *Angew. Chem. Int. Ed.* **1965**, *4*, 1075-1077; b) E. J. Corey, D. Seebach, *Angew. Chem. Int. Ed.* **1965**, *4*, 1077-1078.
- [5] a) D. Enders, O. Niemeier, A. Henseler, *Chem. Rev.* **2007**, *107*, 5606-5655; b) D. M. Flanigan, F. Romanov-Michailidis, N. A. White, T. Rovis, *Chem. Rev.* **2015**, *115*, 9307-9387.
- [6] D. E. Lewis, *Angew. Chem. Int. Ed.* **2013**, *52*, 11704-11712.
- [7] J. A. Leitch, T. Rossolini, T. Rogova, J. A. P. Maitland, D. J. Dixon, *ACS Catal.* **2020**, *10*, 2009-2025.
- [8] M. Huang, *J. Am. Chem. Soc.* **1946**, *68*, 2487-2488.
- [9] D. Barton, D. Ives, B. Thomas, *J. Chem. Soc.* **1955**, 2056.
- [10] D. J. Cram, M. R. V. Sahyun, *J. Am. Chem. Soc.* **1962**, *84*, 1734-1735.
- [11] M. F. Grundon, H. B. Henbest, M. D. Scott, *J. Chem. Soc.* **1963**, 1855-1858.
- [12] L. Caglioti, M. Magi, *Tetrahedron* **1963**, *19*, 1127-1131.
- [13] M. E. Furrow, A. G. Myers, *J. Am. Chem. Soc.* **2004**, *126*, 5436-5445.
- [14] a) S. Chandrasekhar, M. Venkat Reddy, K. Srinivasa Reddy, C. Ramarao, *Tetrahedron Lett.* **2000**, *41*, 2667-2670; b) A. G. Myers, M. Movassaghi, *J. Am. Chem. Soc.* **1998**, *120*, 8891-8892.
- [15] H. Wang, X.-J. Dai, C.-J. Li, *Nat. Chem.* **2017**, *9*, 374-378.
- [16] X.-J. Dai, C.-J. Li, *J. Am. Chem. Soc.* **2016**, *138*, 5433-5440.
- [17] a) N. Chen, X.-J. Dai, H. Wang, C.-J. Li, *Angew. Chem. Int. Ed.* **2017**, *56*, 6260-6263; b) Y.-Z. Wang, Q. Liu, L. Cheng, S.-C. Yu, L. Liu, C.-J. Li, *Tetrahedron* **2021**, *80*, 131889.
- [18] X.-J. Dai, H. Wang, C.-J. Li, *Angew. Chem. Int. Ed.* **2017**, *56*, 6302-6306.
- [19] L. Lv, C.-J. Li, *Chem. Sci.* **2021**, *12*, 2870-2875.
- [20] S.-S. Yan, L. Zhu, J.-H. Ye, Z. Zhang, H. Huang, H. Zeng, C.-J. Li, Y. Lan, D.-G. Yu, *Chem. Sci.* **2018**, *9*, 4873-4878.
- [21] L. Lv, L. Yu, Z. Qiu, C. J. Li, *Angew. Chem. Int. Ed.* **2020**, *59*, 6466-6472.
- [22] D. Cao, P. Pan, H. Zeng, C.-J. Li, *Chem. Commun.* **2019**, *55*, 9323-9326.
- [23] W. Wei, X.-J. Dai, H. Wang, C. Li, X. Yang, C.-J. Li, *Chem. Sci.* **2017**, *8*, 8193-8197.
- [24] a) C.-C. Li, H. Wang, M. M. Sim, Z. Qiu, Z.-P. Chen, R. Z. Khaliullin, C.-J. Li, *Nat. Commun.* **2020**, *11*, 6022; b) C.-C. Li, J. Kan, Z. Qiu, J. Li, L. Lv, C.-J. Li, *Angew. Chem. Int. Ed.* **2020**, *59*, 4544-4549.
- [25] C.-C. Li, X.-J. Dai, H. Wang, D. Zhu, J. Gao, C.-J. Li, *Org. Lett.* **2018**, *20*, 3801-3805.
- [26] a) C. Zhu, J. Zhang, *Chem. Commun.* **2019**, *55*, 2793-2796; b) D. Zhu, L. Lv, Z. Qiu, C.-J. Li, *J. Org. Chem.* **2019**, *84*, 6312-6322.
- [27] L. Lv, D. Zhu, Z. Qiu, J. Li, C.-J. Li, *ACS Catal.* **2019**, *9*, 9199-9205.
- [28] L. Lv, D. Zhu, C.-J. Li, *Nat. Commun.* **2019**, *10*, 715.
- [29] L. Lv, D. Zhu, J. Tang, Z. Qiu, C.-C. Li, J. Gao, C.-J. Li, *ACS Catal.* **2018**, *8*, 4622-4627.
- [30] J. Tang, L. Lv, X.-J. Dai, C.-C. Li, L. Li, C.-J. Li, *Chem. Commun.* **2018**, *54*, 1750-1753.
- [31] J. Yao, Z. Chen, L. Yu, L. Lv, D. Cao, C.-J. Li, *Chem. Sci.* **2020**, *11*, 10759-10763.
- [32] L. Yu, L. Lv, Z. Qiu, Z. Chen, Z. Tan, Y. F. Liang, C. J. Li, *Angew. Chem. Int. Ed.* **2020**, *59*, 14009-14013.
- [33] D. Zhu, L. Lv, C.-C. Li, S. Ung, J. Gao, C.-J. Li, *Angew. Chem. Int. Ed.* **2018**, *57*, 16520-16524.

- [34] L. Lv, C.-J. Li, *Angew. Chem. Int. Ed.*, **2021**, DOI: <https://doi.org/10.1002/anie.202102240>.
- [35] S. Kim, J. R. Cho, *Synlett* **1992**, *1992*, 629-630.
- [36] N. E. Campbell, G. M. Sammis, *Angew. Chem. Int. Ed.* **2014**, *53*, 6228-6231.
- [37] G. K. Friestad, in *Radicals in Synthesis III* (Eds.: M. Heinrich, A. Gansäuer), Springer Berlin Heidelberg, Berlin, Heidelberg, **2012**, pp. 61-91.
- [38] P. Xu, W. Li, J. Xie, C. Zhu, *Acc. Chem. Res.* **2018**, *51*, 484-495.
- [39] H. T. Dao, C. Li, Q. Michaudel, B. D. Maxwell, P. S. Baran, *J. Am. Chem. Soc.* **2015**, *137*, 8046-8049.
- [40] M. Saladrigas, J. Bonjoch, B. Bradshaw, *Org. Lett.* **2020**, *22*, 684-688.
- [41] a) L. Marzo, S. K. Pagire, O. Reiser, B. König, *Angew. Chem. Int. Ed.* **2018**, *57*, 10034-10072; b) J. M. R. Narayanam, C. R. J. Stephenson, *Chem. Soc. Rev.* **2011**, *40*, 102-113; c) C. K. Prier, D. A. Rankic, D. W. C. MacMillan, *Chem. Rev.* **2013**, *113*, 5322-5363; d) D. Ravelli, S. Protti, M. Fagnoni, *Chem. Rev.* **2016**, *116*, 9850-9913; e) N. A. Romero, D. A. Nicewicz, *Chem. Rev.* **2016**, *116*, 10075-10166; f) K. L. Skubi, T. R. Blum, T. P. Yoon, *Chem. Rev.* **2016**, *116*, 10035-10074.
- [42] S. Wang, B.-Y. Cheng, M. Sršen, B. König, *J. Am. Chem. Soc.* **2020**, *142*, 7524-7531.
- [43] a) T. Nishino, Y. Nishiyama, N. Sonoda, *Heteroat. Chem.* **2002**, *13*, 131-135; b) B. K. Banik, O. Zegrocka, I. Banik, L. Hackfeld, F. F. Becker, *Tetrahedron Lett.* **1999**, *40*, 6731-6734; c) M. Szostak, N. J. Fazakerley, D. Parmar, D. J. Procter, *Chem. Rev.* **2014**, *114*, 5959-6039.
- [44] A. F. Garrido-Castro, M. C. Maestro, J. Alemán, *Catalysts* **2020**, *10*, 562.
- [45] T. Ju, Q. Fu, J.-H. Ye, Z. Zhang, L.-L. Liao, S.-S. Yan, X.-Y. Tian, S.-P. Luo, J. Li, D.-G. Yu, *Angew. Chem. Int. Ed.* **2018**, *57*, 13897-13901.
- [46] a) X. Fan, X. Gong, M. Ma, R. Wang, P. J. Walsh, *Nat. Commun.* **2018**, *9*, 4936. b) R. Wang, M. Ma, X. Gong, G. B. Panetti, X. Fan, P. J. Walsh, *Org. Lett.* **2018**, *20*, 2433-2436.
- [47] R. Wang, M. Ma, X. Gong, X. Fan, P. J. Walsh, *Org. Lett.* **2019**, *21*, 27-31.
- [48] J. Zhu, C. Dai, M. Ma, Y. Yue, X. Fan, *Org. Chem. Front.* **2021**, *8*, 1227-1232.
- [49] D. J. van As, T. U. Connell, M. Brzozowski, A. D. Scully, A. Polyzos, *Org. Lett.* **2018**, *20*, 905-908.
- [50] J. J. Li. Bouveault-Blanc reduction. In: Name Reactions. Springer, Berlin, Heidelberg. 2003. pp. 48-48
- [51] a) S. K. Pradhan, S. R. Kadam, J. N. Kolhe, T. V. Radhakrishnan, S. V. Sohani, V. B. Thaker, *J. Org. Chem.* **1981**, *46*, 2622-2633; b) D. Guijarro, B. Mancheño, M. Yus, *Tetrahedron* **1993**, *49*, 1327-1334.
- [52] T. Hirao, *Chem. Rev.* **1997**, *97*, 2707-2724.
- [53] A. Gansäuer, M. Moschioni, D. Bauer, *Eur. J. Org. Chem.* **1998**, *1998*, 1923-1927.
- [54] T. Naito, K. Tajiri, T. Harimoto, I. Ninomiya, T. Kiguchi, *Tetrahedron Lett.* **1994**, *35*, 2205-2206.
- [55] C.-H. Yeh, R. P. Korivi, C.-H. Cheng, *Adv. Synth. Catal.* **2013**, *355*, 1338-1344.
- [56] K. C. Nicolaou, S. P. Ellery, J. S. Chen, *Angew. Chem. Int. Ed.* **2009**, *48*, 7140-7165.
- [57] a) B. Qiao, Z. Jiang, *ChemPhotoChem* **2018**, *2*, 703-714; b) K. N. Lee, M.-Y. Ngai, *Chem. Commun.* **2017**, *53*, 13093-13112; c) Q. Xia, J. Dong, H. Song, Q. Wang, *Chem. Eur. J.* **2018**.
- [58] O. Ishitani, C. Pac, H. Sakurai, *J. Org. Chem.* **1983**, *48*, 2941-2942.
- [59] I. Willner, T. Tsfania, Y. Eichen, *J. Org. Chem.* **1990**, *55*, 2656-2662.
- [60] L. Lin, X. Bai, X. Ye, X. Zhao, C.-H. Tan, Z. Jiang, *Angew. Chem. Int. Ed.* **2017**, *56*, 13842-13846.
- [61] a) B. Qiao, C. Li, X. Zhao, Y. Yin, Z. Jiang, *Chem. Commun.* **2019**, *55*, 7534-7537; b) T. Shao, Y. Li, N. Ma, C. Li, G. Chai, X. Zhao, B. Qiao, Z. Jiang, *iScience* **2019**, *16*, 410-419.
- [62] S. Wang, N. Lokesh, J. Hioe, R. M. Gschwind, B. König, *Chem. Sci.* **2019**, *10*, 4580-4587.



## 2. Photoinitiated Carbonyl-Metathesis: Deoxygenative Reductive Olefination of Aromatic Aldehydes via Photoredox Catalysis



### Abstract:

Carbonyl–carbonyl olefination, known as McMurry reaction, represents a powerful strategy for the construction of olefins. However, catalytic variants that directly couple two carbonyl groups in a single reaction are less explored. Here, we report a photoredox-catalysis that uses B<sub>2</sub>pin<sub>2</sub> as terminal reductant and oxygen trap allowing for deoxygenative olefination of aromatic aldehydes under mild conditions. This strategy provides access to a diverse range of symmetrical and unsymmetrical alkenes with moderate to high yield (up to 83%) and functional-group tolerance. To follow the reaction pathway, a series of experiments were conducted including radical inhibition, deuterium labelling, fluorescence quenching and cyclic voltammetry. Furthermore, NMR studies and DFT calculations were combined to detect and analyze three active intermediates: a cyclic three-membered anionic species, an α-oxyboryl carbanion and a 1,1-benzylidiboronate ester. Based on these results, we propose a mechanism for the C=C bond generation involving a sequential radical borylation, “bora-Brook” rearrangement, B<sub>2</sub>pin<sub>2</sub>-mediated deoxygenation and a boron-Wittig process.

**This chapter has been published in:** S. Wang, N. Lokesh, J. Hioe, R. Gschwind\* and B. König\*. *Chem. Sci.* **2019**, *10*, 4580–4587. Reproduced with permission from RSC.

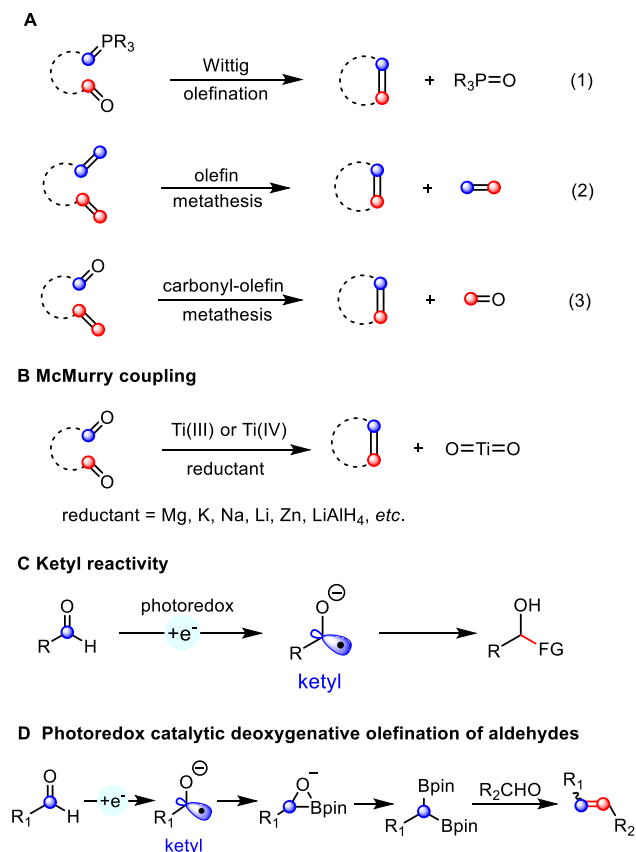
### Author Contributions:

S. W. carried out all photo reactions and wrote the manuscript and supporting information, S.W. and N. L. performed all the NMR mechanistic investigations and wrote the NMR chapter of the manuscript and the Supporting Information, J. H. performed the chemical shift calculations. R. G. and B. K. supervised the project. R. G. and B. K. are the corresponding author.

## 2.1 Introduction

Alkenes are omnipresent in natural compounds and essential functional groups for many chemical transformations. Among many methods that have been developed for the generation of alkenes, olefination and metathesis reactions converting two functional groups into one alkene are particularly useful for the synthesis of complex molecules. The classic Wittig olefination uses phosphonium ylide reagents (Scheme 1A, eqn (1))<sup>[1]</sup> and many related carbonyl olefination processes, such as the Horner–Wadsworth–Emmons,<sup>[1b]</sup> Peterson,<sup>[2]</sup> Julia<sup>[3]</sup> and Tebbe<sup>[4]</sup> reactions utilizing different ylide or carbene precursors have been developed. Olefin cross-metathesis reactions catalyzed by metal alkylidenes allow the exchange between two olefins to form a pair of distinct alkenes (Scheme 1A, eqn (2)).<sup>[5]</sup> The related catalytic olefin–carbonyl metathesis strategy for the synthesis of alkenes was discovered just recently (Scheme 1A, eqn (3)).<sup>[6]</sup>

Contrary to these olefination and metathesis processes, catalytic bicarbonyl olefination reactions remain less developed. The McMurry reaction provides an attractive route to alkenes from two carbonyl groups (Scheme 1B).<sup>[7]</sup> The net result of such a carbonyl–carbonyl olefination could be viewed as a “metathesis” process although the oxygen atom is generally not released as oxygen gas,



**Scheme 1.** Divergent functionalization of carbonyl

but bounded to reagents. Classic McMurry protocols use titanium salts in combination with a reducing reagent under heating. The whole process is driven thermodynamically by the formation of strong Ti–O bonds. Despite being very effective and widely used, this system generally requires relatively harsh reaction conditions, such as the use of stoichiometric amounts of the titanium reagent and strong reductants at high temperature, lowering the overall functional group tolerance.<sup>[7–8]</sup> Therefore, several

milder and catalytic methods were developed. A variant using only catalytic amounts of titanium with an excess of chlorosilane was developed by Fürstner and co-workers.<sup>[9]</sup> Wagner used hexachlorodisilane at high temperature (160 °C) for converting diarylmethanones into tetraarylethylenes.<sup>[10]</sup> More recently, Ott et al. reported the stereoselective preparation of *E*-alkenes from two aldehydes by using phosphanylphosphonate.<sup>[11]</sup> After that, Li described a stepwise Ru-catalyzed carbonyl-carbonyl olefination method wherein hydrazine was employed as the mediator to transform one carbonyl into its carbanion equivalent.<sup>[12]</sup> Despite these advances, the direct catalytic carbonyl-carbonyl olefination in one step and under mild reaction conditions remains a challenge.

In recent years, photoredox catalysis has evolved into an attractive alternative to traditional strategies for generating radical intermediates.<sup>[13]</sup> For instance, ketyl radicals can be easily accessed from carbonyl compounds by using a photoredox-mediated single-electron reduction strategy.<sup>[14]</sup> The obtained ketyl radicals have been used in C-C bond formation by addition to  $\pi$  systems or radical-radical coupling (Scheme 1C). However, a photoredox catalyzed reductive coupling of carbonyls followed by deoxygenation yielding a carbon-carbon double bond has not been achieved so far. Herein, we report the first deoxygenative olefination coupling of aromatic aldehydes enabled by the cooperative action of bis(pinacolato)diboron and a photoredox catalytic system (Scheme 1D).

The anticipated deoxygenative olefination process requires a four-electron reduction and an efficient oxygen acceptor. Moreover, a careful design of the catalytic system is required to suppress the competing pinacol coupling.<sup>[15]</sup> With these mechanistic challenges in mind, we envisioned the possibility of combining the photocatalytic carbonyl reduction system with a diboron reagent allowing an efficient McMurry-type process based on the following considerations: 1) the Lewis acidity of the boron atom of the diboronate compounds could potentially activate the carbonyl groups thus facilitating the single-electron reduction process.<sup>[16]</sup> 2) the formation of a strong B-O bond would provide a significant thermodynamic driving force for the deoxygenation process.<sup>[16b],[17]</sup>

## 2.2 Results and discussion

### 2.2.1 Optimization of reaction condition

To examine the feasibility of our hypothesis, we chose *para*-tolualdehyde **1a** as the model substrate in combination with bis(pinacolato)diboron ( $B_2pin_2$ ) as the oxygen acceptor. A promising result was obtained when irradiating a mixture containing **1a**,  $B_2pin_2$ , DIPEA,  $CS_2CO_3$ ,  $[Ir(dFCF_3ppy)_2dtbbpy]PF_6$  (1 mol%) and DMF with a blue LED lamp giving trace amounts of alkene **2a** (see Supplementary Information Table S1, entry 1). Interestingly, removing the electron donor DIPEA from the system also yielded the product in 6% yield with full conversion of **1a** (Table S1, entry 2). Moreover, the alkene **2a** was not detected in the absence of either  $CS_2CO_3$  or  $B_2pin_2$  (Table S1, entry 3-4). As the formation of the product does not require an additional electron donor, we reasoned that  $B_2Pin_2$  may serve as the terminal reductant and the oxygen acceptor in this reaction. Next, we explored the effect of another co-catalyst, which could potentially shuttle electrons from the boron species to the photocatalytic system.<sup>[18]</sup> To our delight, a significant increase in yield (39%, Table S1, entry 6) was observed upon adding benzyl thiol (10 mol%) as co-catalyst, whereas quinuclidine proved ineffective (Table S1, entry 5). Testing the reaction with other bases resulted in lower yields (Table S1 entry 7-15). Further evaluation of other thiols revealed that only benzyl thiol (20 mol%) and 4-Me-benzyl thiol (20 mol%) gave comparably

good yields (Table S2, entry 6 and entry 14). A variety of photocatalysts were tested for this transformation; using a slightly modified catalyst [Ir(FCF<sub>3</sub>ppy)<sub>2</sub>dtbbpy]PF<sub>6</sub> increased the yield to 74% (*Z/E* = 2.2/1). Screening of the solvents revealed that DMF was the optimal solvent for this reaction (Table S3). Better yield and *Z/E* selectivity were achieved by employing a combination of [Ir(FCF<sub>3</sub>ppy)<sub>2</sub>dtbbpy]PF<sub>6</sub> with 4-Me-benzyl thiol (Table S4, entry 3). Subsequently, the effect of concentration was examined, subtly varying the concentration to 0.33 M increased the yield to 87% with a better *Z/E* selectivity of the product (*Z/E* = 2.6/1) (Table S5, entry 3). Interestingly, small amounts of product **2a** (17%, Table 1, entry 10) were also detected in the absence of the photocatalyst. Presumably, small amount of benzaldehyde could be excited by visible light in the presence of B<sub>2</sub>pin<sub>2</sub> to form ketyl radical that leads to the formation of product. However, further control experiments confirmed that both the photocatalyst and light were crucial for efficient transformation (Table 1, entry 9 and 10).

**Table 1.** Screening of reaction conditions

Entry	Change from standard conditions	Yield of <b>2a</b> ( <i>Z</i> and <i>E</i> ) [%]	<i>Z/E</i> <sup>[b]</sup>
1	none	87	2.6/1
2	without thiol	trace	-
3	without B <sub>2</sub> in <sub>2</sub>	0	-
4	without Cs <sub>2</sub> CO <sub>3</sub>	trace	-
5	Na <sub>2</sub> CO <sub>3</sub> instead of Cs <sub>2</sub> CO <sub>3</sub>	trace	-
6	CsF instead of Cs <sub>2</sub> CO <sub>3</sub>	trace	-
7	DMF (1 mL)	77	2.5/1
8	DMF (0.4 mL)	68	2.4/1
9	without light	0	-
10	without photocatalyst	17	3.5/1

<sup>a</sup>Unless otherwise noted, all reactions were carried out with **1a** (0.2 mmol), [Ir(FCF<sub>3</sub>ppy)<sub>2</sub>dtbbpy]PF<sub>6</sub> (0.002 mmol), B<sub>2</sub>pin<sub>2</sub> (0.24 mmol), Cs<sub>2</sub>CO<sub>3</sub> (0.24 mmol), 4-Me-BnSH (0.04 mmol) in anhydrous DMF (0.6 mL) under nitrogen, irradiation with 3 W blue LED for 24 h at 25 °C. Yields were determined by crude NMR using 1,3,5-trimethoxybenzene as an internal standard. <sup>b</sup>*Z* : *E* ratio determined by <sup>1</sup>H NMR analysis.

### 2.2.2 Synthetic scope

With the optimized reaction conditions in hand, we then investigated the scope of this reaction with substituted aromatic aldehydes as substrates. A broad range of aromatic aldehydes bearing *para*-(**1a-1g**), *meta*-(**1h-1p**) or *ortho*-(**1q-1s**) substituents reacted smoothly to afford the corresponding alkenes. Many synthetically useful functional groups including alkyl (**1a**, **1c** and **1q**), alkoxy (**1d-e**, **1h**, **1r** and **1t**), acetal (**1u**), silyl (**1m**), boronic ester (**1n**) are tolerated in this transformation.

Importantly, the presence of acidic protons in amides (**1f-g**, and **1i**) and amines (**1j**) did not interfere with the reaction, giving yields of the isolated alkenes ranging from 47% to 63%. Aromatic substituents,



such as phenyl (**1k**, **1s**) and thiophenyl (**1l**) furnished alkene products, albeit in lower yields. Furthermore, the reaction was compatible with halogen substituents on the benzaldehydes and gave the chloro- and fluoro-substituted alkenes in 40% and 32% yield, respectively (**1o-p**). However, benzaldehydes possessing strong electron-withdrawing groups, such as nitro or nitrile, were not tolerated. *ortho*-Substituted 2-methyl benzaldehyde gave an excellent *Z/E* selectivity (*Z/E*:16/1) and good yield (60%). More sterically hindered groups such as methoxy (**1r**) and phenyl (**1s**) at the *ortho*-position showed a similarly high *Z/E* selectivity up to (39:1), albeit a decreased yield. This significant increase in *Z/E* selectivity may be attributable to the increase in triplet energy of the *Z* isomers caused by a larger twisting angle in the presence of an *ortho*-substitution, while a small increase in triplet energy in the less-congested *E* isomer is expected.<sup>[19]</sup> Additionally, heteroarenes including benzothiophene (**1v**), benzofuran (**1w**) as well as indole (**1x**) performed well in this transformation. However, aliphatic aldehydes and aromatic ketones gave only trace amounts of products with low conversions, presumably due to their higher reduction potentials and steric hindrance, respectively.

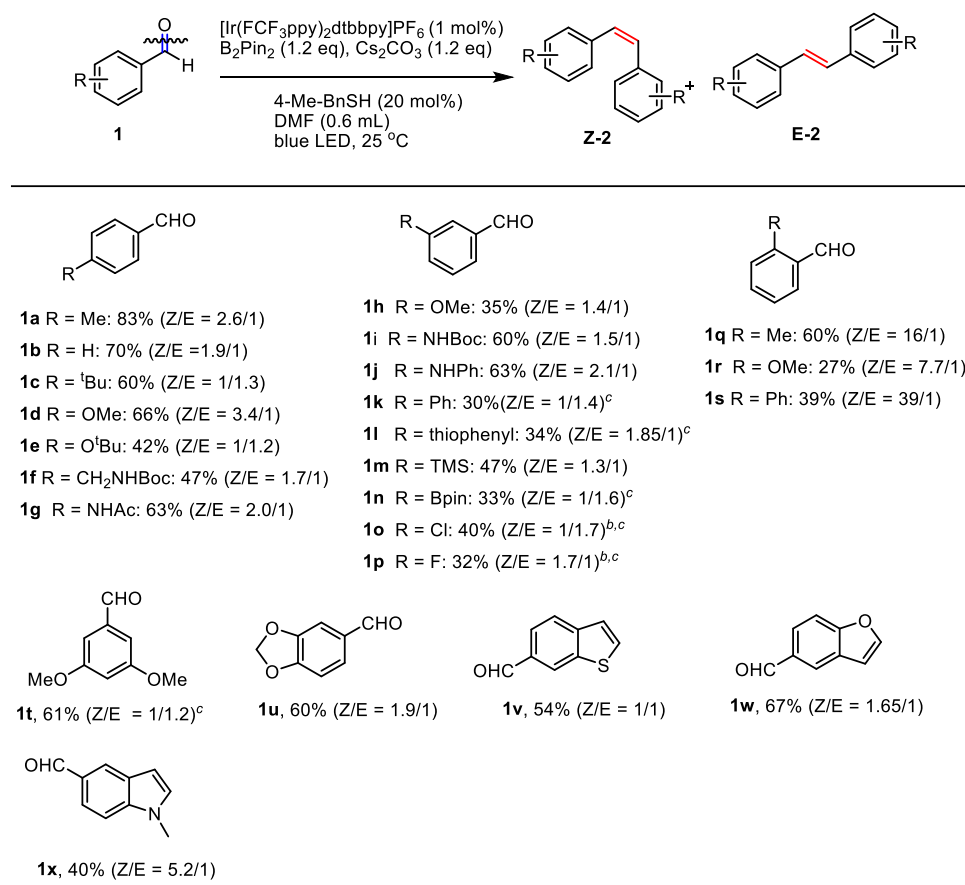


**Figure 1.** Scope of aldehydes for the homo-coupling deoxygenative olefination<sup>a</sup>. <sup>a</sup>Reaction conditions: **1** (0.2 mmol), [Ir(FCF<sub>3</sub>ppy)<sub>2</sub>dtbbpy]PF<sub>6</sub> (0.002 mmol), B<sub>2</sub>pin<sub>2</sub> (0.24 mmol), Cs<sub>2</sub>CO<sub>3</sub> (0.24 mmol), 4-MeBnSH (0.04 mmol) in anhydrous DMF (0.6 mL), irradiation with 3 W blue LED for 24 h at 25 °C, isolated yields. Yield refers to combined yield of *Z* and *E* isomers. <sup>b</sup>Ethyl 2-mercaptopropionate (0.04 mmol) was used in place of 4-MeBnSH. <sup>c</sup>Isolated yield, average of two parallel reactions.

After having established the scope of aldehydes in homo-coupling reactions, we turned our attention to more challenging cross-coupling reactions between two different aldehydes. As shown in Figure 2, using slightly modified reaction conditions, the coupling between two different aldehydes proceeds well to

give a range of unsymmetrical alkenes. Aldehydes bearing amides and amine groups at the aromatic ring react smoothly with *para*-tolualdehyde to give the corresponding alkenes in moderate to good yields (**5a-5c**). Aldehydes carrying alkoxy groups at the phenyl ring were tolerated under our reaction conditions, affording the alkenes in modest to good yields with modest *Z/E* selectivity (**5d-5f**). However, this cross-coupling reaction is sensitive to steric hindrance and *ortho*-substituents led to a decreased reactivity (**5e**). The reaction of heteroaromatic aldehydes furnished a heterocycle-containing stilbene (**5g**). Coupling between benzaldehyde and 3,5-dimethoxybenzaldehyde afforded the alkene in 57% yield with good selectivity (*Z/E* = 1/3.5).<sup>[20]</sup>

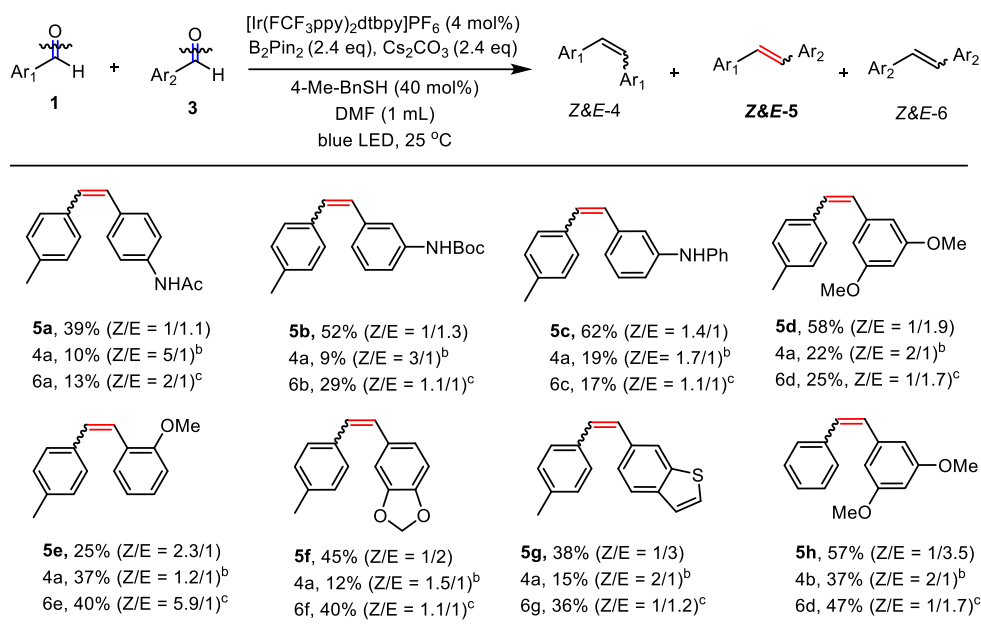


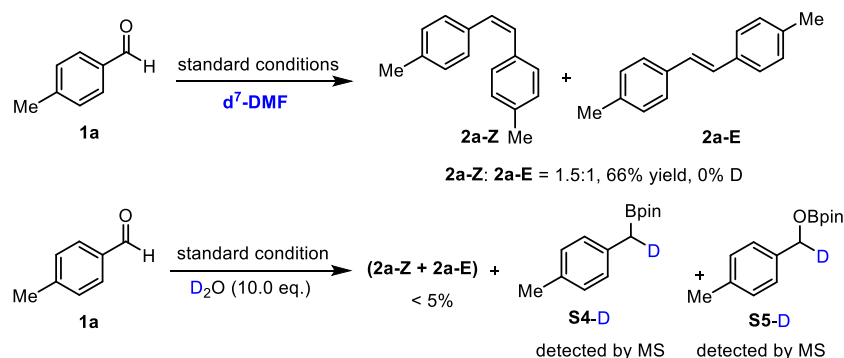
**Figure 2.** Scope of aldehydes for the cross-coupling deoxygenative olefination<sup>a</sup> <sup>a</sup>Reaction conditions: **1** (0.1 mmol), **3** (0.15 mmol), [Ir(FCF<sub>3</sub>ppy)<sub>2</sub>dtbbpy]PF<sub>6</sub> (0.004 mmol), B<sub>2</sub>pin<sub>2</sub> (0.24 mmol), Cs<sub>2</sub>CO<sub>3</sub> (0.24 mmol), 4-Me-BnSH (0.04 mmol) in anhydrous DMF (1 mL), irradiation with 3 W blue LED for 24 h at room temperature, isolated average yield of two parallel reactions. Yield refers to combined yield of *Z* and *E* isomers. <sup>b</sup>Yields and *Z/E* ratio values were determined with <sup>1</sup>H NMR using 1,3,5-methoxybenzene as internal standard; based on the amount of aldehyde **1**. <sup>c</sup>Yields and *Z/E* ratio values were determined with <sup>1</sup>H NMR using 1,3,5-methoxybenzene as internal standard; based on the amount of aldehyde **3**.

### 2.2.3 Mechanistic investigation

To gain insights into the reaction mechanism, a series of chemical experiments, spectroscopic investigations and *in situ* illumination NMR experiments<sup>[21]</sup> were conducted.

The initial Stern-Volmer luminescence quenching experiments revealed that phenylmethanethiolate quenches the excited state of the photocatalyst much more efficiently than the corresponding thiol, while the aldehyde and B<sub>2</sub>pin<sub>2</sub> do not quench at all (see Supplementary Information, Figure S6). This indicates a potential electron transfer from the sulfur anion to the excited state of the photocatalyst. This reduced [Ir(FCF<sub>3</sub>ppy)<sub>2</sub>dtbbpy]PF<sub>6</sub> (II) (*Ir*<sup>0</sup><sub>1/2</sub><sup>III/II</sup> = -1.38V vs SCE in DMF, Figure S1) catalyst causes the single-electron reduction of **1a**. Even though the *E*<sub>red</sub> of **1a** is higher (*E*<sub>red</sub> = -2.07 V vs SCE in DMF, Figure S3), the decrease of reduction potential of aldehyde **1a** on addition of Lewis acidic B<sub>2</sub>pin<sub>2</sub> (Figure S4 and S5) facilitates this single-electron reduction.

Next, the presence of radical species in the catalytic cycle was tested by addition of 2,2,6,6-tetramethylpiperidin-1-oxyl (TEMPO, 1.0 eq.) to the mixture, which shows a dramatic drop in product yield (down to 8 % see Supplementary Information). This was also evidenced in the  $^{13}\text{C}$  NMR spectrum, which shows a line broadened signal for the carbonyl of the benzaldehyde (see Supplementary Information Figure S9), possibly due to exchange of the radical species (ketyl radical) with benzaldehyde. Subsequently, a series of control experiments were performed to identify key intermediates. 1,2-Diol, benzyl alcohol and 1,2-diketone were excluded as intermediates, since using them in place of benzaldehyde did not lead to alkene formation (Supplementary Information, Scheme S1). Furthermore, benzylboronic esters **S4** and benzyloxyborate ester **S5** were identified as by-products in the reaction (Figure S7). Most interestingly, control experiments in the presence of  $\text{D}_2\text{O}$  (10.0 eq.) quenched the reaction significantly, affording the alkene in trace amounts along with the formation of deuterated (at the benzylic position) boronic esters **S4-D** and borate ester **S5-D** (Scheme 2). In contrast, with only  $\text{d}^7\text{-DMF}$  as solvent, deuterium was not incorporated in either the products or the boronic ester **S4** and borate ester **S5**. These findings suggest the involvement of boron-related species such as an  $\alpha$ -oxyboryl carbanion<sup>[22]</sup> and an  $\alpha$ -boryl carbanion<sup>[23]</sup> in the reaction mechanism.



**Scheme 2.** Deuteration experiments

Next, a systematic *in situ* illumination NMR study was carried out to directly detect these reaction intermediates. To monitor this unusual transformation from carbonyl groups to double bonds and to boost sensitivity of otherwise insensitive  $^{13}\text{C}$  signals, benzaldehyde specifically  $^{13}\text{C}$  labelled at the carbonyl position was used (see Figure 3A). This enabled us not only to predominately track the chemical modulations at the carbonyl position, but also to identify the number of protons bound to the carbon in several intermediate species by  $^1\text{H}$  coupled 1D  $^{13}\text{C}$  experiments (see below); therefore, in the following only the  $^{13}\text{C}$  signals of the labelled carbon are discussed.

On irradiation (455 nm, blue LED) of the reaction mixture, besides starting material and product resonances, several new  $^{13}\text{C}$  signals are detected, indicating the generation of possible reaction intermediates. Figure 3A shows the *in situ*  $^1\text{H}$  decoupled  $^{13}\text{C}$  spectrum of the reaction mixture after 18 hours of irradiation. Besides benzaldehyde, the two products (P and P' in Figure 3A), and the by-products **S4** and **S5**, several additional peaks appeared. Among them three intermediates were assigned, which are marked with **G**, **F** and **H** and highlighted with different colors in Figure 3A. To identify and characterize the intermediates, a combined approach of chemical exchange information from  $^{13}\text{C}$  CEST (chemical exchange saturation transfer), chemical shift information and multiplicity pattern accessed from  $^1\text{H}$  coupled 1D  $^{13}\text{C}$  spectra was applied. Furthermore, theoretical calculations and spectra of individually synthesized intermediates were used to corroborate the assignment.

To identify the next intermediate formed from benzaldehyde, the spectra are scanned by  $^{13}\text{C}$  CEST NMR (detailed information about CEST is given in Supplementary Information ).<sup>[24]</sup> In case there is any chemical exchange on the ms time scale with benzaldehyde, saturation can be transferred from the exchanging intermediate onto benzaldehyde and hence the intermediate becomes detectable. The most pronounced intensity drop observed for the benzaldehyde  $^{13}\text{C}=\text{O}$  signal at 193 ppm is on saturation at 78.5 ppm (Figure 3B<sup>1</sup>). However, at 300 K, the peak at 78.5 ppm is very broad (blue, Figure 3B) suggesting a transient nature of the intermediate. To characterize this intermediate further, the temperature was lowered to 270 K resulting in a considerable narrowing of this  $^{13}\text{C}$  signal. In addition, the  $^1\text{H}$  coupled  $^{13}\text{C}$  spectrum reveals a  $^{13}\text{C}$ -H moiety by appearance of a doublet. From the literature, it was considered that the base might react with the diboron reagent to generate  $\text{sp}^3$ - $\text{sp}^2$  diboron species that participates in ketyl radical borylation<sup>[25]</sup> to give  $\alpha$ -boryl alkoxide. Furthermore, theoretical calculations predict a  $^{13}\text{C}$  chemical shift of 70.4 ppm for a cyclic three-membered anionic species **F** (Figure 3B). The open form of the  $\alpha$ -boryl alkoxide **E** was found to be energetically less favorable by theoretical calculations. However, we cannot distinguish experimentally between **E** and **F**. Based on this evidence, the  $^{13}\text{C}$  peak at 78.5 ppm is assigned to the cyclic three-membered species **F** or to the  $\alpha$ -boryl carbonyl peak of benzaldehyde indicate a fast chemical alkoxide **E**; thus, the above discussed line broadening of exchange with the ketyl radical. In addition, CEST exchange saturation transfer reveals a slow exchange of benzaldehyde with the cyclic three-membered anionic species **F** or **E**. Combining these experimental observations we conclude that a sequential exchange process takes place from benzaldehyde through a very short-lived ketyl radical to **E** or **F**.

Next, the assignment of the  $\alpha$ -oxyboryl carbanion intermediate **G** is discussed (see Figure 3C). In a “bora-Brook” rearrangement process this  $\alpha$ -oxyboryl carbanion **G** was found to be generated from the isomerization of  $\alpha$ -boryl alkoxide **E**.<sup>[22]</sup> Furthermore, Nozaki et al. proposed a three-membered-ring species similar to **F** as the transition state of the C to O boryl migration in the “bora-Brook” rearrangement.<sup>[22c]</sup> Given these reports and the oxophilicity of boron (B-O bond BDE = 193 kcal/mol),<sup>[26]</sup> such a carbon to oxygen boryl migration in the cyclic three-membered anionic species **F** to generate  $\alpha$ -oxyboryl carbanion **G** is highly probable. The aforementioned control experiments, wherein deuterium-trapped benzyloxyborate ester **S5-D** was observed, further corroborates the existence of **G**. Indeed, we could detect a relatively broad peak of very small intensity at 102 ppm in the reaction mixture corresponding to the benzylic carbon of  $\alpha$ -oxyboryl carbanion **G** (Figure 3A and 3C). The  $^1\text{H}$  coupled  $^{13}\text{C}$  spectrum shows a doublet (Figure 3C) indicating a  $^{13}\text{CH}$  group and the calculated chemical shifts ( $^{13}\text{C}$  108 ppm and  $^1\text{H}$  6 ppm) are in good agreement with the assignment to the benzylic carbon of  $\alpha$ -oxyboryl carbanion **G**. Moreover, the essential role of DMF and  $\text{Cs}_2\text{CO}_3$  in our reaction is in line with the observation by Nozaki that the presence of a polar solvent and larger alkali metal cation could enhance the nucleophilicity of the anionic oxygen atom in such processes.<sup>[22c]</sup> Overall, we conclude that the  $\alpha$ -oxyboryl carbanion **G** is generated via a “bora-Brook” rearrangement from the cyclic three-membered anionic species **F**.

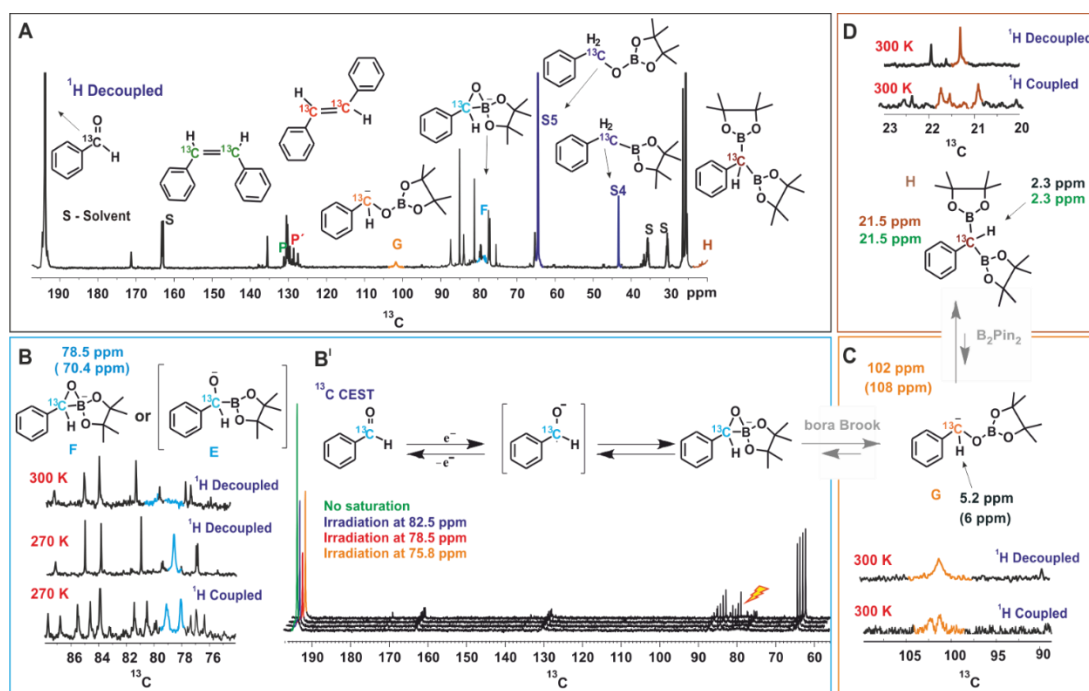
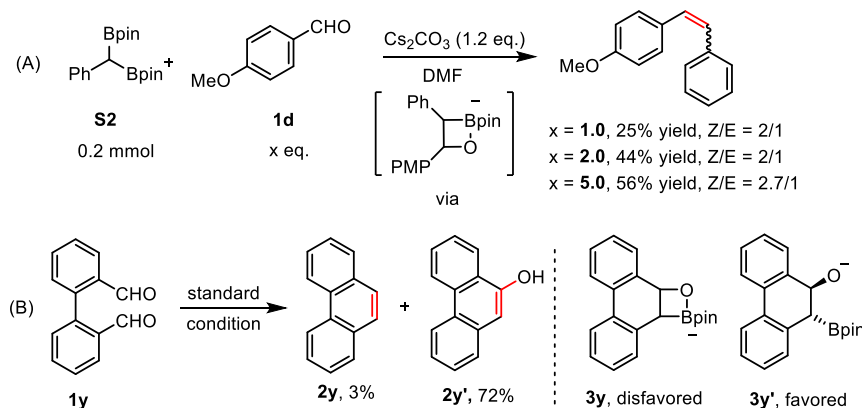


**Figure 3** NMR Studies of the Reaction Intermediates. (A) *In situ*  $^{13}\text{C}$  spectrum of the reaction mixture after 18 hours of illumination, the observed intermediate peaks are marked with respective colors and stable intermediates are directly compared to independently synthesized compounds. (B) Stabilization and characterization of transient intermediate **F** is achieved at low temperature (270 K) and characterized from  $^1\text{H}$  decoupled and coupled  $^{13}\text{C}$  spectra. (B')  $^{13}\text{C}$  CEST spectra establishing initial chemical transformation between benzaldehyde and primary key intermediate **F**. (C) Identification of  $\alpha$ -oxyboryl carbanion **G** from  $^{13}\text{C}$  and  $^1\text{H}$  chemical shifts (for HSQC see ESI $^\dagger$ ) and the multiplicity pattern of  $^{13}\text{C}$  at the benzylic position. (D) Assignment of intermediate **H** from the multiplicity pattern of  $^{13}\text{C}$  at the benzylic position and  $^{13}\text{C}$  and  $^1\text{H}$  chemical shifts (for HSQC see ESI $^\dagger$ ). The  $^1\text{H}$  and  $^{13}\text{C}$  chemical shifts of independently synthesized **H** are given in green. The values inside brackets are calculated chemical shift values. Unless otherwise mentioned, all spectra were measured at 300 K, in a 600 MHz NMR spectrometer.

Previous theoretical calculations showed that the transformation of an  $\alpha$ -oxyboryl carbanion **G** to a 1,1-benzylidiboronate ester **H** (for structure see Figure 3D) is thermodynamically and kinetically favorable.<sup>[27]</sup> Therefore, the intermediacy of **H** in our reaction process was examined with NMR. To identify the chemical shifts of **H**, a  $^{13}\text{C}$ - $^1\text{H}$  HSQC spectrum (see, Supplementary Information) of the pure independently synthesized intermediate **H** was measured and revealed a benzylic carbon at 21.5 ppm and the corresponding proton at 2.50 ppm. Indeed, careful observation of the  $^{13}\text{C}$  spectra of the reaction mixture revealed a very small peak of **H** at 21.5 ppm (Figure 3A and 3D). The assignment to **H** was confirmed by a doublet ( $^{-13}\text{CH}$ ) in the  $^1\text{H}$  coupled  $^{13}\text{C}$  spectrum (Figure 3D) and HSQC spectra of the reaction mixture (Supplementary information). At present, we can only suggest that **H** is formed via a nucleophilic attack of the carbanion **G** to  $\text{B}_2\text{pin}_2$  followed by a deoxygenation step. A related mechanism was proposed by Liu and Lan et al. for a borylation of an  $\alpha$ -oxyboronic species, in which similar *gem*-diboron compounds are generated via an oxoanion instead of a carbanion attacking  $\text{B}_2\text{pin}_2$ .<sup>[27]</sup>

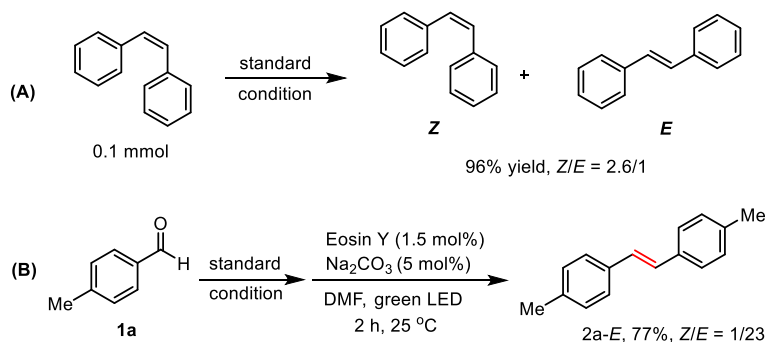
*Gem*-Diborylalkanes, such as intermediate **H**, treated with a suitable base, are known to be deprotonated or mono-deborylated to boryl carbanions.<sup>[23a],[23b-d, 23g]</sup> The resulting  $\alpha$ -boryl anions react with carbonyl

groups through a boron-Wittig pathway to give olefins.<sup>[23a],[23b-d, 23g]</sup> Indeed, the olefinic product could be obtained in an independent experiment treating benzaldehyde **1d** with 1,1-benzylidiboronate ester **H** in the presence of Cs<sub>2</sub>CO<sub>3</sub> (Scheme 3A). Moreover, we could trap the α-boryl anion as boronic esters **S4-D** in the presence of D<sub>2</sub>O (10.0 eq) (Scheme 2). This is a strong hint that an α-boryl carbanion is involved in our reaction pathway, although we could not directly identify it via *in situ* NMR.



**Scheme 3.** Further mechanistic studies

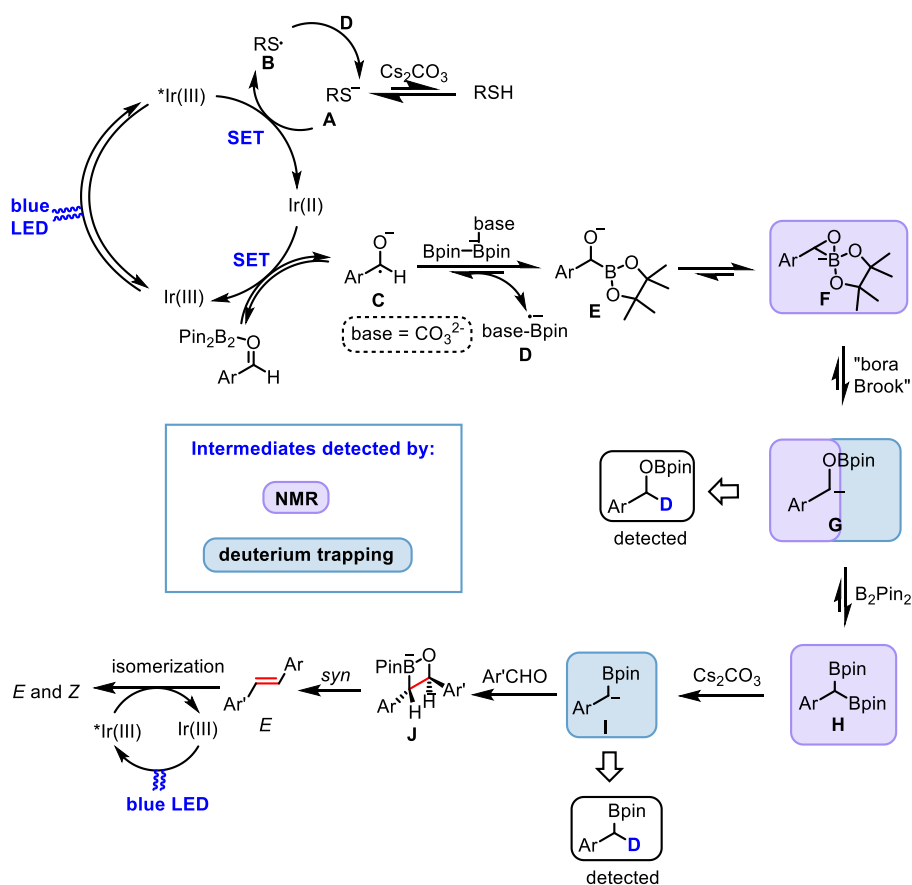
Next, we turned our attention to explore the origin of the *Z/E* selectivity in the reaction. By NMR we observed that the more thermodynamically stable *E* isomer was formed dominantly at the early stage of the reaction. Later, a *E* to *Z* isomerization occurs, with the *Z* isomer being the major product (Table S8). We rationalize the formation of *E*-alkenes as the major configuration at the early reaction stage as a consequence of a *syn* boron-oxygen elimination.<sup>[23a, 28]</sup> Additional evidence for the photo-induced alkene isomerization process was obtained when *E*-alkene was subjected to the standard reaction condition. The corresponding product was obtained in a similar *Z/E* ratio (*Z/E* = 2.6/1, 96% yield) as in our reaction system. (Scheme 4A).<sup>[29]</sup> We also found that alkene *E-2a* could be obtained in one pot using the reported photo-sensitized *Z* to *E* isomerization strategy, giving alkene *E-2a* in 77% (Scheme 4B).<sup>[30]</sup>



**Scheme 4.** Isomerization studies

Based on the above experimental evidence and mechanistic pathways previously reported in literature, we propose the mechanism depicted in Scheme 5 for the reported photocatalytic carbonyl-carbonyl olefination of aromatic aldehydes. Initially, the photoexcited state of [Ir<sup>III</sup>(FCF<sub>3</sub>ppy)<sub>2</sub>dtbbpy]<sup>+</sup> is reductively quenched by the sulfur anion **A**, formed by the deprotonation of thiol by base, affording sulfur radical **B** and [Ir<sup>II</sup>(FCF<sub>3</sub>ppy)<sub>2</sub>dtbbpy] (Ir<sub>1/2</sub><sup>III/II</sup> = -1.38V vs SCE in DMF). Single-electron transfer (SET) from the Ir(II) species to benzaldehyde in the presence of B<sub>2</sub>pin<sub>2</sub> gives the ground-state Ir(III) and ketyl radical **C**. Subsequent radical borylation<sup>[31]</sup> of **C** produces radical anion **D** and anion **E** or **F**. The

resulting radical anion **D** reduces the sulfur radical **B** back to the anion **A**. The three-membered cyclic



**Scheme 5.** Proposed reaction mechanism

anion **F** undergoes a “bora-Brook” rearrangement to form  $\alpha$ -oxyboryl carbanion **G**. The resulting carbanion **G** subsequently reacts with another molecule of  $B_2pin_2$  leading to the formation of 1,1-benzylidiboronate ester **H**. The base-promoted mono-deborylation of **H** gives rise to the formation of  $\alpha$ -boryl carbanion **I**. After nucleophilic attack to the carbonyl group of a second aldehyde, a four-membered cyclic intermediate **J** is most probably formed, which affords *E*-alkene via a B-O *syn* elimination. Finally, energy transfer from the excited state of the photocatalyst to the *E*-alkene produces a mixture of *Z* and *E* isomers as the final product.

### 2.3 Conclusions

In summary, we have developed a photoredox-catalyzed reaction for reductive carbonyl-carbonyl olefination of aromatic aldehydes using  $B_2pin_2$  as both the oxygen atom trap and the terminal reductant. The reaction system provides a mild and efficient method to prepare both symmetrical and unsymmetrical diarylalkenes through intermolecular bicarbonyl olefination and tolerates a broad range of functional groups. Combining our in situ illumination NMR technique with a series of mechanistic studies,  $\alpha$ -oxyboryl carbanion,  $\alpha$ -boryl carbanion and 1,1-benzylidiboronate esters were detected as key intermediate species in the reaction. Furthermore, theoretical calculations corroborate the NMR observation of the cyclic three-membered anionic species involved in the “bora-Brook” rearrangement. Mechanistic studies support the hypothesis that the formation of the double bond is facilitated by a boron-Wittig process. This combination of photoredox catalysis with boron chemistry constitutes a unique example of an Umploung strategy to convert an aldehyde into a boryl-functionalized carbanion.

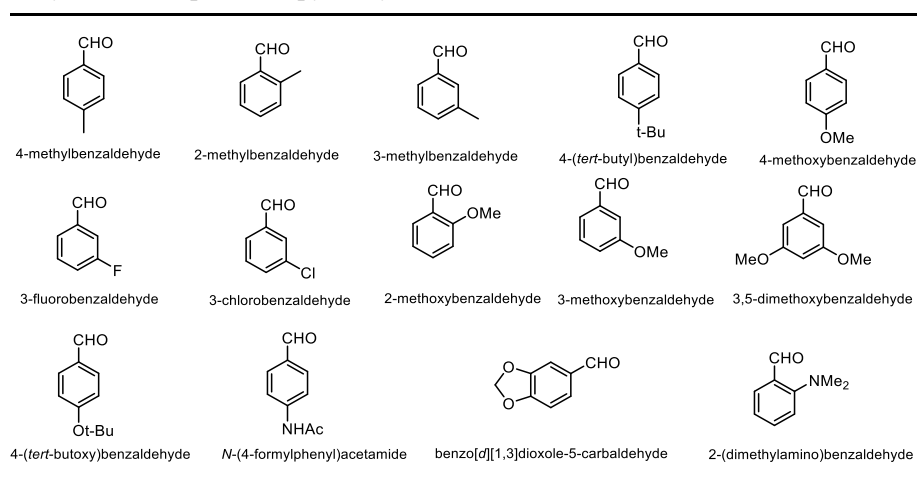
## 2.4 Experimental part

### 2.4.1 Generation information

Starting materials and reagents were purchased from commercial suppliers (Sigma Aldrich, Alfa Aesar, Acros, Fluka or abcr) and were used without further purification. Solvents were used as p.a. grade. Industrial grade of solvents was used for automated flash column chromatography. Dry nitrogen was used as inert gas atmosphere. Liquids were added via syringe, needle and septum technique unless stated differently. All NMR spectra were recorded on a Bruker Avance 300 or 400 spectrometer. Chemical shifts ( $\delta$  scale) are reported in parts per million and calibrated using the solvent residue peak as the internal standard.<sup>[32]</sup> Data are reported as follows: chemical shift ( $\delta$  ppm), multiplicity (s = singlet, d = doublet, t = triplet, q = quartet, m = multiplet, dd = doublet of doublets, dt = doublet of triplets, br = broad), coupling constant (Hz), and integration. High-resolution mass spectra (HRMS) were obtained from the central analytic mass spectrometry facilities of the Faculty of Chemistry and Pharmacy, University of Regensburg. GC/MS measurements were performed on a 7890A GC system from Agilent Technologies with an Agilent 5975 MSD Detector. Data acquisition and evaluation were done with MSD ChemStation E.02.02.1431. Photocatalytic reactions were performed with 455 nm LEDs (OSRAM Oslon SSL 80 royal-blue LEDs ( $\lambda = 455$  nm ( $\pm 15$  nm), 3.5 V, 700 mA). Analytical TLC was performed on silica gel coated alumina plates (MN TLC sheets ALUGRAM® Xtra SIL G/UV254). Visualization was done by UV light (254 or 366 nm). Flash column chromatography for photocatalytic reactions was performed with silica gel (particle size: 40-63  $\mu\text{m}$  or 25  $\mu\text{m}$ ) on a Biotage® Isolera™ Spektra system. Solvents were dried over activated (at 250 °C for 2 hours) 3 Å molecular sieves.

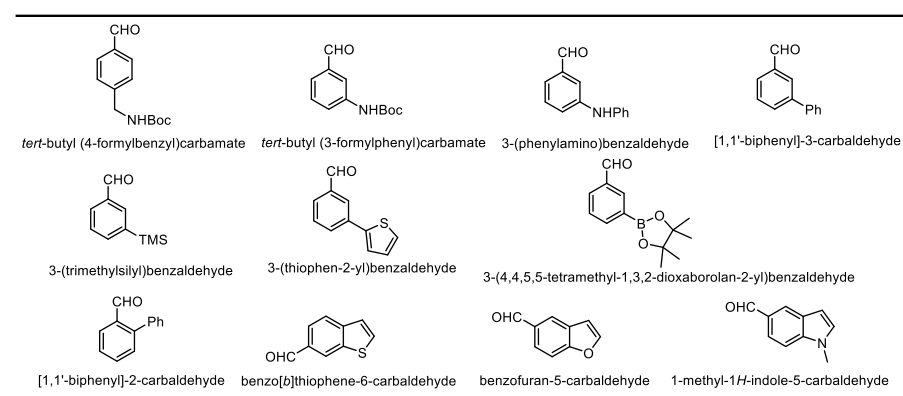
### 2.4.2 Starting materials

The following starting materials were commercially available and purified by distilling (if liquid) prior to use; aldehydes (if solid) were purified by washing with saturated  $\text{Na}_2\text{CO}_3$  solution and then the purity was checked by  $^1\text{H}$  NMR spectroscopy analysis.

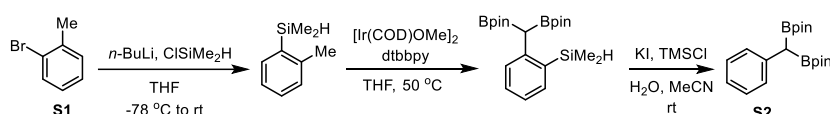


The following starting materials were synthesized according to literature reports<sup>[33]</sup>





### Synthesis of 1,1-benzylidiboronate ester.<sup>[34]</sup>

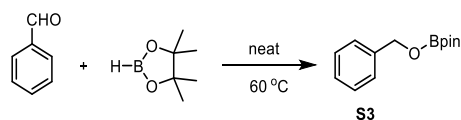


**Step 1:** To a 50 mL round bottom flask containing a stir bar was added the 2-bromomethylbenzene **S1** (10.00 mmol). The flask was sealed with a septum, and dry THF (30 mL) was added under N<sub>2</sub>. The reaction mixture was cooled to  $-78\text{ }^{\circ}\text{C}$ , then a solution of *n*-BuLi (7.4mL, 15 mmol, 1.60 M in hexane) was added dropwise to the reaction mixture. The reaction was stirred for 30 minutes, and chlorodimethylsilane (1.42 g, 15 mmol) was added in one portion at the same temperature. The reaction mixture was then warmed to room temperature and stirred for overnight. The reaction was quenched with a saturated NH<sub>4</sub>Cl solution (15.0 mL) and extracted with Et<sub>2</sub>O (15.0 mL x 3). The combined organic layers were washed with brine, dried over Na<sub>2</sub>SO<sub>4</sub>, and concentrated under vacuum. The crude product was purified by flash column chromatography on silica gel (hexane as eluent) to give 2-methylphenyl dimethylsilane derivative as colorless liquid (1.15 g, 85%).

**Step 2:** To a 50 mL round bottom flask containing a stir bar was added B<sub>2</sub>pin<sub>2</sub> (2.0 eq, 10 mmol, 2.54 g). The flask was sealed with a septum, evacuated with pump and refilled with N<sub>2</sub> for three cycles, then (2-methylphenyl)dimethylsilane (5 mmol, 750 mg), freshly prepared stock solutions of [Ir(COD)OMe]<sub>2</sub> (0.025 mmol, 0.5 mol %) in THF (5.00 mL), and 4,4'-di-*tert*-butyl-2,2'-bipyridine (0.05 mmol, 1.00 mol %) were added in sequence by syringes. The flask was stirred at 50 °C overnight, the resulting reaction mixture filtered through a pad of Celite and concentrated under reduced pressure. The obtained yellowish solid was directly used for the next step.

**Step 3:** To a 20 mL snap vial containing a stir bar was added 1,1-benzylidiboronate ester, KI (1.20 equiv.), TMSCl (1.20 equiv.), H<sub>2</sub>O (1.20 equiv.), and CH<sub>3</sub>CN (0.100 M). The reaction was sealed and stirred for 2 h at room temperature. The mixture was filtered through a pad of SiO<sub>2</sub> and concentrated under reduced pressure. The crude mixture was purified by flash column chromatography (PE:EA = 100:0 to 90:10) to give the 1,1-benzylidiboronate ester **S2** as a white solid (1.2 g, 70% yield over 2 steps). <sup>1</sup>H NMR (400 MHz, CDCl<sub>3</sub>) δ 7.30 – 7.16 (m, 4H), 7.12 – 7.03 (m, 1H), 2.30 (s, 1H), 1.22 (s, 12H). <sup>13</sup>C NMR (101 MHz, CDCl<sub>3</sub>) δ 139.47, 129.12, 127.90, 124.14, 83.33, 24.66, 24.58.

### Synthesis of 2-(Benzyloxy)pinacolborane<sup>[35]</sup>



To a 10 mL snap vial containing a stir bar was added benzaldehyde (5.0 mmol, 530 mg) and pinacolborane (7.0 mmol, 1.4 eq., 1.0 mL). The reaction mixture was stirred at 60 °C for 30 minutes. The reaction mixture was concentrated under reduced pressure. Next, the potassium carbonate (0.75 mmol, 0.15 eq., 103.5 mg.) and 5 mL of DCM were added and stirred with the crude product for 25 minutes. After that, the solution was filtrated through a pad of Celite and concentrated under reduced pressure to give the product **S3** as a colorless oil (1.11g, 95%). <sup>1</sup>H NMR (300 MHz, CDCl<sub>3</sub>) δ 7.37 – 7.27 (m, 5H), 4.93 (s, 2H), 1.27 (s, 12H). <sup>13</sup>C NMR (75 MHz, CDCl<sub>3</sub>) δ 139.14 , 128.22 , 127.30 , 126.65 , 82.93 , 66.61 , 24.56 .

### 2.4.3 Experimental procedures

#### General procedure A for the homo-coupling olefination of aldehydes

To a 5 mL snap vial with a stirring bar, B<sub>2</sub>pin<sub>2</sub> (0.24 mmol, 1.2 equiv.), [Ir(FCF<sub>3</sub>ppy)<sub>2</sub>dtbbpy] (1 mol%) and Cs<sub>2</sub>CO<sub>3</sub> (0.24 mmol, 1.2 equiv.) were added. The vial was evacuated and back filled with nitrogen for three times. A solution of 4-Me-BnSH (20 mol%) and aldehyde (0.2 mmol) in dry DMF (0.6 mL) was added by syringe. After degassed with two freeze-pump-thaw cycles via a syringe needle, the reaction mixture was irradiated with a 455 nm LED (~3W) for 24 hours at 25 °C. The reaction mixture was then diluted with water and extracted with ethyl acetate (10 mL \*3). The combined organic phase was then washed with H<sub>2</sub>O (10 mL) and brine, dried over sodium sulfate, concentrated under vacuum and subjected to flash column chromatography.

#### General procedure B for the homo-coupling olefination of aldehydes

To a 5 mL snap vial with a stirring bar, B<sub>2</sub>pin<sub>2</sub> (0.24 mmol, 1.2 equiv.), [Ir(FCF<sub>3</sub>ppy)<sub>2</sub>dtbbpy] (1 mol%) and Cs<sub>2</sub>CO<sub>3</sub> (0.24 mmol, 1.2 equiv.) were added. The vial was evacuated and back filled with nitrogen for three times. A solution of 4-Me-BnSH (20 mol%) and aldehyde (0.2 mmol) in dry DMF (0.6 mL) was added by syringe. After degassed with two freeze-pump-thaw cycles via a syringe needle, the reaction mixture was irradiated with a 455 nm LED (~3W) for 24 hours at 25 °C. The reaction mixture was diluted with water and ethyl acetate. NaBO<sub>3</sub> (2.0 equiv.) was then added into the mixture and stirred for 30 minutes. The solution was extracted with ethyl acetate (10 mL \*3). The combined organic phase was then washed by H<sub>2</sub>O (10 mL) and brine, dried over sodium sulfate, concentrated under vacuum and subjected to flash column chromatography.

#### General procedure C for the cross-coupling olefination of two aldehydes

To a 5 mL snap vial with stirring bar, B<sub>2</sub>pin<sub>2</sub> (0.24 mmol, 2.4 equiv.), [Ir(FCF<sub>3</sub>ppy)<sub>2</sub>dtbbpy] (4 mol%) and Cs<sub>2</sub>CO<sub>3</sub> (0.24 mmol, 2.4 equiv.) were added. The vial was evacuated and back filled with nitrogen three times. A solution of 4-Me-BnSH (40 mol%) and aldehyde **1a** (0.1 mmol) and aldehyde **2a** (0.15 mmol) in dry DMF (1.0 mL) was added by syringe. After degassed with two freeze-pump-thaw cycles via a syringe needle, the reaction mixture was irradiated with a 455 nm LED (~3W) for 24 hours at 25 °C. The reaction mixture was diluted with water and extracted with ethyl acetate (10 mL \*3). The combined organic phase was then washed with H<sub>2</sub>O (10 mL) and brine, dried over sodium sulfate, concentrated under vacuum and subjected to flash column chromatography.

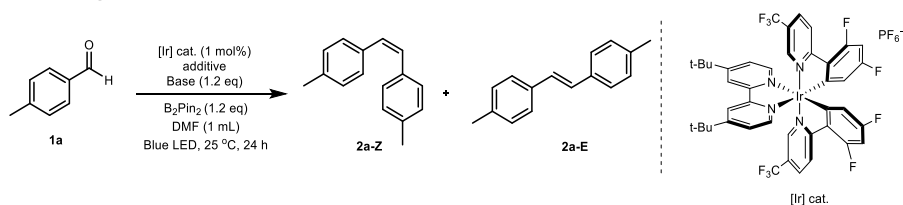
#### General procedure D for the cross-coupling olefination of two aldehydes

To a 5 mL snap vial with stirring bar, B<sub>2</sub>pin<sub>2</sub> (0.24 mmol, 2.4 equiv.), [Ir(FCF<sub>3</sub>ppy)<sub>2</sub>dtbbpy] (4 mol%) and Cs<sub>2</sub>CO<sub>3</sub> (0.24 mmol, 2.4 equiv.) were added. The vial was evacuated and back filled with nitrogen three times. A solution of 4-Me-BnSH (40 mol%) and aldehyde **1a** (0.1 mmol) and aldehyde **2a** (0.15 mmol) in dry DMF (1.0 mL) was added by syringe. After degassed with two freeze-pump-thaw cycles via a syringe needle, the

reaction mixture was irradiated with a 455 nm LED (~3W) for 24 hours at 25 °C. The reaction mixture was diluted with water and ethyl acetate. NaBO<sub>3</sub> (2.0 equiv.) was then added into the mixture and stirred for 30 minutes. The solution was extracted with ethyl acetate (10 mL \*3). The combined organic phase was then washed by H<sub>2</sub>O (10 mL) and brine, dried over sodium sulfate, concentrated under vacuum and subjected to flash column chromatography.

#### 2.4.4 Optimization of the reaction conditions

**Table S1.** Screening of bases and additives

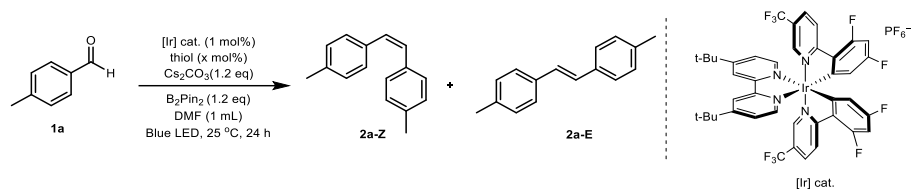


Entry <sup>[a]</sup>	Base	Additive	Yield [%]	Z:E <sup>[b]</sup>
1	Cs <sub>2</sub> CO <sub>3</sub>	DIPEA (3.0 eq)	trace	-
2	Cs <sub>2</sub> CO <sub>3</sub>	-	6	-
3	-	-	0	-
4 <sup>[c]</sup>	Cs <sub>2</sub> CO <sub>3</sub>	-	0	-
5	Cs <sub>2</sub> CO <sub>3</sub>	quinuclidine (10 mol%)	trace	-
6	Cs <sub>2</sub> CO <sub>3</sub>	BnSH (10 mol%)	39	1/2.6
7	K <sub>3</sub> PO <sub>4</sub>	BnSH (10 mol%)	8	1.3/1
8	K <sub>2</sub> CO <sub>3</sub>	BnSH (10 mol%)	15	1.2/1
9	Na <sub>2</sub> CO <sub>3</sub>	BnSH (10 mol%)	trace	-
10	NaOAc	BnSH (10 mol%)	trace	-
11	Na <sub>2</sub> HPO <sub>4</sub>	BnSH (10 mol%)	n.r	-
12	t-BuOK	BnSH (10 mol%)	9	1/1.6
13	pyridine	BnSH (10 mol%)	trace	-
14	DMAP	BnSH (10 mol%)	trace	-
15	DBU	BnSH (10 mol%)	trace	-

[a] Reaction condition: *p*-tolualdehyde **1a** (0.2 mmol), B<sub>2</sub>pin<sub>2</sub> (0.24 mmol), base (0.24 mmol), BnSH (10 mol%) and photocatalyst (1 mol%) in 1 mL DMF, irradiation with blue LED at 25 °C. Yields were determined

by  $^1\text{H}$  NMR analysis of crude reaction mixture; 1,3,5-trimethoxybenzene was used as internal standard. [b] Determined by  $^1\text{H}$  NMR. [c] without  $\text{B}_2\text{pin}_2$ .

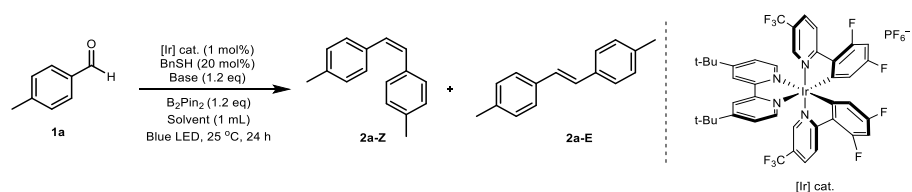
**Table S2.** Screening of thiols



Entry <sup>[a]</sup>	Thiol (x mol%)	Yield [%]	Z:E <sup>[b]</sup>
1	BnSH (10 mol%)	39	1/2.6
2	PhSH (10 mol%)	11	1/1.5
3	$i\text{Pr}_3\text{SiSH}$ (10 mol%)	20	1.1/1
4	AcCH(Me)SH (10 mol%)	29	1.7/1
5	BnCH <sub>2</sub> SH (10 mol%)	trace	-
<b>6</b>	<b>BnSH (20%)</b>	<b>66</b>	<b>1/1.8</b>
7	BnSH (5%)	8	1.4/1
8	BnSH (30%)	63	1.9/1
9	BnSH (50%)	36	1.5/1
10	BnSSBn (20%)	30	1/1.6
11	4-CF <sub>3</sub> -BnSH (20%)	39	1/1.8
12	PhCH(Me)SH (20%)	53	1/1.4
13	4- $t\text{Bu}$ -BnSH (20%)	39	1/2.2
<b>14</b>	<b>4-Me-BnSH (20%)</b>	<b>63</b>	<b>1/1</b>
15	2,4,6-trimethyl-BnSH (20%)	52	1/2.2
16	-	7	1.5/1

[a] Reaction condition: *p*-tolaldehyde **1a** (0.2 mmol),  $\text{B}_2\text{pin}_2$  (0.24 mmol),  $\text{Cs}_2\text{CO}_3$  (0.24 mmol), thiol and photocatalyst (1 mol%) in 1 mL DMF, irradiation with blue LED at 25 °C. Yields were determined by  $^1\text{H}$  NMR analysis of crude reaction mixture; 1,3,5-trimethoxybenzene was used as internal standard. [b] Determined by  $^1\text{H}$  NMR.

**Table S3.** Screening of solvents

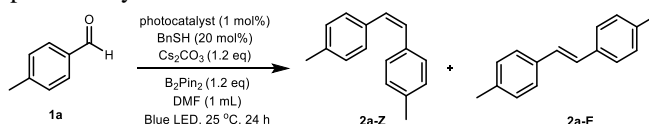


Entry <sup>[a]</sup>	Solvent	Yield [%]	Z/E <sup>[b]</sup>
----------------------	---------	-----------	--------------------

1	DMF	66	1/1.8
2	DMA	56	1/1.1
3	DMSO	9	1/5.4
4	acetone	trace	-
5	MeNO <sub>2</sub>	0	-
6	DCE	trace	-
7	EtOH	10	3.2/1
8	NMP	4	only Z
10	DMPU	17	1.1/1
11	DMF/MeCN=4/1	36	2.2/1
12	DMF/DMA=4/1	19	2.4/1
13	DMF/DMSO=4/1	61	1.3/1
14	DMF/EtOAc=4/1	58	1.6/1
15	DMF/NMP=4/1	23	1.8/1
16	DMF+10 eq H <sub>2</sub> O	trace	-

[a] Reaction condition: *p*-tolualdehyde **1a** (0.2 mmol), B<sub>2</sub>pin<sub>2</sub> (0.24 mmol), base (0.24 mmol), BnSH (20 mol%) and photocatalyst (1 mol%) in 1 mL solvent, irradiation with blue LED at 25 °C. Yields were determined by <sup>1</sup>H NMR analysis of crude reaction mixture; 1,3,5-trimethoxybenzene was used as internal standard. [b] Determined by <sup>1</sup>H NMR.

**Table S4.** Screening of photocatalysts

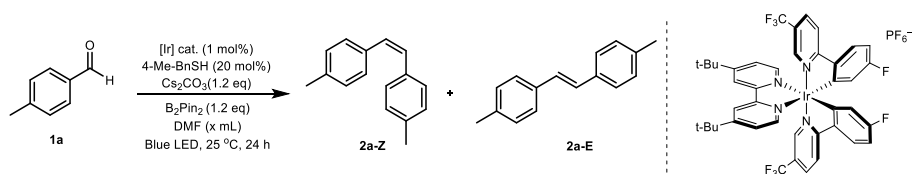


Entry <sup>[a]</sup>	Photocatalyst (x mol%)	Yield [%]	Z:E <sup>[b]</sup>
1	[Ir(dFCF <sub>3</sub> ppy) <sub>2</sub> dtbbpy]PF <sub>6</sub> (1 mol%)	66	1/1.8
2	[Ir(FCF <sub>3</sub> ppy) <sub>2</sub> dtbbpy]PF <sub>6</sub> (1 mol%)	74	2.2/1
3 <sup>[c]</sup>	[Ir(FCF <sub>3</sub> ppy) <sub>2</sub> dtbbpy]PF <sub>6</sub> (1 mol%)	77	2.5/1
4	[Ir(dFCF <sub>3</sub> ppy) <sub>2</sub> (5,5'-dCF <sub>3</sub> bpy)]PF <sub>6</sub> (1 mol%)	41	1/1.3
5	4CzIPN (5 mol%)	trace	-
6	EoSIn Y (5 mol%)	trace	-
7	[Ir(ppy) <sub>2</sub> dtbbpy]PF <sub>6</sub> (1 mol%)	14	2.4/1
8	[Ir(ppy) <sub>2</sub> bpy]PF <sub>6</sub> (1 mol%)	9	1.4/1

9	Ru(bpy) <sub>3</sub> Cl <sub>2</sub> (1 mol%)	11	1/4.8
10	[Ru(bpz) <sub>3</sub> ][PF <sub>6</sub> ] <sub>2</sub> (1 mol%)	11	1/5.3

[a] Reaction condition: *p*-tolualdehyde **1a** (0.2 mmol), B<sub>2</sub>pin<sub>2</sub> (0.24 mmol), Cs<sub>2</sub>CO<sub>3</sub> (0.24 mmol), BnSH (20 mol%) and photocatalyst (x mol%) in 1 mL DMF, irradiation with blue LED at 25 °C. Yields were determined by <sup>1</sup>H NMR analysis of crude reaction mixture; 1,3,5-trimethoxybenzene was used as internal standard. [b] Determined by <sup>1</sup>H NMR. [c] 4-Methyl benzyl thiol (20 mol%) was used.

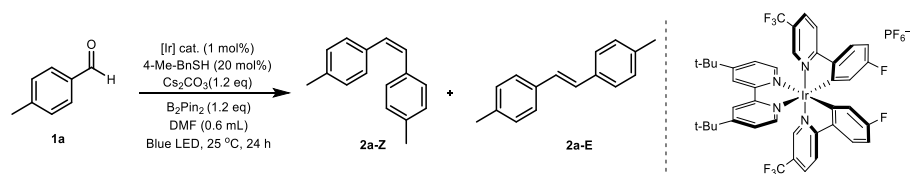
**Table S5.** Screening of reaction concentration



Entry <sup>[a]</sup>	PC	Thiol	Concentration	Yield[%]	Z/E <sup>[b]</sup>
1	[Ir(FCF <sub>3</sub> ppy) <sub>2</sub> dtbbpy] ]PF <sub>6</sub> (1 mol%)	4-MeBnSH (20 mol%)	0.1 M	25	1/1
2	[Ir(FCF <sub>3</sub> ppy) <sub>2</sub> dtbbpy] ]PF <sub>6</sub> (1 mol%)	4-MeBnSH (20 mol%)	0.13 M	71	1.8/1
3	[Ir(FCF <sub>3</sub> ppy) <sub>2</sub> dtbbpy] ]PF <sub>6</sub> (1 mol%)	4-MeBnSH (20 mol%)	0.33 M	<b>87(83)<sup>[c]</sup></b>	<b>2.6/1</b>
4	[Ir(FCF <sub>3</sub> ppy) <sub>2</sub> dtbbpy] ]PF <sub>6</sub> (1 mol%)	4-MeBnSH (20 mol%)	0.5 M	68	2.4/1

[a] Reaction condition: *p*-tolualdehyde **1a** (0.2 mmol), B<sub>2</sub>pin<sub>2</sub> (0.24 mmol), Cs<sub>2</sub>CO<sub>3</sub> (0.24 mmol), BnSH (20 mol%) and [Ir(FCF<sub>3</sub>ppy)<sub>2</sub>dtbbpy]PF<sub>6</sub> (1 mol%) in DMF, irradiation with blue LED at 25 °C. Yields were determined by <sup>1</sup>H NMR analysis of crude reaction mixture; 1,3,5-trimethoxybenzene was used as internal standard. [b] Determined by <sup>1</sup>H NMR. [c] Isolated yield.

**Table S6.** Control experiments



Entry <sup>[a]</sup>	Photocatalyst	Light	Thiol	Yield [%]	Z/E <sup>[b]</sup>
1 <sup>[c]</sup>	[Ir(FCF <sub>3</sub> ppy) <sub>2</sub> dtbbpy]PF <sub>6</sub> (1 mol%)	OFF	4-MeBnSH (20 mol%)	0	-
2 <sup>[d]</sup>	-	ON	4-MeBnSH	17	3.5/1

			(20 mol%)		
3 <sup>[e]</sup>	[Ir(FCF <sub>3</sub> ppy) <sub>2</sub> dtbbpy]PF <sub>6</sub> (1 mol%)	ON	4-MeBnSH (20 mol%)	8	1.8/1

[a]: Reaction condition: *p*-tolualdehyde **1a** (0.2 mmol), B<sub>2</sub>pin<sub>2</sub> (0.24 mmol), Cs<sub>2</sub>CO<sub>3</sub> (0.24 mmol), 4-MeBnSH (20 mol%) and catalyst (1 mol%) in 0.6 mL solvent, irradiation with blue LED at 25 °C. Yields were determined by <sup>1</sup>H NMR analysis of crude reaction mixture; 1,3,5-trimethoxybenzene was used as internal standard. [b]: Determined by <sup>1</sup>H NMR [c]: In the dark. [d]: Without photocatalyst. [e] Adding TEMPO (1.0 eq.)

## 2.4.5 Mechanistic studies

### Cyclic Voltammetry

CV measurements were taken on a three-electrode potentiostat galvanostat PGSTAT302N from Metrohm Autolab by using a glassy carbon working electrode, a platinum wire counter electrode, a silver wire as a reference electrode. The voltammograms were taken at room temperature in a degassed DMF or MeCN solution ([n-Bu<sub>4</sub>NBF<sub>4</sub>] = 0.1 M, [substrate] = 1 mM, ferrocene as the internal standard) under Argon atmosphere. The scan rate was 0.1 V/s. Potentials vs. SCE were reported according to E<sub>SCE</sub> = E<sub>Fc/Fc+</sub> + 0.38 V.

#### Index Peak position

1	-1.1783
2	-1.6013
3	-1.2991
4	-1.1078
5	0.65964
6	0.58411

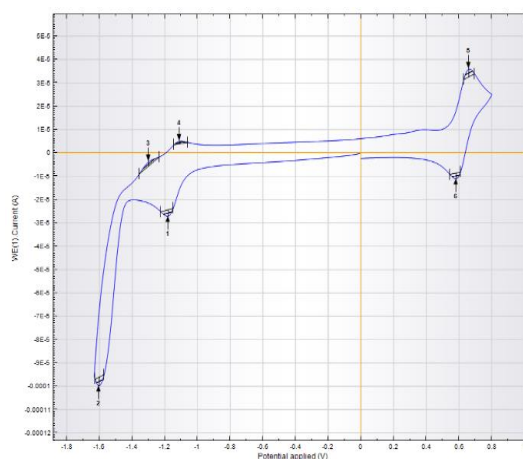


**Figure S1.** Cyclic voltammogram of [Ir(FCF<sub>3</sub>ppy)<sub>2</sub>dtbbpy]PF<sub>6</sub> in MeCN (with Ferrocene)

E<sub>red</sub> [Ir(III)/Ir(II)] = -1.38V vs. SCE

#### Index Peak position

1	1.5056
2	1.0725
3	0.9718

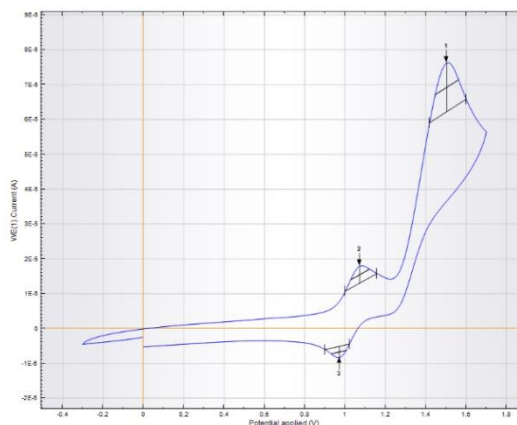


**Figure S2.** Cyclic voltammogram of 4-Me-BnSH in DMF (with Ferrocene)

$E_{\text{ox}}(4\text{-Me-BnSH}) = 0.86 \text{ V vs. SCE}$

**Index Peak position**

1	-1.5056
2	0.99701
3	0.8963

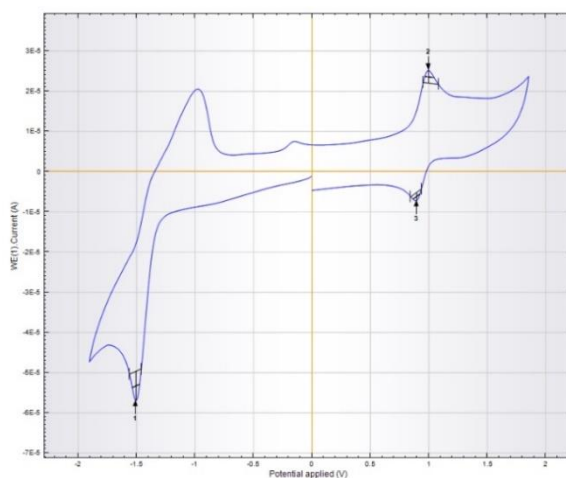


**Figure S3.** Cyclic voltammogram of benzaldehyde **1a** in DMF (with Ferrocene)

$E_{\text{red}}(\mathbf{1a}) = -2.07 \text{ V vs. SCE}$

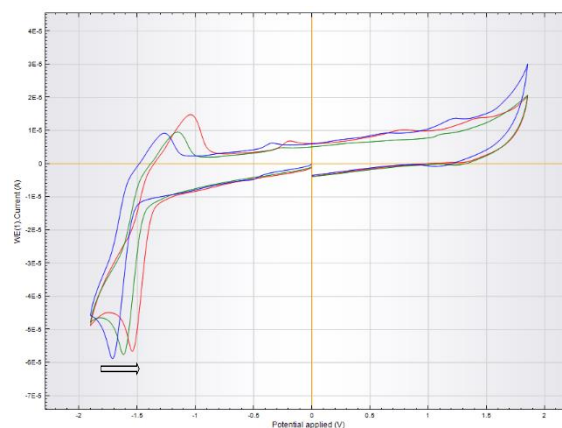


**Figure S4.** Cyclic voltammogram of benzaldehyde **1a** in DMF (blue curve) and a mixture of **1a** with  $\text{B}_2\text{pin}_2$  (2.0 eq.) in DMF after stirring for 3 minutes (green curve). The reduction potential of **1a** after adding more  $\text{B}_2\text{pin}_2$  (red curve). The corresponding reduction peak of **1a** shifted towards lower potential after adding  $\text{B}_2\text{pin}_2$ .

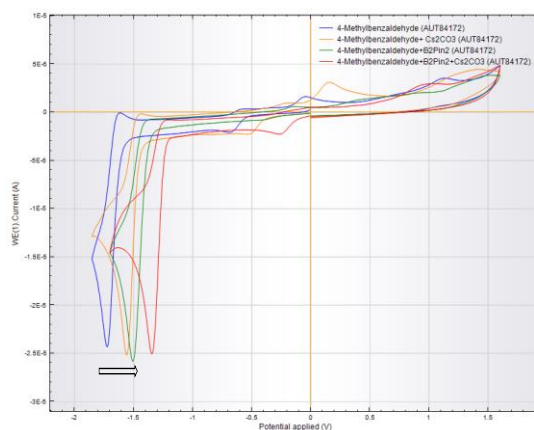




**Figure S5.** Cyclic voltammogram of benzaldehyde **1a** (blue curve) in DMF in the presence of different additives. Adding Cs<sub>2</sub>CO<sub>3</sub> (4.0 eq) (orange curve). Adding B<sub>2</sub>pin<sub>2</sub> (4.0 eq) (green curve). Adding Cs<sub>2</sub>CO<sub>3</sub> (4.0 eq) and B<sub>2</sub>pin<sub>2</sub> (4.0 eq) (red curve).

### Fluorescence quenching study

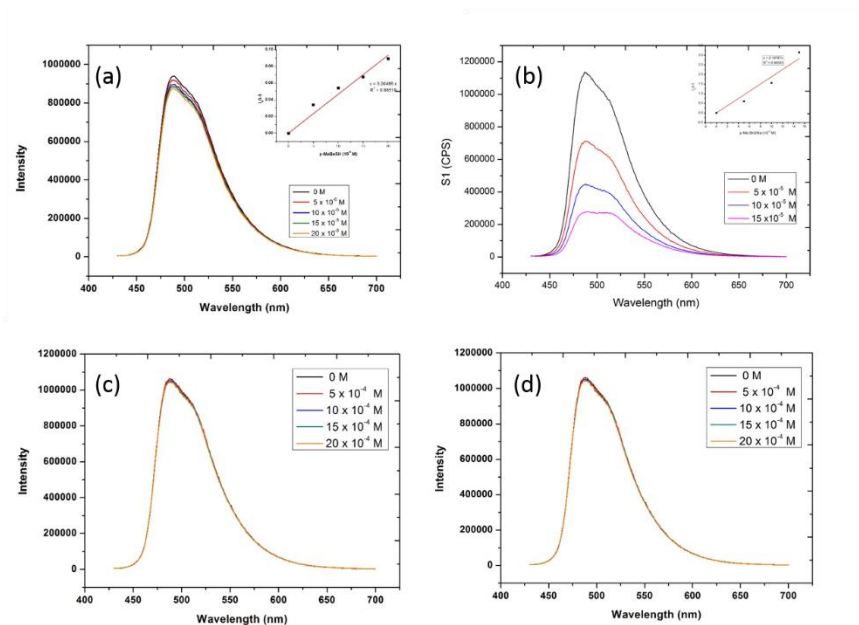


**Figure S6.** Luminescence spectra of [Ir(FCF<sub>3</sub>ppy)<sub>2</sub>dtbbpy]PF<sub>6</sub> ( $1.0 \times 10^{-5}$  M) was collected as a function of different quenchers in degassed DMF with excitation at 420 nm. Inset is the Stern-Volmer plot of [Ir(FCF<sub>3</sub>ppy)<sub>2</sub>dtbbpy]PF<sub>6</sub> by different quenchers. a) A solution of *p*-Me-BnSH in DMF was added and its concentration was changed from 0 to  $20 \times 10^{-5}$  M. b) A solution of *p*-Me-BnSNa in DMF was added and its concentration was changed from 0 to  $15 \times 10^{-5}$  M. c) A solution of B<sub>2</sub>pin<sub>2</sub> in DMF was added and its concentration was changed from 0 to  $20 \times 10^{-4}$  M. d) A solution of *p*-Me-PhCHO in DMF was added and its concentration was changed from 0 to  $20 \times 10^{-4}$  M.

## Detection of by-products

### GC-MS analysis of reaction mixtures

To a 5 mL snap vial with stirring bar,  $B_2pin_2$  (0.24 mmol, 1.2 equiv.),  $[Ir(FCF_3ppy)_2dtbbpy]$  (1 mol%) and  $Cs_2CO_3$  (0.24 mmol, 1.2 equiv.) were added. The vial was evacuated and back filled with nitrogen three times. A solution of 4-Me-BnSH (20 mol%) and aldehyde **1a** (0.2 mmol) in dry DMF (0.6 mL) was added by syringe. After degassing by the freeze-pump-thaw via a syringe needle for two circles, the reaction mixture was irradiated with a 455 nm LED for 6 hours at 25 °C. Then the resulting reaction mixture was filtered and subjected for GC-MS measurement. Boronic ester **S4** and borate ester **S5** were detected along with the generation of products.

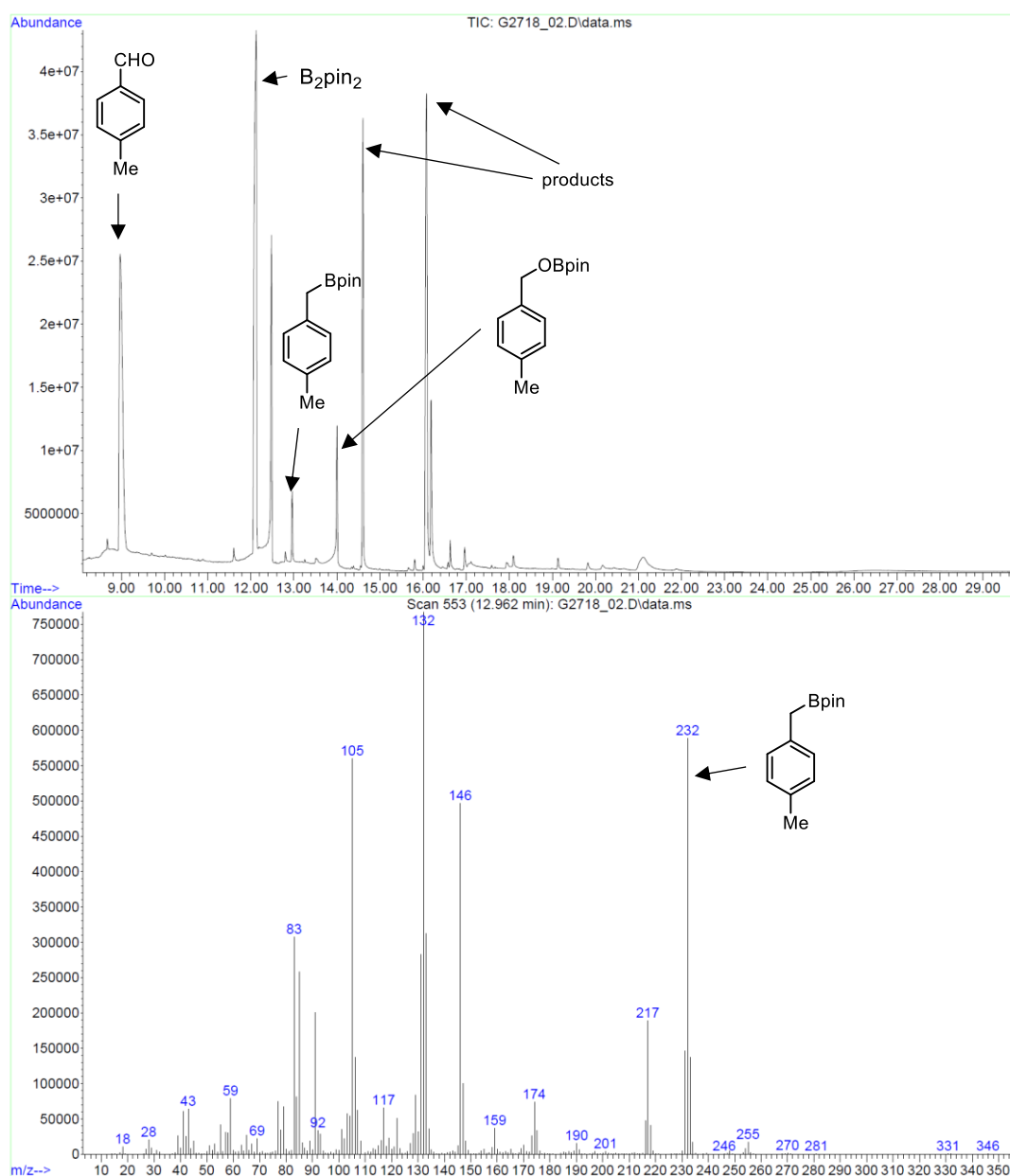
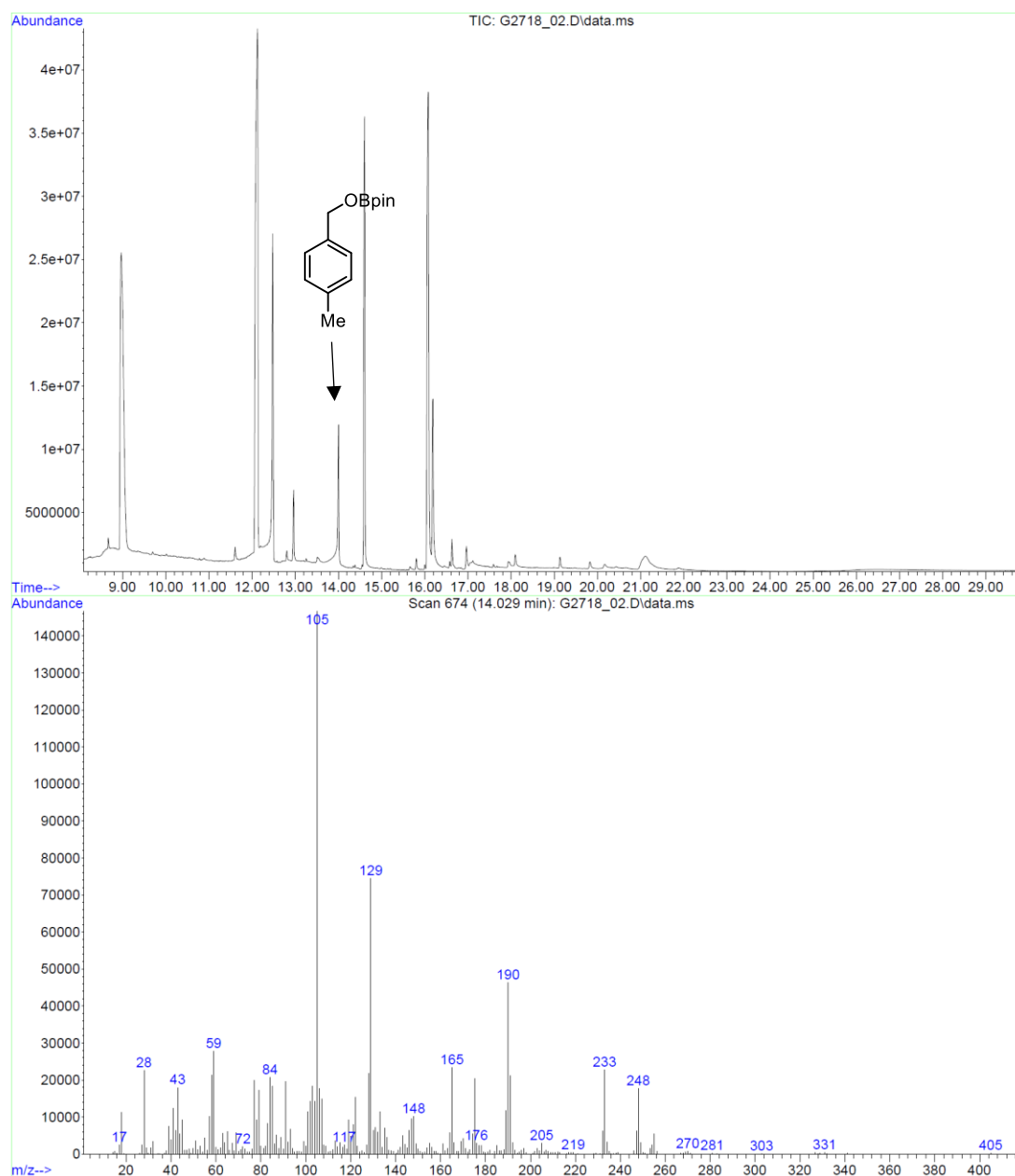
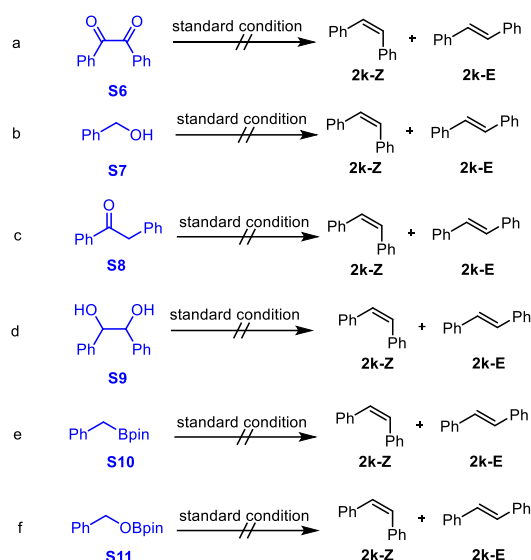


Figure S7-1. GC-MS report of the reaction mixtures after 6 hours



**Figure S7-2.** GC-MS report of the reaction mixtures after 6 hours

## Control experiments

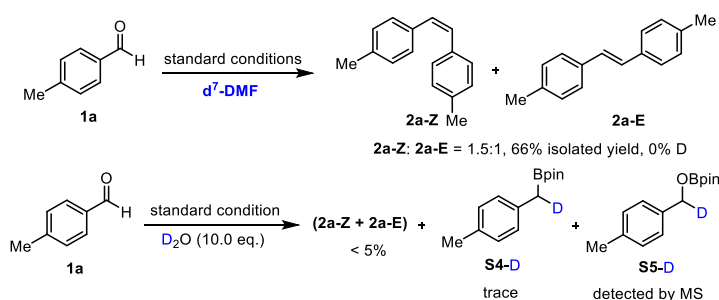


**Scheme S1.** Control experiments with potential intermediates

In order to detect the possible intermediates involved in the reaction processes, several control experiments employing the possible intermediates **S4-S7** in the place of benzaldehyde were carried out (Scheme S1a-1d). However, none of them gave detectable yields of alkenes as the products.

Moreover, considering that the boronic ester **S4** and borate ester **S5** were detected in the reaction mixtures after irradiation, we also tested the possible intermediacy of boronic esters during the reaction process. When non-substituted boronates **S10** and **S11** were used as the starting material in place of benzaldehyde, the generation of product **2k** was not observed. So the direct intermediacy of boronic ester **S4** and borate ester **S5** in the product generation process was excluded. In addition, this result inspired us to investigate the possible intermediates involved for the generation of boronic ester **S4** and borate ester **S5**.

## Deuteration experiments



**Scheme S2.** Deuteration experiments with deuterated solvent

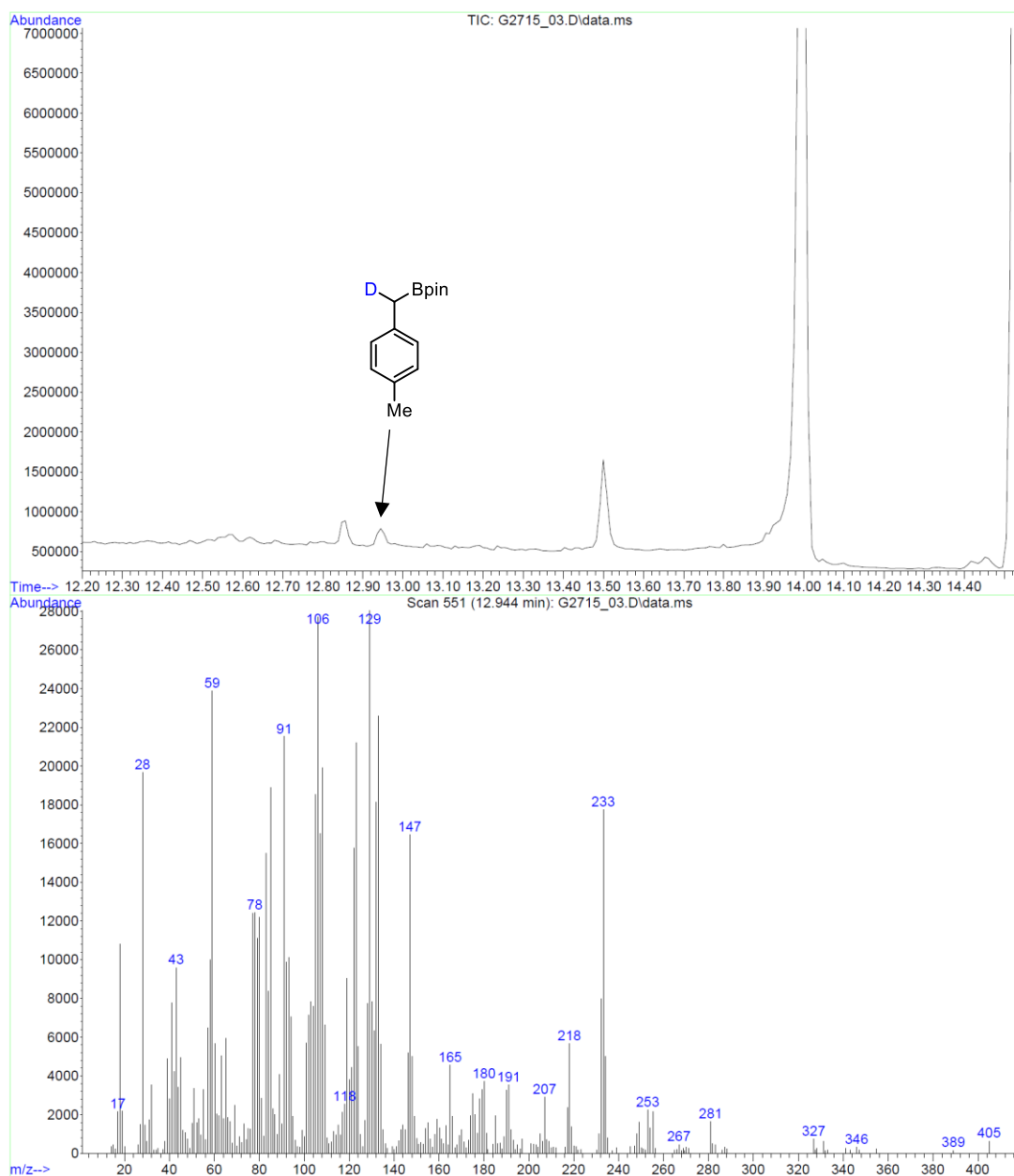


**Figure S8-1.** GC-MS report of the deuterated boronic ester S4-D

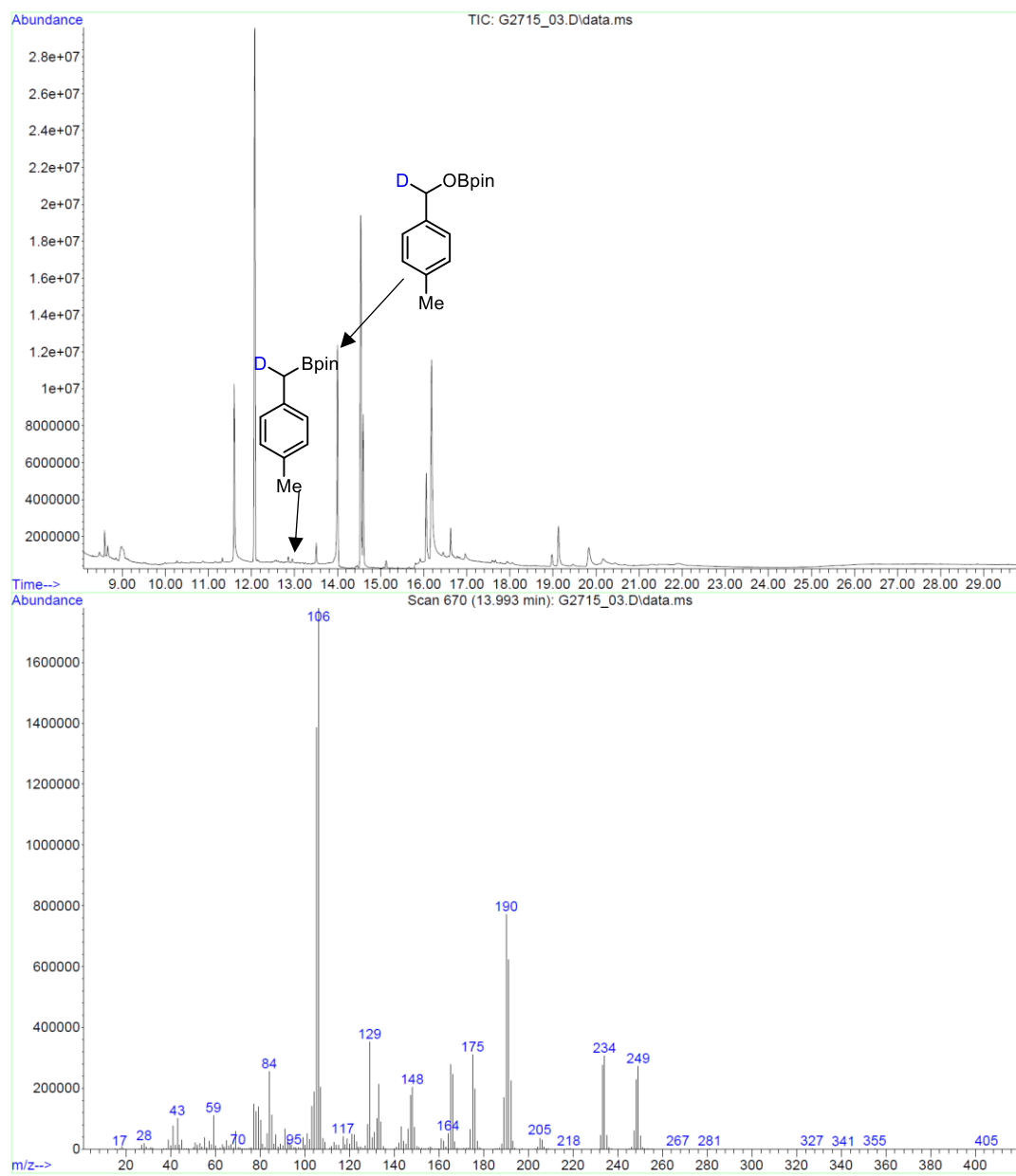


**Figure S8-2.** GC-MS report of the deuterated borate ester S5-D

## NMR Mechanistic Study

For mechanistic studies, specifically  $^{13}\text{C}$ -labelled benzaldehyde (labelled at carbonyl position) substrate is used, while keeping the other reaction conditions identical as mentioned above. Both *in situ* NMR sample and batch reaction sample studies were carried out. In case of batch reaction, prior to the NMR measurements the reaction mixture was irradiated for 3 hours (*ex situ*). For *in situ* NMR sample, the samples were prepared in argon atmosphere directly inside NMR tube. To minimize light expose to the sample, the NMR tube was covered with aluminum foil during the sample preparation.

The NMR experiments were measured on a Bruker Avance III HD 600 MHz spectrometer with a 5 mm TBI-F probe and a Bruker Avance III 600 MHz with Prodigy BBO-probe, equipped with BCU II temperature control unit. The  $^{13}\text{C}$  of C=O group in solvent DMF was used as the reference in  $^{13}\text{C}$  NMR spectra. NMR experiments are modified to minimize NOE enhancement from  $^1\text{H}$  nuclei and predominantly observe the labelled  $^{13}\text{C}$  peaks.

For the *in situ* illumination, the LED-based optical fiber connected device was used.<sup>[36]</sup> The sample was prepared in 5 mm amberized NMR tubes of spintec which were used together with an insert for the optical fiber and a transistor circuit operated by the spectrometer to switch the LED automatically. The temperature was controlled by the BCU II unit of the spectrometer. For light source a Lumitronix Cree XT-E (royalblue) with a peak wavelength of 450 nm and 500 mW optical output was used.

## CEST NMR

CEST NMR experiment is analogous to EXSY method for study of chemical exchange. CEST is more sensitive than EXSY.<sup>[37]</sup> The higher sensitivity of the method can be exploited to detect low-populated reaction intermediates.<sup>[38]</sup> CEST involves selective saturation of peaks or spectra, and observing intensity modulations in the peak of corresponding exchanged peaks. In the present study, following 1D  $^{13}\text{C}$  CEST pulse sequence is used

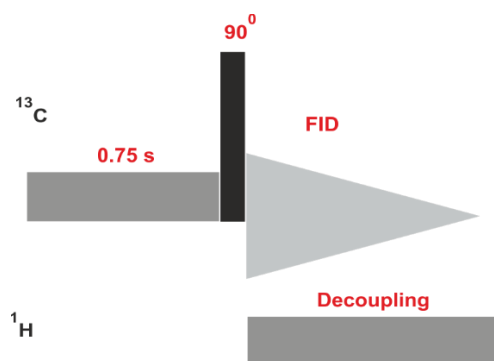


**Figure S9.** 1D  $^{13}\text{C}$  CEST pulse sequence. Saturation pulse is applied for 0.75 s duration with 200 Hz RF field strength. To maximize the intensity and enhance the effect,  $^1\text{H}$  decoupling is applied during the acquisition.

## Identification and characterization of intermediates

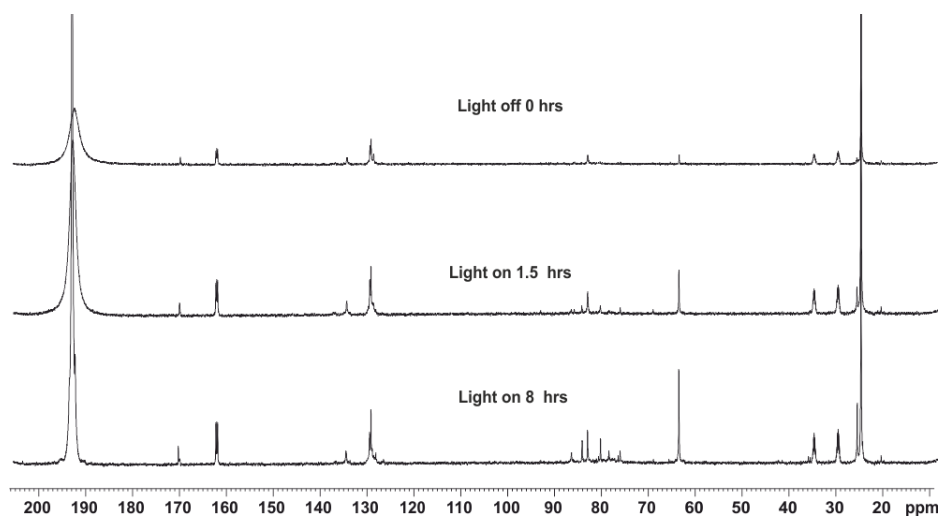


**Figure S10.** *In situ*  $^1\text{H}$  decoupled  $^{13}\text{C}$  spectra of reaction mixture at different time. The  $^{13}\text{C}$  resonance of aldehyde shows relatively broader peak, possibly indicating a radical formation at carbonyl position. Upon irradiation, the spectra show development of new set of signals with time, corresponding to intermediates, by-products and products.

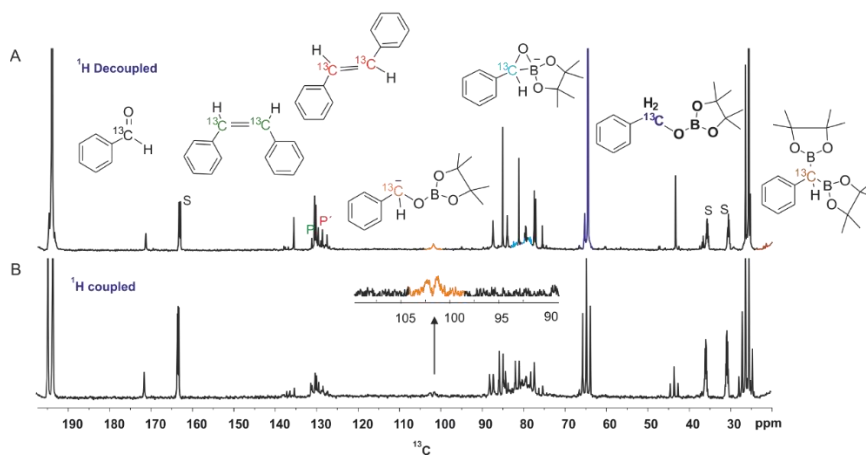


**Figure S11.** Complete *in situ*  $^1\text{H}$  decoupled (A) and coupled (B)  $^{13}\text{C}$  spectra of reaction mixture after 18 hours.



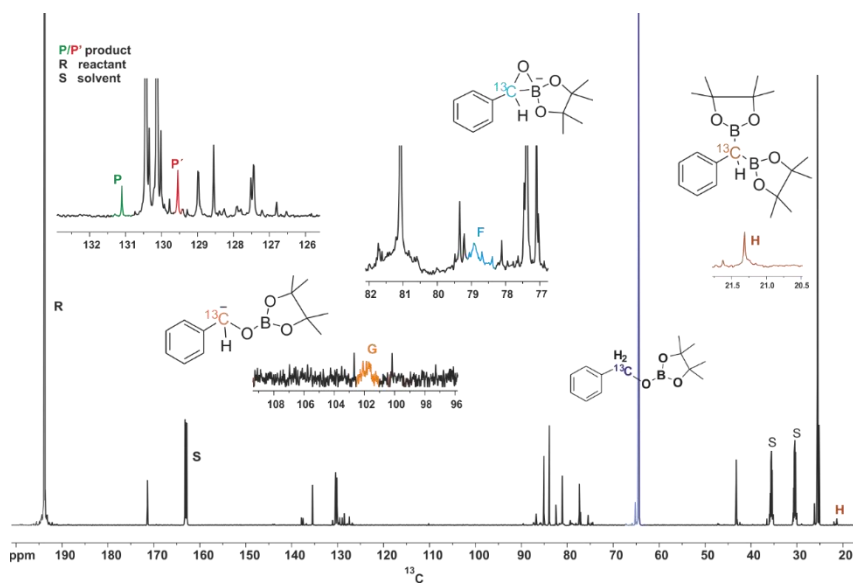


**Figure S12.**  $^1\text{H}$  decoupled  $^{13}\text{C}$  spectra of batch reaction mixture after 3 hours of irradiation. All identified peaks assigned to product, reactant, solvent and intermediates are distinctively marked.

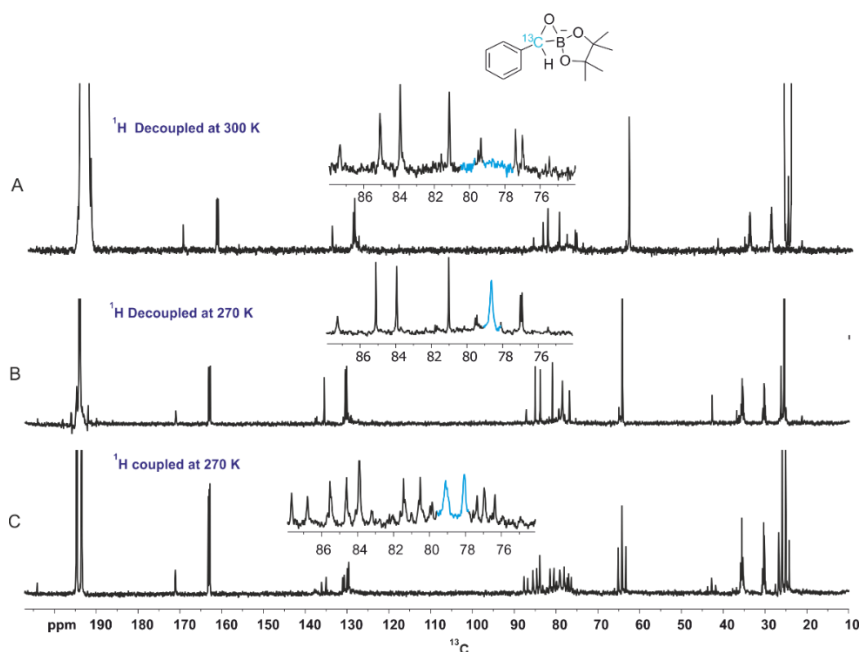


**Figure S13.** Stabilization and characterization of intermediate **F**, shown is the complete spectra at 300 K (A) and 270 K (B). The doublet in  $^1\text{H}$  coupled spectrum (C) indicates  $-\text{CH}$  moiety.

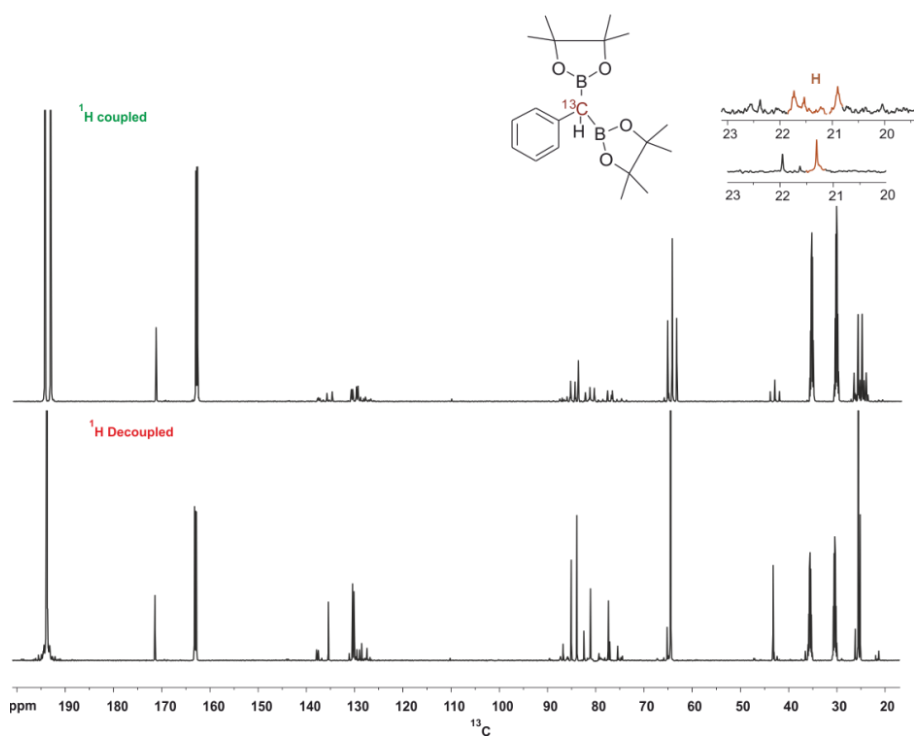


**Figure S14.**  $^1\text{H}$  coupled (top), and decoupled (bottom)  $^{13}\text{C}$  spectra of batch reaction mixture. Marked peaks correspond to the intermediate **H**. The  $^1\text{H}$  coupled spectrum indicates C-H moiety, which corroborates the intermediate **H**.

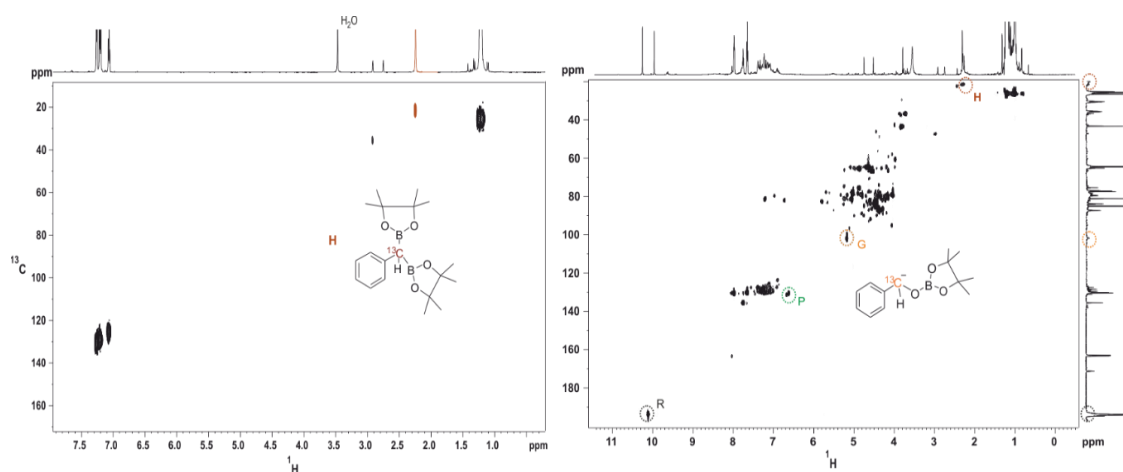


**Figure S15.** HSQC spectra of batch reaction mixture (right), and independently synthesized intermediates **H** (left). The marked peak **H** corresponds to the intermediate **H** in the reaction mixture.

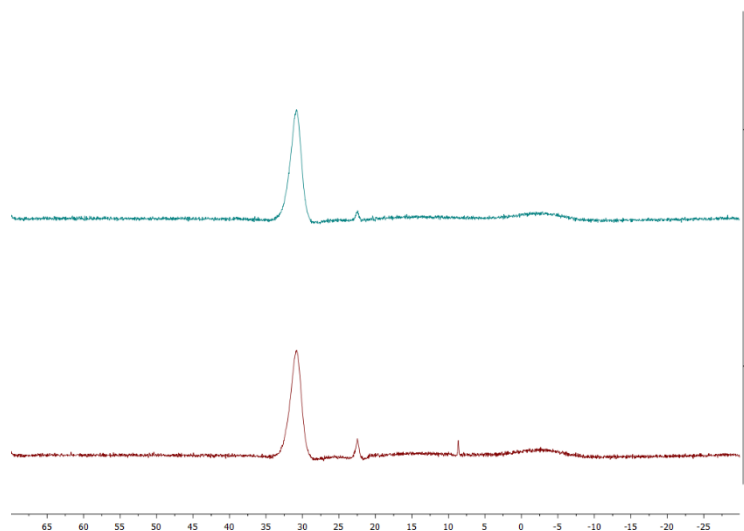
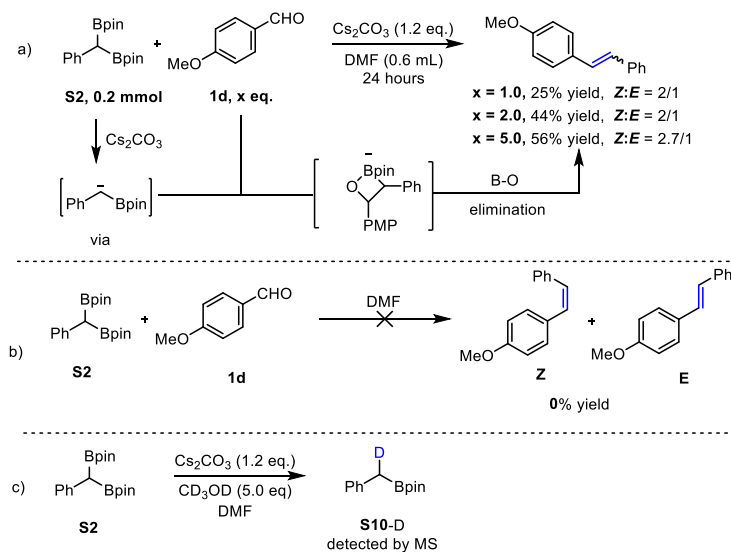


**Figure S16.**  $^{11}\text{B}$  NMR spectra of  $\text{B}_2\text{pin}_2$  (top signal) and a mixture of  $\text{B}_2\text{pin}_2$  and  $\text{Cs}_2\text{CO}_3$  (bottom signal) in  $d^7\text{-DMF}$ . The scale is recorded in ppm.

### Further control experiments

#### Scheme S3. Control experiments with 1,1-benzylidiboronate ester **S2**



The reaction between **S2** and **1d** in the presence of  $\text{Cs}_2\text{CO}_3$  (1.2 equiv.) afforded the corresponding unsymmetrical alkene in 25% yield ( $Z/E = 2/1$ ). When increasing the amount of aldehyde **1d** used, higher reaction efficiency was observed. However, no product could be detected in the absence of  $\text{Cs}_2\text{CO}_3$ . When  $\text{CD}_3\text{OD}$  (5.0 eq) was added into the mixture containing **S2**,  $\text{Cs}_2\text{CO}_3$  (1.2 eq) and DMF (0.6 mL), the corresponding deuterated benzyl boronic ester **S10-D** was detected as the main product which suggests that  $\text{Cs}_2\text{CO}_3$  could promote the mono-deborylation of **S2** to give  $\alpha$ -boryl carbanion.<sup>[39]</sup> **S10-D**: MS (EI)  $m/z$ : 219. HRMS (EI): 219.1531. Moreover, according to the literatures report we suggest the nucleophilic attack of  $\alpha$ -boryl carbanion towards carbonyl of **1d** followed by the B-O elimination is responsible for the generation of alkene.

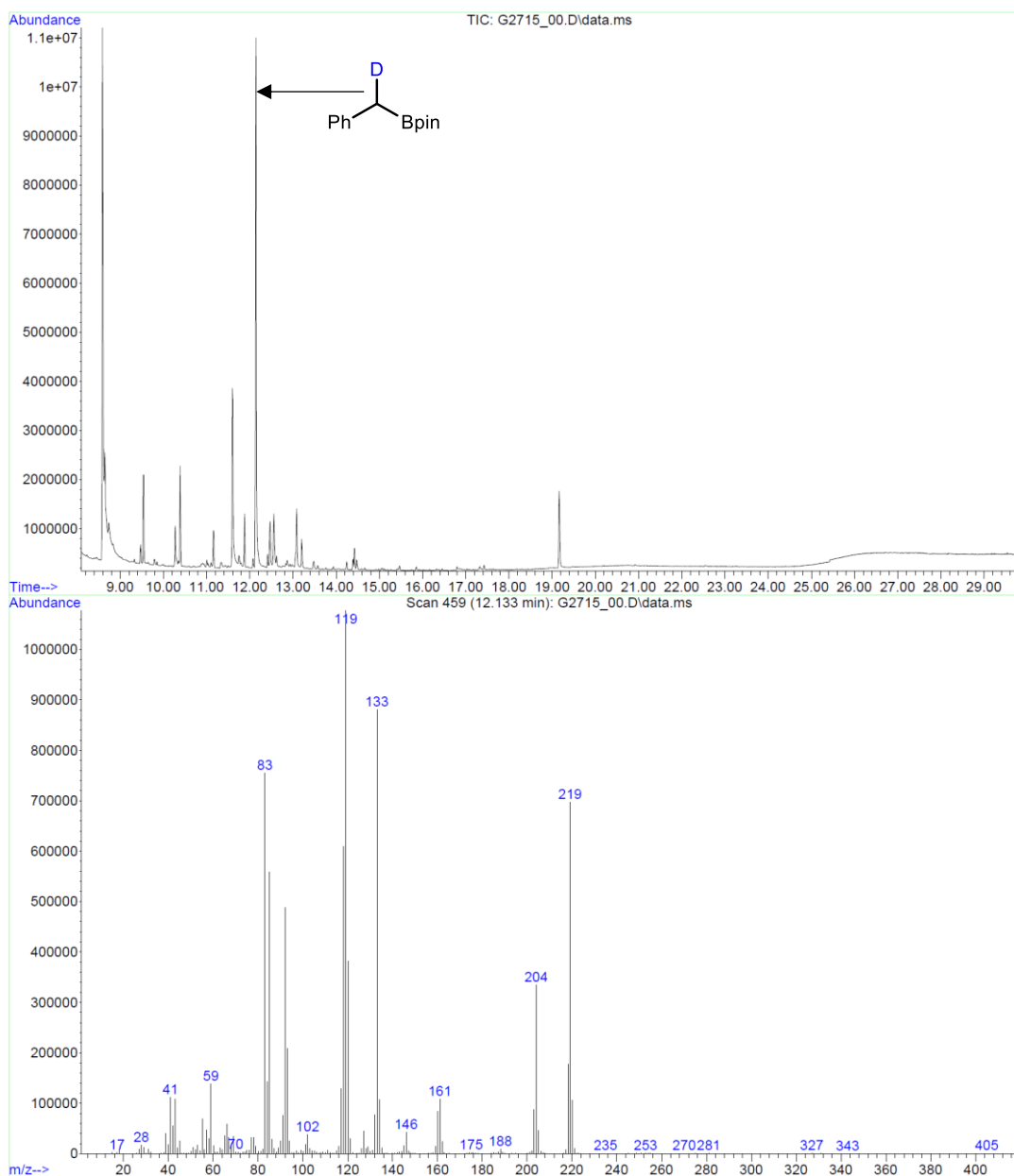
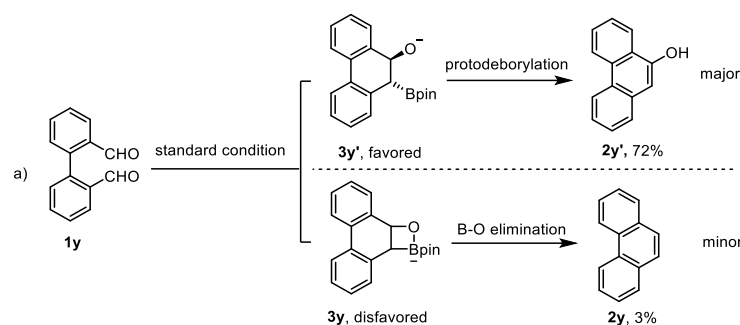


**Figure S17.** GC-MS report of S10-D in Scheme S3c

#### Scheme S4. Control reaction with 2,2'-diphenyldicarboxaldehyde **1y**

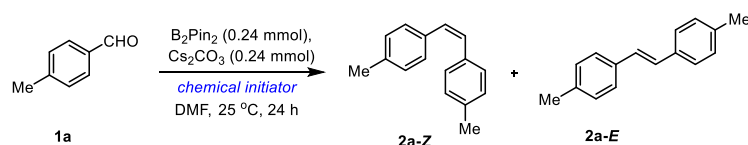


When using 2,2'-diphenyldicarboxaldehyde **1y** as the testing substrate for a potential intramolecular coupling reaction, anticipated intramolecular coupling product **2y** was obtained in only 3% yield and partially deoxygenative coupling product **2y'** was isolated as the major product (72%). We propose two possible intermediates to explain the distribution of these two products. Firstly,  $\alpha$ -boryl stabilized carbanion was generated as the key intermediate, subsequent intramolecular attack towards vicinal carbonyl group led to four-membered ring intermediate **3y** and species **3y'**. The formation of **3y'** outcompetes the generation of highly twisted **3y**. Further deborylation<sup>[40]</sup> and elimination in the presence of  $\text{Cs}_2\text{CO}_3$  to give 9-phenanthrenol **2y'** as the major product.

#### Evaluation of potential propagation pathway

**Hypothesis:** The proposed Bpin-base radical (**D**) is potentially capable of reducing another molecule of benzaldehyde to give ketyl radical anion (**C**), leading to a radical chain propagation mechanism. In order to determine this potential propagative process, experiments using chemical initiator ( $\text{SmI}_2$  or Na) in place of the photocatalytic system (photocatalyst, blue light and thiol) were conducted.

#### Scheme S5. (Sub)-stoichiometric experiment



To a 5 mL snap vial with stirring bar,  $\text{B}_2\text{pin}_2$  (0.24 mmol, 2.4 equiv.),  $\text{Cs}_2\text{CO}_3$  (0.24 mmol, 2.4 equiv.) and Sodium (when Na was used as chemical initiator) were added. The vial was evacuated and back filled with nitrogen three times. A solution of aldehyde **1a** (0.2 mmol) in dry DMF (0.6 mL) and  $\text{SmI}_2$  in THF (when  $\text{SmI}_2$  was used as chemical initiator) was added by syringe. After degassed with two freeze-pump-thaw cycles via a syringe needle, the reaction mixture was stirred for 24 hours at 25 °C. After this time, the reaction mixture was quenched by adding water and added ethyl acetate. 1,3,5-trimethoxybenzene was added then the reaction mixture was analyzed by  $^1\text{H}$  NMR. Results are shown in Table S7.

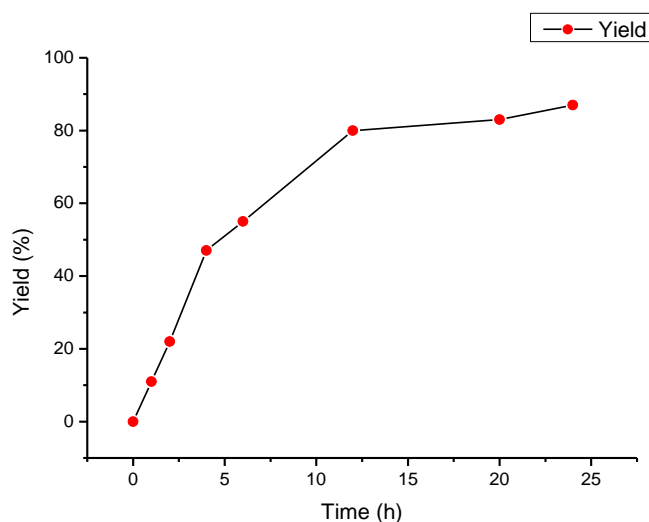
**Table S7.** Yields obtained in the presence of chemical initiators

Initiator	2a (Z+E), yield (%)
SmI <sub>2</sub> (20 mol%)	0
SmI <sub>2</sub> (100 mol%)	0
Na (20 mol%)	0
Na (100 mol%)	0

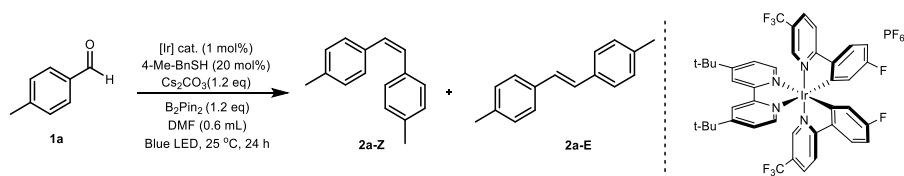
### Reaction Kinetics and Isomerization Experiments

#### Reaction profile and time/isomerization experiments

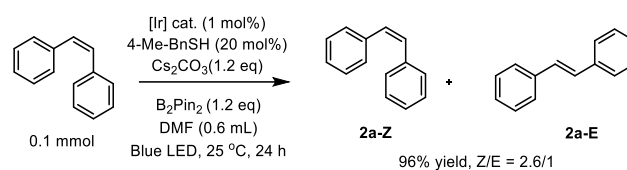
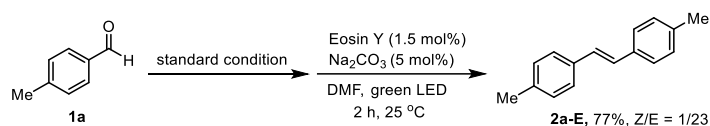
To a 5 mL snap vial with a stirring bar, B<sub>2</sub>pin<sub>2</sub> (0.24 mmol, 1.2 equiv.), [Ir(FCF<sub>3</sub>ppy)<sub>2</sub>dtbbpy] (1 mol%) and Cs<sub>2</sub>CO<sub>3</sub> (0.24 mmol, 1.2 equiv.) were added. The vial was evacuated and back filled with nitrogen three times. A solution of 4-Me-BnSH (20 mol%) and *p*-tolualdehyde (0.2 mmol, 24 mg) in dry DMF (0.6 mL) was added by syringe. After degassing by the freeze-pump-thaw via a syringe needle for two cycles, the reaction mixture was irradiated with a 455 nm LED for indicated time at 25 °C. The yield of **2a** and Z/E ratio were determined by <sup>1</sup>H NMR analysis of crude reaction mixture using 1,3,5-trimethoxybenzene as internal standard.



**Figure S18.** Reaction profile plot

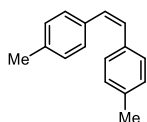
**Table S8.** Time/Isomerization studies

Time (h)	Yield of <b>2a</b> [%]	Z/E
1 h	11	1/8.5
2 h	22	1/4.8
4 h	47	1/2.6
6 h	55	1/2.3
12 h	80	1.3/1
20 h	83	2.7/1
24 h	<b>87</b>	<b>2.6/1</b>

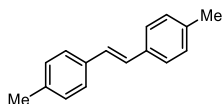
**Scheme S6.** Z to E isomerization of **2a**

To a 5 mL snap vial with stirring bar, B<sub>2</sub>pin<sub>2</sub> (0.24 mmol, 1.2 equiv.), [Ir(FCF<sub>3</sub>ppy)<sub>2</sub>dtbbpy] (1 mol%) and Cs<sub>2</sub>CO<sub>3</sub> (0.24 mmol, 1.2 equiv.) were added. The vial was evacuated and back filled with nitrogen three times. A solution of 4-Me-BnSH (20 mol%) and **1a** (0.2 mmol, 24 mg) in dry DMF (0.6 mL) was added by syringe. After degassing by the freeze-pump-thaw via a syringe needle for two cycles, the reaction mixture was irradiated with a 455 nm LED for 24 hours at 25 °C. Reaction mixture was then diluted with DMF (2 mL) and filtered through a pad of celite. To the filtrate was added Eosin Y (3 μmol, 1.5 mol%, based on **1a**), Na<sub>2</sub>CO<sub>3</sub> (5 mol%, 10 μmol, based on **1a**), the reaction was irradiated with green LED for 2 hours after degassing. The resulting solution was added 1,3,5-trimethoxybenzene as internal standard, concentrated with vacuum and subjected to <sup>1</sup>H NMR analysis.

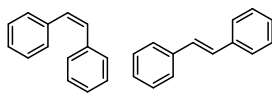
## 2.5 Characterization of products



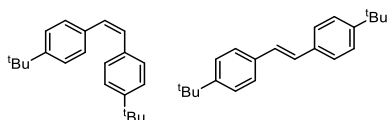
**(Z)-1,2-di-p-tolylene:** Following the general procedure A, the product was obtained as the oily liquid 12.5 mg.  $^1\text{H NMR}$  (400 MHz,  $\text{CDCl}_3$ )  $\delta$  7.18 (d,  $J = 8.1$  Hz, 2H), 7.05 (d,  $J = 7.6$  Hz, 2H), 6.53 (s, 1H), 2.33 (s, 3H).  $^{13}\text{C NMR}$  (101 MHz,  $\text{CDCl}_3$ )  $\delta$  136.69, 134.48, 129.49, 128.85, 128.72, 21.22. **HRMS** (EI) calculated for  $\text{C}_{16}\text{H}_{16}$   $[\text{M}]^+$ :208.1247, found 208.1245.



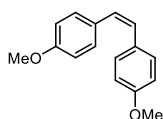
**(E)-1,2-di-p-tolylene:** Following the general procedure A, the product was obtained as the white solid 4.8 mg.  $^1\text{H NMR}$  (300 MHz,  $\text{CDCl}_3$ )  $\delta$  7.40 (m, 4H), 7.16 (d,  $J = 7.9$  Hz, 4H), 7.04 (s, 2H), 2.36 (s, 6H).  $^{13}\text{C NMR}$  (101 MHz,  $\text{CDCl}_3$ )  $\delta$  137.25, 134.72, 129.34, 127.61, 126.28, 21.23. **HRMS** (EI) calculated for  $\text{C}_{16}\text{H}_{16}$   $[\text{M}]^+$ :208.1247, found 208.1247.



**(Z)-1,2-diphenylethene and (E)-1,2-diphenylethene:** Following the general procedure A, the product was obtained as the white solid 12.6 mg (70% yield,  $Z/E = 2/1$ ).  $^1\text{H NMR}$  (300 MHz,  $\text{CDCl}_3$ )  $\delta$  7.57 – 7.51 (m, 2H), 7.42 – 7.35 (m, 2H), 7.32 – 7.26 (m, 5H), 7.26 – 7.17 (m, 6H), 7.14 (s, 1H), 6.62 (s, 2H).  $^{13}\text{C NMR}$  (75 MHz,  $\text{CDCl}_3$ )  $\delta$  137.3, 137.2, 130.21, 128.84, 128.65, 128.18, 127.60, 127.05, 126.48. **HRMS** (EI) calculated for  $\text{C}_{14}\text{H}_{12}$   $[\text{M}]^+$ :180.0934, found 180.0926.

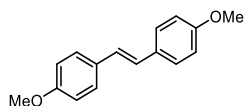


**(Z)-1,2-bis(4-(tert-butyl)phenyl)ethene and (E)-1,2-bis(4-(tert-butyl)phenyl)ethene:** Following the general procedure A, the product was obtained as the colorless oil 19.2 mg (60% yield,  $Z/E = 1/1.3$ ).  $^1\text{H NMR}$  (300 MHz,  $\text{CDCl}_3$ )  $\delta$  7.49 – 7.36 (m, 10H), 7.24 (s, 1H), 7.23 – 7.14 (m, 3H), 7.07 (s, 2H), 7.06 – 7.01 (m, 2H), 6.51 (s, 2H), 1.34 (s, 18H), 1.32 (s, 14H).  $^{13}\text{C NMR}$  (75 MHz,  $\text{CDCl}_3$ )  $\delta$  150.52, 149.98, 134.74, 134.47, 129.51, 129.48, 129.37, 129.34, 128.85, 128.72, 128.69, 128.47, 127.69, 126.12, 125.55, 125.05, 34.59, 31.30. **HRMS** (EI) calculated for  $\text{C}_{22}\text{H}_{28}$   $[\text{M}]^+$ :292.2186, found 292.2189.

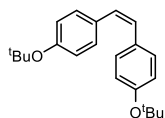


**(Z)-1,2-bis(4-methoxyphenyl)ethene:** Following the general procedure A, the product was obtained as the colorless oil 12.2 mg.  $^1\text{H NMR}$  (300 MHz,  $\text{CDCl}_3$ )  $\delta$  7.24 – 7.17 (m, 4H), 6.81 – 6.74 (m, 4H), 6.45 (s, 2H), 3.80 (s, 6H).  $^{13}\text{C NMR}$  (75 MHz,  $\text{CDCl}_3$ )  $\delta$  158.46, 130.01, 129.95, 128.33, 113.56, 55.17. **HRMS** (EI) calculated for  $\text{C}_{16}\text{H}_{16}\text{O}_2$   $[\text{M}]^+$ :240.1145, found 240.1145.

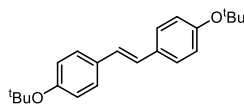




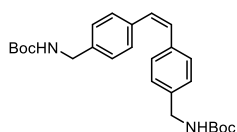
**(E)-1,2-bis(4-methoxyphenyl)ethene:** Following the general procedure A, the product was obtained as the white solid 3.6 mg.  $^1\text{H NMR}$  (300 MHz,  $\text{CDCl}_3$ )  $\delta$  7.46 – 7.39 (m, 4H), 6.93 (s, 2H), 6.92 – 6.86 (m, 4H), 3.83 (s, 6H).  $^{13}\text{C NMR}$  (75 MHz,  $\text{CDCl}_3$ )  $\delta$  158.96 , 130.44 , 127.38 , 126.14 , 114.07 , 55.31 . **HRMS** (EI) calculated for  $\text{C}_{16}\text{H}_{16}\text{O}_2$   $[\text{M}]^+$ : 240.1145, found 240.1134.



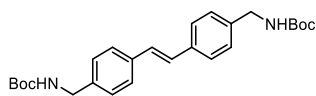
**(Z)-1,2-bis(4-(tert-butoxy)phenyl)ethene:** Following the general procedure A, the product was obtained as clear oil 6.2 mg.  $^1\text{H NMR}$  (400 MHz,  $\text{CDCl}_3$ )  $\delta$  7.18 – 7.11 (m, 4H), 6.86 – 6.81 (m, 4H), 6.49 (s, 2H), 1.34 (s, 18H).  $^{13}\text{C NMR}$  (101 MHz,  $\text{CDCl}_3$ )  $\delta$  154.33 , 132.40 , 129.40 , 128.99 , 123.71 , 78.48 , 28.84 . **HRMS** (EI) calculated for  $\text{C}_{22}\text{H}_{28}\text{O}_2$   $[\text{M}]^+$ : 324.2084, found 324.2090.



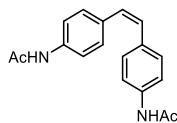
**(E)-1,2-bis(4-(tert-butoxy)phenyl)ethene:** Following the general procedure A, the product was obtained as clear crystal 7.8 mg.  $^1\text{H NMR}$  (400 MHz,  $\text{CDCl}_3$ )  $\delta$  7.42 – 7.37 (m, 4H), 6.98 (d,  $J = 2.7$  Hz, 4H), 6.97 (s, 2H), 1.36 (s, 18H).  $^{13}\text{C NMR}$  (101 MHz,  $\text{CDCl}_3$ )  $\delta$  154.89 , 132.74 , 127.07 , 126.81 , 124.28 , 78.70 , 28.86. **HRMS** (EI) calculated for  $\text{C}_{22}\text{H}_{28}\text{O}_2$   $[\text{M}]^+$ : 324.2084, found 324.2093.



**Di-tert-butyl ((ethene-1,2-diylbis(4,1-phenylene))bis(methylene))(Z)-dicarbamate:** Following the general procedure A, the product was obtained as clear oil 13 mg.  $^1\text{H NMR}$  (400 MHz,  $\text{CDCl}_3$ )  $\delta$  7.19 (m, 4H), 7.12 (d,  $J = 8.0$  Hz, 4H), 6.55 (s, 2H), 4.85 (s, 2H), 4.28 (d,  $J = 5.9$  Hz, 4H), 1.45 (s, 18H).  $^{13}\text{C NMR}$  (101 MHz,  $\text{CDCl}_3$ )  $\delta$  155.84 , 137.70 , 136.20 , 129.82 , 129.01 , 127.25 , 79.47 , 44.37 , 28.38 . **HRMS** (ESI) calculated for  $\text{C}_{26}\text{H}_{35}\text{N}_2\text{O}_4$   $[\text{M}+\text{H}]^+$ : 439.2591, found 439.2590.

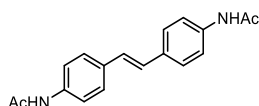


**Di-tert-butyl ((ethene-1,2-diylbis(4,1-phenylene))bis(methylene))(E)-dicarbamate:** Following the general procedure A, the product was obtained as white solid 7.6 mg.  $^1\text{H NMR}$  (400 MHz,  $\text{CDCl}_3$ )  $\delta$  7.47 (d,  $J = 8.2$  Hz, 4H), 7.27 (d,  $J = 7.5$  Hz, 5H), 7.07 (s, 2H), 4.86 (s, 2H), 4.32 (d,  $J = 5.9$  Hz, 4H), 1.47 (s, 18H).  $^{13}\text{C NMR}$  (101 MHz,  $\text{CDCl}_3$ )  $\delta$  155.86 , 138.32 , 136.39 , 128.14 , 127.83 , 126.67 , 79.53 , 44.43 , 28.40 , 28.38 . **HRMS** (ESI) calculated for  $\text{C}_{26}\text{H}_{35}\text{N}_2\text{O}_4$   $[\text{M}+\text{H}]^+$ : 439.2591, found 439.2594.

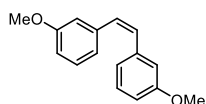


**(Z)-N,N'-(ethene-1,2-diylbis(4,1-phenylene))diacetamide:** Following the general procedure A, the product was obtained as white solid 12.3 mg.  $^1\text{H NMR}$  (300 MHz,  $\text{CDCl}_3$ )  $\delta$  7.61 (s, 2H), 7.36 – 7.29 (m, 4H), 7.20 – 7.13 (m, 4H), 6.49 (s, 2H), 2.14 (s, 6H).  $^{13}\text{C NMR}$  (75 MHz,  $\text{CDCl}_3$ )  $\delta$  168.53 , 136.75 , 133.21 , 129.47 ,

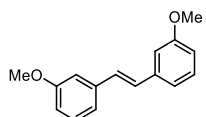
129.19 , 127.78 , 119.58 , 24.55 . **HRMS** (ESI) calculated for  $C_{18}H_{19}N_2O_2$   $[M+H]^+$ :295.1441, found 295.1444.



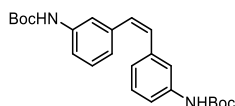
**(E)-N,N'-(ethene-1,2-diylbis(4,1-phenylene))diacetamide:** Following the general procedure A, the product was obtained as white solid 6.2 mg.  **$^1H$  NMR** (300 MHz,  $DMSO-d_6$ )  $\delta$  10.00 (s, 2H), 7.60 – 7.47 (m, 8H), 7.07 (s, 2H), 3.34 (s, 2H), 2.04 (s, 6H).  **$^{13}C$  NMR** (75 MHz,  $DMSO-d_6$ )  $\delta$  168.22 , 138.63 , 132.04 , 126.67 , 126.54 , 119.04 , 24.06 . **HRMS** (ESI) calculated for  $C_{18}H_{19}N_2O_2$   $[M+H]^+$ :295.1441, found 295.1445.



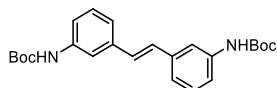
**(Z)-1,2-bis(3-methoxyphenyl)ethene:** Following the general procedure A, the product was obtained as clear oil 9.8 mg (total amount from two parallel reactions).  **$^1H$  NMR** (300 MHz,  $CDCl_3$ )  $\delta$  7.15 (t,  $J = 7.9$  Hz, 2H), 6.88 – 6.78 (m, 4H), 6.75 (ddd,  $J = 8.3, 2.6, 1.0$  Hz, 2H), 6.58 (s, 2H). 3.67 (s, 6H)  **$^{13}C$  NMR** (75 MHz,  $CDCl_3$ )  $\delta$  159.32 , 138.50 , 130.32 , 129.17 , 128.88 , 121.48 , 113.75 , 113.27 , 55.04 . **HRMS** (EI) calculated for  $C_{16}H_{16}O_2$   $[M]^+$  240.1145, found 240.1145.



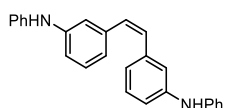
**(E)-1,2-bis(3-methoxyphenyl)ethene:** Following the general procedure A, the product was obtained as white solid 6.8 mg (total amount from two parallel reactions).  **$^1H$  NMR** (300 MHz,  $CDCl_3$ )  $\delta$  7.31 – 7.25 (m, 3H), 7.12 (dt,  $J = 7.7, 1.3$  Hz, 2H), 7.08 (s, 2H), 7.05 (dd,  $J = 2.6, 1.6$  Hz, 2H), 6.83 (ddd,  $J = 8.2, 2.5, 1.0$  Hz, 2H), 3.86 (s, 6H).  **$^{13}C$  NMR** (75 MHz,  $CDCl_3$ )  $\delta$  159.85 , 138.65 , 129.62 , 128.87 , 119.25 , 113.36 , 111.72 , 55.25. **HRMS** (EI) calculated for  $C_{16}H_{16}O_2$  240.1145, found 240.1138  $[M]^+$ .



**Di-tert-butyl (ethene-1,2-diylbis(3,1-phenylene))(Z)-dicarbamate:** Following the general procedure B, the product was obtained as white solid 14.8 mg.  **$^1H$  NMR** (400 MHz,  $CDCl_3$ )  $\delta$  7.32 (d,  $J = 8.1$  Hz, 2H), 7.27 (d,  $J = 1.9$  Hz, 2H), 7.16 (t,  $J = 7.9$  Hz, 2H), 6.91 (dt,  $J = 7.7, 1.3$  Hz, 2H), 6.53 (s, 2H), 6.52 (s, 2H), 1.50 (s, 18H).  **$^{13}C$  NMR** (101 MHz,  $CDCl_3$ )  $\delta$  152.92 , 138.09 , 137.66 , 130.05 , 128.83 , 124.26 , 119.33 , 118.11 , 80.42 , 28.35. **HRMS** (ESI) calculated for  $C_{24}H_{34}N_3O_4$   $[M+NH_4]^+$ :428.2544, found 428.2555.

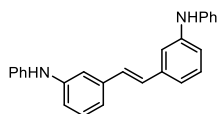


**Di-tert-butyl (ethene-1,2-diylbis(3,1-phenylene))(E)-dicarbamate:** Following the general procedure B, the product was obtained as white solid 9.8 mg.  **$^1H$  NMR** (300 MHz,  $CDCl_3$ )  $\delta$  7.58 (t,  $J = 1.9$  Hz, 2H), 7.28–7.19 (m, 6H), 7.06 (s, 2H), 6.52 (s, 2H), 1.54 (s, 18H).  **$^{13}C$  NMR** (75 MHz,  $CDCl_3$ )  $\delta$  152.70 , 138.68 , 138.11 , 129.18 , 128.80 , 121.37 , 117.74 , 116.35 , 80.57 , 28.34 . **HRMS** (ESI) calculated for  $C_{24}H_{34}N_3O_4$   $[M+NH_4]^+$ :428.2544, found 428.2553.

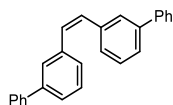


**(Z)-3,3'-(ethene-1,2-diyl)bis(N-phenylaniline).** Following the general procedure B, the product was

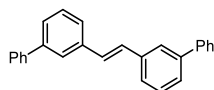
obtained as yellowish solid 15.4 mg.  $^1\text{H NMR}$  (300 MHz,  $\text{CDCl}_3$ )  $\delta$  7.20 (m, 6H), 7.03 (t,  $J = 2.0$  Hz, 2H), 6.95 – 6.84 (m, 10H), 6.58 (s, 2H), 5.64 (s, 2H).  $^{13}\text{C NMR}$  (75 MHz,  $\text{CDCl}_3$ )  $\delta$  142.88 , 142.70 , 138.41 , 130.55 , 129.27 , 129.23 , 121.59 , 120.83 , 117.66 , 117.63 , 116.39 . **HRMS** (ESI) calculated for  $\text{C}_{26}\text{H}_{23}\text{N}_2$   $[\text{M}+\text{H}]^+$ :363.1856, found 363.1854.



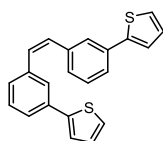
**(E)-3,3'-(ethene-1,2-diyl)bis(N-phenylaniline)**. Following the general procedure B, the product was obtained as yellowish solid 7.4 mg.  $^1\text{H NMR}$  (300 MHz,  $\text{CDCl}_3$ )  $\delta$  7.34 – 7.27 (m, 4H), 7.26 – 7.19 (m, 4H), 7.13 – 7.06 (m, 6H), 7.02 (s, 2H), 7.00 – 6.91 (m, 4H), 5.73 (s, 2H).  $^{13}\text{C NMR}$  (75 MHz,  $\text{CDCl}_3$ )  $\delta$  143.46 , 142.98, 138.46 , 129.60 , 129.39 , 128.78 , 121.13 , 119.41 , 117.98 , 117.18 , 115.65 . **HRMS** (ESI) calculated for  $\text{C}_{26}\text{H}_{23}\text{N}_2$   $[\text{M}+\text{H}]^+$ :363.1856, found 363.1859



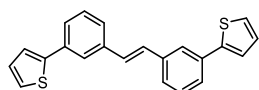
**(Z)-1,2-di([1,1'-biphenyl]-3-yl)ethene**. Following the general procedure A, the product was obtained as white solid 8.3 mg (total amount from two parallel reactions).  $^1\text{H NMR}$  (300 MHz,  $\text{CDCl}_3$ )  $\delta$  7.55 (t,  $J = 1.8$  Hz, 2H), 7.47 – 7.42 (m, 6H), 7.40 – 7.26 (m, 10H), 6.72 (s, 2H).  $^{13}\text{C NMR}$  (75 MHz,  $\text{CDCl}_3$ )  $\delta$  141.13 , 140.94 , 137.64 , 130.48 , 128.74 , 128.65 , 127.82 , 127.79 , 127.21 , 127.03 , 125.98 . **HRMS** (EI) calculated for  $\text{C}_{26}\text{H}_{20}$   $[\text{M}]^+$ :332.1560, found 332.1566.



**(E)-1,2-di([1,1'-biphenyl]-3-yl)ethene**. Following the general procedure A, the product was obtained as white solid 11.6 mg (total amount from two parallel reactions).  $^1\text{H NMR}$  (300 MHz,  $\text{CDCl}_3$ )  $\delta$  7.76 (t,  $J = 1.8$  Hz, 2H), 7.67 – 7.62 (m, 4H), 7.56 – 7.44 (m, 10H), 7.42 – 7.37 (m, 2H), 7.26 (s, 2H).  $^{13}\text{C NMR}$  (75 MHz,  $\text{CDCl}_3$ )  $\delta$  141.72 , 141.05 , 137.70 , 129.11 , 128.92 , 128.77 , 127.40 , 127.19 , 126.59 , 125.45 , 125.40 . **HRMS** (EI) calculated for  $\text{C}_{26}\text{H}_{20}$   $[\text{M}]^+$ :332.1560, found 332.1563.

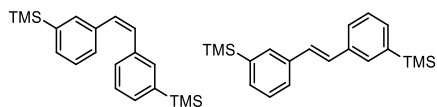


**(Z)-1,2-bis(3-(thiophen-2-yl)phenyl)ethene**: Following the general procedure A, the product was obtained as clear oil 15.2 mg (total amount from two parallel reactions).  $^1\text{H NMR}$  (300 MHz,  $\text{CDCl}_3$ )  $\delta$  7.56 (t,  $J = 1.8$  Hz, 2H), 7.46 (dt,  $J = 7.4, 1.7$  Hz, 2H), 7.28 (s, 1H), 7.25 – 7.16 (m, 7H), 7.03 (dd,  $J = 5.1, 3.6$  Hz, 2H), 6.67 (s, 2H).  $^{13}\text{C NMR}$  (75 MHz,  $\text{CDCl}_3$ )  $\delta$  137.63 , 134.37 , 130.35 , 128.84 , 127.98 , 127.92 , 126.39 , 124.83 , 124.81 , 123.1 . **HRMS** (EI) calculated for  $\text{C}_{22}\text{H}_{16}\text{S}_2$   $[\text{M}]^+$ :344.0688, found 344.0682.

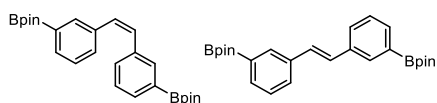


**(E)-1,2-bis(3-(thiophen-2-yl)phenyl)ethene**: Following the general procedure A, the product was obtained as clear oil. Following the general procedure A, the product was obtained as a white solid 8.2 mg (total amount from two parallel reactions).  $^1\text{H NMR}$  (300 MHz,  $\text{CDCl}_3$ )  $\delta$  7.76 (t,  $J = 1.8$  Hz, 2H), 7.50 (ddt,  $J = 17.3, 7.8, 1.5$  Hz, 4H), 7.41 (s, 1H), 7.39 – 7.35 (m, 3H), 7.31 (dd,  $J = 5.1, 1.2$  Hz, 2H), 7.20 (s, 2H), 7.11 (dd,  $J = 5.1,$

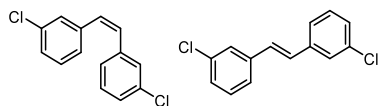
3.6 Hz, 2H).  $^{13}\text{C}$  NMR (75 MHz,  $\text{CDCl}_3$ )  $\delta$  144.15 , 137.77 , 134.83 , 129.23 , 128.86 , 128.02 , 125.52 , 125.37 , 124.96 , 124.24 , 123.31 . **HRMS** (EI) calculated for  $\text{C}_{22}\text{H}_{16}\text{S}_2$   $[\text{M}]^+$ :344.0688, found 344.0679.



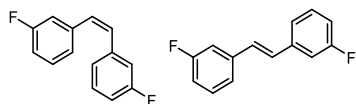
**(Z)-1,2-bis(3-(trimethylsilyl)phenyl)ethene and (E)-1,2-bis(3-(trimethylsilyl)phenyl)ethene:** Following the general procedure A, the product (mixture of Z and E products, Z/E = 1.6/1) was obtained as clear oil 15.2 mg.  $^1\text{H}$  NMR (300 MHz,  $\text{CDCl}_3$ )  $\delta$  7.63 (dt,  $J$  = 1.9, 0.8 Hz, 1H), 7.52 (dt,  $J$  = 7.5, 1.7 Hz, 1H), 7.43 – 7.35 (m, 3H), 7.34 – 7.28 (m, 5H), 7.22 – 7.16 (m, 5H), 7.12 (s, 2H), 6.61 (s, 2H), 0.29 (s, 13H), 0.13 (s, 18H).  $^{13}\text{C}$  NMR (75 MHz,  $\text{CDCl}_3$ )  $\delta$  140.83 , 140.17 , 136.56 , 136.53 , 133.89 , 132.59 , 131.88 , 131.72 , 130.53 , 129.23 , 128.88 , 128.86 , 128.79 , 128.72 , 128.69 , 128.04 , 127.55 , 126.65 , 126.39 , -1.10 , -1.27 . **HRMS** (EI) calculated for  $\text{C}_{20}\text{H}_{28}\text{Si}_2$   $[\text{M}]^+$ :324.1724, found 324.1733.



**(Z)-1,2-bis(3-(4,4,5,5-tetramethyl-1,3,2-dioxaborolan-2-yl)phenyl)ethene and (E)-1,2-bis(3-(4,4,5,5-tetramethyl-1,3,2-dioxaborolan-2-yl)phenyl)ethene:** Following the general procedure A, the product (mixture of Z and E products, Z/E = 1/1.6) was obtained as clear oil 28.6 mg (total amount from two parallel reactions).  $^1\text{H}$  NMR (300 MHz,  $\text{CDCl}_3$ )  $\delta$  8.01 – 7.95 (m, 2H), 7.70 (ddd,  $J$  = 5.5, 2.5, 1.2 Hz, 3H), 7.61 (m, 3H), 7.43 – 7.33 (m, 3H), 7.30 (dt,  $J$  = 7.9, 1.6 Hz, 1H), 7.18 (s, 2H), 7.17 – 7.09 (m, 2H), 6.61 (s, 1H), 1.37 (s, 24H), 1.33 (s, 17H).  $^{13}\text{C}$  NMR (75 MHz,  $\text{CDCl}_3$ )  $\delta$  136.66 , 136.56 , 135.56 , 133.84 , 133.36 , 132.88 , 131.38 , 130.14 , 129.36 , 129.27 , 128.52 , 128.07 , 127.37 , 126.26 , 83.85 , 83.75 , 24.88 , 24.83 . **HRMS** (EI) calculated for  $\text{C}_{26}\text{H}_{34}\text{B}_2\text{O}_4$   $[\text{M}]^+$ :432.2643, found 432.2647 and 432.2645.

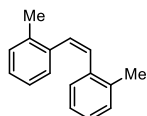


**(Z)-1,2-bis(3-chlorophenyl)ethene and (E)-1,2-bis(3-chlorophenyl)ethene:** Following the general procedure A, the product (mixture of Z and E products, Z/E = 1/1.2) was obtained as white solid 19.8 mg (total amount from two parallel reactions).  $^1\text{H}$  NMR (300 MHz,  $\text{CDCl}_3$ )  $\delta$  7.50 (t,  $J$  = 1.8 Hz, 2H), 7.37 (dt,  $J$  = 7.4, 1.7 Hz, 2H), 7.33 – 7.26 (m, 3H), 7.24 – 7.20 (m, 2H), 7.20 – 7.12 (m, 2H), 7.08 (dt,  $J$  = 7.0, 1.7 Hz, 1H), 7.03 (s, 2H), 6.57 (s, 1H).  $^{13}\text{C}$  NMR (75 MHz,  $\text{CDCl}_3$ )  $\delta$  138.66 , 138.42 , 134.69 , 134.17 , 129.99 , 129.93 , 129.53 , 128.80 , 128.59 , 127.88 , 127.47 , 126.90 , 126.39 , 124.88 . **HRMS** (EI) calculated for  $\text{C}_{14}\text{H}_{10}\text{Cl}_2$   $[\text{M}]^+$ :248.0154, found 248.0147.

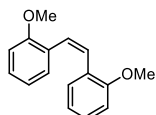


**(Z)-1,2-bis(3-fluorophenyl)ethene and (E)-1,2-bis(3-fluorophenyl)ethene:** Following the general procedure A, the product (mixture of Z and E products, Z/E = 1.7/1) was obtained as white solid 14 mg (total amount from two parallel reactions).  $^1\text{H}$  NMR (300 MHz,  $\text{CDCl}_3$ )  $\delta$  7.37 – 7.26 (m, 2H), 7.26 – 7.22 (m, 1H), 7.22 – 7.16 (m, 2H), 7.06 (s, 1H), 7.00 (dt,  $J$  = 7.7, 1.3 Hz, 3H), 6.96 – 6.87 (m, 4H), 6.60 (s, 2H).  $^{13}\text{C}$  NMR (75 MHz,  $\text{CDCl}_3$ )  $\delta$  164.77, 164.29, 161.52, 161.04 , 139.20, 139.10, 138.92 , 138.81 , 130.22 , 130.10 , 130.06 , 129.85 , 129.74 , 128.78 , 128.75 , 124.61 , 124.57 , 122.61 , 122.58 , 115.63 , 115.34 , 114.91 , 114.63 , 114.43 , 114.15 , 113.03 , 112.74 .  $^{19}\text{F}$  NMR (282 MHz,  $\text{CDCl}_3$ )  $\delta$  -113.73, -113.77. **HRMS** (EI)

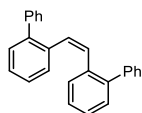
calculated for  $C_{14}H_{10}F_2 [M]^+$ :216.0745, found 216.0741.



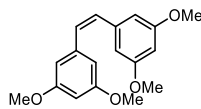
**(Z)-1,2-di-o-tolylolethene and (E)-1,2-di-o-tolylolethene:** Following the general procedure A, the products (mixture of Z and E configuration product, Z/E = 16/1) were obtained as clear oil 12.5 mg.  $^1H$  NMR (300 MHz,  $CDCl_3$ )  $\delta$  7.23 – 7.18 (m, 1H), 7.18 – 7.13 (m, 2H), 7.09 (m, 2H), 7.01 – 6.89 (m, 5H), 6.73 (s, 2H), 2.30 (s, 6H).  $^{13}C$  NMR (75 MHz,  $CDCl_3$ )  $\delta$  136.47 , 136.11 , 129.91 , 129.42 , 129.07 , 126.97 , 125.36 , 19.88 . **HRMS** (EI) calculated for  $C_{16}H_{16}O_2 [M]^+$  208.1247, found 208.1241.



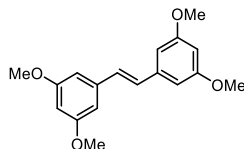
**(Z)-1,2-bis(2-methoxyphenyl)ethene and (E)-1,2-bis(2-methoxyphenyl)ethene:** Following the general procedure A, the products (Z/E = 8.1/1) were obtained as clear oil 13.0 mg.  $^1H$  NMR (300 MHz,  $CDCl_3$ )  $\delta$  7.20 – 7.10 (m, 4H), 6.87 (dd,  $J$  = 8.3, 1.1 Hz, 2H), 6.77 (s, 2H), 6.70 (td,  $J$  = 7.5, 1.1 Hz, 2H), 3.89 (s, 1H), 3.83 (s, 6H).  $^{13}C$  NMR (75 MHz,  $CDCl_3$ )  $\delta$  157.08 , 129.97 , 128.26 , 126.30 , 125.57 , 120.03 , 110.46 , 55.42 . **HRMS** (EI) calculated for  $C_{16}H_{16}O_2 [M]^+$  240.1145, found 240.1151.



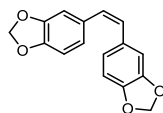
**(Z)-1,2-di([1,1'-biphenyl]-2-yl)ethene:** Following the general procedure A, the product was obtained as clear oil 13.0 mg.  $^1H$  NMR (300 MHz,  $CDCl_3$ )  $\delta$  7.39 – 7.36 (m, 3H), 7.36 (s, 7H), 7.34 (t,  $J$  = 1.6 Hz, 3H), 7.32 – 7.27 (m, 3H), 7.15 (td,  $J$  = 7.4, 1.6 Hz, 2H), 6.38 (s, 2H).  $^{13}C$  NMR (75 MHz,  $CDCl_3$ )  $\delta$  141.43 , 141.03 , 135.30 , 129.96 , 129.71 , 129.48 , 127.94 , 127.23 , 127.02 , 126.85 . **HRMS** (EI) calculated for  $C_{26}H_{20} [M]^+$ :332.1560, found 332.1566.



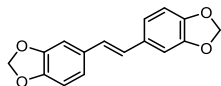
**(Z)-1,2-bis(3,5-dimethoxyphenyl)ethene:** Following the general procedure A, the product was obtained as white solid 16.8 mg (total amount from two parallel reactions).  $^1H$  NMR (400 MHz,  $CDCl_3$ )  $\delta$  6.54 (s, 2H), 6.44 (d,  $J$  = 2.4 Hz, 4H), 6.32 (t,  $J$  = 2.3 Hz, 2H), 3.67 (s, 12H).  $^{13}C$  NMR (101 MHz,  $CDCl_3$ )  $\delta$  160.46 , 138.96 , 130.54 , 106.73 , 99.90 , 55.22 . **HRMS** (EI) calculated for  $C_{18}H_{20}O_4 [M]^+$ :300.1356, found 300.1360.



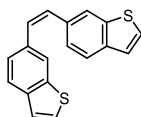
**(E)-1,2-bis(3,5-dimethoxyphenyl)ethene:** Following the general procedure A, the product was obtained as white solid 19.8 mg (total amount from two parallel reactions).  $^1H$  NMR (400 MHz,  $CDCl_3$ )  $\delta$  7.01 (s, 2H), 6.67 (d,  $J$  = 2.3 Hz, 4H), 6.40 (t,  $J$  = 2.3 Hz, 2H), 3.83 (s, 12H).  $^{13}C$  NMR (101 MHz,  $CDCl_3$ )  $\delta$  160.94 , 139.11 , 129.15 , 104.59 , 100.08 , 55.36 . **HRMS** (EI) calculated for  $C_{18}H_{20}O_4 [M]^+$ :300.1356, found 300.1355.



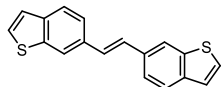
**(Z)-1,2-bis(benzo[d][1,3]dioxol-5-yl)ethene.** Following the general procedure A, the product was obtained as white solid 10.5 mg.  $^1\text{H NMR}$  (300 MHz,  $\text{CDCl}_3$ )  $\delta$  6.75 – 6.69 (m, 6H), 6.41 (s, 2H), 5.93 (s, 4H).  $^{13}\text{C NMR}$  (75 MHz, 300 MHz,  $\text{CDCl}_3$ )  $\delta$  147.36 , 146.54 , 128.84 , 122.82 , 108.87 , 108.23 , 100.89. **HRMS** (EI) calculated for  $\text{C}_{16}\text{H}_{12}\text{O}_4$   $[\text{M}]^+$ :268.0730, found 268.0733



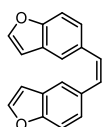
**(E)-1,2-bis(benzo[d][1,3]dioxol-5-yl)ethene:** Following the general procedure A, the product was obtained as white solid 5.5 mg.  $^1\text{H NMR}$  (300 MHz,  $\text{CDCl}_3$ )  $\delta$  7.03 (d,  $J = 1.7$  Hz, 2H), 6.90 (dd,  $J = 8.1, 1.7$  Hz, 2H), 6.85 (s, 2H), 6.79 (d,  $J = 8.0$  Hz, 2H), 5.97 (s, 4H).  $^{13}\text{C NMR}$  (75 MHz,  $\text{CDCl}_3$ )  $\delta$  148.10 , 147.08 , 131.93 , 126.68 , 121.16 , 108.40 , 105.36 , 101.08 . **HRMS** (EI) calculated for  $\text{C}_{16}\text{H}_{12}\text{O}_4$   $[\text{M}]^+$ :268.0730, found 268.0728.



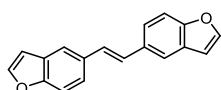
**(Z)-1,2-bis(benzo[b]thiophen-5-yl)ethene:** Following the general procedure A, the product was obtained as white solid 7.9 mg.  $^1\text{H NMR}$  (300 MHz,  $\text{CDCl}_3$ )  $\delta$  7.77 – 7.73 (m, 2H), 7.69 (dd,  $J = 8.4, 0.8$  Hz, 2H), 7.41 (d,  $J = 5.4$  Hz, 2H), 7.28 (d,  $J = 1.7$  Hz, 1H), 7.25 (d,  $J = 1.6$  Hz, 1H), 7.23 (dd,  $J = 5.5, 0.8$  Hz, 2H), 6.76 (s, 2H).  $^{13}\text{C NMR}$  (75 MHz,  $\text{CDCl}_3$ )  $\delta$  139.76 , 138.45 , 133.45 , 129.99 , 126.55 , 125.32 , 123.96 , 123.90 , 122.09 . **HRMS** (EI) calculated for  $\text{C}_{18}\text{H}_{12}\text{S}_2$   $[\text{M}]^+$ :292.0375, found 292.0373.



**(E)-1,2-bis(benzo[b]thiophen-6-yl)ethene:** Following the general procedure A, the product was obtained as white solid 7.9 mg. **Note: this compound shows poor solubility in common solvent like  $\text{CDCl}_3$ ,  $\text{DMSO-D}_6$ ,  $\text{acetone-D}_6$  and dissolves only slight amount in  $\text{TCE-D}_2$ .**  $^1\text{H NMR}$  (400 MHz,  $\text{TCE-D}_2$ )  $\delta$  7.97 (d,  $J = 1.6$  Hz, 2H), 7.91 (d,  $J = 8.4$  Hz, 2H), 7.62 (dd,  $J = 8.5, 1.7$  Hz, 2H), 7.51 (d,  $J = 5.4$  Hz, 2H), 7.39 (dd,  $J = 5.4, 0.8$  Hz, 2H), 7.31 (s, 2H).  $^{13}\text{C NMR}$  (101 MHz,  $\text{TCE-D}_2$ )  $\delta$  139.98 , 138.69 , 133.69 , 128.35 , 127.19 , 123.93 , 122.64 , 122.45 , 121.76 , 120.18. **HRMS** (EI) calculated for  $\text{C}_{18}\text{H}_{12}\text{S}_2$   $[\text{M}]^+$ :292.0375, found 292.0373.

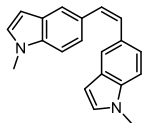


**(Z)-1,2-bis(benzo[b]thiophen-5-yl)ethene:** Following the general procedure A, the product was obtained as white solid 10.9 mg.  $^1\text{H NMR}$  (300 MHz,  $\text{CDCl}_3$ )  $\delta$  7.58 (d,  $J = 2.2$  Hz, 2H), 7.50 (dd,  $J = 1.9, 0.6$  Hz, 2H), 7.35 (d,  $J = 0.8$  Hz, 1H), 7.32 (t,  $J = 0.8$  Hz, 1H), 7.22 (d,  $J = 1.8$  Hz, 1H), 7.19 (d,  $J = 1.7$  Hz, 1H), 6.70 (s, 2H), 6.66 (dd,  $J = 2.2, 1.0$  Hz, 2H).  $^{13}\text{C NMR}$  (75 MHz,  $\text{CDCl}_3$ )  $\delta$  154.03 , 145.17 , 132.10 , 129.61 , 127.43 , 125.54 , 121.45 , 111.06 , 106.66 . **HRMS** (EI) calculated for  $\text{C}_{18}\text{H}_{12}\text{O}_2$   $[\text{M}]^+$ :260.0832, found 260.0833.

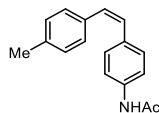


**(E)-1,2-bis(benzo[b]thiophen-5-yl)ethene:** Following the general procedure A, the product was obtained

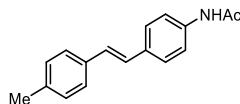
as white solid 6.6 mg.  $^1\text{H NMR}$  (400 MHz,  $\text{CDCl}_3$ )  $\delta$  7.73 (t,  $J = 1.2$  Hz, 2H), 7.63 (d,  $J = 2.2$  Hz, 2H), 7.54 – 7.46 (m, 4H), 7.20 (s, 2H), 6.80 – 6.75 (m, 2H).  $^{13}\text{C NMR}$  (101 MHz,  $\text{CDCl}_3$ )  $\delta$  154.59, 145.51, 132.69, 127.96, 127.89, 122.90, 119.01, 111.53, 106.68. **HRMS** (EI) calculated for  $\text{C}_{18}\text{H}_{12}\text{O}_2$   $[\text{M}]^+$ :260.0832, found 260.0828.



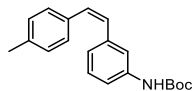
**(Z)-1,2-bis(1-methyl-1H-indol-5-yl)ethene:** Following the general procedure B, the products ( $Z/E = 5.2/1$ ) were obtained as white solid 11.4 mg.  $^1\text{H NMR}$  (400 MHz,  $\text{CDCl}_3$ )  $\delta$  7.77 – 7.73 (m, 0.45H), 7.61 (dd,  $J = 1.6, 0.8$  Hz, 2H), 7.51 (dd,  $J = 8.6, 1.7$  Hz, 0.5H), 7.31 (d,  $J = 8.5$  Hz, 0.56H), 7.22 (dd,  $J = 8.6, 1.7$  Hz, 3H), 7.13 (dt,  $J = 8.5, 0.8$  Hz, 2H), 7.04 (d,  $J = 3.1$  Hz, 0.51H), 7.00 (d,  $J = 3.1$  Hz, 2H), 6.67 (s, 2H), 6.49 (dd,  $J = 3.1, 0.8$  Hz, 0.4H), 6.39 (dd,  $J = 3.1, 0.9$  Hz, 2H), 3.81 (s, 1.2H), 3.76 (s, 6H).  $^{13}\text{C NMR}$  (101 MHz,  $\text{CDCl}_3$ )  $\delta$  136.21, 135.75, 129.20, 129.10, 128.86, 128.31, 127.28, 123.08, 121.35, 120.02, 119.07, 109.35, 108.70, 101.17, 101.15, 32.92, 32.83. **HRMS** (EI) calculated for  $\text{C}_{20}\text{H}_{18}\text{N}_2$   $[\text{M}]^+$ :286.1465, found 286.1462.



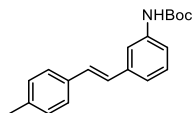
**(Z)-N-(4-(4-methylstyryl)phenyl)acetamide:** Following the general procedure C, the products were obtained as white solid 9.3 mg (total amount from two parallel reactions).  $^1\text{H NMR}$  (300 MHz,  $\text{CDCl}_3$ )  $\delta$  7.39 – 7.31 (m, 2H), 7.24 – 7.18 (m, 2H), 7.17 – 7.11 (m, 2H), 7.03 (d,  $J = 7.9$  Hz, 2H), 6.56 – 6.43 (m, 2H), 2.31 (s, 3H), 2.16 (s, 3H). H on NH was not observed.  $^{13}\text{C NMR}$  (75 MHz,  $\text{CDCl}_3$ )  $\delta$  168.16, 136.83, 136.62, 134.25, 133.42, 129.81, 129.51, 128.92, 128.82, 128.68, 119.34, 24.63, 21.22. **HRMS** (EI) calculated for  $\text{C}_{17}\text{H}_{17}\text{NO}$   $[\text{M}]^+$ :251.1305, found 251.1310.



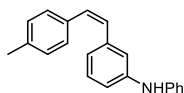
**(E)-N-(4-(4-methylstyryl)phenyl)acetamide:** Following the general procedure C, the products were obtained as white solid 10.1 mg (total amount from two parallel reactions).  $^1\text{H NMR}$  (300 MHz,  $\text{DMSO}-d_6$ )  $\delta$  10.00 (s, 1H), 7.61 – 7.48 (m, 4H), 7.46 (d,  $J = 7.9$  Hz, 2H), 7.17 (d,  $J = 7.8$  Hz, 2H), 7.11 (s, 2H), 2.30 (s, 3H), 2.05 (s, 3H).  $^{13}\text{C NMR}$  (75 MHz,  $\text{DMSO}-d_6$ )  $\delta$  168.26, 138.72, 136.72, 134.47, 131.97, 129.32, 127.05, 126.82, 126.78, 126.22, 119.04, 24.07, 20.87. **HRMS** (EI) calculated for  $\text{C}_{17}\text{H}_{17}\text{NO}$   $[\text{M}]^+$ :251.1305, found 251.1309.



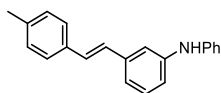
**Tert-butyl (Z)-N-(3-(4-methylstyryl)phenyl)carbamate:** Following the general procedure D, the products were obtained as clear oil 14 mg (total amount from two parallel reactions).  $^1\text{H NMR}$  (300 MHz,  $\text{CDCl}_3$ )  $\delta$  7.17 – 7.10 (m, 4H), 7.02 (d,  $J = 8.0$  Hz, 2H), 6.93 (dt,  $J = 7.6, 1.4$  Hz, 1H), 6.58 – 6.46 (m, 2H), 6.36 (s, 1H), 2.31 (s, 3H), 1.50 (s, 8H).  $^{13}\text{C NMR}$  (75 MHz,  $\text{CDCl}_3$ )  $\delta$  152.66, 138.30, 138.28, 136.90, 134.94, 134.03, 130.45, 129.15, 128.87, 128.83, 128.81, 123.55, 118.71, 117.14, 80.50, 28.31, 21.23. **HRMS** (ESI) calculated for  $\text{C}_{20}\text{H}_{23}\text{NNaO}_2$   $[\text{M}+\text{Na}]^+$ :332.1621, found 332.1621.



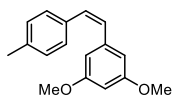
**Tert-butyl (E)-(3-(4-methylstyryl)phenyl)carbamate:** Following the general procedure D, the product was obtained as white solid 18.2 mg (total amount from two parallel reactions).  $^1\text{H NMR}$  (300 MHz,  $\text{CDCl}_3$ )  $\delta$  7.60 (d,  $J = 1.8$  Hz, 1H), 7.43 – 7.38 (m, 2H), 7.30 – 7.23 (m, 2H), 7.20 – 7.14 (m, 4H), 7.13 – 6.98 (m, 2H), 6.49 (s, 1H), 2.36 (s, 3H), 1.54 (s, 9H).  $^{13}\text{C NMR}$  (75 MHz,  $\text{CDCl}_3$ )  $\delta$  152.70 , 138.66 , 138.42 , 137.56 , 134.41 , 129.37 , 129.16 , 128.98 , 127.42 , 126.44 , 121.21 , 117.47 , 116.19 , 28.35 , 21.26 . **HRMS** (ESI) calculated for  $\text{C}_{20}\text{H}_{23}\text{NNaO}_2$   $[\text{M}+\text{Na}]^+$ :332.1621, found 332.1625.



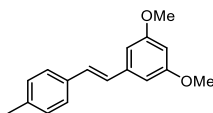
**(Z)-3-(4-methylstyryl)-N-phenylaniline:** Following the general procedure D, the product was obtained as white solid 20.6 mg (total amount from two parallel reactions).  $^1\text{H NMR}$  (400 MHz,  $\text{CDCl}_3$ )  $\delta$  7.20 – 7.13 (m, 5H), 7.07 (d,  $J = 7.9$  Hz, 2H), 7.00 (t,  $J = 1.9$  Hz, 1H), 6.93 – 6.81 (m, 5H), 6.59 – 6.49 (m, 2H), 5.59 (s, 1H), 2.34 (s, 3H).  $^{13}\text{C NMR}$  (101 MHz,  $\text{CDCl}_3$ )  $\delta$  142.77 , 142.76 , 138.64 , 134.25 , 136.71 , 134.25 , 130.39 , 129.64 , 129.21 , 129.19 , 128.94 , 128.89 , 121.58 , 120.78 , 117.62 , 117.57 , 116.49 , 21.27 . **HRMS** (ESI) calculated for  $\text{C}_{21}\text{H}_{20}\text{N}$   $[\text{M}+\text{H}]^+$ :286.1590, found 286.1594.



**(E)-3-(4-methylstyryl)-N-phenylaniline:** Following the general procedure D, the product was obtained as white solid 14.7 mg (total amount from two parallel reactions).  $^1\text{H NMR}$  (400 MHz,  $\text{CDCl}_3$ )  $\delta$  7.42 – 7.38 (m, 2H), 7.32 – 7.25 (m, 3H), 7.22 (t,  $J = 2.0$  Hz, 1H), 7.17 (d,  $J = 7.9$  Hz, 2H), 7.10 (m, 3H), 7.03 (d,  $J = 6.3$  Hz, 2H), 6.99 – 6.93 (m, 2H), 5.76 (s, 1H), 2.36 (s, 3H).  $^{13}\text{C NMR}$  (101 MHz,  $\text{CDCl}_3$ )  $\delta$  143.37 , 143.00 , 138.71 , 137.55 , 134.44 , 129.57 , 129.38 , 128.76 , 127.58 , 126.42 , 121.11 , 119.34 , 117.97 , 117.02 , 115.59 , 21.26 . **HRMS** (ESI) calculated for  $\text{C}_{21}\text{H}_{20}\text{N}$   $[\text{M}+\text{H}]^+$ :286.1590, found 286.1592.

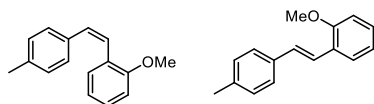


**(Z)-1,3-dimethoxy-5-(4-methylstyryl)benzene:** Following the general procedure C, the product was obtained as white solid 10.2 mg (total amount from two parallel reactions).  $^1\text{H NMR}$  (400 MHz,  $\text{CDCl}_3$ )  $\delta$  7.17 (d,  $J = 7.9$  Hz, 2H), 7.04 (d,  $J = 7.9$  Hz, 2H), 6.59 – 6.45 (m, 2H), 6.42 (d,  $J = 2.3$  Hz, 2H), 6.31 (t,  $J = 2.3$  Hz, 1H), 3.66 (s, 6H), 2.30 (s, 3H).  $^{13}\text{C NMR}$  (101 MHz,  $\text{CDCl}_3$ )  $\delta$  160.48 , 139.33 , 136.91 , 134.17 , 130.62 , 129.47 , 128.85 , 128.81 , 106.67 , 99.71 , 55.19 , 21.21 . **HRMS** (EI) calculated for  $\text{C}_{17}\text{H}_{18}\text{O}_2$   $[\text{M}]^+$ :254.1301, found 254.1303.

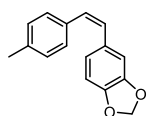


**(E)-1,3-dimethoxy-5-(4-methylstyryl)benzene:** Following the general procedure C, the product was obtained as white solid 19.3 mg (total amount from two parallel reactions).  $^1\text{H NMR}$  (400 MHz,  $\text{CDCl}_3$ )  $\delta$  7.43 – 7.38 (m, 2H), 7.17 (d,  $J = 7.9$  Hz, 2H), 7.03 (q,  $J = 16.3$  Hz, 2H), 6.67 (d,  $J = 2.2$  Hz, 2H), 6.39 (t,  $J = 2.2$  Hz, 1H), 3.83 (s, 6H), 2.36 (s, 3H).  $^{13}\text{C NMR}$  (100 MHz,  $\text{CDCl}_3$ )  $\delta$  160.95 , 139.54 , 137.65 , 134.33 , 129.39 , 129.13 , 127.65 , 126.48 , 104.45 , 99.81 , 55.36 , 21.25 . **HRMS** (EI) calculated for  $\text{C}_{17}\text{H}_{18}\text{O}_2$   $[\text{M}]^+$ :254.1301, found 254.1306.

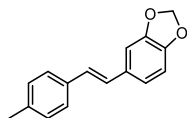




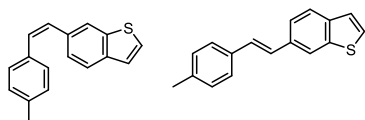
**(Z)-1-methoxy-2-(4-methylstyryl)benzene and (E)-1-methoxy-2-(4-methylstyryl)benzene:** Following the general procedure C, the products (mixture of Z and E configuration of products, Z/E = 1.9/1) were obtained as clear oil 11.2 mg (total amount from two parallel reactions).  $^1\text{H NMR}$  (300 MHz,  $\text{CDCl}_3$ )  $\delta$  7.60 (dd,  $J = 7.7, 1.8$  Hz, 0.4 H), 7.48 – 7.39 (m, 1.5H), 7.25 – 7.16 (m, 3H), 7.14 (d,  $J = 8.3$  Hz, 3H), 7.00 (dq,  $J = 6.9, 1.3, 0.8$  Hz, 2H), 6.90 (dt,  $J = 8.9, 1.2$  Hz, 1.5H), 6.77 (td,  $J = 7.5, 1.1$  Hz, 1H), 6.67 – 6.56 (m, 2H), 3.89 (s, 1.2H), 3.84 (s, 3H), 2.36 (s, 1.55H), 2.30 (s, 3H).  $^{13}\text{C NMR}$  (75 MHz,  $\text{CDCl}_3$ )  $\delta$  157.13, 156.78, 137.17, 136.63, 134.29, 130.14, 130.04, 129.27, 129.01, 128.74, 128.71, 128.44, 128.40, 126.45, 126.39, 126.25, 124.96, 122.39, 120.70, 120.17, 110.88, 110.60, 55.50, 55.46, 21.25, 21.21. **HRMS** (EI) calculated for  $\text{C}_{16}\text{H}_{16}\text{O}$   $[\text{M}]^+$ :224.1196, found 224.1189.



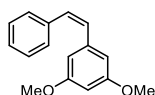
**(Z)-5-(4-methylstyryl)benzo[d][1,3]dioxole:** Following the general procedure C, the product was obtained as white solid 7.1 mg (total amount from two parallel reactions).  $^1\text{H NMR}$  (300 MHz,  $\text{CDCl}_3$ )  $\delta$  7.20 – 7.12 (m, 2H), 7.08 – 7.02 (m, 2H), 6.78 – 6.66 (m, 3H), 6.52 – 6.40 (m, 2H), 5.92 (s, 2H), 2.32 (s, 3H).  $^{13}\text{C NMR}$  (75 MHz,  $\text{CDCl}_3$ )  $\delta$  147.28, 146.48, 136.77, 134.25, 131.38, 129.20, 129.08, 128.95, 128.68, 122.87, 108.88, 108.15, 100.86, 21.24. **HRMS** (EI) calculated for  $\text{C}_{16}\text{H}_{14}\text{O}_2$   $[\text{M}]^+$ :238.0988, found 238.0982.



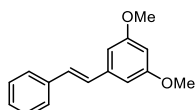
**(E)-5-(4-methylstyryl)benzo[d][1,3]dioxole:** Following the general procedure C, the product was obtained as white solid 14.3 mg (total amount from two parallel reactions).  $^1\text{H NMR}$  (300 MHz,  $\text{CDCl}_3$ )  $\delta$  7.41 – 7.34 (m, 2H), 7.16 (d,  $J = 7.9$  Hz, 2H), 7.06 (d,  $J = 1.7$  Hz, 1H), 6.97 – 6.87 (m, 3H), 6.80 (d,  $J = 8.0$  Hz, 1H), 5.98 (s, 2H), 2.36 (s, 3H).  $^{13}\text{C NMR}$  (75 MHz,  $\text{CDCl}_3$ )  $\delta$  148.09, 147.10, 137.22, 134.57, 132.05, 129.35, 127.33, 126.93, 126.19, 121.25, 108.38, 105.44, 101.07, 21.23. **HRMS** (EI) calculated for  $\text{C}_{16}\text{H}_{14}\text{O}_2$   $[\text{M}]^+$ :238.0988, found 238.0988.



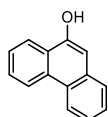
**(Z)-6-(4-methylstyryl)benzo[b]thiophene and (E)-6-(4-methylstyryl)benzo[b]thiophene:** Following the general procedure C, the product (mixture of mixture of Z and E configuration of products, Z/E = 1/3) was obtained as white solid 19 mg (total amount from two parallel reactions).  $^1\text{H NMR}$  (400 MHz,  $\text{CDCl}_3$ )  $\delta$  7.75 – 7.73 (m, 1H), 7.71 (d,  $J = 8.4$  Hz, 1H), 7.41 (d,  $J = 5.4$  Hz, 1.5H), 7.28 (d,  $J = 1.6$  Hz, 0.5H), 7.24 (dd,  $J = 5.5, 0.8$  Hz, 1H), 7.20 – 7.15 (m, 3H), 7.03 (dd,  $J = 7.3, 5.0$  Hz, 2.6H), 6.70 – 6.57 (m, 2H), 6.52 (s, 0.2H), 2.37 (s, 0.8H), 2.32 (s, 3H).  $^{13}\text{C NMR}$  (101 MHz,  $\text{CDCl}_3$ )  $\delta$  139.74, 138.31, 137.24, 136.88, 136.70, 134.22, 133.69, 130.02, 129.48, 129.45, 129.40, 129.34, 128.90, 128.85, 128.80, 128.71, 127.59, 126.47, 126.34, 126.27, 125.32, 123.95, 123.78, 122.04, 21.23. **HRMS** (EI) calculated for  $\text{C}_{17}\text{H}_{14}\text{S}$   $[\text{M}]^+$ :250.0811, found 250.0808.



**(Z)-1,3-dimethoxy-5-styrylbenzene:** Following the general procedure C, the product was obtained as clear oil 10.7 mg (total amount from two parallel reactions). **<sup>1</sup>H NMR** (300 MHz, CDCl<sub>3</sub>) δ 7.26 – 7.22 (m, 2H), 7.22 – 7.11 (m, 3H), 6.61 – 6.46 (m, 2H), 6.36 (d, *J* = 2.3 Hz, 2H), 6.27 (t, *J* = 2.3 Hz, 1H), 3.59 (s, 6H). **<sup>13</sup>C NMR** (75 MHz, CDCl<sub>3</sub>) δ 160.47, 139.02, 137.23, 130.66, 130.19, 128.92, 128.15, 127.15, 106.70, 99.89, 55.17. **HRMS** (EI) calculated for C<sub>16</sub>H<sub>16</sub>O<sub>2</sub> [M]<sup>+</sup>:240.1145, found 240.1144.



**(E)-1,3-dimethoxy-5-styrylbenzene:** Following the general procedure C, the product was obtained as white solid 37.3 mg (total amount from two parallel reactions). **<sup>1</sup>H NMR** (300 MHz, CDCl<sub>3</sub>) δ 7.56 – 7.47 (m, 2H), 7.41 – 7.31 (m, 2H), 7.31 – 7.24 (m, 1H), 7.15 – 6.99 (m, 2H), 6.69 (d, *J* = 2.3 Hz, 2H), 6.42 (t, *J* = 2.3 Hz, 1H), 3.84 (s, 6H). **<sup>13</sup>C NMR** (75 MHz, CDCl<sub>3</sub>) δ 160.94, 139.31, 137.08, 129.17, 128.65, 128.63, 127.70, 126.54, 104.54, 99.95, 55.35. **HRMS** (EI) calculated for C<sub>16</sub>H<sub>16</sub>O<sub>2</sub> [M]<sup>+</sup>:240.1145, found 240.1140.

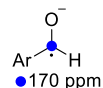


**Phenanthren-9-ol**<sup>[41]</sup>: Following the general procedure A, the product was obtained as white solid. **<sup>1</sup>H NMR** (300 MHz, CDCl<sub>3</sub>) δ 8.71 – 8.65 (m, 1H), 8.64 – 8.57 (m, 1H), 8.36 – 8.27 (m, 1H), 7.75 – 7.62 (m, 3H), 7.58 – 7.47 (m, 2H), 7.01 (s, 1H), 5.46 (s, 1H). **<sup>13</sup>C NMR** (75 MHz, CDCl<sub>3</sub>) δ 149.47, 132.62, 131.51, 127.20, 126.92, 126.70, 126.68, 126.40, 125.50, 124.25, 122.68, 122.56, 122.32, 106.06.

## 2.6 Computational details

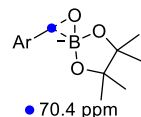
All structures were calculated at (U)M06-2X/def2-SVP level of theory in continuum of DMF using SMD.<sup>[42]</sup> Subsequently all minima were confirmed by the frequency analysis at the same level as the geometry optimization. NMR calculation were performed at (U)M06-2X/IGLO-III level of theory. Software used for the calculations was Gaussian09 D.01.<sup>[43]</sup>

### Intermediate C



```
1\1\GINC-LOGIN\SP\UM062X\Gen\C7H6O1(1-,2)\JHIOE\16-Aug-2018\0\#p m062 x/gen int=ultrafine
nmr geom=check guess=read\title\|-1,2\C,0,-4.1792437331,0.5576305262,-0.0000088375\C,0,-
2.7986641095,0.5528389664,0.0005837628\C,0,-2.0428430643,1.7711929493,0.0002024268\C,0,-
2.8014042074,.9920048314,-0.0008485131\C,0,-4.1811901914,2.9772926615,-0.001444854\C,0,-
4.9099641818,1.7671752092,-0.001033192\H,0,-4.7173522911,-0.3964207066,0.0003281258\H,0,-
2.2546220491,-0.3981825076,0.0013866246\H,0,-2.2369469939,3.9267638514,-0.0011473426\H,0,-
4.7248909401,3.9286338431-0.0022408523\H,0,-6.0015764488,1.7656757921,-0.0014977491\C,0,-
0.6173375442,1.7941980402,0.0008133736\O,0,0.1121905789,2.8090339425,-0.0000359792\H,0,-
0.1486804239,0.7704197211,0.0017419062\Version=ES64L-G09RevD.01\State=2-A\HF=-
345.5776769\S2=0.769017\S2-1=0.\S2A=0.750186\RMSD=4.659e-09\Dipole=-1.6246434,-
0.7094793,0.0000402\Quadrupole=-10.6825062,5.8154287,4.8670776,-5.5916524,-0.0007838,-
0.001827\PG=C01 [X(C7H6O1)]\@
```

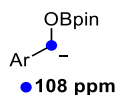
### Intermediate F



```
1\1\GINC-WORKER1\SP\RM062X\Gen\C13H18B1O3(1-)\JHIOE\16-Aug-2018\0\#p
m062x/gen int=ultrafinemrgeom=checkguess=read\title\|-1,1\B,0,0.8025139948,0.3887627412,-
0.6612617005\O,0,1.4369555543,-0.9124944769,-0.6439264473\O,0,1.8464338421,1.3706643402,-
0.4836905038\C,0,2.955522464,0.6992284989,0.0767190418\C,0,2.8363346008,-0.7272956109,-
0.56325231 14\C,0,2.7842585379,0.6478604804,1.5983221868\H,0,3.6541746597,0.20294
72637,2.1036476959\H,0,2.6530150152,1.674145734,1.9729577572\H,0,1.8872623611,0.069047274,1.86
55507328\C,0,4.2364555852,1.4438596282,-
0.2704388125\H,0,4.2506490945,2.4174622362,0.243075019\H,0,5.1255404934,0.8784007031,0.0492664
955\H,0,4.3061988252,1.6311303561,-1.350260776\C,0,3 .4583568145,-
1.8411824578,0.2685594718\H,0,3.3713016351,-2.7994617285,-0.2660776274\H,0,4.5271806244,-
1.6519388593,0.4541644896\H,0,2.9451343177,-1.9463360599,1.2335378252\C,0,3.4157754782,-
0.758926363,-1.980085642\H,0,4.5149956456,-0.7059595872,-1.985945976\H,0,3.1129122288,-
1.6993962599,-2.4642945908\H,0,3.0195302311,0.075786834,-2.5772801646\C,0,-1.6218180412,-
0.5039479644,0.2184518453\C,0,-1.7491111351,-1.6345667673,-0.613075291\C,0,-2.3556076112,-
0.4995514219,1.4233363823\C,0,-2.5662156216,-2.7052010233,-0.2544202819\H,0,-1.1870334504,-
1.6458423519,-1.5478417842\C,0,-3.1670469421,-1.5732906884,1.7822834094\H,0,-2.285
2745099,0.3694828246,2.084025033\C,0,-3.2810031569,-2.6885805915,0.9465350756\H,0,-
```

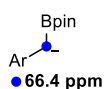
2.6475756883,-3.5674878875,-0.9211974685\H,0,-3.7230820022,-1.5381073181,2.7224066762\H,0,-  
 3.9191000617,-3.5288589707,1.2260024192\C,0,-0.7267563833,0.604629704,-0.1280111646\O,0,-  
 0.2976254265,0.6709910608,-1.506822266\H,0,-  
 1.0416444532,1.5780340291,0.2821281036\\Version=ES64L-G09RevD.01\State=1-A\HF=-  
 756.9035343\RMSD=6.172e-09\Dipole=1.470795,-0.6760783,0.8835049\Quadrupole=-  
 7.3982423,1.9382182,5.4600241,-3.8719754,0.0993767,4.8661149\PG=C01 [X(C13H18B1O3)]\@

### Intermediate G



1\1\GINC-LOGIN\SP\RM062X\Gen\C13H18B1O3(1-)\JHIOE\16-Aug-2018\0\#p m0 62x/gen  
 int=ultrafine nmr geom=check guess=read\\title\|-1,1\C,0,-5.1665668202,-  
 1.0011423153,0.1598778365\C,0,-3.8174672924,-1.2920876112,0.1708424172\C,0,-2.8022887926,-  
 0.2602980211,0.0164482383\C,0,-3.3354705463,1.0832318183,-0.1505002077\C,0,-  
 4.6971261383,1.3317587236,-0.1554132639\C,0,-5.6562049865,0.3133158072,-0.0012808228\H,0,-  
 5.8765434468,-1.8263084626,0.2817986484\H,0,-3.4911108448,-2.3289648915,0.2990328095\H,0,-  
 2.6312727676,1.9080811823,-0.2744942146\H,0,-5.0336173914,2.3665256115,-0.2847457153\H,0,-  
 6.7252460086,0.527992261,-0.0070463642\C,0,-1.4606079293,-0.5462233741,0.0306606191\O,0,-  
 0.5299863077,0.4939237104 , -0.119114358\B,0,0.7942653033,0.2768309382,-  
 0.0746683198\O,0,1.3878303824,-0.9466875224,0.1539690697\O,0,1.7143561716,1.2877074282,-  
 0.2556547351\C,0,2.9955161994,0.752128753,0.1184393335\C,0,2.7921147749,-0.7852226136,-  
 0.1159091878\C,0,3.2191553961,1.0884642086,1.5899468238\H,0,4.2135659697,0.7689206113,1.931661  
 8664\H,0,3.1392014818,2.1769718286,1.7214069537\H,0,2.4589412011,0.6078720168,2.2238197025\C,0  
 ,4.076952882 ,1.3837867815,-0.7391597606\H,0,4.1613695063,2.4535368634,-  
 0.4987311093\H,0,5.0507036774,0.9113295756,-0.5421816684\H,0,3.8479132967,1.2901447161,-  
 1.8083472535\C,0,3.5908169899,-1.6787072959,0.815388368\H,0,3.3934824844,-  
 2.7332871052,0.5737680337\H,0,4.6687784038,-1.4952845839,0.6947927932\H,0,3.3181534567,-  
 1.5109789526,1.8650930491\C,0,3.026322090 7,-1.1859784789,-1.5692470069\H,0,4.093272135,-  
 1.1522483273,-1.8303665927\H,0,2.6636740439,-2.2130172687,-1.7180339214\H,0,2.4755116641,-  
 0.5238811941,-2.2539639664\H,0,-1.0421232386,-1.545733817,0.1561039054\\Version=ES64L-  
 G09RevD.01\State=1-A\HF=-756.8875119\RMSD=9.027e-09\Dipole=6.1732203,-  
 0.3029483,0.0614667\Quadrupole=-29.5106229,14.5748531,14. 9357698,-  
 0.189417,0.2296481,0.5941862\PG=C01 [X(C13H18B1O3)]\@

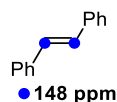
### Intermediate I



1\1\GINC-LOGIN\SP\RM062X\Gen\C13H18B1O2(1-)\JHIOE\16-Aug-  
 2018\0\#pm062x/genint=ultrafinenmrgeom=checkguess=read\\title\|-1,1\C,0,3.7882225827,-  
 2.6124857025,-0.1400350777\C,0,2.999497242,-1.4793838659,0.0234632562\C,0,1.570391986,-  
 1.5196209061,-0.0234026358\C,0,1.0180448517,-2.8210364965,-0.2541773951\C,0,1.8160900788,-  
 3.9465404182,-0.4153900104\C,0,3.2150856365,-3.8703024027,-0.363082723\H,0,4.8766705567,-

2.5131063076,-0.0926217174\H,0,3.4848798376,-0.5136577633,0.1959686309\H,0,-0.0683559656,-  
 2.9149571292,-0.3017297187\H,0,1.3351388753,-4.91411160 , -0.5882029485\H,0,3.8345249467,-  
 4.7593011113,-0.4916864019\C,0,0.7772687117,-0.3422448645,0.1451190665\B,0,-0.7125143694,-  
 0.2142195782,0.0923865907\O,0,-1.406441886,0.9895928571,0.3150502314\O,0,-1.643086951 , -  
 1.2352683663,-0.1811717144\C,0,-2.9494819271,-0.7396279328,0.1116668537\C,0,-  
 2.7634460601,0.8011865593,-0.0797536033\C,0,-3.2756949026,-1 .10578416,1.5591736622\H,0,-  
 4.3008511336,-0.8189135403,1.8345637945\H,0,-3.1759191181,-2.1942277671,1.6806490665\H,0,-  
 2.5753748387,-0.6168178686,2.2528795914\C,0,-3.9579519705,-1.3788370343,-0.8288778218\H,0,-  
 4 .0385240237,-2.454285392,-0.6116852112\H,0,-4.95405682,-0.9292768788,-0.6987913876\H,0,-  
 3.6529160343,-1.2649696678,-1.8771201972\C,0,-3.6708086167,1.6612552876,0.7852696246\H,0,-  
 3.4863088695,2.7247256148,0.5721211391\H,0,-4.7301509691,1.4501638539,0.574139539\H,0,-  
 3.4820979211,1.4914315504,1.8532609939\C,0,-2.8894728214,1.2176522517,-1.5451845948\H ,0,-  
 3.9282683456,1.1611037625,-1.9010143998\H,0,-2.5435232102,2.2564108155,-1.6496668402\H,0,-  
 2.2621940382,0.5817314152,-  
 2.1878853654\H,0,1.3542061273,0.5762126578,0.3190755932\\Version=ES64L-G09RevD.01\State=1-  
 A\HF=-681.6507621\RMSD=3.077e-09\Dipole=-3.2774466,0.6913671,-0.0583084\Quadrupole=-  
 8.8271727,0.8248718,8.002301,10.3571073,0.8081531,-1.15 02448\PG=C01 [X(C13H18B1O2)]\@

**E-Stilbene**



1\1\GINC-LOGIN\SP\RM062X\Gen\C14H12\JHIOE\21-Aug-  
 2018\0\#pm062x/genint=ultrafinenmrgeom=checkguess=read\\title\0,1\C,0,-3.077834829,0.0286242605,-  
 0.4723232408\C,0,-1.686276038,0.0909490003,-0.5294393081\C,0,-0.9928148458,1.2335137843,-  
 0.0971053299\C,0,-1.7405127227,2.318046496,0.3969691768\C,0,-  
 3.129368542,2.2554359611,0.4537760719\C,0,-3.8057164835,1.1114290873,0.0199007814\H,0,-  
 3.5950194352,-0.8698783335,-0 .8139401929\H,0,-1.1187713797,-0.7590001724,-0.9155805779\H,0,-  
 1.234586236,3.2216488175,0.741299131\H,0,-3.6915661658,3.1074897768,0.8403981966\H,0,-  
 4.8952027702,1.0673728907,0.0665318217\C,0,0.4763461488,1.2387116712,-  
 0.1825598736\C,0,1.2889267672,2.244400186,0.186811481\C,0,2.7580988929,2.2495231727,0.10127305  
 1\C,0,3.5056391781,1.1652403732,-  
 0.3936059429\C,0,3.4517020459,3.3917566583,0.5342282197\C,0,4.8944908051,1.2277570289,-  
 0.4505290928\H,0,2.9995526394,0.2619413802,-  
 0.7384978035\C,0,4.84326943,3.4539718905,0.4770249424\H,0,2.8843336402,4.2415255467,0.92096217  
 76\C,0,5.5709926927,2.371411863,-0.0159603339\H,0,5.4565733291,0.3759184528,-  
 0.8377946439\H,0,5.3605869157,4.3521933366,0.8191806338\H,0,6.6604776628,2.4154064869,-  
 0.0626807249\H,0,0.9095757241,0.3200368998,-  
 0.5898063083\H,0,0.8557191858,3.1630297711,0.5941834483\\Version=ES64L-G09RevD.01\State=1-  
 A\HF=-540.6806169\RMSD=6.333e-09\Dipole=-.0000301,0.0000036,-  
 0.0000083\Quadrupole=4.7427015,2.6050902,-7.3477917,0.3341779,-0.707642,4.9858681\PG=C01  
 [X(C14H12)]\@

## 2.7 References

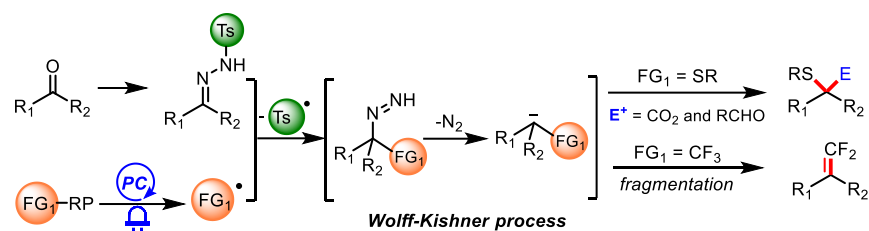
- [1] a) T. Takeda, *Modern carbonyl olefination: Methods and applications*, John Wiley & Sons, **2006**; b) B. E. Maryanoff, A. B. Reitz, *Chem. Rev.* **1989**, *89*, 863-927.
- [2] D. J. Peterson, *J. Org. Chem.* **1968**, *33*, 780-784.
- [3] J. B. Baudin, G. Hareau, S. A. Julia, O. Ruel, *Tetrahedron Lett.* **1991**, *32*, 1175-1178.
- [4] F. Tebbe, G. Parshall, G. d. Reddy, *J. Am. Chem. Soc.* **1978**, *100*, 3611-3613.
- [5] a) A. H. Hoveyda, A. R. Zhugralin, *Nature* **2007**, *450*, 243-251; b) O. Eivgi, N. G. Lemcoff, *Synthesis* **2018**, *50*, 49-63; c) Y. Vidavsky, N. G. Lemcoff, *Beilstein J. Org. Chem.* **2010**, *6*, 1106-1119.
- [6] a) J. R. Ludwig, C. S. Schindler, *Synlett* **2017**, *28*, 1501; b) L. Ravindar, R. Lekkala, K. Rakesh, A. M. Asiri, H. M. Marwani, H.-L. Qin, *Org. Chem. Front.* **2018**, *5*, 1381-1391; c) M. R. Becker, R. B. Watson, C. S. Schindler, *Chem. Soc. Rev.* **2018**, *47*, 7867-7881.
- [7] J. E. McMurry, *Chem. Rev.* **1989**, *89*, 1513-1524.
- [8] A. Fürstner, B. Bogdanović, *Angew. Chem. Int. Ed.* **1996**, *35*, 2442-2469.
- [9] A. Fürstner, A. Hupperts, *J. Am. Chem. Soc.* **1995**, *117*, 4468-4475.
- [10] M. Moxter, J. Tillmann, M. Füser, M. Bolte, H.-W. Lerner, M. Wagner, *Chem. Eur. J.* **2016**, *22*, 16028-16031.
- [11] K. Esfandiari, J. Mai, S. Ott, *J. Am. Chem. Soc.* **2017**, *139*, 2940-2943.
- [12] W. Wei, X.-J. Dai, H. Wang, C. Li, X. Yang, C.-J. Li, *Chem. Sci.* **2017**, *8*, 8193-8197.
- [13] a) J. M. R. Narayanam, C. R. J. Stephenson, *Chem. Soc. Rev.* **2011**, *40*, 102-113; b) J. Xuan, W.-J. Xiao, *Angew. Chem. Int. Ed.* **2012**, *51*, 6828-6838; c) C. K. Prier, D. A. Rankic, D. W. C. MacMillan, *Chem. Rev.* **2013**, *113*, 5322-5363; d) N. A. Romero, D. A. Nicewicz, *Chem. Rev.* **2016**, *116*, 10075-10166; e) M. H. Shaw, J. Twilton, D. W. C. MacMillan, *J. Org. Chem.* **2016**, *81*, 6898-6926; f) D. Ravelli, S. Protti, M. Fagnoni, *Chem. Rev.* **2016**, *116*, 9850-9913; g) K. L. Skubi, T. R. Blum, T. P. Yoon, *Chem. Rev.* **2016**, *116*, 10035-10074; h) L. Marzo, S. K. Pagire, O. Reiser, B. König, *Angew. Chem. Int. Ed.* **2018**, *57*, 10034-10072.
- [14] a) H. G. Yayla, R. R. Knowles, *Synlett* **2014**, *25*, 2819-2826; b) E. C. Gentry, R. R. Knowles, *Acc. Chem. Res.* **2016**, *49*, 1546-1556; c) N. Hoffmann, *Eur. J. Org. Chem.* **2017**, *2017*, 1982-1992; d) K. N. Lee, M.-Y. Ngai, *Chem. Commun.* **2017**, *53*, 13093-13112; e) Q. Wang, Q. Xia, J. Dong, H. Song, *Chem. Eur. J.* **2019**, *25*, 2949-2961.
- [15] M. Nakajima, E. Fava, S. Loescher, Z. Jiang, M. Rueping, *Angew. Chem. Int. Ed.* **2015**, *54*, 8828-8832.
- [16] a) L. Deloux, M. Srebnik, *Chem. Rev.* **1993**, *93*, 763-784; b) A. Maity, T. S. Teets, *Chem. Rev.* **2016**, *116*, 8873-8911; c) E. Dimitrijević, M. S. Taylor, *ACS Catal.* **2013**, *3*, 945-962; d) K. Ishihara, H. Yamamoto, *Eur. J. Org. Chem.* **1999**, *1999*, 527-538.
- [17] a) D. S. Laitar, P. Müller, J. P. Sadighi, *J. Am. Chem. Soc.* **2005**, *127*, 17196-17197; b) S. Bae, M. K. Lakshman, *J. Org. Chem.* **2008**, *73*, 1311-1319; c) V. Gurram, H. K. Akula, R. Garlapati, N. Pottabathini, M. K. Lakshman, *Adv. Synth. Catal.* **2015**, *357*, 451-462; d) J. Kim, C. R. Bertozzi, *Angew. Chem. Int. Ed.* **2015**, *54*, 15777-15781; e) H. Lu, Z. Geng, J. Li, D. Zou, Y. Wu, Y. Wu, *Org. Lett.* **2016**, *18*, 2774-2776; f) K. Yang, F. Zhou, Z. Kuang, G. Gao, T. G. Driver, Q. Song, *Org. Lett.* **2016**, *18*, 4088-4091; g) M. Rauser, C. Ascheberg, M. Niggemann, *Angew. Chem. Int. Ed.* **2017**, *56*, 11570-11574; h) W. Fu, Q. Song, *Org. Lett.* **2018**, *20*, 393-396.
- [18] a) D. A. Nicewicz, D. S. Hamilton, *Synlett* **2014**, *25*, 1191-1196; b) N. A. Romero, D. A. Nicewicz, *J. Am. Chem. Soc.* **2014**, *136*, 17024-17035; c) M. Weiser, S. Hermann, A. Penner, H.-A. Wagenknecht, *Beilstein J. Org. Chem.* **2015**, *11*, 568-575.

- [19] a) Y.-P. Zhao, L.-Y. Yang, R. S. H. Liu, *Green Chem.* **2009**, *11*, 837-842; b) W. Cai, H. Fan, D. Ding, Y. Zhang, W. Wang, *Chem. Commun.* **2017**, *53*, 12918-12921; c) X.-J. Wei, W. Boon, V. Hessel, T. Noël, *ACS Catal.* **2017**, *7*, 7136-7140; d) K. Singh, S. J. Staig, J. D. Weaver, *J. Am. Chem. Soc.* **2014**, *136*, 5275-5278.
- [20] However, in all cases, the homo-coupled products of two aldehydes were observed (the yields were given in Table 2).
- [21] a) C. Feldmeier, H. Bartling, E. Riedle, R. M. Gschwind, *J. Magn. Reson.* **2013**, *232*, 39-44; b) C. Feldmeier, H. Bartling, K. Magerl, R. M. Gschwind, *Angew. Chem. Int. Ed.* **2015**, *54*, 1347-1351; c) H. Bartling, A. Eisenhofer, B. König, R. M. Gschwind, *J. Am. Chem. Soc.* **2016**, *138*, 11860-11871.
- [22] a) D. S. Matteson, *Aust. J. Chem.* **2011**, *64*, 1425-1429; b) D. S. Matteson, *J. Org. Chem.* **2013**, *78*, 10009-10023; c) H. Kisu, H. Sakaino, F. Ito, M. Yamashita, K. Nozaki, *J. Am. Chem. Soc.* **2016**, *138*, 3548-3552.
- [23] a) I. Marek, J.-F. Normant, *Chem. Rev.* **1996**, *96*, 3241-3268; b) T. Klis, S. Lulinski, J. Serwatowski, *Curr. Org. Chem.* **2010**, *14*, 2549-2566; c) R. Nallagonda, K. Padala, A. Masarwa, *Org. Biomol. Chem.* **2018**, *16*, 1050-1064; d) C. Wu, J. Wang, *Tetrahedron Lett.* **2018**, *59*, 2128-2140; e) K. Hong, X. Liu, J. P. Morken, *J. Am. Chem. Soc.* **2014**, *136*, 10581-10584; f) A. Noble, R. S. Mega, D. Pflästerer, E. L. Myers, V. K. Aggarwal, *Angew. Chem. Int. Ed.* **2018**, *57*, 2155-2159; g) N. Miralles, R. J. Maza, E. Fernández, *Adv. Synth. Catal.* **2018**, *360*, 1306-1327.
- [24] N. Lokesh, A. Seegerer, J. Hioe, R. M. Gschwind, *J. Am. Chem. Soc.* **2018**, *140*, 1855-1862.
- [25] a) A. Fawcett, J. Pradeilles, Y. Wang, T. Mutsuga, E. L. Myers and V. K. Aggarwal, *Science*, **2017**, *357*, 283-286; b) D. Hu, L. Wang and P. Li, *Org. Lett.* **2017**, *19*, 2770-2773; c) L. Candish, M. Teders and F. Glorius, *J. Am. Chem. Soc.* **2017**, *139*, 7440-7443; d) Y. Cheng, C. Mück-Lichtenfeld and A. Studer, *J. Am. Chem. Soc.* **2018**, *140*, 6221-6225; e) J. Wu, L. He, A. Noble and V. K. Aggarwal, *J. Am. Chem. Soc.* **2018**, *140*, 10700-10704; f) F. Sandfort, F. Strieth-Kalthoff, F. J. R. Klauck, M. J. James and F. Glorius, *Chem. Eur. J.* **2018**, *24*, 17210-17214. g) Y. Cheng, C. Mück-Lichtenfeld and A. Studer, *Angew. Chem. Int. Ed.* **2018**, *57*, 16832-16836; h) J.-J. Zhang, X.-H. Duan, Y. Wu, J.-C. Yang and L.-N. Guo, *Chem. Sci.* **2019**, *10*, 161-166; i) G. Yan, D. Huang and X. Wu, *Adv. Synth. Catal.* **2018**, *360*, 1040-1053.
- [26] J. A. Dean, (ed.) *Lange's Handbook of Chemistry* 15th edn (McGraw-Hill, New York, NY, 1998)
- [27] L. Wang, T. Zhang, W. Sun, Z. He, C. Xia, Y. Lan, C. Liu, *J. Am. Chem. Soc.* **2017**, *139*, 5257-5264.
- [28] A. Pelter, D. Buss, E. Colclough, B. Singaram, *Tetrahedron* **1993**, *49*, 7077-7103.
- [29] J. Metternich, R. Gilmour, *Synlett* **2016**, *27*, 2541-2552.
- [30] J.-J. Zhong, Q. Liu, C.-J. Wu, Q.-Y. Meng, X.-W. Gao, Z.-J. Li, B. Chen, C.-H. Tung, L.-Z. Wu, *Chem. Commun.* **2016**, *52*, 1800-1803.
- [31] a) A. Fawcett, J. Pradeilles, Y. Wang, T. Mutsuga, E. L. Myers, V. K. Aggarwal, *Science* **2017**, *357*, 283-286; b) D. Hu, L. Wang, P. Li, *Org. Lett.* **2017**, *19*, 2770-2773; c) L. Candish, M. Teders, F. Glorius, *J. Am. Chem. Soc.* **2017**, *139*, 7440-7443; d) Y. Cheng, C. Mück-Lichtenfeld, A. Studer, *J. Am. Chem. Soc.* **2018**, *140*, 6221-6225; e) J. Wu, L. He, A. Noble, V. K. Aggarwal, *J. Am. Chem. Soc.* **2018**, *140*, 10700-10704; f) Y. Cheng, C. Mück-Lichtenfeld, A. Studer, *Angew. Chem. Int. Ed.* **2018**, *57*, 16832-16836; g) J.-J. Zhang, X.-H. Duan, Y. Wu, J.-C. Yang, L.-N. Guo, *Chem. Sci.* **2019**, *10*, 161-166; h) G. Yan, D. Huang, X. Wu, *Adv. Synth. Catal.* **2018**, *360*, 1040-1053.
- [32] H. E. Gottlieb, V. Kotlyar, A. Nudelman, *J. Org. Chem.* **1997**, *62*, 7512-7515.
- [33] a) S. Bensaid, J. Roger, K. Beydoun, D. Roy, H. Doucet, *Synth. Commun.* **2011**, *41*, 3524-3531; b) L. V. Dunkerton, B. C. Barot, A. Nigam, *J. Heterocycl. Chem.* **1987**, *24*, 749-755; c) P. B.

- Dzhevakov, M. A. Topchiy, D. A. Zharkova, O. S. Morozov, A. F. Asachenko, M. S. Nechaev, *Adv. Synth. Catal.* **2016**, 358, 977-983; d) M. J. Harper, E. J. Emmett, J. F. Bower, C. A. Russell, *J. Am. Chem. Soc.* **2017**, 139, 12386-12389; e) E. Lee, Y. An, J. Kwon, K. I. Kim, R. Jeon, *Bioorg. Med. Chem.* **2017**, 25, 3614-3622; f) K. Nishikawa, H. Fukuda, M. Abe, K. Nakanishi, T. Taniguchi, T. Nomura, C. Yamaguchi, S. Hiradate, Y. Fujii, K. Okuda, *Phytochemistry* **2013**, 96, 132-147; g) A. Rafai Far, Y. Lag Cho, A. Rang, D. M. Rudkevich, J. Rebek, *Tetrahedron* **2002**, 58, 741-755; h) Y. Yu, J. Srogl, L. S. Liebeskind, *Org. Lett.* **2004**, 6, 2631-2634; i) S. Zhang, B. An, J. Li, J. Hu, L. Huang, X. Li, A. S. Chan, *Org. Biomol. Chem.* **2017**, 15, 7404-7410; j) Y. Zhang, Z. Zhang, B. Wang, L. Liu, Y. Che, *Bioorg. Med. Chem. Lett.* **2016**, 26, 1885-1888.
- [34] S. H. Cho, J. F. Hartwig, *Chem. Sci.* **2014**, 5, 694-698.
- [35] H. Stachowiak, J. Kaźmierczak, K. Kuciński, G. Hreczycho, *Green Chem.* **2018**, 20, 1738-1742.
- [36] C. Feldmeier, H. Bartling, E. Riedle, R. M. Gschwind, *J. Magn. Reson.* **2013**, 232, 39-44.
- [37] V. Guivel-Scharen, T. Sinnwell, S. D. Wolff, R. S. Balaban, *J. Magn. Reson.* **1998**, 133, 36-45.
- [38] N. Lokesh, A. Seegerer, J. Hioe, R. M. Gschwind, *J. Am. Chem. Soc.* **2018**, 140, 1855-1862.
- [39] a) K. Hong, X. Liu, J. P. Morken, *J. Am. Chem. Soc.* **2014**, 136, 10581-10584; b) A. J. Wommack, J. S. Kingsbury, *Tetrahedron Lett.* **2014**, 55, 3163-3166.
- [40] a) P. A. Cox, M. Reid, A. G. Leach, A. D. Campbell, E. J. King, G. C. Lloyd-Jones, *J. Am. Chem. Soc.* **2017**, 139, 13156-13165; b) X. Huang, J. Hu, M. Wu, J. Wang, Y. Peng, G. Song, *Green Chem.* **2018**, 20, 255-260; c) D. V. Partyka, *Chem. Rev.* **2011**, 111, 1529-1595; d) C. Sandford, V. K. Aggarwal, *Chem. Commun.* **2017**, 53, 5481-5494.
- [41] J. F. Guastavino, R. A. Rossi, *J. Org. Chem.* **2012**, 77, 460-472.
- [42] a) Y. Zhao, D. G. Truhlar, *Theor. Chem. Acc.* **2008**, 120, 215-241; b) A. V. Marenich, C. J. Cramer, D. G. Truhlar, *J. Phys. Chem. B* **2009**, 113, 6378-6396.
- [43] Gaussian 09, Revision D.01, M. J. Frisch, G. W. Trucks, H. B. Schlegel, G. E. Scuseria, M. A. Robb, J. R. Cheeseman, G. Scalmani, V. Barone, G. A. Petersson, H. Nakatsuji, X. Li, M. Caricato, A. Marenich, J. Bloino, B. G. Janesko, R. Gomperts, B. Mennucci, H. P. Hratchian, J. V. Ortiz, A. F. Izmaylov, J. L. Sonnenberg, D. Williams-Young, F. Ding, F. Lipparini, F. Egidi, J. Goings, B. Peng, A. Petrone, T. Henderson, D. Ranasinghe, V. G. Zakrzewski, J. Gao, N. Rega, G. Zheng, W. Liang, M. Hada, M. Ehara, K. Toyota, R. Fukuda, J. Hasegawa, M. Ishida, T. Nakajima, Y. Honda, O. Kitao, H. Nakai, T. Vreven, K. Throssell, J. A. Montgomery, Jr., J. E. Peralta, F. Ogliaro, M. Bearpark, J. J. Heyd, E. Brothers, K. N. Kudin, V. N. Staroverov, T. Keith, R. Kobayashi, J. Normand, K. Raghavachari, A. Rendell, J. C. Burant, S. S. Iyengar, J. Tomasi, M. Cossi, J. M. Millam, M. Klene, C. Adamo, R. Cammi, J. W. Ochterski, R. L. Martin, K. Morokuma, O. Farkas, J. B. Foresman, and D. J. Fox, Gaussian, Inc., Wallingford CT, 2016.



### 3 Umpolung Difunctionalization of Carbonyls via Visible-Light Photoredox Catalytic Radical-Carbanion Relay



- Combination of photocatalysis with Wolff-Kishner process
- Generation of functionalized alkyl carbanions under mild conditions
  - >85 examples & up to 87% yield
  - Mechanistic insights

#### Abstract:

The combination of photoredox catalysis with the Wolff–Kishner (WK) reaction allows the difunctionalization of carbonyl groups by a radical-carbanion relay sequence (photo-Wolff–Kishner reaction). Photoredox initiated radical addition to N-sulfonylhydrazones yields  $\alpha$ -functionalized carbanions following the WK-type mechanism. With sulfur-centered radicals, the carbanions are further functionalized by reaction with electrophiles including  $\text{CO}_2$  and aldehydes, whereas  $\text{CF}_3$  radical addition furnishes a wide range of gem-difluoroalkenes through  $\beta$ -fluoride elimination of the generated  $\alpha$ - $\text{CF}_3$  carbanions. More than 80 substrate examples demonstrate the broad applicability of this reaction sequence. A series of investigations including radical inhibition, deuterium labeling, fluorescence quenching, cyclic voltammetry, and control experiments support the proposed radical-carbanion relay mechanism.

**This chapter has been published in:** S. Wang, B. Cheng, M. Sršen and B. König\*. *J. Am. Chem. Soc.* **2020**, *142*, 7524–7531. Reproduced with permission from ACS.

#### Author Contributions:

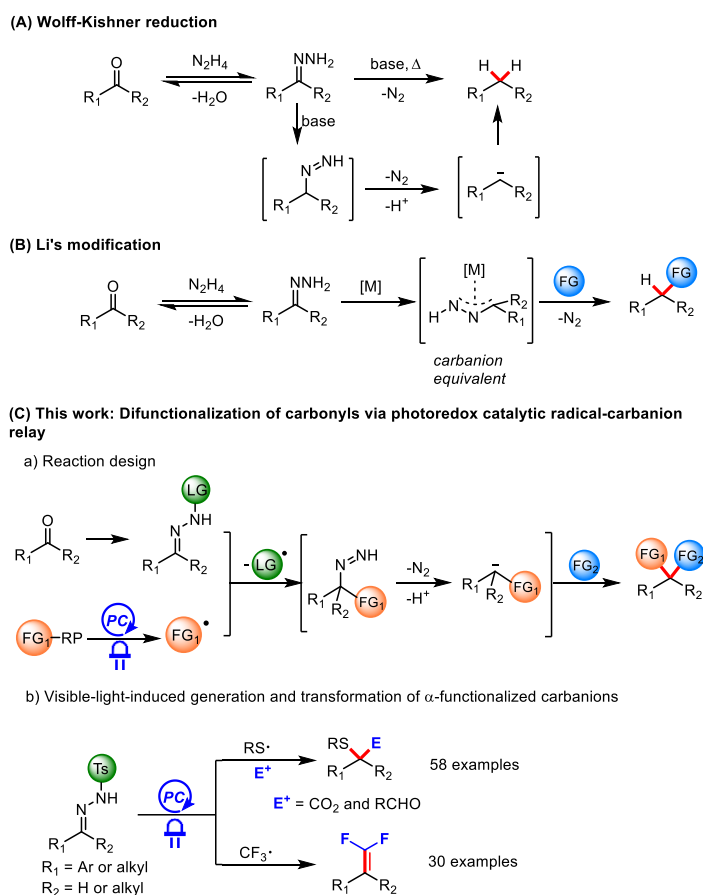
S.W. developed the reaction and investigated substrate scope in table 3, 4, and 6. S.W. and B.C. explored the substrate scope in table 2. S.W. and M.S. synthesized the starting materials. S.W. carried out the mechanistic studies and wrote the manuscript and SI. B.K. supervised the project and corrected the manuscript from S.W.

### 3.1 Introduction

The inversion of the inherent polarity of organic functionalities, termed as *umpolung*, is a key bond-forming strategy in organic synthesis.<sup>[1]</sup> The *umpolung* of a carbonyl group places a negative charge on the carbon atom, making it nucleophilic and prone to attack electrophiles. Carbonyl *umpolung* is achieved in many ways: Acyl anion equivalents are obtained by the *umpolung* of electrophilic aldehydes in stoichiometric dithiane chemistry<sup>[2]</sup> and catalytic N-heterocyclic carbene (NHC) chemistry<sup>[3]</sup>. Synthetically important alkyl carbanion intermediates can be obtained from carbonyl groups using the Wolff–Kishner (WK) reduction. The polarity inversion is accomplished by sequential hydrazone formation, tautomerization, and N<sub>2</sub>-extrusion to generate a nucleophilic alkyl carbanionic species (Scheme 1A). With elegant modifications from Huang Minlon<sup>[4]</sup> and others,<sup>[5]</sup> the WK process has evolved over the past century into a powerful carbonyl deoxygenation tool in the synthesis of complex molecules.<sup>[5]</sup> Despite being a very effective way of producing carbanions, synthetic applications of this chemistry have long been underexplored considering that the alkyl carbanion in such an *umpolung* can, in principle, react with many electrophiles other than a proton. Few examples based on the modified WK process have been developed for the construction of C–C bonds, wherein highly reactive alkyllithium reagents were employed to react with sulfonylhydrazones.<sup>[6]</sup> More recently, pioneering work by Li and co-workers demonstrated the direct functionalization of the carbanion in a Wolff–Kishner reaction by nucleophilic addition to carbonyl compounds,<sup>[7]</sup> imines,<sup>[8]</sup> CO<sub>2</sub>,<sup>[9]</sup> and Michael acceptors<sup>[10]</sup> under ruthenium catalysis. The same group utilized such carbanions in metal-catalyzed Negishi-type coupling,<sup>[11]</sup> Heck-type coupling,<sup>[12]</sup> Tsuji-Trost alkylation,<sup>[13]</sup> and olefination reactions<sup>[14]</sup> or metal-free C–C bond-forming reactions.<sup>[15]</sup> In these cases, the functional groups are installed through metal-assisted nucleophilic trapping of nonfunctionalized alkyl carbanions (Scheme 1B). Inspired by the facile generation of carbanions in the classic WK process, we questioned if functionalized carbanions can be produced catalytically for a subsequent nucleophilic reaction allowing the simultaneous installation of two functional groups at a geminal position. The scope of such a reaction sequence has remained unexplored although its realization represents a desirable synthetic tool for carbonyl group functionalization.

As part of our ongoing research activities in photoredox catalytic generation of functionalized carbanions from carbonyls,<sup>[16]</sup> we envisioned that a combination of a conventional WK process with photoredox catalysis might furnish functionalized alkyl carbanions for a subsequent derivatization. In the anticipated radical-carbanion relay sequence, radicals generated by the photoredox catalytic system would be captured by Nsulfonylhydrazone,<sup>[17]</sup> thus installing the first functional group. Subsequently, the diazene intermediate, resulting from radical fragmentation,<sup>[17b, 17c, 18]</sup> enters a similar reaction sequence as involved in the WK reduction to give functionalized carbanions, which offers a second opportunity for further transformations (Scheme 1C, a). Herein we report the successful implementation of this radical-carbanion relay functionalization concept. The combination of photoredox catalysis with a Wolff–Kishner process allows the facile generation of  $\alpha$ -sulfenyl and  $\alpha$ -CF<sub>3</sub> carbanions that undergo further nucleophilic attack or fragmentation, respectively (Scheme 1C, b).

## Scheme 1. Umpolung generation of alkyl carbanions from carbonyls



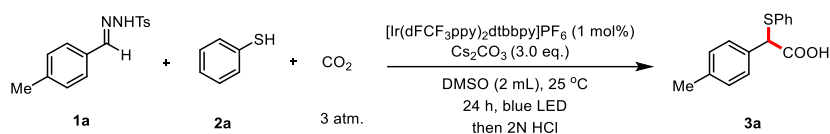
## 3.2 Results and discussion

### 3.2.1 Generation of $\alpha$ -sulfenyl carbanions and their reactions with electrophiles.

Carbon–sulfur bonds are found in pharmaceuticals or natural products and are widely used in synthesis. Recent years have witnessed increasing attention to develop an efficient approach to forge C–S bonds.<sup>[19]</sup> We postulate that photogenerated thiyl radicals<sup>[20]</sup> from various thiols can engage in the radical-carbanion relay functionalization sequence. Such a process would yield synthetically useful  $\alpha$ -sulfenyl carbanions, which are traditionally produced through deprotonation of sulfides with strong bases such as <sup>n</sup>BuLi and NaNH<sub>2</sub>.<sup>[21]</sup> Building on the facile carbanion trapping by CO<sub>2</sub><sup>[22]</sup> and our continued interest in utilization of CO<sub>2</sub> as the C1 feedstock for photocatalytic carboxylation reactions,<sup>[22e][23]</sup> we selected N-tosylhydrazone as the radical acceptor in the anticipated sequence based on the following considerations: (1) they can be easily prepared through condensation of carbonyl compounds with TsNHNH<sub>2</sub>; (2) after radical addition to N-tosylhydrazone, rapid  $\beta$ -sulfone elimination was anticipated to produce a sulfinyl radical which should undergo single-electron transfer with the photocatalyst.<sup>[17],[24]</sup> We commenced our study by utilizing aldehyde hydrazone **1a**, thiophenol **2a**, and CO<sub>2</sub> as model substrates for the optimization of the reaction conditions. After systematic screening of all reaction parameters (see the SI for details), we were delighted to obtain the desired functionalized carboxylic acid **3a** in 81% yield using [Ir(dFCF<sub>3</sub>ppy)<sub>2</sub>dtbbpy]PF<sub>6</sub> (1 mol %) under 3 atm of CO<sub>2</sub> in DMSO (Table 1, entry 1). Polar solvents like DMSO and DMF were effective for this thiocarboxylation reaction (see the SI, Table S2). Moreover, we successfully converted p-tolualdehyde into the desired product **3a** in one pot by means of a condensation and photocatalytic sequence with similar efficiency (Table 1, entry

2). Rigorous control experiments revealed that photocatalyst, base, and light were crucial for the transformation to occur (Table 1, entries 6–8).

**Table 1.** Screening of Reaction Conditions for Thiocarboxylation of N-Tosylhydrazone<sup>a</sup>



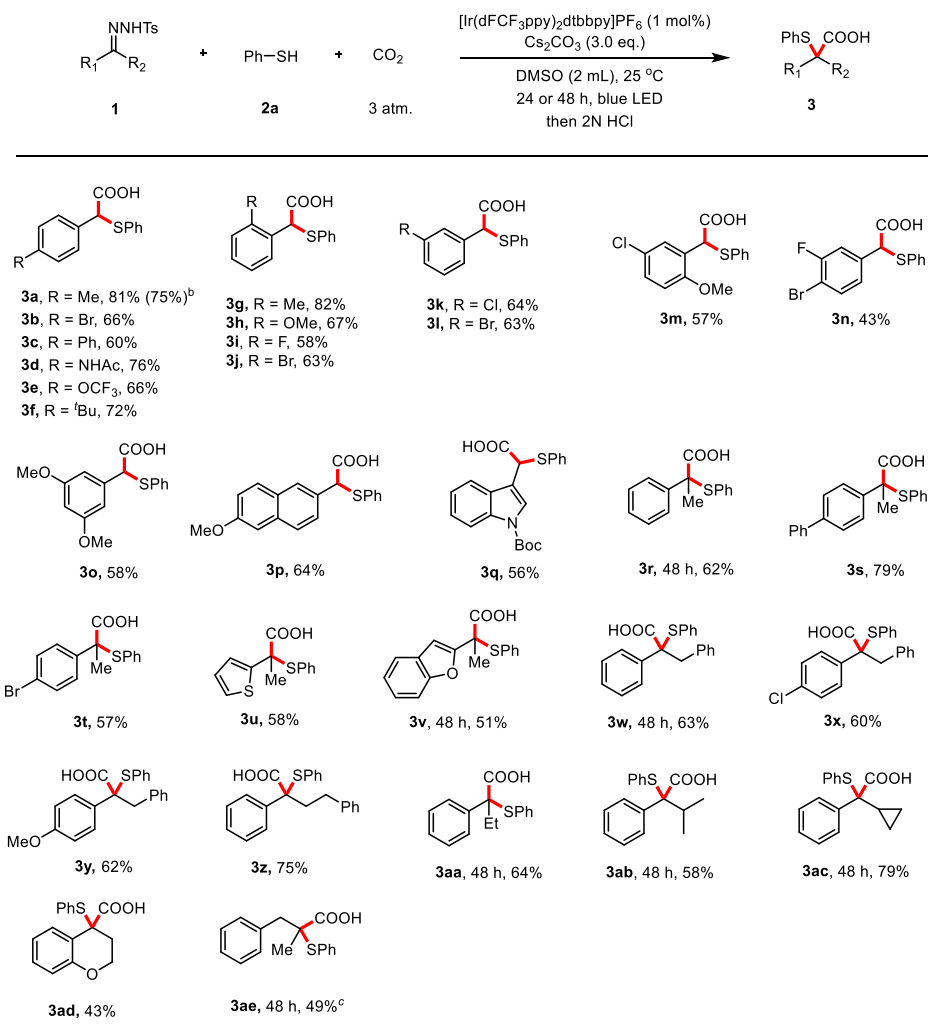
Entry	Change from standard conditions	Yield <sup>b</sup>
1	none	81%
2	one-pot process	80% <sup>c</sup>
3	MeCN instead of DMSO	n.d.
4	THF instead of DMSO	n.d.
5	4CzIPN instead of Ir-F	n.d.
6	without Cs <sub>2</sub> CO <sub>3</sub>	n.d.
7	without PC	n.d.
8	in the dark	n.d.

<sup>a</sup>Reaction conditions: compound **1a** (0.2 mmol), **2a** (0.3 mmol), Cs<sub>2</sub>CO<sub>3</sub> (0.6 mmol), [Ir(dFCF<sub>3</sub>ppy)<sub>2</sub>dtbbpy]PF<sub>6</sub> (1 mol %), and 3 atm of CO<sub>2</sub> in 2 mL of solvent, irradiation with blue LED (455 nm) at 25 °C for 24 h. n.d. = not detected. <sup>b</sup>Yields were determined by <sup>1</sup>H NMR analysis of the crude reaction mixture using 1,3,5-trimethoxybenzene as the internal standard. <sup>c</sup>**1a** was formed in one pot starting from p-tolualdehyde and used directly without purification. 4CzIPN = 2,4,5,6-tetra(carbazol-9-yl)isophthalonitrile. Ir-F = [Ir(dFCF<sub>3</sub>ppy)<sub>2</sub>dtbbpy]PF<sub>6</sub>. PC = photocatalyst.

With the optimized reaction conditions in hand, we examined the scope of the method (Table 2). The reaction gave good yields of the corresponding products with a series of aromatic aldehyde-derived N-tosylhydrazones bearing electron-neutral (**3a–3c**, **3f**, **3g**, **3j**, and **3l**), electron-donating (**3d**, **3h**, and **3o**), or electron-withdrawing (**3i**, **3k**, and **3n**) groups at para-, meta-, or ortho- positions. The reaction was compatible with N-tosylhydrazones containing two substituents on the aromatic ring, affording the desired carboxylic acids (**3m–3o**) in reasonable yields (43–58%). Heterocyclic and naphthalene containing substituents were also well tolerated by the catalytic system (**3p**, **3q**). The reaction system could also be extended to N-tosylhydrazones derived from ketones, affording a wide range of carboxylic acids with quaternary carbon-centers (**3r–3ae**). Gratifyingly, functional groups including phenyl (**3s**), halogen (**3t** and **3x**), thiophene (**3u**), benzofuran (**3v**), and methoxy (**3y**) on the aromatic rings of substrates were well tolerated. The reaction proceeded with similar efficiencies for electron rich or electron poor substrates. Moreover, N-tosylhydrazones bearing more sterically hindered substituents at the α-position such as ethyl (**3aa**), isopropyl (**3ab**), and cyclopropyl (**3ac**) gave the desired products in good yields, but longer reaction times were required. The reaction could be utilized for the thiocarboxylation of N-tosylhydrazone derived from 4-chromanone, yielding the heterocyclic product **3ad** in 43% yield. To our delight, N-tosylhydrazone derived from an aliphatic ketone reacted at 0 °C yielding product **3ae** in moderate yield. The decreased efficiency and required low reaction temperature were rationalized by the instability of the aliphatic α-sulfonyl carbanion. Importantly, this reaction is

easily scalable, as demonstrated by the gram scale synthesis of **3a** in 75% yield.

**Table 2.** Scope of N-tosylhydrazones for thiocarboxylation<sup>a</sup>

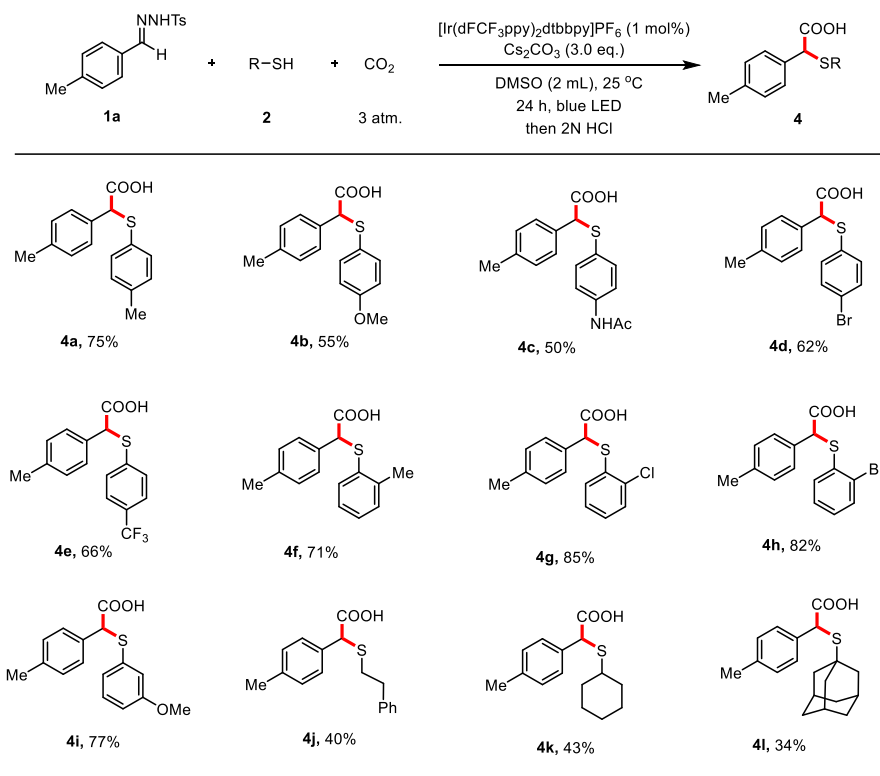


<sup>a</sup>Reaction conditions: Unless otherwise noted, all reactions were carried out with **1** (0.2 mmol), **2a** (0.3 mmol), Cs<sub>2</sub>CO<sub>3</sub> (0.6 mmol), [Ir(dFCF<sub>3</sub>ppy)<sub>2</sub>dtbbpy]PF<sub>6</sub> (1 mol%) and 3 atm of CO<sub>2</sub> in 2 mL DMSO, irradiation with blue LED (455 nm) at 25 °C for 24 hours, and isolated yields were shown.<sup>b</sup>6 mmol scale, CO<sub>2</sub> was bubbled into the reaction continuously.<sup>c</sup>Reaction was conducted at 0 °C in DMF (2 mL)

Next, we explored the scope of the reaction with respect to thiols. As shown in Table 3, thiophenols bearing either electron-donating (**4a–4c**) or electron-withdrawing groups (**4e**) on the para position of the aromatic ring reacted smoothly to generate the expected products in mostly good yields. Both ortho- and meta-substituted thiophenols were suitable substrates, affording the products in high yields (71–85%). However, 4-nitrothiophenol failed to give the desired product. Notably, besides aromatic thiophenols, our method could be extended to primary, secondary, and tertiary aliphatic thiols (**4j–4l**), albeit with moderate efficiencies. After successful application of this radical-carbanion relay sequence for carboxylation, we tested other electrophiles, like aldehydes or ketones, to realize a visible-light driven Barbier-type reaction.<sup>[22b, 25]</sup> Barbier-type reactions are well-known carbon-carbon forming reactions utilizing the nucleophilic attack of organometallic species to carbonyl compounds.<sup>[26]</sup> Using slightly modified reaction conditions, we discovered that photo-Wolff-Kishner generated carbanions can be

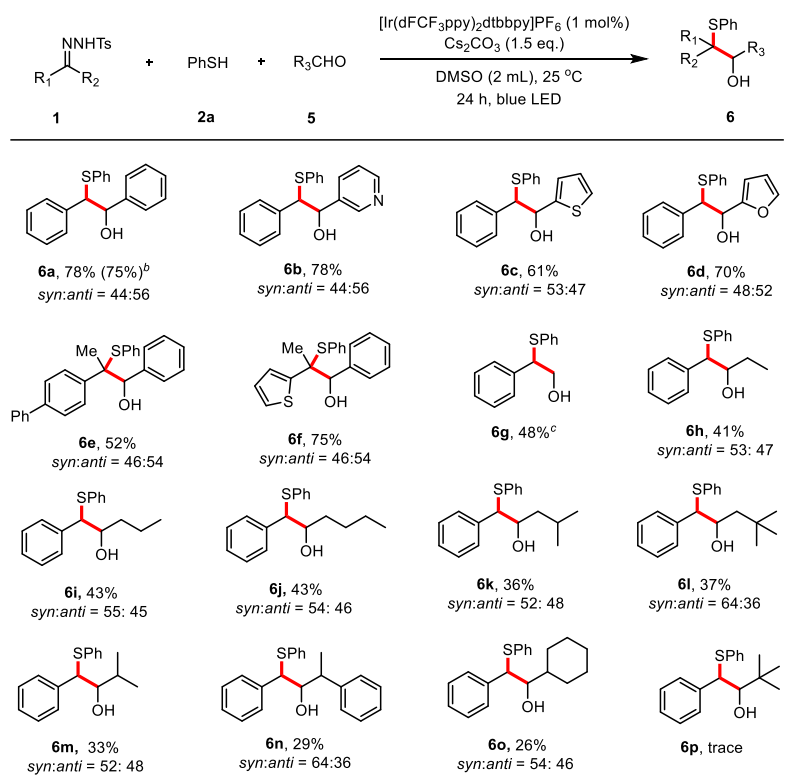
efficiently trapped with a wide range of aldehydes (Table 4).

**Table 3.** Scope of the thiols for thiocarboxylation<sup>a</sup>



<sup>a</sup>Reaction conditions: Unless otherwise noted, all reactions were carried out with **1a** (0.2 mmol), **2** (0.3 mmol), Cs<sub>2</sub>CO<sub>3</sub> (0.6 mmol), [Ir(dFCF<sub>3</sub>ppy)<sub>2</sub>dtbbpy]PF<sub>6</sub> (1 mol%) and 3 atm of CO<sub>2</sub> in 2 mL DMSO, irradiation with blue LED (455 nm) at 25 °C for 24 hours, and isolated yields were shown.

Benzaldehyde reacted smoothly to give the desired alcohol **6a** in 78% yield. We were delighted to find that heteroaryl aldehydes readily participated in the coupling reaction to give products **6b–6d**. When ketone-derived N-tosylhydrazones were employed, densely functionalized sulfides (**6e–6f**) were constructed in synthetically useful yields. Besides aromatic aldehydes, aliphatic aldehydes bearing short or long chains were suitable electrophiles in our system, giving the desired products in moderate yields (**6g–6o**).<sup>[27]</sup> Notably, solid paraformaldehyde reacted to provide the desired product (**6g**) in 48% yield. This transformation was however sensitive to steric hindrance. The presence of additional substituents at the  $\alpha$ -carbon on the trapping aldehyde decreased the yield considerably (**6m–6o**), and only a trace amount of the product was detected when pivalaldehyde was employed. Moreover, ketones failed to trap the generated carbanion in the catalytic system, which may be explained by the undesired deprotonation of the  $\alpha$ -protons to the carbonyl yielding benzyl phenyl sulfide.<sup>[28]</sup>

**Table 4.** Scope of the aldehydes for thiohydroxyalkylation<sup>a</sup>

<sup>a</sup>Reaction conditions: Unless otherwise noted, all reactions were carried out with **1** (0.2 mmol), **2a** (0.3 mmol), **5** (0.8 mmol), Cs<sub>2</sub>CO<sub>3</sub> (0.3 mmol), [Ir(dFCF<sub>3</sub>ppy)<sub>2</sub>dtbbpy]PF<sub>6</sub> (1 mol%) in 2 mL DMSO, irradiation with blue LED (455 nm) at 25 °C for 24 hours, and isolated yields were shown. <sup>b</sup>6 mmol scale. <sup>c</sup>Paraformaldehyde (0.8 mmol) and DMSO (4 mL) were used.

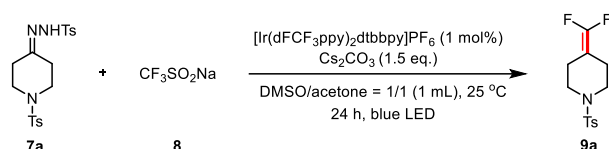
### 3.2.2 Generation of $\alpha$ -CF<sub>3</sub> carbanions and their fragmentation reactions.

Organic molecules containing a fluorine moiety generally exhibit improved reactivity, bioactivity, and metabolic stability compared to their nonfluorinated counterparts.<sup>[29]</sup> An important privileged fluorocontaining group is the gem-difluoroethylene moiety based on their unique property in medicinal chemistry.<sup>[30]</sup> Moreover, gem-difluoroalkenes are versatile building blocks for the synthesis of other fluorine-containing molecules.<sup>[31]</sup> Traditional methods such as Wittig<sup>[32]</sup> and Julia<sup>[33]</sup> reactions for the synthesis of 1,1-difluoroalkenes generally suffer from limited scope, modest efficiency, or harsh conditions. Another efficient pathway is the gem-difluorination of diazo compounds under metal catalytic<sup>[34]</sup> or metal-free reaction conditions.<sup>[35]</sup> This strategy is generally restricted to aromatic diazo compounds or diazo esters. Recently, several elegant defluorination strategies starting from  $\alpha$ -trifluoromethyl alkenes based on metal catalysis<sup>[36]</sup> or photoredox catalysis<sup>[37]</sup> have been developed for the synthesis of gem-difluoroalkenes. Nevertheless, this route requires the presence of trifluoromethyl groups on the alkene moieties, and the product scope is limited by the accessibility of such trifluoromethylated alkenes.

Following the proposal shown in Scheme 1C and encouraged by the success in the generation of  $\alpha$  sulfenyl carbanions as described in section 2.1, we wondered whether difluoroalkenes could be produced involving CF<sub>3</sub> radicals in the radical-carbanion relay sequence. The feasibility of this approach was supported by the facile E1cB elimination of  $\alpha$ -CF<sub>3</sub> carbanions to yield the difluoroalkenes.<sup>[37a, 37f, 38]</sup> We

used sodium triflinate (Langlois reagent,  $\text{CF}_3\text{SO}_2\text{Na}$ ), a benchstable and commercially available trifluoromethylation reagent, as the  $\text{CF}_3$  radical precursor and N-tosylhydrazone **7a** as the model substrate.<sup>[39]</sup> The optimized conditions (see the SI, Tables S5–S7), which include the use of  $[\text{Ir}(\text{dFCF}_3\text{ppy})_2\text{dtbbpy}]\text{PF}_6$  (2 mol %) as photocatalyst and  $\text{Cs}_2\text{CO}_3$  (1.5 equiv.) as the base in 1 mL of solvent (DMSO/acetone = 1/1), delivered the desired 1,1-difluoroalkene **9a** in 77% yield (Table 5, entry 2). Likewise, this transformation demonstrated retained efficiency when the reaction was carried out in a one-pot process (Table 5, entry 3). Control experiments indicated that the base, photocatalyst, and light irradiation were essential for this reaction (Table 5, entries 4–6).

**Table 5.** Screening of reaction conditions for the 1,1-difluoroolefination of N-tosylhydrazone<sup>a</sup>



Entry	Change from standard conditions	Yield <sup>b</sup>
1	none	70%
2	PC (2 mol%)	77% (73%) <sup>c</sup>
3	one-pot, PC (2 mol%)	75% <sup>d</sup>
4	without $\text{Cs}_2\text{CO}_3$	n.d.
5	without PC	n.d.
6	in the dark	n.d.

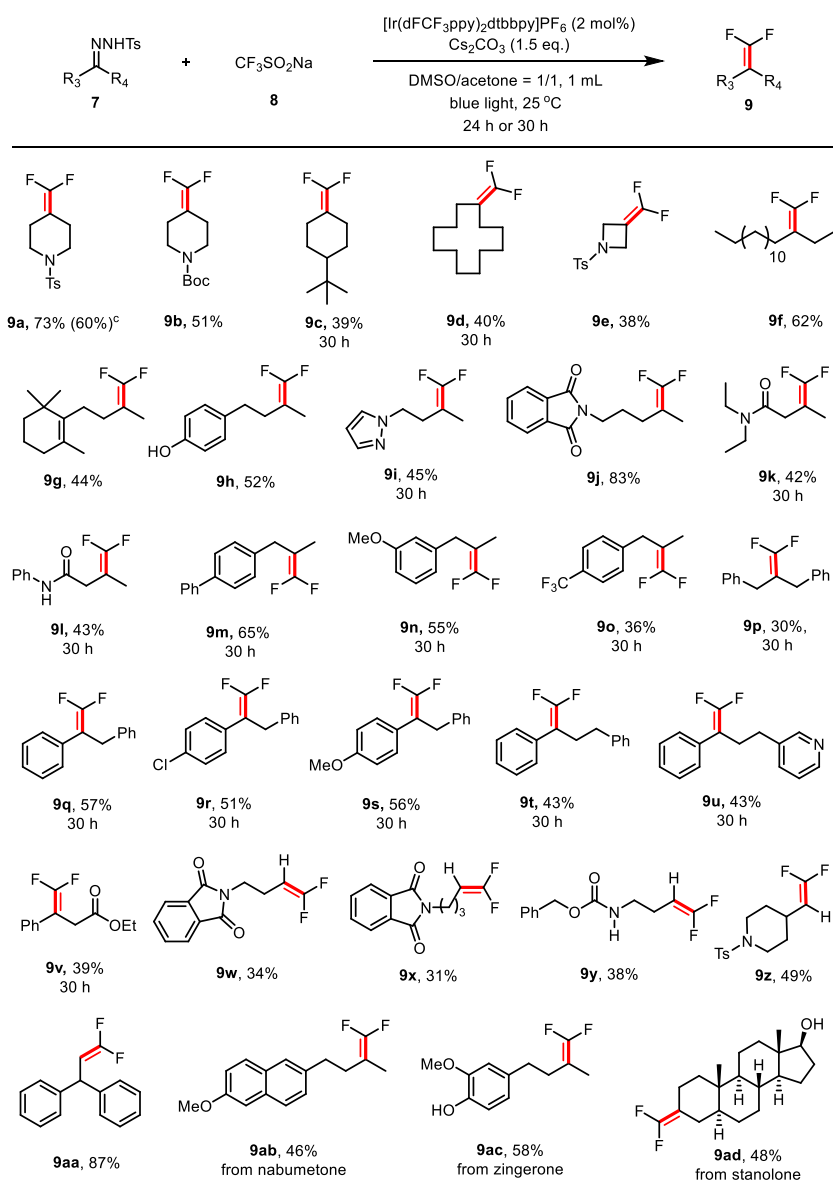
<sup>a</sup>Reaction conditions: Compound **7a** (0.2 mmol), **8** (0.3 mmol),  $\text{Cs}_2\text{CO}_3$  (0.3 mmol),  $[\text{Ir}(\text{dFCF}_3\text{ppy})_2\text{dtbbpy}]\text{PF}_6$  (1 mol%) in 1 mL solvent, irradiation with blue LED (455 nm) at 25 °C for 24 hours. n.d. = not detected. <sup>b</sup> Yields were determined by  $^{19}\text{F}$  NMR analysis of crude reaction mixture using 4,4'-difluorobenzophenone as internal standard. <sup>c</sup> Isolated yield. <sup>d</sup>**7a** was formed in one pot starting from corresponding ketone and used directly without purification. PC = photocatalyst.

Using the optimized reaction conditions for the gem-difluoroolefination, the scope of this methodology was evaluated. As summarized in Table 6, the reaction proceeded smoothly with a variety of N-tosylhydrazones, affording the expected gem-difluoroalkenes in moderate to good yields. The reactions of sodium triflinate with cycloketone-derived N-tosylhydrazones led to the corresponding products **9a–9e** in 38–73% yields. Interestingly, a strained substrate like azetidinone-derivatized N-tosylhydrazone could be successfully functionalized yielding difluoroalkene **9e** in modest yield.<sup>[40]</sup> Our method could be also extended to acyclic N-tosylhydrazones. For instance, tosylhydrazone derived from 3-hexadecanone performed well in our reaction affording the desired product **9f** in 62% yield. Moreover, the mild reaction conditions were compatible with ketone-based tosylhydrazones bearing a wide range of functional groups including alkene (**9g**), phenol (**9h**), and amide (**9j–9l**). With N-tosylhydrazones derived from phenylacetones, functional groups such as phenyl, methoxy, and trifluoromethyl on the aromatic ring were well tolerated (**9m–9o**). A sterically hindered substrate **7p** participated in the reaction well to yield the gemdifluoroalkene. Tosylhydrazones derived from aromatic ketones were also applicable affording the desired products (**9q–9u**) in reasonable yields. The reactions proceeded smoothly with heterocycle-containing substrates (e.g., pyrazole **7i** and pyridine **7u**). Notably, ester groups on the carbon chain remained untouched (**9v**). This catalytic system was also suitable for aliphatic aldehyde-based N-tosylhydrazones, delivering the corresponding products in moderate to excellent yields (**9w–9aa**). The utility of this method was further demonstrated by applying it to



functionalize structurally and functionally complex natural products like nabumetone, zingerone, and stanolone, providing the desired products (**9ab–9ad**) in good yields.

**Table 6.** Scope of the *gem*-difluoroolefination of N-tosylhydrazones<sup>a</sup>



<sup>a</sup>Reaction conditions: Unless otherwise noted, all reactions were carried out with **7** (0.2 mmol), **8** (0.3 mmol), Cs<sub>2</sub>CO<sub>3</sub> (0.3 mmol), [Ir(dFCF<sub>3</sub>ppy)<sub>2</sub>dtbbpy]PF<sub>6</sub> (2 mol%) in (DMSO/acetone = 1/1) 1 mL, irradiation with blue LED (455 nm) at 25 °C for 24 or 30 hours, and isolated yields were shown. <sup>b</sup>8 mmol scale, reaction time: 48 hours.

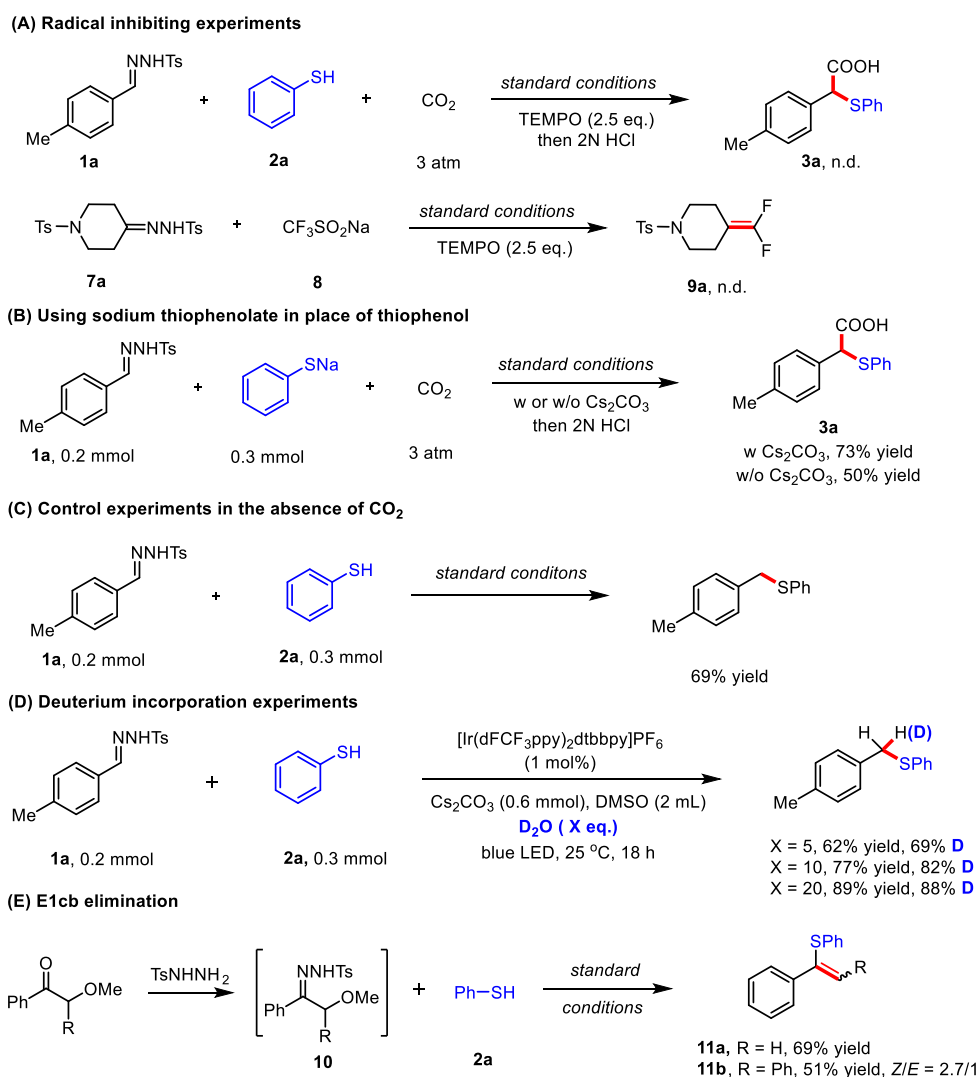
### 3.2.3 Reaction mechanism

To gain insights into the reaction mechanism, a series of spectroscopic investigations and control experiments were conducted. First, no desired products were detected when the radical scavenger TEMPO (2.5 equiv) was added to the thiocarboxylation or gemdifluoroolefination reaction. The radical nature of this type of reaction was further confirmed by the formation of TEMPO–SPh and TEMPO–CF<sub>3</sub> adducts, which were detected by the HRMS (Scheme 2A and the SI). Based on our results and literature

reports about the radical functionalization of N-sulfonylhydrazones,<sup>[17]</sup> we postulate that the sulfur-centered radical and CF<sub>3</sub> radical follow a similar mechanism to react with N-tosylhydrazones to give the carbanions. We chose the thiocarboxylation reaction as a model reaction to study the mechanism more closely.

A control experiment using sodium thiophenolate in place of the corresponding thiophenol **2a** yielded the desired carboxylic acid **3a** in 73% yield. Moreover, we found that the product could be generated in 50% yield with sodium thiophenolate even in the absence of Cs<sub>2</sub>CO<sub>3</sub>, suggesting that the base (Cs<sub>2</sub>CO<sub>3</sub>) merely serves to deprotonate the thiols (Scheme 2B). The Stern–Volmer luminescence quenching experiments revealed that sodium thiophenolate quenches the excited state of the photocatalyst much more efficiently than N-tosylhydrazone **1a** and thiophenol **2a** (see the SI, Figures S8–S11). Light “on–off” experiments indicated that continuous light irradiation was essential for the reaction to proceed (see the SI). Additionally, the quantum yield of this transformation was determined to be 2.1%. Hence, a radical chain process is unlikely for this reaction. The combined results suggest a transient sulfur-centered radical, generated by single-electron oxidation of thiophenolate by the excited state of photocatalyst in a reductive quenching photocatalytic cycle.

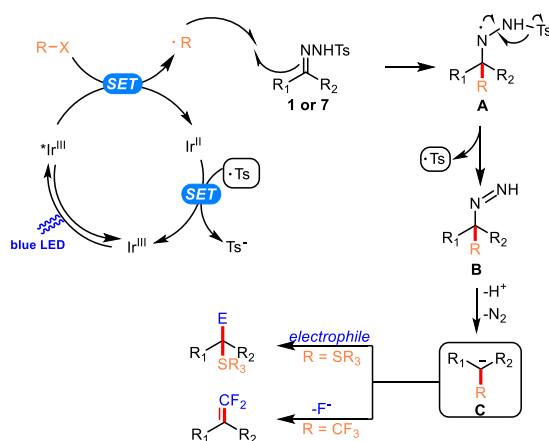
## Scheme 2. Mechanistic studies



Further control experiments showed that (4-methylbenzyl)-(phenyl)sulfide could be obtained in 69% yield in the absence of CO<sub>2</sub> (Scheme 2C). This finding suggests that the sulfur-centered radical could interact with N-tosylhydrazone **1a** irrespective of the existence of CO<sub>2</sub>. The result is in accordance with the hypothesis that a transient  $\alpha$ -sulfenyl carbanion might occur in the reaction process. On this basis, we conducted isotope-labeling experiments. Indeed, when D<sub>2</sub>O was added in the absence of CO<sub>2</sub>, up to 88% deuterium incorporation into sulfide was observed (Scheme 2D). In addition, a carbanion intermediate should in principle undergo E1cB elimination when the adjacent carbon atom bears an appropriate leaving group.<sup>[41]</sup> Therefore, N-tosylhydrazones bearing a methoxyl group at the vicinal carbon were prepared and subjected to the standard reaction conditions in the absence of CO<sub>2</sub> giving the corresponding alkenes **11a** and **11b** in good yields (Scheme 2E).

Based on the above experimental evidence and mechanistic pathways reported in the literature, we propose a plausible mechanism as depicted in Scheme 3 for the reported photocatalytic generation of functionalized carbanions. Initially, the photoexcited state of [Ir<sup>III</sup>(dFCF<sub>3</sub>ppy)<sub>2</sub>dtbbpy]<sup>+</sup> ( $E_{1/2}[^*Ir^{III/II}] = +1.21$  V vs SCE)<sup>[42]</sup> is reductively quenched by sodium triflate ( $E_{ox} = +1.05$  V vs SCE)<sup>[22a]</sup> or thiophenolate ( $E_{ox} = \sim 0.75$  V vs SCE),<sup>[43]</sup> formed through the deprotonation of thiophenol by base, affording a sulfur centered radical and a CF<sub>3</sub> radical, respectively. Subsequent radical addition to the C-N bond of N-tosylhydrazone generates the aminyl radical species **A**.<sup>[44]</sup> Fragmentation of the arenesulfonyl radical from intermediate **A** leads to a functionalized diazene intermediate **B**,<sup>[18]</sup> and the following Wolff-Kishner type N<sub>2</sub> extrusion process proceeds to give  $\alpha$ -CF<sub>3</sub> or sulfur carbanion **C** for further reactions. In the case of the  $\alpha$ -sulfenyl carbanion, subsequent nucleophilic attack to CO<sub>2</sub> or aliphatic aldehydes give carboxylic acids or alcohols. When  $\alpha$ -CF<sub>3</sub> carbanions were produced,  $\beta$ -fluoride elimination occurred to furnish the gem-difluoroalkenes. Finally, single-electron transfer (SET) from the reduced photoredox catalyst Ir<sup>II</sup> ( $E_{1/2}[Ir^{III/II}] = -1.37$  V vs SCE)<sup>[42]</sup> to the arenesulfonyl radical ( $E_{red} = +0.50$  V vs SCE)<sup>[24b]</sup> yields a sulfinate anion and regenerates the photocatalyst.

**Scheme 3.** Proposed mechanism of the photo-Wolff-Kishner carbanion generation



### 3.3. Conclusion

In summary, we have established a new reaction sequence for the generation of  $\alpha$ -functionalized alkyl carbanions through the merger of photoredox catalytic radical generation with the classic Wolff-Kishner (WK) reaction. This radical-carbanion relay for carbonyl functionalization involves the radical addition to N-sulfonylhydrazones, which enables the formation of  $\alpha$ -substituted carbanion intermediates.

Subsequent reaction with electrophiles including CO<sub>2</sub> and aldehydes or fragmentation results in thiocarboxylation, thiohydroxyalkylation, and gem-difluoroolefination with broad substrate scope and good tolerance of many functional groups. Mechanistic studies support the hypothesis that a tandem photocatalytic radical addition/Wolff–Kishner process starting from N-sulfonylhydrazones facilitates the formation of the carbanion. This strategy greatly expands the synthetic potential of Wolff–Kishner reaction. Further studies aiming to generate non-stabilized carbanions by this strategy are currently under investigation.

## 3.4 Experimental part

### 3.4.1 General information

All NMR spectra were recorded at room temperature using a Bruker Avance 300 (300 MHz for <sup>1</sup>H, 75 MHz for <sup>13</sup>C, 282 MHz for <sup>19</sup>F), or a Bruker Avance 400 (400 MHz for <sup>1</sup>H, 101 MHz for <sup>13</sup>C, 376 MHz for <sup>19</sup>F) NMR spectrometer. All chemical shifts are reported in δ-scale as parts per million [ppm] (multiplicity, coupling constant *J*, number of protons) relative to the solvent residual peaks as the internal standard. Coupling constants *J* are given in Hertz [Hz]. Abbreviations used for signal multiplicity: <sup>1</sup>H-NMR: br = broad, s = singlet, d = doublet, t = triplet, q = quartet, dd = doublet of doublets, dt = doublet of triplets, and m = multiplet. High resolution mass spectra (HRMS) were obtained from the central analytic mass spectrometry facilities of the Faculty of Chemistry and Pharmacy, Regensburg University, and are reported according to the IUPAC recommendations 2013. All mass spectra were recorded on a Finnigan MAT 95, Thermo Quest Finnigan TSQ 7000, Finnigan MATSSQ 710 A or an Agilent Q-TOF 6540 UHD instrument. GC measurements were performed on a GC 7890 from Agilent Technologies. Data acquisition and evaluation was done with Agilent ChemStation Rev.C.01.04. [35]. Analytical TLC was performed on silica gel coated alumina plates (MN TLC sheets ALUGRAM® Xtra SIL G/UV254). Visualization was done by UV light (254 or 366 nm). If necessary, potassium permanganate was used for chemical staining. Purification by column chromatography was performed with silica gel 60 M (40–63 μm, 230–440 mesh, Merck) on a Biotage® Isolera TM Spektra One device. All photocatalytic reactions were performed with 455 nm LEDs (OSRAM Oslon SSL 80 royal-blue LEDs (λ = 455 nm (± 15 nm), 3.5 V, 700 mA).

The sample was irradiated with a LED through the vial's plane bottom side and cooled from the side using custom-made aluminum cooling blocks connected to a thermostat (Figure S1). Gram-scale reactions were in a classic glass tube photochemical reactor setup irradiated from the outside (Figure S2). The glass tube with reaction mixture and LED cooling block were thermostated at 25 °C. CO<sub>2</sub> was bubbled continuously through the reaction mixture in the large-scale carboxylation reactions. UV–Vis and fluorescence measurements were performed with a Varian Cary 100 UV/Vis spectrophotometer and FluoroMax-4 spectrofluorometer, respectively. Electrochemical studies were carried out under argon atmosphere. The measurements were performed in anhydrous solvent containing 0.1 M tetra-n-butylammonium tetrafluoroborate using ferrocene/ferrocenium (Fc/Fc<sup>+</sup>) as an internal reference. A glassy carbon electrode (working electrode), platinum wire counter electrode, and Ag quasi-reference electrode were employed. Commercially available starting materials and solvents were used without further purification.

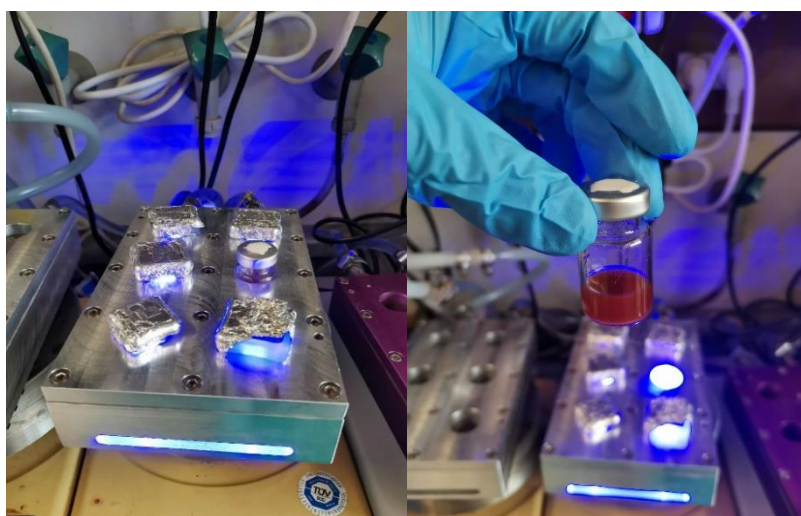
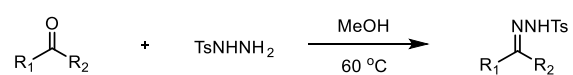


**Figure S1.** Photochemical set-up for regular-scale reactions



**Figure S2.** Photochemical set-up for large-scale reactions

### 3.4.2 Starting materials



N-tosylhydrazone was prepared according a reported procedure.<sup>[45]</sup> To a stirred solution of tosylhydrazide (10 mmol) in MeOH (10 mL) at 60 °C, aldehyde or ketone (1 equiv.) was added dropwise (or portionwise if solid). The reaction was completed within 0.5 h. After that, the solvent was removed directly under reduced pressure, and the crude mixture was either directly used or further purified by recrystallization.

### 3.4.3 Experimental procedures

#### General procedure A

To a 9 mL snap vial with magnetic stirring bar, tosylhydrazone (0.2 mmol), Cs<sub>2</sub>CO<sub>3</sub> (0.6 mmol), [Ir(dFCF<sub>3</sub>ppy)<sub>2</sub>dtbbpy]PF<sub>6</sub> (0.002 mmol) were added. The vial was evacuated and back filled with CO<sub>2</sub> for three times. A solution of thiol (0.3 mmol) in dry DMSO (2 mL) was added by syringe. Then the solution was bubbled with CO<sub>2</sub> for 3 minutes. After CO<sub>2</sub> (14 mL) was injected by syringe the vial was sealed with wax. The mixture was irradiated with a 455 nm LED at 25 °C. After 24 or 48 h, the mixture was quenched with 2N HCl and extracted with EtOAc (10 mL \*3). The combined organic phase was then washed with H<sub>2</sub>O (10 mL) and brine, dried over sodium sulfate, concentrated under vacuum. The residue was purified by silica gel flash chromatography (gradient eluent: petroleum ether/EtOAc/HOAc=50/1/0.1% to 10/1/0.1%) to give the desired product.

#### General procedure B

To a 9 mL snap vial with magnetic stirring bar, tosylhydrazone (0.2 mmol), Cs<sub>2</sub>CO<sub>3</sub> (0.3 mmol), [Ir(dFCF<sub>3</sub>ppy)<sub>2</sub>dtbbpy]PF<sub>6</sub> (0.002 mmol) were added. The vial was evacuated and back filled with N<sub>2</sub> for three times. A solution of thiophenol (0.3 mmol) and carbonyl compound (0.8 mmol) in dry DMSO (2 mL) was added by syringe. The mixture was irradiated with a 455 nm LED at 25 °C. After 24 h, the mixture was quenched with H<sub>2</sub>O and extracted with EtOAc (10 mL \*3). The combined organic phase was then washed with H<sub>2</sub>O (10 mL) and brine, dried over sodium sulfate, concentrated under vacuum. The residue was purified by silica gel flash chromatography (gradient eluent: pentane/EtOAc =50/1 to 10/1) to give the desired product.

#### General procedure C

To a 9 mL snap vial with magnetic stirring bar, tosylhydrazone (0.2 mmol), Cs<sub>2</sub>CO<sub>3</sub> (0.3 mmol), [Ir(dFCF<sub>3</sub>ppy)<sub>2</sub>dtbbpy]PF<sub>6</sub> (0.004 mmol) and CF<sub>3</sub>SO<sub>2</sub>Na (0.3 mmol) were added. The vial was evacuated and back filled with N<sub>2</sub> for three times, DMSO/acetone = 1/1 (1 mL) was added by syringe. The mixture was irradiated with a 455 nm LED at 25 °C. After the indicated time, the mixture was quenched with H<sub>2</sub>O and extracted with EtOAc (10 mL \*3). The combined organic phase was then washed with H<sub>2</sub>O (10 mL) and brine, dried over sodium sulfate, concentrated under vacuum. The residue was purified by silica gel flash chromatography (eluent: pentane/EA) to give the desired product.

#### General procedure D-for “one-pot” thiocarboxylation of N-tosylhydrazone

To a 9 mL snap vial with magnetic stirring bar, carbonyl compound (0.2 mmol), tosylhydrazide (0.2 mmol) and MeOH (1 mL), the mixture was stirred at 60 °C for 30 minutes. After the solvent was removed under vacuum, [Ir(dFCF<sub>3</sub>ppy)<sub>2</sub>dtbbpy]PF<sub>6</sub> (0.002 mmol) and Cs<sub>2</sub>CO<sub>3</sub> (0.6 mmol) were added. The vial was evacuated and back filled with CO<sub>2</sub> for three times. A solution of thiophenol (0.3 mmol) in dry DMSO (2 mL) was added by syringe. Then the solution was bubbled with CO<sub>2</sub> for 3 minutes. After CO<sub>2</sub> (14 mL) was injected by syringe the vial was sealed with wax. The mixture was irradiated with a 455 nm LED at 25 °C. After 24 or 48 h, the mixture was quenched with 2N HCl and extracted with EtOAc (10 mL \*3). The combined organic phase was then washed with H<sub>2</sub>O (10 mL) and brine, dried over sodium sulfate, concentrated under vacuum. The residue was purified by silica gel flash chromatography (gradient eluent: petroleum ether/EtOAc/HOAc=50/1/0.1% to 10/1/0.1%) to give the desired product.

#### General procedure E-for “one-pot” 1,1-difluoroolefination of N-tosylhydrazone

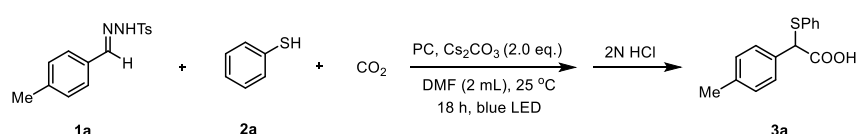
To a 9 mL snap vial with magnetic stirring bar, carbonyl compound (0.2 mmol), tosylhydrazide (0.2 mmol) and MeOH (1 mL), the mixture was stirred at 60 °C for 30 minutes. After the solvent was removed

under vacuum,  $[\text{Ir}(\text{dFCF}_3\text{ppy})_2\text{dtbbpy}]\text{PF}_6$  (0.004 mmol),  $\text{Cs}_2\text{CO}_3$  (0.3 mmol) and  $\text{CF}_3\text{SO}_2\text{Na}$  (0.3 mmol) were added. The vial was evacuated and back filled with  $\text{N}_2$  for three times,  $\text{DMSO}/\text{acetone} = 1/1$  (1 mL) was added by syringe. The mixture was irradiated with a 455 nm LED at 25 °C. After the indicated time, the mixture was quenched with  $\text{H}_2\text{O}$  and extracted with  $\text{EtOAc}$  (10 mL \*3). The combined organic phase was then washed with  $\text{H}_2\text{O}$  (10 mL) and brine, dried over sodium sulfate, concentrated under vacuum. The residue was purified by silica gel flash chromatography (eluent: pentane/EA) to give the desired product.

### 3.4.4 Optimization details for the reaction conditions

#### Optimization details for thiocarboxylation of tosylhydrazone 1a

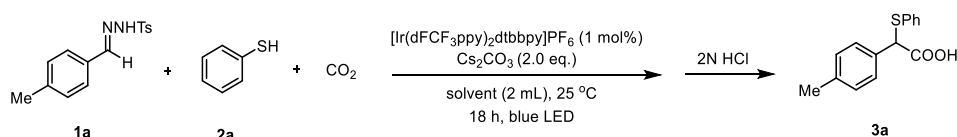
**Table S1.** Screening of photocatalysts<sup>a</sup>



Entry	PC (mol%)	CO <sub>2</sub>	Yield (%) <sup>b</sup>
1	$[\text{Ir}(\text{dFCF}_3\text{ppy})_2\text{dtbbpy}]\text{PF}_6$ (1 mol%)	4 atm	55
2	$[\text{Ir}(\text{dFCF}_3\text{ppy})_2\text{bpy}]\text{PF}_6$ (1 mol%)	4 atm	40
3	4CzIPN (2 mol%)	4 atm	0
4	Eosin Y (2 mol%)	4 atm	0
5	$[\text{Ir}(\text{ppy})_2\text{dtbbpy}]\text{PF}_6$ (1 mol%)	4 atm	13
6	$\text{Ru}(\text{bpy})_3\text{Cl}_2 \cdot 6\text{H}_2\text{O}$ (1 mol%)	4 atm	34
7	-	4 atm	0

<sup>a</sup> Reaction conditions: Unless otherwise noted, all reactions were carried out with **1a** (0.2 mmol), **2a** (0.4 mmol),  $\text{Cs}_2\text{CO}_3$  (0.4 mmol), photocatalyst and 4 atm of  $\text{CO}_2$  in 2 mL DMF, irradiation with a blue LED at 25 °C for 24 hours. <sup>b</sup> Yields were determined by  $^1\text{H}$  NMR analysis of crude reaction mixture using 1,3,5-trimethoxybenzene as internal standard.

**Table S2.** Screening of solvents<sup>a</sup>

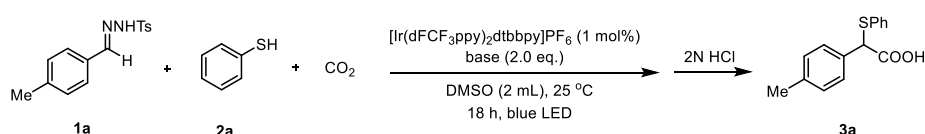


Entry	Solvent	CO <sub>2</sub>	Yield (%) <sup>b</sup>
1	DMF	4 atm	55
2	DMSO	4 atm	68

3	MeCN	4 atm	0
4	toluene	4 atm	0
5	THF	4 atm	0
6	PhCF <sub>3</sub>	4 atm	0

<sup>a</sup> Reaction conditions: Unless otherwise noted, all reactions were carried out with **1a** (0.2 mmol), **2a** (0.4 mmol), Cs<sub>2</sub>CO<sub>3</sub> (0.4 mmol), [Ir(dFCF<sub>3</sub>ppy)<sub>2</sub>dtbbpy]PF<sub>6</sub> (1 mol%) and 4 atm of CO<sub>2</sub> in 2 mL solvent, irradiation with blue LED at 25 °C for 24 hours. <sup>b</sup> Yields were determined by <sup>1</sup>H NMR analysis of crude reaction mixture using 1,3,5-trimethoxybenzene as internal standard.

**Table S3.** Screening of bases<sup>a</sup>



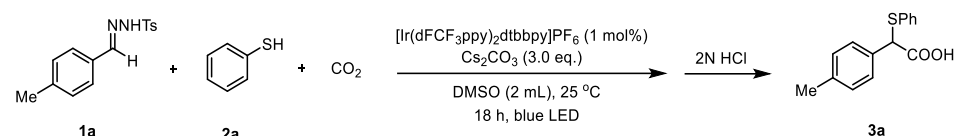
Entry	Base	CO <sub>2</sub>	Yield (%) <sup>b</sup>
1	Cs <sub>2</sub> CO <sub>3</sub>	4 atm.	68
2	K <sub>2</sub> CO <sub>3</sub>	4 atm.	39
3	Na <sub>2</sub> CO <sub>3</sub>	4 atm.	50
4	Li <sub>2</sub> CO <sub>3</sub>	4 atm.	10
5	NaHCO <sub>3</sub>	4 atm.	16
6	K <sub>3</sub> PO <sub>4</sub>	4 atm.	53
7	CsOAc	4 atm.	55
8	KOAc	4 atm.	58
9	NaOAc	4 atm.	38
10	NaOH	4 atm.	47
11	DBU	4 atm.	44
12	Cs <sub>2</sub> CO <sub>3</sub> (1.0 eq.)	4 atm.	57
13	Cs <sub>2</sub> CO <sub>3</sub> (1.5 eq.)	4 atm.	66
14	Cs <sub>2</sub> CO <sub>3</sub> (2.5 eq.)	4 atm.	71
15	Cs <sub>2</sub> CO <sub>3</sub> (3.0 eq.)	4 atm.	<b>76</b>
16	-	4 atm.	<b>0</b>

<sup>a</sup> Reaction conditions: Unless otherwise noted, all reactions were carried out with **1a** (0.2 mmol), **2a** (0.4 mmol), base, [Ir(dFCF<sub>3</sub>ppy)<sub>2</sub>dtbbpy]PF<sub>6</sub> (1 mol%) and 4 atm of CO<sub>2</sub> in 2 mL DMSO, irradiation with blue LED at 25 °C for 24 hours. <sup>b</sup> Yields were determined by <sup>1</sup>H NMR analysis of crude reaction mixture using



1,3,5-trimethoxybenzene as internal standard.

**Table S4.** Screening of substrate ratios and control experiments<sup>a</sup>

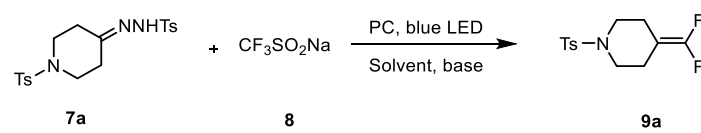


Entry	1a : 2a	CO <sub>2</sub>	Yield (%) <sup>b</sup>
1 <sup>c</sup>	1 : 2.0	4 atm.	21
2	1 : 2.0	4 atm.	76
3	1 : 1.5	4 atm.	<b>81</b>
4	1 : 1.0	4 atm.	62
5	1 : 2.5	4 atm.	72
6	1 : 3.0	4 atm.	48
7	1 : 1.5	2 atm.	65
8	1 : 1.5	balloon	70
9	1 : 1.5	3 atm.	<b>81</b>
10 <sup>d</sup>	1 : 1.5	3 atm.	0
11 <sup>e</sup>	1 : 1.5	3 atm.	0

<sup>a</sup> Reaction conditions: Unless otherwise noted, all reactions were carried out with **7a** (0.2 mmol), **8** (0.4 mmol), base (0.6 mmol), [Ir(dFCF<sub>3</sub>ppy)<sub>2</sub>dtbbpy]PF<sub>6</sub> (1 mol%) and 4 atm of CO<sub>2</sub> in 2 mL DMSO, irradiation with a blue LED at 25 °C for 24 hours. <sup>b</sup> Yields were determined by <sup>1</sup>H NMR analysis of crude reaction mixture using 1,3,5-trimethoxybenzene as internal standard. <sup>c</sup> **2a** was replaced by 2.0 eq. of PhSSPh (diphenyl disulfide). <sup>d</sup> without light. <sup>e</sup> without photocatalyst.

### Optimization details for *gem*-difluoroolefination of tosylhydrazone **7a**

**Table S5.** Optimization of the reaction conditions<sup>a</sup>



Entry	Base (1.5 eq)	Photocatalyst	Solvent	Yield [%] <sup>b</sup>
1	Cs <sub>2</sub> CO <sub>3</sub>	[Ir(dFCF <sub>3</sub> ppy) <sub>2</sub> dtbbpy]PF <sub>6</sub> (1 mol%)	DMSO	<b>59</b>
2	K <sub>2</sub> CO <sub>3</sub>	[Ir(dFCF <sub>3</sub> ppy) <sub>2</sub> dtbbpy]PF <sub>6</sub> (1 mol%)	DMSO	25

3	Na <sub>2</sub> CO <sub>3</sub>	[Ir(dFCF <sub>3</sub> ppy) <sub>2</sub> dtbbpy]PF <sub>6</sub> (1 mol%)	DMSO	n.d
4	NaOH	[Ir(dFCF <sub>3</sub> ppy) <sub>2</sub> dtbbpy]PF <sub>6</sub> (1 mol%)	DMSO	n.d
5	CH <sub>3</sub> COOCs	[Ir(dFCF <sub>3</sub> ppy) <sub>2</sub> dtbbpy]PF <sub>6</sub> (1 mol%)	DMSO	n.d
6	K <sub>3</sub> PO <sub>4</sub>	[Ir(dFCF <sub>3</sub> ppy) <sub>2</sub> dtbbpy]PF <sub>6</sub> (1 mol%)	DMSO	n.d
7	KO <sup>t</sup> Bu	[Ir(dFCF <sub>3</sub> ppy) <sub>2</sub> dtbbpy]PF <sub>6</sub> (1 mol%)	DMSO	n.d
8	2,4,6-collidine	[Ir(dFCF <sub>3</sub> ppy) <sub>2</sub> dtbbpy]PF <sub>6</sub> (1 mol%)	DMSO	n.d
9	CsF	[Ir(dFCF <sub>3</sub> ppy) <sub>2</sub> dtbbpy]PF <sub>6</sub> (1 mol%)	DMSO	n.d
10	-	[Ir(dFCF <sub>3</sub> ppy) <sub>2</sub> dtbbpy]PF <sub>6</sub> (1 mol%)	DMSO	n.d

<sup>a</sup>Unless otherwise noted, all the reactions were carried out with **7a** (0.2 mmol), **8** (0.3 mmol), base (0.3 mmol), [Ir(dFCF<sub>3</sub>(ppy)<sub>2</sub>dtbbpy]PF<sub>6</sub> (1 mol%, 0.002 mmol) in DMSO (1 mL), irradiation with a blue LED at 25 °C for 24 h. <sup>b</sup><sup>19</sup>F NMR yield using 4,4'-difluorobenzophenone as an internal standard. n.d = not detected

**Table S6.** Photocatalyst screening

Entry	Base	Photocatalyst	Solvent	Yield[%] <sup>b</sup>
1	Cs <sub>2</sub> CO <sub>3</sub>	[Ir(dFCF <sub>3</sub> ppy) <sub>2</sub> dtbbpy]PF <sub>6</sub> (1 mol%)	DMSO	59
2	Cs <sub>2</sub> CO <sub>3</sub>	[Ir(dFCF <sub>3</sub> ppy) <sub>2</sub> dtbbpy]PF <sub>6</sub> (2 mol%)	DMSO	61
3	Cs <sub>2</sub> CO <sub>3</sub>	[Ir(dFCF <sub>3</sub> ppy) <sub>2</sub> dtbbpy]PF <sub>6</sub> (0.5 mol%)	DMSO	44
4	Cs <sub>2</sub> CO <sub>3</sub>	[Ir(dFCF <sub>3</sub> ppy) <sub>2</sub> dtbbpy]PF <sub>6</sub> (1 mol%)	DMSO	41
5	Cs <sub>2</sub> CO <sub>3</sub>	[IrdF(Me)(ppy) <sub>2</sub> dtbbpy]PF <sub>6</sub> (1 mol%)	DMSO	trace
6	Cs <sub>2</sub> CO <sub>3</sub>	[Ir(ppy) <sub>2</sub> dtbbpy]PF <sub>6</sub> (1 mol%)	DMSO	n.d
7	Cs <sub>2</sub> CO <sub>3</sub>	4CzIPN (5 mol%)	DMSO	18
8	Cs <sub>2</sub> CO <sub>3</sub>	EoSIn Y (2 mol%)	DMSO	n.d
9	Cs <sub>2</sub> CO <sub>3</sub>	Rh-6G (10 mol%)	DMSO	n.d
10	Cs <sub>2</sub> CO <sub>3</sub>	Fukuzumi ClO <sub>4</sub> <sup>-</sup> (5 mol%)	DMSO	n.d
11	Cs <sub>2</sub> CO <sub>3</sub>	Carbon Nitride	DMSO	n.d

20 mg

<sup>a</sup> Unless otherwise noted, all the reactions were carried out with **7a** (0.2 mmol), **8** (0.3 mmol), base (0.3 mmol), photocatalyst (1 mol%, 0.002 mmol) in DMSO (1 mL), irradiation with a blue LED at 25 °C for 24 h. <sup>b</sup> <sup>19</sup>F NMR yield using 4,4'-difluorobenzophenone as an internal standard. n.d = not detected.

**Table S7.** Optimization of the reaction conditions<sup>a</sup>

Entry	Base	Photocatalyst	Solvent	Yield [%] <sup>b</sup>
1	Cs <sub>2</sub> CO <sub>3</sub>	[Ir(dFCF <sub>3</sub> ppy) <sub>2</sub> dtbbpy]PF <sub>6</sub> (1 mol%)	DMF	38
2	Cs <sub>2</sub> CO <sub>3</sub>	[Ir(dFCF <sub>3</sub> ppy) <sub>2</sub> dtbbpy]PF <sub>6</sub> (1 mol%)	DMA	30
3	Cs <sub>2</sub> CO <sub>3</sub>	[Ir(dFCF <sub>3</sub> ppy) <sub>2</sub> dtbbpy]PF <sub>6</sub> (1 mol%)	MeCN	trace
4	Cs <sub>2</sub> CO <sub>3</sub>	[Ir(dFCF <sub>3</sub> ppy) <sub>2</sub> dtbbpy]PF <sub>6</sub> (1 mol%)	DCE	n.d
5	Cs <sub>2</sub> CO <sub>3</sub>	[Ir(dFCF <sub>3</sub> ppy) <sub>2</sub> dtbbpy]PF <sub>6</sub> (1 mol%)	THF	n.d
6	Cs <sub>2</sub> CO <sub>3</sub>	[Ir(dFCF <sub>3</sub> ppy) <sub>2</sub> dtbbpy]PF <sub>6</sub> (1 mol%)	toluene	n.d
7	Cs <sub>2</sub> CO <sub>3</sub>	[Ir(dFCF <sub>3</sub> ppy) <sub>2</sub> dtbbpy]PF <sub>6</sub> (1 mol%)	dioxane	n.d
8	Cs <sub>2</sub> CO <sub>3</sub>	[Ir(dFCF <sub>3</sub> ppy) <sub>2</sub> dtbbpy]PF <sub>6</sub> (1 mol%)	MeOH	n.d
9	Cs <sub>2</sub> CO <sub>3</sub>	[Ir(dFCF <sub>3</sub> ppy) <sub>2</sub> dtbbpy]PF <sub>6</sub> (1 mol%)	NMP	n.d
10	Cs <sub>2</sub> CO <sub>3</sub>	[Ir(dFCF <sub>3</sub> ppy) <sub>2</sub> dtbbpy]PF <sub>6</sub> (1 mol%)	DMSO/THF=4:1	52
11	Cs <sub>2</sub> CO <sub>3</sub>	[IrdFCF <sub>3</sub> (ppy) <sub>2</sub> dtbpy]PF <sub>6</sub> (1 mol%)	DMSO/1,4-dioxane=4:1	53
12	Cs <sub>2</sub> CO <sub>3</sub>	[Ir(dFCF <sub>3</sub> ppy) <sub>2</sub> dtbbpy]PF <sub>6</sub> (1 mol%)	DMSO/MeCN=4:1	62
13	Cs <sub>2</sub> CO <sub>3</sub>	[Ir(dFCF <sub>3</sub> ppy) <sub>2</sub> dtbbpy]PF <sub>6</sub> (1 mol%)	DMSO/EA=4:1	62
14	Cs <sub>2</sub> CO <sub>3</sub>	[Ir(dFCF <sub>3</sub> ppy) <sub>2</sub> dtbbpy]PF <sub>6</sub> (1 mol%)	DMSO/toluene=4:1	38
15	Cs <sub>2</sub> CO <sub>3</sub>	[Ir(dFCF <sub>3</sub> ppy) <sub>2</sub> dtbbpy]PF <sub>6</sub> (1 mol%)	DMSO/DME=4:1	46
16	Cs <sub>2</sub> CO <sub>3</sub>	[Ir(dFCF <sub>3</sub> ppy) <sub>2</sub> dtbbpy]PF <sub>6</sub> (1 mol%)	DMSO/H <sub>2</sub> O=4:1	n.d
17	Cs <sub>2</sub> CO <sub>3</sub>	[Ir(dFCF <sub>3</sub> ppy) <sub>2</sub> dtbbpy]PF <sub>6</sub> (1 mol%)	DMSO/acetone=4:1	65
18	Cs <sub>2</sub> CO <sub>3</sub>	[Ir(dFCF <sub>3</sub> ppy) <sub>2</sub> dtbbpy]PF <sub>6</sub>	DMSO/acetone=2:1	67

		(1 mol%)		
19	Cs <sub>2</sub> CO <sub>3</sub>	[Ir(dFCF <sub>3</sub> ppy) <sub>2</sub> dtbbpy]PF <sub>6</sub> (1 mol%)	DMSO/acetone=1:1	70
20	Cs <sub>2</sub> CO <sub>3</sub>	[Ir(dFCF <sub>3</sub> ppy) <sub>2</sub> dtbbpy]PF <sub>6</sub> (1 mol%)	DMSO/acetone=1:2	70
21	Cs <sub>2</sub> CO <sub>3</sub>	[Ir(dFCF <sub>3</sub> ppy) <sub>2</sub> dtbbpy]PF <sub>6</sub> (1 mol%)	DMSO/acetone=1:1 (0.6 mL in total)	65
22	Cs <sub>2</sub> CO <sub>3</sub>	[Ir(dFCF <sub>3</sub> ppy) <sub>2</sub> dtbbpy]PF <sub>6</sub> (1 mol%)	DMSO/acetone=1:1 (1.5 mL in total)	70
23	Cs <sub>2</sub> CO <sub>3</sub>	[Ir(dFCF <sub>3</sub> ppy) <sub>2</sub> dtbbpy]PF <sub>6</sub> (2 mol%)	DMSO/acetone=1:1	77 (73) <sup>c</sup>
24	Cs <sub>2</sub> CO <sub>3</sub>	-	DMSO/acetone=1:1	n.d
25 <sup>d</sup>	Cs <sub>2</sub> CO <sub>3</sub>	[Ir(dFCF <sub>3</sub> ppy) <sub>2</sub> dtbbpy]PF <sub>6</sub> (2 mol%)	DMSO/acetone=1:1	n.d

<sup>a</sup>Unless otherwise noted, all the reactions were carried out with **7a** (0.2 mmol), **8** (0.3 mmol), Cs<sub>2</sub>CO<sub>3</sub> (0.3 mmol), [Ir(dFCF<sub>3</sub>ppy)<sub>2</sub>dtbbpy]PF<sub>6</sub> (1 mol%, 0.002 mmol) in solvent (1 mL), irradiation with a blue LED at 25 °C for 24 h. <sup>b</sup><sup>19</sup>F NMR yield using 4,4'-difluorobenzophenone as an internal standard. n.d = not detected. <sup>c</sup> isolated yield. <sup>d</sup> in the dark.

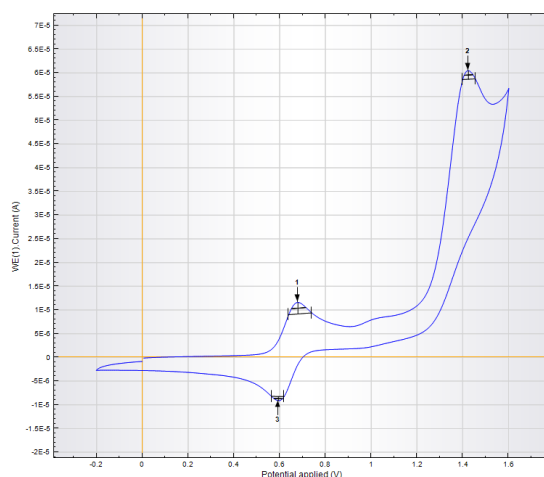
### 3.4.5 Mechanistic studies

#### CV measurements

CV measurements were taken on a three-electrode potentiostat galvanostat PGSTAT302N from Metrohm Autolab by using a glassy carbon working electrode, a platinum wire counter electrode, a silver wire as a reference electrode. The voltammograms were taken at room temperature in a degassed DMF or MeCN solution ([n-Bu<sub>4</sub>NBF<sub>4</sub>] = 0.1 M, [substrate] = 1 mM, ferrocene as the internal standard) under Argon atmosphere. The scan rate was 0.1 V/s. Potentials vs. SCE were reported according to E<sub>SCE</sub> = E<sub>Fc/Fc+</sub> + 0.38 V.

Index Peak position

- 1 0.67978
- 2 1.425
- 3 0.59418

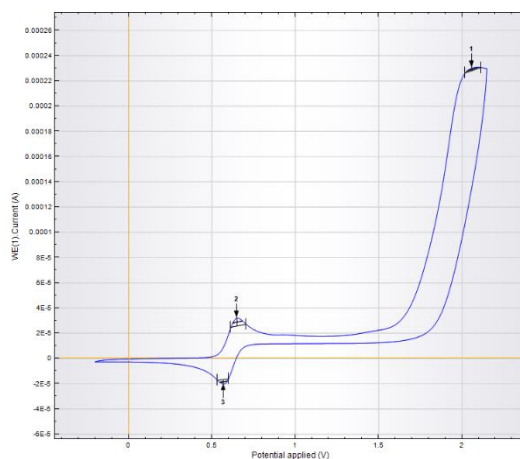


E<sub>ox</sub>(**1a**) = 1.17 V vs. SCE

**Figure S3.** Cyclic voltammogram of N-tosylhydrazone **1a** in DMSO (with Ferrocene)

Index Peak position

1	2.0595
2	0.64957
3	0.569

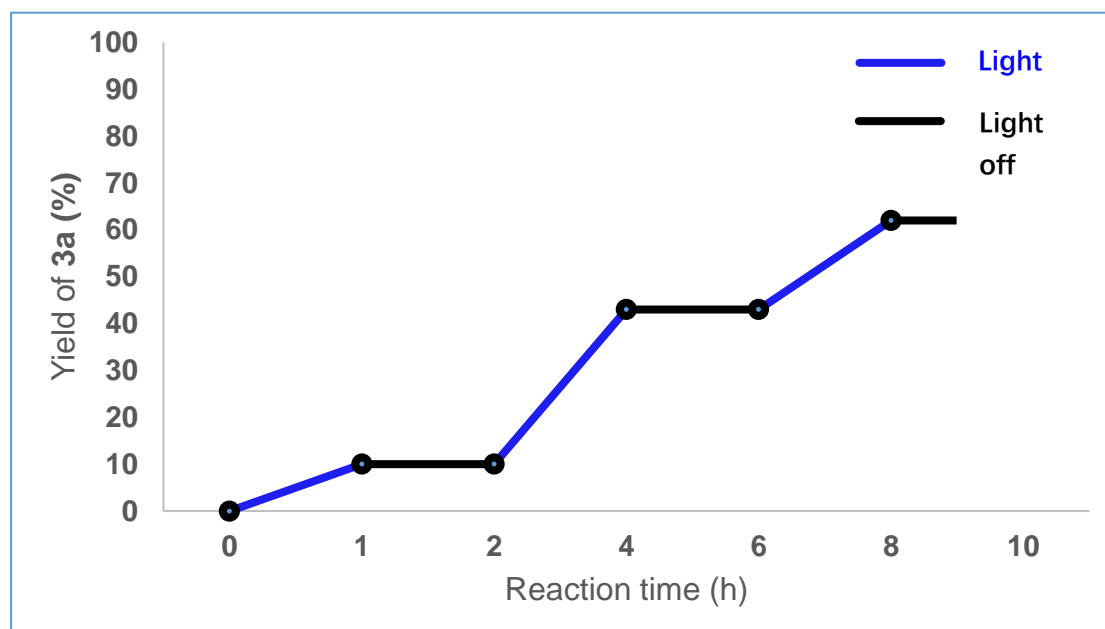


$E_{\text{ox}}(\mathbf{1a}) = 1.83 \text{ V vs. SCE}$

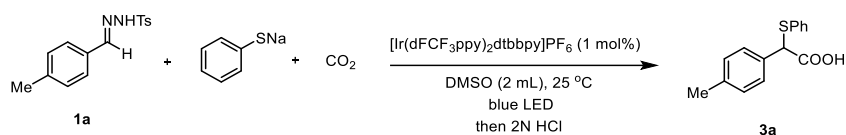
**Figure S4.** Cyclic voltammogram of N-tosylhydrazone **7a** in MeCN (with Ferrocene)

### “On-off” Experiments

Tosylhydrazone **1a** (0.2 mmol, 57.6 mg),  $\text{Cs}_2\text{CO}_3$  (0.6 mmol, 195.5 mg),  $[\text{Ir}(\text{dFCF}_3\text{ppy})_2\text{dtbbpy}]\text{PF}_6$  (0.002 mmol, 2.2 mg) were added into a 9 mL snap vial equipped with a stirring bar. The vial was evacuated and back filled with  $\text{CO}_2$  for three times. A solution of thiophenol **2a** (0.3 mmol) in dry DMSO (2 mL) was added by syringe. Then the solution was bubbled with  $\text{CO}_2$  for 3 minutes. After  $\text{CO}_2$  (14 mL) was injected by syringe the vial was sealed with wax. The reaction mixture was irradiated by a blue LED at 25 °C. Parallel reactions were carried out for various reaction times. The yield of carboxylic acid was determined by  $^1\text{H}$  NMR analysis using 1,3,5-trimethoxybenzene as internal standard after acidified with 2N HCl.



## Determination of the reaction quantum yield



To a 9 mL snap vial, **1a** (0.2 mmol, 1.0 eq), sodium thiophenolate (0.3 mmol, 1.5 eq), [Ir(dFCF<sub>3</sub>ppy)<sub>2</sub>dtbbpy]PF<sub>6</sub> (0.002 mmol, 1 mol%) were added. The vial was evacuated and back filled with CO<sub>2</sub> for three times, and then dry DMSO (6 mL) was added by syringe. After that, 2 mL solution was transferred from the vial into the cuvette by syringe, the solution in cuvette was bubbled with CO<sub>2</sub> for 5 minutes and equipped with a CO<sub>2</sub> balloon. The sample was placed in the quantum yield spectrometer and irradiated with a 455 nm LED for 300.76 s. After irradiation, the yield of the formed product was determined by <sup>1</sup>H NMR analysis of acidified crude reaction mixture using 1,3,5-trimethoxybenzene as internal standard. The yield of the formed product **3a** was determined to be 28.5%.

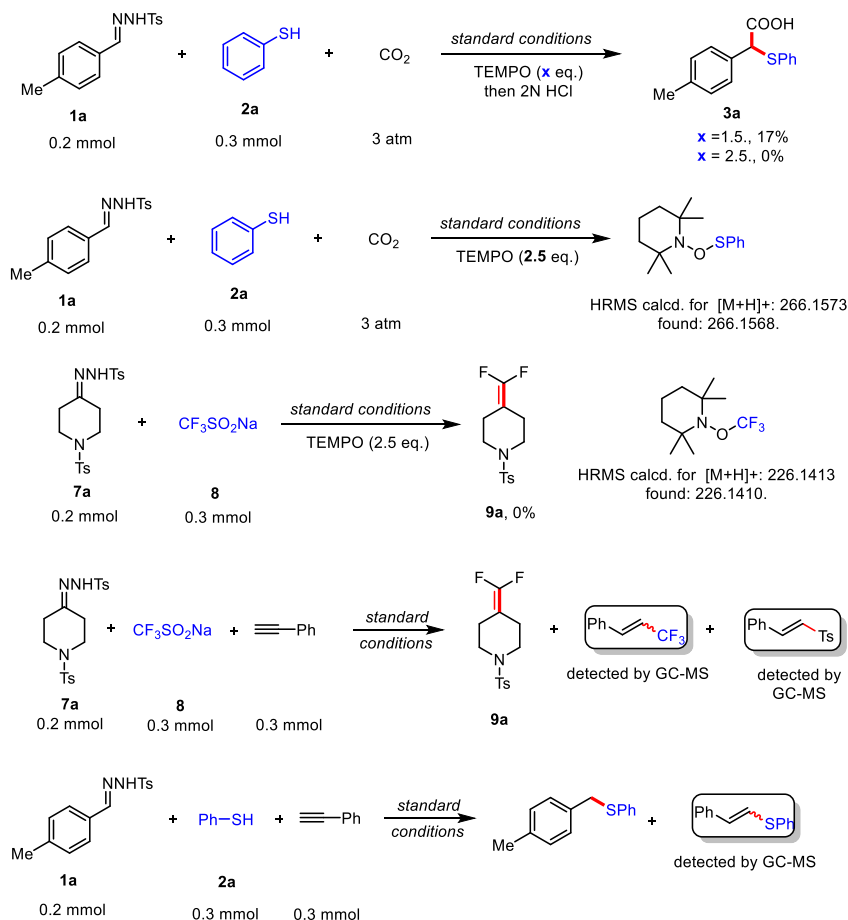
$$\Phi = \frac{\text{Number of product molecules}}{\text{Number of absorbed photons}} = \frac{N_{\text{prod}}}{N_{\text{ph,abs}}} = \frac{c_{\text{prod}} \cdot V \cdot N_A \cdot h \cdot c}{P_{\text{abs}} \cdot \Delta t \cdot \lambda} = 2.1\%$$

$c_{\text{prod}}$ : concentration of product **3a**;  $V$ : 2 mL;  $N_A$ :  $6.02 \cdot 10^{23}$ /mol;  $h$ : planck constant;  $c$ : speed of light;  $P_{\text{abs}}$ : absorbed optical power = 131.7 mW;  $\Delta t$ : illumination time = 300.76 s;  $\lambda$ : 455 nm.

The quantum yield ( $\Phi$ ) was calculated to be 2.1%

## Control experiments

### (A) Radical inhibiting and trapping experiments



To further prove the existence of radicals (thiyl radicals, trifluoromethyl radical and tosyl radical) in the proposed catalytic cycle, we attempted to use trapping reagents including TEMPO and phenylacetylene under the standard conditions. First, products **3a** and **9a** were not formed when the radical scavenger TEMPO (2.5 eq.) was added to the thiocarboxylation and *gem*-difluoroolefination reaction respectively, TEMPO-SPh and TEMPO-CF<sub>3</sub> adducts were detected by HRMS. Moreover, hydrotrifluoromethylation and hydrothiolation products were detected by GC-MS when phenylacetylene was added. It is to be noted that the proposed tosyl radical could be trapped in the reaction of **7a** with **8** by the phenylacetylene to give hydrosulfonylation product.

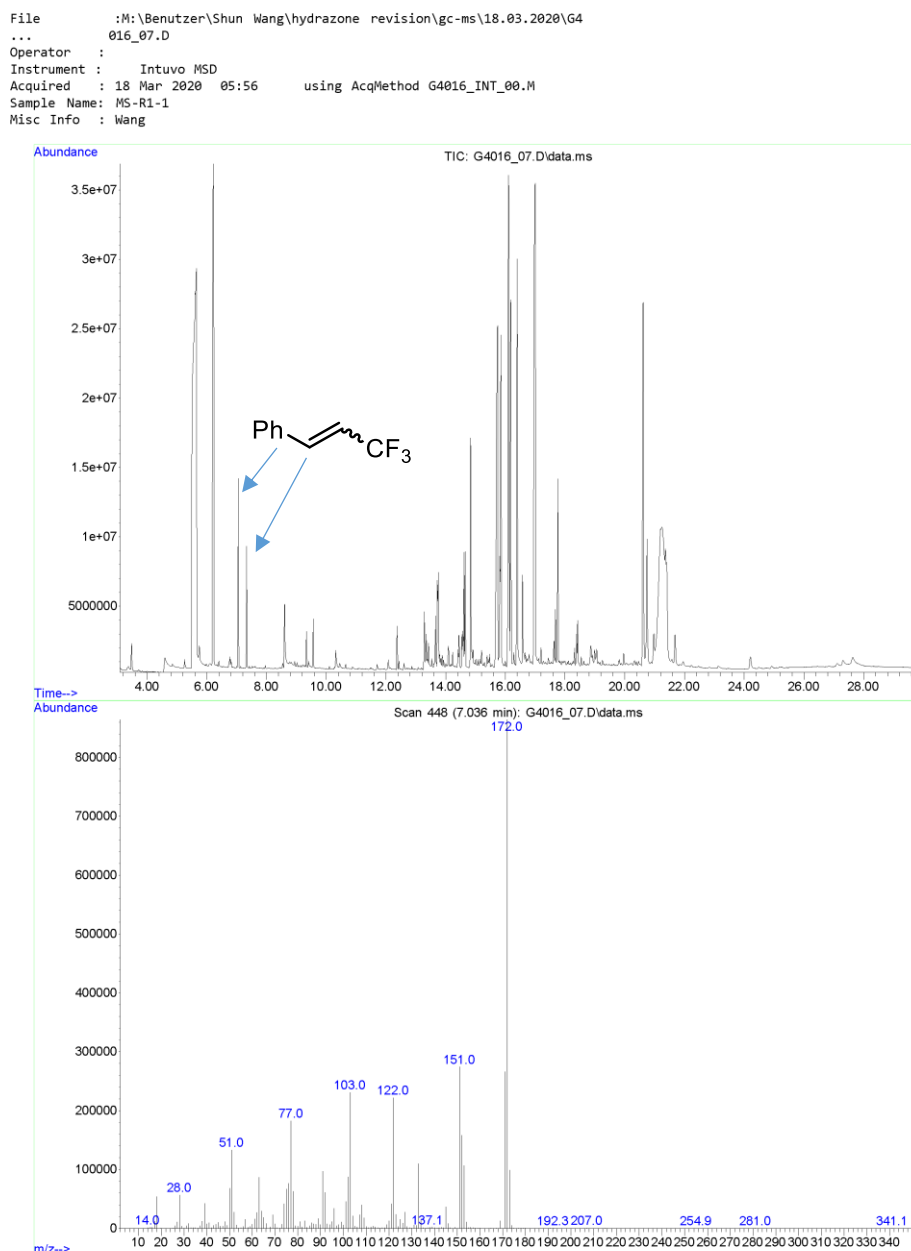
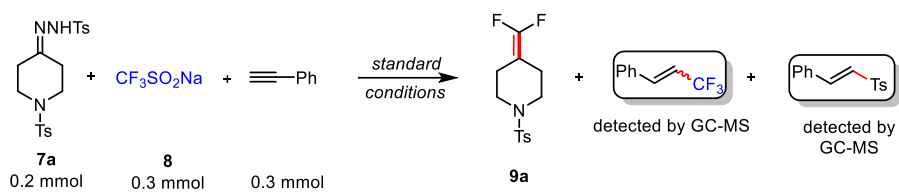


**Figure S5.** GC-MS report of hydrotrifluoromethylation product



File : M:\GCMS\_TEMP\Wang\G4016\_07.D  
 Operator :  
 Acquired : 18 Mar 2020 05:56 using AcqMethod G4016\_INT\_00.M  
 Instrument : Intuvo MSD  
 Sample Name : MS-R1-1  
 Misc Info : Wang  
 Vial Number : 33

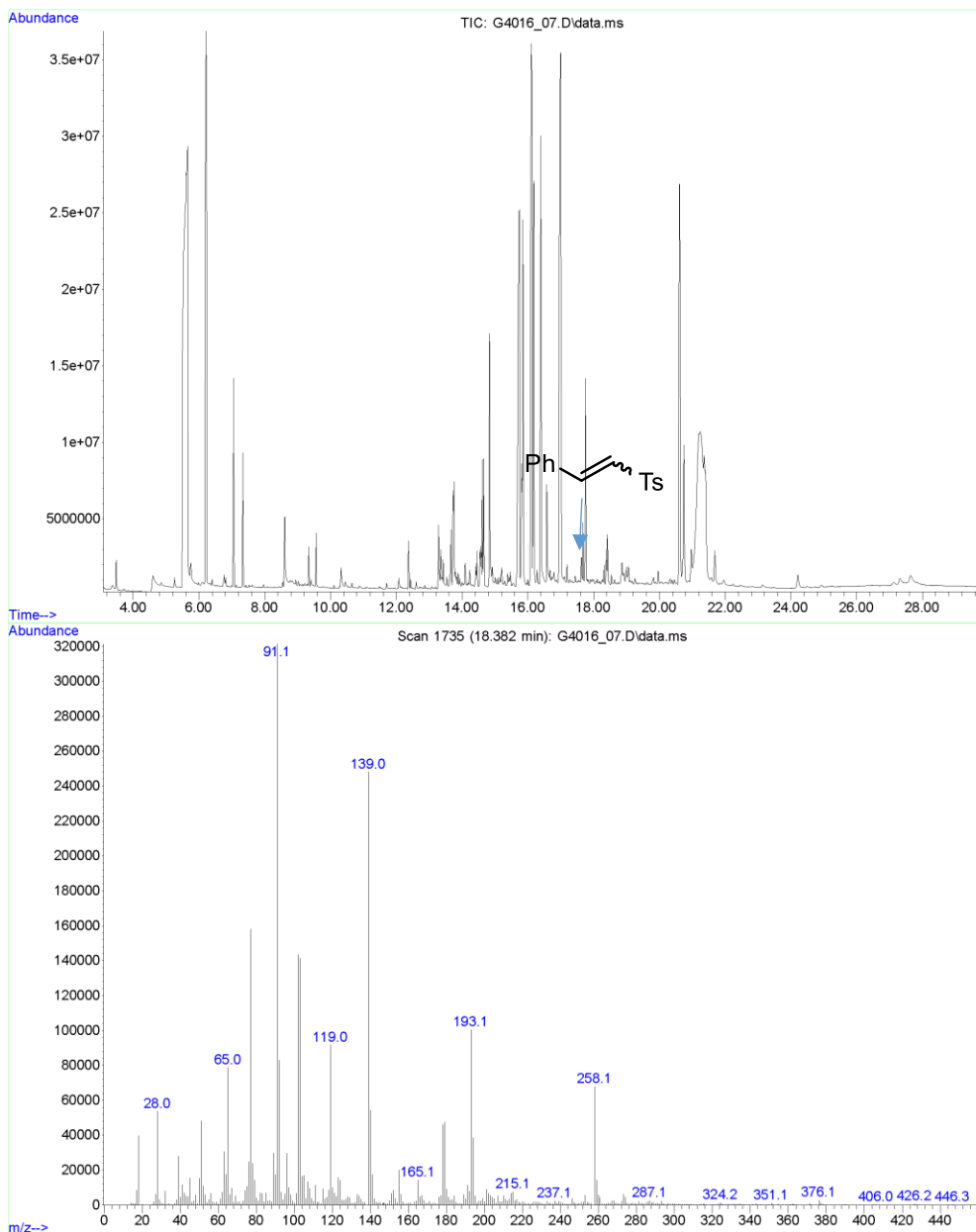
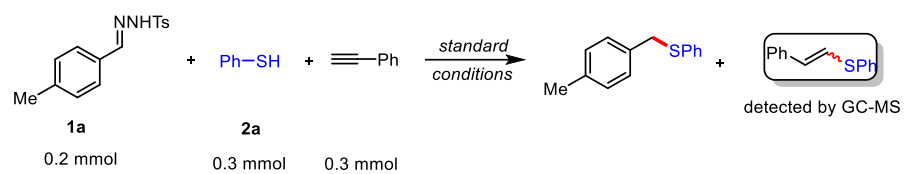


**Figure S6.** GC-MS report of hydrosulfonylation product





File : M:\GCMS\_TEMP\Wang\G3986\_00.D  
 Operator :  
 Acquired : 03 Mar 2020 22:09 using AcqMethod G3986\_INT\_00.M  
 Instrument : Intuvo MSD  
 Sample Name : SC-R 1  
 Misc Info : Wang  
 Vial Number: 13

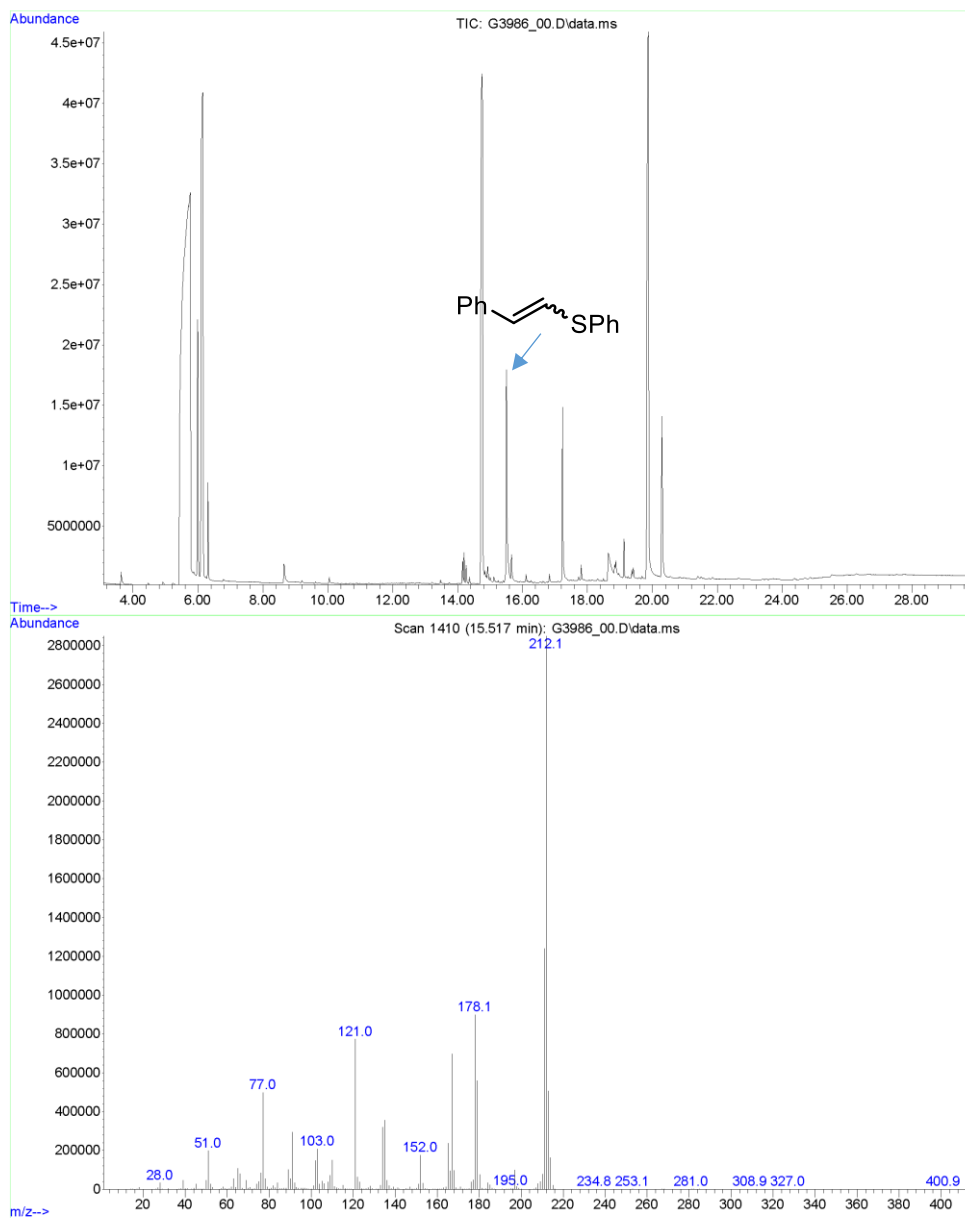
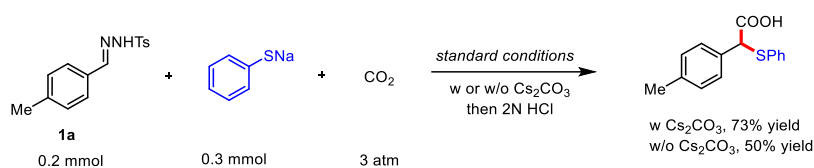
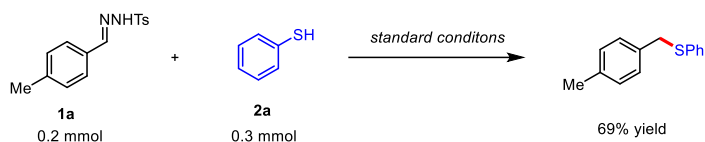


**Figure S7.** GC-MS report of hydrosulfonylation product

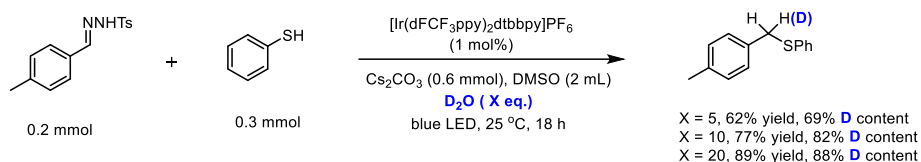
## (B) Using sodium thiophenolate in place of thiophenol



## (C) Control experiments in the absence of $\text{CO}_2$

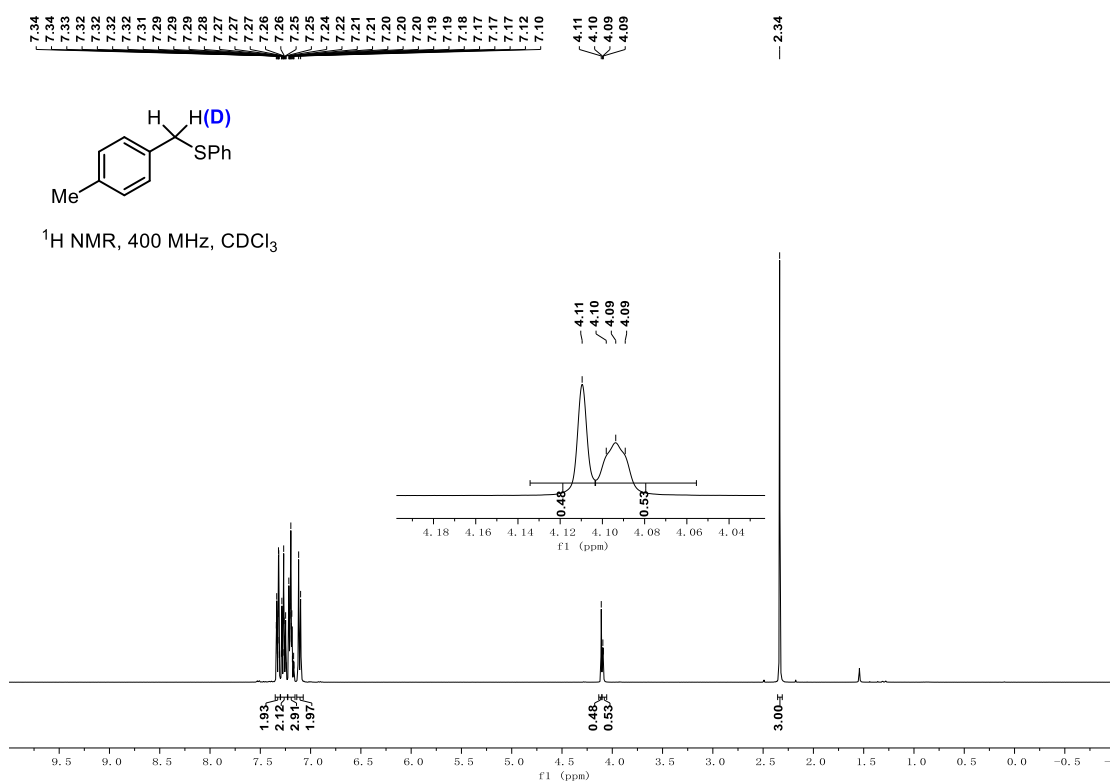


## (D) Deuterium incorporation experiments

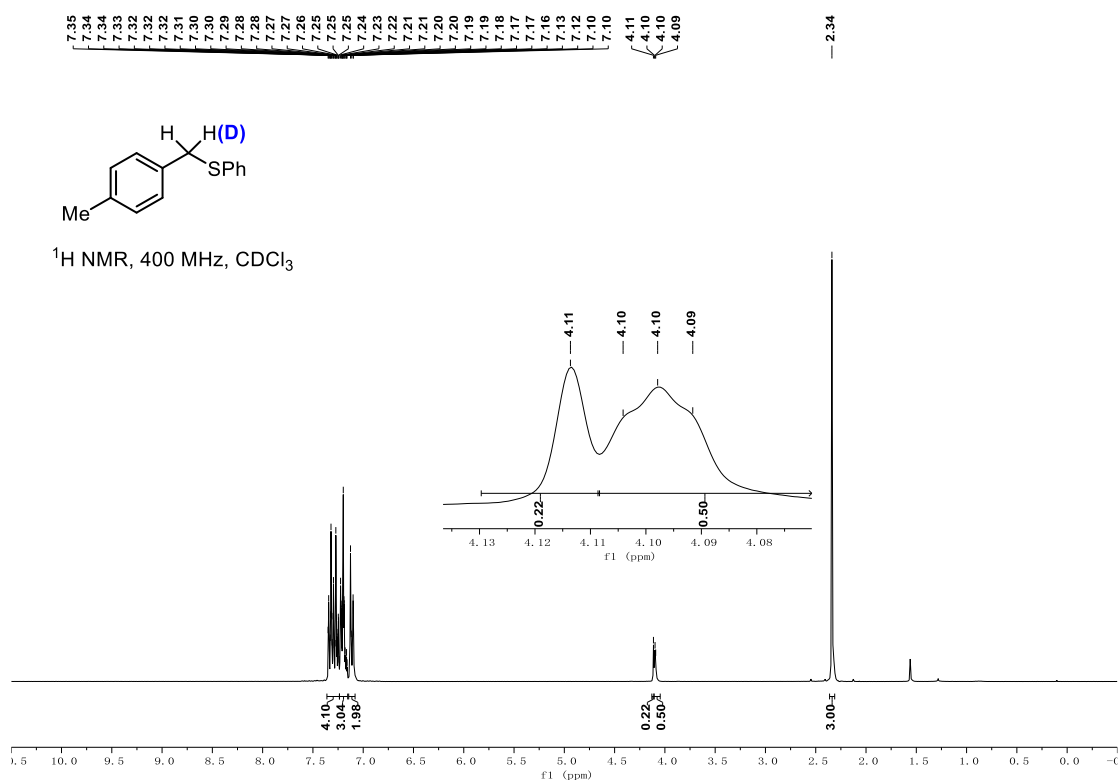


Tosylhydrazone **1a** (0.2 mmol, 57.6 mg),  $\text{Cs}_2\text{CO}_3$  (0.6 mmol, 195.5 mg),  $[\text{Ir}(\text{dFCF}_3\text{ppy})_2\text{dtbbpy}]\text{PF}_6$  (0.002 mmol, 2.2 mg) were added into a 9 mL snap vial equipped with a stirring bar. The vial was evacuated and back filled with  $\text{N}_2$  for three times. Then PhSH (0.3 mmol), dry DMSO (2.0 mL) and  $\text{D}_2\text{O}$  (x eq.) were added sequentially by syringes. The reaction mixtures were irradiated with a blue LED at 25 °C for 24 h. The reaction mixture was quenched with  $\text{H}_2\text{O}$  and extracted with EtOAc (10 mL \*3). The combined organic phase was then washed with  $\text{H}_2\text{O}$  (10 mL) and brine, dried over sodium sulfate, concentrated under vacuum. The residue was purified by silica gel flash chromatography (eluent: petroleum ether) to give the desired product. The recorded  $^1\text{H}$ -NMR spectra are depicted below.

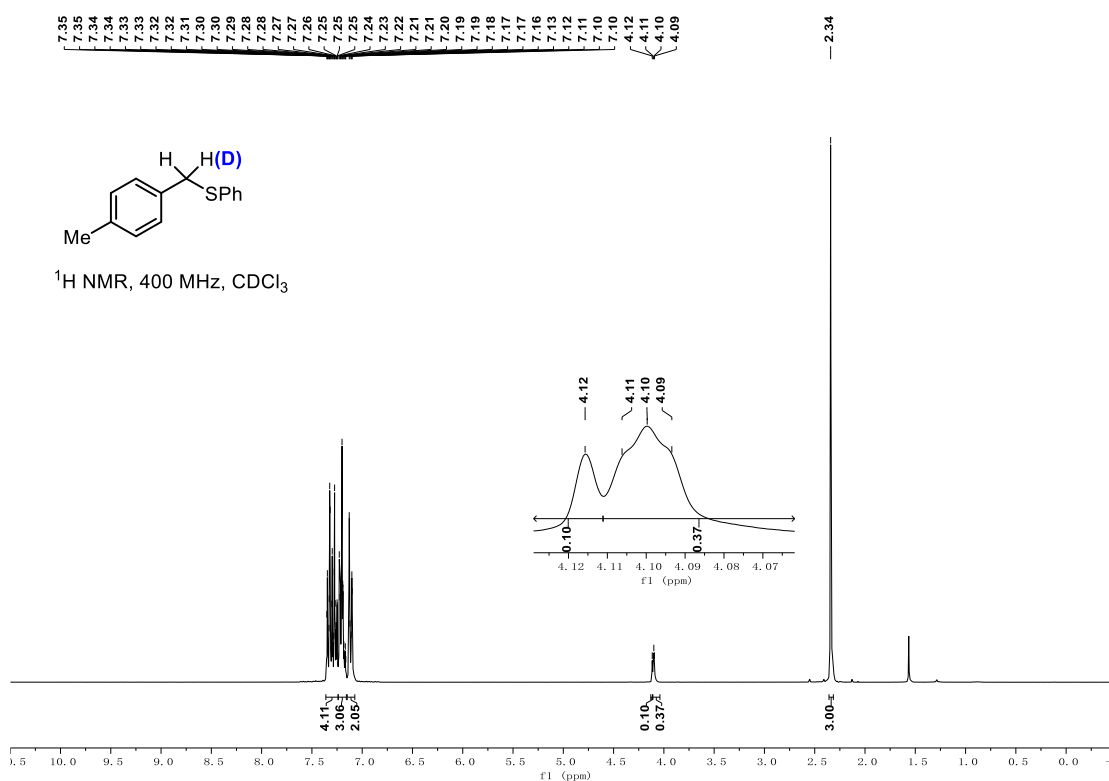
X = 5.0 eq.



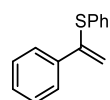
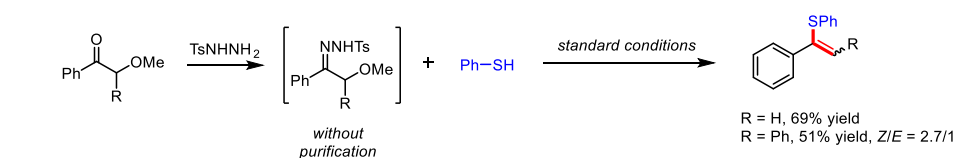
X = 10.0 eq.



X = 20 eq.

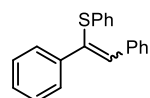


### (E) E1cb elimination



### phenyl(1-phenylvinyl)sulfane

The product was obtained as a colorless oil, 29.3 mg, yield = 69%. <sup>1</sup>H NMR (300 MHz, CDCl<sub>3</sub>) δ 7.56 – 7.50 (m, 2H), 7.32 – 7.28 (m, 2H), 7.22 – 7.11 (m, 4H), 7.16 – 7.11 (m, 2H), 5.57 (s, 1H), 5.21 (s, 1H). <sup>13</sup>C NMR (75 MHz, CDCl<sub>3</sub>) δ 144.43, 138.69, 133.75, 131.90, 129.01, 128.44, 128.26, 127.28, 127.12, 115.81. HRMS (EI) calcd for C<sub>14</sub>H<sub>12</sub>S [M]<sup>+</sup>: 212.0654, found: 212.0653.



### (Z) and (E)-(1,2-diphenylvinyl)(phenyl)sulfane

The product was obtained as a colorless oil, 29.4 mg, yield = 51% (Z/E = 2.7/1). <sup>1</sup>H NMR (400 MHz, CDCl<sub>3</sub>) (Z and E isomer) δ 7.75 (dd, J = 7.5, 1.7 Hz, 3H), 7.67 – 7.61 (m, 3H), 7.43 – 7.33 (m, 7H), 7.32 – 7.18 (m, 16H), 7.14 – 7.07 (m, 6H), 7.06 – 7.00 (m, 1H), 6.98 – 6.94 (m, 2H), 6.80 (s, 1H). <sup>13</sup>C NMR (101 MHz, CDCl<sub>3</sub>) (Z and E isomer) δ 145.19, 144.59, 139.96, 138.15, 136.94, 134.73, 126.94, 125.75, 124.94, 124.72,

124.51, 123.82, 122.37, 121.91, 121.38, 120.96, 120.40, 119.63, 116.34, 111.60, 109.92, 109.45, 109.40.  
HRMS (EI) calcd for  $C_{20}H_{16}S [M]^+$ : 288.0967, found: 288.0962.

### Luminescence quenching experiments

Luminescence spectra of  $[Ir(dFCF_3ppy)_2dtbbpy]PF_6$  ( $1.0 \times 10^{-5}M$ ) was collected as a function of different quenchers in degassed DMSO with excitation at 420 nm and data of emission intensity at 480 nm was recorded.

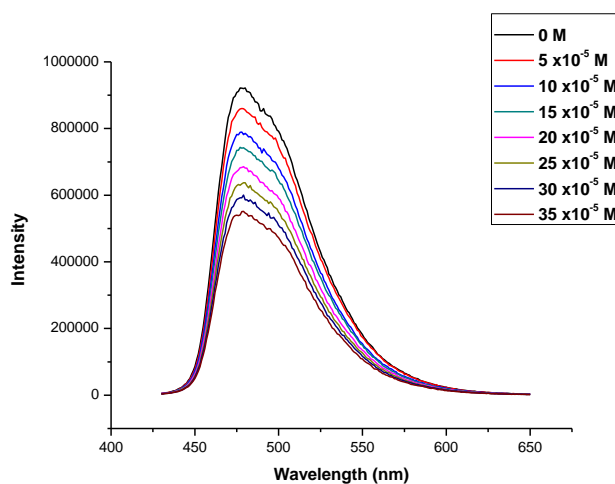


**Figure S8.** A solution of PhSNa in DMSO was added and its concentration was changed from 0 to  $35 \times 10^{-5} M$

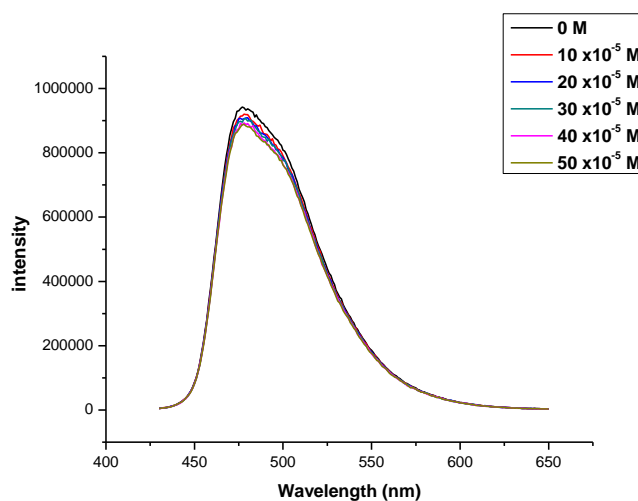


**Figure S9.** A solution of PhSH in DMSO was added and its concentration was changed from 0 to  $50 \times 10^{-5} M$

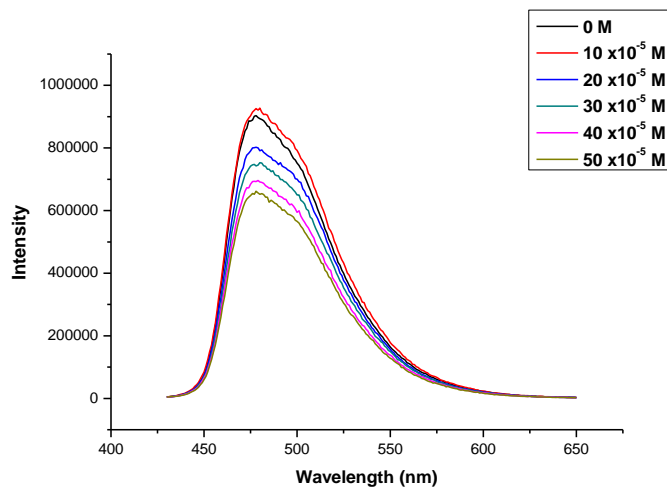


**Figure S10.** A solution of **1a** in DMSO was added and its concentration was changed from 0 to  $50 \times 10^{-5} \text{ M}$

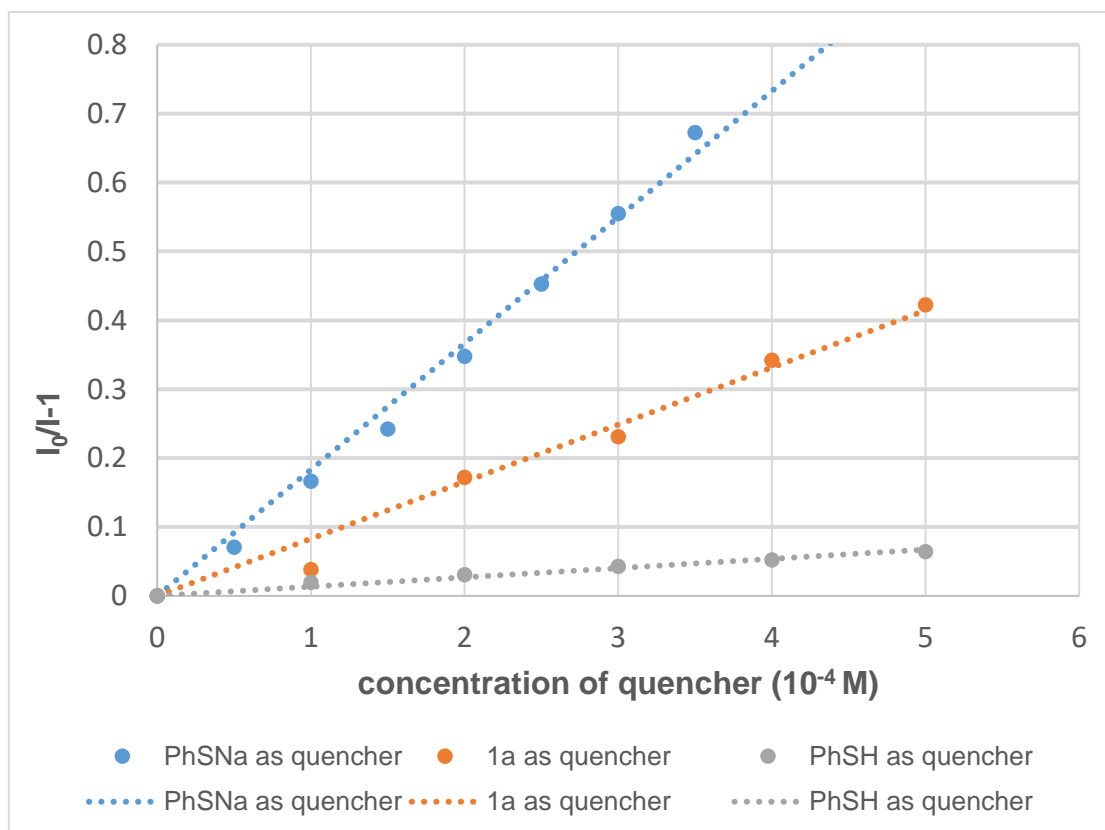


**Figure S11.** Stern-Volmer plot of  $[\text{Ir}(\text{dFCF}_3\text{ppy})_2\text{dtbbpy}]\text{PF}_6$  by different components

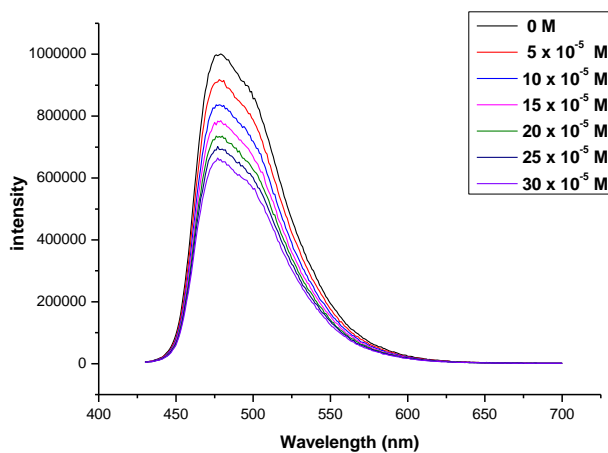


**Figure S12.** A solution of **8** ( $\text{CF}_3\text{SO}_2\text{Na}$ ) in DMSO was added and its concentration was changed from 0 to  $30 \times 10^{-5} \text{ M}$

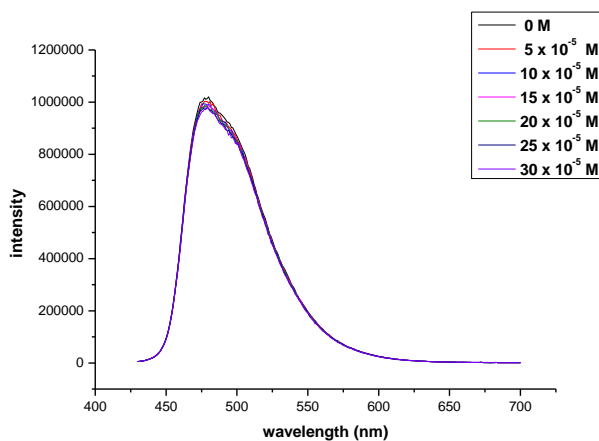


**Figure S13.** A solution of **7a** in DMSO was added and its concentration was changed from 0 to  $30 \times 10^{-5} \text{ M}$

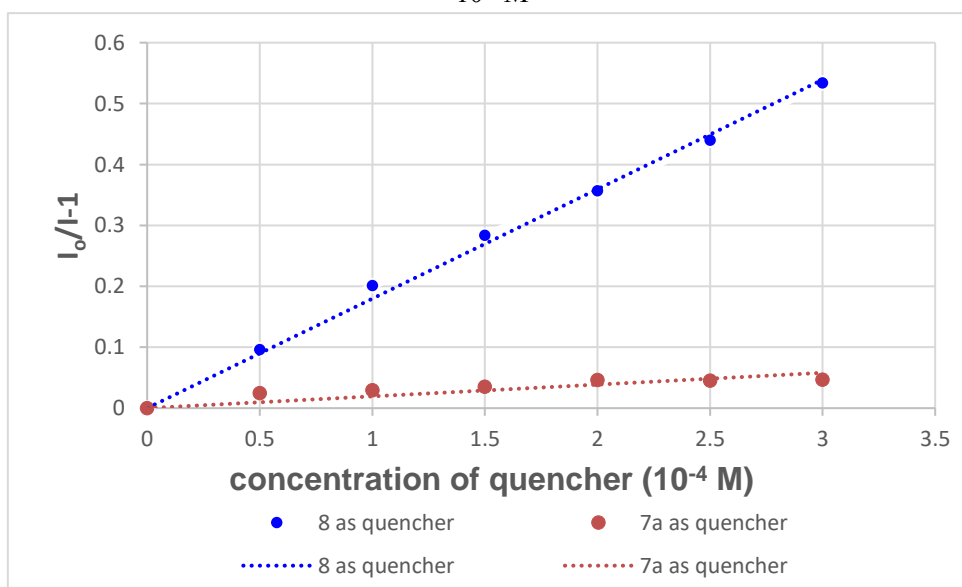
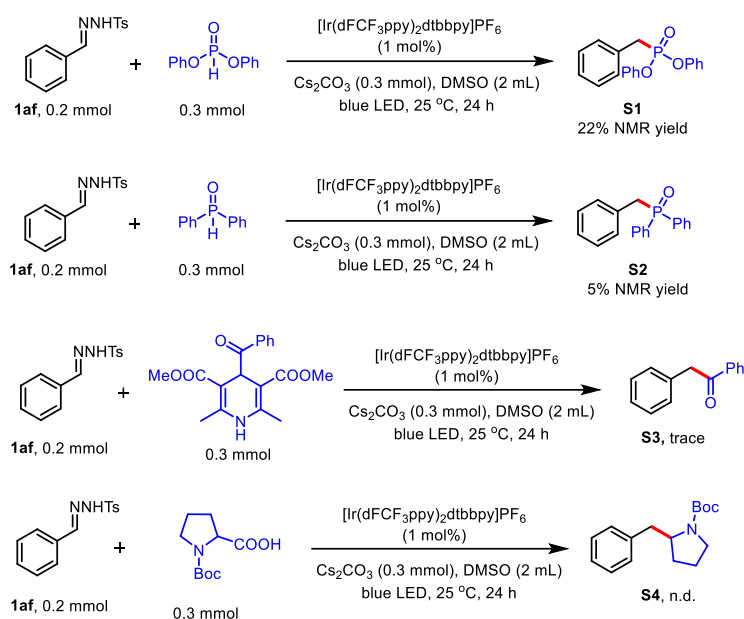


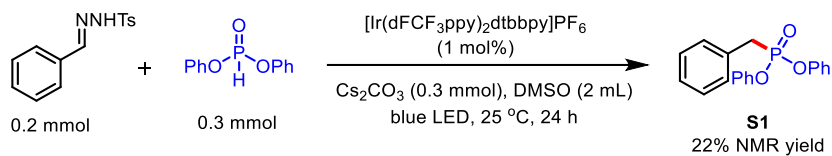
**Figure S14.** Stern-Volmer plot of  $[\text{Ir}(\text{dFCF}_3\text{ppy})_2\text{dtbbpy}]\text{PF}_6$  by different components

**Scheme S1.** Testing other radical precursors in the photoredox catalytic Wolff-Kishner processes



In addition to  $\text{CF}_3\text{SO}_2\text{Na}$  and thiols, other radical precursors including phosphite, phosphine oxide, 1,4-dihydropyridine and carboxylic acid are tested in this photocatalytic radical-anion relay sequence. As summarized in **Scheme S1**, under the unoptimized reaction conditions phosphite, phosphine oxide and dihydropyridine could react with N-tosylhydrazone **1af** to give corresponding carbanions which are then trapped by the protons in the reaction mixture. These results demonstrated that this novel strategy could be further extended in the production and transformation of other functionalized carbanions. Further studies along this lines are currently underway in our laboratory.





File :M:\GCMS\_TEMP\Wang\G4016\_03.D  
Operator :  
Acquired : 18 Mar 2020 03:37 using AcqMethod G4016\_INT\_00.M  
Instrument : Intuvo MSD  
Sample Name: SC-MR-3  
Misc Info : Wang  
Vial Number: 29

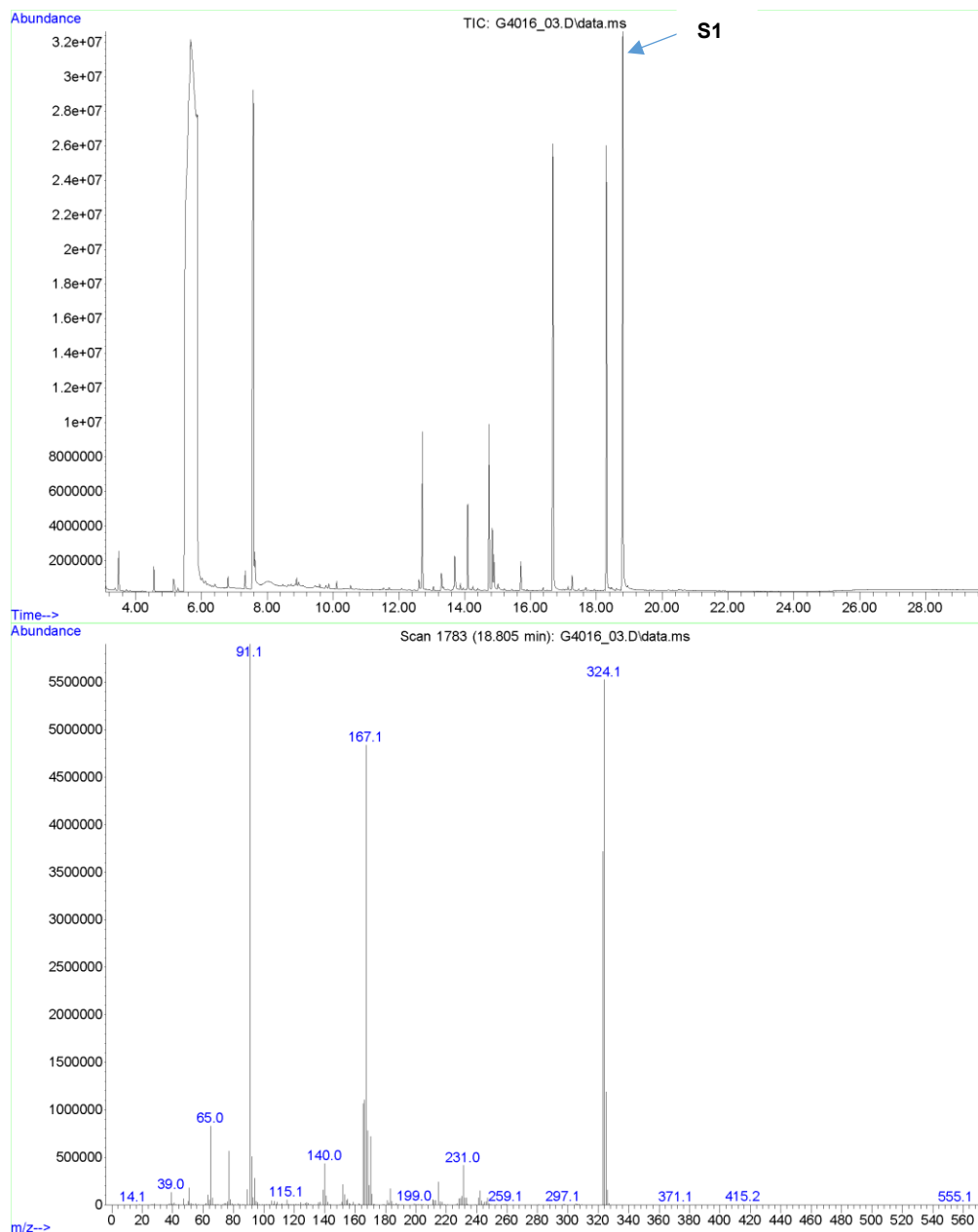


**Figure S15.** GC-MS report of product **S1**

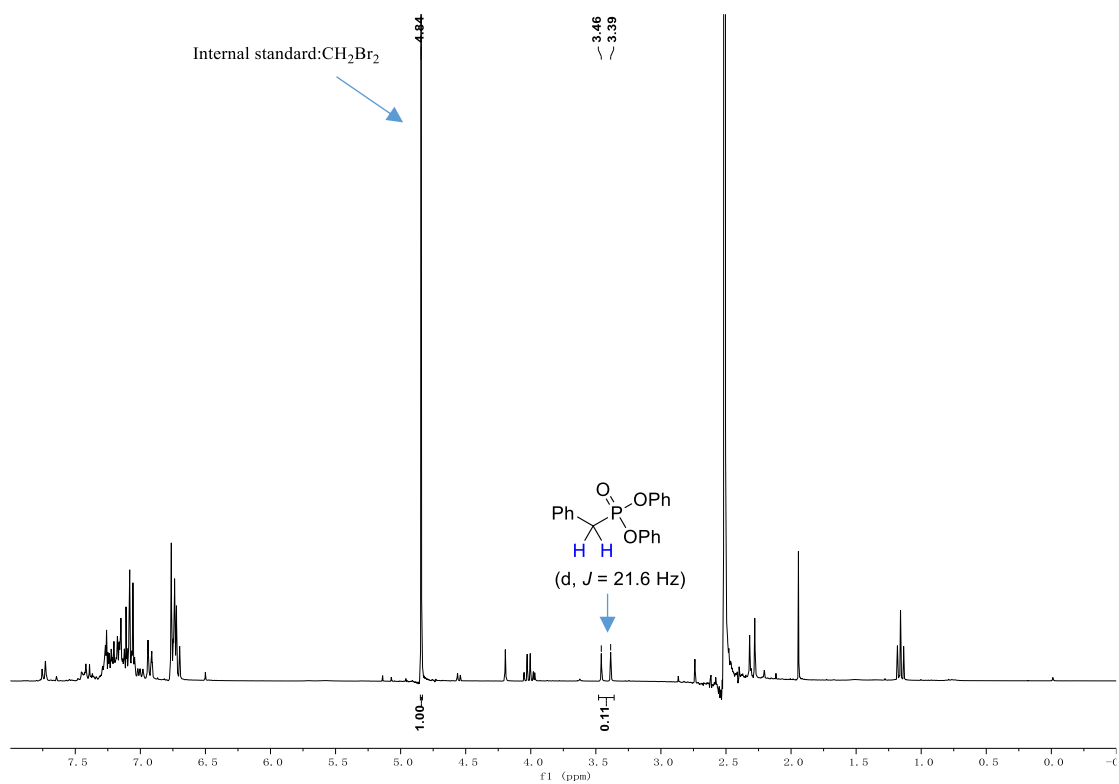
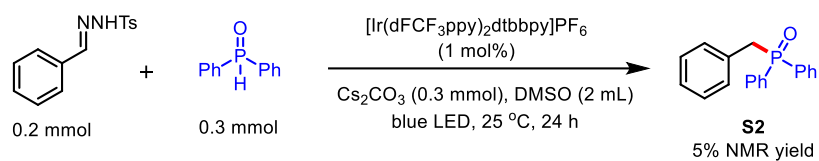


**Figure S16.** Crude <sup>1</sup>H NMR spectrum of the reaction between **1af** and diphenylphosphite<sup>[46]</sup>



File : M:\GCMS\_TEMP\Wang\G4016\_04.D  
 Operator :  
 Acquired : 18 Mar 2020 04:12 using AcqMethod G4016\_INT\_00.M  
 Instrument : Intuvo MSD  
 Sample Name: SC-MR-4  
 Misc Info : Wang  
 Vial Number: 30

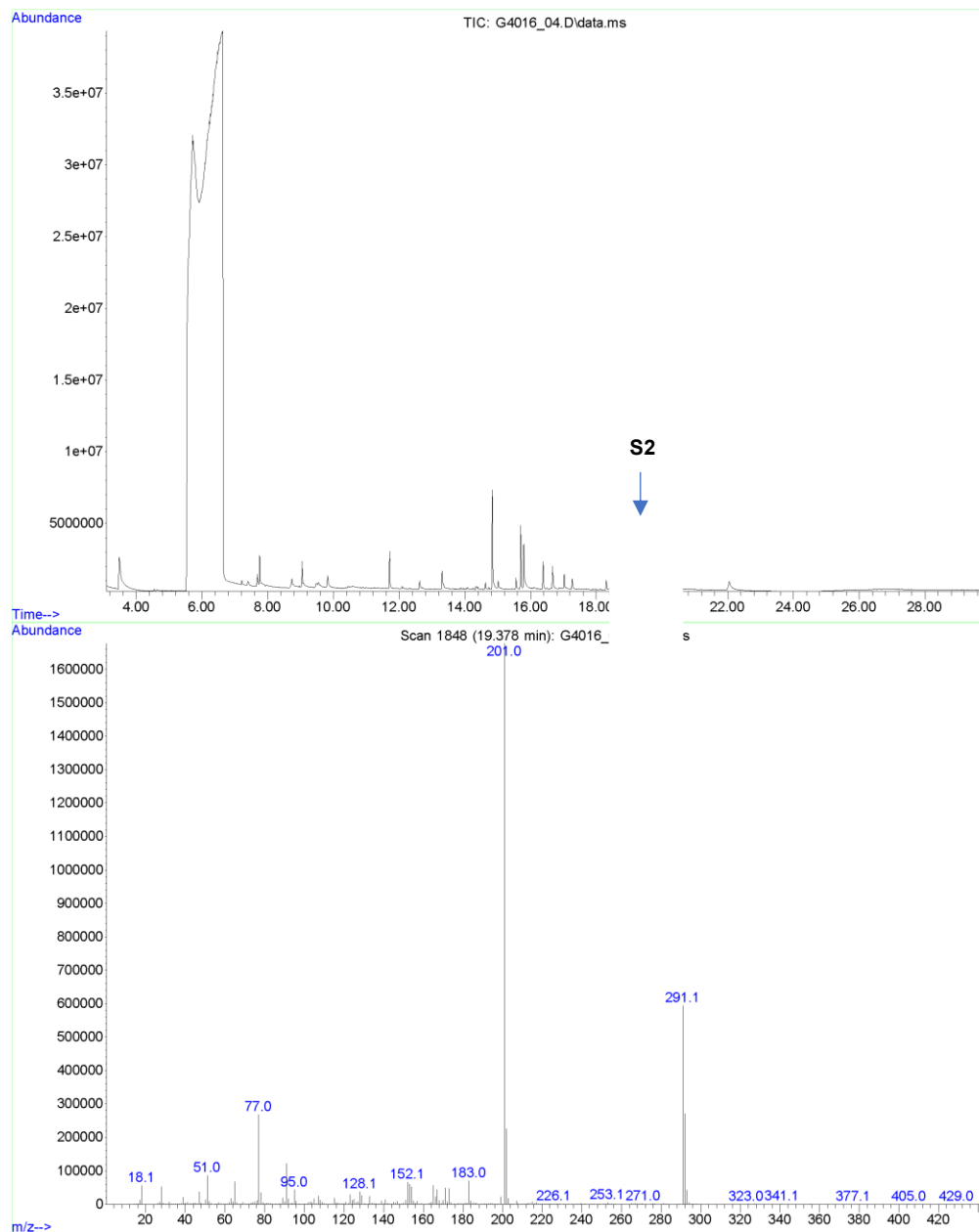
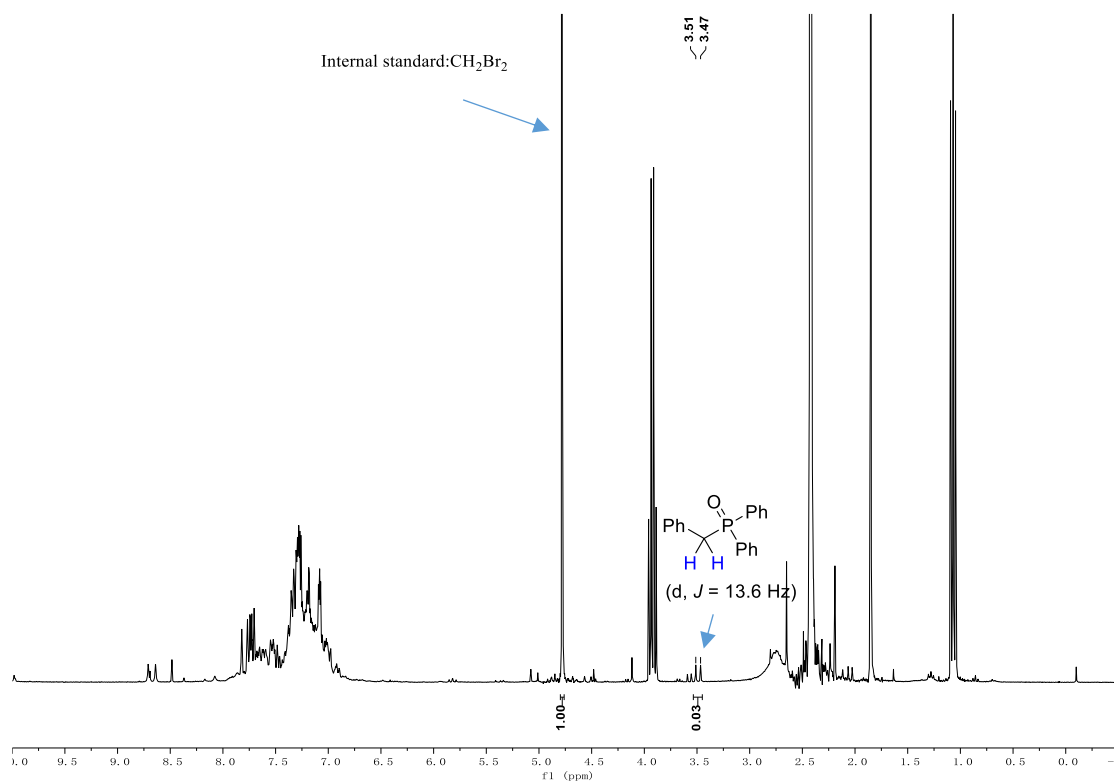
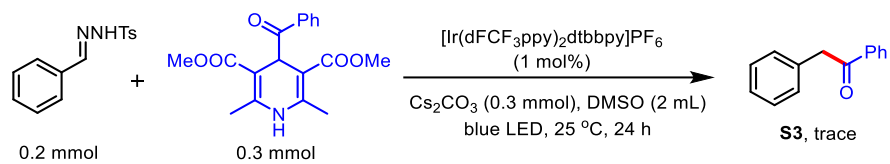


Figure S17. GC-MS report of product S2



**Figure S18.** Crude  $^1\text{H}$  NMR spectrum of the reaction between **1af** and diphenylphosphine oxide<sup>[47]</sup>



File : M:\GCMS\_TEMP\Wang\G4016\_01.D  
 Operator :  
 Acquired : 18 Mar 2020 02:28 using AcqMethod G4016\_INT\_00.M  
 Instrument : Intuvo MSD  
 Sample Name : SC-MR-1-1  
 Misc Info : Wang  
 Vial Number : 27

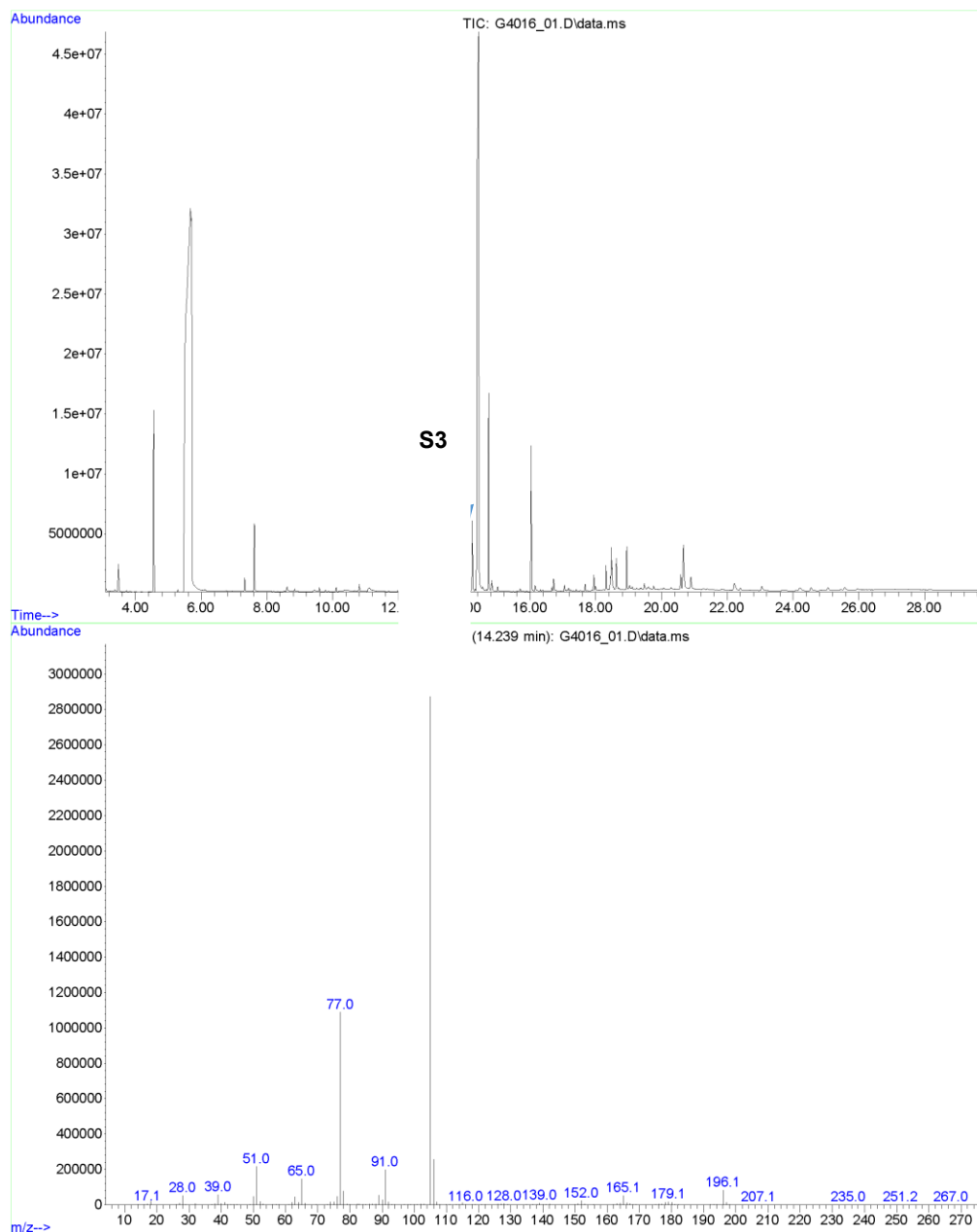


**Figure S19.** GC-MS report of product **S3**

**Table S8.** Diastereoselectivity of  $\alpha$ -sulfenyl carbanion addition to benzaldehyde<sup>a</sup>

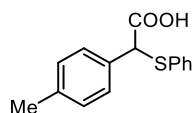
Reaction scheme showing the synthesis of **6a** from **1af**, **2a**, and **5**. The reaction conditions are:  $[\text{Ir}(\text{dFCF}_3\text{ppy})_2\text{dtbbpy}]\text{PF}_6$  (1 mol%), base (1.5 eq.), additive (1.5 eq.), DMSO (2 mL), blue LED, 25 °C.

Entry	Base	Additive	Yield of <b>6a</b>	<i>Syn:Anti</i> <sup>b</sup>
1	$\text{Cs}_2\text{CO}_3$	-	78%	44:56
2	$\text{Li}_2\text{CO}_3$	-	15%	44:56
3	$\text{MgCO}_3$	-	n.d.	-
4	$\text{Cs}_2\text{CO}_3$	$\text{MgClO}_4$	25%	43:57
5	$\text{Cs}_2\text{CO}_3$	$\text{LiCl}$	80%	51:49

<sup>a</sup>Reaction conditions: Unless otherwise noted, all reactions were carried out with **1af** (0.2 mmol), **2a** (0.3 mmol), **5** (0.8 mmol), base (0.3 mmol),  $[\text{Ir}(\text{dFCF}_3\text{ppy})_2\text{dtbbpy}]\text{PF}_6$  (1 mol%) in 2 mL DMSO, irradiation with blue LED (455 nm) at 25 °C for 24 hours, NMR yields were shown. <sup>b</sup>Determined by <sup>1</sup>H NMR analysis.

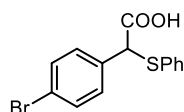
Regarding the diastereoselectivity of  $\alpha$ -sulfenyl carbanion addition to benzaldehyde, we attempted to improve the syn/anti ratio by adding chelating bases or additives. We tested commonly used chelating metal cation including  $\text{Li}^+$  and  $\text{Mg}^{2+}$  in this reaction. As demonstrated above, when  $\text{Cs}_2\text{CO}_3$  was replaced by  $\text{Li}_2\text{CO}_3$  or  $\text{MgCO}_3$ , the reaction efficiencies dropped dramatically whereas the diastereoselectivity remained unchanged. Adding  $\text{MgClO}_4$  (1.5 eq) did not improve diastereoselectivity but decreased the yield significantly. Moreover, using  $\text{LiCl}$  as additive afforded the product in retained efficiency and poor diastereoselectivity.

### 3.4.6 Characterization of products



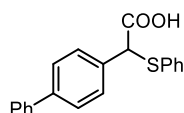
#### 2-(phenylthio)-2-(p-tolyl)acetic acid (3a)

Following the general procedure A, the product was obtained as a white solid, 41.2 mg, 81% yield; mp 108.3-110.6 °C.  $^1\text{H NMR}$  (300 MHz,  $\text{CDCl}_3$ )  $\delta$  7.41 – 7.36 (m, 2H), 7.36 – 7.30 (m, 2H), 7.28 – 7.24 (m, 3H), 7.14 (d,  $J = 7.8$  Hz, 2H), 4.87 (s, 1H), 2.34 (s, 3H).  $^{13}\text{C NMR}$  (75 MHz,  $\text{CDCl}_3$ )  $\delta$  175.69, 138.47, 133.56, 132.38, 131.90, 129.47, 129.05, 128.36, 128.03, 55.83, 21.16. **HRMS** (ESI) Calcd. for  $[\text{M}+\text{H}]^+$ : 259.0787. Found: 259.0791.



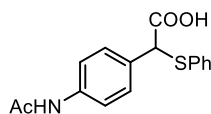
#### 2-(4-bromophenyl)-2-(phenylthio)acetic acid (3b)

Following the general procedure A, the product was obtained as a white solid, 42.4 mg, 66% yield. mp 110.5-114.8 °C.  $^1\text{H NMR}$  (300 MHz,  $\text{CDCl}_3$ )  $\delta$  9.12 (s, 1H), 7.41 – 7.33 (m, 2H), 7.32 – 7.25 (m, 2H), 7.25 – 7.13 (m, 5H), 4.74 (s, 1H).  $^{13}\text{C NMR}$  (75 MHz,  $\text{CDCl}_3$ )  $\delta$  175.86, 134.08, 132.97, 132.66, 131.85, 130.21, 129.15, 128.50, 122.70, 55.63. **HRMS** (ESI) Calcd. for  $[\text{M}+\text{H}]^+$ : 322.9736. Found: 322.9737.



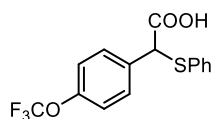
#### 2-(1,1'-biphenyl-4-yl)-2-(phenylthio)acetic acid (3c)

Following the general procedure A, the product was obtained as a white solid, 38.7 mg, 60% yield. mp 150.4-154.6 °C.  $^1\text{H NMR}$  (300 MHz,  $\text{CDCl}_3$ )  $\delta$  9.07 (s, 1H), 7.61 – 7.50 (m, 6H), 7.48 – 7.33 (m, 5H), 7.31 – 7.27 (m, 3H), 4.95 (s, 1H).  $^{13}\text{C NMR}$  (75 MHz,  $\text{CDCl}_3$ )  $\delta$  176.31, 141.45, 140.31, 133.89, 133.29, 132.64, 129.10, 128.94, 128.78, 128.22, 127.53, 127.46, 127.07, 55.94. **HRMS** (ESI) Calcd. for  $[\text{M}+\text{NH}_4]^+$ : 338.1209. Found: 338.1214.



#### 2-(4-acetamidophenyl)-2-(phenylthio)acetic acid (3d)

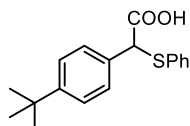
Following the general procedure A, the product was obtained as a white solid, 45.6 mg, 76% yield. mp 212.3-215.1 °C.  $^1\text{H NMR}$  (400 MHz,  $\text{DMSO}-d_6$ )  $\delta$  9.98 (s, 1H), 7.56 – 7.51 (m, 2H), 7.41 – 7.33 (m, 4H), 7.32 – 7.25 (m, 2H), 7.24 – 7.19 (m, 1H), 5.17 (s, 1H), 2.03 (s, 3H).  $^{13}\text{C NMR}$  (101 MHz,  $\text{DMSO}-d_6$ )  $\delta$  171.28, 168.39, 139.11, 134.36, 130.55, 130.40, 129.02, 128.80, 127.04, 118.99, 54.20, 24.02. **HRMS** (ESI) Calcd. for  $[\text{M}+\text{H}]^+$ : 302.0845. Found: 302.0852.



#### 2-(phenylthio)-2-(4-(trifluoromethoxy)phenyl)acetic acid (3e)

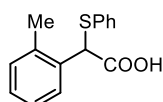
Following the general procedure A, the product was obtained as a white solid, 43.2 mg, 66% yield. mp

78.9-83.2 °C. **<sup>1</sup>H NMR** (300 MHz, CDCl<sub>3</sub>) δ 8.18 (s, 1H), 7.42 – 7.34 (m, 2H), 7.32 – 7.25 (m, 2H), 7.22 – 7.14 (m, 3H), 7.13 – 7.05 (m, 2H), 4.79 (s, 1H). **<sup>13</sup>C NMR** (75 MHz, CDCl<sub>3</sub>) δ 175.88, 149.20 (q, *J* = 2.1 Hz), 133.68, 133.08, 132.59, 130.11, 129.16, 128.57, 121.06, 55.43. **<sup>19</sup>F NMR** (282 MHz, CDCl<sub>3</sub>) δ -58.32. **HRMS** (ESI) Calcd. for [M+H]<sup>+</sup>: 329.0454. Found: 329.0456.



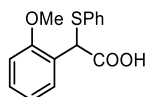
### 2-(4-(tert-butyl)phenyl)-2-(phenylthio)acetic acid (3f)

Following the general procedure, the product was obtained as a white solid, 43.3 mg, 72% yield. mp 105.7-110.8 °C. **<sup>1</sup>H NMR** (400 MHz, CDCl<sub>3</sub>) δ 8.42 (s, 1H), 7.35 – 7.25 (m, 6H), 7.20 – 7.14 (m, 3H), 4.79 (s, 1H), 1.22 (s, 9H). **<sup>13</sup>C NMR** (101 MHz, CDCl<sub>3</sub>) δ 176.42, 151.63, 133.74, 132.27, 131.71, 129.05, 128.14, 127.99, 125.75, 55.76, 34.59, 31.24. **HRMS** (ESI) Calcd. for [M+NH<sub>4</sub>]<sup>+</sup>: 318.1522. Found: 318.1529.



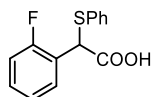
### 2-(phenylthio)-2-(o-tolyl)acetic acid (3g)

Following the general procedure A, the product was obtained as a yellow gel-like solid, 42.2 mg, 82% yield. **<sup>1</sup>H NMR** (400 MHz, CDCl<sub>3</sub>) δ 8.57 (s, 1H), 7.50 – 7.44 (m, 1H), 7.31 (dd, *J* = 6.5, 2.9 Hz, 2H), 7.21 – 7.15 (m, 3H), 7.14 – 7.05 (m, 3H), 5.05 (s, 1H), 2.28 (s, 3H). **<sup>13</sup>C NMR** (101 MHz, CDCl<sub>3</sub>) δ 176.41, 136.24, 133.63, 133.34, 132.58, 130.61, 129.06, 128.39, 128.25, 128.13, 126.60, 52.67, 19.50. **HRMS** (ESI) Calcd. for [M+H]<sup>+</sup>: 259.0787. Found: 259.0787.



### 2-(phenylthio)-2-(3-methoxyphenyl)acetic acid (3h)

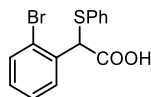
Following the general procedure A, the product was obtained as yellow gel-like solid, 36.9 mg, 67% yield. **<sup>1</sup>H NMR** (400 MHz, CDCl<sub>3</sub>) δ 7.97 (s, 1H), 7.40 (dd, *J* = 7.7, 1.7 Hz, 1H), 7.37 – 7.29 (m, 2H), 7.21 – 7.14 (m, 4H), 6.86 (td, *J* = 7.5, 1.1 Hz, 1H), 6.79 (dd, *J* = 8.3, 1.1 Hz, 1H), 5.30 (s, 1H), 3.72 (s, 3H). **<sup>13</sup>C NMR** (101 MHz, CDCl<sub>3</sub>) δ 176.22, 156.44, 134.04, 132.37, 129.59, 129.41, 128.89, 127.80, 123.85, 120.86, 110.86, 55.69, 49.53. **HRMS** (ESI) Calcd. for [M+H]<sup>+</sup>: 275.0739. Found: 275.0736.



### 2-(2-fluorophenyl)-2-(phenylthio)acetic acid (3i)

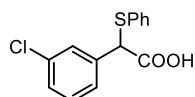
Following the general procedure A, the product was obtained as yellow gel-like solid, 30.2 mg, 58% yield. **<sup>1</sup>H NMR** (400 MHz, CDCl<sub>3</sub>) δ 10.69 (s, 1H), 7.48 (td, *J* = 7.6, 1.8 Hz, 1H), 7.35 – 7.30 (m, 2H), 7.23 – 7.14 (m, 4H), 7.04 (td, *J* = 7.6, 1.3 Hz, 1H), 6.95 (ddd, *J* = 9.7, 8.2, 1.2 Hz, 1H), 5.17 (s, 1H). **<sup>13</sup>C NMR** (101 MHz, CDCl<sub>3</sub>) δ 175.87, 161.15, 158.68, 133.10, 132.78, 130.09 (d, *J* = 8.4 Hz), 130.01 (d, *J* = 2.6 Hz), 129.08, 128.46, 124.42 (d, *J* = 3.6 Hz), 122.66 (d, *J* = 13.9 Hz), 115.43 (d, *J* = 21.8 Hz), 48.39 (d, *J* = 3.2 Hz). **HRMS** (ESI) Calcd. for [M+H]<sup>+</sup>: 263.0538. Found: 263.0537.





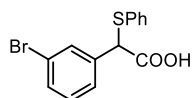
### 2-(2-bromophenyl)-2-(phenylthio)acetic acid (3j)

Following the general procedure A, the product was obtained as yellow gel-like solid, 40.4 mg, 63% yield.  $^1\text{H NMR}$  (400 MHz,  $\text{CDCl}_3$ )  $\delta$  7.57 (dd,  $J = 7.9, 1.7$  Hz, 1H), 7.48 (dd,  $J = 8.0, 1.3$  Hz, 1H), 7.39 – 7.32 (m, 2H), 7.24 – 7.18 (m, 4H), 7.09 (td,  $J = 7.7, 1.7$  Hz, 1H), 5.40 (s, 1H).  $^{13}\text{C NMR}$  (101 MHz,  $\text{CDCl}_3$ )  $\delta$  174.98, 134.84, 133.03, 132.95, 132.84, 130.26, 129.80, 129.09, 128.42, 127.85, 124.49, 54.92. **HRMS** (ESI) Calcd. for  $[\text{M}+\text{H}]^+$ : 322.9737. Found: 322.9736.



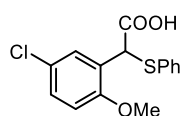
### 2-(3-chlorophenyl)-2-(phenylthio)acetic acid (3k)

Following the general procedure A, the product was obtained as a yellow gel-like solid, 35.6 mg, 64% yield.  $^1\text{H NMR}$  (300 MHz,  $\text{CDCl}_3$ )  $\delta$  8.95 (s, 1H), 7.45 (t,  $J = 1.8$  Hz, 1H), 7.40 – 7.35 (m, 2H), 7.33 – 7.23 (m, 6H), 4.82 (s, 1H).  $^{13}\text{C NMR}$  (75 MHz,  $\text{CDCl}_3$ )  $\delta$  175.78, 136.93, 134.53, 133.01, 132.62, 129.90, 129.16, 128.72, 128.69, 128.54, 126.77, 55.74. **HRMS** (ESI) Calcd. for  $[\text{M}-\text{H}]^-$ : 277.0092. Found: 277.0096.



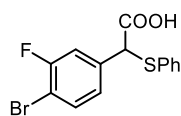
### 2-(3-bromophenyl)-2-(phenylthio)acetic acid (3l)

Following the general procedure A, the product was obtained as a white solid, 40.3 mg, 63% yield, mp 92.8 - 93.5 °C.  $^1\text{H NMR}$  (400 MHz,  $\text{CDCl}_3$ )  $\delta$  7.59 (d,  $J = 1.8$  Hz, 1H), 7.46 (d,  $J = 7.9$  Hz, 1H), 7.37 (t,  $J = 7.7$  Hz, 3H), 7.32 – 7.26 (m, 3H), 7.20 (t,  $J = 7.9$  Hz, 1H), 6.27 (s, 1H), 4.82 (s, 1H).  $^{13}\text{C NMR}$  (101 MHz,  $\text{CDCl}_3$ )  $\delta$  175.09, 137.26, 133.05, 132.66, 131.64, 131.59, 130.18, 129.17, 128.57, 127.24, 122.65, 55.67. **HRMS** (ESI) Calcd. for  $[\text{M}+\text{H}]^+$ : 322.9735. Found: 322.9736.



### 2-(5-chloro-2-methoxyphenyl)-2-(phenylthio)acetic acid (3m)

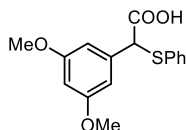
Following the general procedure A, the product was obtained as a white solid, 35.2 mg, 57% yield. mp 136.3-140.0 °C.  $^1\text{H NMR}$  (300 MHz,  $\text{CDCl}_3$ )  $\delta$  8.06 (s, 1H), 7.46 (d,  $J = 2.6$  Hz, 1H), 7.45 – 7.37 (m, 2H), 7.31 – 7.26 (m, 3H), 7.23 (dd,  $J = 8.8, 2.6$  Hz, 1H), 6.79 (d,  $J = 8.8$  Hz, 1H), 5.30 (s, 1H), 3.77 (s, 3H).  $^{13}\text{C NMR}$  (75 MHz,  $\text{CDCl}_3$ )  $\delta$  175.96, 155.06, 133.29, 132.79, 129.39, 129.24, 128.99, 128.21, 125.75, 125.54, 111.96, 55.99, 49.05. **HRMS** (ESI) Calcd. for  $[\text{M}+\text{H}]^+$ : 309.0347. Found: 309.0353.



### 2-(4-bromo-3-fluorophenyl)-2-(phenylthio)acetic acid (3n)

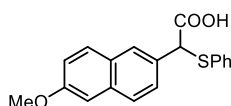
Following the general procedure A, the product was obtained as a white solid, 29.4 mg, 43% yield.  $^1\text{H NMR}$  (300 MHz,  $\text{CDCl}_3$ )  $\delta$  9.51 (s, 1H), 7.53 – 7.46 (m, 1H), 7.37 – 7.32 (m, 2H), 7.31 – 7.23 (m, 4H), 7.09

-7.04 (m, 1H), 4.80 (s, 1H).  $^{13}\text{C}$  NMR (75 MHz,  $\text{CDCl}_3$ )  $\delta$  175.40, 158.94 (d,  $J = 248.4$  Hz), 136.72 (d,  $J = 6.8$  Hz), 133.59, 133.16, 132.24, 129.23, 128.74, 125.44 (d,  $J = 3.5$  Hz), 116.76 (d,  $J = 23.7$  Hz), 109.30 (d,  $J = 21.0$  Hz), 55.43.  $^{19}\text{F}$  NMR (282 MHz,  $\text{CDCl}_3$ )  $\delta$  -106.44. HRMS (ESI) Calcd. for  $[\text{M}+\text{H}]^+$ : 340.9642. Found: 340.9644.



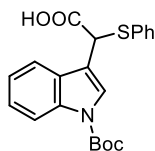
### 2-(3,5-dimethoxyphenyl)-2-(phenylthio)acetic acid (3o)

Following the general procedure A, the product was obtained as a white solid, 35.1 mg, 58% yield. mp 115.3-119.9 °C.  $^1\text{H}$  NMR (400 MHz,  $\text{CDCl}_3$ )  $\delta$  9.55 (s, 1H), 7.33 – 7.27 (m, 2H), 7.19 – 7.16 (m, 3H), 6.51 (d,  $J = 2.3$  Hz, 2H), 6.32 (t,  $J = 2.3$  Hz, 1H), 4.71 (s, 1H), 3.67 (s, 6H).  $^{13}\text{C}$  NMR (101 MHz,  $\text{CDCl}_3$ )  $\delta$  175.89, 160.86, 136.97, 133.37, 132.52, 129.08, 128.16, 106.54, 100.76, 56.35, 55.40. HRMS (ESI) Calcd. for  $[\text{M}+\text{H}]^+$ : 305.0842. Found: 305.0846.



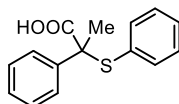
### 2-(6-methoxynaphthalen-2-yl)-2-(phenylthio)acetic acid (3p)

Following the general procedure A, the product was obtained as a white solid, 41.2 mg, 64% yield. mp 162.8-168.4 °C.  $^1\text{H}$  NMR (300 MHz,  $\text{CDCl}_3$ )  $\delta$  8.45 (s, 1H), 7.78 – 7.64 (m, 3H), 7.57 (dd,  $J = 8.5, 1.9$  Hz, 1H), 7.41 – 7.35 (m, 2H), 7.26 – 7.20 (m, 3H), 7.17 – 7.08 (m, 2H), 5.02 (s, 1H), 3.92 (s, 3H).  $^{13}\text{C}$  NMR (75 MHz,  $\text{CDCl}_3$ )  $\delta$  176.17, 158.12, 134.38, 133.37, 132.62, 129.86, 129.53, 129.05, 128.53, 128.14, 127.63, 127.48, 126.46, 119.25, 105.57, 56.36, 55.31. HRMS (ESI) Calcd. for  $[\text{M}+\text{H}]^+$ : 325.0893. Found: 325.0901.



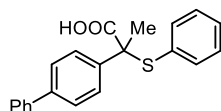
### 2-(1-(tert-butoxycarbonyl)-1H-indol-3-yl)-2-(phenylthio)acetic acid (3q)

Following the general procedure A, the product was obtained as a yellowish oil, 40.6 mg, 56% yield.  $^1\text{H}$  NMR (400 MHz,  $\text{CDCl}_3$ )  $\delta$  8.16 (d,  $J = 8.3$  Hz, 1H), 7.70 (d,  $J = 7.8$  Hz, 1H), 7.64 (s, 1H), 7.46 – 7.40 (m, 2H), 7.38 – 7.27 (m, 5H), 5.12 (s, 1H), 1.65 (s, 9H).  $^{13}\text{C}$  NMR (101 MHz,  $\text{CDCl}_3$ )  $\delta$  174.96, 149.34, 135.46, 133.26, 133.14, 129.03, 128.48, 128.43, 125.42, 124.90, 122.84, 119.40, 115.39, 113.75, 84.06, 47.68, 28.14. HRMS (ESI) Calcd. for  $[\text{M}-\text{H}]^-$ : 382.1119. Found: 382.1119.



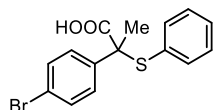
### 2-phenyl-2-(phenylthio)propanoic acid (3r)

Following the general procedure A, the product was obtained as a white solid, 31.2 mg, 62% yield. mp 96.4-98.9 °C.  $^1\text{H}$  NMR (300 MHz,  $\text{CDCl}_3$ )  $\delta$  7.57 – 7.50 (m, 2H), 7.39 -7.27 (m, 7H), 7.25 – 7.20 (m, 1H), 1.82 (s, 3H).  $^{13}\text{C}$  NMR (75 MHz,  $\text{CDCl}_3$ )  $\delta$  177.40, 139.85, 136.69, 130.86, 129.47, 128.69, 128.36, 127.92, 127.10, 59.57, 25.20. HRMS (ESI) Calcd. for  $[\text{M}+\text{NH}_4]^+$ : 276.1053. Found: 276.1055.



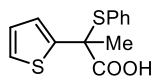
### 2-([1,1'-biphenyl]-4-yl)-2-(phenylthio)propanoic acid (3s)

Following the general procedure A, the product was obtained as a white solid, 52.9 mg, 79% yield. mp 138.4-142.3 °C.  $^1\text{H NMR}$  (300 MHz,  $\text{CDCl}_3$ )  $\delta$  8.90 (s, 1H), 7.56 – 7.46 (m, 6H), 7.39 – 7.21 (m, 6H), 7.19 – 7.11 (m, 2H), 1.77 (s, 3H).  $^{13}\text{C NMR}$  (75 MHz,  $\text{CDCl}_3$ )  $\delta$  178.57 , 140.68 , 140.28 , 138.80 , 136.75 , 130.91 , 129.48 , 128.78 , 128.69 , 127.62 , 127.48 , 127.04 , 126.95 , 59.21 , 25.00 . **HRMS** (ESI) Calcd. for  $[\text{M}+\text{NH}_4]^+$ : 352.1366. Found: 352.1373.



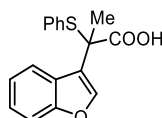
### 2-(4-bromophenyl)-2-(phenylthio)propanoic acid (3t)

Following the general procedure A, the product was obtained as a white solid, 38.3 mg, 57% yield. mp 111.7-114.5 °C.  $^1\text{H NMR}$  (400 MHz,  $\text{CDCl}_3$ )  $\delta$  8.99 (s, 1H), 7.41 – 7.31 (m, 4H), 7.27 (ddt,  $J = 10.0$ , 7.3, 1.6 Hz, 3H), 7.20 – 7.14 (m, 2H), 1.71 (s, 3H).  $^{13}\text{C NMR}$  (100 MHz,  $\text{CDCl}_3$ )  $\delta$  178.09 , 139.00 , 136.74 , 131.37 , 130.55 , 129.64 , 129.07 , 128.76 , 122.05 , 58.87 , 24.89 . **HRMS** (ESI) Calcd. for  $[\text{M}+\text{H}]^+$ : 336.9892. Found: 336.9889.



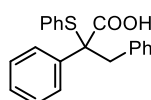
### 2-(phenylthio)-2-(thiophen-2-yl)propanoic acid (3u)

Following the general procedure A, the product was obtained as a white solid, 30.7 mg, 58% yield, mp 68.5 -69.6 °C.  $^1\text{H NMR}$  (400 MHz,  $\text{CDCl}_3$ )  $\delta$  7.43 – 7.36 (m, 3H), 7.32 – 7.26 (m, 3H), 7.14 (dd,  $J = 3.7$ , 1.2 Hz, 1H), 6.96 (dd,  $J = 5.1$ , 3.7 Hz, 1H), 1.92 (s, 3H).  $^{13}\text{C NMR}$  (101 MHz,  $\text{CDCl}_3$ )  $\delta$  176.91, 143.40, 136.69, 130.90, 129.81, 128.74, 126.95, 126.55, 126.12, 56.04, 25.72. **HRMS** (ESI) Calcd. for  $[\text{M}-\text{H}]^-$ : 263.0206. Found: 263.0213.



### 2-(benzofuran-3-yl)-2-(phenylthio)propanoic acid (3v)

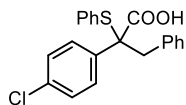
Following the general procedure A, the product was obtained as a white solid, 30.6 mg, 51% yield, mp 131.5 - 133.0 °C.  $^1\text{H NMR}$  (400 MHz,  $\text{CDCl}_3$ )  $\delta$  7.51 (t,  $J = 8.5$  Hz, 2H), 7.38 – 7.29 (m, 4H), 7.22 (dtd,  $J = 8.4$ , 4.1, 2.1 Hz, 3H), 6.64 (d,  $J = 0.9$  Hz, 1H), 1.92 (s, 3H).  $^{13}\text{C NMR}$  (101 MHz,  $\text{CDCl}_3$ )  $\delta$  174.74, 154.75, 154.11, 137.13, 130.00, 129.87, 128.69, 127.80, 124.71, 122.95, 121.17, 111.31, 106.15, 55.09, 23.03. **HRMS** (ESI) Calcd. for  $[\text{M}+\text{H}]^+$ : 299.0736. Found: 299.0737.



### 2,3-diphenyl-2-(phenylthio)propanoic acid (3w)

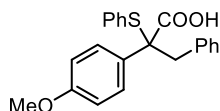
Following the general procedure A, the product was obtained as a oily solid, 42.1 mg, 63% yield.  $^1\text{H NMR}$  (400 MHz,  $\text{CDCl}_3$ )  $\delta$  7.32 – 7.28 (m, 2H), 7.26 – 7.15 (m, 6H), 7.14 – 7.00 (m, 5H), 6.83 (dt,  $J = 6.8$ , 1.5 Hz, 2H), 3.40 (dd,  $J = 93.5$ , 13.7 Hz, 2H).  $^{13}\text{C NMR}$  (101 MHz,  $\text{CDCl}_3$ )  $\delta$  176.41, 137.97, 136.21, 135.65,

130.92, 130.90, 129.37, 128.72, 128.51, 127.85, 127.66, 127.62, 126.76, 65.49, 44.50. **HRMS** (EI) Calcd. for [M-H]<sup>-</sup>: 333.0955. Found: 333.0962.



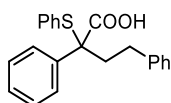
### 2-(4-chlorophenyl)-3-phenyl-2-(phenylthio)propanoic acid (3x)

Following the general procedure A, the product was obtained as a oily solid, 44.2 mg, 60% yield. **<sup>1</sup>H NMR** (300 MHz, CDCl<sub>3</sub>) δ 10.22 (s, 1H), 7.31 – 7.23 (m, 2H), 7.23 – 6.98 (m, 10H), 6.84 – 6.76 (m, 2H), 3.36 (dd, *J* = 92.5, 13.6 Hz, 2H). **<sup>13</sup>C NMR** (101 MHz, CDCl<sub>3</sub>) δ 176.28, 136.48, 136.12, 135.27, 133.51, 130.83, 130.63, 130.17, 129.58, 128.82, 127.89, 127.80, 126.96, 64.87, 44.67. **HRMS** (ESI) Calcd. for [M+H]<sup>+</sup>: 369.0711. Found: 369.0708.



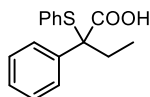
### 2-(4-methoxyphenyl)-3-phenyl-2-(phenylthio)propanoic acid (3y)

Following the general procedure A, the product was obtained as a oily solid, 44.8 mg, 62% yield. **<sup>1</sup>H NMR** (300 MHz, CDCl<sub>3</sub>) δ 7.85 (s, 1H), 7.41 – 7.36 (m, 2H), 7.35 – 7.10 (m, 8H), 6.97 – 6.86 (m, 2H), 6.84 – 6.75 (m, 2H), 3.81 (s, 3H), 3.46 (dd, *J* = 69.9, 13.5 Hz, 2H). **<sup>13</sup>C NMR** (75 MHz, CDCl<sub>3</sub>) δ 176.88, 158.78, 136.13, 135.78, 131.07, 130.93, 129.97, 129.78, 129.29, 128.69, 127.61, 126.68, 113.14, 64.91, 55.26, 44.50. **HRMS** (ESI) Calcd. for [M+Na]<sup>+</sup>: 387.1025. Found: 387.1027.



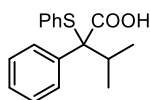
### 2,4-diphenyl-2-(phenylthio)butanoic acid (3z)

Following the general procedure A, the product was obtained as a oily solid, 51.9 mg, 75% yield. **<sup>1</sup>H NMR** (300 MHz, CDCl<sub>3</sub>) δ 8.53 (s, 1H), 7.41 – 7.34 (m, 2H), 7.31 – 7.14 (m, 8H), 7.13 – 7.00 (m, 5H), 2.67 (dtd, *J* = 50.4, 13.1, 4.7 Hz, 2H), 2.29 (dddd, *J* = 33.5, 13.9, 12.1, 4.7 Hz, 2H). **<sup>13</sup>C NMR** (75 MHz, CDCl<sub>3</sub>) δ 177.66, 141.31, 139.04, 136.48, 130.30, 129.47, 128.67, 128.40, 128.37, 128.31, 127.82, 127.52, 126.00, 64.53, 38.12, 31.29. **HRMS** (ESI) Calcd. for [M+H]<sup>+</sup>: 349.1257. Found: 349.1259.



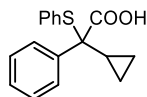
### 3-methyl-2-phenyl-2-(phenylthio)butanoic acid (3aa)

Following the general procedure A, the product was obtained as a yellow gel-like solid, 34.8 mg, 64% yield. **<sup>1</sup>H NMR** (300 MHz, CDCl<sub>3</sub>) δ 7.35 – 7.30 (m, 2H), 7.26 (d, *J* = 5.8 Hz, 2H), 7.23 – 7.20 (m, 2H), 7.18 – 7.07 (m, 4H), 2.16 – 1.91 (m, 2H), 0.94 (t, *J* = 7.3 Hz, 3H). **<sup>13</sup>C NMR** (75 MHz, CDCl<sub>3</sub>) δ 177.13, 139.04, 136.59, 130.43, 129.34, 128.58, 128.14, 127.62, 127.59, 65.55, 29.12, 9.27. **HRMS** (ESI) Calcd. for [M-H]<sup>-</sup>: 271.0798. Found: 271.0801.



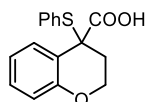
### 3-methyl-2-phenyl-2-(phenylthio)butanoic acid (3ab)

Following the general procedure A, the product was obtained as a white solid, mp 130.1-131.2 °C, 33.2 mg, 58% yield. <sup>1</sup>H NMR (400 MHz, CDCl<sub>3</sub>) δ 7.46 – 7.42 (m, 2H), 7.35 (d, *J* = 1.2 Hz, 1H), 7.33 – 7.31 (m, 2H), 7.28 (dd, *J* = 8.2, 1.6 Hz, 2H), 7.23 – 7.17 (m, 2H), 2.60 (p, *J* = 6.7 Hz, 1H), 1.00 (d, *J* = 6.7 Hz, 6H). <sup>13</sup>C NMR (101 MHz, CDCl<sub>3</sub>) δ 175.90, 135.99, 135.10, 131.26, 129.74, 129.25, 128.61, 127.42, 127.23, 70.22, 33.74, 19.36, 18.01. HRMS (ESI) Calcd. for [M-H]<sup>-</sup>: 285.0955. Found: 285.0958.



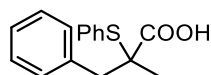
### 2-cyclopropyl-2-phenyl-2-(phenylthio)acetic acid (3ac)

Following the general procedure A, the product was obtained as a yellow gel-like solid, 45.1 mg, 79% yield. <sup>1</sup>H NMR (400 MHz, CDCl<sub>3</sub>) δ 7.43 – 7.38 (m, 2H), 7.37 – 7.32 (m, 2H), 7.24 (d, *J* = 7.8 Hz, 3H), 7.21 – 7.11 (m, 3H), 1.45 (ddd, *J* = 14.0, 8.4, 5.5 Hz, 1H), 0.51 (qq, *J* = 8.8, 4.4 Hz, 2H), 0.31 (dq, *J* = 10.5, 5.3, 4.8 Hz, 1H), 0.19 (dq, *J* = 8.6, 4.6, 4.1 Hz, 1H). <sup>13</sup>C NMR (101 MHz, CDCl<sub>3</sub>) δ 177.20, 136.67, 136.48, 130.92, 129.31, 129.06, 128.56, 127.83, 127.70, 66.06, 17.87, 4.25, 2.33. HRMS (ESI) Calcd. for [M-H]<sup>-</sup>: 283.0798. Found: 283.0803.



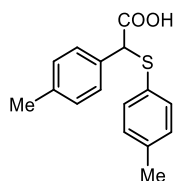
### 4-(phenylthio)chromane-4-carboxylic acid (3ad)

Following the general procedure A, the product was obtained as a white solid, mp 130.2 -131.4 °C, 24.3 mg, 43% yield. <sup>1</sup>H NMR (400 MHz, CDCl<sub>3</sub>) δ 7.75 (dd, *J* = 8.0, 1.5 Hz, 1H), 7.43 – 7.37 (m, 2H), 7.33 – 7.27 (m, 1H), 7.24 – 7.11 (m, 3H), 6.91 – 6.84 (m, 1H), 6.76 (dd, *J* = 8.3, 1.2 Hz, 1H), 4.32 (ddd, *J* = 11.4, 6.5, 3.2 Hz, 1H), 4.02 (ddd, *J* = 11.5, 8.9, 2.5 Hz, 1H), 2.47 (ddd, *J* = 14.4, 6.5, 2.5 Hz, 1H), 2.12 (ddd, *J* = 14.4, 8.9, 3.2 Hz, 1H). <sup>13</sup>C NMR (101 MHz, CDCl<sub>3</sub>) δ 177.23, 154.57, 136.66, 130.83, 130.49, 129.91, 129.84, 129.00, 120.52, 119.27, 117.37, 63.48, 53.80, 31.74. HRMS (ESI) Calcd. for [M+Na]<sup>+</sup>: 309.0556. Found: 309.0556.



### 2-methyl-3-phenyl-2-(phenylthio)propanoic acid (3ae)

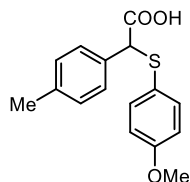
Following the slightly modified procedure A (reaction was conducted at 0 °C in 2 mL DMF, reaction time: 48 h), the product was obtained as a white solid, 26.5 mg, 49% yield. mp 101.5-105.3 °C. <sup>1</sup>H NMR (300 MHz, CDCl<sub>3</sub>) δ 7.42 – 7.27 (m, 6H), 7.26 – 7.14 (m, 4H), 6.50 (s, 1H), 2.21 – 2.00 (m, 2H), 1.01 (t, *J* = 7.2 Hz, 3H). <sup>13</sup>C NMR (75 MHz, CDCl<sub>3</sub>) δ 177.09, 139.03, 136.59, 130.43, 129.35, 128.58, 128.14, 127.63, 127.59, 65.55, 29.14, 9.27. HRMS (ESI) Calcd. for [M-H]<sup>-</sup>: 271.0798. Found: 271.0799.



### 2-(p-tolyl)-2-(p-tolylthio)acetic acid (4a)

Following the general procedure A, the product was obtained as a white solid, 40.6 mg, 75% yield. mp

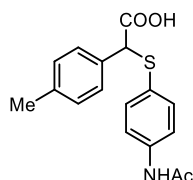
124.7-128.8 °C. **<sup>1</sup>H NMR** (300 MHz, CDCl<sub>3</sub>) δ 8.32 (s, 1H), 7.35 – 7.26 (m, 4H), 7.17 – 7.11 (m, 2H), 7.10 – 7.03 (m, 2H), 4.79 (s, 1H), 2.34 (s, 3H), 2.31 (s, 3H). **<sup>13</sup>C NMR** (75 MHz, CDCl<sub>3</sub>) δ 176.40 , 138.44 , 138.36 , 133.12 , 132.03 , 129.83 , 129.74 , 129.41 , 128.38 , 56.35 , 21.16 . **HRMS** (ESI) Calcd. for [M+H]<sup>+</sup>: 273.0944. Found: 273.0951.



#### 2-((4-methoxyphenyl)thio)-2-(p-tolyl)acetic acid (4b)

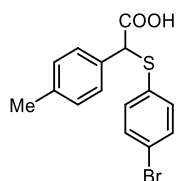
Following the general procedure A, the product was obtained as a white solid, 29.7 mg, 55% yield. mp 136.9-141.5 °C. **<sup>1</sup>H NMR** (400 MHz, CDCl<sub>3</sub>) δ 7.37 – 7.32 (m, 2H), 7.31 – 7.27 (m, 2H), 7.13 (d, *J* = 7.9 Hz, 2H), 6.83 – 6.75 (m, 2H), 4.71 (s, 1H), 3.78 (s, 3H), 2.34 (s, 3H). **<sup>13</sup>C NMR** (101 MHz, CDCl<sub>3</sub>) δ 176.34 , 160.22 , 138.27 , 136.03 , 132.12 , 129.35 , 128.43 , 123.53 , 114.58 , 57.04 , 55.28 , 21.15 .

**HRMS** (ESI) Calcd. for [M+NH<sub>4</sub>]<sup>+</sup>: 306.1158. Found: 306.1165.



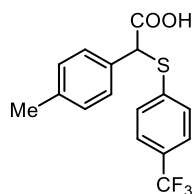
#### 2-((4-acetamidophenyl)thio)-2-(p-tolyl)acetic acid (4c)

Following the general procedure A, the product was obtained as a yellowish solid, 31.3 mg, 50% yield. mp 208.9-220.4 °C. **<sup>1</sup>H NMR** (400 MHz, DMSO-*d*<sub>6</sub>) δ 12.94 (s, 1H), 9.98 (s, 1H), 7.51 – 7.45 (m, 2H), 7.32 – 7.25 (m, 4H), 7.12 (d, *J* = 7.9 Hz, 2H), 5.01 (s, 1H), 2.26 (s, 3H), 2.02 (s, 3H). **<sup>13</sup>C NMR** (101 MHz, DMSO-*d*<sub>6</sub>) δ 171.32 , 168.37 , 138.92 , 137.23 , 133.43 , 132.57 , 129.00 , 128.26 , 126.97 , 119.29 , 55.40 , 24.01 , 20.69 . **HRMS** (ESI) Calcd. for [M+H]<sup>+</sup>: 316.1002. Found: 316.1009.



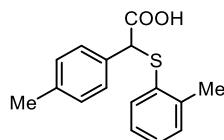
#### 2-((4-bromophenyl)thio)-2-(p-tolyl)acetic acid (4d)

Following the general procedure A, the product was obtained as a white solid, 41.5 mg, 62% yield. mp 118.5-122.4 °C. **<sup>1</sup>H NMR** (300 MHz, CDCl<sub>3</sub>) δ 8.10 (s, 1H), 7.45 – 7.35 (m, 2H), 7.33 – 7.27 (m, 2H), 7.25 – 7.18 (m, 2H), 7.17 – 7.12 (m, 2H), 4.83 (s, 1H), 2.34 (s, 3H). **<sup>13</sup>C NMR** (75 MHz, CDCl<sub>3</sub>) δ 176.00 , 138.68 , 134.09 , 132.49 , 132.14 , 131.49 , 129.55 , 128.36 , 122.50 , 55.80 , 21.17 . **HRMS** (ESI) Calcd. for [M+H]<sup>+</sup>: 336.9892. Found: 336.9890.



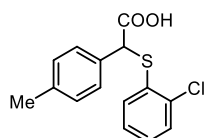
#### 2-(p-tolyl)-2-((4-(trifluoromethyl)phenyl)thio)acetic acid (4e)

Following the general procedure A, the product was obtained as a white solid, 43.1 mg, 66% yield. mp 109.1-119.8 °C. <sup>1</sup>H NMR (300 MHz, CDCl<sub>3</sub>) δ 9.11 (s, 1H), 7.54 – 7.46 (m, 2H), 7.45 – 7.39 (m, 2H), 7.38 – 7.33 (m, 2H), 7.21 – 7.12 (m, 2H), 4.97 (s, 1H), 2.35 (s, 3H). <sup>13</sup>C NMR (75 MHz, CDCl<sub>3</sub>) δ 176.05, 139.02 (d, *J* = 1.2 Hz), 138.96, 131.10, 130.50, 129.69, 128.32, 125.84 (q, *J* = 3.8 Hz), 54.74, 21.15. <sup>19</sup>F NMR (282 MHz, CDCl<sub>3</sub>) δ -63.14. HRMS (ESI) Calcd. for [M+NH<sub>4</sub>]<sup>+</sup>: 344.0927. Found: 344.0931.



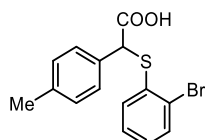
#### 2-(p-tolyl)-2-(o-tolylthio)acetic acid (4f)

Following the general procedure A, the product was obtained as a white solid, 38.7 mg, 71% yield. mp 91.3-93.9 °C. <sup>1</sup>H NMR (400 MHz, CDCl<sub>3</sub>) δ 9.51 (s, 1H), 7.37 – 7.34 (m, 3H), 7.21 – 7.13 (m, 4H), 7.10 (ddd, *J* = 8.7, 5.1, 2.5 Hz, 1H), 4.80 (s, 1H), 2.39 (s, 3H), 2.35 (s, 3H). <sup>13</sup>C NMR (101 MHz, CDCl<sub>3</sub>) δ 176.62, 140.17, 138.44, 132.90, 132.59, 131.93, 130.42, 129.43, 128.35, 128.06, 126.60, 55.04, 21.15, 20.54. HRMS (ESI) Calcd. for [M+H]<sup>+</sup>: 273.0944. Found: 273.0948.



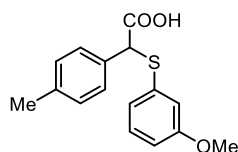
#### 2-((2-chlorophenyl)thio)-2-(p-tolyl)acetic acid (4g)

Following the general procedure A, the product was obtained as a white solid, 49.7 mg, 85% yield. mp 107.4-109.9 °C. <sup>1</sup>H NMR (300 MHz, CDCl<sub>3</sub>) δ 9.11 (s, 1H), 7.42-7.35 (m, 4H), 7.23 – 7.10 (m, 4H), 5.03 (s, 1H), 2.34 (s, 3H). <sup>13</sup>C NMR (75 MHz, CDCl<sub>3</sub>) δ 176.08, 138.65, 136.13, 132.88, 132.76, 131.21, 129.92, 129.53, 128.87, 128.38, 127.28, 53.87, 21.15. HRMS (ESI) Calcd. for [M+H]<sup>+</sup>: 293.0398. Found: 293.0395.



#### 2-((2-bromophenyl)thio)-2-(p-tolyl)acetic acid (4h)

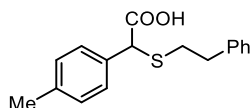
Following the general procedure A, the product was obtained as a white solid, 55.1 mg, 82% yield. mp 91.9-93.8 °C. <sup>1</sup>H NMR (400 MHz, CDCl<sub>3</sub>) δ 7.86 (s, 1H), 7.58 (dd, *J* = 7.9, 1.4 Hz, 1H), 7.41 – 7.36 (m, 2H), 7.35 (dd, *J* = 7.8, 1.7 Hz, 1H), 7.21 – 7.13 (m, 3H), 7.09 (td, *J* = 7.7, 1.7 Hz, 1H), 5.02 (s, 1H), 2.34 (s, 3H). <sup>13</sup>C NMR (101 MHz, CDCl<sub>3</sub>) δ 175.89, 138.70, 134.92, 133.26, 132.50, 131.11, 129.56, 128.86, 128.42, 127.94, 126.47, 54.22, 21.16. HRMS (ESI) Calcd. for [M+H]<sup>+</sup>: 336.9892. Found: 336.9895.



#### 2-((3-methoxyphenyl)thio)-2-(p-tolyl)acetic acid (4i)

Following the general procedure A, the product was obtained as a white solid, 44.3 mg, 77% yield. mp

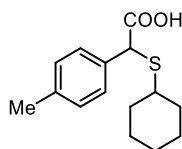
96.1-99.4 °C. **<sup>1</sup>H NMR** (400 MHz, CDCl<sub>3</sub>) δ 9.56 (s, 1H), 7.35 (d, *J* = 7.9 Hz, 2H), 7.21 – 7.12 (m, 3H), 6.98 (dt, *J* = 7.8, 1.2 Hz, 1H), 6.90 (t, *J* = 2.0 Hz, 1H), 6.80 (ddd, *J* = 8.3, 2.5, 1.0 Hz, 1H), 4.89 (s, 1H), 3.72 (s, 3H), 2.34 (s, 3H). **<sup>13</sup>C NMR** (101 MHz, CDCl<sub>3</sub>) δ 176.53, 159.67, 138.48, 134.80, 131.88, 129.83, 129.47, 128.37, 124.15, 116.87, 114.19, 55.69, 55.19, 21.12. **HRMS** (ESI) Calcd. for [M+H]<sup>+</sup>: 289.0893. Found: 289.0897.



#### 2-(phenethylthio)-2-(p-tolyl)acetic acid (4j)

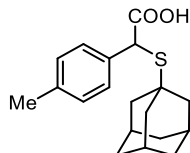
Following the general procedure A, the product was obtained as a yellowish oil, 23.1 mg, 40% yield.

**<sup>1</sup>H NMR** (400 MHz, CDCl<sub>3</sub>) δ 8.00 (s, 1H), 7.24 (d, *J* = 8.0 Hz, 2H), 7.22 – 7.16 (m, 2H), 7.15 – 7.10 (m, 1H), 7.09 – 7.04 (m, 4H), 4.43 (s, 1H), 2.81 – 2.64 (m, 4H), 2.26 (s, 3H). **<sup>13</sup>C NMR** (101 MHz, CDCl<sub>3</sub>) δ 176.72, 139.95, 138.29, 132.18, 129.42, 128.50, 128.48, 128.39, 126.44, 51.70, 35.68, 33.45, 21.13. **HRMS** (ESI) Calcd. for [M+H]<sup>+</sup>: 287.1100. Found: 287.1107.



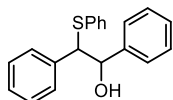
#### 2-(cyclohexylthio)-2-(p-tolyl)acetic acid (4k)

Following the general procedure A, the product was obtained as a white solid, 22.8 mg, 43% yield. mp 62.9-64.6 °C. **<sup>1</sup>H NMR** (400 MHz, CDCl<sub>3</sub>) δ 7.38 – 7.31 (m, 2H), 7.15 (d, *J* = 8.0 Hz, 2H), 4.61 (s, 1H), 2.74 (tt, *J* = 10.4, 3.7 Hz, 1H), 2.33 (s, 3H), 2.00 – 1.91 (m, 2H), 1.79 – 1.68 (m, 2H), 1.63 – 1.54 (m, 1H), 1.40 – 1.19 (m, 5H). **<sup>13</sup>C NMR** (101 MHz, CDCl<sub>3</sub>) δ 177.21, 138.10, 132.86, 129.38, 128.29, 50.17, 44.25, 33.19, 33.09, 25.79, 25.76, 25.68, 21.12. **HRMS** (ESI) Calcd. for [M+H]<sup>+</sup>: 265.1257. Found: 265.1262.



#### 2-(adamantan-1-ylthio)-2-(p-tolyl)acetic acid (4l)

Following the general procedure A, the product was obtained as a white solid, 21.6 mg, 34% yield. mp 173.3-175.6 °C. **<sup>1</sup>H NMR** (400 MHz, CDCl<sub>3</sub>) δ 10.80 (s, 1H), 7.37 – 7.31 (m, 2H), 7.13 (d, *J* = 7.9 Hz, 2H), 4.62 (s, 1H), 2.32 (s, 3H), 2.04 (q, *J* = 3.2 Hz, 3H), 1.93 – 1.85 (m, 6H), 1.73 – 1.60 (m, 6H). **<sup>13</sup>C NMR** (101 MHz, CDCl<sub>3</sub>) δ 178.34, 137.78, 134.01, 129.36, 128.14, 47.28, 46.77, 43.28, 36.05, 29.66, 21.07. **HRMS** (ESI) Calcd. for [M+H]<sup>+</sup>: 317.1570. Found: 317.1576.

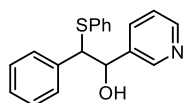


#### 1,2-diphenyl-2-(phenylthio)ethan-1-ol (6a)

Following the general procedure B, the product was obtained as a colorless oil, 47.0 mg, 78% yield; *syn*: *anti* = 44: 56; **<sup>1</sup>H NMR of (*syn*)- and (*anti*)-6a** (300 MHz, CDCl<sub>3</sub>) δ 7.23 – 7.01 (m, 26H), 6.97 – 6.89 (m, 2H), 4.95 (d, *J* = 5.8 Hz, 1H, *anti*), 4.85 (d, *J* = 8.6 Hz, 1H, *syn*), 4.36 (d, *J* = 5.8 Hz, 1H, *anti*), 4.27 (d, *J* = 8.6 Hz, 1H, *syn*), 3.24 (s, 1H, *syn*), 2.52 (s, 1H, *anti*). **<sup>13</sup>C NMR of (*syn*)- and (*anti*)-6a** (75 MHz, CDCl<sub>3</sub>) δ

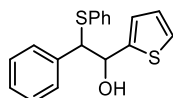


140.47, 140.31, 139.13, 137.50, 134.27, 134.06, 132.32, 132.21, 129.09, 128.83, 128.50, 128.15, 128.07, 127.96, 127.93, 127.80, 127.73, 127.60, 127.38, 127.30, 127.21, 126.83, 126.62, 76.80, 75.77, 63.87, 61.34. **HRMS** (ESI) Calcd. for  $[M+H]^+$ : 307.1151. Found: 307.1161.



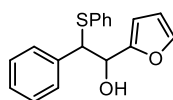
### 2-phenyl-2-(phenylthio)-1-(pyridin-3-yl)ethan-1-ol (6b)

Following the general procedure B, the product was obtained as a sticky oil, 46.7 mg, 76% yield; *syn: anti* = 44: 56; **<sup>1</sup>H NMR** of (*syn*)- and (*anti*)-6b (300 MHz, CDCl<sub>3</sub>) δ 8.23 – 8.10 (m, 4H), 7.41 (dt, *J* = 7.9, 2.0 Hz, 1H), 7.33 (dt, *J* = 7.9, 2.0 Hz, 1H), 7.21 – 7.12 (m, 9H), 7.12 – 7.02 (m, 8H), 7.02 – 6.89 (m, 4H), 4.96 (d, *J* = 5.8 Hz, 1H), 4.87 (d, *J* = 8.0 Hz, 1H), 4.29 (d, *J* = 5.8 Hz, 2H), 4.25 (d, *J* = 8.0 Hz, 1H). **<sup>13</sup>C NMR** of (*syn*)- and (*anti*)-6b (75 MHz, CDCl<sub>3</sub>) δ 148.38, 148.32, 148.06, 147.90, 138.47, 137.23, 136.84, 136.71, 134.72, 134.61, 134.06, 133.82, 132.23, 132.09, 129.05, 128.88, 128.82, 128.50, 128.21, 127.70, 127.50, 127.38, 127.35, 122.95, 122.90, 74.46, 73.52, 63.14, 61.14. **HRMS** (EI) Calcd. for C<sub>19</sub>H<sub>17</sub>NOS  $[M]^+$ : 307.1019. Found: 307.1018.



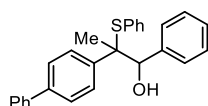
### 2-phenyl-2-(phenylthio)-1-(thiophen-2-yl)ethan-1-ol (6c)

Following the general procedure B, the product was obtained as a sticky oil, 38 mg, 61% yield; *syn: anti* = 53:47. **<sup>1</sup>H NMR** (400 MHz, CDCl<sub>3</sub>) δ 7.37 – 7.26 (m, 10H), 7.26 – 7.22 (m, 5H), 7.22 – 7.17 (m, 6H), 7.16 (dd, *J* = 5.1, 1.2 Hz, 1H), 7.13 – 7.06 (m, 2H), 6.95 – 6.86 (m, 2H), 6.78 (dd, *J* = 5.1, 3.6 Hz, 1H), 6.63 (dt, *J* = 3.6, 0.9 Hz, 1H), 5.33 (d, *J* = 6.1 Hz, 1H), 5.25 (d, *J* = 8.5 Hz, 1H), 4.50 (d, *J* = 6.1 Hz, 1H), 4.38 (d, *J* = 8.5 Hz, 1H), 3.50 (s, 1H), 2.76 (s, 1H). **<sup>13</sup>C NMR** (101 MHz, CDCl<sub>3</sub>) δ 144.15, 143.85, 139.00, 137.66, 134.07, 133.45, 132.83, 132.35, 129.02, 128.86, 128.41, 128.32, 128.16, 127.77, 127.67, 127.42, 126.24, 126.21, 125.32, 125.26, 125.03, 124.78, 72.82, 72.38, 63.73, 61.74. **HRMS** (ESI) Calcd. for  $[M+H]^+$ : 313.0715. Found: 313.0710.



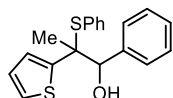
### 1-(furan-2-yl)-2-phenyl-2-(phenylthio)ethan-1-ol (6d)

Following the general procedure B, the product was obtained as a sticky oil, 41.6 mg, 70% yield; *syn: anti* = 48:52; **<sup>1</sup>H NMR** (400 MHz, CDCl<sub>3</sub>) δ 7.29 – 7.19 (m, 11H), 7.19 – 7.11 (m, 9H), 7.11 – 7.05 (m, 2H), 6.23 (dd, *J* = 3.3, 1.8 Hz, 1H), 6.16 – 6.11 (m, 2H), 6.07 – 6.04 (m, 1H), 5.03 (dd, *J* = 6.7, 2.2 Hz, 1H), 4.95 (dd, *J* = 8.2, 1.8 Hz, 1H), 4.61 (d, *J* = 6.7 Hz, 1H), 4.58 (d, *J* = 8.2 Hz, 1H), 3.21 (d, *J* = 3.8 Hz, 1H), 2.48 (d, *J* = 4.7 Hz, 1H). **<sup>13</sup>C NMR** (101 MHz, CDCl<sub>3</sub>) δ 153.09, 152.56, 141.91, 138.94, 137.90, 134.04, 133.39, 132.80, 132.34, 128.81, 128.78, 128.66, 128.37, 128.14, 128.12, 127.70, 127.58, 127.37, 127.33, 110.23, 110.10, 108.23, 108.16, 77.32, 77.00, 76.68, 70.36, 70.24, 60.35, 58.71. **HRMS** (ESI) Calcd. for  $[M+H]^+$ : 297.0944. Found: 297.0937.



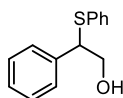
### 2-([1,1'-biphenyl]-4-yl)-1-phenyl-2-(phenylthio)propan-1-ol (6e)

Following the general procedure B, the product was obtained as a colorless oil, 41.4 mg, 52% yield; *syn:anti* = 46:54. **<sup>1</sup>H NMR** (400 MHz, CDCl<sub>3</sub>) δ 7.57 – 7.49 (m, 5H), 7.44 (s, 5H), 7.39 – 7.29 (m, 9H), 7.29 – 7.21 (m, 6H), 7.20 – 7.14 (m, 3H), 7.14 – 7.04 (m, 8H), 7.04 – 6.95 (m, 4H), 6.88 (ddt, *J* = 13.9, 7.0, 1.5 Hz, 4H), 5.19 (s, 1H), 4.78 (s, 1H), 3.23 (s, 1H), 3.14 (s, 1H), 1.47 (s, 3H), 1.43 (s, 3H). **<sup>13</sup>C NMR** (101 MHz, CDCl<sub>3</sub>) δ 141.51, 140.41, 140.28, 139.83, 139.49, 139.36, 138.54, 138.50, 136.89, 136.29, 131.30, 130.90, 129.06, 128.94, 128.80, 128.75, 128.68, 128.63, 128.53, 128.34, 127.83, 127.73, 127.35, 127.33, 127.31, 127.19, 126.94, 126.83, 126.19, 126.08, 79.54, 78.66, 62.60, 60.30, 22.89, 18.78. **HRMS** (ESI) Calcd. for [M+Na]<sup>+</sup>: 419.1440. Found: 419.1441.



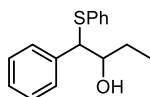
### phenyl-2-(phenylthio)-2-(thiophen-2-yl)propan-1-ol (6f)

Following the general procedure B, the product was obtained as a colorless oil, 48.9 mg, 75% yield; *syn:anti* = 46:54. **<sup>1</sup>H NMR** (400 MHz, CDCl<sub>3</sub>) δ 7.53 – 7.47 (m, 2H), 7.45 – 7.38 (m, 1H), 7.37 – 7.29 (m, 7H), 7.27 – 7.14 (m, 9H), 7.14 – 7.08 (m, 2H), 7.03 – 6.97 (m, 2H), 6.94 (dd, *J* = 5.1, 3.6 Hz, 1H), 6.87 (dd, *J* = 3.7, 1.2 Hz, 1H), 6.80 (dd, *J* = 5.1, 3.6 Hz, 1H), 6.49 (dd, *J* = 3.6, 1.2 Hz, 1H), 5.15 (s, 1H), 4.77 (s, 1H), 3.73 – 3.23 (m, 2H), 1.56 (s, 3H), 1.53 (s, 4H). **<sup>13</sup>C NMR** (101 MHz, CDCl<sub>3</sub>) δ 148.27, 144.28, 138.41, 138.05, 136.93, 136.48, 130.83, 130.59, 129.41, 129.11, 128.77, 128.58, 128.04, 127.93, 127.67, 127.55, 127.41, 127.28, 126.80, 126.15, 126.10, 125.96, 125.63, 124.68, 79.16, 78.97, 60.84, 59.18, 24.67, 20.61. **HRMS** (ESI) Calcd. for [M+Na]<sup>+</sup>: 349.0691. Found: 349.0697.



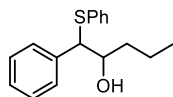
### 2-phenyl-2-(phenylthio)ethan-1-ol (6g)

Following the modified general procedure B, paraformaldehyde (4.0 eq., 0.8 mmol) and DMSO (4 mL) were used, the product was obtained as a colorless oil, 22.1 mg, 48% yield. **<sup>1</sup>H NMR** (400 MHz, CDCl<sub>3</sub>) δ 7.29 – 7.21 (m, 6H), 7.21 – 7.14 (m, 4H), 4.24 (t, *J* = 6.9 Hz, 1H), 3.89 – 3.79 (m, 2H), 1.79 (s, 1H). **<sup>13</sup>C NMR** (100 MHz, CDCl<sub>3</sub>) δ 138.88, 133.68, 132.55, 128.92, 128.71, 128.05, 127.79, 127.56, 65.24, 56.07. **HRMS** (ESI) Calcd. for [M+H]<sup>+</sup>: 231.0838. Found: 231.0840.



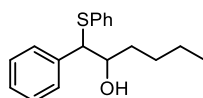
### 1-phenyl-1-(phenylthio)butan-2-ol (6h)

Following the general procedure B, the product was obtained as a colorless oil, 21.3 mg, 41% yield; *syn:anti* = 53:47; **<sup>1</sup>H NMR of (syn)- and (anti)-6c** (400 MHz, CDCl<sub>3</sub>) δ 7.41 – 7.36 (m, 2H), 7.36 – 7.30 (m, 3H), 7.30 – 7.23 (m, 8H), 7.23 – 7.15 (m, 8H), 4.25 (d, *J* = 5.0 Hz, 1H, *anti*), 4.08 (d, *J* = 8.3 Hz, 1H, *syn*), 3.83 – 3.88 (m, 2H), 1.63 – 1.49 (m, 2H, *anti*), 1.45 – 1.28 (m, 3H, *syn*), 0.95 (td, *J* = 7.4, 5.9 Hz, 7H, mix). **<sup>13</sup>C NMR of (syn)- and (anti)-6c** (101 MHz, CDCl<sub>3</sub>) δ 140.05, 138.29, 134.46, 133.99, 132.66, 132.09, 128.99, 128.91, 128.81, 128.43, 128.20, 127.58, 127.45, 127.36, 127.28, 74.77, 74.47, 62.21, 59.89, 27.12, 27.05, 10.28, 9.97. **HRMS** (ESI) Calcd. for [M+H]<sup>+</sup>: 259.1151. Found: 259.1153.



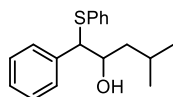
#### phenyl-1-(phenylthio)pentan-2-ol (6i)

Following the modified general procedure B, the product was obtained as a colorless oil, 23.4 mg, 43% yield; *syn:anti* = 55:45;  $^1\text{H NMR}$  of (*syn*)- and (*anti*)-**6d** (400 MHz,  $\text{CDCl}_3$ )  $\delta$  7.34 – 7.07 (m, 22H), 4.16 (d,  $J$  = 4.9 Hz, 1H, *anti*), 4.00 (d,  $J$  = 8.1 Hz, 1H, *syn*), 3.84 (td,  $J$  = 7.8, 3.1 Hz, 2H), 2.03 (d,  $J$  = 49.7 Hz, 2H), 1.51 – 1.20 (m, 9H), 0.77 (dt,  $J$  = 12.9, 6.5 Hz, 7H).  $^1\text{H NMR}$  of (*syn*)- and (*anti*)-**6c** (101 MHz,  $\text{CDCl}_3$ )  $\delta$  140.03, 138.29, 134.48, 134.05, 132.60, 132.05, 129.00, 128.90, 128.81, 128.44, 128.42, 128.22, 127.56, 127.41, 127.35, 127.26, 73.31, 72.85, 62.53, 60.23, 36.28, 36.26, 19.16, 18.96, 13.93, 13.90. **HRMS** (ESI) Calcd. for  $[\text{M}+\text{H}]^+$ : 273.1308. Found: 273.1310.



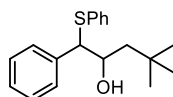
#### phenyl-1-(phenylthio)hexan-2-ol (6j)

Following the general procedure B, the product was obtained as a colorless oil, 24.4 mg, 43% yield; *syn:anti* = 54:46;  $^1\text{H NMR}$  of (*syn*)- and (*anti*)-**6e** (400 MHz,  $\text{CDCl}_3$ )  $\delta$  7.33 – 7.28 (m, 2H, mix), 7.28 – 7.22 (m, 3H), 7.21 – 7.14 (m, 9H), 7.14 – 7.06 (m, 7H), 4.16 (d,  $J$  = 5.0 Hz, 1H, *anti*), 4.00 (d,  $J$  = 8.1 Hz, 1H, *syn*), 3.83 (dtt,  $J$  = 7.6, 4.0, 2.2 Hz, 2H), 2.62 (s, 1H, *anti*), 2.00 (s, 1H, *syn*), 1.53 – 1.05 (m, 16H), 0.76 (dt,  $J$  = 11.5, 7.1 Hz, 7H).  $^{13}\text{C NMR}$  of (*syn*)- and (*anti*)-**6e** (101 MHz,  $\text{CDCl}_3$ )  $\delta$  140.05, 138.29, 134.49, 134.04, 132.61, 132.05, 128.99, 128.90, 128.80, 128.43, 128.21, 127.56, 127.41, 127.35, 127.26, 73.52, 73.11, 62.49, 60.19, 33.87, 33.83, 28.10, 27.89, 22.57, 22.51, 13.98, 13.95. **HRMS** (ESI) Calcd. for  $[\text{M}+\text{H}]^+$ : 287.1464. Found: 287.1467.



#### 4-methyl-1-phenyl-1-(phenylthio)pentan-2-ol (6k)

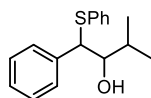
Following the general procedure B, the product was obtained as a colorless oil, 20.6 mg, 36% yield; *syn:anti* = 52:48;  $^1\text{H NMR}$  of (*syn*)- and (*anti*)-**6f** (400 MHz,  $\text{CDCl}_3$ )  $\delta$  7.33 – 7.28 (m, 2H), 7.27 – 7.22 (m, 3H), 7.21 – 7.17 (m, 7H), 7.16 – 7.06 (m, 9H), 4.14 (d,  $J$  = 4.8 Hz, 1H, *anti*), 3.98 (d,  $J$  = 8.0 Hz, 1H, *syn*), 3.96 – 3.87 (m, 2H), 2.03 (s, 2H), 1.81 – 1.67 (m, 2H), 1.33 – 1.01 (m, 6H), 0.77 (dt,  $J$  = 10.8, 6.6 Hz, 13H).  $^{13}\text{C NMR}$  of (*syn*)- and (*anti*)-**6f** (101 MHz,  $\text{CDCl}_3$ )  $\delta$  140.01, 138.26, 134.53, 134.11, 132.59, 131.97, 129.03, 128.89, 128.82, 128.45, 128.42, 128.23, 127.56, 127.41, 127.35, 127.23, 71.71, 71.19, 62.95, 60.61, 43.33, 43.26, 24.81, 24.78, 23.68, 23.47, 21.76, 21.36. **HRMS** (ESI) Calcd. for  $[\text{M}+\text{H}]^+$ : 287.1464. Found: 287.1466.



#### 4,4-dimethyl-1-phenyl-1-(phenylthio)pentan-2-ol (6l)

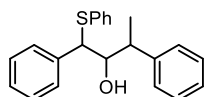
Following the general procedure B, the product was obtained as a colorless oil, 22.1 mg, 37% yield; *syn:anti* = 64:36;  $^1\text{H NMR}$  of (*syn*)- and (*anti*)-**6g** (400 MHz,  $\text{CDCl}_3$ )  $\delta$  7.49 – 7.43 (m, 2H), 7.37 (ddd,  $J$  = 6.8, 3.9, 1.9 Hz, 3H), 7.35 – 7.20 (m, 14H), 4.24 (d,  $J$  = 5.0 Hz, 1H, *syn*), 4.11 (tt,  $J$  = 4.3, 2.4 Hz, 3H), 2.12 (s, 2H, mix), 1.60 (dd,  $J$  = 14.6, 1.6 Hz, 1H), 1.46 – 1.37 (m, 2H), 0.94 (s, 9H), 0.93 (s, 9H).  $^{13}\text{C NMR}$  of (*syn*)- and (*anti*)-**6g** (101 MHz,  $\text{CDCl}_3$ )  $\delta$  140.07, 138.35, 134.64, 134.26, 132.45, 131.74, 129.06, 128.89, 128.81,

128.42, 128.36, 127.53, 127.35, 127.33, 127.14, 77.32, 77.00, 76.68, 71.42, 70.85, 63.55, 61.70, 47.72, 47.52, 30.34, 29.98, 29.95. **HRMS** (ESI) Calcd. for  $[M+H]^+$ : 301.1621. Found: 301.1624.



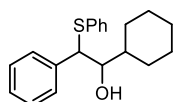
### 3-methyl-1-phenyl-1-(phenylthio)butan-2-ol (6m)

Following the general procedure B, the product was obtained as a colorless oil, 17.8 mg, 33% yield; *syn:anti* = 51:49; **<sup>1</sup>H NMR of (syn)- and (anti)-6h** (300 MHz, CDCl<sub>3</sub>) δ 7.43 – 7.37 (m, 2H), 7.37 – 7.28 (m, 4H), 7.28 – 7.19 (m, 14H), 7.18 – 7.10 (m, 3H), 4.32 (d, *J* = 5.5 Hz, 1H, *anti*), 4.16 (d, *J* = 8.8 Hz, 1H, *syn*), 3.76 (dd, *J* = 8.7, 3.5 Hz, 1H), 3.61 (dd, *J* = 6.7, 5.5 Hz, 1H), 1.89 – 1.72 (m, *J* = 6.7 Hz, 1H), 1.62 (pd, *J* = 6.8, 3.5 Hz, 1H), 1.02 – 0.84 (m, 14H). **<sup>13</sup>C NMR of (syn)- and (anti)-6h** (75 MHz, CDCl<sub>3</sub>) δ 140.26, 138.38, 134.12, 133.81, 132.92, 132.49, 129.14, 128.91, 128.77, 128.46, 128.42, 128.06, 127.57, 127.50, 127.45, 127.29, 60.70, 57.65, 30.51, 29.76, 20.56, 19.53, 17.52, 14.82. **HRMS** (ESI) Calcd. for  $[M+H]^+$ : 273.1308. Found: 273.1309.



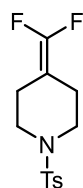
### 1,3-diphenyl-1-(phenylthio)butan-2-ol (6n)

Following the general procedure B, the product was obtained as a colorless oil, 19.2 mg, 29% yield; *syn:anti* = 53:47; **<sup>1</sup>H NMR of (syn)- and (anti)-6i** (400 MHz, CDCl<sub>3</sub>) δ 7.24 – 7.05 (m, 26H), 6.94 – 6.89 (m, 2H), 4.08 – 4.00 (m, 2H), 3.99 – 3.93 (m, 2H), 2.91 – 2.80 (m, 1H, *syn*), 2.72 – 2.63 (m, 1H, *anti*), 2.47 (s, 1H), 2.34 (s, 1H), 1.24 (d, *J* = 7.0 Hz, 3H), 1.20 (d, *J* = 6.9 Hz, 3H). **<sup>13</sup>C NMR of (syn)- and (anti)-6i** (101 MHz, CDCl<sub>3</sub>) δ 144.69, 144.10, 140.66, 137.33, 134.08, 134.01, 132.52, 132.09, 129.56, 128.93, 128.71, 128.58, 128.50, 128.44, 128.23, 128.02, 127.80, 127.71, 127.68, 127.37, 127.23, 126.58, 126.49, 78.81, 76.11, 59.53, 56.42, 42.91, 42.22, 18.48, 14.94. **HRMS** (ESI) Calcd. for  $[M+H]^+$ : 335.1464. Found: 335.1463.



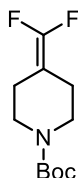
### cyclohexyl-2-phenyl-2-(phenylthio)ethan-1-ol (6o)

Following the general procedure B, the product was obtained as a colorless oil, 16.5 mg, 26% yield; *syn:anti* = 54:46; **<sup>1</sup>H NMR of (syn)- and (anti)-6i** (300 MHz, CDCl<sub>3</sub>) δ 7.42 – 7.37 (m, 2H), 7.36 – 7.29 (m, 4H), 7.27 (d, *J* = 2.2 Hz, 2H), 7.26 – 7.15 (m, 14H), 4.36 (d, *J* = 5.4 Hz, 1H, *anti*), 4.26 (d, *J* = 8.0 Hz, 1H, *syn*), 3.72 – 3.63 (m, 2H), 2.65 (s, 1H), 2.17 (s, 1H), 1.96 – 1.51 (m, 14H), 1.50 – 1.29 (m, 4H), 1.23 – 0.92 (m, 11H). **<sup>13</sup>C NMR of (syn)- and (anti)-6i** (75 MHz, CDCl<sub>3</sub>) δ 140.40, 138.40, 134.28, 134.14, 132.50, 132.34, 129.13, 128.90, 128.75, 128.48, 128.43, 128.09, 127.53, 127.37, 127.29, 127.27, 77.75, 76.85, 39.94, 39.73, 30.56, 29.66, 27.74, 26.35, 26.31, 25.98, 25.91, 25.82, 25.76. **HRMS** (ESI) Calcd. for  $[M+H]^+$ : 313.1621. Found: 313.1624.



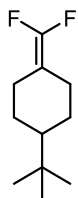
#### 4-(difluoromethylene)-1-tosylpiperidine (9a)

Following the general procedure C, the product was obtained as a white solid, 42 mg, 73% yield.  $^1\text{H NMR}$  (400 MHz,  $\text{CDCl}_3$ )  $\delta$  7.65 – 7.59 (m, 2H), 7.31 (d,  $J = 8.0$  Hz, 2H), 3.02 (t,  $J = 5.7$  Hz, 4H), 2.42 (s, 3H), 2.30 – 2.23 (m, 4H).  $^{13}\text{C NMR}$  (101 MHz,  $\text{CDCl}_3$ )  $\delta$  151.23 (t,  $J = 283.0$  Hz), 143.67, 133.14, 129.67, 127.56, 83.64 (t,  $J = 20.7$  Hz), 46.20 (t,  $J = 2.1$  Hz), 23.62 (t,  $J = 1.9$  Hz), 21.47.  $^{19}\text{F NMR}$  (377 MHz,  $\text{CDCl}_3$ )  $\delta$  -96.51. **HRMS** (ESI) Calcd. for  $\text{C}_{13}\text{H}_{16}\text{F}_2\text{NO}_2\text{S}$   $[\text{M}+\text{H}]^+$ : 288.0864, found: 288.0866.



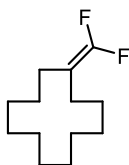
#### tert-butyl 4-(difluoromethylene)piperidine-1-carboxylate (9b)

Following the general procedure C, the product was obtained as a colorless oil, 23.7 mg, 51% yield.;  $^1\text{H NMR}$  (400 MHz,  $\text{CDCl}_3$ )  $\delta$  3.44 – 3.35 (m, 4H), 2.16 – 2.12 (m, 4H), 1.46 (s, 9H).  $^{13}\text{C NMR}$  (101 MHz,  $\text{CDCl}_3$ )  $\delta$  154.60, 151.41 (t,  $J = 281.9$  Hz), 84.97 (t,  $J = 20.2$  Hz), 79.76, 43.83, 28.39, 23.95.  $^{19}\text{F NMR}$  (376 MHz,  $\text{CDCl}_3$ )  $\delta$  -97.37. **HRMS** (ESI) calcd for  $\text{C}_{11}\text{H}_{18}\text{F}_2\text{NO}_2$   $[\text{M}+\text{H}]^+$ : 234.1300, found: 234.1299.



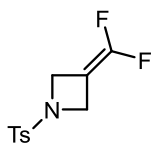
#### 1-(tert-butyl)-4-(difluoromethylene)cyclohexane (9c)

Following the general procedure C, the product was obtained as a colorless oil, 14.8 mg, 39% yield.  $^1\text{H NMR}$  (400 MHz,  $\text{CDCl}_3$ )  $\delta$  2.54 – 2.45 (m, 2H), 1.88 – 1.80 (m, 2H), 1.77 – 1.64 (m, 2H), 1.10 – 0.94 (m, 3H), 0.85 (s, 9H).  $^{13}\text{C NMR}$  (101 MHz,  $\text{CDCl}_3$ )  $\delta$  150.42 (t,  $J = 280.0$  Hz), 88.00 (t,  $J = 18.6$  Hz), 47.81, 32.47, 27.51, 27.22 (t,  $J = 1.9$  Hz), 24.61 (t,  $J = 1.9$  Hz).  $^{19}\text{F NMR}$  (376 MHz,  $\text{CDCl}_3$ )  $\delta$  -99.99. **HRMS** (EI) calcd for  $\text{C}_{13}\text{H}_{22}\text{F}_2$   $[\text{M}]^+$ : 188.1377, found: 188.1367.



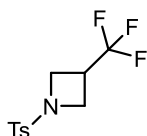
#### (difluoromethylene)cyclododecane (9d)

Following the general procedure C, the product was obtained as a colorless oil, 17.1 mg, 40% yield.  $^1\text{H NMR}$  (300 MHz,  $\text{CDCl}_3$ )  $\delta$  2.02 (tt,  $J = 7.0, 2.4$  Hz, 4H), 1.48 (p,  $J = 6.7, 6.3$  Hz, 4H), 1.38 – 1.31 (m, 14H).  $^{13}\text{C NMR}$  (75 MHz,  $\text{CDCl}_3$ )  $\delta$  153.64, (t,  $J = 281.25$  Hz), 87.05 (t,  $J = 16.0$  Hz), 25.12 (t,  $J = 1.5$  Hz), 24.34, 24.17 (t,  $J = 1.5$  Hz), 23.38, 23.05.  $^{19}\text{F NMR}$  (282 MHz,  $\text{CDCl}_3$ )  $\delta$  -94.71. **HRMS** (EI) calcd for  $\text{C}_{13}\text{H}_{22}\text{F}_2$   $[\text{M}]^+$ : 216.1684, found: 216.1688.



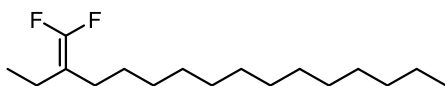
### 3-(difluoromethylene)-1-tosylazetidine (9e)

Following the general procedure C, the product was obtained as a white solid, 19.8 mg, 38% yield. **<sup>1</sup>H NMR** (300 MHz, CDCl<sub>3</sub>) δ 7.80 – 7.70 (m, 2H), 7.43 – 7.34 (m, 2H), 4.38 (t, *J* = 3.8 Hz, 4H), 2.46 (s, 3H). **<sup>13</sup>C NMR** (75 MHz, CDCl<sub>3</sub>) δ 150.19 (t, *J* = 284.6 Hz), 144.69, 131.34, 130.04, 128.41, 78.24 (t, *J* = 30.1 Hz), 53.06 (t, *J* = 2.8 Hz), 21.66. **<sup>19</sup>F NMR** (282 MHz, CDCl<sub>3</sub>) δ -91.60. **HRMS** (ESI) calcd for [M+H]<sup>+</sup>: 260.0551, found: 260.0558.



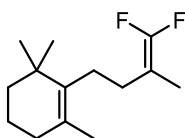
### tosyl-3-(trifluoromethyl)azetidine (9e')

Following the general procedure C, the product was obtained as a white solid (by product), 14.8 mg, 21% yield. **<sup>1</sup>H NMR** (400 MHz, CDCl<sub>3</sub>) δ 7.75 – 7.70 (m, 2H), 7.39 (d, *J* = 8.0 Hz, 2H), 3.97 (t, *J* = 8.8 Hz, 2H), 3.81 (dd, *J* = 8.8, 6.4 Hz, 2H), 3.10 (ht, *J* = 8.5, 6.4 Hz, 1H), 2.46 (s, 3H). **<sup>13</sup>C NMR** (101 MHz, CDCl<sub>3</sub>) δ 144.60, 131.04, 129.92, 128.27, 125.26 (q, *J* = 275.5 Hz), 49.61 (q, *J* = 3.8 Hz), 31.10 (q, *J* = 32.9 Hz), 21.59. **<sup>19</sup>F NMR** (376 MHz, CDCl<sub>3</sub>) δ -73.79. **HRMS** (ESI) calcd for [M+H]<sup>+</sup>: 280.0614, found: 280.0617.



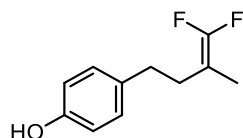
### 3-(difluoromethylene)hexadecane (9f)

Following the general procedure C, the product was obtained as a colorless oil, 33.9 mg, 62% yield. **<sup>1</sup>H NMR** (300 MHz, CDCl<sub>3</sub>) δ 2.03 – 1.92 (m, 4H), 1.43 – 1.33 (m, 2H), 1.26 (s, 20H), 0.99 (t, *J* = 7.5 Hz, 3H), 0.92 – 0.84 (m, 3H). **<sup>13</sup>C NMR** (75 MHz, CDCl<sub>3</sub>) δ 152.95 (t, *J* = 282.5 Hz), 90.33 (t, *J* = 16.4 Hz), 31.95, 29.71, 29.68, 29.62, 29.44, 29.39, 29.20, 27.45 (t, *J* = 2.6 Hz), 26.01 – 25.19 (m), 22.71, 19.28 (t, *J* = 2.0 Hz), 14.12, 12.43 (t, *J* = 2.7 Hz). **<sup>19</sup>F NMR** (282 MHz, CDCl<sub>3</sub>) δ -97.45 (d, *J* = 59.2 Hz, 1F), δ -97.69 (d, *J* = 59.2 Hz, 1F), **HRMS** (EI) calcd for C<sub>17</sub>H<sub>32</sub>F<sub>2</sub> [M]<sup>+</sup>: 274.2467, found: 274.2461.



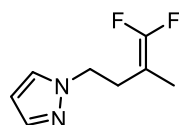
### 2-(4,4-difluoro-3-methylbut-3-en-1-yl)-1,3,3-trimethylcyclohex-1-ene (9g)

Following the general procedure C, the product was obtained as a colorless oil, 20.0 mg, 44% yield. **<sup>1</sup>H NMR** (400 MHz, CDCl<sub>3</sub>) δ 2.09 – 2.03 (m, 2H), 2.03 – 1.95 (m, 2H), 1.95 – 1.88 (m, 2H), 1.61 (q, *J* = 3.4 Hz, 6H), 1.59 – 1.54 (m, 2H), 1.45 – 1.39 (m, 2H), 1.00 (s, 6H). **<sup>13</sup>C NMR** (101 MHz, CDCl<sub>3</sub>) δ 152.72 (dd, *J* = 282.8, 280.7 Hz), 136.31, 127.72, 85.25 (dd, *J* = 20.4, 16.9 Hz), 39.78, 34.94, 32.75, 28.99 (d, *J* = 2.1 Hz), 28.52, 26.76 (dd, *J* = 2.6, 2.3 Hz), 22.35, 19.65, 19.50, 14.06, 11.92 (t, *J* = 2.1 Hz). **<sup>19</sup>F NMR** (377 MHz, CDCl<sub>3</sub>) δ -97.41 (d, *J* = 59.5 Hz, 1F), -98.25 (d, *J* = 59.3 Hz, 1F). **HRMS** (EI) calcd for C<sub>14</sub>H<sub>22</sub>F<sub>2</sub> [M]<sup>+</sup>: 228.1684, found: 228.1683.



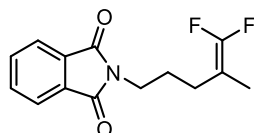
#### 4-(4,4-difluoro-3-methylbut-3-en-1-yl)phenol (9h)

Following the general procedure C, the product was obtained as a colorless oil, 20.6 mg, 52% yield.  $^1\text{H NMR}$  (300 MHz,  $\text{CDCl}_3$ )  $\delta$  7.11 – 6.99 (m, 2H), 6.82 – 6.70 (m, 2H), 4.78 (s, 1H), 2.63 (dd,  $J = 9.1, 6.7$  Hz, 2H), 2.23 (ddt,  $J = 7.5, 6.5, 2.1$  Hz, 2H), 1.57 (t,  $J = 3.2$  Hz, 3H).  $^{13}\text{C NMR}$  (101 MHz,  $\text{CDCl}_3$ )  $\delta$  153.69, 152.96 (t,  $J = 281.2$  Hz), 150.16, 133.50, 129.41, 115.18, 84.12 (dd,  $J = 19.5, 18.2$  Hz) 32.67 (t,  $J = 2.0$  Hz), 30.38 (d,  $J = 2.4$  Hz), 11.95 (t,  $J = 2.1$  Hz).  $^{19}\text{F NMR}$  (376 MHz,  $\text{CDCl}_3$ )  $\delta$  -96.81 (d,  $J = 57.6$  Hz, 1F), -97.10 (d,  $J = 57.6$  Hz, 1F).



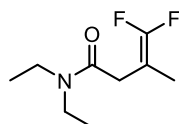
#### 1-(4,4-difluoro-3-methylbut-3-en-1-yl)-1H-pyrazole (9i)

Following the general procedure C, the product was obtained as a colorless oil, 15.5 mg, 45% yield.  $^1\text{H NMR}$  (400 MHz,  $\text{CDCl}_3$ )  $\delta$  7.54 – 7.46 (m, 1H), 7.35 (dd,  $J = 2.3, 0.6$  Hz, 1H), 6.24 (t,  $J = 2.1$  Hz, 1H), 4.20 (t,  $J = 7.1$  Hz, 2H), 2.52 (tt,  $J = 7.1, 2.1$  Hz, 2H), 1.51 (t,  $J = 3.2$  Hz, 3H).  $^{13}\text{C NMR}$  (101 MHz,  $\text{CDCl}_3$ )  $\delta$  153.44 (t,  $J = 284.8$  Hz), 139.37, 128.90, 105.52, 81.77 (t,  $J = 19.7$  Hz), 49.83 (t,  $J = 3.2$  Hz), 29.72 (d,  $J = 2.7$  Hz), 11.90 (t,  $J = 1.9$  Hz).  $^{19}\text{F NMR}$  (377 MHz,  $\text{CDCl}_3$ )  $\delta$  -94.76 (d,  $J = 53.2$  Hz), -95.25 (d,  $J = 53.2$  Hz). **HRMS** (EI) Calcd. for  $\text{C}_8\text{H}_9\text{F}_2\text{N}_2$   $[\text{M}]^+$ : 171.0728. Found: 171.0731.



#### 2-(5,5-difluoro-4-methylpent-4-en-1-yl)isoindoline-1,3-dione (9j)

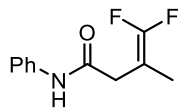
Following the general procedure C, the product was obtained as a white solid, 44.2 mg, 83% yield.  $^1\text{H NMR}$  (300 MHz,  $\text{CDCl}_3$ )  $\delta$  7.86 – 7.78 (m, 2H), 7.75 – 7.65 (m, 2H), 3.68 – 3.60 (m, 2H), 2.03 (tt,  $J = 8.1, 2.2$  Hz, 2H), 1.77 (tt,  $J = 9.3, 6.5$  Hz, 2H), 1.56 (t,  $J = 3.2$  Hz, 3H).  $^{13}\text{C NMR}$  (75 MHz,  $\text{CDCl}_3$ )  $\delta$  168.24, 152.74 (t,  $J = 282.1$  Hz), 133.88, 132.01, 123.15, 83.61 (t,  $J = 19.0$  Hz), 37.39, 25.86 (t,  $J = 2.6$  Hz), 25.57 (t,  $J = 1.8$  Hz), 11.54 (t,  $J = 1.9$  Hz).  $^{19}\text{F NMR}$  (282 MHz,  $\text{CDCl}_3$ )  $\delta$  -96.39 (d,  $J = 57.2$  Hz, 1F), -96.41 (d,  $J = 57.2$  Hz, 1F). **HRMS** (EI) calcd for  $\text{C}_{14}\text{H}_{13}\text{NO}_2\text{F}_2$   $[\text{M}]^+$ : 265.0909, found: 265.0905.



#### N,N-diethyl-4,4-difluoro-3-methylbut-3-enamide (9k)

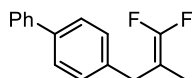
Following the general procedure C, the product was obtained as a colorless oil, 16.1 mg, 42% yield.  $^1\text{H NMR}$  (300 MHz,  $\text{CDCl}_3$ )  $\delta$  3.32 (m, 3.39-3.25, 4H), 2.99 (t,  $J = 2.0$  Hz, 2H), 1.64 (t,  $J = 3.2$  Hz, 3H), 1.13 (dt,  $J = 19.9, 7.1$  Hz, 6H).  $^{13}\text{C NMR}$  (75 MHz,  $\text{CDCl}_3$ )  $\delta$  168.41 (t,  $J = 3.0$  Hz), 153.27 (t,  $J = 280.7$  Hz), 81.33 (dd,  $J = 22.1, 19.0$  Hz), 41.98, 40.27, 33.17 (d,  $J = 2.8$  Hz), 14.15, 12.93, 12.31.  $^{19}\text{F NMR}$  (282 MHz,  $\text{CDCl}_3$ )

$\delta$  -95.76 (d,  $J$  = 54.5 Hz, 1F), -96.06 (d,  $J$  = 54.5 Hz, 1F). **HRMS** (ESI) calcd for  $C_9H_{16}F_2NO$   $[M+H]^+$ : 192.1194, found: 192.1196.



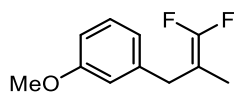
#### 4,4-difluoro-3-methyl-N-phenylbut-3-enamide (9l)

Following the general procedure C, the product was obtained as a white solid, 18.3 mg, 43% yield.;  **$^1H$  NMR** (300 MHz,  $CDCl_3$ )  $\delta$  7.53 – 7.47 (m, 3H), 7.36 – 7.27 (m, 2H), 7.17 – 7.08 (m, 1H), 3.05 (t,  $J$  = 2.0 Hz, 2H), 1.71 (t,  $J$  = 3.3 Hz, 3H).  **$^{13}C$  NMR** (75 MHz,  $CDCl_3$ )  $\delta$  167.54 (t,  $J$  = 3.0 Hz), 154.07 (t,  $J$  = 282.7 Hz), 137.43, 128.98, 124.61, 120.02, 80.79 (t,  $J$  = 20.6 Hz), 37.22, 12.43.  **$^{19}F$  NMR** (282 MHz,  $CDCl_3$ )  $\delta$  -93.82. **HRMS** (ESI) calcd for  $C_{11}H_{12}F_2NO$   $[M+H]^+$ : 212.0881, found: 212.0885.



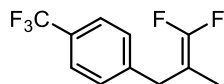
#### 4-(3,3-difluoro-2-methylallyl)-1,1'-biphenyl (9m)

Following the general procedure C, the product was obtained as a colorless oil, 31.8 mg, 65% yield.  **$^1H$  NMR** (300 MHz,  $CDCl_3$ )  $\delta$  7.64 – 7.53 (m, 4H), 7.50 – 7.42 (m, 2H), 7.39 – 7.33 (m, 1H), 7.30 – 7.24 (m, 2H), 3.35 (t,  $J$  = 2.1 Hz, 2H), 1.56 (t,  $J$  = 3.2 Hz, 3H).  **$^{13}C$  NMR** (75 MHz,  $CDCl_3$ )  $\delta$  153.1 (dd,  $J$  = 280.5 Hz, 279.8 Hz), 140.86, 139.43, 137.62 (t,  $J$  = 2.7 Hz), 128.96, 128.73, 127.21, 127.15, 126.99, 84.61 (t,  $J$  = 19.0 Hz), 34.14 (q,  $J$  = 1.6 Hz), 11.84 (t,  $J$  = 1.6 Hz).  **$^{19}F$  NMR** (282 MHz,  $CDCl_3$ )  $\delta$  -96.97 (d,  $J$  = 56.2 Hz, 1F), -97.23 (d,  $J$  = 56.2 Hz, 1F). **HRMS** (EI) calcd for  $C_{16}H_{14}F_2$   $[M]^+$ : 244.1058, found: 244.1054.



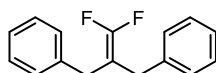
#### 1-(3,3-difluoro-2-methylallyl)-3-methoxybenzene (9n)

Following the general procedure C, the product was obtained as a colorless oil, 21.8 mg, 55% yield.  **$^1H$  NMR** (300 MHz,  $CDCl_3$ )  $\delta$  7.23 (dd,  $J$  = 8.3, 7.4 Hz, 1H), 6.82 – 6.71 (m, 3H), 3.81 (s, 3H), 3.27 (t,  $J$  = 2.1 Hz, 2H), 1.51 (t,  $J$  = 3.2 Hz, 3H).  **$^{13}C$  NMR** (75 MHz,  $CDCl_3$ )  $\delta$  159.72, 153.27 (dd, 280.5 Hz, 279.8 Hz), 140.15 (t,  $J$  = 2.6 Hz), 129.42, 120.96, 114.36, 111.57, 84.57 (t,  $J$  = 19.0 Hz), 55.13, 34.50 (t,  $J$  = 2.0 Hz), 11.78 (t,  $J$  = 1.7 Hz).  **$^{19}F$  NMR** (282 MHz,  $CDCl_3$ )  $\delta$  -97.11 (d,  $J$  = 56.4 Hz, 1F), -97.36 (d,  $J$  = 56.4 Hz, 1F). **HRMS** (EI) calcd for  $C_{11}H_{12}OF_2$   $[M]^+$ : 198.0851, found: 198.0852.



#### 1-(3,3-difluoro-2-methylallyl)-4-(trifluoromethyl)benzene (9o)

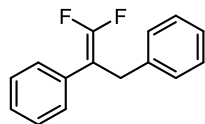
Following the general procedure C, the product was obtained as a colorless oil, 17 mg, 36% yield. Colorless oil;  **$^1H$  NMR** (400 MHz,  $CDCl_3$ )  $\delta$  7.52 (d,  $J$  = 8.0 Hz, 2H), 7.25 (d,  $J$  = 8.0 Hz, 2H), 3.31 (d,  $J$  = 2.0 Hz, 2H), 1.46 (t,  $J$  = 3.2 Hz, 3H).  **$^{13}C$  NMR** (101 MHz,  $CDCl_3$ )  $\delta$  153.47 (dd, 283.8 Hz, 283.7 Hz), 142.67, 129.10, 128.84, 125.45 (q,  $J$  = 3.8 Hz), 122.87, 84.03 (t,  $J$  = 19.4 Hz), 34.39 (t,  $J$  = 1.9 Hz), 11.75 (d,  $J$  = 1.9 Hz).  **$^{19}F$  NMR** (377 MHz,  $CDCl_3$ )  $\delta$  -62.98 (s, 3H), -96.37 (d,  $J$  = 56.6 Hz, 1F), -96.59 (d,  $J$  = 56.6 Hz, 1F). **HRMS** (EI) calcd for  $C_{11}H_9F_5$   $[M]^+$ : 236.0624, found: 236.0623.





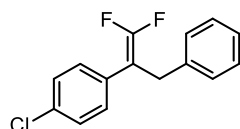
### (2-(difluoromethylene)propane-1,3-diyl)dibenzene (9p)

Following the general procedure C, the product was obtained as a colorless oil, 14.6 mg, 30% yield.  $^1\text{H NMR}$  (400 MHz,  $\text{CDCl}_3$ )  $\delta$  7.34 – 7.28 (m, 4H), 7.26 – 7.20 (m, 2H), 7.17 – 7.11 (m, 4H), 3.21 (d,  $J = 2.1$  Hz, 4H).  $^{13}\text{C NMR}$  (101 MHz,  $\text{CDCl}_3$ )  $\delta$  154.22 (t,  $J = 284.6$  Hz), 138.30 (t,  $J = 2.6$  Hz), 128.76, 128.50, 126.49, 88.97 (t,  $J = 17.4$  Hz), 31.54 (t,  $J = 1.6$  Hz).  $^{19}\text{F NMR}$  (376 MHz,  $\text{CDCl}_3$ )  $\delta$  -96.59. **HRMS** (EI) calcd for  $\text{C}_{16}\text{H}_{14}\text{F}_2$  [ $\text{M}$ ] $^+$ : 244.1058, found: 244.1051.



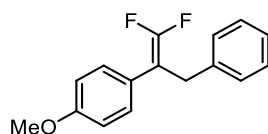
### (3,3-difluoroprop-2-ene-1,2-diyl)dibenzene (9q)

Following the general procedure C, the product was obtained as a colorless oil, 26.3 mg, 57% yield.  $^1\text{H NMR}$  (300 MHz,  $\text{CDCl}_3$ )  $\delta$  7.33 – 7.27 (m, 4H), 7.27 – 7.22 (m, 3H), 7.22 – 7.14 (m, 3H), 3.75 (t,  $J = 2.3$  Hz, 2H).  $^{13}\text{C NMR}$  (75 MHz,  $\text{CDCl}_3$ )  $\delta$  154.38 (dd,  $J = 291.8, 287.4$  Hz), 138.43 (t,  $J = 2.7$  Hz), 133.48 (t,  $J = 3.8$  Hz), 128.45, 128.33, 128.24 (t,  $J = 3.4$  Hz), 127.25, 126.37, 91.66 (dd,  $J = 21.4, 13.6$  Hz), 33.89 (d,  $J = 1.9$  Hz).  $^{19}\text{F NMR}$  (282 MHz,  $\text{CDCl}_3$ )  $\delta$  -90.87 (d,  $J = 40.1$  Hz, 1F), -91.43 (d,  $J = 40.0$  Hz, 1F). **HRMS** (EI) calcd for  $\text{C}_{15}\text{H}_{12}\text{F}_2$  [ $\text{M}$ ] $^+$ : 230.0902, found: 230.0904.



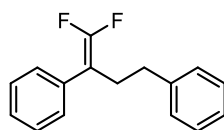
### chloro-4-(1,1-difluoro-3-phenylprop-1-en-2-yl)benzene (9r)

Following the general procedure C, the product was obtained as a colorless oil, 26.9 mg, 51% yield.  $^1\text{H NMR}$  (300 MHz,  $\text{CDCl}_3$ )  $\delta$  7.31 – 7.23 (m, 4H), 7.23 – 7.20 (m, 2H), 7.19 – 7.12 (m, 3H), 3.72 (t,  $J = 2.3$  Hz, 2H).  $^{13}\text{C NMR}$  (75 MHz,  $\text{CDCl}_3$ )  $\delta$  154.35 (dd,  $J = 292.2, 288.1$  Hz), 138.00 (t,  $J = 2.6$  Hz), 133.10, 131.89 (t,  $J = 3.7$  Hz), 129.56 (t,  $J = 3.6$  Hz), 128.56 (d,  $J = 1.7$  Hz), 128.21, 126.54, 90.96 (dd,  $J = 22.0, 13.6$  Hz), 33.75.  $^{19}\text{F NMR}$  (282 MHz,  $\text{CDCl}_3$ )  $\delta$  -90.21 (d,  $J = 38.7$  Hz, 1F), -90.63 (d,  $J = 38.8$  Hz, 1F). **HRMS** (EI) calcd for  $\text{C}_{15}\text{H}_{11}\text{F}_2\text{Cl}$  [ $\text{M}$ ] $^+$ : 254.0512, found: 254.0506.



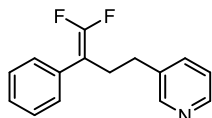
### 1-(1,1-difluoro-3-phenylprop-1-en-2-yl)-4-methoxybenzene (9s)

Following the general procedure C, the product was obtained as a colorless oil, 29.2 mg, 56% yield.  $^1\text{H NMR}$   $\delta$  7.18 – 7.12 (m, 2H), 7.12 – 7.05 (m, 5H), 6.76 – 6.70 (m, 2H), 3.68 (s, 3H), 3.62 (t,  $J = 2.3$  Hz, 2H).  $^{13}\text{C NMR}$  (101 MHz,  $\text{CDCl}_3$ )  $\delta$  158.62, 154.23 (dd,  $J = 290.6, 286.8$  Hz), 138.56 (t,  $J = 2.6$  Hz), 129.38 (t,  $J = 3.5$  Hz), 128.43, 128.27, 126.33, 113.79, 91.13 (dd,  $J = 21.3, 13.9$  Hz), 55.15, 33.99 (d,  $J = 2.5$  Hz).  $^{19}\text{F NMR}$  (376 MHz,  $\text{CDCl}_3$ )  $\delta$  -92.01 (d,  $J = 42.9$  Hz, 1F), -92.41 (d,  $J = 42.9$  Hz, 1F). **HRMS** (EI) calcd for  $\text{C}_{16}\text{H}_{14}\text{OF}_2\text{Cl}$  [ $\text{M}$ ] $^+$ : 260.1007, found: 260.1003.



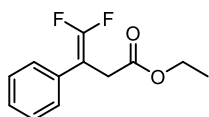
### (4,4-difluorobut-3-ene-1,3-diyl)dibenzene (9t)

Following the general procedure C, the product was obtained as a colorless oil, 21.1 mg, 43% yield.  $^1\text{H NMR}$  (300 MHz,  $\text{CDCl}_3$ )  $\delta$  7.44 – 7.26 (m, 7H), 7.25 – 7.07 (m, 3H), 2.78 – 2.59 (m, 4H).  $^{13}\text{C NMR}$  (101 MHz,  $\text{CDCl}_3$ )  $\delta$  153.72 (dd,  $J = 290.8, 287.0$  Hz), 141.00, 133.46 (dd,  $J = 4.5, 3.2$  Hz), 128.48, 128.36 (d,  $J = 3.2$  Hz), 128.28 (t,  $J = 3.2$  Hz), 127.30, 126.07, 91.81 (dd,  $J = 21.6, 13.3$  Hz), 34.01 (t,  $J = 2.6$  Hz), 29.67 (d,  $J = 1.6$  Hz).  $^{19}\text{F NMR}$  (282 MHz,  $\text{CDCl}_3$ )  $\delta$  -91.58 (d,  $J = 42.5$  Hz, 1F), -92.02 (d,  $J = 42.5$  Hz, 1F). **HRMS** (EI) calcd for  $\text{C}_{16}\text{H}_{14}\text{F}_2$   $[\text{M}]^+$ : 244.1058, found: 244.1056.



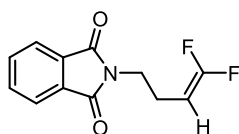
### 3-(4,4-difluoro-3-phenylbut-3-en-1-yl)pyridine (9u)

Following the general procedure C, the product was obtained as a colorless oil, 23.5 mg, 48% yield.  $^1\text{H NMR}$  (400 MHz,  $\text{CDCl}_3$ )  $\delta$  8.41 (dd,  $J = 4.9, 1.6$  Hz, 1H), 8.33 (d,  $J = 2.2$  Hz, 1H), 7.42 (dt,  $J = 7.8, 2.0$  Hz, 1H), 7.37 – 7.30 (m, 2H), 7.29 – 7.22 (m, 3H), 7.20 – 7.14 (m, 1H), 2.73 – 2.59 (m, 4H).  $^{13}\text{C NMR}$  (101 MHz,  $\text{CDCl}_3$ )  $\delta$  153.76 (dd,  $J = 291.2, 287.5$  Hz), 149.58, 147.35, 136.24, 136.11, 132.92 (dd,  $J = 14.3, 11.3$  Hz), 128.61, 128.23 (t,  $J = 3.2$  Hz), 127.51, 123.36, 91.23 (dd,  $J = 21.3, 14.2$  Hz), 30.97 (t,  $J = 2.7$  Hz), 29.12 (d,  $J = 1.7$  Hz).  $^{19}\text{F NMR}$  (377 MHz,  $\text{CDCl}_3$ )  $\delta$  -91.24 (d,  $J = 41.5$  Hz), -91.53 (d,  $J = 41.5$  Hz). **HRMS** (EI) Calcd. for  $\text{C}_{15}\text{H}_{13}\text{F}_2\text{N}$   $[\text{M}]^+$ : 245.1009. Found: 245.1008.



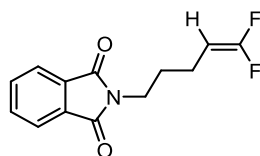
### ethyl 4,4-difluoro-3-phenylbut-3-enoate (9v)

Following the general procedure C, the product was obtained as a colorless oil, 17.6 mg, 39% yield.  $^1\text{H NMR}$  (300 MHz,  $\text{CDCl}_3$ )  $\delta$  7.40 – 7.26 (m, 5H), 4.13 (q,  $J = 7.1$  Hz, 2H), 3.40 (dd,  $J = 2.5, 2.0$  Hz, 2H), 1.20 (t,  $J = 7.1$  Hz, 3H).  $^{13}\text{C NMR}$  (75 MHz,  $\text{CDCl}_3$ )  $\delta$  170.13 (dd,  $J = 3.0$  Hz, 2.6 Hz), 154.78 (dd,  $J = 292.4, 289.0$  Hz), 133.02 (t,  $J = 3.8$  Hz), 128.48, 127.83 (t,  $J = 3.5$  Hz), 127.52, 87.16 (dd,  $J = 21.5, 17.7$  Hz), 61.09, 33.88 (d,  $J = 2.6$  Hz), 14.05.  $^{19}\text{F NMR}$  (282 MHz,  $\text{CDCl}_3$ )  $\delta$  -88.41 (d,  $J = 35.3$  Hz, 1F), -89.69 (d,  $J = 35.3$  Hz, 1F). **HRMS** (EI) calcd for  $\text{C}_{12}\text{H}_{12}\text{F}_2\text{O}_2$   $[\text{M}]^+$ : 226.0805, found: 226.0808.



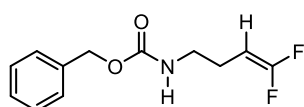
### 2-(4,4-difluorobut-3-en-1-yl)isoindoline-1,3-dione (9w)

Following the general procedure C, the product was obtained as a white solid, 15.9 mg, 34% yield.  $^1\text{H NMR}$  (300 MHz,  $\text{CDCl}_3$ )  $\delta$  7.89 – 7.79 (m, 2H), 7.76 – 7.67 (m, 2H), 4.18 (dtd,  $J = 24.9, 7.9, 2.1$  Hz, 1H), 3.73 (td,  $J = 7.0, 0.8$  Hz, 2H), 2.44 – 2.32 (m, 2H).  $^{13}\text{C NMR}$  (75 MHz,  $\text{CDCl}_3$ )  $\delta$  168.31, 156.36 (dd,  $J = 287.6, 285.4$  Hz), 133.93, 132.04, 123.21, 76.92 (d,  $J = 2.1$  Hz), 37.18, 28.25 (t,  $J = 2.4$  Hz), 19.71 (d,  $J = 4.6$  Hz).  $^{19}\text{F NMR}$  (282 MHz,  $\text{CDCl}_3$ )  $\delta$  -87.00 (d,  $J = 42.6$  Hz, 1F), -90.05 (d,  $J = 42.6$  Hz, 1F). **HRMS** (EI) calcd for  $\text{C}_{12}\text{H}_9\text{NF}_2\text{O}_2$   $[\text{M}]^+$ : 237.0596, found: 237.0597.



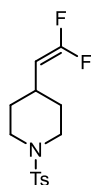
#### 2-(5,5-difluoropent-4-en-1-yl)isoindoline-1,3-dione (9x)

Following the general procedure C, the product was obtained as a white solid, 15.8 mg, 31% yield.  $^1\text{H NMR}$  (400 MHz,  $\text{CDCl}_3$ )  $\delta$  7.84 (dd,  $J = 5.4, 3.0$  Hz, 2H), 7.71 (dd,  $J = 5.5, 3.0$  Hz, 2H), 4.20 (dtd,  $J = 25.2, 7.8, 2.4$  Hz, 1H), 3.73 – 3.66 (m, 2H), 2.04 (qt,  $J = 7.8, 1.9$  Hz, 2H), 1.76 (p,  $J = 7.4$  Hz, 2H).  $^{13}\text{C NMR}$  (101 MHz,  $\text{CDCl}_3$ )  $\delta$  168.31, 159.21, 156.37, 156.35, 153.52, 133.93, 132.04, 123.21, 77.32, 77.14, 77.00, 76.93, 76.91, 76.68, 37.18, 28.27, 28.25, 28.23, 19.73, 19.69.  $^{19}\text{F NMR}$  (282 MHz,  $\text{CDCl}_3$ )  $^{19}\text{F NMR}$  (377 MHz,  $\text{CDCl}_3$ )  $\delta$  -88.91 (d,  $J = 46.4$  Hz), -91.13 (d,  $J = 46.4$  Hz). **HRMS** (EI) calcd for  $\text{C}_{13}\text{H}_{11}\text{NO}_2\text{F}_2$   $[\text{M}]^+$ :251.0752, found: 251.0748.



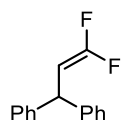
#### benzyl (4,4-difluorobut-3-en-1-yl)carbamate (9y)

Following the general procedure C, the product was obtained as a white solid, 18.5 mg, 38% yield.  $^1\text{H NMR}$  (300 MHz,  $\text{CDCl}_3$ )  $\delta$  7.35 (m, 5H), 5.10 (s, 2H), 4.87 (s, 1H), 4.15 (dtd,  $J = 25.1, 7.9, 2.2$  Hz, 1H), 3.24 (q,  $J = 6.6$  Hz, 2H), 2.28 – 2.11 (m, 2H).  $^{13}\text{C NMR}$  (75 MHz,  $\text{CDCl}_3$ )  $^{13}\text{C NMR}$  (75 MHz, Chloroform-*d*)  $\delta$  156.31, 156.94 (dd, 285.0 Hz, 284.3 Hz), 136.40, 128.51, 128.13, 128.07, 74.95 (dd, 21.0 Hz, 20.3 Hz), 66.73, 40.43, 23.18 (d,  $J = 4.3$  Hz).  $^{19}\text{F NMR}$  (282 MHz,  $\text{CDCl}_3$ )  $\delta$  -87.37 (d,  $J = 44.0$  Hz, 1F), -90.39 (d,  $J = 44.1$  Hz, 1F). **HRMS** (ESI) calcd for  $[\text{M}+\text{H}]^+$ :242.0987, found: 242.0988.



#### 4-(2,2-difluorovinyl)-1-tosylpiperidine (9z)

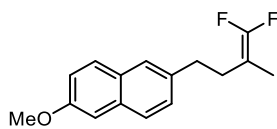
Following the general procedure C, the product was obtained as a colorless oil, 29.5 mg, 49% yield.  $^1\text{H NMR}$  (400 MHz,  $\text{CDCl}_3$ )  $\delta$  7.66 – 7.59 (m, 2H), 7.32 (d,  $J = 7.9$  Hz, 2H), 4.02 (ddd,  $J = 25.4, 9.3, 2.7$  Hz, 1H), 3.71 (dt,  $J = 11.6, 3.5$  Hz, 2H), 2.43 (s, 3H), 2.30 (td,  $J = 11.9, 2.7$  Hz, 2H), 2.18 – 2.00 (m, 1H), 1.78 – 1.68 (m, 2H), 1.54 – 1.42 (m, 2H).  $^{13}\text{C NMR}$  (101 MHz,  $\text{CDCl}_3$ )  $\delta$  155.87 (t,  $J = 288.8$  Hz), 143.51, 132.93, 129.59, 127.65, 81.77 (dd,  $J = 20.8, 19.7$  Hz), 45.85, 31.46 (t,  $J = 2.3$  Hz), 29.86 (d,  $J = 4.5$  Hz), 21.47.  $^{19}\text{F NMR}$  (377 MHz,  $\text{CDCl}_3$ )  $\delta$  -89.08 (d,  $J = 46.0$  Hz, 1F), -89.82 (d,  $J = 45.9$  Hz, 1F). **HRMS** (ESI) calcd for  $[\text{M}+\text{H}]^+$ : 302.1021, found: 302.1026.



#### (3,3-difluoroprop-2-ene-1,1-diyl)dibenzene (9aa)

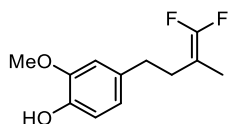
Following the general procedure C, the product was obtained as a white solid, 40 mg, 87% yield.  $^1\text{H NMR}$  (400 MHz,  $\text{CDCl}_3$ )  $\delta$  7.26 – 7.19 (m, 4H), 7.17 – 7.06 (m, 6H), 4.83 – 4.77 (m, 1H), 4.69 (ddd,  $J = 23.8, 10.5, 2.4$  Hz, 1H).  $^{13}\text{C NMR}$  (101 MHz,  $\text{CDCl}_3$ )  $\delta$  155.96 (dd,  $J = 288.7, 287.4$  Hz), 143.09 (t,  $J = 2.1$  Hz), 128.60, 127.89, 126.69, 82.00 (dd,  $J = 22.3, 19.1$  Hz), 44.52 (d,  $J = 4.9$  Hz).  $^{19}\text{F NMR}$  (377 MHz,  $\text{CDCl}_3$ )  $\delta$  -88.70

(d,  $J = 42.7$  Hz, 1F), -90.43 (d,  $J = 42.8$  Hz, 1F). **HRMS** (EI) calcd. for  $C_{15}H_{11}F_2$   $[M]^+$ : 229.0823, found: 229.0826.



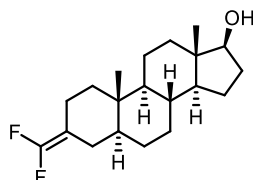
#### 2-(4,4-difluoro-3-methylbut-3-en-1-yl)-6-methoxynaphthalene (9ab)

Following the general procedure C, the product was obtained as a colorless oil, 24.3 mg, 46% yield.  **$^1H$  NMR** (300 MHz,  $CDCl_3$ )  $\delta$  7.72 – 7.65 (m, 2H), 7.56 (dt,  $J = 1.4, 0.8$  Hz, 1H), 7.31 (dd,  $J = 8.4, 1.7$  Hz, 1H), 7.17 – 7.11 (m, 2H), 3.92 (s, 3H), 2.84 (dd,  $J = 9.2, 6.7$  Hz, 2H), 2.36 (ddt,  $J = 7.7, 6.4, 2.2$  Hz, 2H), 1.62 (t,  $J = 3.2$  Hz, 3H).  **$^{13}C$  NMR** (75 MHz,  $CDCl_3$ )  $\delta$  157.20, 152.95 (dd,  $J = 280.5$  Hz, 279.8 Hz), 136.39, 133.05, 129.03, 128.90, 127.54, 126.79, 126.26, 118.72, 105.59, 84.22 (dd,  $J = 18.8$  Hz, 18.0 Hz), 55.25, 33.57 (t,  $J = 2.6$  Hz), 30.18 (d,  $J = 2.3$  Hz), 12.02 (t,  $J = 2.1$  Hz).  **$^{19}F$  NMR** (282 MHz,  $CDCl_3$ )  $\delta$  -96.62 (d,  $J = 57.4$  Hz, 1F), -96.97 (d,  $J = 57.4$  Hz, 1F). **HRMS** (EI) calcd for  $C_{16}H_{16}F_2O$   $[M]^+$ : 262.1164, found: 262.1164.



#### 4-(4,4-difluoro-3-methylbut-3-en-1-yl)-2-methoxyphenol (9ac)

Following the general procedure C, the product was obtained as a colorless oil, 26.5 mg, 58% yield.  **$^1H$  NMR** (400 MHz,  $CDCl_3$ )  $\delta$  6.84 (d,  $J = 8.5$  Hz, 1H), 6.70 – 6.65 (m, 2H), 5.50 (s, 1H), 3.88 (s, 3H), 2.64 (dd,  $J = 9.1, 6.7$  Hz, 2H), 2.25 (tt,  $J = 8.0, 2.1$  Hz, 2H), 1.58 (t,  $J = 3.2$  Hz, 3H).  **$^{13}C$  NMR** (101 MHz,  $CDCl_3$ )  $\delta$  152.95 (dd,  $J = 282.3, 281.4$  Hz), 146.36, 143.83, 133.14, 120.91, 114.20, 110.79, 84.18 (dd,  $J = 19.4, 18.3$  Hz), 55.86, 33.22 (t,  $J = 2.7$  Hz), 30.35 (d,  $J = 2.2$  Hz), 11.94.  **$^{19}F$  NMR** (377 MHz,  $CDCl_3$ )  $\delta$  -96.79 (d,  $J = 57.8$  Hz, 1F), -97.11 (d,  $J = 57.7$  Hz, 1F). **HRMS** (EI) calcd for  $C_{12}H_{14}F_2O_2$   $[M]^+$ : 228.0956, found: 228.0956.



#### 3-(difluoromethylene)-10,13-dimethylhexadecahydro-1H-cyclopenta[a]phenanthren-17-ol (9ad)

Following the general procedure C, the product was obtained as a white solid, 27.2 mg, 48% yield.  **$^1H$  NMR** (300 MHz,  $CDCl_3$ )  $\delta$  3.62 (dd,  $J = 9.0, 8.0$  Hz, 1H), 2.34 – 2.20 (m, 1H), 2.04 (dtd,  $J = 13.2, 9.2, 5.7$  Hz, 2H), 1.90 (tddd,  $J = 14.7, 6.2, 3.4, 1.4$  Hz, 1H), 1.83 – 1.61 (m, 4H), 1.61 – 1.51 (m, 2H), 1.48 – 1.29 (m, 4H), 1.29 – 0.83 (m, 8H), 0.84 (d,  $J = 0.7$  Hz, 3H), 0.73 (d,  $J = 0.7$  Hz, 3H), 0.65 (ddd,  $J = 12.3, 10.4, 4.2$  Hz, 1H).  **$^{13}C$  NMR** (75 MHz,  $CDCl_3$ )  $\delta$  150.62 (t,  $J = 280.3$  Hz), 87.60 (t,  $J = 18.5$  Hz), 81.90, 54.22, 50.95, 46.22 (t,  $J = 1.8$  Hz), 42.91, 37.92 (t,  $J = 1.5$  Hz), 36.67, 36.09, 35.43, 31.35, 30.47, 28.43, 26.62 (d,  $J = 1.8$  Hz), 23.34, 20.54, 19.86 (t,  $J = 2.3$  Hz), 11.38, 11.12.  **$^{19}F$  NMR** (282 MHz,  $CDCl_3$ )  $\delta$  -99.52 (d,  $J = 63.3$  Hz, 1F), -99.92 (d,  $J = 63.2$  Hz, 1F). **HRMS** (EI) calcd for  $C_{20}H_{30}F_2O$   $[M]^+$ : 324.2259, found: 324.2258.

### 3.5. References

- [1] D. Seebach, *Angew. Chem. Int. Ed.* **1979**, *18*, 239-258.
- [2] a) B.-T. Gröbel, D. SEEBACH, *Synthesis* **1977**, *1977*, 357-402; b) D. Seebach, E. J. Corey, *J. Org. Chem.* **1975**, *40*, 231-237; c) A. B. Smith, C. M. Adams, *Acc. Chem. Res.* **2004**, *37*, 365-377.

- [3] a) X. Bugaut, F. Glorius, *Chem. Soc. Rev.* **2012**, *41*, 3511-3522; b) D. M. Flanigan, F. Romanov-Michailidis, N. A. White, T. Rovis, *Chem. Rev.* **2015**, *115*, 9307-9387; c) N. Marion, S. Díez-González, S. P. Nolan, *Angew. Chem. Int. Ed.* **2007**, *46*, 2988-3000.
- [4] M. Huang, *J. Am. Chem. Soc.* **1946**, *68*, 2487-2488.
- [5] Lewis, D. E. *The Wolff-Kishner Reduction and Related Reactions: Discovery and Development*; Elsevier, 2019
- [6] a) A. G. Myers, P. J. Kukkola, *J. Am. Chem. Soc.* **1990**, *112*, 8208-8210; b) A. G. Myers, M. Movassaghi, *J. Am. Chem. Soc.* **1998**, *120*, 8891-8892; c) E. Vedejs, J. M. Dolphin, W. T. Stolle, *J. Am. Chem. Soc.* **1979**, *101*, 249-251; d) E. Vedejs, W. T. Stolle, *Tetrahedron Lett.* **1977**, *18*, 135-138.
- [7] H. Wang, X.-J. Dai, C.-J. Li, *Nat. Chem.* **2017**, *9*, 374-378.
- [8] N. Chen, X.-J. Dai, H. Wang, C.-J. Li, *Angew. Chem. Int. Ed.* **2017**, *56*, 6260-6263.
- [9] S.-S. Yan, L. Zhu, J.-H. Ye, Z. Zhang, H. Huang, H. Zeng, C.-J. Li, Y. Lan, D.-G. Yu, *Chem. Sci.* **2018**, *9*, 4873-4878.
- [10] X.-J. Dai, H. Wang, C.-J. Li, *Angew. Chem. Int. Ed.* **2017**, *56*, 6302-6306.
- [11] J. Tang, L. Lv, X.-J. Dai, C.-C. Li, L. Li, C.-J. Li, *Chem. Commun.* **2018**, *54*, 1750-1753.
- [12] L. Lv, D. Zhu, C.-J. Li, *Nat. Commun.* **2019**, *10*, 715.
- [13] D. Zhu, L. Lv, C.-C. Li, S. Ung, J. Gao, C.-J. Li, *Angew. Chem. Int. Ed.* **2018**, *57*, 16520-16524.
- [14] W. Wei, X.-J. Dai, H. Wang, C. Li, X. Yang, C.-J. Li, *Chem. Sci.* **2017**, *8*, 8193-8197.
- [15] H. Zeng, Z. Luo, X. Han, C.-J. Li, *Org. Lett.* **2019**, *21*, 5948-5951.
- [16] S. Wang, N. Lokesh, J. Hioe, R. M. Gschwind, B. König, *Chem. Sci.* **2019**, *10*, 4580-4587.
- [17] a) H. T. Dao, C. Li, Q. Michaudel, B. D. Maxwell, P. S. Baran, *J. Am. Chem. Soc.* **2015**, *137*, 8046-8049; b) S. Kim, J. R. Cho, *Synlett* **1992**, *1992*, 629-630; c) N. E. Campbell, G. M. Sammis, *Angew. Chem. Int. Ed.* **2014**, *53*, 6228-6231.
- [18] a) J. E. Baldwin, R. M. Adlington, J. C. Bottaro, J. N. Kolhe, I. M. Newington, M. W. D. Perry, *Tetrahedron* **1986**, *42*, 4235-4246; b) J. E. Baldwin, J. C. Bottaro, J. N. Kolhe, R. M. Adlington, *J. Chem. Soc., Chem. Commun.* **1984**, 22-23; c) J. R. Reyes, V. H. Rawal, *Angew. Chem. Int. Ed.* **2016**, *55*, 3077-3080.
- [19] a) P. Chauhan, S. Mahajan, D. Enders, *Chem. Rev.* **2014**, *114*, 8807-8864; b) C. Shen, P. Zhang, Q. Sun, S. Bai, T. S. A. Hor, X. Liu, *Chem. Soc. Rev.* **2015**, *44*, 291-314; c) F. Minghao, T. Bingqing, H. L. Steven, J. Xuefeng, *Curr. Top. Med. Chem.* **2016**, *16*, 1200-1216; d) N. Wang, P. Saidharedy, X. Jiang, *Nat. Prod. Rep.* **2020**, *37*, 246-275.
- [20] a) W. Guo, K. Tao, W. Tan, M. Zhao, L. Zheng, X. Fan, *Org. Chem. Front.* **2019**, *6*, 2048-2066; b) A. Wimmer, B. König, *Beilstein J. Org. Chem.* **2018**, *14*, 54-83.
- [21] R. Fernández de la Pradilla, A. Viso, in *Comprehensive Organic Synthesis II (Second Edition)* (Ed.: P. Knochel), Elsevier, Amsterdam, **2014**, pp. 157-208.
- [22] a) V. R. Yatham, Y. Shen, R. Martin, *Angew. Chem. Int. Ed.* **2017**, *56*, 10915-10919; b) L.-L. Liao, G.-M. Cao, J.-H. Ye, G.-Q. Sun, W.-J. Zhou, Y.-Y. Gui, S.-S. Yan, G. Shen, D.-G. Yu, *J. Am. Chem. Soc.* **2018**, *140*, 17338-17342; c) J. Hou, A. Ee, H. Cao, H.-W. Ong, J.-H. Xu, J. Wu, *Angew. Chem. Int. Ed.* **2018**, *57*, 17220-17224; d) W.-J. Yoo, J. Kondo, J. A. Rodríguez-Santamaría, T. V. Q. Nguyen, S. Kobayashi, *Angew. Chem. Int. Ed.* **2019**, *58*, 6772-6775; e) Q.-Y. Meng, T. E. Schirmer, A. L. Berger, K. Donabauer, B. König, *J. Am. Chem. Soc.* **2019**, *141*, 11393-11397.
- [23] a) Q.-Y. Meng, S. Wang, B. König, *Angew. Chem. Int. Ed.* **2017**, *56*, 13426-13430; b) Q.-Y. Meng, S. Wang, G. S. Huff, B. König, *J. Am. Chem. Soc.* **2018**, *140*, 3198-3201; c) B. Sahoo, P. Bellotti, F. Juliá-Hernández, Q.-Y. Meng, S. Crespi, B. König, R. Martin, *Chem. Eur. J.* **2019**, *25*, 9001-9005.

- [24] a) A. Noble, D. W. C. MacMillan, *J. Am. Chem. Soc.* **2014**, *136*, 11602-11605; b) D. R. Heitz, K. Rizwan, G. A. Molander, *J. Org. Chem.* **2016**, *81*, 7308-7313.
- [25] A. L. Berger, K. Donabauer, B. König, *Chem. Sci.* **2018**, *9*, 7230-7235.
- [26] a) Y. Yamamoto, N. Asao, *Chem. Rev.* **1993**, *93*, 2207-2293. b) P. Barbier. *C. R. Acad. Sci.* **1899**, *128*, 110-111.
- [27] In the examples of 6h and 6i, benzyl phenyl sulfide was formed in 29% and 32% yield, respectively.
- [28] S. Nakamura, R. Nakagawa, Y. Watanabe, T. Toru, *J. Am. Chem. Soc.* **2000**, *122*, 11340-11347.
- [29] a) K. Müller, C. Faeh, F. Diederich, *Science* **2007**, *317*, 1881-1886; b) E. P. Gillis, K. J. Eastman, M. D. Hill, D. J. Donnelly, N. A. Meanwell, *J. Med. Chem.* **2015**, *58*, 8315-8359.
- [30] a) V. Gouverneur, *Fluorine in Pharmaceutical and Medicinal Chemistry: from biophysical aspects to clinical applications*, World Scientific, **2012**; b) I. Ojima, *Fluorine in medicinal chemistry and chemical biology*, John Wiley & Sons, **2009**.
- [31] a) G. Chelucci, *Chem. Rev.* **2012**, *112*, 1344-1462; b) X. Zhang, S. Cao, *Tetrahedron Lett.* **2017**, *58*, 375-392; c) S. Koley, R. A. Altman, *Isr. J. Chem.* **2020**, *60*, 313-339.
- [32] a) J. Zheng, J. Cai, J.-H. Lin, Y. Guo, J.-C. Xiao, *Chem. Commun.* **2013**, *49*, 7513-7515; b) D. J. Burton, Z.-Y. Yang, W. Qiu, *Chem. Rev.* **1996**, *96*, 1641-1716.
- [33] a) Y. Zhao, W. Huang, L. Zhu, J. Hu, *Org. Lett.* **2010**, *12*, 1444-1447; b) B. Gao, Y. Zhao, M. Hu, C. Ni, J. Hu, *Chem. Eur. J.* **2014**, *20*, 7803-7810.
- [34] a) Z. Zhang, Q. Zhou, W. Yu, T. Li, G. Wu, Y. Zhang, J. Wang, *Org. Lett.* **2015**, *17*, 2474-2477; b) M. Hu, Z. He, B. Gao, L. Li, C. Ni, J. Hu, *J. Am. Chem. Soc.* **2013**, *135*, 17302-17305; c) Z. Yang, M. Möller, R. M. Koenigs, *Angew. Chem. Int. Ed.* **2020**, *59*, 5572-5576.
- [35] M. Hu, C. Ni, L. Li, Y. Han, J. Hu, *J. Am. Chem. Soc.* **2015**, *137*, 14496-14501.
- [36] a) D. Ding, Y. Lan, Z. Lin, C. Wang, *Org. Lett.* **2019**, *21*, 2723-2730; b) Y. Lan, F. Yang, C. Wang, *ACS Catal.* **2018**, *8*, 9245-9251; c) Z. Lin, Y. Lan, C. Wang, *Org. Lett.* **2019**, *21*, 8316-8322; d) Z. Lin, Y. Lan, C. Wang, *ACS Catal.* **2018**, *9*, 775-780; e) X. Lu, X.-X. Wang, T.-J. Gong, J.-J. Pi, S.-J. He, Y. Fu, *Chem. Sci.* **2019**, *10*, 809-814; f) X. Zhao, C. Li, B. Wang, S. Cao, *Tetrahedron Lett.* **2019**, *60*, 129-132.
- [37] a) S. B. Lang, R. J. Wiles, C. B. Kelly, G. A. Molander, *Angew. Chem. Int. Ed.* **2017**, *56*, 15073-15077; b) T. Xiao, L. Li, L. Zhou, *J. Org. Chem.* **2016**, *81*, 7908-7916; c) H. Chen, D. Anand, L. Zhou, *Asian J. Org. Chem.* **2019**, *8*, 661-664; d) J. P. Phelan, S. B. Lang, J. Sim, S. Berritt, A. J. Peat, K. Billings, L. Fan, G. A. Molander, *J. Am. Chem. Soc.* **2019**, *141*, 3723-3732; e) R. J. Wiles, J. P. Phelan, G. A. Molander, *Chem. Commun.* **2019**, *55*, 7599-7602; f) L. H. Wu, J. K. Cheng, L. Shen, Z. L. Shen, T. P. Loh, *Adv. Synth. Catal.* **2018**, *360*, 3894-3899; g) Y.-Q. Guo, R. Wang, H. Song, Y. Liu, Q. Wang, *Org. Lett.* **2020**, *22*, 709-713.
- [38] K. Uneyama, T. Katagiri, H. Amii, *Acc. Chem. Res.* **2008**, *41*, 817-829.
- [39] a) C. Zhang, *Adv. Synth. Catal.* **2014**, *356*, 2895-2906; b) T. Koike, M. Akita, *Chem* **2018**, *4*, 409-437; c) C. Alonso, E. Martinez de Marigorta, G. Rubiales, F. Palacios, *Chem. Rev.* **2015**, *115*, 1847-1935; d) X. Pan, H. Xia, J. Wu, *Org. Chem. Front.* **2016**, *3*, 1163-1185.
- [40] In this case, the protonated byproduct was isolated in 24% yield.
- [41] K. Donabauer, M. Maity, A. L. Berger, G. S. Huff, S. Crespi, B. König, *Chem. Sci.* **2019**, *10*, 5162-5166.
- [42] M. S. Lowry, J. I. Goldsmith, J. D. Slinker, R. Rohl, R. A. Pascal, G. G. Malliaras, S. Bernhard, *Chem. Mater.* **2005**, *17*, 5712-5719.
- [43] a) M. Jiang, H. Li, H. Yang, H. Fu, *Angew. Chem. Int. Ed.* **2017**, *56*, 874-879; b) D. Liu, H. X. Ma,

- P. Fang, T. S. Mei, *Angew. Chem. Int. Ed.* **2019**, *58*, 5033-5037.
- [44] P. Xu, W. Li, J. Xie, C. Zhu, *Acc. Chem. Res.* **2018**, *51*, 484-495.
- [45] B.-H. Zhang, L.-S. Lei, S.-Z. Liu, X.-Q. Mou, W.-T. Liu, S.-H. Wang, J. Wang, W. Bao, K. Zhang, *Chem. Commun.* **2017**, *53*, 8545-8548.
- [46] L. Gavara, C. Petit, J.-L. Montchamp, *Tetrahedron Lett.* **2012**, *53*, 5000-5003.
- [47] A. J. Stepen, M. Bursch, S. Grimme, D. W. Stephan, J. Paradies, *Angew. Chem. Int. Ed.* **2018**, *57*, 15253-1525





## 4. Light-Induced Single-Electron Transfer Processes Involving Sulfur

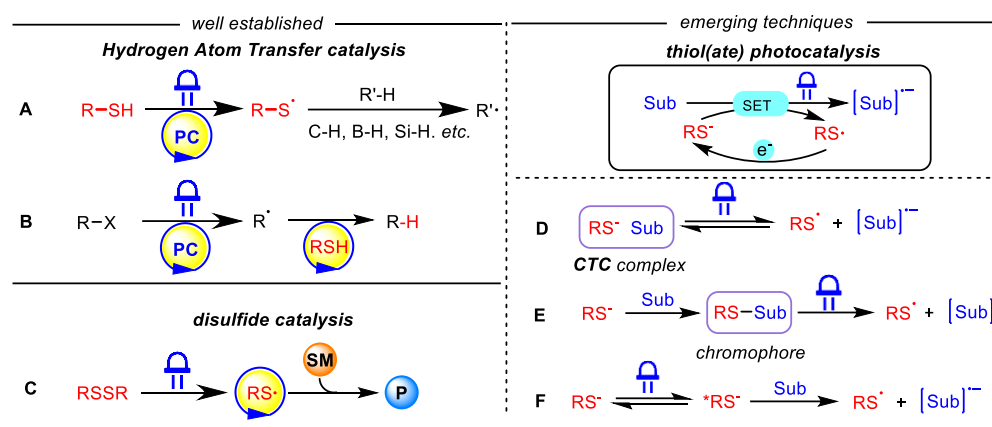
### Anions as Catalysts

#### 4.1 Introduction

Photoredox catalysis has experienced a dramatic prosperity over the past decade and enabled many new chemical transformations in a sustainable way. Since most organic molecules do not absorb visible light, their direct activation requires irradiation with ultraviolet (UV) light, which can cause undesired side reactions and requires specialized setups limiting the broader application of classic photochemistry in organic synthesis. The use of visible-light-absorbing photocatalysts to sensitize organic molecules through energy transfer processes or initiate photoredox reactions have practical advantages and can lead to better reaction selectivity.<sup>[1]</sup> Chemical photocatalysis has been proved to be a powerful strategy for the activation and the formation of different chemical bonds mainly via radical and radical ion intermediates. A variety of molecular photocatalysts including transition-metal complexes<sup>[1b, 1c, 1g]</sup> (e.g., based on Ru and Ir) and organic dyes,<sup>[1e]</sup> improved existing methods and enabled new chemical transformations. Recently, the potential of excited anionic species for triggering electron transfer processes owing to their enhanced electron-donating power and bathochromically shifted absorption as compared to the neutral species has attracted increasing interest.<sup>[2]</sup> This has endowed a broad range of structurally simple anionic species with unique catalytic behaviors. A key advantage of anionic photocatalysis is the effortless availability of anionic catalysts by deprotonation with base from the corresponding acids.

In this context, sulfur-based anionic species (e.g., sulfide, thiolate), have found applications as catalysts or co-catalysts in photochemical transformations. In visible-light photocatalysis, thiolates are readily oxidized by an excited photoredox catalysts to generate thiyl radicals, which are employed for the construction of organosulfur molecules, and used as hydrogen atom transfer agents (Scheme 1A-B).<sup>[3]</sup> Additionally, thiyl radicals are produced from photolysis of disulfides, which have been utilized in a variety of chemical transformations in a catalytic manner (Scheme 1C).<sup>[4]</sup> Excited sulfur-based anions are potent electron donors as a photocatalyst and can be used for inert bond activation. Moreover, upon photo-induced ET between thiolates and substrates, the resulting thiyl radicals and substrate radical anions are valuable intermediates in subsequent reaction steps. We will discuss the key aspects for the successful design of such a photo-thiolate catalytic system in the following section. These include: 1) What is the light-absorbing species? 2) How does the electron transfer event occurs between thiolate catalyst and substrate and 3) how is the thiolate catalyst after the electron transfer process regenerated.

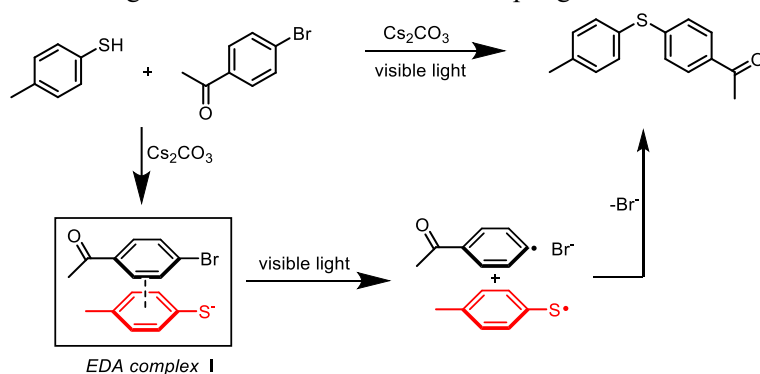
Guided by these questions we provide a brief overview of the emerging photo-induced sulfur-based anion-catalyzed approaches for new chemical transformations. Electron transfer modes from thiolate to substrates under photochemical conditions have been categorized into three groups; 1) ET through excitation of a charge-transfer complex (Scheme 1D); 2) photoexcitation of the *in-situ* formed chromophore (Scheme 1E); 3) ET between the excited state of a sulfur-based anion with a substrate. We will not include photocatalytic reactions that use thiols or thiolates as a co-catalyst for the generation of radicals as key intermediates by way of sulfur-mediated hydrogen atom transfer (HAT) processes. Research advance in this field has been summarized in several comprehensive reviews.<sup>[5]</sup>



**Scheme 1.** Thiol(ate) catalysis in photo-induced reactions

## 4.2 Light-induced thiolate catalysis mediated by an electron donor–acceptor (EDA) complex

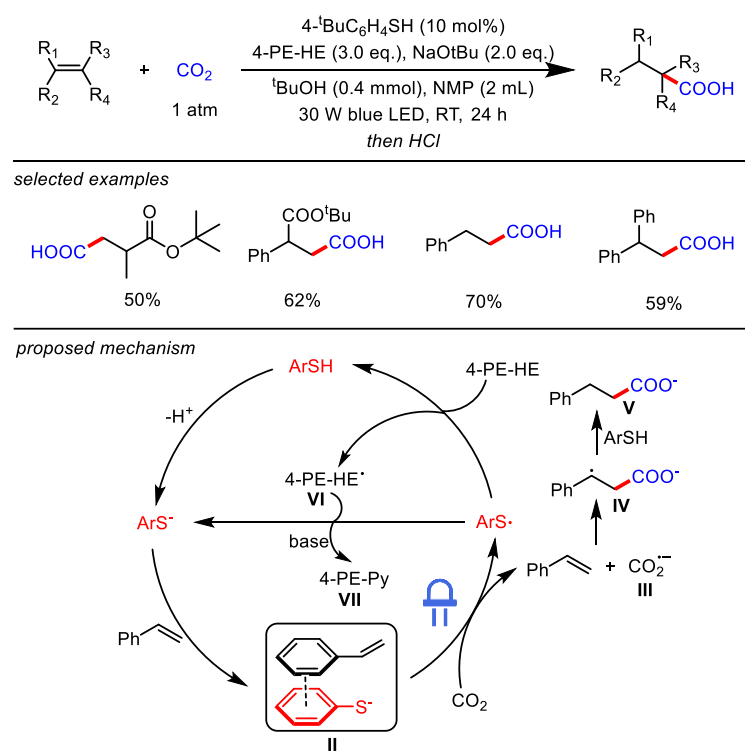
Thiolate nucleophiles are known to participate in photo-induced  $S_{RN}1$  reactions with aryl halides to construct C-S bonds.<sup>[6]</sup> Nevertheless, in the classical  $S_{RN}1$  processes the photo-induced electron transfer from thiolate to aryl halides requires the use of UV light and liquid ammonia as reaction medium.<sup>[7]</sup> In 2017, pioneering work by Miyake and co-workers demonstrated that a thiolate anion could form an electron donor-acceptor (EDA) complex with the aryl halide (Scheme 3).<sup>[8]</sup> The resulting EDA complex was then irradiated by visible light to generate the corresponding thiyl radical and aryl radical, and a C-S coupled product was then generated from radical-radical coupling.<sup>[8-9]</sup>



**Scheme 3.** Stoichiometric EDA complex formation between thiolate and aryl halide

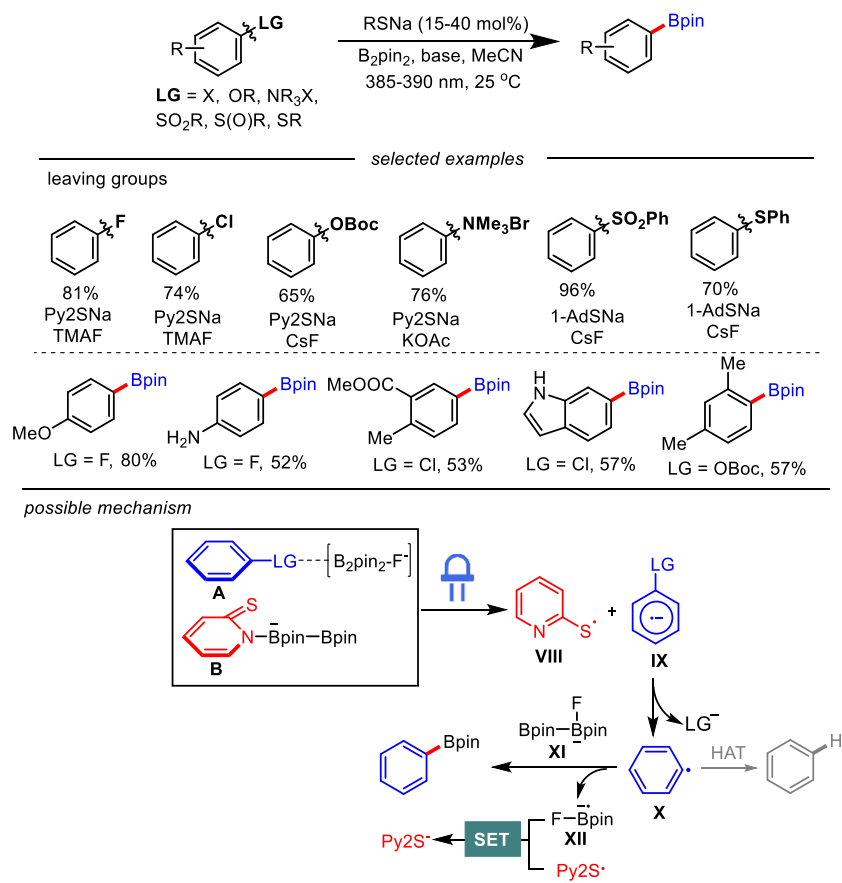
Recently, the Yu group investigated the catalytic potential of thiolates in a photoreaction through the EDA complex formation with substrates. They developed a visible-light-driven thiolate-catalyzed hydrocarboxylation of alkenes with  $CO_2$  by using 4-phenethyl Hantzsch ester (4-PE-HE) as the terminal reductant.<sup>[10]</sup> In their proposed mechanism, the reaction commences with the deprotonation of thiol by base to yield a thiolate. Then, the formation of EDA complex II between thiolate and alkene is followed by light excitation and electron transfer to  $CO_2$  to give a thiyl radical, alkene and a  $CO_2$  radical anion III. Radical addition of III to the alkene yields intermediate IV, capable of abstracting a hydrogen atom from thiophenol to give carboxylate V, which is then protonated to produce the desired carboxylic acid. Two reaction pathways are proposed to recycle the thiol and thiolate. The thiyl radical undergoes a HAT process to regenerate the thiol and concomitantly produce 4-PE-HE radical VI. The thiolate can also be recycled from the reduction of the thiyl radical by VI. The catalytic system was suitable for the hydrocarboxylation of acrylates and styrenes with superior functional group tolerance and moderate to

good product yields.



**Scheme 4.** Visible-light-induced thiolate-catalytic hydrocarboxylation of alkenes with CO<sub>2</sub>

In 2020, our group developed a photo-induced thiolate-catalyzed ipso-borylation of substituted arenes with B<sub>2</sub>pin<sub>2</sub>.<sup>[11]</sup> Inspired by the work by Miyake, we envisioned that a similar light-induced electron transfer from the anion to the aryl halide might occur to result in a thiyl radical and an aryl radical after releasing a halide anion. We anticipated that a fast aryl radical borylation with diboron compounds would outcompete the undesired C-S coupling to yield the desired aryl boronate and a boryl radical anion **XII**. The thiolate catalyst could then be regenerated from the single-electron reduction of a thiyl radical by a boryl radical anion **XII**.<sup>[12]</sup> As shown in Scheme 5, this photo-induced thiolate catalysis concept has been successfully applied for the borylation of a broad range of substrates that have low activity in most photocatalytic strategies. Specifically, by using 2-pyridinyl sodium thiolate or 1-AdSNa as a catalyst, B<sub>2</sub>pin<sub>2</sub> (Bispinacolato diboron) as a borylation reagent with purple light (385-390 nm) irradiation, inert C<sub>aryl</sub>-X bonds were borylated with moderate to good efficiencies. Compared with typical photoredox catalysis, the reaction system exhibited stronger reducing ability and engages non-activated C<sub>aryl</sub>-F, C<sub>aryl</sub>-Cl, C<sub>aryl</sub>-Br, C<sub>aryl</sub>-O, C<sub>aryl</sub>-N and C<sub>aryl</sub>-S bonds in productive radical borylation reactions, thus expanding the available aryl radical precursor scope. Notably, despite its high reducing power, the reaction showed a broad substrate scope. Mechanistic studies suggest that the formation of a charge-transfer complex is key for the reduction of the substrate to generate the aryl radical. It is proposed that the activation effect of substrates including C-X, C-OR, and C-NMe<sub>3</sub>X bonds by a [B<sub>2</sub>pin<sub>2</sub>-F<sup>-</sup>] adduct is essential for the photo-induced electron transfer process (Scheme 5).

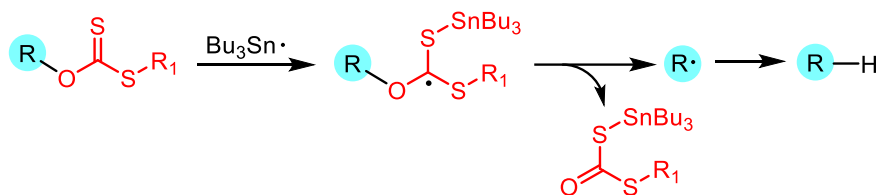


**Scheme 5.** Photo-induced thiolate-catalytic ipso-borylation of substituted arenes

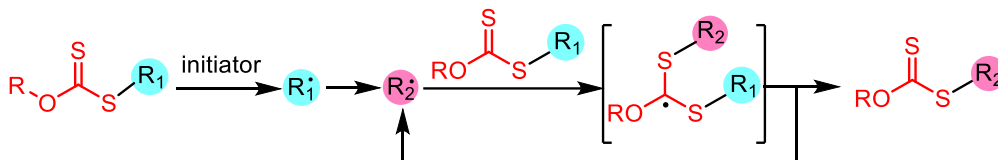
### 4.3 Photo-induced xanthate anion catalysis via *in-situ* formation of the light-absorbing species

Xanthates (or dithiocarbonates) are useful radical precursors in Barton–McCombie radical deoxygenation<sup>[13]</sup> reactions and the degenerative radical xanthate transfer as pioneered by the Zard group<sup>[14]</sup> (Scheme 6A and 6B). A variety of synthetically valuable free radicals can thus be produced and employed for various transformations such as decarboxylation, polymerization as well as C-C bond coupling reactions. The radical generation from xanthates in these processes is based on the radical addition-fragmentation processes in the presence of radical initiators such as peroxides, AIBN/Bu<sub>3</sub>SnH, or BEt<sub>3</sub>/O<sub>2</sub>.<sup>[13a, 15]</sup> Alternatively, a visible-light-driven approach has been developed for the cleavage of C-S bonds of *S*-acyl xanthates<sup>[14c, 14d, 16]</sup> and *N*-xanthylamide<sup>[17]</sup> (Scheme 6C). The photophysical properties of xanthates have also inspired the use of xanthate anions as a catalyst or initiator in photochemical reactions.

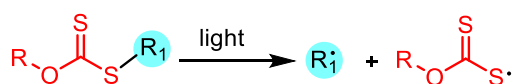
(A) Barton McCombie deoxygenation



(B) Zard's degenerative radical xanthate transfer

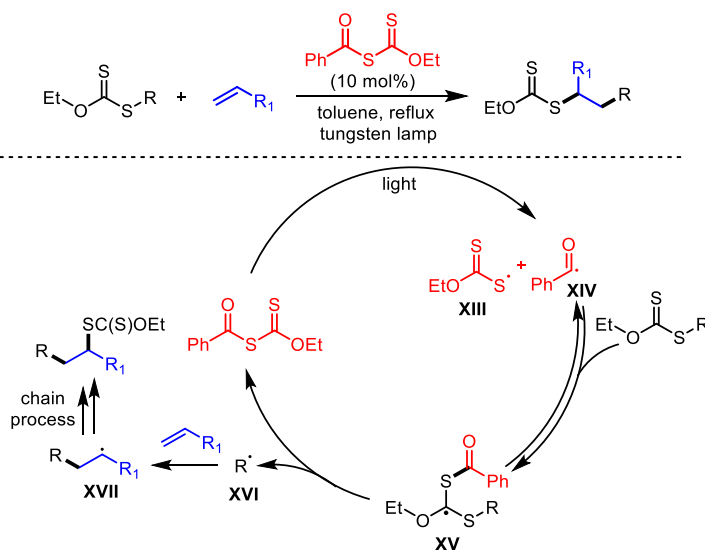


(C) Photo-induced radical generation from xanthate



**Scheme 6.** Radical generation from xanthates

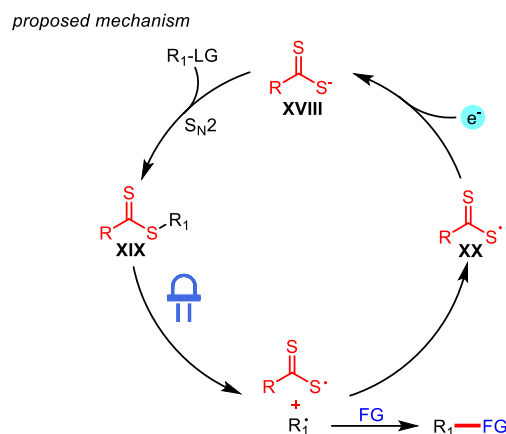
As early as 1988, Zard et al. reported the degenerative xanthate transfer from alkylxanthates to alkenes by using S-benzoyl O-ethyl xanthate as an initiator under irradiation with a tungsten lamp.<sup>[18]</sup> The reaction is initiated by photolysis of the S-benzoyl O-ethyl xanthate to give benzoyl radical **XIV** and a sulfur-centered radical **XIII**. A reversible benzoyl radical addition to the thiocarbonyl group affords radical intermediate **XV** which is followed by the  $\beta$ -scission to generate a carbon-centered radical **XVI**, concomitantly recycling the S-benzoyl O-ethyl xanthate. Subsequent addition of **XVI** to the C=C bond of an alkene radical trapping reagent produces radical species **XVII** capable of participating in the chain reaction process to give the desired product (Scheme 7).



**Scheme 7.** Light-induced degenerative radical transfer of xanthates to olefins

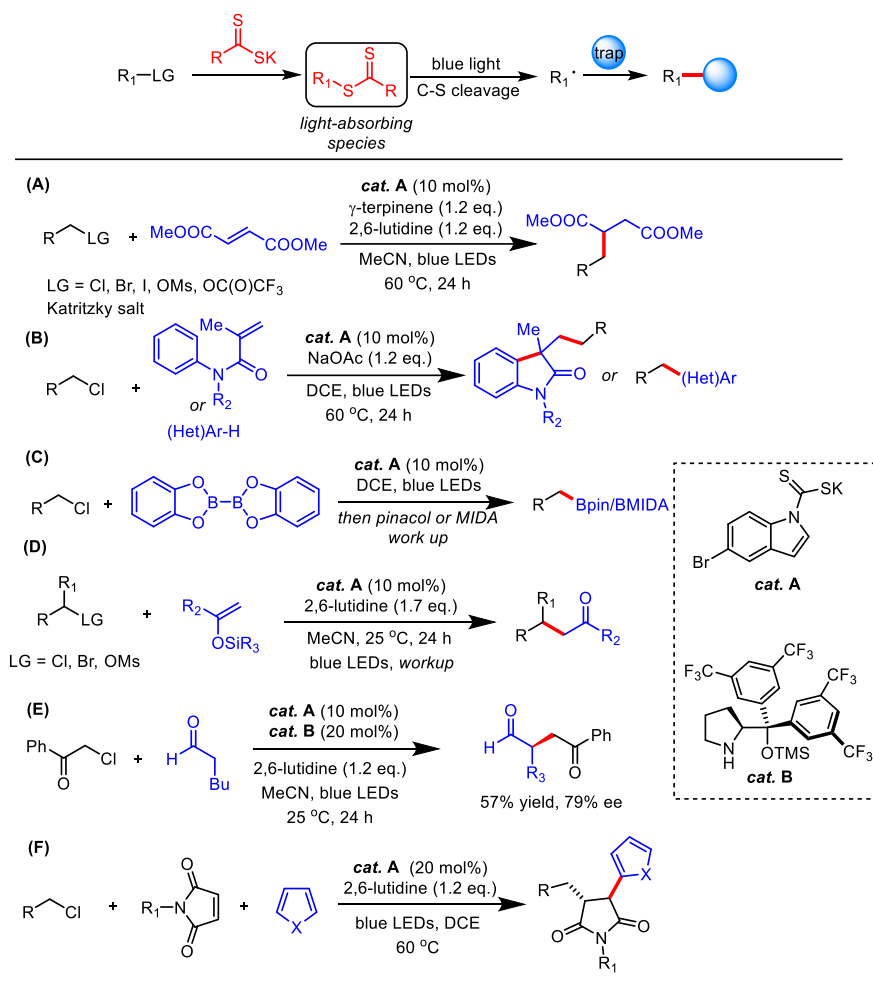
Despite being a very powerful radical generation pathway, the synthetic use of S-acyl xanthates in photochemical reactions is confined to xanthate transfer reactions wherein the alkylxanthates are

required as substrates for the radical chain initiation. Very recently, Melchiorre and co-workers reported a visible-light-induced generation of radicals from alkyl electrophiles by using a nucleophilic thiocarbamate anion catalyst.<sup>[19]</sup> The proposed catalytic cycle begins with the photolytic cleavage of a weak C-S bond of the *in-situ* generated xanthate intermediate, affording an alkyl radical and the sulfur-centered radical **XX**. The resulting sulfur-centered radical **XX** undergoes single-electron reduction to regenerate the anionic catalyst **XVIII** while the carbon-centered radical can be employed for C-X bond forming reactions (Scheme 8).



**Scheme 8.** Proposed mechanism for the photo-induced dithiocarbamate anion-catalyzed radical generation

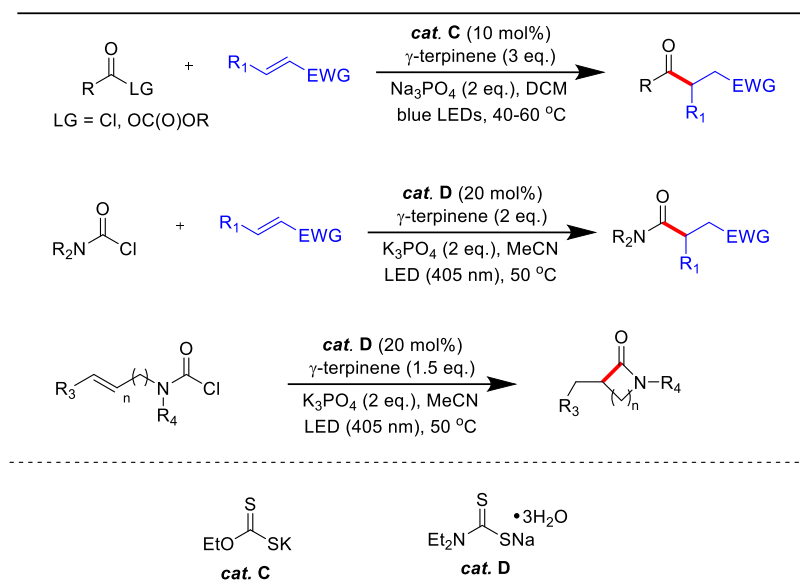
Under blue LED irradiation, various types of alkyl radical precursors including chlorides, bromides, mesylates and Katritzky salts were compatible with the reaction system using potassium dithiocarbamate as a catalyst. The produced alkyl radicals could be trapped by Michael acceptors, acrylamides, bis(catecholato)diboron ( $B_2cat_2$ ), silyl enol ethers, or (hetero) arenes with the formation of the desired functionalized products (Scheme 9A-D).<sup>[19-20]</sup> Notably, alkyl radicals generated in this photocatalytic system were successfully employed for the direct enantioselective  $\alpha$ -alkylation of aliphatic aldehydes (Scheme 9E).<sup>[19]</sup> The methodology was further applied to a visible-light mediated three-component radical type reaction wherein coupling reactions with alkyl chlorides, maleimides, and heteroarenes allowed the consecutive formation of two C-C bonds in one reaction (Scheme 9F).<sup>[21]</sup>



**Scheme 9.** Photo-induced dithiocarbamate anion-catalyzed generation of alkyl radicals and their use in C-C bond construction

Additionally, the Melchiorre group further extended the photocatalytic approach to the generation of acyl radicals /carbamoyl radicals from acyl/carbamoyl chlorides via a nucleophilic acyl substitution pathway. The resulting radicals were then involved in a Giese-type addition process to C=C bonds of alkenes in both intermolecular and intramolecular manner to yield the C-C coupled products (Scheme 10).<sup>[22]</sup>

This chemistry relies on the formation of a photoactive species from the xanthate or dithiocarbamate anion and electrophiles via S<sub>N</sub>2 substitution, capable of activating inert substrates with high reduction potentials which are normally challenging in a SET-based activation mechanism. Furthermore, this photocatalysis demonstrates an excellent functional group tolerance, a broad substrate scope and may find further synthetic applications in organic synthesis.

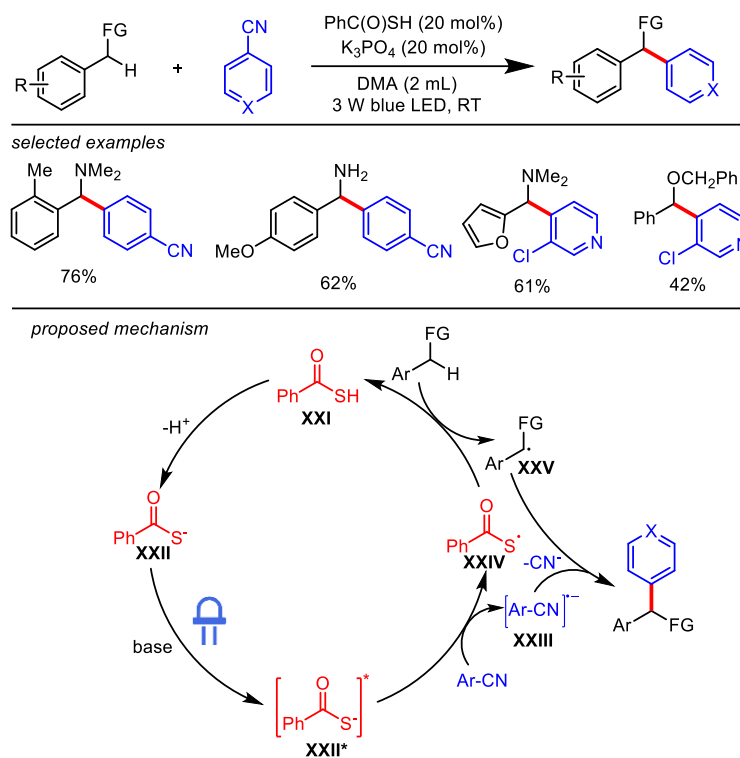


**Scheme 10.** Photo-induced dithiocarbamate and ethyl xanthate anion-catalyzed generation of acyl radicals and carbamoyl radicals and their use in C-C bond construction

#### 4.4 Light-induced thiolate catalysis enabled by the excited state of thiolate

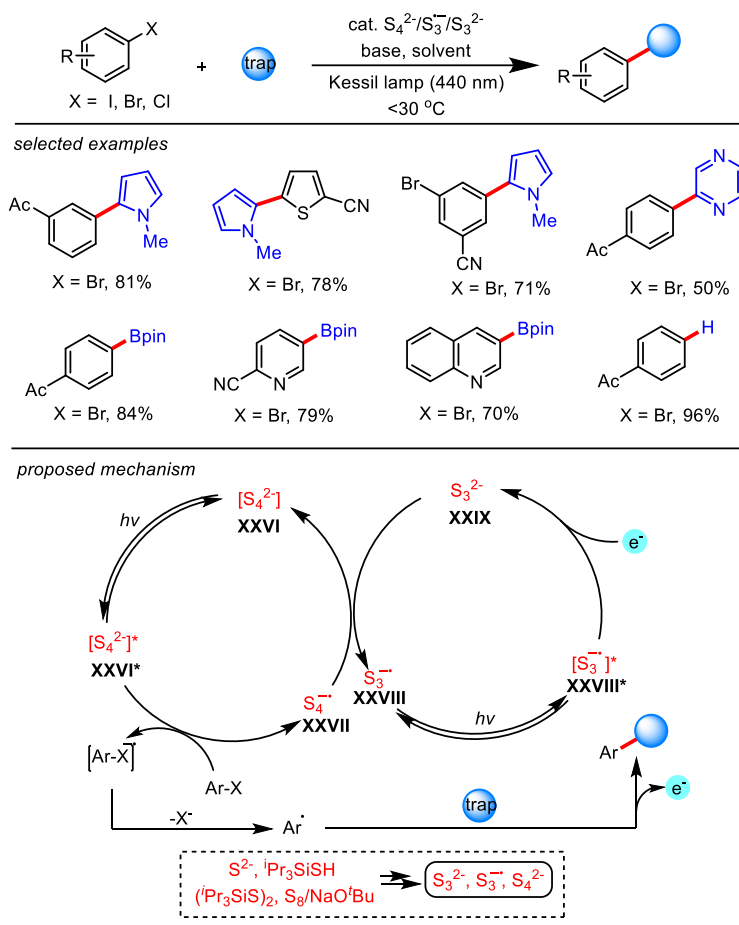
Apart from the aforementioned reactions, the excited state of sulfur-based anions has been explored for photocatalytic reactions. This process is driven by the reducing ability of the excited state thiolate anions triggering the electron transfer to a substrate generating the corresponding thiyl radical and substrate radical anion. Recently, Hamashima et al. have shown that the excited state of a thiobenzoate anion could be engaged in the catalytic single-electron reduction of cyanoarenes (Scheme 11).<sup>[23]</sup> By leveraging the dual role of the thiobenzoate anion catalyst, namely a one-electron reducing catalyst and as HAT catalyst, this method allowed the direct benzylic Csp<sup>3</sup>-H arylation with cyanoarenes in the presence of a catalytic amount (20 mol%) of thiobenzoic acid under blue light irradiation. The proposed mechanism of this transformation starts with deprotonation of **XXI** by base to produce thiobenzoate **XXII**, which could be excited by visible light. Subsequent SET from the photoexcited thiobenzoate to cyanoarenes generates the thiyl radical **XXIV** and a radical anion **XXIII**. The resulting thiyl radical **XXIV** abstracts a hydrogen atom from the substrate to give a carbon radical **XXV**, simultaneously regenerating the catalyst **XXI**. Further radical-radical coupling between **XXIII** and **XXV** affords the target product after releasing the cyanide anion. This unique catalytic system demonstrates good to excellent catalytic efficiency and a wide substrate scope with a broad range of functional groups being tolerated.





**Scheme 11.** Photo-induced thiobenzoate anion-catalyzed  $\text{Csp}^3\text{-H}$  arylation

Anionic polysulfides are used in various research fields including alkali-metal-sulfur batteries, biological chemistry, material science, and organic synthesis.<sup>[24]</sup> Despite their well-explored photophysical properties,<sup>[24a, 24b, 24e]</sup> their use as photocatalysts for chemical reactions has been reported only recently by Chiba and co-workers.<sup>[25]</sup> They showed that polysulfide anions possess a high reduction power after visible light excitation, capable of single-electron reduction of aryl halides to generate synthetically valuable aryl radicals. The resulting aryl radicals were exploited in aryl-aryl cross-coupling, borylation, and hydrogenation reactions. The protocol showed a broad scope, tolerating a wide range of substituents including carbonyls, pyridine, indole, and thiophene heterocycles. However, a decreased reaction efficiency was observed with electron-rich bromoarenes (e.g., 4-bromoanisole) as substrate. They demonstrated that dilithium sulfide, thiol ( $i\text{Pr}_3\text{SiSH}$ ; triisopropylsilanethiol), disulfide ( $i\text{Pr}_3\text{SiS}_2$ ) and  $\text{S}_8/\text{NaOtBu}$  were suitable precatalysts for the polysulfide anion generation. The presence of  $[\text{S}_3^-]$ ,  $[\text{S}_4^{2-}]$ , and  $[\text{S}_3^{2-}]$  species in a DMSO solution of  $\text{K}_2\text{S}_x$  (potassium polysulfide) was confirmed by UV/Vis spectroscopy. The proposed mechanism involves two coupled photoredox cycles:  $[\text{S}_4^-]/[\text{S}_4^{2-}]$  and  $[\text{S}_3^-]/[\text{S}_3^{2-}]$ . Upon photoexcitation of  $[\text{S}_4^{2-}]$  by blue light, electron transfer occurs between the resulting  $[\text{S}_4^{2-}]^*$  and an aryl halide produces the aryl radical along with the generation of  $[\text{S}_4^-]$ . Another SET event then takes place between  $[\text{S}_4^-]$  and  $[\text{S}_3^{2-}]$  to recycle the  $[\text{S}_4^{2-}]$  species and concomitantly produce  $[\text{S}_3^-]$ , which could be photo-excited to participate in another  $[\text{S}_3]$  photocatalytic cycle. The aryl radical was trapped by different reagents to give the desired coupling product after one-electron oxidation. The  $[\text{S}_3^{2-}]$  species was recycled by single-electron reduction of photo-excited  $[\text{S}_3^-]$  (Scheme 12).



**Scheme 12.** Photo-induced polysulfide anion-catalyzed reduction of aryl halides

## 4.5 Conclusion and outlook

We have highlighted recent progress exploring the catalytic property of sulfur-based anions in photo reactions. Although thiolates and their corresponding radicals are well-established HAT catalysts in photoredox catalysis, their direct use as catalysts to induce chemical transformations with light irradiation is still in its fancy. Thiolates show great potential to catalyze photoreactions via in-situ formation of chromophores or generating charge-transfer-complexes with substrates. Additionally, the excited states of anionic sulfur species show catalytic activity. A key advantage of thiolate photocatalysis is the possibility of using the generated thiyl radicals within the same catalytic cycle for hydrogen abstraction reactions.

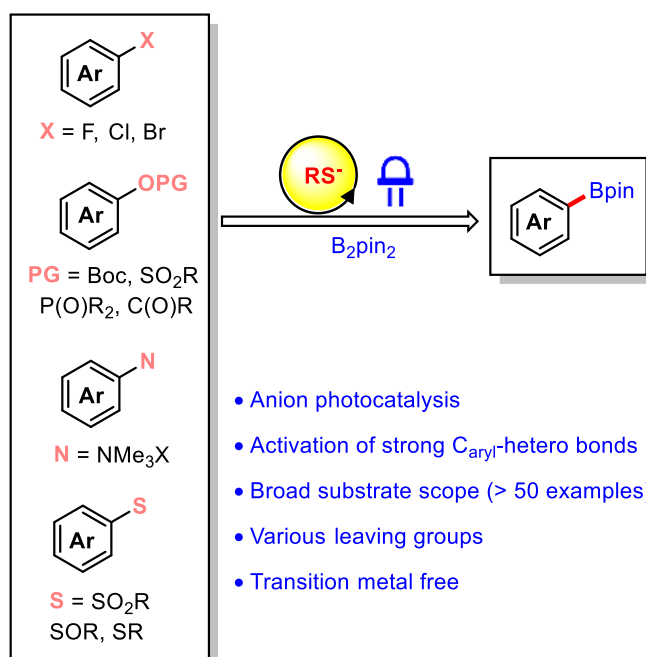
We expect in the near future an increasing attention to this field of research. Novel synthetic developments may arise from the identification of other substrates that can engage in sulfur-anion photocatalysis. Current catalytic systems require high catalyst loadings, which could be ascribed to the instability of catalysts and low activity of the catalytic systems. To improve, the design and development of new sulfur anionic catalysts for more efficient catalysts is a logic next step. Finally, the mechanistic details of most sulfur anion catalytic photoreactions are little understood and insights from mechanistic studies will be essential for the rational design of the next generation of thiolate photocatalytic systems.

## 4.6 References

- [1] a) L. Marzo, S. K. Pagire, O. Reiser, B. König, *Angew. Chem. Int. Ed.* **2018**, *57*, 10034-10072; b) J. M. R. Narayanam, C. R. J. Stephenson, *Chem. Soc. Rev.* **2011**, *40*, 102-113; c) C. K. Prier, D. A. Rankic, D. W. C. MacMillan, *Chem. Rev.* **2013**, *113*, 5322-5363; d) D. Ravelli, S. Protti, M. Fagnoni, *Chem. Rev.* **2016**, *116*, 9850-9913; e) N. A. Romero, D. A. Nicewicz, *Chem. Rev.* **2016**, *116*, 10075-10166; f) K. L. Skubi, T. R. Blum, T. P. Yoon, *Chem. Rev.* **2016**, *116*, 10035-10074; g) M. H. Shaw, J. Twilton, D. W. C. MacMillan, *J. Org. Chem.* **2016**, *81*, 6898-6926.
- [2] a) M. Schmalzbauer, M. Marcon, B. König, *Angew. Chem. Int. Ed.* **2020**; b) M. A. Fox, *Chem. Rev.* **1979**, *79*, 253-273; c) J.-P. Soumillion, *Photoinduced Electron Transfer V* **1993**, 93-141.
- [3] F. Dénès, M. Pichowicz, G. Povie, P. Renaud, *Chem. Rev.* **2014**, *114*, 2587-2693.
- [4] a) Y. Patehebieke, *Beilstein J. Org. Chem.* **2020**, *16*, 1418-1435; b) D. M. Lynch, E. M. Scanlan, *Molecules* **2020**, *25*, 3094.
- [5] a) Y. Wang, Y. Li, X. Jiang, *Chem. Asian J.* **2018**, *13*, 2208-2242; b) R. S. Glass, *Top Curr Chem.* **2018**, *376*; c) A. Breder, S. Ortgies, *Tetrahedron Lett.* **2015**, *56*, 2843-2852; d) A. Breder, C. Depken, *Angew. Chem. Int. Ed.* **2019**, *58*, 17130-17147; e) L. Capaldo, D. Ravelli, *Eur. J. Org. Chem.* **2017**, *2017*, 2056-2071.
- [6] R. A. Rossi, A. B. Pierini, A. B. Peññory, *Chem. Rev.* **2003**, *103*, 71-168.
- [7] J. F. Bunnett, X. Creary, *J. Org. Chem.* **1974**, *39*, 3173-3174.
- [8] B. Liu, C.-H. Lim, G. M. Miyake, *J. Am. Chem. Soc.* **2017**, *139*, 13616-13619.
- [9] a) G. Li, Q. Yan, Z. Gan, Q. Li, X. Dou, D. Yang, *Org. Lett.* **2019**, *21*, 7938-7942; b) M. Yang, T. Cao, T. Xu, S. Liao, *Org. Lett.* **2019**, *21*, 8673-8678.
- [10] H. Huang, J.-H. Ye, L. Zhu, C.-K. Ran, M. Miao, W. Wang, H. Chen, W.-J. Zhou, Y. Lan, B. Yu, D.-G. Yu, *CCS Chem.* **2020**, *2*, 1746-1756.
- [11] S. Wang, Shun, H. Wang, B. Koenig, *ChemRxiv* **2020**. Preprint. <https://doi.org/10.26434/chemrxiv.13298837.v1>.
- [12] S. Wang, N. Lokesh, J. Hioe, R. M. Gschwind, B. König, *Chem. Sci.* **2019**, *10*, 4580-4587.
- [13] a) D. Crich, L. Quintero, *Chem. Rev.* **1989**, *89*, 1413-1432; b) D. H. R. Barton, S. W. McCombie, *J. Chem. Soc., Perkin Trans. 1.* **1975**, 1574-1585.
- [14] a) B. Quiclet-Sire, S. Z. Zard, *Chem. Eur. J.* **2006**, *12*, 6002-6016; b) B. Quiclet-Sire, S. Z. Zard, *Beilstein J. Org. Chem.* **2013**, *9*, 557-576; c) B. Quiclet-Sire, S. Z. Zard, *Sci. China Chem.* **2019**, *62*, 1450-1462; d) S. Z. Zard, *Angew. Chem. Int. Ed.* **1997**, *36*, 672-685; e) S. Z. Zard, *Helv. Chim. Acta* **2019**, *102*, e1900134.
- [15] S. W. McCombie, B. Quiclet-Sire, S. Z. Zard, *Tetrahedron* **2018**, *74*, 4969-4979.
- [16] D. H. R. Barton, M. V. George, M. Tomoeda, *J. Chem. Soc.* **1962**, 1967-1974.
- [17] a) S. K. Ayer, J. L. Roizen, *J. Org. Chem.* **2019**, *84*, 3508-3523; b) W. L. Czaplyski, C. G. Na, E. J. Alexanian, *J. Am. Chem. Soc.* **2016**, *138*, 13854-13857; c) J. B. Williamson, W. L. Czaplyski, E. J. Alexanian, F. A. Leibfarth, *Angew. Chem. Int. Ed.* **2018**, *57*, 6261-6265; d) C. G. Na, D. Ravelli, E. J. Alexanian, *J. Am. Chem. Soc.* **2020**, *142*, 44-49.
- [18] a) F. Mestre, C. Tailhan, S. Zard, *Heterocycles (Sendai)* **1989**, *28*, 171-174; b) P. Delduc, C. Tailhan, S. Z. Zard, *J. Chem. Soc., Chem. Commun.* **1988**, 308-310.
- [19] B. Schweitzer-Chaput, M. A. Horwitz, E. de Pedro Beato, P. Melchiorre, *Nat. Chem.* **2019**, *11*, 129-135.
- [20] a) D. Mazzarella, G. Magagnano, B. Schweitzer-Chaput, P. Melchiorre, *ACS Catal.* **2019**, *9*, 5876-5880; b) D. Spinnato, B. Schweitzer-Chaput, G. Goti, M. Ošeka, P. Melchiorre, *Angew. Chem. Int.*

- Ed.* **2020**, *59*, 9485-9490.
- [21] S. Cuadros, M. A. Horwitz, B. Schweitzer-Chaput, P. Melchiorre, *Chem. Sci.* **2019**, *10*, 5484-5488.
- [22] E. de Pedro Beato, D. Mazzarella, M. Balletti, P. Melchiorre, *Chem. Sci.* **2020**, *11*, 6312-6324.
- [23] F. Kobayashi, M. Fujita, T. Ide, Y. Ito, K. Yamashita, H. Egami, Y. Hamashima, *ACS Catal.* **2021**, *11*, 82-87.
- [24] a) T. Chivers, P. J. W. Elder, *Chem. Soc. Rev.* **2013**, *42*, 5996-6005; b) R. Steudel, T. Chivers, *Chem. Soc. Rev.* **2019**, *48*, 3279-3319; c) Z.-Y. Gu, J.-J. Cao, S.-Y. Wang, S.-J. Ji, *Chem. Sci.* **2016**, *7*, 4067-4072; d) J.-H. Li, Q. Huang, S.-Y. Wang, S.-J. Ji, *Org. Lett.* **2018**, *20*, 4704-4708; e) W. Tan, C. Wang, X. Jiang, *Chin. J. Chem.* **2019**, *37*, 1234-1238; f) G. Zhang, H. Yi, H. Chen, C. Bian, C. Liu, A. Lei, *Org. Lett.* **2014**, *16*, 6156-6159.
- [25] H. Li, X. Tang, J. H. Pang, X. Wu, E. K. L. Yeow, J. Wu, S. Chiba, *J. Am. Chem. Soc.* **2021**, *143*, 481-487.

## 5. Photo-Induced Thiolate Catalytic Activation of Inert C<sub>aryl</sub>-Hetero Bonds for Radical Borylation



### Abstract:

Substantial effort is currently devoted to obtaining photoredox catalysts with high redox power. Yet, it remains challenging to apply the currently established methods to the activation of bonds with high bond dissociation energy and to substrates with high reduction potentials. Herein, we introduce a novel photocatalytic strategy for the activation of inert substituted arenes for aryl borylation by using thiolate as a catalyst. This catalytic system exhibits strong reducing ability and engages non-activated C<sub>aryl</sub>-F, C<sub>aryl</sub>-X, C<sub>aryl</sub>-O, C<sub>aryl</sub>-N and C<sub>aryl</sub>-S bonds in productive radical borylation reactions, thus expanding the available aryl radical precursor scope. Despite its high reducing power, the method has a broad substrate scope and good functional group tolerance. Spectroscopic investigations and control experiments suggest the formation of a charge-transfer complex as the key step to activate the substrates.

**This chapter has been published in:** Wang, Shun; Wang, Hua; Koenig, Burkhard (2020): Photo-Induced Thiolate Catalytic Activation of Inert C<sub>aryl</sub>-Hetero Bonds for Radical Borylation. ChemRxiv. Preprint. <https://doi.org/10.26434/chemrxiv.13298837.v1>

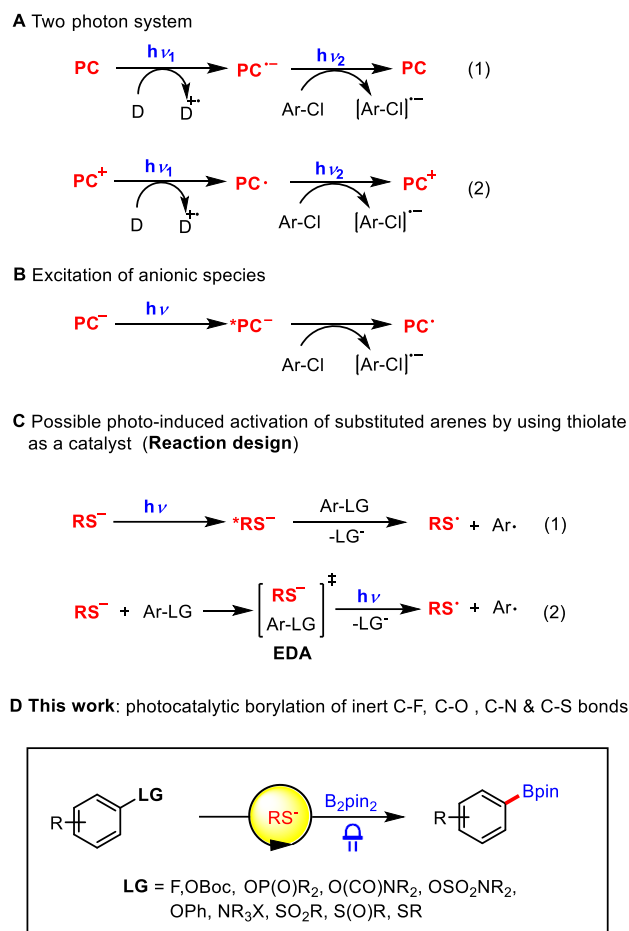
### Author Contributions:

S.W. developed the catalytic system, conducted the experiments and analyzed the data; S.W. and H.W. conducted the mechanistic studies; S.W. and B.K. wrote the manuscript with input from all of the authors. B.K. supervised the project.

## 5.1 Introduction

Photoredox catalysis has emerged as a powerful technique in organic synthesis over the past decade through converting the energy of photons into redox potentials for chemical processes. This empowers organic chemists to realize a number of unprecedented chemical transformations under mild conditions for organic synthesis.<sup>[1]</sup> However, the range of attainable redox potentials in typical photocatalysis system is governed by the energy of the absorbed photon. Intersystem crossing and non-radiative pathways diminished this energy inevitably.<sup>[2]</sup> Thus, it is challenging to activate high redox power demanding substrates by visible-light-irradiation. For instance, reductive transformations, particularly those that require highly reducing power, remain an underdeveloped field. To this end, considerable efforts have been devoted towards the development of new photocatalytic systems with high reduction ability over past few years. To overcome the thermodynamic limits, several approaches to accumulate the energy of two or more photons enhancing the reducing power of a photocatalyst have been established.<sup>[2-3]</sup> We have reported a consecutive photoinduced electron transfer (conPET) utilizing two photons via excitation of photogenerated radical anions (**Scheme 1A**, equation 1).<sup>[4]</sup> Likewise, photoexcitation of electrochemically generated radical anions was shown to be capable of generating high reduction power.<sup>[5]</sup> Nicewicz et al. showed that the acridine radical ACR• could act as an extremely potent photoreductant upon excitation with light (**Scheme 1A**, equation 2).<sup>[6]</sup> Moreover, direct photoexcitation of an organo-anionic species has been demonstrated to provide exciting opportunities to access highly reducing reactive intermediates (**Scheme 1B**).<sup>[3c, 7]</sup>

Arylboronates are recognized as essential building blocks in organic synthesis, material science, and drug discovery.<sup>[8][9]</sup> Transition-metal-catalyzed Miyaura borylation of aryl halides has been developed as one of the most efficient method for synthesizing arylboron reagents.<sup>[10]</sup> In recent years, photocatalytic borylation has attracted considerable research interest and opened a new avenue to access arylboronates.<sup>[11]</sup> A number of photo-induced systems were developed that allow for the borylation of aryl-X bonds from a wide range of substrates such as aryldiazonium salts,<sup>[12]</sup> aryl ammonium salts,<sup>[13]</sup> aryl (pseudo) halides,<sup>[5b, 13-14]</sup> and redox-active esters.<sup>[15]</sup> However, most established photo-induced borylation methods are limited to substrates with labile aryl-hetero bonds or low reduction potentials. Thus, it remains highly challenging to apply the current methods to the borylation of inert bonds such as unactivated C<sub>aryl</sub>-F, C<sub>aryl</sub>-O, C<sub>aryl</sub>-N and C<sub>aryl</sub>-S bonds owing to their high bond dissociation energy and high reduction potentials of substrates. The development of a strategy for the borylation of these bonds would not only greatly widen the available substrate types to access arylboronates but also might represent a significant step towards utilizing unreactive bonds as functional groups in cross-coupling reactions.



**Scheme 1.** Photocatalytic strategies to access high reduction power for SET activation of substituted arenes

Continuing our research in exploring the reducing ability of anionic species in photoredox catalysis,<sup>[16]</sup> we wondered whether we could generate aryl radicals from inert bonds ( $\text{C}_{\text{aryl}}\text{-F}$ ,  $\text{C}_{\text{aryl}}\text{-O}$ ,  $\text{C}_{\text{aryl}}\text{-N}$  and  $\text{C}_{\text{aryl}}\text{-S}$  bonds) for borylation by using a sulfur-centered anion (*e.g.*, thiolate) as a photocatalyst. The proposed catalytic system was inspired by our previous finding wherein thiolate could efficiently shuttle electrons from the boronate radical anion, a species that is produced in radical borylation processes, to the photocatalytic system.<sup>[17]</sup> It was therefore hypothesized that using thiolate direct as a photocatalyst might offer an exciting opportunity for the activation of inert  $\text{C}_{\text{aryl}}\text{-X}$  bonds to generate aryl radicals. In the anticipated activation of substituted arenes by thiolate photocatalysis, two possible reaction modes might be involved as shown in **Scheme 1C**: (1) direct interaction of substituted arenes with the excited state of thiolate. (2) formation of a charge transfer complex between thiolate catalyst and substituted arenes.<sup>[18]</sup> We report herein the successful application of thiolate catalysis for the photoinduced borylation of substituted arenes through the cleavage of non-activated  $\text{C}(\text{sp}^2)\text{-F}$ ,  $\text{C}(\text{sp}^2)\text{-O}$ ,  $\text{C}(\text{sp}^2)\text{-N}$  and  $\text{C}(\text{sp}^2)\text{-S}$  bonds (**Scheme 1D**).

## 5.2 Results and discussion

### 5.2.1 Investigation of reaction conditions

We commenced the study by evaluating the defluoroborylation reaction of fluorobenzene **1a** with  $\text{B}_2\text{pin}_2$  (bis(catecholato)diboron). Owing to the high bond dissociation energy of Ar-F bonds (*e.g.* BDE of Ph-F bond is  $526 \text{ kJ}\cdot\text{mol}^{-1}$ ), only few examples are available for the borylation of unactivated aryl fluoride

under transition-metal-free conditions at present.<sup>[13a, 14h, 19]</sup> To our delight, the desired borylated product **2a** was obtained in 33% yield at room temperature by irradiation with a 385-390 nm LED using CsF as a base and sodium 3-methyl-phenyl thiolate (30% mol) as the catalyst (Table 1, entry 1). Studies with other thiolates revealed that 2-PySNa (pyridine-2-thiolate) is the optimal catalyst yielding the product in 56% yield (entries 2-4). It is worth mentioning that CySNa (sodium cyclohexanethiolate) and 1-AdSNa (Sodium 1-Adamantanethiolate) showed comparably good catalytic performances affording the product while pyridine as a catalyst did not give the product (entry 5), thus indicating that in our reaction the reactivity stems from the thiolate under photocatalytic conditions. Changing the solvent from MeCN to DMSO or THF gave either a poor yield or trace amount of the product (entry 6 and 7). To further increase the yield, a variety of bases were examined. Tetramethylammonium fluoride (TMAF) turned out to be the optimal base, resulting in the formation of **2a** in 74% yield, the increase of reactivity likely attributed to its superior solubility in MeCN (entry 8). Using other bases such as KF, Cs<sub>2</sub>CO<sub>3</sub> and CsOAc failed to improve the yield (entries 9-11). In the absence of base, the reaction afforded **2a** in only 13% yield (entry 12). To our delight, the yield was further improved to 81% when slight excess amounts of B<sub>2</sub>pin<sub>2</sub> and TMAF were employed (entry 13). The use of the more Lewis-acidic diboron source B<sub>2</sub>cat<sub>2</sub> afforded only trace amount of compound **2a** (entry 14). Control experiments showed that both thiolate catalyst 2-PySNa and light irradiation (385-390 nm) were essential for this reaction (entries 15-17). This method is easily scalable, with boronic ester **2a** obtained in 70% yield on a 6 mmol scale.

**Table 1.** Evaluation of reaction conditions for the borylation of fluorobenzene with B<sub>2</sub>pin<sub>2</sub>

Entry	Base	Catalyst	Solvent	Yield <sup>a</sup>
1	CsF	3-Me-PhSNa	MeCN	33%
2	CsF	CySNa	MeCN	48%
3	CsF	1-AdSNa	MeCN	40%
4	CsF	Py2SNa	MeCN	56%
5	CsF	pyridine	MeCN	n.d.
6	CsF	Py2SNa	DMSO	24%
7	CsF	Py2SNa	THF	trace
8	TMAF	Py2SNa	MeCN	74%
9	KF	Py2SNa	MeCN	19%
10	Cs <sub>2</sub> CO <sub>3</sub>	Py2SNa	MeCN	33%
11	CsOAc	Py2SNa	MeCN	27%
12	-	Py2SNa	MeCN	13%
Entry	Change from entry 8		Yield	
13	B <sub>2</sub> pin <sub>2</sub> (3.0 eq.), TMAF (3.0)		81% (78%) <sup>b</sup> , 70% <sup>c</sup>	
14	B <sub>2</sub> cat <sub>2</sub> in place of B <sub>2</sub> pin <sub>2</sub>		trace <sup>d</sup>	
15	455 nm LED		n.d.	
16	in the dark		trace	
17	no Py2SNa		10%	

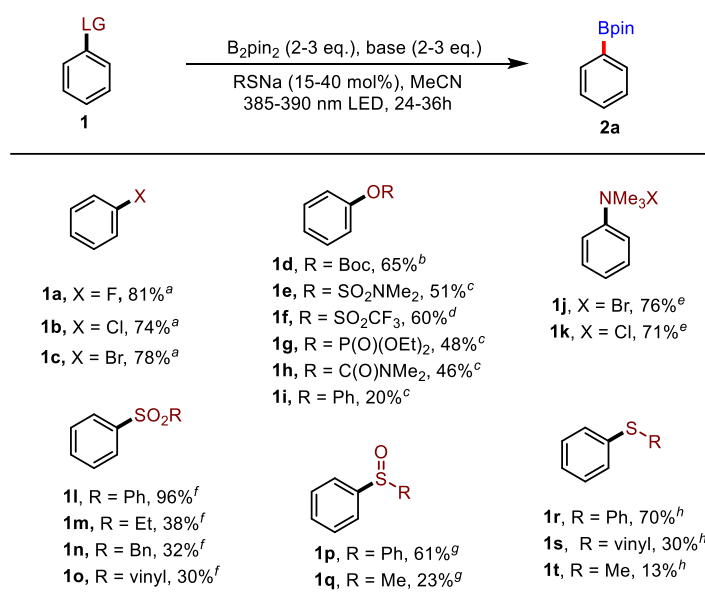


Reaction conditions: **1a** (0.2 mmol), B<sub>2</sub>pin<sub>2</sub> (0.4 mmol), base (0.4 mmol), catalyst (30 mol%), and in 2 mL of solvent, irradiation with a 385-390 nm LED (3.8 W) at 30-35 °C (internal temperature) for 24 h under N<sub>2</sub> atmosphere. n.d. = not detected. TMAF= tetramethylammonium fluoride; B<sub>2</sub>pin<sub>2</sub> = bis(pinacolato)diboron; CySNa = sodium cyclohexanethiolate; 1-AdSNa = Sodium 1-Adamantanethiolate; Py2SNa = pyridine-2-thiolate; B<sub>2</sub>cat<sub>2</sub> = bis(catecholato)diboron. <sup>a</sup>Yields were determined by GC-FID analysis of the crude reaction mixture using dodecane as an internal standard. <sup>b</sup>Isolated yield. <sup>c</sup>6 mmol scale. <sup>d</sup>Work up with Et<sub>3</sub>N (0.5 mL) and pinacol (0.8 mmol).

## 5.2.2 Scope of leaving group for ipso-borylation

Encouraged by these results, we next turned our attention to test the feasibility of this catalytic system with arene substrates bearing different leaving groups (Table 2). When the same reaction was attempted with chlorobenzene **1b** ( $E_{\text{red}}^{\text{p}} = -2.78$  V vs SCE) and bromobenzene **1c** ( $E_{\text{red}}^{\text{p}} = -2.44$  V vs SCE), borylation product **2a** was obtained in 74% and 78% yield, respectively. We then focused on the borylation of C-O bonds of phenol derivatives considering that phenols have emerged as versatile and cost-efficient alternatives to aryl halides.<sup>[11c, 20]</sup> It is worth mentioning that, unlike the use of reactive aryl sulfonates such as aryl triflates, mesylates or tosylates, only few methods are known for the catalytic radical borylation of less or even non-activated aryl esters as coupling partners via C-O bond cleavage.<sup>[11c, 13b, 14d]</sup> In particular, using slightly modified reaction conditions (see the SI for details), O-Boc-protected phenol **1d** could be borylated efficiently to give product **2a** in 65% yield. To the best of our knowledge, this is the first example of transition metal-free borylation of aryl carbonates via C-O bond cleavage. Furthermore, we found that the reaction system was feasible for sulfamate **1e**, triflate **1f**, phosphate **1g** and carbamate **1h**. Interestingly, even C-O bonds of diphenylether showed a certain degree of reactivity in the reaction. Arylammonium salts **1j** and **1k** were also viable for this transformation leading to C-N borylated products in 76% and 71% yield, respectively.

**Table 2.** Leaving group scope for photo-induced *ipso*-borylation of substituted arenes<sup>a</sup>



<sup>a</sup>Reaction condition: **1** (0.2 mmol), B<sub>2</sub>pin<sub>2</sub> (3.0 eq.) base (3.0 eq.), Py2SNa (15-40 %mol), in 2 mL of MeCN, irradiation with a 385-390 nm LED (3.8 W) at 30-35 °C (internal temperature) for 24 h under N<sub>2</sub> atmosphere. Yields were determined by GC-FID using n-dodecane as an internal standard. Potentials are reported vs SCE.

<sup>b</sup>CsF (3.0 eq.), Py2SNa (40 mol%), 36 h. <sup>c</sup>TMAF (3.0 eq.), MeCN (1.5 mL), 36 h. <sup>d</sup>CsOAc (3.0 eq.), AcSK (20 mol%). <sup>e</sup>KOAc (3.0 eq.), Py2SNa (15 mol%), MeCN (1.5 mL). <sup>f</sup>CsF (3.0 eq.), 1-AdSNa (30 mol%). <sup>g</sup>B<sub>2</sub>pin<sub>2</sub> (2.0 eq.), CsF (2.0 eq.), CySNa (30 mol%). <sup>h</sup>B<sub>2</sub>pin<sub>2</sub> (2.0 eq.), CsF (2.0 eq.), 1-AdSNa (30 mol%).

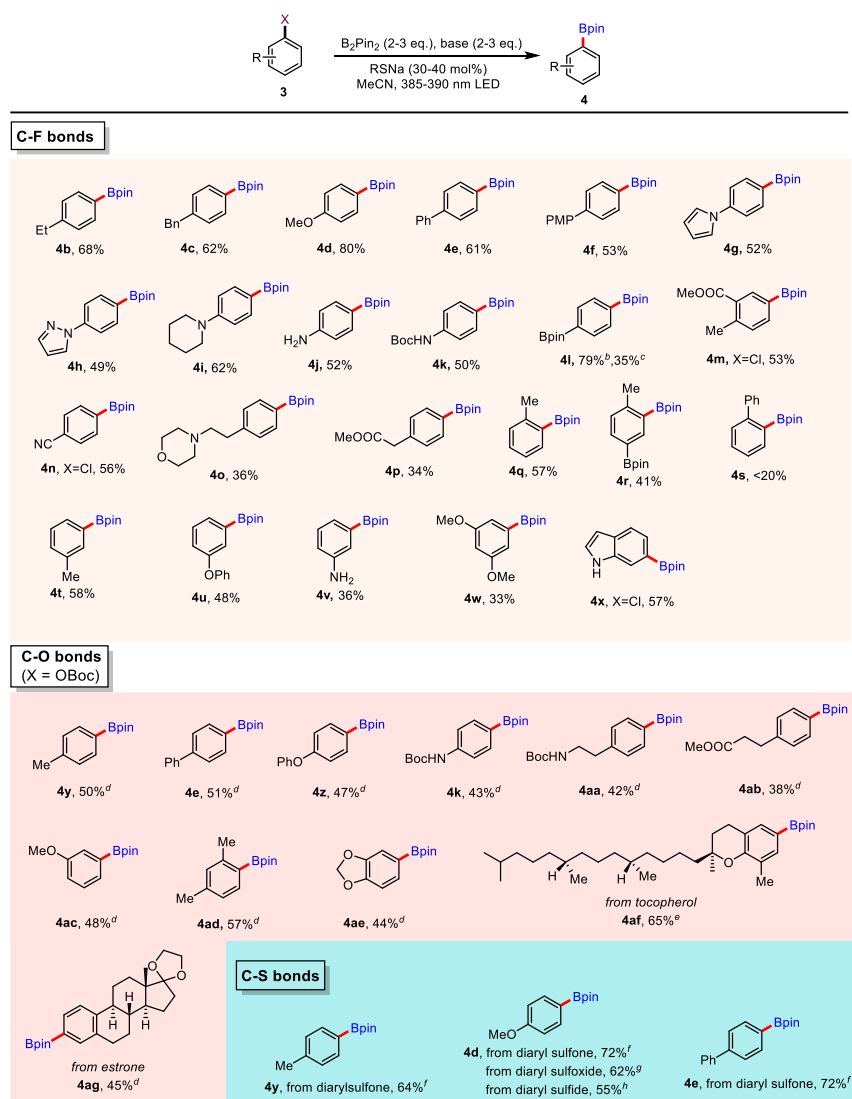
Given that organosulfur compounds are widely present in natural products, drugs and proteins, our protocol was briefly examined as a viable route for the C–S bond borylation of sulfur-containing molecules, which allows modification of their structures.<sup>[21]</sup> Indeed, the C–S bond of diphenyl sulfone **1l** ( $E_{\text{red}}^p = -2.06$  V vs SCE) could be borylated to give product **2a** in excellent yield. When alkyl phenyl sulfones (**1m** and **1n**) and vinyl phenyl sulfone **1o** were used, the borylation occurred selectively at the phenyl-SO<sub>2</sub> bonds to give aryl boronic ester product **2a**, while the alkyl boronic esters were merely observed in trace amounts. The reactivity is in contrast to Nambo and Crudden's observation, wherein the borylation of alkyl phenyl sulfones occurred predominately to afford alkyl boronic esters in a pyridine catalytic system.<sup>[22]</sup> Other than sulfones, our strategy permitted the use of diphenyl sulfoxide **1p** ( $E_{\text{red}}^p = -2.42$  V vs SCE) and methyl phenyl sulfoxide **1q** ( $E_{\text{red}}^p = -2.58$  V vs SCE) as the phenyl radical precursors for borylation, albeit the reaction in the latter case proceeds with lower efficiency. Subsequently, we were glad to find that this methodology was applicable to convert aryl sulfides to aryl boronic esters through C–S cleavage. Specifically, diphenyl sulfide **1r** ( $E_{\text{red}}^p = -2.8$  V vs SCE) reacted smoothly to give **2a** in a 70% yield, while vinyl phenyl sulfide demonstrated diminished reactivity. Attempts to borylate thioanisole **1t** was unsuccessful, affording the target product **2a** in 13% yield. These results are particularly noteworthy considering the fact that thiolate anions are rarely used as leaving groups in radical arylation reactions and sulfides possess more negative reduction potentials, which are caused by the electron-donating property of SR groups.<sup>[3a, 23]</sup>

### 5.2.3 Substrate scope for the borylation of C-X, C-O and C-S bonds

After surveying the scope of phenyl radical precursors, we next sought to study the preparative scope of our reaction utilizing substituted aryl fluorides and chlorides, O-Boc protected phenols as well as organosulfur compounds. We were pleased to see a wide variety of aryl fluorides bearing *para*-(**3b–3p**), *ortho*-(**3q** and **3r**) and *meta*-(**3t–3v**) substituents reacting smoothly to afford the corresponding boronic esters. A broad range of substituents at the *para*-position, including strongly electron-donating groups such as –OMe (**3d**), piperidinyll (**3i**), –NH<sub>2</sub> (**3j**), as well as electron-neutral ethyl (**3b**), benzyl (**3c**) and boronic ester (**3l**) groups, were all tolerated and provided the desired products in good yields. The presence of acidic protons in amine (**3j** and **3v**) and amide (**3k**) did not interfere with the reaction. Aromatic substituents, such as aryl (**3e** and **3f**), pyrrole (**3g**) and pyrazole (**3h**) were compatible with the reaction conditions. The use of aryl fluorides bearing electron-withdrawing groups (e.g., acetyl, CN, CF<sub>3</sub>) afforded the products in low yields, although the starting materials were completely consumed under the reaction conditions. However, corresponding arylchlorides bearing strong EWGs (e.g., COOMe and CN) were compatible with the reaction system and delivered the desired products **4m** and **4n** in moderate yields. This observation might be attributed to the strong electron withdrawing property of fluoro substituents, leading to over-reduction of substrates bearing other EWGs on the aromatic ring. Substrates bearing functional groups such as morpholine and ester on the alkyl chains also reacted smoothly to give the products (**3o** and **3p**). *Ortho*-methyl substituted aryl fluorides (**3q** and **3r**) reacted smoothly to provide the products in 57% and 41% yield, respectively, whereas more sterically hindered phenyl groups at the *ortho*-position inhibited the reactivity with the hydrodefluorination product being detected as the major byproduct. *Meta*-substituted aryl fluorides bearing various functional groups such as phenoxy and amine showed good reactivity in the reaction conditions. Aryl fluorides bearing two

methoxy groups also reacted to furnish the corresponding product (**4w**) in 33% yield, highlighting the high reactivity of the catalytic system. In addition, an unprotected indole functionality was preserved in the borylation process. It should be noted that hydrodehalogenation products were detected as the main side products in most cases due to a competing HAT pathway (**Scheme S2**).

**Table 3.** Substrate scope for photo-induced ipso-borylation<sup>a</sup>



<sup>a</sup>Reaction conditions: **3** (0.2 mmol), B<sub>2</sub>pin<sub>2</sub> (3.0 eq.), TMAF (3.0 eq.), Py<sub>2</sub>SNa (30% mol), in 2 mL of MeCN, irradiation with a 385-390 nm LED (3.8 W) at 30-35 °C for 24 h under N<sub>2</sub> atmosphere, and isolated yields were shown. <sup>b</sup>CsF (3.0 eq.), B<sub>2</sub>pin<sub>2</sub> (3.0 eq.). <sup>c</sup>from 1,4-difluorobenzene, TMAF (4.0 eq.), B<sub>2</sub>pin<sub>2</sub> (4.0 eq.), mono-borylation product was obtained in 25% yield. <sup>d</sup>CsF (3.0 eq.), Py<sub>2</sub>SNa (40 mol%), 36 h. <sup>e</sup>X = OSO<sub>2</sub>NMe<sub>2</sub>, Py<sub>2</sub>SNa (40 % mol), MeCN (1.5 mL). <sup>f</sup>CsF (3.0 eq.), 1-AdSNa (30 mol %). <sup>g</sup>CsF (2.0 eq.), B<sub>2</sub>pin<sub>2</sub> (2.0 eq.), CySNa (30 mol%). <sup>h</sup>CsF (2.0 eq.), B<sub>2</sub>pin<sub>2</sub> (2.0 eq.), 1-AdSNa (30 mol%).

Prompted by these results, we next proceeded to explore the scope of the *ipso*-borylation of Ar-OBoc and Ar-S bonds. We were delighted to find that many synthetically useful functional groups including alkyl (**4y** and **4ad**), phenyl (**4e**), phenoxy (**4z**), amide (**4k**) and alkoxy (**4ac** and **4ae**) substituents on the phenyl ring of Boc-protected phenols could be tolerated, providing the products in moderate yields. These results are noteworthy considering that the electron rich Boc-protected phenols should possess

very negative reduction potentials. Moreover, amide **4aa** and ester **4ab** functionalities on the alkyl chain of the phenolic compounds remained untouched in the reaction conditions. The synthetic utility of this chemistry was further demonstrated by the successful borylation of a  $\delta$ -tocopherol and estrone derivatives, affording the product **4af** and **4ag** in 65% and 45% yield respectively. Likewise, we observed hydrodefunctionalized products as the major side products for the borylation of Boc-protected phenols. In these cases lower conversions were observed compared to the results for fluoroarenes (**Scheme S3**). Finally, the borylation of diarylsulfones bearing methyl, methoxy and phenyl groups were fruitful in giving product yields of the isolated boronic esters (**4y**, **4d** and **4e**) ranging from 64% to 72%. Besides, methoxy-substituted diaryl sulfoxide and sulfide were also suitable substrates for borylation.

### 5.2.4 Mechanistic insights

To obtain mechanistic insights into the reaction mechanism, a number of experimental studies were carried out. At the outset, the effect of radical scavengers on the current borylation system was examined (**Scheme S4** and **Figure 1A**). The presence of 1,1-DPE (1,1-diphenylethylene) inhibited

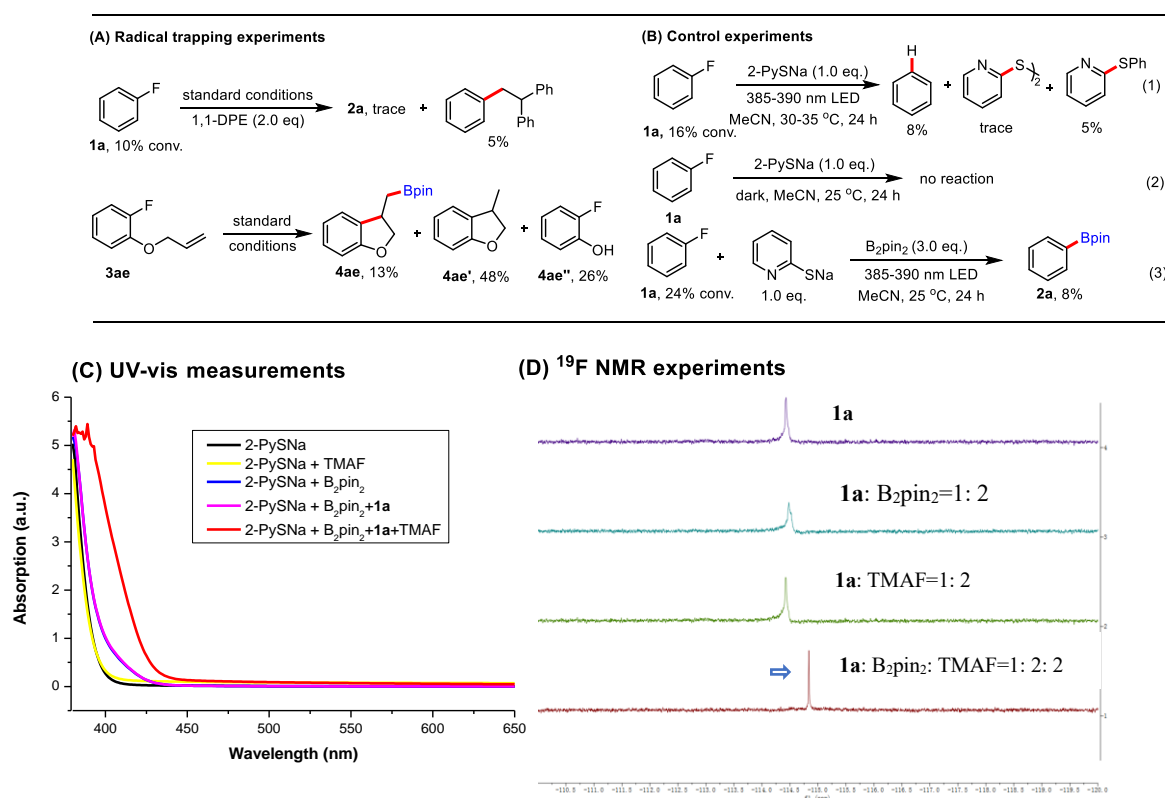


**Figure 1.** Mechanistic studies. (A) Radical trapping experiments. (B) Control experiments to elucidate the mechanism. (C) UV-vis spectra of reaction components. (D) <sup>19</sup>F NMR spectra of **1a** in the presence of B<sub>2</sub>pin<sub>2</sub>, and/or TMAF.

the reaction completely, and the corresponding trapping adducts were formed in 5% yield. When aryl fluoride **3ae** with an *ortho*-allyloxy side chain was subjected to the standard conditions, cyclic alkylboronate **4ae** derived from a radical addition-borylation sequence was detected in 13% yield. These results collectively suggest the intermediacy of the phenyl radical in the reaction. To elucidate the radical generation process, further control experiments were conducted. Under light irradiation (385-390 nm), fluorobenzene **1a** reacted with 2-PySNa to give benzene, disulfide and sulfide albeit in low conversion

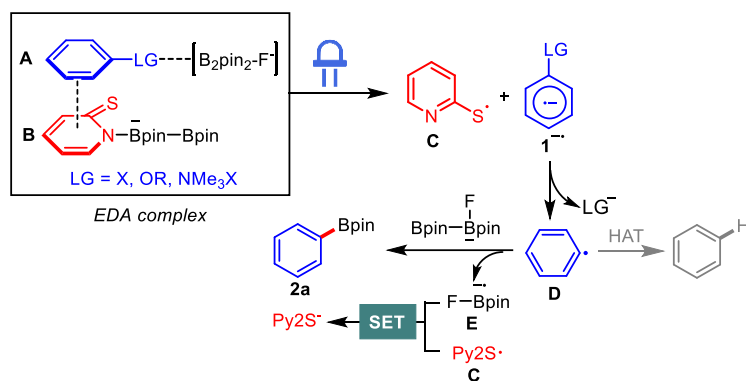
(16%), whereas no reaction could be observed in the dark (**Figure 1B**, equation 1-2). These results imply that phenyl radical and sulfur radical could be generated through direct photo-induced electron transfer between the thiolate and fluorobenzene with low efficiency.

Next, we performed UV-vis spectroscopic measurements of reaction components to explore the electron transfer process between 2-PySNa and **1a**. It turned out that absorption spectra of B<sub>2</sub>pin<sub>2</sub>, substrate **1a**, and TMAF showed bands exclusively in the UV region (<300 nm) (**Figure S10**). However, 2-PySNa was observed to absorb light at 390 nm, addition of B<sub>2</sub>pin<sub>2</sub> (1.0 eq.) led to a clear redshift by ~50 nm in absorption. A further significant redshift appeared when TMAF and **1a** were added to the mixture of 2-PySNa and B<sub>2</sub>pin<sub>2</sub>, while this signal change was not observed in the absence of TMAF (**Figure 1C**). Likewise, obvious redshifts were observed in the mixture of 2-PySNa and B<sub>2</sub>pin<sub>2</sub>, TMAF (or CsF) with other type of substrates (**1b-1h**) (**Figure S11-17**). In contrast, new absorption bands were directly observed upon mixing **1j**, **1l**, **1p** or **1r** with the corresponding optimal thiolate (**Figure S18-21**). These results might support the formation of charge-transfer complexes in the reaction processes.<sup>[24]</sup>

Moreover, we were intrigued by the redshift in the UV-vis spectrum of 2-PySNa by adding B<sub>2</sub>pin<sub>2</sub>. <sup>11</sup>B NMR spectroscopic analysis revealed that a new peak with a chemical shift of 8.8 ppm appeared upon mixing B<sub>2</sub>pin<sub>2</sub> with 2-PySNa, suggesting the formation of an anionic diboron species (**Figure S24**). Meanwhile, it was observed that, both <sup>1</sup>H NMR and <sup>13</sup>C NMR signals of 2-PySNa were shifted with 1.0 equivalent of B<sub>2</sub>pin<sub>2</sub> added, confirming the formation of a new boryl species. Considering the ease with which diboronate esters can react with pyridine type bases to form the corresponding Lewis base adducts,<sup>[15, 25]</sup> it was postulated that a Lewis acid-base adduct formed between 2-PyS<sup>-</sup> and B<sub>2</sub>pin<sub>2</sub> was responsible for the observed redshift.

To study the photo-induced electron transfer process between substrates and thiolate catalysts, a series of control experiments using substrates **1** and thiolates as reactants were conducted. Firstly, thiolates could react with substrates **1j**, **1p** and **1r** which can directly form an EDA complex with them to afford benzene in high yields under light irradiation (**Scheme S6**). Subsequent control experiments demonstrated that in the absence of fluoride a low conversion of **1a** (24%) and only 8% borylation product **2a** were observed with 1.0 equivalent of 2-PySNa (**Figure 1B**, equation 3). Similarly, reactions of **1b-h** and **1l** between 2-PySNa (1.1 eq.) gave low conversions (**Scheme S6**) under light irradiation. We thus suspect that it is very likely that the activation of substrates by the co-existence of fluoride and B<sub>2</sub>pin<sub>2</sub> could facilitate the SET between thiolate and **1a-h**.

Subsequently, we chose fluorobenzene **1a** as the model substrate to study the potential activation effect by fluoride and B<sub>2</sub>pin<sub>2</sub>. We first observed a C-F chemical shift moving upfield from -114.51 to -114.84 ppm after mixing **1a** with 2.0 equivalents of B<sub>2</sub>pin<sub>2</sub> and TMAF, while the C-F chemical shift was not affected by B<sub>2</sub>pin<sub>2</sub> or TMAF separately (**Figure 1D**). On the other hand, we observed the formation of a sp<sup>2</sup>-sp<sup>3</sup> fluoride diborane adduct between TMAF and B<sub>2</sub>pin<sub>2</sub> by <sup>19</sup>F NMR measurements (**Figure S27**).<sup>[14g, 26]</sup> We thus propose that an *in-situ* generated nucleophilic boryl anion species [B<sub>2</sub>pin<sub>2</sub>-F<sup>-</sup>] could activate fluorobenzene **1a**, facilitating the single electron transfer and subsequent fluoride leaving process. We speculate that this activation effect is also essential for the photo-induced electron transfer event between substrates **1b-1h** or **1l** and the catalyst to occur.



**Scheme 2.** Mechanistic proposal

Based on the aforementioned results and mechanistic pathways previously reported in literature, we propose the mechanism depicted in **Scheme 2** and **Scheme S7-S9**. The reaction sequence is initiated by photo-induced electron transfer process between boryl anion-activated **1** (LG = X, O, N) (**A**) and 2-PySNa/B<sub>2</sub>pin<sub>2</sub> adduct **B** to afford thiyl radical and radical anion of **1**.<sup>[27]</sup> In the case of **1j**, **1p** and **1r**, EDA complexes were directly formed between substrates and thiolates. Upon photoexcitation of the EDA complexes, an inner-sphere electron transfer occurs to arrive at thiyl radical and radical anion of **1**.<sup>[28]</sup> The resulting radical anion undergoes cleavage of the C-LG bond to form the phenyl radical, which then reacts with a sp<sup>3</sup>-sp<sup>2</sup> diboron species [F-B<sub>2</sub>pin<sub>2</sub>]<sup>-</sup> to give the desired borylation product **2a** and boryl radical anion **E**. Finally, the thiyl radical **C** was reduced by boryl radical anion **E** to regenerate thiolate closing the catalytic cycle.

### 5.3 Conclusion

In summary, we have developed a new photocatalytic strategy for the *ipso*-borylation of substituted arenes using thiolate as a catalyst. This strategy realized the borylation of a very broad range of inert C-X bonds including non-activated C-F, C-O bonds of phenol derivatives (carbonate, sulfamate, phosphate and carbamate), C-N bond of ammonium salts and C-S bonds (sulfone, sulfoxide and sulfide) with very negative reduction potentials, which are challenging using existing photoredox activation. In this manner, this system allows the utilization of a range of unconventional leaving groups for radical borylation reactions, thus expanding available substrate types to access arylboronates. Despite the generated high reducing power, this reaction displays broad functional group tolerance, and furnishes borylated products in moderate to excellent yields. We propose the formation of an EDA complex between thiolate/B<sub>2</sub>pin<sub>2</sub> and boryl-anion-activated substrates as the key step to obtain the reactivity, which is supported by UV-vis measurements, NMR analysis and control experiments. This combination of photochemistry with thiolate catalysis constitutes a unique activation mode of substituted arenes in cross-coupling reactions. Further studies regarding elucidation the detailed reaction mechanism and the extension of this catalytic system to other coupling partners are currently underway in our laboratory.

## 5.4 Experimental part

### 5.4.1 General information

All NMR spectra were recorded at room temperature using a Bruker Avance 300 (300 MHz for  $^1\text{H}$ , 75 MHz for  $^{13}\text{C}$ , 282 MHz for  $^{19}\text{F}$ ), or a Bruker Avance 400 (400 MHz for  $^1\text{H}$ , 101 MHz for  $^{13}\text{C}$ , 376 MHz for  $^{19}\text{F}$ ) NMR spectrometer. All chemical shifts are reported in  $\delta$ -scale as parts per million [ppm] (multiplicity, coupling constant  $J$ , number of protons) relative to the solvent residual peaks as the internal standard. Coupling constants  $J$  are given in Hertz [Hz]. Abbreviations used for signal multiplicity:  $^1\text{H}$ -NMR: br = broad, s = singlet, d = doublet, t = triplet, q = quartet, dd = doublet of doublets, dt = doublet of triplets, and m = multiplet. High resolution mass spectra (HRMS) were obtained from the central analytic mass spectrometry facilities of the Faculty of Chemistry and Pharmacy, University of Regensburg, and are reported according to the IUPAC recommendations 2013. All mass spectra were recorded on a Finnigan MAT 95, Thermo Quest Finnigan TSQ 7000, Finnigan MATSSQ 710 A or an Agilent Q-TOF 6540 UHD instrument. GC measurements were performed on a GC 7890 from Agilent Technologies. Data acquisition and evaluation was done with Agilent ChemStation Rev.C.01.04. [35]. Analytical TLC was performed on silica gel coated alumina plates (MN TLC sheets ALUGRAM<sup>®</sup> Xtra SIL G/UV254). Visualization was done by UV light (254 or 366 nm). If necessary, potassium permanganate was used for chemical staining. Purification by column chromatography was performed with silica gel 60 M (40-63  $\mu\text{m}$ , 230-440 mesh, Merck) on a Biotage<sup>®</sup> Isolera TM Spektra One device. Unless otherwise noticed, all photocatalytic reactions were performed with 3.8W 385-390 nm LEDs (OSRAM Oslon SSL 80 royal-LEDs ( $\lambda = 385\text{-}390\text{ nm}$  ( $\pm 15\text{ nm}$ ), 3.5 V, 700 mA). The sample was irradiated with a LED through the vial's plane bottom side and cooled from the side using custom-made aluminum cooling blocks connected to a thermostat (Figure S1). The glass tube with reaction mixture and LED cooling block were thermostated at 25  $^\circ\text{C}$ , internal temperature was measured to be 30-35  $^\circ\text{C}$ . UV-Vis and fluorescence measurements were performed with a Varian Cary 100 UV/Vis spectrophotometer and FluoroMax-4 spectrofluorometer, respectively. Electrochemical studies were carried out under argon atmosphere. The measurements were performed in anhydrous solvent containing 0.1 M tetra-*n*-butylammonium tetrafluoroborate using ferrocene/ferrocenium ( $\text{Fc}/\text{Fc}^+$ ) as an internal reference. A glassy carbon electrode (working electrode), platinum wire counter electrode, and Ag quasi-reference electrode were employed. Commercially available starting materials and solvents were used without further purification.



**Figure S1.** Photochemical reaction setup-regular scale

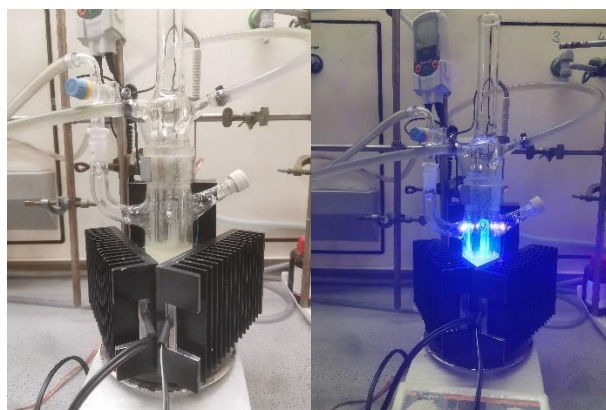
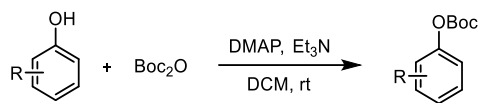


**Figure S2.** Photochemical reaction setup-large scale



## 5.4.2 Starting materials

### General procedure for the synthesis of Boc-protected phenols



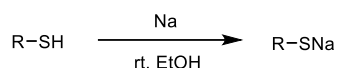
To a solution of Et<sub>3</sub>N (0.56 mL, 4 mmol) and DMAP (12.2 mg, 0.1 mmol) in dry DCM (10 ml), phenol (2 mmol) was added and the clear solution allowed to stir for 15 min. Boc<sub>2</sub>O (524 mg, 2.4 mmol) was added, and the solution was allowed to stir for a further 2 h. The reaction was quenched with water and extracted with DCM (10 mL × 2). The combined organic layers were dried over anhydrous Na<sub>2</sub>SO<sub>4</sub>, filtered, and concentrated by rotary evaporation. Purification by column chromatography using PE/EtOAc as the eluent to afford the product.

### General procedure for the synthesis of sulfamate

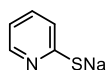


A round bottom flask was charged with NaH (0.431 g, 10.76 mmol, 1.2 equiv, 60% dispersion in oil), and cooled to 0 °C. Then a solution of phenol (1.0 g, 8.97 mmol, 1 equiv) in DME (24 mL) was added dropwise via syringe to the NaH. The resulting solution was warmed to rt for 10 min, and then cooled to 0 °C. A solution of dimethyl sulfamoyl chloride (1.34 g, 10.76 mmol, 1.2 equiv) in DME (6 mL) was then added dropwise via syringe to the reaction mixture. The reaction mixture was warmed to rt, allowed to stir overnight, and then quenched with 10 mL water and extracted with ethyl acetate (20 mL × 3). The combined organic layers were dried over anhydrous Na<sub>2</sub>SO<sub>4</sub>, filtered, and concentrated by rotary evaporation. Purification by column chromatography using PE/EtOAc as the eluent to afford the product.

### General procedure for the synthesis of sodium aryl or alkyl thiolates



Sodium aryl or alkyl thiolates were prepared in similar a procedure described in the literature.<sup>[29]</sup> Under N<sub>2</sub> atmosphere, sodium (10 mmol, 1.0 eq., 240 mg) was dissolved in 30 mL of absolute ethanol at room temperature. Careful: strong gas evolution (H<sub>2</sub>)! To the generated solution was added 2-mercaptopyridine (10 mmol, 1.0 eq, 1.11 g) portion wise with stirring. The reaction was stirred at the rt for 3h. The solvent was removed on the rotary evaporator. The resulting yellowish solid was suspended in 50 ml of diethyl ether and sonicated for 3 hours. The solid was washed with Et<sub>2</sub>O (100 mL) and collected by filtration and dried under high vacuum to afford the corresponding sodium thiolate salt in quantitative yield.



### Sodium pyridine-2-thiolate

<sup>1</sup>H NMR (400 MHz, DMSO-d<sub>6</sub>) δ 7.79 (ddd, *J* = 5.0, 2.1, 0.9 Hz, 1H), 6.97 (dt, *J* = 8.1, 1.1 Hz, 1H), 6.89 (ddd, *J* = 8.1, 6.9, 2.1 Hz, 1H), 6.36 (ddd, *J* = 6.7, 5.0, 1.3 Hz, 1H). <sup>13</sup>C NMR (101 MHz, DMSO-d<sub>6</sub>) δ 180.26, 147.36, 132.49, 128.25, 112.04. HRMS (ESI) Calcd. for [M-Na<sup>+</sup>+H<sup>+</sup>]: 112.0215. Found: 112.0216.

The following sodium thiolate salts were prepared according to this procedure: sodium cyclohexanethiolate, sodium adamantane thiolate.

### 5.4.3 Experimental procedures

#### General procedure for the photo-induced C-F borylation of fluoroarenes (GP1)

To a 9 mL snap vial with magnetic stirring bar,  $B_2pin_2$  (0.6 mmol), TMAF (0.6 mmol), sodium pyridine-2-thiolate (30 mol%) were added. The vial was evacuated and back filled with  $N_2$  for three times. A solution of fluoroarene (0.2 mmol) in dry MeCN (2 mL) was added by syringe. The mixture was irradiated with a 385-390 nm LED (with aluminum block cooling to keep the internal temperature of the reaction mixture at 30-35 °C) under  $N_2$  atmosphere. After 24 h, the reaction mixture was diluted with EA (5 mL) and filtered through a pad of Celite. After filtration, the filtrate was concentrated under reduced pressure. The residue was purified by silica gel column chromatography (eluent: hexane/EtOAc) to give the corresponding boronate esters.

#### General procedure for the photo-induced C-O borylation of Boc-protected phenols (GP2)

To a 9 mL snap vial with magnetic stirring bar,  $B_2pin_2$  (0.6 mmol), CsF (0.6 mmol), sodium pyridine-2-thiolate (40 mol%) were added. The vial was evacuated and back filled with  $N_2$  for three times. A solution of substrate (0.2 mmol) in dry MeCN (1.5 mL) was added by syringe. The mixture was irradiated with a 385-390 nm LED (with aluminum block cooling to keep the internal temperature of the reaction mixture at 30-35 °C) under  $N_2$  atmosphere. After 36 h, the reaction mixture was diluted with EA (5 mL) and filtered through a pad of Celite. After filtration, the filtrate was concentrated under reduced pressure. The residue was purified by silica gel column chromatography (eluent: hexane/EtOAc) to give the corresponding boronate esters.

#### General procedure for the photo-induced C-S borylation of sulfones (GP3)

To a 9 mL snap vial with magnetic stirring bar,  $B_2pin_2$  (0.6 mmol), CsF (0.6 mmol), 1-AdSNa (30 mol%) were added. The vial was evacuated and back filled with  $N_2$  for three times. A solution of substrate (0.2 mmol) in dry MeCN (2 mL) was added by syringe. The mixture was irradiated with a 385-390 nm LED (with aluminum block cooling to keep the internal temperature of the reaction mixture at 30-35 °C) under  $N_2$  atmosphere. After 24 h, the reaction mixture was diluted with EA (5 mL) and filtered through a pad of Celite. After filtration, the filtrate was concentrated under reduced pressure. The residue was purified by silica gel column chromatography (eluent: hexane/EtOAc) to give the corresponding boronate esters.

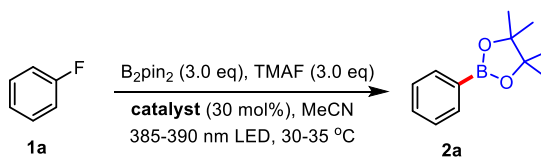
#### General procedure for the photo-induced C-S borylation of sulfoxides and sulfides (GP4)

To a 9 mL snap vial with magnetic stirring bar,  $B_2pin_2$  (0.4 mmol), CsF (0.4 mmol), RSNa (30 mol%) were added. The vial was evacuated and back filled with  $N_2$  for three times. A solution of substrate (0.2 mmol) in dry MeCN (2 mL) was added by syringe. The mixture was irradiated with a 385-390 nm LED (with aluminum block cooling to keep the internal temperature of the reaction mixture at 30-35 °C) under  $N_2$  atmosphere. After 24 h, the reaction mixture was diluted with EA (5 mL) and filtered through a pad of Celite. After filtration, the filtrate was concentrated under reduced pressure. The residue was purified by silica gel column chromatography (eluent: hexane/EtOAc) to give the corresponding boronate esters.

#### 5.4.4 Optimization details for the reaction conditions

General procedure: To a 9 mL snap vial with magnetic stirring bar, B<sub>2</sub>pin<sub>2</sub>, base, sodium pyridine-2-thiolate (30 mol%) were added. The vial was evacuated and back filled with N<sub>2</sub> for three times. A solution of fluoroarene (0.2 mmol) in dry MeCN (2 mL) was added by syringe. The mixture was irradiated with a 385-390 nm LED (with aluminum block cooling to keep the internal temperature of the reaction mixture at 30-35 °C) under N<sub>2</sub> atmosphere. After 24 h, the reaction mixture was diluted with EA (5 mL), dodecane was added as an internal standard, followed by water. After shaking for 1 min, the organic layer was separated and analyzed by GC to determine conversion and yield of the reaction.

**Table S1. Evaluation of catalysts for the borylation of fluorobenzene**

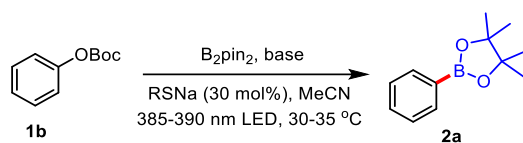


Reaction scheme: Fluorobenzene (**1a**) reacts with B<sub>2</sub>pin<sub>2</sub> (3.0 eq) and TMAF (3.0 eq) in the presence of a catalyst (30 mol%), MeCN, and irradiation with 385-390 nm LED at 30-35 °C to yield the pinacol boronate ester (**2a**).

Entry	Catalyst	Yield (%) <sup>b</sup>
1	2-PySNa (30 mol%)	81%
2	2-PySLi (30 mol%)	75%
3	2-PySK (30 mol%)	78%
4	2-PySO <sub>2</sub> Na (30 mol%)	29%
5	2-PySO <sub>3</sub> Na	trace

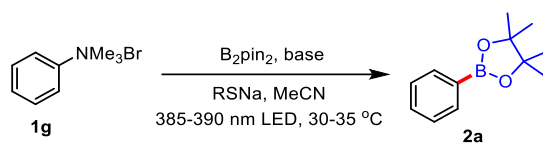
<sup>a</sup>All reactions were carried out with **1a** (0.2 mmol), B<sub>2</sub>pin<sub>2</sub> (0.6 mmol), TMAF (0.6 mmol), catalyst (30 mol%), and in 2 mL MeCN, irradiation with a 385-390 nm LED (3.8 W) at 25 °C under N<sub>2</sub> atmosphere for 24 h.

<sup>b</sup>Yields were determined by GC-FID analysis of the crude reaction mixture using dodecane as an internal standard.

**Table S2.** Optimization details for borylation of tert-butyl phenyl carbonate

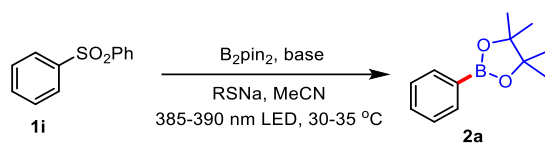
Entry	Base (equiv.)	Thiolate	Solvent	Yield (%) <sup>b</sup>
<b>1</b>	TMAF (3.0 eq.)	2-PySNa (30 mol%)	MeCN (2 mL)	13%
<b>2</b>	CsF (3.0 eq.)	2-PySNa (30 mol%)	MeCN (2 mL)	53%
<b>3</b>	Cs <sub>2</sub> CO <sub>3</sub> (3.0 eq.)	2-PySNa (30 mol%)	MeCN (2 mL)	30%
<b>4</b>	CsOAc (3.0 eq.)	2-PySNa (30 mol%)	MeCN (2 mL)	17%
<b>5</b>	CsF (3.0 eq.)	-	MeCN (2 mL)	6%
<b>6</b>	CsF (3.0 eq.)	CySNa (30 mol%)	MeCN (2 mL)	31%
<b>7</b>	CsF (3.0 eq.)	1-AdSNa (30 mol%)	MeCN (2 mL)	21%
<b>8</b>	CsF (3.0 eq.)	4-PySNa (30 mol%)	MeCN (2 mL)	36%
<b>9</b>	CsF (3.0 eq.)	2-PySNa (20 mol%)	MeCN (2 mL)	56%
<b>10</b>	CsF (3.0 eq.)	2-PySNa (40 mol%)	MeCN (2 mL)	59.5%
<b>11</b>	CsF (3.0 eq.)	2-PySNa (50 mol%)	MeCN (2 mL)	42%
<b>12</b>	CsF (3.0 eq.)	2-PySNa (40 mol%)	MeCN (1.5 mL)	<b>65%</b> <sup>c</sup>

<sup>a</sup>Unless otherwise noted, all the reactions were carried out with **1b** (0.2 mmol),  $B_2pin_2$  (0.6 mmol), base (0.6 mmol), thiolate (30 mol%), and in 2 mL MeCN, irradiation with a 385-390 nm LED (3.8 W) at 30-35 °C (internal temperature) under N<sub>2</sub> atmosphere for 24 h. n.d. = not detected. <sup>b</sup>Yields were determined by GC-FID analysis of the crude reaction mixture using dodecane as an internal standard. <sup>c</sup>Reaction time: 36 h.

**Table S3.** Optimization details for borylation of trimethylphenylammonium bromide

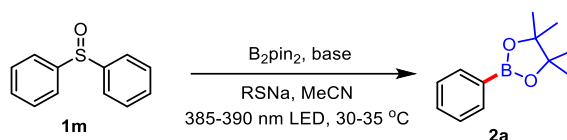
Entry	Base (equiv.)	$B_2pin_2$ (equiv.)	Thiolate	Solvent	Yield (%) <sup>b</sup>
<b>1</b>	CsF	(2.0 eq.)	2-PySNa	MeCN	53%
	(2.0 eq.)		(30 mol%)	(2 mL)	
<b>2</b>	CsF	(2.0 eq.)	-	MeCN	8%
	(2.0 eq.)			(2 mL)	
<b>3</b>	CsF	(3.0 eq.)	2-PySNa	MeCN	46%
	(3.0 eq.)		(30 mol%)	(2 mL)	
<b>4</b>	CsF	(3.0 eq.)	2-PySNa	MeCN	55%
	(3.0 eq.)		(15 mol%)	(2 mL)	
<b>5</b>	CsOAc	(3.0 eq.)	2-PySNa	MeCN	61%
	(3.0 eq.)		(15 mol%)	(2 mL)	
<b>6</b>	KOAc	(3.0 eq.)	2-PySNa	MeCN	65%
	(3.0 eq.)		(15 mol%)	(2 mL)	
<b>7</b>	-	(3.0 eq.)	2-PySNa	MeCN	19%
			(15 mol%)	(2 mL)	
<b>8</b>	KOAc	(3.0 eq.)	2-PySNa	MeCN	59%
	(3.0 eq.)		(10 mol%)	(2 mL)	
<b>9</b>	KOAc	(3.0 eq.)	2-PySNa	MeCN	17%
	(3.0 eq.)		(5 mol%)	(2 mL)	
<b>10</b>	KOAc	(3.0 eq.)	2-PySNa	MeCN	<b>76%</b>
	(3.0 eq.)		(15 mol%)	(1.5 mL)	

<sup>a</sup>Unless otherwise noted, all the reactions were carried out with **1g** (0.2 mmol),  $B_2pin_2$  (0.6 mmol), base (0.6 mmol), thiolate (30 mol%), and in 2 mL of solvent, irradiation with a 385-390 nm LED (3.8 W) at 30-35 °C (internal temperature) under  $N_2$  atmosphere for 24 h. n.d. = not detected. <sup>b</sup>Yields were determined by GC-FID analysis of the crude reaction mixture using dodecane as an internal standard.

**Table S4.** Optimization details for borylation of diphenyl sulfone

Entry	Base (equiv.)	$B_2pin_2$ (equiv.)	Thiolate	Solvent	Yield (%) <sup>b</sup>
<b>1</b>	CsF	(2.0 eq.)	2-PySNa	MeCN	50%
	(2.0 eq.)		(30 mol%)	(2 mL)	
<b>2</b>	CsF	(2.0 eq.)	1-AdSNa	MeCN	68%
	(2.0 eq.)		(30 mol%)	(2 mL)	
<b>3</b>	CsF	(2.0 eq.)	CySNa	MeCN	48%
	(2.0 eq.)		(30 mol%)	(2 mL)	
<b>4</b>	CsF	(3.0 eq.)	1-AdSNa	MeCN	<b>96%</b>
	(3.0 eq.)		(30 mol%)	(2 mL)	

<sup>a</sup>Unless otherwise noted, all the reactions were carried out with **1i** (0.2 mmol),  $B_2pin_2$  (0.4 mmol), base (0.4 mmol), thiolate (30 mol%), and in 2 mL of solvent, irradiation with a 385-390 nm LED (3.8 W) at 30-35 °C (internal temperature) under  $N_2$  atmosphere for 24 h. n.d. = not detected. <sup>b</sup>Yields were determined by GC-FID analysis of the crude reaction mixture using dodecane as an internal standard.

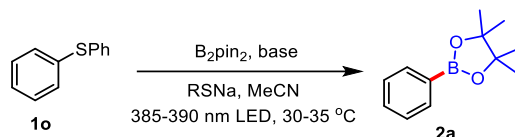
**Table S5.** Optimization details for borylation of diphenyl sulfoxide

Entry	Base (equiv.)	$B_2pin_2$ (equiv.)	Thiolate	Solvent	Yield (%) <sup>b</sup>
<b>1</b>	CsF	(2.0 eq.)	2-PySNa	MeCN	37%
	(2.0 eq.)		(30 mol%)	(2 mL)	
<b>2</b>	CsF	(2.0 eq.)	1-AdSNa	MeCN	44%
	(2.0 eq.)		(30 mol%)	(2 mL)	
<b>3</b>	CsF	(2.0 eq.)	CySNa	MeCN	<b>61%</b>
	(2.0 eq.)		(30 mol%)	(2 mL)	
<b>4</b>	CsF	(3.0 eq.)	1-AdSNa	MeCN	53%
	(3.0 eq.)		(30 mol%)	(2 mL)	

<sup>a</sup>Unless otherwise noted, all the reactions were carried out with **1m** (0.2 mmol),  $B_2pin_2$  (0.4 mmol), base (0.4 mmol), thiolate (30 mol%), and in 2 mL of solvent, irradiation with a 385-390 nm LED (3.8 W) at 30-35 °C

(internal temperature) under N<sub>2</sub> atmosphere for 24 h. n.d. = not detected. <sup>b</sup>Yields were determined by GC-FID analysis of the crude reaction mixture using dodecane as an internal standard.

**Table S6.** Optimization details for borylation of diphenyl sulfide

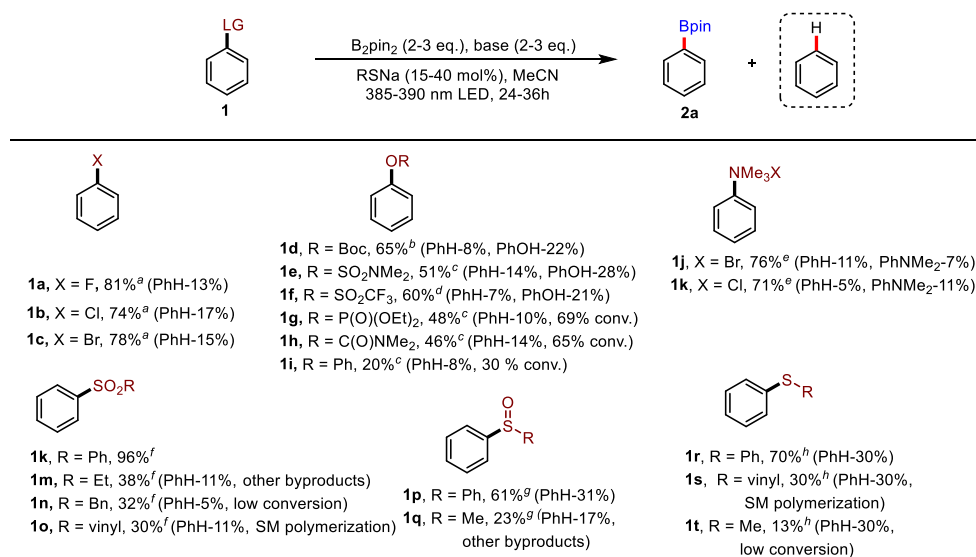


Entry	Base (equiv.)	B <sub>2</sub> pin <sub>2</sub> (equiv.)	Thiolate	Solvent	Yield (%) <sup>b</sup>
<b>1</b>	CsF	(2.0 eq.)	2-PySNa	MeCN	48%
	(2.0 eq.)		(30 mol%)	(2 mL)	
<b>2</b>	CsF	(2.0 eq.)	1-AdSNa	MeCN	<b>70%</b>
	(2.0 eq.)		(30 mol%)	(2 mL)	
<b>3</b>	CsF	(2.0 eq.)	CySNa	MeCN	50%
	(2.0 eq.)		(30 mol%)	(2 mL)	
<b>4</b>	CsF	(3.0 eq.)	1-AdSNa	MeCN	61%
	(3.0 eq.)		(30 mol%)	(2 mL)	

<sup>a</sup>Unless otherwise noted, all the reactions were carried out with **1o** (0.2 mmol), B<sub>2</sub>pin<sub>2</sub> (0.4 mmol), base (0.4 mmol), thiolate (30 mol%), and in 2 mL of solvent, irradiation with a 385-390 nm LED (3.8 W) at 30-35 °C (internal temperature) under N<sub>2</sub> atmosphere for 24 h. n.d. = not detected. <sup>b</sup>Yields were determined by GC-FID analysis of the crude reaction mixture using dodecane as an internal standard.

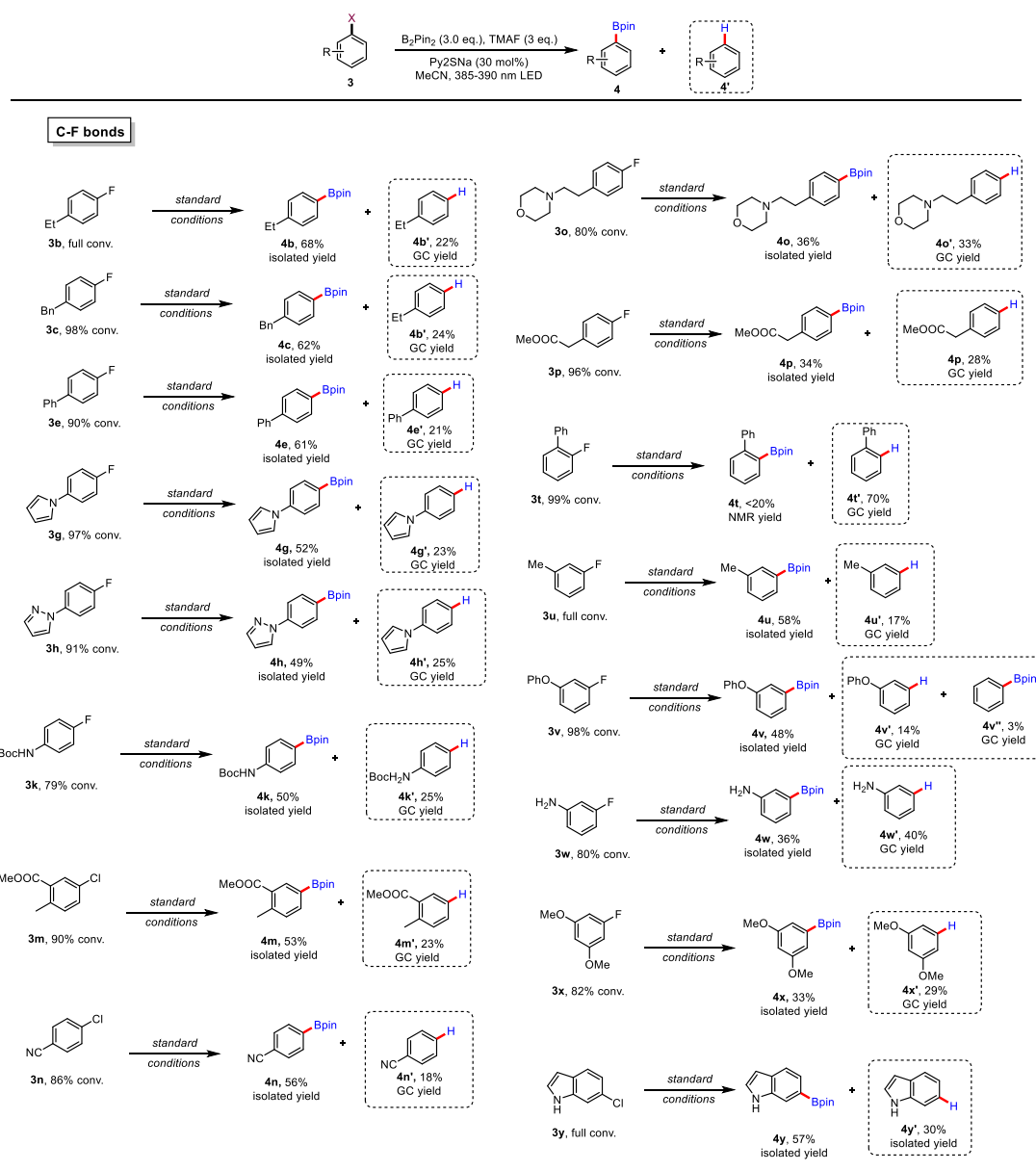
#### 5.4.5 Side product detection and unsuccessful substrates

**Scheme S1.** Side products detection in the borylation of C<sub>aryl</sub>-X bonds



<sup>a</sup>Reaction conditions: **1** (0.2 mmol), B<sub>2</sub>pin<sub>2</sub> (3.0 eq.), base (3.0 eq.), Py<sub>2</sub>SNa (15-40 % mol), in 2 mL of MeCN, irradiation with a 385-390 nm LED (3.8 W) at 30-35 °C (internal temperature) for 24 h under N<sub>2</sub> atmosphere. Yields were determined by GC-FID using n-dodecane as an internal standard. <sup>b</sup>CsF (3.0 eq.), Py<sub>2</sub>SNa (40 mol%), 36 h. <sup>c</sup>TMAF (3.0 eq.), MeCN (1.5 mL), 36 h. <sup>d</sup>CsOAc (3.0 eq.), AcSK (20 mol%). <sup>e</sup>KOAc (3.0 eq.), Py<sub>2</sub>SNa (15 mol%), MeCN (1.5 mL). <sup>f</sup>CsF (3.0 eq.), 1-AdSNa (30 mol%). <sup>g</sup>B<sub>2</sub>pin<sub>2</sub> (2.0 eq.), CsF (2.0 eq.), CsSNa (30 mol%). <sup>h</sup>B<sub>2</sub>pin<sub>2</sub> (2.0 eq.), CsF (2.0 eq.), 1-AdSNa (30 mol%).

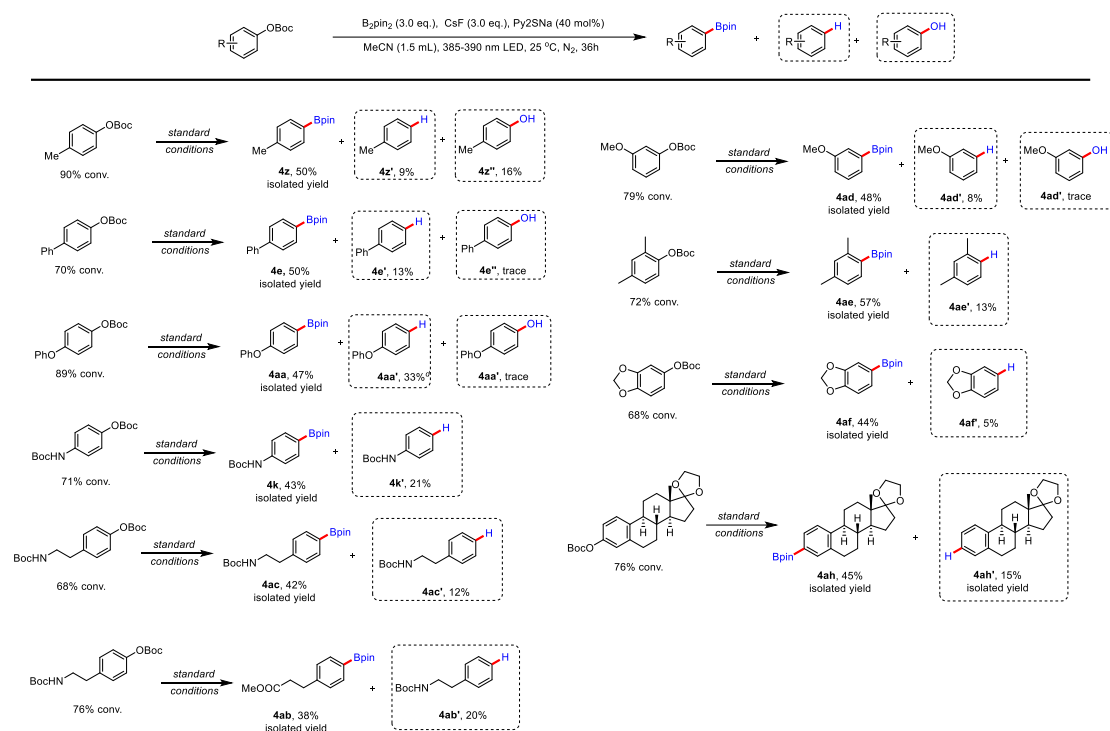
**Scheme S2.** Side products detection in the borylation of substituted C<sub>aryl</sub>-X bonds



<sup>a</sup>Unless otherwise noted, all the reactions were carried out with **3** (0.2 mmol), B<sub>2</sub>pin<sub>2</sub> (0.6 mmol), base (0.6 mmol), thiolate (30 mol%), and in 2 mL MeCN, irradiation with a 385-390 nm LED (3.8 W) at 30-35 °C (internal temperature) under N<sub>2</sub> atmosphere for 24 h. <sup>b</sup>Yields of byproducts were determined by GC-FID analysis of the crude reaction mixture using dodecane as an internal standard.

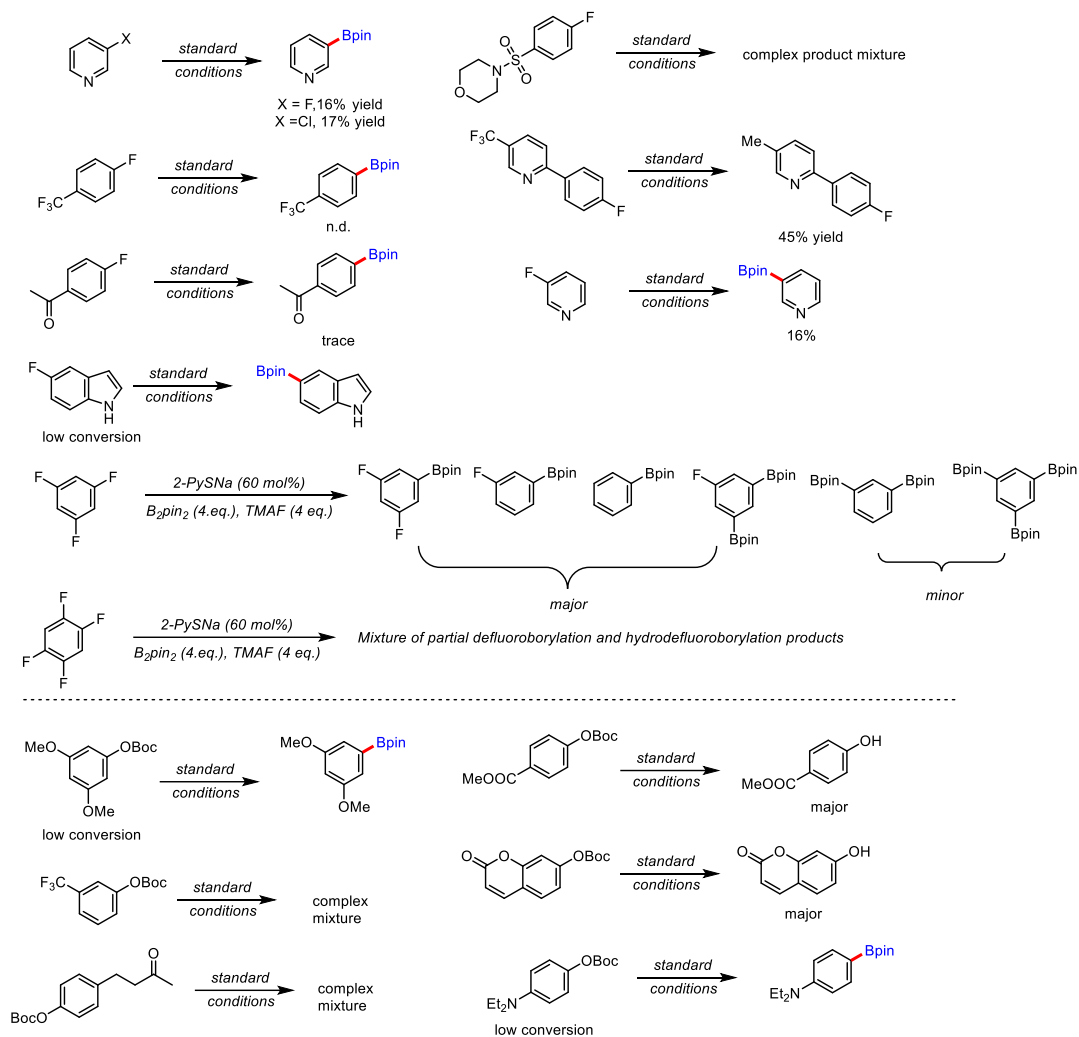


### Scheme S3. Side products detection in the borylation of C<sub>aryl</sub>-OBoc bonds



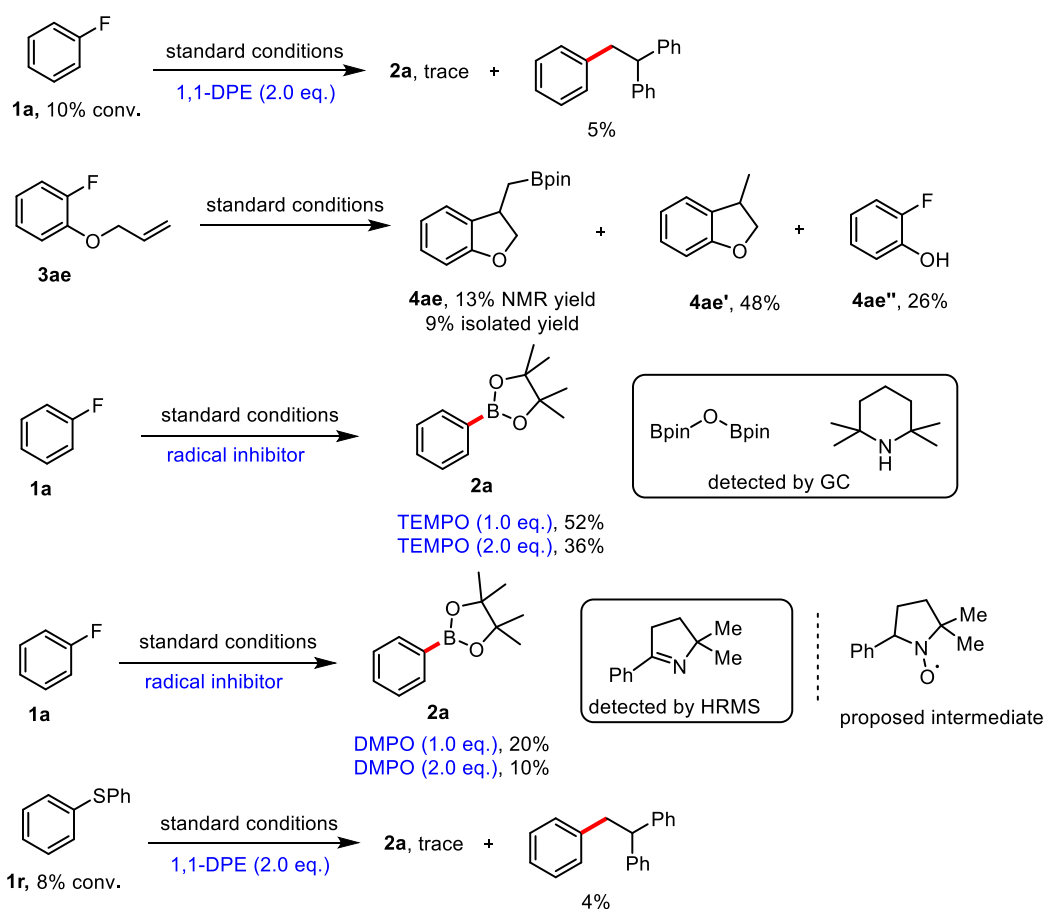
<sup>a</sup>Unless otherwise noted, all the reactions were carried out with **3** (0.2 mmol), B<sub>2</sub>pin<sub>2</sub> (0.6 mmol), base (0.6 mmol), thiolate (40 mol%), and in 1.5 mL MeCN, irradiation with a 385-390 nm LED (3.8 W) at 30-35 °C (internal temperature) under N<sub>2</sub> atmosphere for 36 h. <sup>b</sup>Yields of byproducts were determined by GC-FID analysis of the crude reaction mixture using dodecane as an internal standard.

## Unsuccessful substrates



## 5.4.6 Mechanistic studies

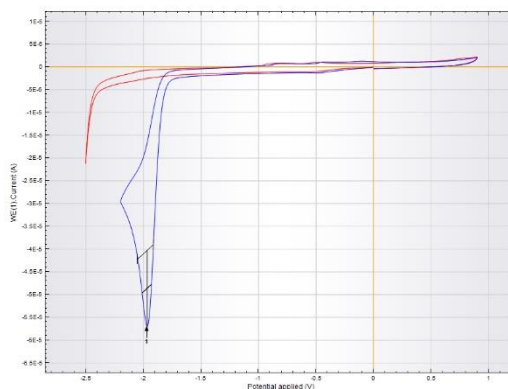
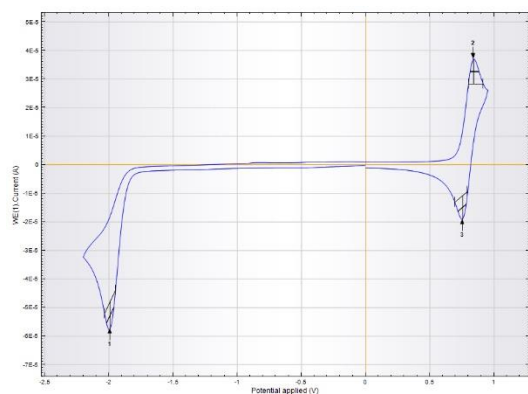
### Scheme S4. Radical trapping experiments



Besides 1,1-diphenylethane, we attempted to use other radical inhibition reagents including TEMPO (2,2,6,6-Tetramethylpiperidine-1-oxyl) and DMPO (5,5-Dimethyl-1-pyrroline N-oxide) under the standard conditions. The desired product could still be obtained in 36% yield when 2 equivalents of TEMPO was added. GC-MS measurements demonstrated that instead of forming the TEMPO-Ph adduct, tetramethylpiperidine and borate were detected as the major products in GC. We speculate that TEMPO was deoxygenated rapidly by bis(boronate) reagent and the phenyl radical reacted with the remaining B<sub>2</sub>pin<sub>2</sub> in the reaction to afford **2a**. Our explanation is also supported by the observation of Li et al. where TEMPO could be deoxygenated rapidly by B<sub>2</sub>cat<sub>2</sub> to afford tetramethylpiperidine.<sup>[30]</sup> Moreover, using DMPO (5,5-Dimethyl-1-pyrroline N-oxide), a well-known spin trap, led to a dramatic decrease of yields. 2,2-Dimethyl-5-phenyl-3,4-dihydro-2H-pyrrole was detected by HRMS (EI m/z [M]<sup>+</sup>: 173.1199). We rationalized that the formation of this product was due to the deoxygenation of an oxygen-centered radical, which was generated from the phenyl radical addition to DMPO by boron species in the reaction. In summary, we conclude that the phenyl radical is the key intermediate in our reaction.

## Cyclic Voltammetry

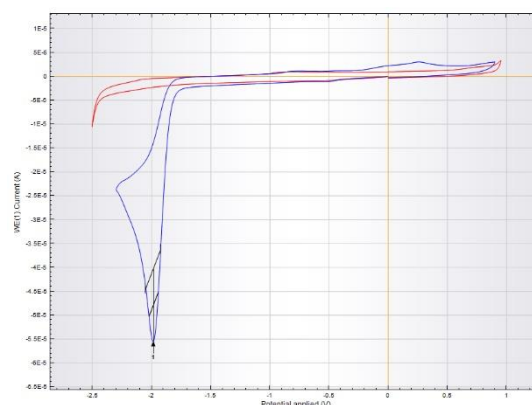
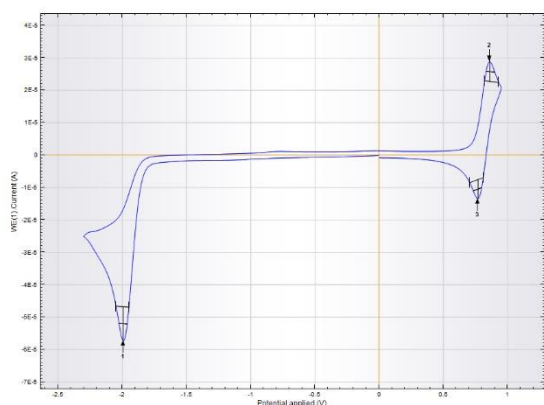
CV measurements were taken on a three-electrode potentiostat galvanostat PGSTAT302N from Metrohm Autolab by using a glassy carbon working electrode (diameter, 3 mm), a platinum wire counter electrode, a silver wire as a reference electrode. The cyclic voltammograms of compounds **1** (1.4 mM) were recorded in an electrolyte of tetra-n-butylammonium tetrafluoroborate (0.1 M) in MeCN or DMF using ferrocene/ferrocenium (Fc/Fc<sup>+</sup>) as an internal reference. Measurements were carried out in degassed MeCN or DMF solution at room temperature under Argon atmosphere. The scan rate was 50 mV/s. Potentials vs SCE were reported according to  $E_{SCE} = E_{Fc/Fc^+} + 0.38$  V.



Index	Peak position	Peak current
1	-1.989	-9.4937E-06
2	0.84091	8.6562E-06
3	0.75531	-8.1274E-06

**Figure S3.** Cyclic voltammogram of **1j** in MeCN

$E_{red}^p(\mathbf{1j}) = -2.41$  V vs SCE

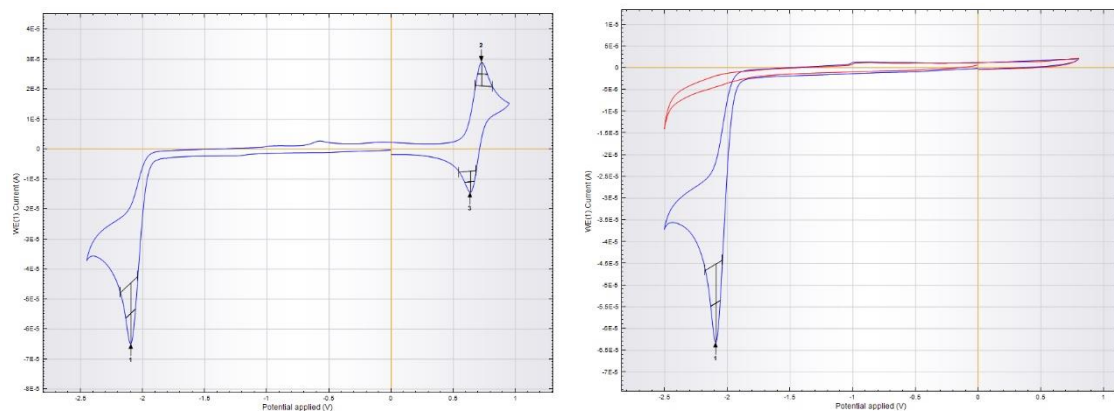


**Index Peak position Peak current**

1	-1.994	-1.0446E-05
2	0.86105	6.0583E-06
3	0.77042	-5.8594E-06

**Figure S4.** Cyclic voltammogram of **1k** in MeCN (with ferrocene)

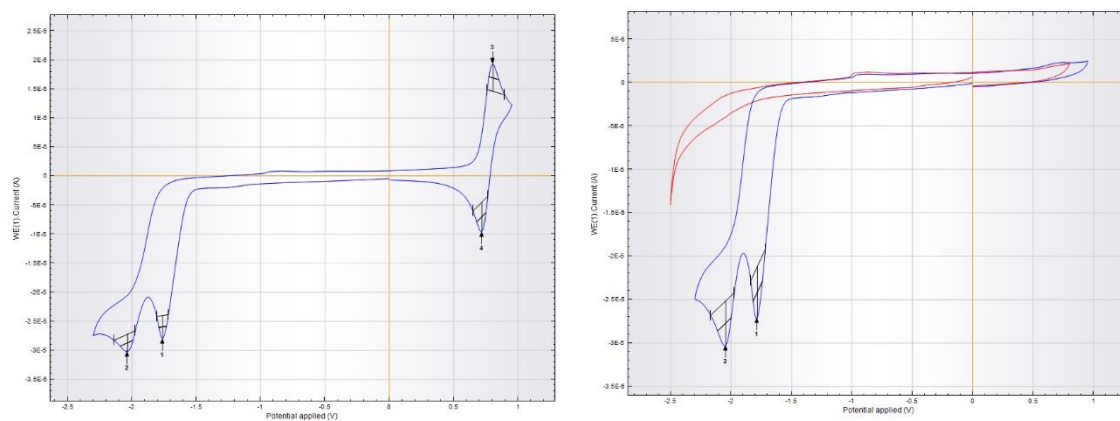
$$E_{red}^p(\mathbf{1k}) = -2.43 \text{ V vs SCE}$$



Index	Peak position	Peak current
1	-2.0947	-2.0314E-05
2	0.73013	7.8443E-06
3	0.6395	-7.0577E-06

**Figure S5.** Cyclic voltammogram of **1m** in MeCN (with ferrocene)

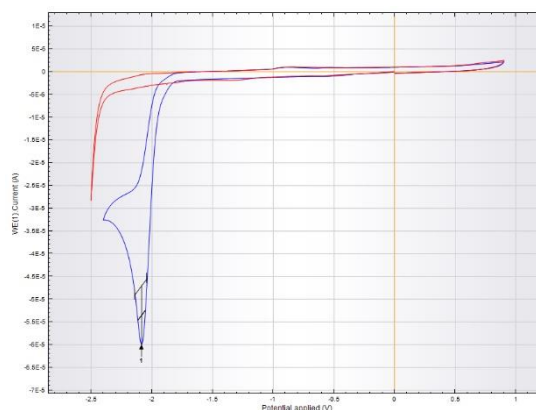
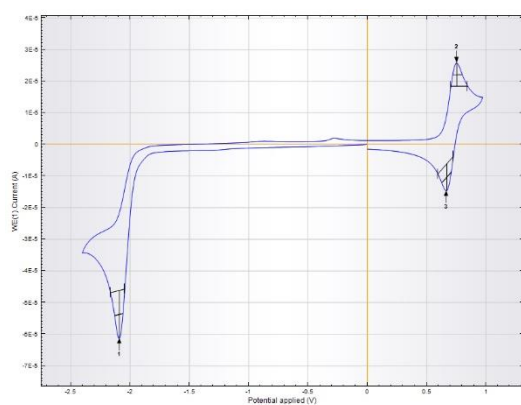
$$E_{red}^p(\mathbf{1m}) = -2.39 \text{ V vs SCE}$$



Index	Peak position	Peak current
1	-1.7624	-3.9124E-06
2	-2.0343	-2.9497E-06
3	0.80566	4.6326E-06
4	0.72006	-5.0087E-06

**Figure S6.** Cyclic voltammogram of **1o** in MeCN (with ferrocene)

$$E_{red,1}^p(\mathbf{1o}) = -2.07 \text{ V vs SCE}, E_{red,2}^p(\mathbf{1o}) = -2.41 \text{ V vs SCE}$$

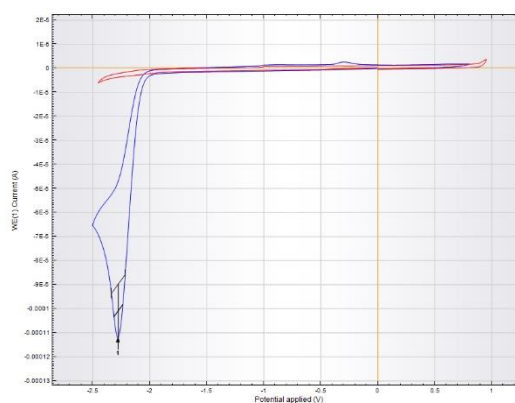
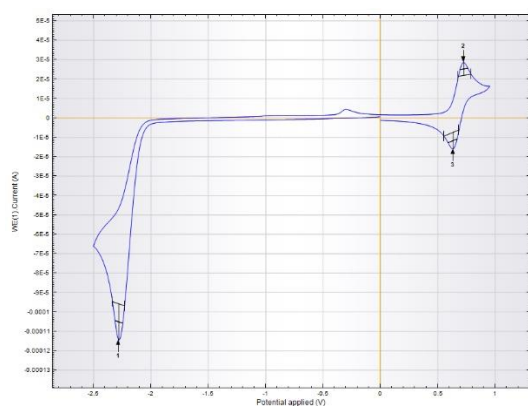


**Index Peak position Peak current**

1	-2.0897	-1.5187E-05
2	0.75531	7.3074E-06
3	0.66971	-8.4685E-06

**Figure S7.** Cyclic voltammogram of **1p** in MeCN (with ferrocene)

$E_{red}^p(\mathbf{1p}) = -2.42 \text{ V vs SCE}$

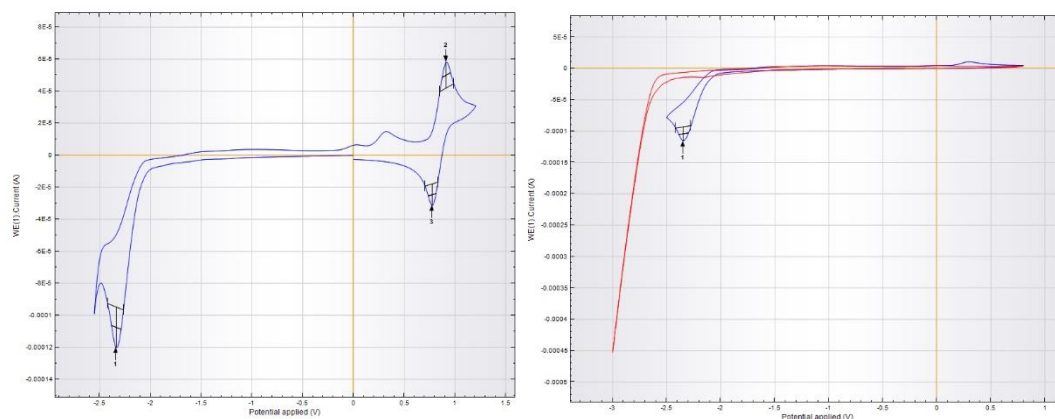


**Index Peak position Peak current**

1	-2.281	-1.8611E-05
2	0.7251	6.6252E-06
3	0.63446	-8.5285E-06

**Figure S8.** Cyclic voltammogram of **1q** in MeCN (with ferrocene)

$E_{red}^p(\mathbf{1q}) = -2.58 \text{ V vs SCE}$

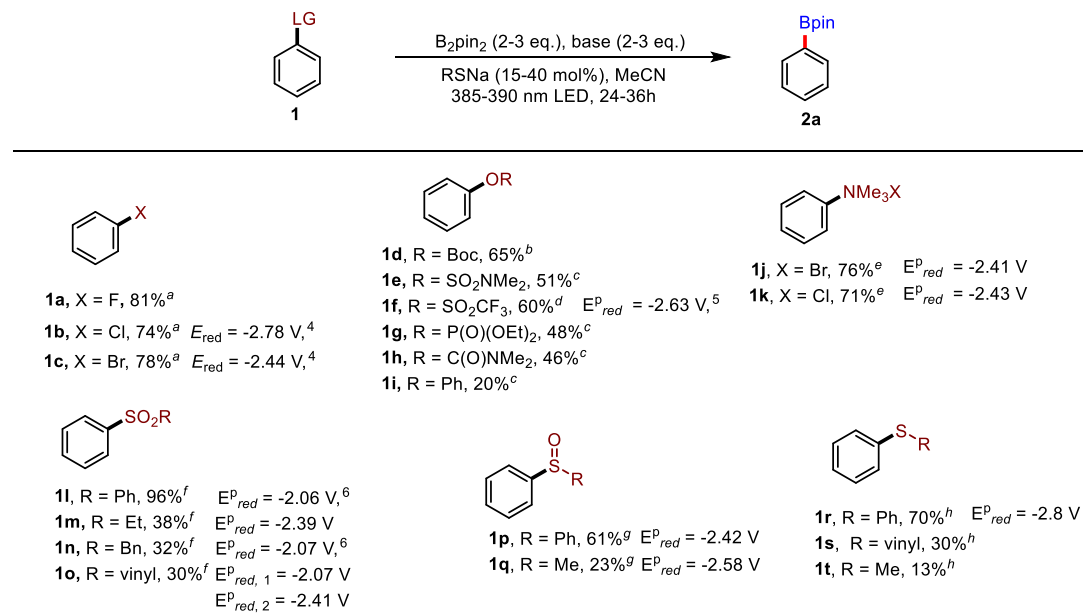


Index	Peak position	Peak current
1	-2.3364	-2.547E-05
2	0.91141	1.6062E-05
3	0.77545	-1.3467E-05

**Figure S9.** Cyclic voltammogram of **1r** in DMF (with ferrocene)

$$E_{red}^p(\mathbf{1r}) = -2.80 \text{ V vs SCE}$$

### Scheme S5. Reduction potential of substrates



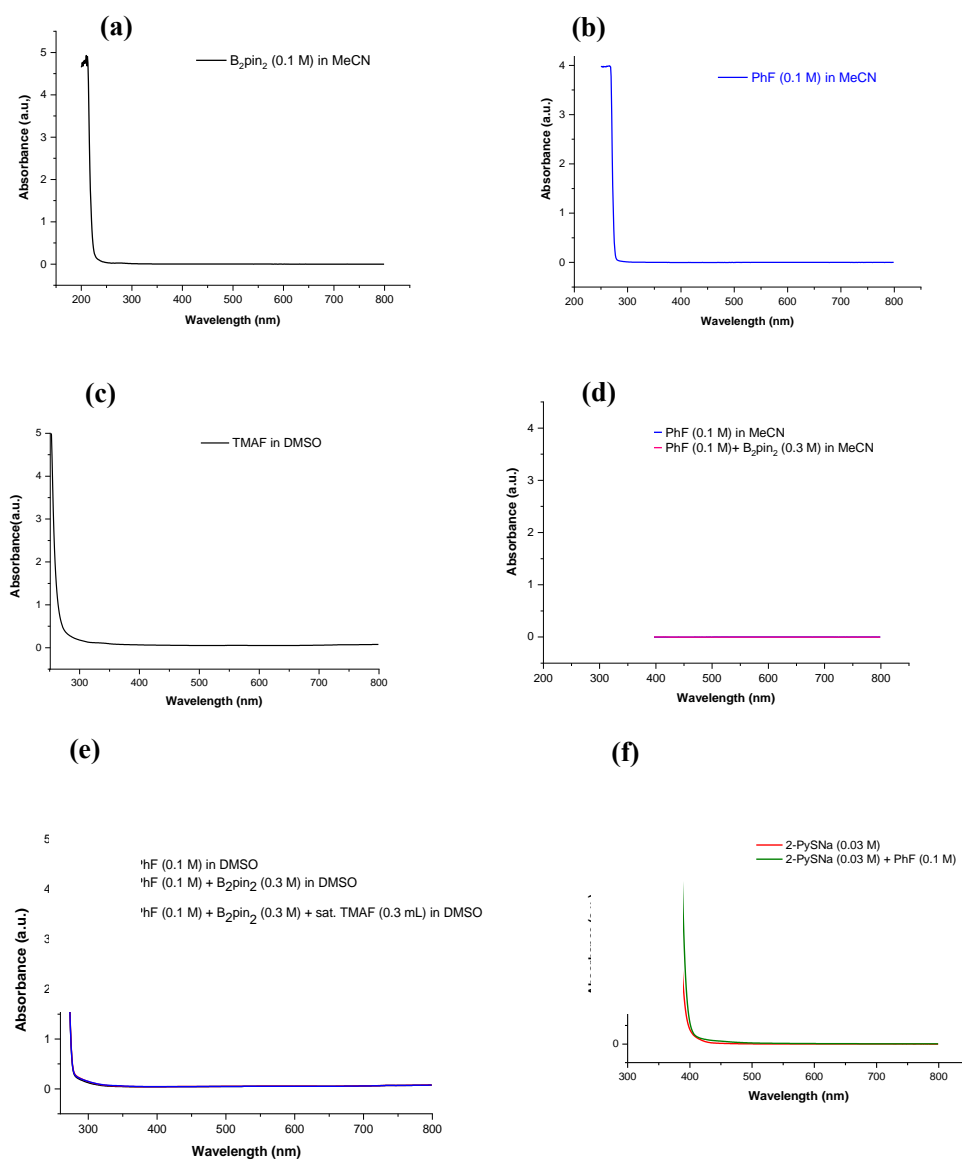
The reductive potentials of **1b**,<sup>[31]</sup>**1c**,<sup>[31]</sup> **1f**,<sup>[32]</sup> **1i**,<sup>[33]</sup> and **1n**<sup>[33]</sup> were taken from the literature. We note that the peak potentials of substrates including **1a**, **1d-e**, **1g-1i**, **1s-t** in our CV measurements are close to the potential window of solvent. It would be difficult to obtain accurate peak potentials in these cases. Therefore, we only show the peak potentials of substrates with a clear reduction in cyclic voltammetry.

Based on our results as shown in Table 2, we conclude that our reaction system is capable of activating the substrates bearing very negative potentials ( $< -3$  V vs SCE).

### Spectroscopic investigations

Optical absorption spectra of the reaction components and their combinations were measured in MeCN or DMSO. Note: considering the poor solubility of TMAF in MeCN, DMSO was selected as the solvent in the measurements when TMAF was used. Control experiments showed that a 42% yield of **2a** was obtained from **1a** when replacing MeCN with DMSO under the optimized conditions.

### UV-vis measurements





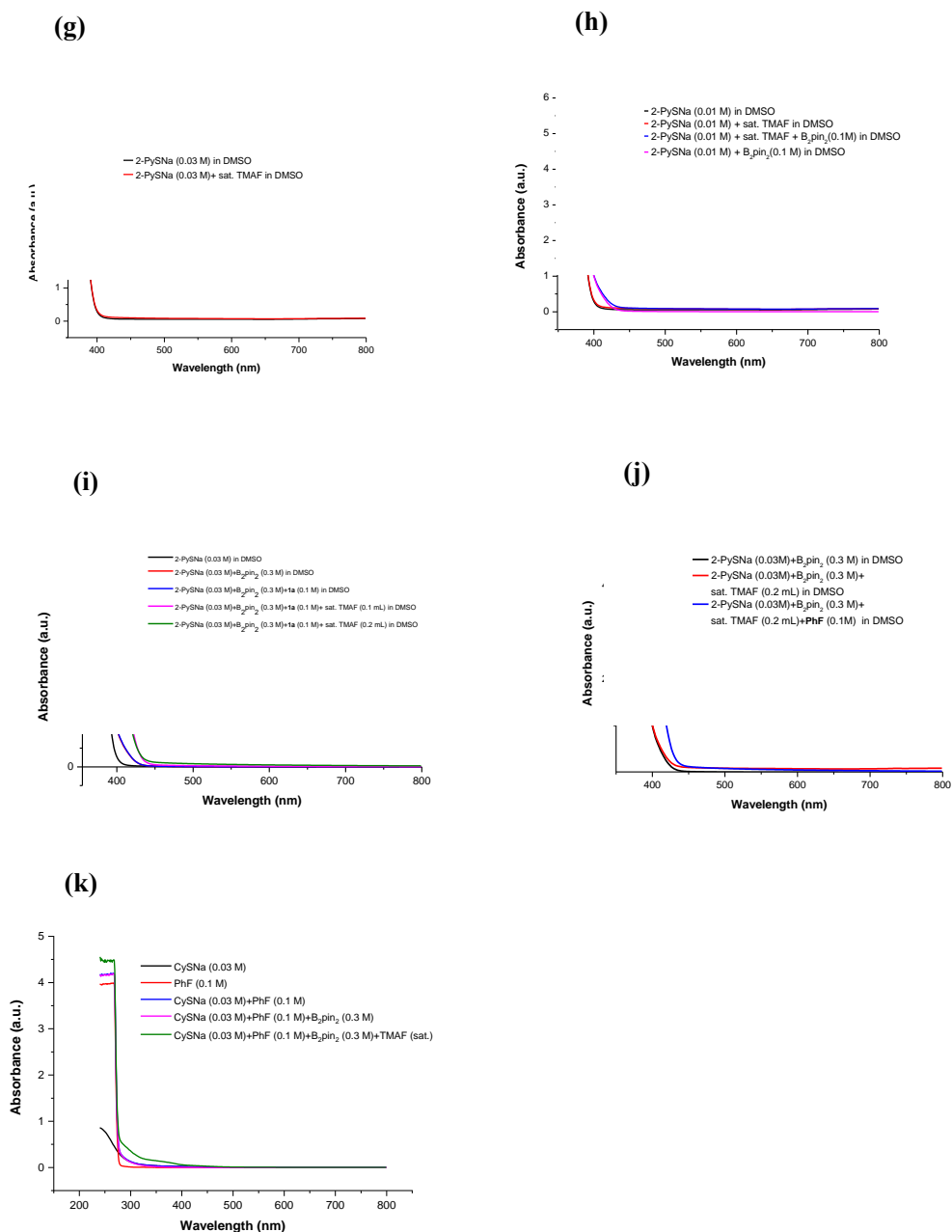


**Figure S10.** (a) UV-vis spectrum of B<sub>2</sub>pin<sub>2</sub> (0.1 M) in MeCN. (b) UV-vis spectrum of **1a** (0.1 M) in MeCN. (c) UV-vis spectrum of TMAF in DMSO. (d) UV-vis spectra of **1a** (0.1 M), **1a** (0.1 M)+B<sub>2</sub>pin<sub>2</sub> (0.3 M) in MeCN. (e) UV-vis spectra of **1a** (0.1 M), **1a** (0.1 M)+B<sub>2</sub>pin<sub>2</sub> (0.3 M), and **1a** (0.1 M)+B<sub>2</sub>pin<sub>2</sub> (0.3 M)+TMAF in DMSO. (f) UV-vis spectra of 2-PySNa (0.03 M), and 2-PySNa (0.03 M)+**1a** (0.1 M) in MeCN. (g) UV-vis spectra of 2-PySNa (0.03 M) and 2-PySNa (0.03 M)+TMAF in DMSO. (h) UV-vis spectra of 2-PySNa (0.03 M), 2-PySNa (0.03 M)+TMAF, 2-PySNa (0.03 M)+TMAF+B<sub>2</sub>pin<sub>2</sub> (0.3 M), and 2-PySNa (0.03 M) +B<sub>2</sub>pin<sub>2</sub> (0.3 M) in DMSO. (i) UV-vis spectra of 2-PySNa (0.03 M), 2-PySNa (0.03 M) +B<sub>2</sub>pin<sub>2</sub> (0.3 M), 2-PySNa (0.03 M) +B<sub>2</sub>pin<sub>2</sub> (0.3 M)+**1a** (0.1 M), 2-PySNa (0.03 M)+B<sub>2</sub>pin<sub>2</sub> (0.3 M)+**1a** (0.1 M) and 2-PySNa (0.03 M) +B<sub>2</sub>pin<sub>2</sub> (0.3 M)+**1a** (0.1 M)+TMAF in DMSO. (j) UV-vis spectra of 2-PySNa (0.03 M) +B<sub>2</sub>pin<sub>2</sub> (0.3 M), 2-PySNa (0.03 M) +B<sub>2</sub>pin<sub>2</sub> (0.3 M) + TMAF, and 2-PySNa (0.03 M) +B<sub>2</sub>pin<sub>2</sub> (0.3 M) + TMAF+**1a** (0.1 M) in DMSO. (k) UV-vis spectra of CySNa (0.03 M), **1a** (0.1 M), **1a** (0.1 M)+CySNa (0.03 M), **1a** (0.1 M)+CySNa (0.03 M)+B<sub>2</sub>pin<sub>2</sub> (0.3 M), **1a** (0.1 M)+CySNa (0.03 M)+B<sub>2</sub>pin<sub>2</sub> (0.3 M)+TMAF in DMSO.

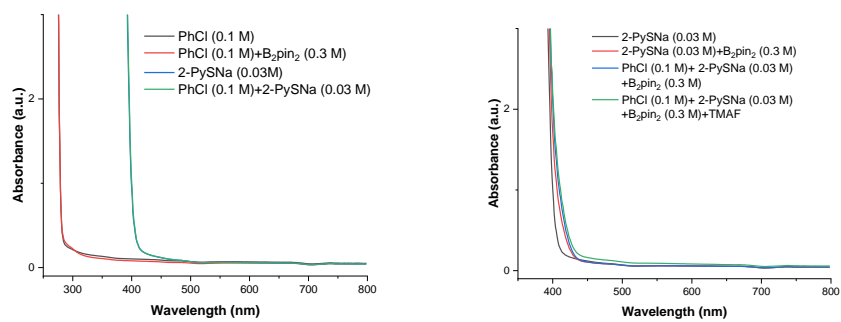


Figure S11. UV-vis spectrum of **1b** in the presence of different components.

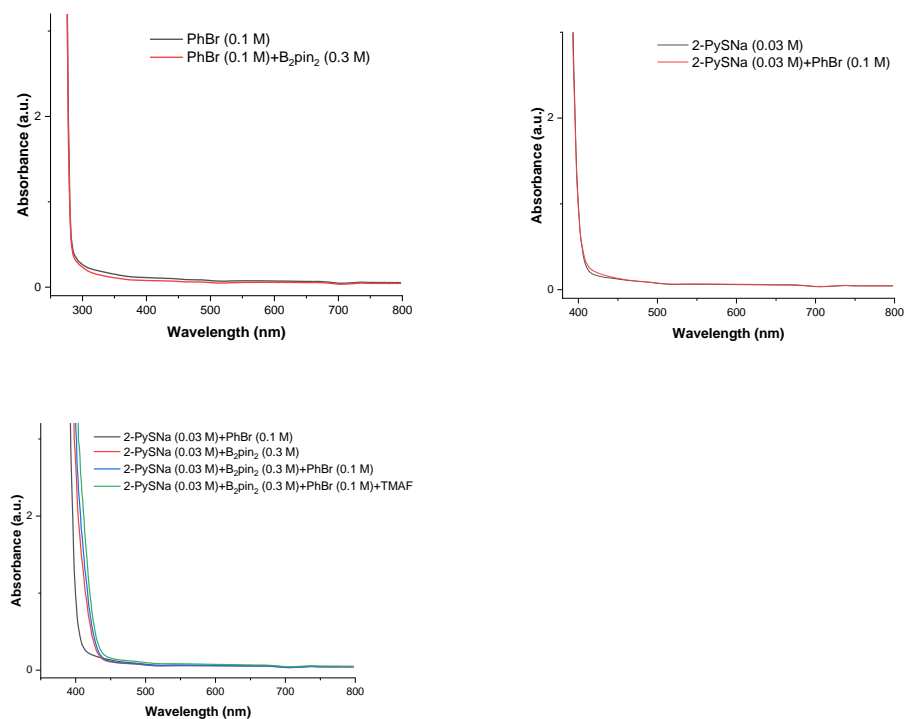


Figure S12. UV-vis spectrum of **1c** in the presence of different components.

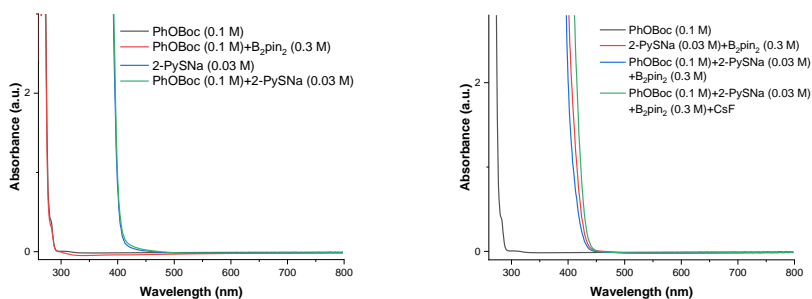


Figure S13. UV-vis spectrum of **1d** in the presence of different components.

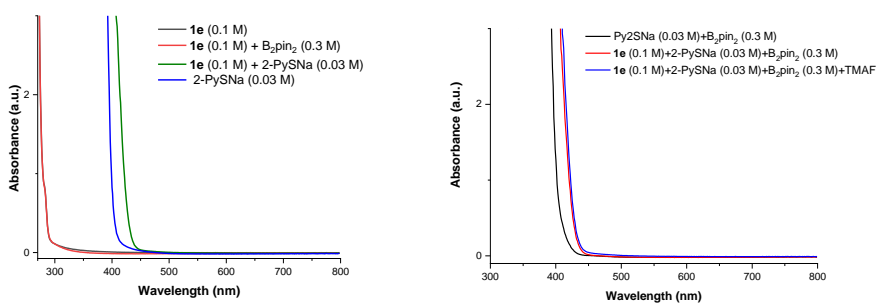


Figure S14. UV-vis spectrum of **1e** in the presence of different components.

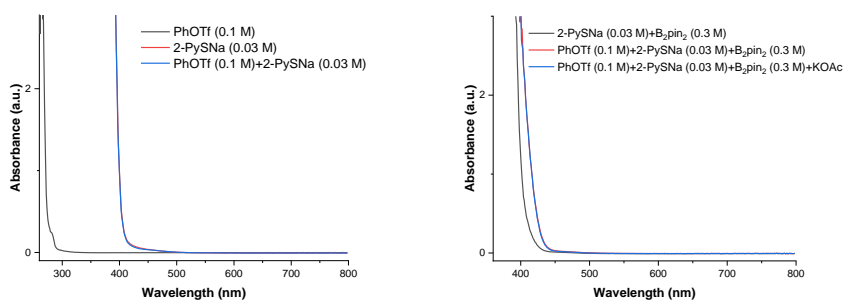


Figure S15. UV-vis spectrum of **1f** in the presence of different components.

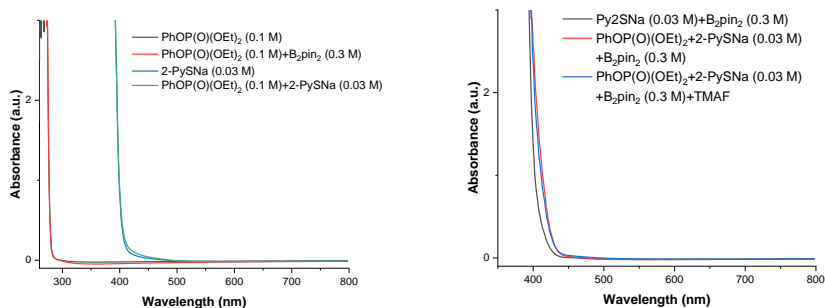


Figure S16. UV-vis spectrum of **1g** in the presence of different components.

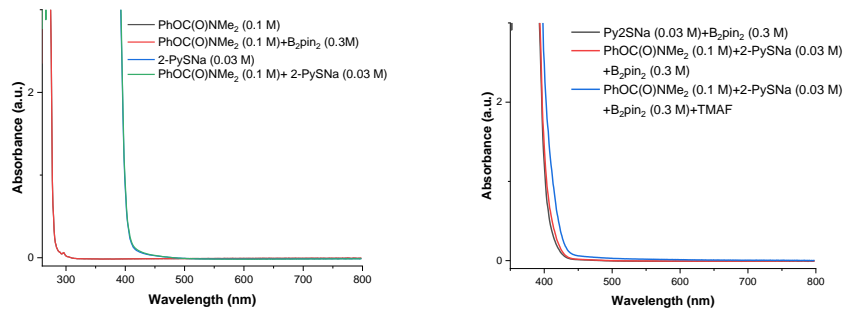


Figure S17. UV-vis spectrum of **1h** in the presence of different components.

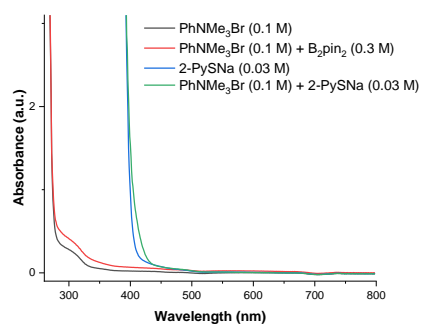


Figure S18. UV-vis spectrum of **1j** in the presence of different components.

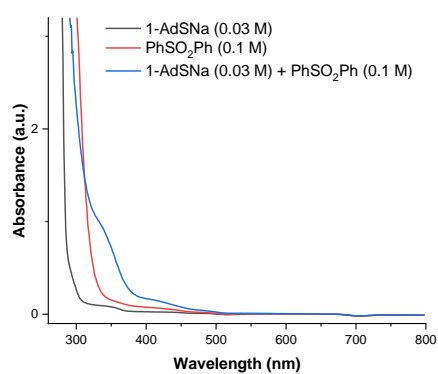


Figure S19. UV-vis spectrum of **1l** in the presence of different components.

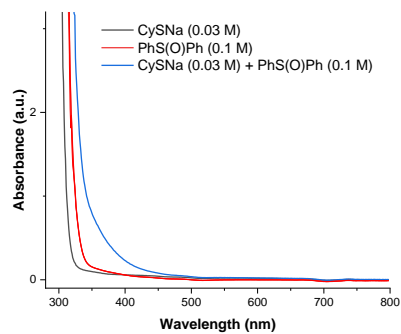
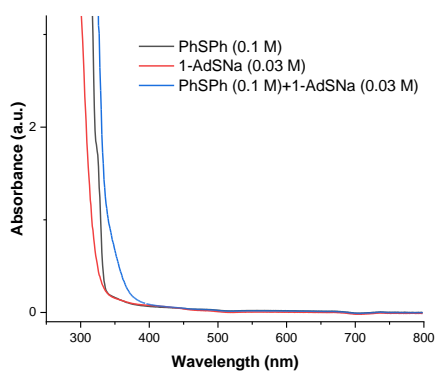
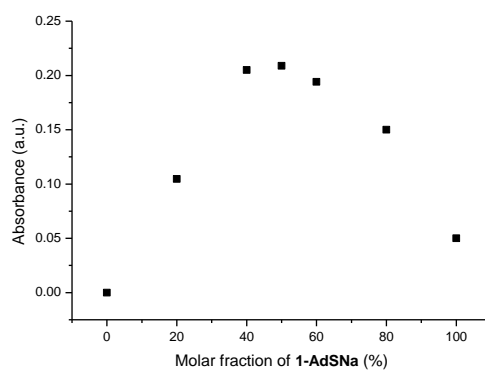


Figure S20. UV-vis spectrum of **1p** in the presence of different components.



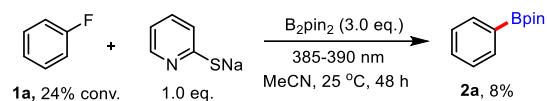
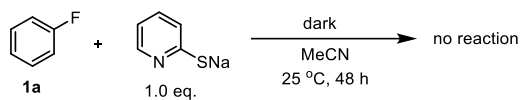
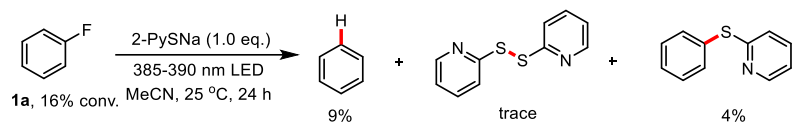
**Figure S21.** UV-vis spectrum of **1r** in the presence of different components.



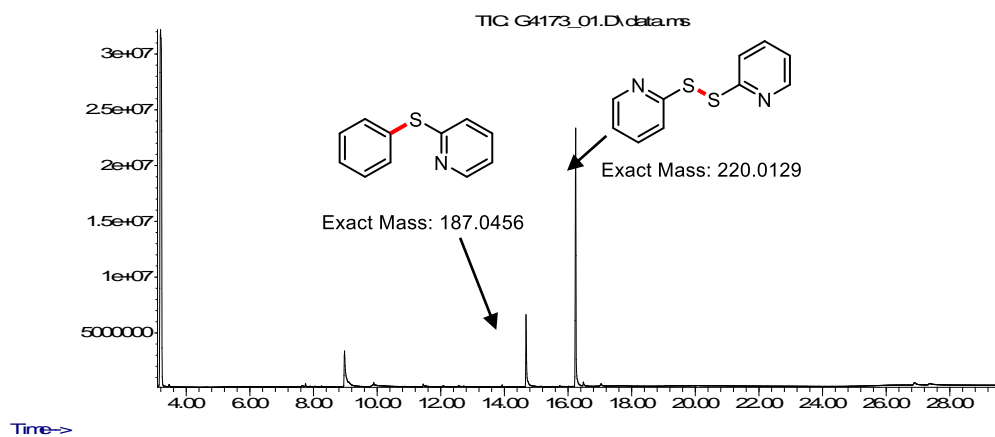
**Figure S22.** Job's plot **1r** with 1-AdSNa in DMSO with intensity of absorption at 360 nm. The total concentration of **1r** and 1-AdSNa was 0.05M and kept the same during the measurements.

## Scheme S6. Control experiments using different radical precursors

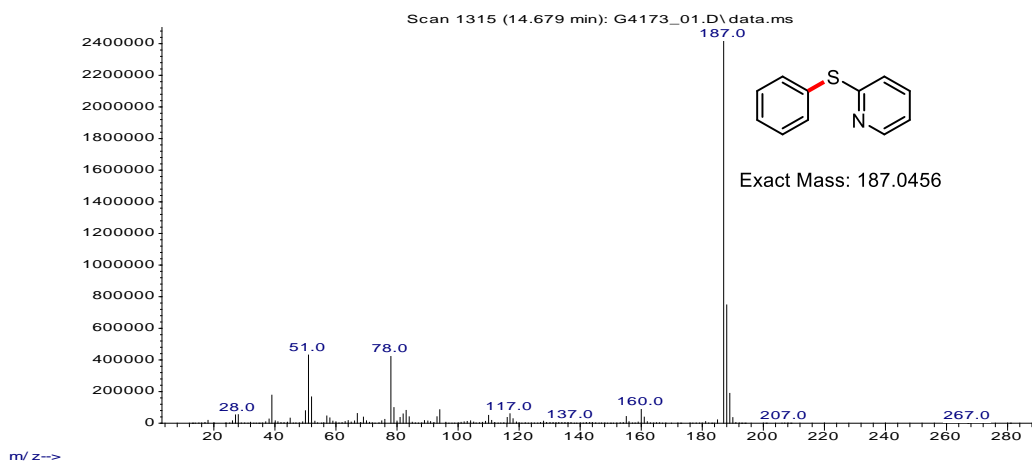
### Control experiments-1a



Abundance



Abundance



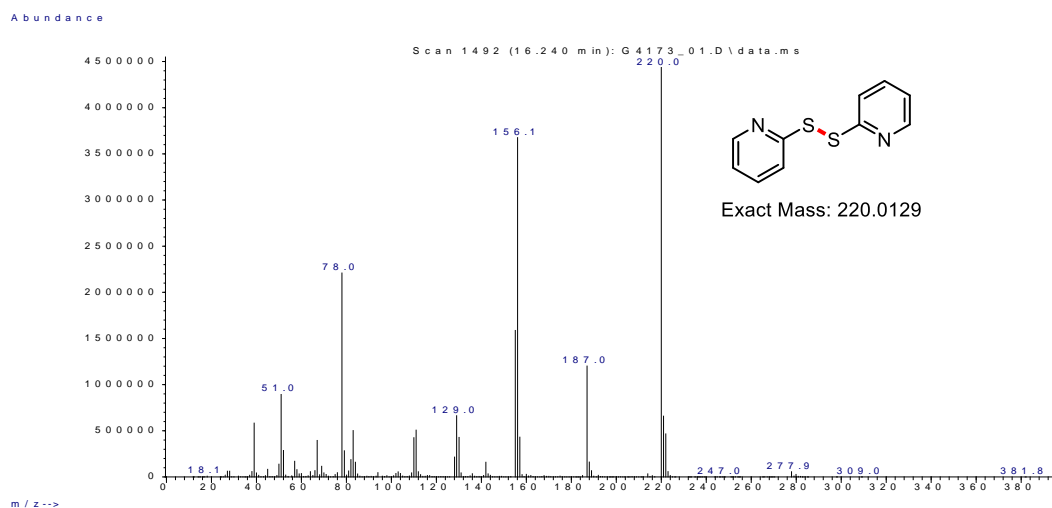
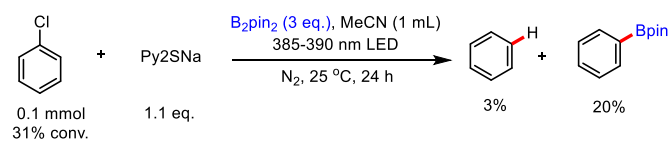
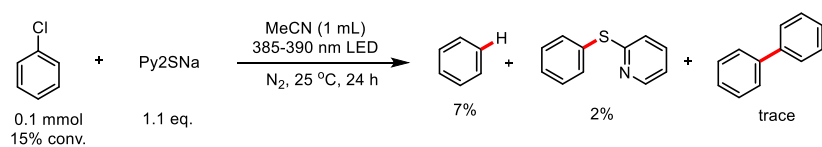
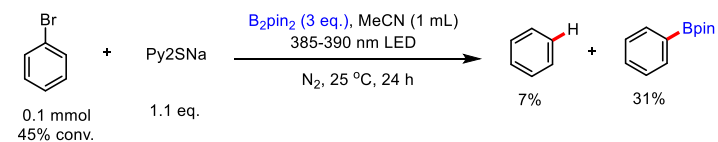
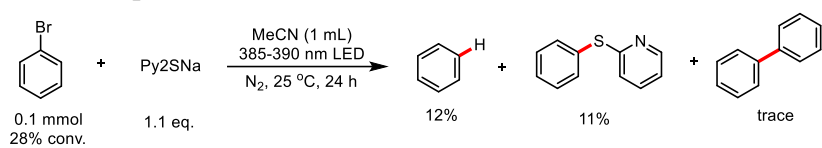


**Figure S23.** GC-MS chromatogram of the reaction mixture of 2-PySNa and **1a** in MeCN after light irradiation (385-390 nm)

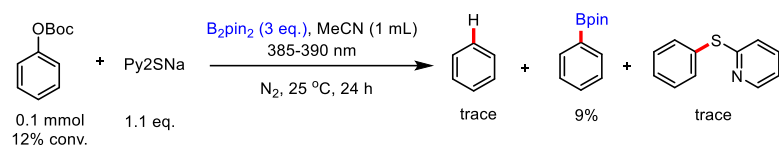
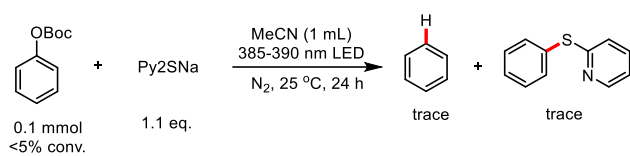
### Control experiments-1b



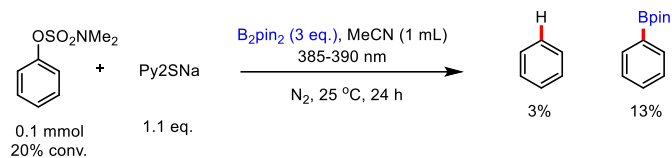
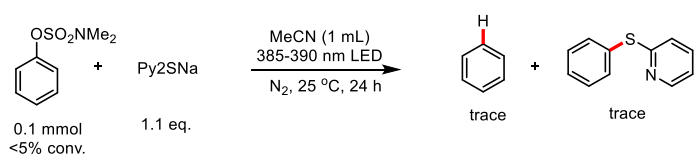
### Control experiments-1c



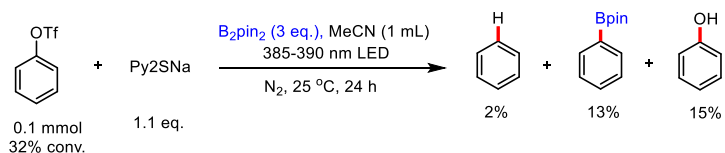
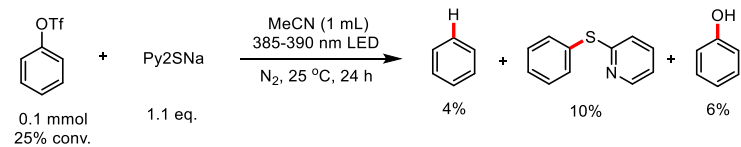
### Control experiments-1d



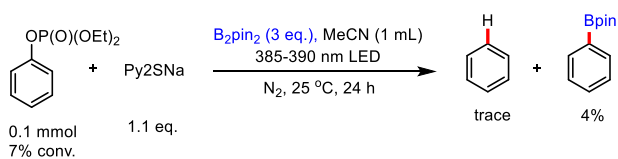
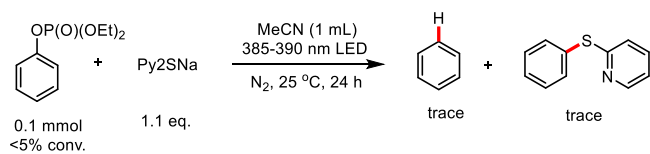
### Control experiments-1e



### Control experiments-1f

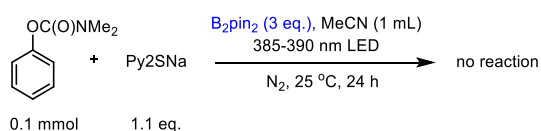
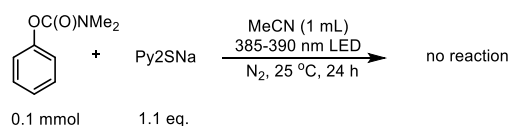


### Control experiments-1g

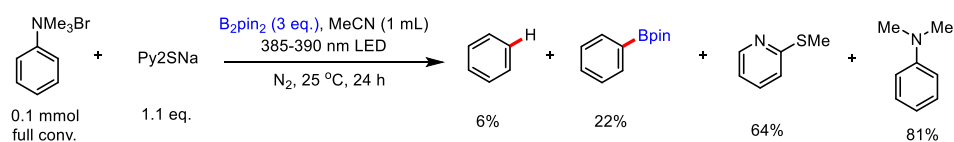
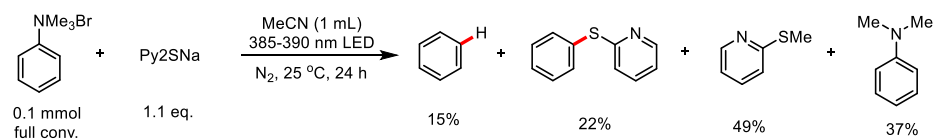




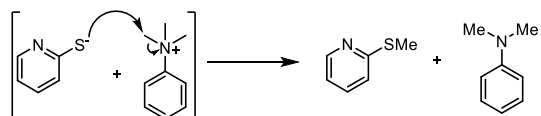
### Control experiments-1h



### Control experiments-1j



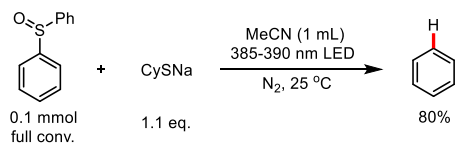
Background reaction process in the absence of base (KOAc)



### Control experiments-1l



### Control experiments-1p



### Control experiments-1r



## NMR studies

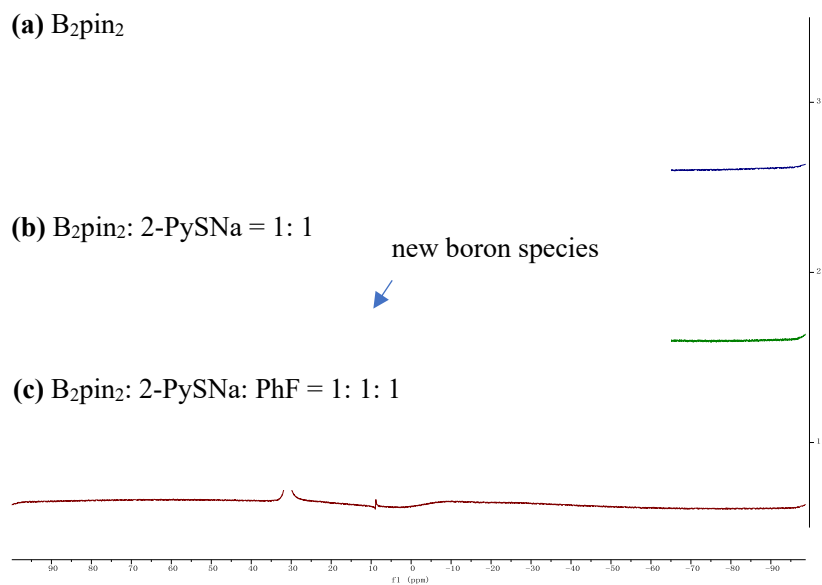


**Figure S24.** (a)  $^{11}B$  NMR spectrum of  $B_2pin_2$  in  $CD_3CN$ . (b)  $^{11}B$  NMR spectrum of  $B_2pin_2$  : 2-PySNa = 1 : 1 in  $CD_3CN$ . (c)  $^{11}B$  NMR spectrum of  $B_2pin_2$ : 2-PySNa: PhF = 1 : 1 : 1 in  $CD_3CN$ .

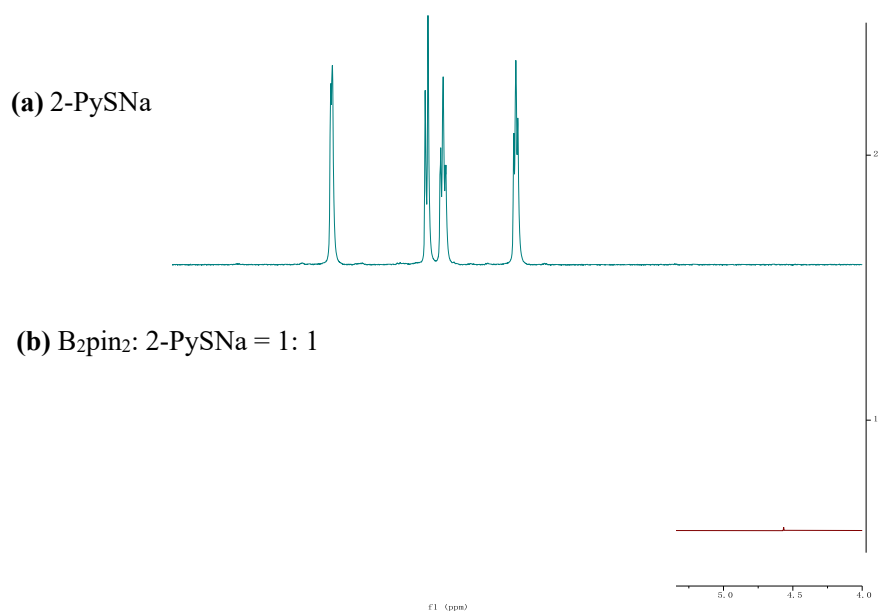


**Figure S25.**  $^1H$  NMR spectra of 2-PySNa in the presence of  $B_2pin_2$ . (a)  $^1H$  NMR spectrum of 2-PySNa in  $CD_3CN$ . (b)  $^1H$  NMR spectrum of 2-PySNa:  $B_2pin_2$  = 1 : 1 in  $CD_3CN$ .

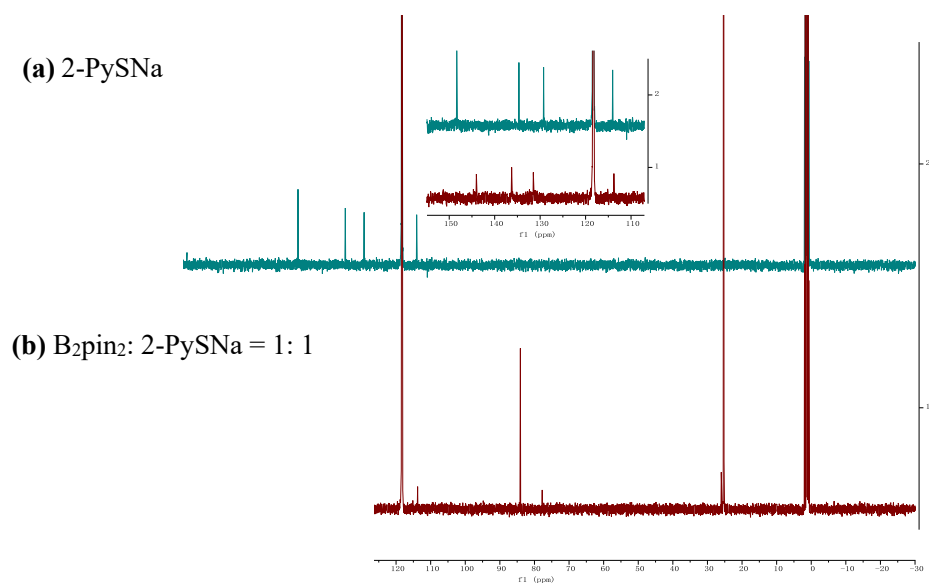


**Figure S26.** (a) <sup>13</sup>C NMR spectrum of 2-PySNa in CD<sub>3</sub>CN. (b) <sup>13</sup>C NMR spectrum of 2-PySNa : B<sub>2</sub>pin<sub>2</sub> = 1 : 1 in CD<sub>3</sub>CN.

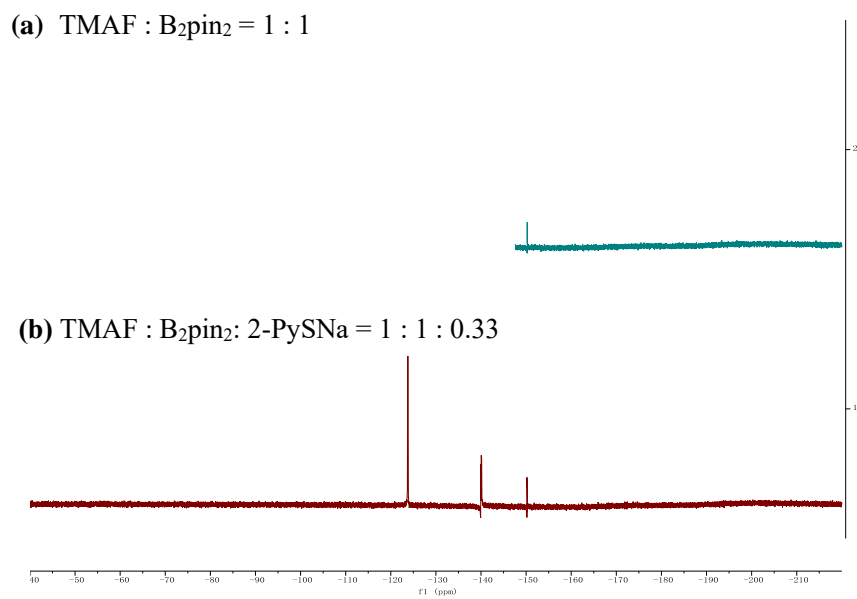


**Figure S27.** (a) <sup>19</sup>F NMR spectrum of TMAF : B<sub>2</sub>pin<sub>2</sub> = 1 : 1 in CD<sub>3</sub>CN. (b) TMAF : B<sub>2</sub>pin<sub>2</sub> : 2-PySNa = 1 : 1 : 0.33 in CD<sub>3</sub>CN. Full conversion of TMAF (<sup>19</sup>F NMR in CD<sub>3</sub>CN, δ -74 ppm) was observed upon mixing with B<sub>2</sub>pin<sub>2</sub> (1.0 eq.) in CD<sub>3</sub>CN. We detected the formation of [Me<sub>4</sub>N][B<sub>2</sub>pin<sub>2</sub>F] (<sup>19</sup>F NMR in CD<sub>3</sub>CN, δ ~125 ppm) and [F<sub>2</sub>Bpin]<sup>-</sup> (<sup>19</sup>F NMR in CD<sub>3</sub>CN, δ ~141 ppm) in the mixture.<sup>[7]</sup>

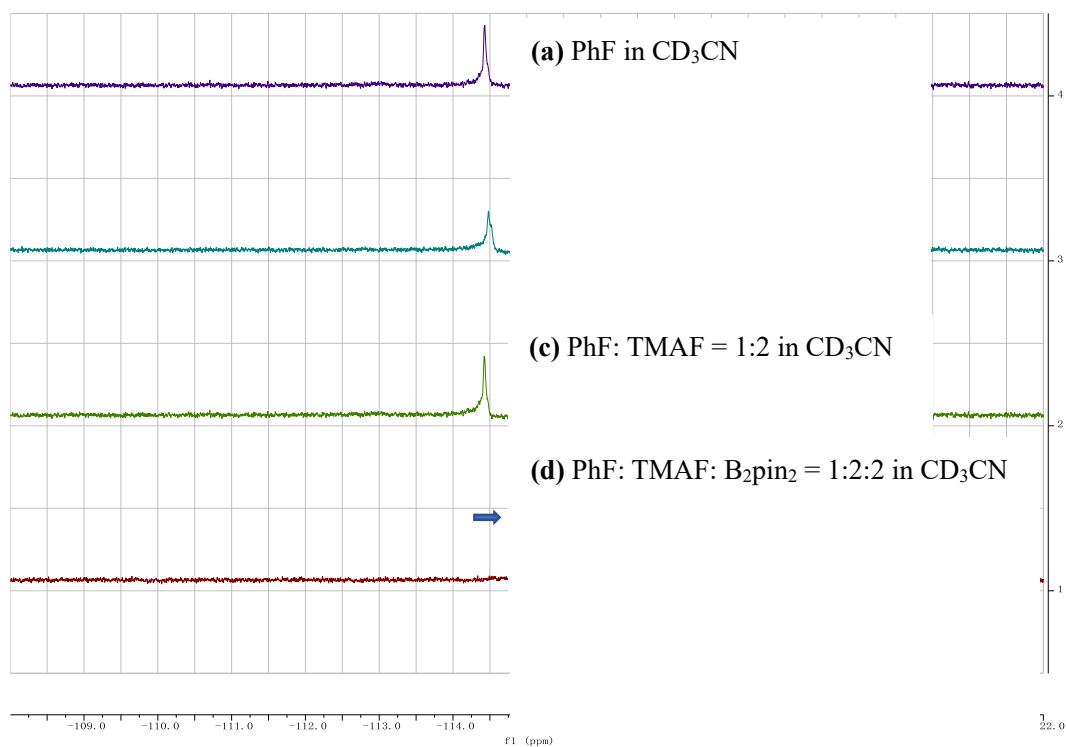
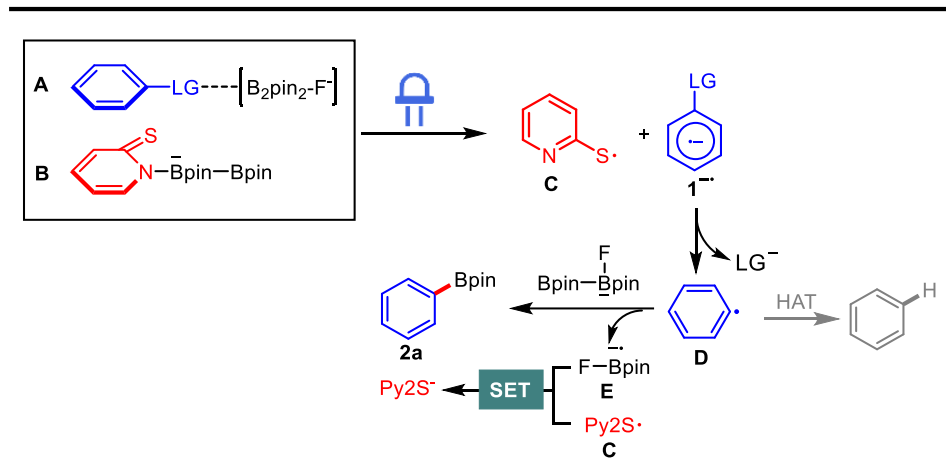


**Figure S28.** <sup>19</sup>F NMR spectra of PhF in the presence of different additives. In order to exclude potential interaction with additives, internal standard (PhCF<sub>3</sub>) was used in a sealed short capillary (~2 cm). (a) <sup>19</sup>F NMR spectrum of PhF in CD<sub>3</sub>CN. (b) <sup>19</sup>F NMR spectrum of PhF : B<sub>2</sub>pin<sub>2</sub> = 1 : 2 in CD<sub>3</sub>CN. (c) <sup>19</sup>F NMR spectrum of PhF : TMAF = 1 : 2 in CD<sub>3</sub>CN. (d) <sup>19</sup>F NMR spectrum of PhF : TMAF: B<sub>2</sub>pin<sub>2</sub>: = 1 : 2: 2 in CD<sub>3</sub>CN.

## Mechanistic proposals and discussions

### Scheme S7. Proposed mechanism for the ipso-borylation of C<sub>aryl</sub>-X, C<sub>aryl</sub>-O and C<sub>aryl</sub>-N bonds

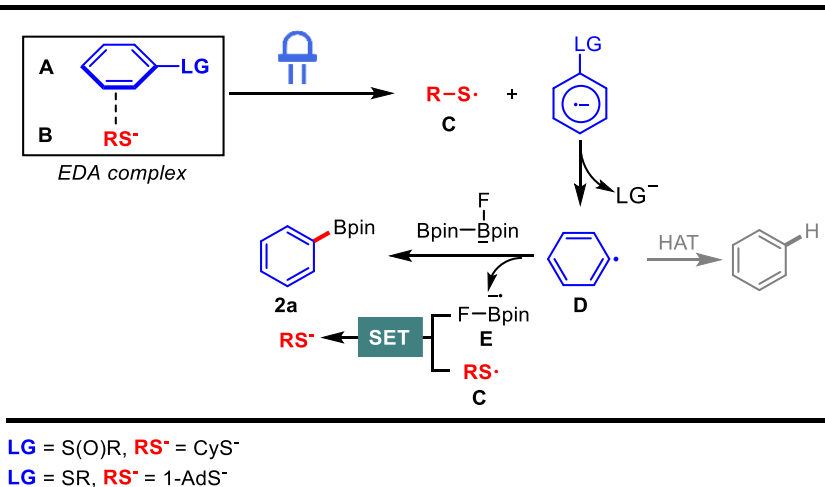


Based on the experimental results, we proposed that the activation effect is essential for the activation of C<sub>aryl</sub>-F, C<sub>aryl</sub>-Cl, C<sub>aryl</sub>-Br and C<sub>aryl</sub>-O bonds during the photo-induced electron transfer process. In the cases of **1a**, **1b**, **1d**, **1f**, **1g** and **1h**, charge transfer complex bands were observed in the reaction mixtures. The co-presence of B<sub>2</sub>pin<sub>2</sub> and fluoride was essential to obtain good conversions of starting materials.

In the case of **1c**, **1e** and **1j**, charge transfer bands were observed in the mixture of **1c**, **1e** or **1j** with 2-PySNa (Figure S12, S14 and S18). However, direct photo-irradiation of the reaction mixtures of **1c** or **1e** with corresponding thiolates gave only low to moderate conversions, which suggests the activation effect of [B<sub>2</sub>pin<sub>2</sub>-F<sup>-</sup>] is also essential for the activation of these substrates.

In the case of **1j**, we observe the nucleophilic attack of 2-PySNa at the substrate to give Py2SMe and N,N-dimethylaniline as the major products in the absence of a fluoride base. Although the charge transfer band was observed between **1j** and 2-PySNa, we speculate the interaction of [B<sub>2</sub>pin<sub>2</sub>-F<sup>-</sup>] with **1j** is key for suppressing the undesired S<sub>N</sub>2 reaction between catalyst and substrate.

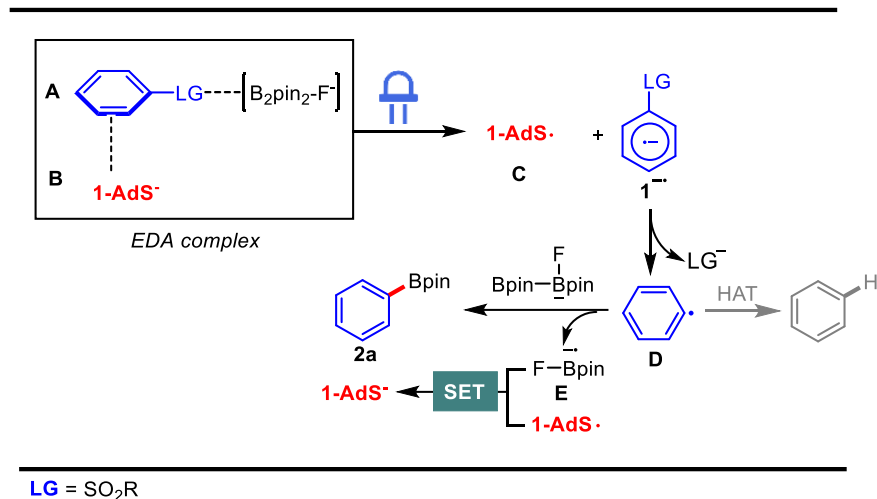
### Scheme S8. Proposed mechanism for the ipso-borylation of C<sub>aryl</sub>-S(O)R and C<sub>aryl</sub>-SR bonds



In the case of sulfoxides and sulfides, clear charge transfer bands were observed in the mixture of **1p** or **1r**

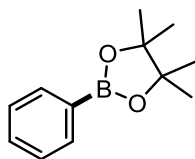
with CySNa or 1-AdSNa (Figure S20 and S21). Moreover, direct photo-irradiation of the reaction mixture of **1p** or **1r** with CySNa or 1-AdSNa afforded benzene in high yields, which suggests the direct photo-induced electron transfer might be the major reaction pathway. Moreover, the Job's plot analysis of the EDA complex **1r**/1-AdSNa showed a maximal absorbance at 50% molar fraction of **1r** indicated the 1:1 stoichiometry of the EDA complex in solution (Figure S22).

**Scheme S9. Proposed mechanism for the ipso-borylation of C<sub>aryl</sub>-SO<sub>2</sub>R bonds**



In the case of **1l**, a clear charge transfer band was observed in the mixture of 1-AdSNa with **1l**. However, direct photo-irradiation of the reaction mixtures of **1l** with 1-AdSNa gave low conversions, which suggests that the activation effect of [B<sub>2</sub>pin<sub>2</sub>-F]<sup>-</sup> is also essential for the cleavage of C-S bonds.

## 5.4.7 Characterization of compounds

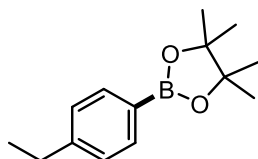


### 4,4,5,5-tetramethyl-2-phenyl-1,3,2-dioxaborolane (**2a**)

**From fluorobenzene:** The general procedure GP1 was followed with fluorobenzene (19.4 mg, 0.2 mmol), B<sub>2</sub>pin<sub>2</sub> (156 mg, 0.6 mmol, 3.0 equiv.), TMAF (56 mg, 0.6 mmol, 3.0 equiv.), Py<sub>2</sub>SNa (8.1 mg, 0.06 mmol, 0.3 equiv.) and CH<sub>3</sub>CN (2 mL). The mixture was irradiated with a 385-390 nm LED light for 24 h. Purification by flash chromatography on silica gel (EtOAc/hexane, 1 : 49 v/v) afford product **2a** (31.8 mg, 78%) as a colorless oil.

**From tert-butyl phenyl carbonate:** The general procedure GP2 was followed with tert-butyl phenyl carbonate (39.6 mg, 0.2 mmol), B<sub>2</sub>pin<sub>2</sub> (156 mg, 0.6 mmol, 3.0 equiv.), CsF (91.2 mg, 0.6 mmol, 3.0 equiv.), Py<sub>2</sub>SNa (10.8 mg, 0.08 mmol, 0.4 equiv.) and CH<sub>3</sub>CN (1.5 mL). The mixture was irradiated with a 385-390 nm LED light for 36 h. Purification by flash chromatography on silica gel (EtOAc/hexane, 1 : 49 v/v) afford product **2a** (26.5 mg, 65%) as a colorless oil.

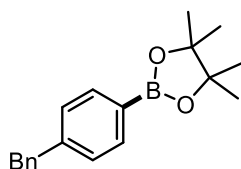
**<sup>1</sup>H NMR** (400 MHz, CDCl<sub>3</sub>) δ 7.88 – 7.77 (m, 2H), 7.51 – 7.42 (m, 1H), 7.42 – 7.33 (m, 2H), 1.36 (s, 12H). **<sup>13</sup>C NMR** (101 MHz, CDCl<sub>3</sub>) δ 134.72, 131.22, 127.68, 83.74, 24.85. **<sup>11</sup>B NMR** (128 MHz, CDCl<sub>3</sub>) δ 30.90. **HRMS** (EI) Calcd. for C<sub>12</sub>H<sub>17</sub>O<sub>2</sub>B [M]<sup>+</sup>: 204.1316. Found: 204.1320.



### 2-(4-ethylphenyl)-4,4,5,5-tetramethyl-1,3,2-dioxaborolane (**4b**)

The general procedure GP1 was followed with 4-ethyl-fluorobenzene (19.4 mg, 0.2 mmol), B<sub>2</sub>pin<sub>2</sub> (156 mg, 0.6 mmol, 3.0 equiv.), TMAF (56 mg, 0.6 mmol, 3.0 equiv.), Py<sub>2</sub>SNa (8.1 mg, 0.06 mmol, 0.3 equiv.) and CH<sub>3</sub>CN (2 mL). The mixture was irradiated with a 385-390 nm LED light for 24 h. Purification by flash chromatography on silica gel (EtOAc/hexane, 1 : 49 v/v) afford product **4b** (31.6 mg, 68%) as a colorless oil.

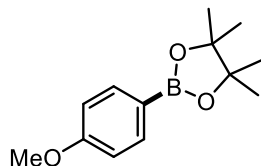
**<sup>1</sup>H NMR** (400 MHz, CDCl<sub>3</sub>) δ 7.78 – 7.71 (m, 2H), 7.25 – 7.19 (m, 2H), 2.67 (q, *J* = 7.6 Hz, 2H), 1.34 (s, 12H), 1.24 (t, *J* = 7.6 Hz, 3H). **<sup>13</sup>C NMR** (101 MHz, CDCl<sub>3</sub>) δ 147.69, 134.89, 127.32, 83.59, 29.10, 24.84, 15.45. **<sup>11</sup>B NMR** (128 MHz, CDCl<sub>3</sub>) δ 30.62. **HRMS** (EI) Calcd. for C<sub>14</sub>H<sub>21</sub>O<sub>2</sub>B [M]<sup>+</sup>: 232.1629. Found: 232.1630.



### 2-(4-benzylphenyl)-4,4,5,5-tetramethyl-1,3,2-dioxaborolane (**4c**)

**From 1-benzyl-4-fluorobenzene:** The general procedure GP1 was followed with 1-benzyl-4-fluorobenzene (37.2 mg, 0.2 mmol), B<sub>2</sub>pin<sub>2</sub> (156 mg, 0.6 mmol, 3.0 equiv.), TMAF (56 mg, 0.6 mmol, 3.0 equiv.), Py<sub>2</sub>SNa (8.1 mg, 0.06 mmol, 0.3 equiv.) and CH<sub>3</sub>CN (2 mL). The mixture was irradiated with a 385-390 nm LED light for 24 h. Purification by flash chromatography on silica gel (EtOAc/hexane, 1 : 49 v/v) afford product **4c** (36.5 mg, 62%) as a transparent oil.

**<sup>1</sup>H NMR** (400 MHz, CDCl<sub>3</sub>) δ 7.77 – 7.70 (m, 2H), 7.30 – 7.24 (m, 2H), 7.23 – 7.14 (m, 5H), 3.99 (s, 2H), 1.33 (s, 12H). **<sup>13</sup>C NMR** (101 MHz, CDCl<sub>3</sub>) δ 144.39, 140.86, 135.00, 128.91, 128.44, 128.42, 126.07, 83.67, 77.32, 77.00, 76.69, 42.12, 24.84. **<sup>11</sup>B NMR** (128 MHz, CDCl<sub>3</sub>) δ 30.76. **HRMS** (EI) Calcd. for C<sub>19</sub>H<sub>23</sub>O<sub>2</sub>B [M]<sup>+</sup>: 294.1786. Found: 294.1782.



#### **2-(4-methoxyphenyl)-4,4,5,5-tetramethyl-1,3,2-dioxaborolane (4d)**

**From 4-fluoroanisole:** The general procedure GP1 was followed with 4-fluoroanisole (25.2 mg, 0.2 mmol), B<sub>2</sub>pin<sub>2</sub> (156 mg, 0.6 mmol, 3.0 equiv.), TMAF (56 mg, 0.6 mmol, 3.0 equiv.), Py<sub>2</sub>SNa (8.1 mg, 0.06 mmol, 0.3 equiv.) and CH<sub>3</sub>CN (2 mL). The mixture was irradiated with a 385-390 nm LED light for 24 h. Purification by flash chromatography on silica gel (EtOAc/hexane, 1 : 49 v/v) afford product **4d** (37.5 mg, 80%) as a white solid.

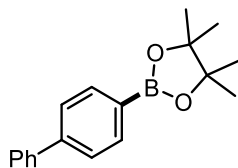
**From 4,4'-sulfonylbis(methoxybenzene):** The general procedure GP3 was followed with 4,4'-sulfonylbis(methoxybenzene) (55.6 mg, 0.2 mmol), B<sub>2</sub>pin<sub>2</sub> (156 mg, 0.6 mmol, 3.0 equiv.), CsF (92 mg, 0.6 mmol, 3.0 equiv.), 1-AdSNa (11.4 mg, 0.06 mmol, 0.3 equiv.) and CH<sub>3</sub>CN (2 mL). The mixture was irradiated with a 385-390 nm LED light for 24 h. Purification by flash chromatography on silica gel (EtOAc/hexane, 1 : 49 v/v) afford product **4d** (33.7 mg, 72%) as a white solid.

**From 4,4'-sulfinylbis(methoxybenzene):** The general procedure GP4 was followed with 4,4'-sulfinylbis(methoxybenzene) (52.4 mg, 0.2 mmol), B<sub>2</sub>pin<sub>2</sub> (103.4 mg, 0.4 mmol, 2.0 equiv.), CsF (62 mg, 0.4 mmol, 2.0 equiv.), CySNa (8.0 mg, 0.06 mmol, 0.3 equiv.) and CH<sub>3</sub>CN (2 mL). The mixture was irradiated with a 385-390 nm LED light for 24 h. Purification by flash chromatography on silica gel (EtOAc/hexane, 1 : 49 v/v) afford product **4d** (29 mg, 62%) as a white solid.

**From bis(4-methoxyphenyl) sulfide:** The general procedure GP4 was followed with bis(4-methoxyphenyl) sulfide (49.2 mg, 0.2 mmol), B<sub>2</sub>pin<sub>2</sub> (103.4 mg, 0.4 mmol, 2.0 equiv.), CsF (62 mg, 0.4 mmol, 2.0 equiv.), 1-AdSNa (11.4 mg, 0.06 mmol, 0.3 equiv.) and CH<sub>3</sub>CN (2 mL). The mixture was irradiated with a 385-390 nm LED light for 24 h. Purification by flash chromatography on silica gel (EtOAc/hexane, 1 : 49 v/v) afford product **4d** (25.7 mg, 55%) as a white solid.

**<sup>1</sup>H NMR** (400 MHz, CDCl<sub>3</sub>) δ 7.81 – 7.66 (m, 2H), 7.00 – 6.70 (m, 2H), 3.83 (s, 3H), 1.33 (s, 12H). **<sup>13</sup>C NMR** (101 MHz, CDCl<sub>3</sub>) δ 162.14, 136.49, 113.29, 83.53, 77.32, 77.00, 76.68, 55.07, 24.84. **<sup>11</sup>B NMR** (128 MHz, CDCl<sub>3</sub>) δ 30.48. **HRMS** (EI) Calcd. for C<sub>18</sub>H<sub>21</sub>O<sub>2</sub>B [M]<sup>+</sup>: 234.1327. Found: 234.1324.





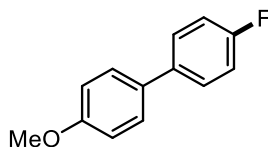
#### 2-([1,1'-biphenyl]-4-yl)-4,4,5,5-tetramethyl-1,3,2-dioxaborolane (**4e**)

**From 4-fluorobiphenyl:** The general procedure GP1 was followed with 4-fluorobiphenyl (34.5 mg, 0.2 mmol), B<sub>2</sub>pin<sub>2</sub> (156 mg, 0.6 mmol, 3.0 equiv.), TMAF (56 mg, 0.6 mmol, 3.0 equiv.), Py<sub>2</sub>SNa (8.1 mg, 0.06 mmol, 0.3 equiv.) and CH<sub>3</sub>CN (2 mL). The mixture was irradiated with a 385-390 nm LED light for 24 h. Purification by flash chromatography on silica gel (EtOAc/hexane, 1 : 40 v/v) afford product **4e** (34.2 mg, 61%) as a transparent oil.

**From [1,1'-biphenyl]-4-yl tert-butyl carbonate:** The general procedure GP2 was followed with [1,1'-biphenyl]-4-yl tert-butyl carbonate (54 mg, 0.2 mmol), B<sub>2</sub>pin<sub>2</sub> (156 mg, 0.6 mmol, 3.0 equiv.), CsF (91.2 mg, 0.6 mmol, 3.0 equiv.), Py<sub>2</sub>SNa (10.8 mg, 0.08 mmol, 0.4 equiv.) and CH<sub>3</sub>CN (1.5 mL). The mixture was irradiated with a 385-390 nm LED light for 36 h. Purification by flash chromatography on silica gel (EtOAc/hexane, 1 : 40 v/v) afford product **4e** (28.6 mg, 51%) as a transparent oil.

**From 4,4''-sulfonyldi-1,1'-biphenyl:** The general procedure GP3 was followed with 4,4''-sulfonyldi-1,1'-biphenyl (74 mg, 0.2 mmol), B<sub>2</sub>pin<sub>2</sub> (156 mg, 0.6 mmol, 3.0 equiv.), CsF (91.2 mg, 0.6 mmol, 3.0 equiv.), 1-AdSNa (11.4 mg, 0.06 mmol, 0.3 equiv.) and CH<sub>3</sub>CN (2 mL). The mixture was irradiated with a 385-390 nm LED light for 24 h. Purification by flash chromatography on silica gel (EtOAc/hexane, 1 : 40 v/v) afford product **4e** (40.3 mg, 72%) as a transparent oil.

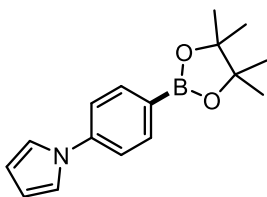
**<sup>1</sup>H NMR** (400 MHz, CDCl<sub>3</sub>) δ 7.93 – 7.85 (m, 2H), 7.65 – 7.57 (m, 4H), 7.47 – 7.39 (m, 2H), 7.37 – 7.30 (m, 1H), 1.35 (s, 12H). **<sup>13</sup>C NMR** (101 MHz, CDCl<sub>3</sub>) δ 143.85, 140.97, 135.23, 128.73, 127.52, 127.19, 126.42, 83.77, 24.84. **<sup>11</sup>B NMR** (128 MHz, CDCl<sub>3</sub>) δ 31.12. **HRMS** (EI) Calcd. for C<sub>18</sub>H<sub>21</sub>O<sub>2</sub>B [M]<sup>+</sup>: 280.1629. Found: 280.1626.



#### 2-(4'-methoxy-[1,1'-biphenyl]-4-yl)-4,4,5,5-tetramethyl-1,3,2-dioxaborolane (**4f**)

**From 4-fluoro-4'-methoxy-1,1'-biphenyl:** The general procedure GP1 was followed with 4-fluoro-4'-methoxy-1,1'-biphenyl (40.4 mg, 0.2 mmol), B<sub>2</sub>pin<sub>2</sub> (156 mg, 0.6 mmol, 3.0 equiv.), TMAF (56 mg, 0.6 mmol, 3.0 equiv.), Py<sub>2</sub>SNa (8.1 mg, 0.06 mmol, 0.3 equiv.) and CH<sub>3</sub>CN (2 mL). The mixture was irradiated with a 385-390 nm LED light for 24 h. Purification by flash chromatography on silica gel (EtOAc/hexane, 1 : 20 v/v) afford product **4f** (32.9 mg, 53%) as a white solid.

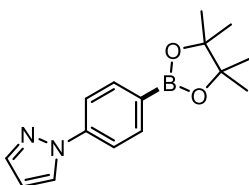
**<sup>1</sup>H NMR** (400 MHz, CDCl<sub>3</sub>) δ 7.91 – 7.83 (m, 2H), 7.62 – 7.54 (m, 4H), 7.02 – 6.94 (m, 2H), 3.86 (s, 3H), 1.37 (s, 12H). **<sup>13</sup>C NMR** (101 MHz, CDCl<sub>3</sub>) δ 159.39, 143.46, 135.24, 133.49, 128.23, 125.96, 114.21, 83.75, 55.33, 24.86. **<sup>11</sup>B NMR** (128 MHz, CDCl<sub>3</sub>) δ 30.68. **HRMS** (EI) Calcd. for C<sub>19</sub>H<sub>23</sub>O<sub>3</sub>B [M]<sup>+</sup>: 310.1735. Found: 310.1741.



#### 1-(4-(4,4,5,5-tetramethyl-1,3,2-dioxaborolan-2-yl)phenyl)-1H-pyrrole (**4g**)

**From 1-(4-fluorophenyl)-1H-pyrrole:** The general procedure GP1 was followed with 1-(4-fluorophenyl)-1H-pyrrole (32.2 mg, 0.2 mmol), B<sub>2</sub>pin<sub>2</sub> (156 mg, 0.6 mmol, 3.0 equiv.), TMAF (56 mg, 0.6 mmol, 3.0 equiv.), Py<sub>2</sub>SNa (8.1 mg, 0.06 mmol, 0.3 equiv.) and CH<sub>3</sub>CN (2 mL). The mixture was irradiated with a 385-390 nm LED light for 24 h. Purification by flash chromatography on silica gel (EtOAc/hexane, 1 : 10 v/v) afford product **4g** (28.0 mg, 52%) as a white solid.

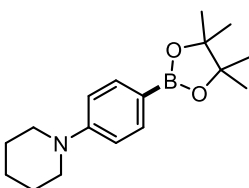
**<sup>1</sup>H NMR** (400 MHz, CDCl<sub>3</sub>) δ 7.86 (d, *J* = 8.4 Hz, 2H), 7.44 – 7.37 (m, 2H), 7.15 (t, *J* = 2.2 Hz, 2H), 6.36 (t, *J* = 2.2 Hz, 2H), 1.36 (s, 12H). **<sup>13</sup>C NMR** (101 MHz, CDCl<sub>3</sub>) δ 142.84, 136.25, 119.23, 119.07, 110.71, 83.89, 24.87. **<sup>11</sup>B NMR** (128 MHz, CDCl<sub>3</sub>) δ 31.00. **HRMS** (EI) Calcd. for C<sub>16</sub>H<sub>20</sub>O<sub>2</sub>NB [M]<sup>+</sup>: 269.1582. Found: 269.1585.



#### 1-(4-(4,4,5,5-tetramethyl-1,3,2-dioxaborolan-2-yl)phenyl)-1H-pyrazole (**4h**)

**From 1-(4-fluorophenyl)-1H-pyrazole:** The general procedure GP1 was followed with 1-(4-fluorophenyl)-1H-pyrazole (32.4 mg, 0.2 mmol), B<sub>2</sub>pin<sub>2</sub> (156 mg, 0.6 mmol, 3.0 equiv.), TMAF (56 mg, 0.6 mmol, 3.0 equiv.), Py<sub>2</sub>SNa (8.1 mg, 0.06 mmol, 0.3 equiv.) and CH<sub>3</sub>CN (2 mL). The mixture was irradiated with a 385-390 nm LED light for 24 h. Purification by flash chromatography on silica gel (EtOAc/hexane, 1 : 8 v/v) afford product **4h** (45.8 mg, 49%) as a white solid. The product was contaminated with B<sub>2</sub>pin<sub>2</sub>, the yield has been calculated taking this into account.

**<sup>1</sup>H NMR** (400 MHz, CDCl<sub>3</sub>) δ 7.97 (dd, *J* = 2.5, 0.6 Hz, 1H), 7.93 – 7.85 (m, 2H), 7.80 – 7.66 (m, 3H), 6.46 (dd, *J* = 2.5, 1.8 Hz, 1H), 1.35 (s, 12H). **<sup>13</sup>C NMR** (101 MHz, CDCl<sub>3</sub>) δ 142.17, 141.27, 136.09, 126.67, 117.95, 107.80, 83.90, 24.85. **<sup>11</sup>B NMR** (128 MHz, CDCl<sub>3</sub>) δ 30.64. **HRMS** (EI) Calcd. for C<sub>15</sub>H<sub>19</sub>O<sub>2</sub>N<sub>2</sub>B [M]<sup>+</sup>: 270.1534. Found: 270.1539.

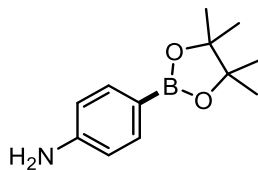


#### 1-(4-(4,4,5,5-tetramethyl-1,3,2-dioxaborolan-2-yl)phenyl)piperidine (**4i**)

**From 1-(4-fluorophenyl)piperidine:** The general procedure GP1 was followed with 1-(4-fluorophenyl)piperidine (36 mg, 0.2 mmol), B<sub>2</sub>pin<sub>2</sub> (156 mg, 0.6 mmol, 3.0 equiv.), TMAF (56 mg, 0.6 mmol, 3.0 equiv.), Py<sub>2</sub>SNa (8.1 mg, 0.06 mmol, 0.3 equiv.) and CH<sub>3</sub>CN (2 mL). The mixture was irradiated with a 385-390 nm LED light for 24 h. Purification by flash chromatography on silica gel (EtOAc/hexane, 1 : 10 v/v) afford product **4i** (35.6 mg, 62%) as a white solid.

**<sup>1</sup>H NMR** (400 MHz, CDCl<sub>3</sub>) δ 7.74 – 7.57 (m, 2H), 6.89 (d, *J* = 8.1 Hz, 2H), 3.32 – 3.18 (m, 4H), 1.68 (p, *J* = 5.6 Hz, 4H), 1.60 (q, *J* = 7.1, 6.1 Hz, 2H), 1.32 (s, 12H). **<sup>13</sup>C NMR** (101 MHz, CDCl<sub>3</sub>) δ 153.93, 136.07,

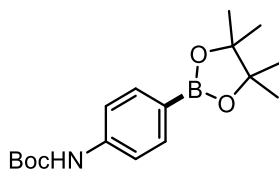
114.54, 83.25, 49.47, 25.50, 24.82, 24.39.  $^{11}\text{B}$  NMR (128 MHz,  $\text{CDCl}_3$ )  $\delta$  31.10. HRMS (EI) Calcd. for  $\text{C}_{17}\text{H}_{26}\text{O}_2\text{NB}$   $[\text{M}]^+$ : 287.2051. Found: 287.2050.



#### 4-(4,4,5,5-tetramethyl-1,3,2-dioxaborolan-2-yl)aniline (**4j**)

**From 4-fluoroaniline:** The general procedure GP1 was followed with 4-fluoroaniline (22.2 mg, 0.2 mmol),  $\text{B}_2\text{pin}_2$  (156 mg, 0.6 mmol, 3.0 equiv.), TMAF (56 mg, 0.6 mmol, 3.0 equiv.),  $\text{Py}_2\text{SNa}$  (8.1 mg, 0.06 mmol, 0.3 equiv.) and  $\text{CH}_3\text{CN}$  (2 mL). The mixture was irradiated with a 385-390 nm LED light for 24 h. Purification by flash chromatography on silica gel (EtOAc/hexane, 1 : 10 v/v) afford product **4j** (22.8 mg, 52%) as a white solid.

$^1\text{H}$  NMR (400 MHz,  $\text{CDCl}_3$ )  $\delta$  7.68 – 7.56 (m, 2H), 6.73 – 6.58 (m, 2H), 3.83 (s, 2H), 1.32 (s, 12H).  $^{13}\text{C}$  NMR (101 MHz,  $\text{CDCl}_3$ )  $\delta$  149.27, 136.39, 114.05, 83.26, 24.82.  $^{11}\text{B}$  NMR (128 MHz,  $\text{CDCl}_3$ )  $\delta$  30.56. HRMS (EI) Calcd. for  $\text{C}_{12}\text{H}_{18}\text{O}_2\text{NB}$   $[\text{M}]^+$ : 219.1425. Found: 219.1431.

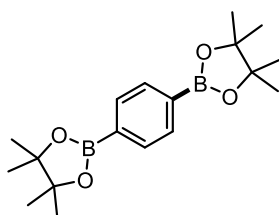


#### tert-butyl (4-(4,4,5,5-tetramethyl-1,3,2-dioxaborolan-2-yl)phenyl)carbamate (**4k**)

**From tert-butyl (4-fluorophenyl)carbamate:** The general procedure GP1 was followed with tert-butyl (4-fluorophenyl)carbamate (42.2 mg, 0.2 mmol),  $\text{B}_2\text{pin}_2$  (156 mg, 0.6 mmol, 3.0 equiv.), TMAF (56 mg, 0.6 mmol, 3.0 equiv.),  $\text{Py}_2\text{SNa}$  (8.1 mg, 0.06 mmol, 0.3 equiv.) and  $\text{CH}_3\text{CN}$  (2 mL). The mixture was irradiated with a 385-390 nm LED light for 24 h. Purification by flash chromatography on silica gel (EtOAc/hexane, 1 : 10 v/v) afford product **4k** (31.9 mg, 50%) as a white solid.

**From tert-butyl (4-((tert-butoxycarbonyl)oxy)phenyl)carbamate:** The general procedure GP2 was followed with tert-butyl (4-((tert-butoxycarbonyl)oxy)phenyl)carbamate (61.8 mg, 0.2 mmol),  $\text{B}_2\text{pin}_2$  (156 mg, 0.6 mmol, 3.0 equiv.), CsF (91.2 mg, 0.6 mmol, 3.0 equiv.),  $\text{Py}_2\text{SNa}$  (10.8 mg, 0.08 mmol, 0.4 equiv.) and  $\text{CH}_3\text{CN}$  (1.5 mL). The mixture was irradiated with a 385-390 nm LED light for 36 h. Purification by flash chromatography on silica gel (EtOAc/hexane, 1 : 40 v/v) afford product **4k** (27.5 mg, 43%) as a transparent oil.

$^1\text{H}$  NMR (300 MHz,  $\text{CDCl}_3$ )  $\delta$  7.77 – 7.69 (m, 2H), 7.40 – 7.32 (m, 2H), 6.58 (s, 1H), 1.51 (s, 9H), 1.33 (s, 12H).  $^{13}\text{C}$  NMR (101 MHz,  $\text{CDCl}_3$ )  $\delta$  152.40, 141.08, 135.83, 117.19, 83.62, 80.69, 28.31, 24.84.  $^{11}\text{B}$  NMR (128 MHz,  $\text{CDCl}_3$ )  $\delta$  30.09. HRMS (ESI) Calcd. for  $[\text{M}+\text{NH}_4]^+$ : 336.2329. Found: 336.2337.

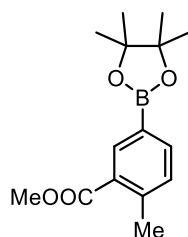


#### 1,4-bis(4,4,5,5-tetramethyl-1,3,2-dioxaborolan-2-yl)benzene (4l)

**From 2-(4-fluorophenyl)-4,4,5,5-tetramethyl-1,3,2-dioxaborolane:** The general procedure GP1 was followed with 2-(4-fluorophenyl)-4,4,5,5-tetramethyl-1,3,2-dioxaborolane (44.4 mg, 0.2 mmol), B<sub>2</sub>pin<sub>2</sub> (156 mg, 0.6 mmol, 3.0 equiv.), CsF (92 mg, 0.6 mmol, 3.0 equiv.), Py<sub>2</sub>SNa (8.1 mg, 0.06 mmol, 0.3 equiv.) and CH<sub>3</sub>CN (2 mL). The mixture was irradiated with a 385-390 nm LED light for 24 h. Purification by flash chromatography on silica gel (EtOAc/hexane, 1 : 20 v/v) afford product **4l** (52.1 mg, 79%) as a white solid.

**From 1,4-difluorobenzene:** The general procedure GP1 was followed with 1,4-difluorobenzene (23 mg, 0.2 mmol), B<sub>2</sub>pin<sub>2</sub> (203.2 mg, 0.8 mmol, 4.0 equiv.), TMAF (75.0 mg, 0.8 mmol, 4.0 equiv.), Py<sub>2</sub>SNa (8.1 mg, 0.06 mmol, 0.3 equiv.) and CH<sub>3</sub>CN (2 mL). The mixture was irradiated with a 385-390 nm LED light for 24 h. Purification by flash chromatography on silica gel (EtOAc/hexane, 1 : 20 v/v) afford product **4l** (23.1 mg, 35%) as a white solid.

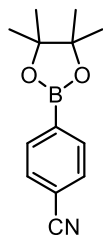
**<sup>1</sup>H NMR** (400 MHz, CDCl<sub>3</sub>) δ 7.80 (s, 4H), 1.35 (s, 24H). **<sup>13</sup>C NMR** (101 MHz, CDCl<sub>3</sub>) δ 133.86, 83.82, 24.85. **<sup>11</sup>B NMR** (128 MHz, CDCl<sub>3</sub>) δ 30.40. **HRMS** (EI) Calcd. for C<sub>18</sub>H<sub>28</sub>O<sub>4</sub>B<sub>2</sub> [M]<sup>+</sup>: 330.2168. Found: 330.2177.



#### methyl 2-methyl-5-(4,4,5,5-tetramethyl-1,3,2-dioxaborolan-2-yl)benzoate (4m)

**From methyl 5-chloro-2-methylbenzoate:** The general procedure GP1 was followed with methyl 5-chloro-2-methylbenzoate (36.8 mg, 0.2 mmol), B<sub>2</sub>pin<sub>2</sub> (156 mg, 0.6 mmol, 3.0 equiv.), TMAF (56 mg, 0.6 mmol, 3.0 equiv.), Py<sub>2</sub>SNa (8.1 mg, 0.06 mmol, 0.3 equiv.) and CH<sub>3</sub>CN (2 mL). The mixture was irradiated with a 385-390 nm LED light for 24 h. Purification by flash chromatography on silica gel (EtOAc/hexane, 1 : 20 v/v) afford product **4m** (29.3 mg, 53%) as a white solid.

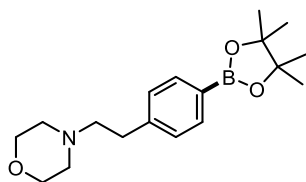
**<sup>1</sup>H NMR** (300 MHz, CDCl<sub>3</sub>) δ 8.41 (d, *J* = 2.0 Hz, 1H), 7.97 (dd, *J* = 8.0, 2.0 Hz, 1H), 7.23 (dt, *J* = 8.1, 0.7 Hz, 1H), 3.90 (s, 3H), 2.58 (s, 3H), 1.35 (s, 12H). **<sup>13</sup>C NMR** (75 MHz, CDCl<sub>3</sub>) δ 167.25, 150.37, 137.01, 131.78, 129.93, 126.71, 83.72, 51.87, 24.87, 22.43. **<sup>11</sup>B NMR** (128 MHz, CDCl<sub>3</sub>) δ 30.72. **HRMS** (EI) Calcd. for C<sub>15</sub>H<sub>21</sub>O<sub>4</sub>B [M]<sup>+</sup>: 276.1527. Found: 276.1530.



#### 4-(4,4,5,5-tetramethyl-1,3,2-dioxaborolan-2-yl)benzonitrile (4n)

**From 4-chlorobenzonitrile:** The general procedure GP1 was followed with methyl 4-chlorobenzonitrile (27.5 mg, 0.2 mmol), B<sub>2</sub>pin<sub>2</sub> (156 mg, 0.6 mmol, 3.0 equiv.), TMAF (56 mg, 0.6 mmol, 3.0 equiv.), Py<sub>2</sub>SNa (8.1 mg, 0.06 mmol, 0.3 equiv.) and CH<sub>3</sub>CN (2 mL). The mixture was irradiated with a 385-390 nm LED light for 24 h. Purification by flash chromatography on silica gel (EtOAc/hexane, 1 : 20 v/v) afford product **4n** (25.6 mg, 56%) as a white solid.

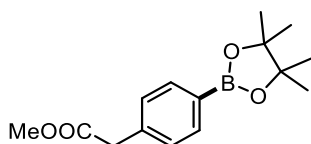
$^1\text{H NMR}$  (400 MHz,  $\text{CDCl}_3$ )  $\delta$  7.90 – 7.84 (m, 2H), 7.66 – 7.60 (m, 2H), 1.35 (s, 12H).  $^{13}\text{C NMR}$  (101 MHz,  $\text{CDCl}_3$ )  $\delta$  135.06, 131.09, 118.83, 114.50, 84.46, 77.32, 77.00, 76.68, 24.83.  $^{11}\text{B NMR}$  (128 MHz,  $\text{CDCl}_3$ )  $\delta$  30.33. **HRMS** (EI) Calcd. for  $\text{C}_{13}\text{H}_{16}\text{O}_2\text{NB}$   $[\text{M}]^+$ : 229.1269. Found: 229.1274.



#### 4-(4-(4,4,5,5-tetramethyl-1,3,2-dioxaborolan-2-yl)phenethyl)morpholine (**4o**)

**From 4-(4-fluorophenethyl)morpholine:** The general procedure GP1 was followed with 4-(4-fluorophenethyl)morpholine (41.8 mg, 0.2 mmol),  $\text{B}_2\text{pin}_2$  (156 mg, 0.6 mmol, 3.0 equiv.), TMAF (56 mg, 0.6 mmol, 3.0 equiv.),  $\text{Py}_2\text{SNa}$  (8.1 mg, 0.06 mmol, 0.3 equiv.) and  $\text{CH}_3\text{CN}$  (2 mL). The mixture was irradiated with a 385-390 nm LED light for 24 h. Purification by flash chromatography on silica gel (EtOAc/hexane, 1 : 6 v/v) afford product **4o** (22.8 mg, 36%) as a white solid.

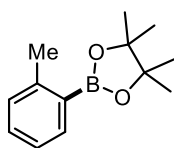
$^1\text{H NMR}$  (300 MHz,  $\text{CDCl}_3$ )  $\delta$  7.81 – 7.74 (m, 2H), 7.28 – 7.22 (m, 2H), 3.84 – 3.71 (m, 4H), 2.95 – 2.80 (m, 2H), 2.68 – 2.61 (m, 2H), 2.60 – 2.52 (m, 4H), 1.37 (s, 12H).  $^{13}\text{C NMR}$  (101 MHz,  $\text{CDCl}_3$ )  $\delta$  143.33, 134.95, 128.12, 83.68, 66.79, 60.48, 53.58, 33.30, 24.83.  $^{11}\text{B NMR}$  (128 MHz,  $\text{CDCl}_3$ )  $\delta$  30.40. **HRMS** (ESI) Calcd. for  $[\text{M}+\text{H}]^+$ : 317.2271. Found: 317.2275.



#### methyl 2-(4-(4,4,5,5-tetramethyl-1,3,2-dioxaborolan-2-yl)phenyl)acetate (**4p**)

**From methyl 2-(4-fluorophenyl)acetate:** The general procedure GP1 was followed with methyl 2-(4-fluorophenyl)acetate (33.6 mg, 0.2 mmol),  $\text{B}_2\text{pin}_2$  (156 mg, 0.6 mmol, 3.0 equiv.), TMAF (56 mg, 0.6 mmol, 3.0 equiv.),  $\text{Py}_2\text{SNa}$  (8.1 mg, 0.06 mmol, 0.3 equiv.) and  $\text{CH}_3\text{CN}$  (2 mL). The mixture was irradiated with a 385-390 nm LED light for 24 h. Purification by flash chromatography on silica gel (EtOAc/hexane, 1 : 20 v/v) afford product **4p** (18.8 mg, 34%) as a transparent oil.

$^1\text{H NMR}$  (400 MHz,  $\text{CDCl}_3$ )  $\delta$  7.80 (d,  $J = 8.1$  Hz, 2H), 7.31 (d,  $J = 8.0$  Hz, 2H), 3.70 (s, 3H), 3.67 (s, 2H), 1.36 (s, 12H).  $^{13}\text{C NMR}$  (101 MHz,  $\text{CDCl}_3$ )  $\delta$  171.74, 137.07, 135.06, 128.63, 83.77, 52.06, 41.42, 24.83.  $^{11}\text{B NMR}$  (128 MHz,  $\text{CDCl}_3$ )  $\delta$  30.83. **HRMS** (EI) Calcd. for  $\text{C}_{15}\text{H}_{21}\text{O}_4\text{B}$   $[\text{M}]^+$ : 276.1527. Found: 276.1522.

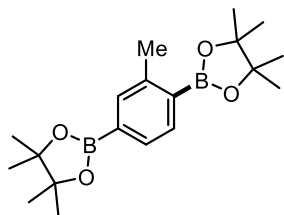


#### 4,4,5,5-tetramethyl-2-(o-tolyl)-1,3,2-dioxaborolane (**4q**)

**From 2-fluorotoluene:** The general procedure GP1 was followed with 2-fluorotoluene (22 mg, 0.2 mmol),  $\text{B}_2\text{pin}_2$  (156 mg, 0.6 mmol, 3.0 equiv.), TMAF (56 mg, 0.6 mmol, 3.0 equiv.),  $\text{Py}_2\text{SNa}$  (8.1 mg, 0.06 mmol, 0.3 equiv.) and  $\text{CH}_3\text{CN}$  (2 mL). The mixture was irradiated with a 385-390 nm LED light for 24 h. Purification by flash chromatography on silica gel (EtOAc/hexane, 1 : 49 v/v) afford product **4q** (24.9 mg, 57%) as a transparent oil.

$^1\text{H NMR}$  (400 MHz,  $\text{CDCl}_3$ )  $\delta$  7.86 (dd,  $J = 7.7, 1.6$  Hz, 1H), 7.42 (td,  $J = 7.5, 1.6$  Hz, 1H), 7.31 – 7.22 (m, 2H), 2.64 (s, 3H), 1.45 (s, 12H).  $^{13}\text{C NMR}$  (101 MHz,  $\text{CDCl}_3$ )  $\delta$  144.81, 135.83, 130.76, 129.75, 124.68,

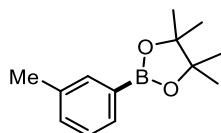
83.38, 24.88, 22.19.  $^{11}\text{B}$  NMR (128 MHz,  $\text{CDCl}_3$ )  $\delta$  31.18. HRMS (EI) Calcd. for  $\text{C}_{13}\text{H}_{19}\text{O}_2\text{B}$   $[\text{M}]^+$ : 218.1473. Found: 218.1472.



#### 2,2'-(2-methyl-1,4-phenylene)bis(4,4,5,5-tetramethyl-1,3,2-dioxaborolane) (**4r**)

**From 2-(4-fluoro-3-methylphenyl)-4,4,5,5-tetramethyl-1,3,2-dioxaborolane:** The general procedure GP1 was followed with 2-(4-fluoro-3-methylphenyl)-4,4,5,5-tetramethyl-1,3,2-dioxaborolane (47.2 mg, 0.2 mmol),  $\text{B}_2\text{pin}_2$  (156 mg, 0.6 mmol, 3.0 equiv.), TMAF (56 mg, 0.6 mmol, 3.0 equiv.),  $\text{Py}_2\text{SNa}$  (8.1 mg, 0.06 mmol, 0.3 equiv.) and  $\text{CH}_3\text{CN}$  (2 mL). The mixture was irradiated with a 385-390 nm LED light for 24 h. Purification by flash chromatography on silica gel (EtOAc/hexane, 1 : 30 v/v) afford product **4r** (28.2 mg, 41%) as a white solid.

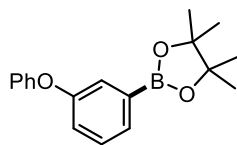
$^1\text{H}$  NMR (400 MHz,  $\text{CDCl}_3$ )  $\delta$  7.75 (d,  $J = 7.3$  Hz, 1H), 7.63 – 7.55 (m, 2H), 2.53 (s, 3H), 1.35 (s, 12H), 1.34 (s, 12H).  $^{13}\text{C}$  NMR (101 MHz,  $\text{CDCl}_3$ )  $\delta$  143.79, 135.85, 135.00, 130.81, 83.75, 83.47, 24.87, 24.84, 21.98.  $^{11}\text{B}$  NMR (128 MHz,  $\text{CDCl}_3$ )  $\delta$  30.89. HRMS (EI) Calcd. for  $\text{C}_{19}\text{H}_{30}\text{O}_4\text{B}_2$   $[\text{M}]^+$ : 344.2325. Found: 344.2330.



#### 4,4,5,5-tetramethyl-2-(m-tolyl)-1,3,2-dioxaborolane (**4t**)

**From 3-fluorotoluene:** The general procedure GP1 was followed with 3-fluorotoluene (22 mg, 0.2 mmol),  $\text{B}_2\text{pin}_2$  (156 mg, 0.6 mmol, 3.0 equiv.), TMAF (56 mg, 0.6 mmol, 3.0 equiv.),  $\text{Py}_2\text{SNa}$  (8.1 mg, 0.06 mmol, 0.3 equiv.) and  $\text{CH}_3\text{CN}$  (2 mL). The mixture was irradiated with a 385-390 nm LED light for 24 h. Purification by flash chromatography on silica gel (EtOAc/hexane, 1 : 49 v/v) afford product **4t** (25.3 mg, 58%) as a transparent oil.

$^1\text{H}$  NMR (400 MHz,  $\text{CDCl}_3$ )  $\delta$  7.64 (s, 1H), 7.61 (q,  $J = 4.6$  Hz, 1H), 7.31 – 7.24 (m, 2H), 2.36 (s, 3H), 1.35 (s, 12H).  $^{13}\text{C}$  NMR (101 MHz,  $\text{CDCl}_3$ )  $\delta$  137.11, 135.32, 132.02, 131.76, 127.67, 83.70, 24.84, 24.78, 21.24.  $^{11}\text{B}$  NMR (128 MHz,  $\text{CDCl}_3$ )  $\delta$  30.89. HRMS (EI) Calcd. for  $\text{C}_{13}\text{H}_{19}\text{O}_2\text{B}$   $[\text{M}]^+$ : 218.1473. Found: 218.1478.

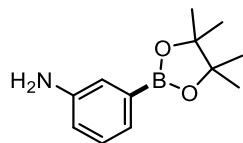


#### 4,4,5,5-tetramethyl-2-(3-phenoxyphenyl)-1,3,2-dioxaborolane (**4u**)

**From 1-fluoro-3-phenoxybenzene:** The general procedure GP1 was followed with 1-fluoro-3-phenoxybenzene (37.6 mg, 0.2 mmol),  $\text{B}_2\text{pin}_2$  (156 mg, 0.6 mmol, 3.0 equiv.), TMAF (56 mg, 0.6 mmol, 3.0 equiv.),  $\text{Py}_2\text{SNa}$  (8.1 mg, 0.06 mmol, 0.3 equiv.) and  $\text{CH}_3\text{CN}$  (2 mL). The mixture was irradiated with a 385-390 nm LED light for 24 h. Purification by flash chromatography on silica gel (EtOAc/hexane, 1 : 49 v/v) afford product **4u** (28.5 mg, 48%) as a transparent oil.

$^1\text{H}$  NMR (400 MHz,  $\text{CDCl}_3$ )  $\delta$  7.56 (dt,  $J = 7.3, 1.1$  Hz, 1H), 7.48 (dd,  $J = 2.6, 1.1$  Hz, 1H), 7.38 – 7.27 (m, 3H), 7.16 – 7.05 (m, 2H), 7.01 – 6.95 (m, 2H), 1.33 (s, 12H).  $^{13}\text{C}$  NMR (101 MHz,  $\text{CDCl}_3$ )  $\delta$  157.67, 156.46,

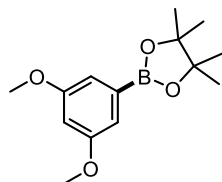
129.83, 129.65, 129.23, 125.29, 122.83, 122.28, 118.45, 83.93, 24.84. **<sup>11</sup>B NMR** (128 MHz, CDCl<sub>3</sub>) δ 29.79. **HRMS** (EI) Calcd. for C<sub>18</sub>H<sub>21</sub>O<sub>3</sub>B [M]<sup>+</sup>: 296.1578. Found: 296.1580.



### 3-(4,4,5,5-tetramethyl-1,3,2-dioxaborolan-2-yl)aniline (4v)

**From 3-fluoroaniline:** The general procedure GP1 was followed with 3-fluoroaniline (22.7 mg, 0.2 mmol), B<sub>2</sub>pin<sub>2</sub> (156 mg, 0.6 mmol, 3.0 equiv.), TMAF (56 mg, 0.6 mmol, 3.0 equiv.), Py<sub>2</sub>SNa (8.1 mg, 0.06 mmol, 0.3 equiv.) and CH<sub>3</sub>CN (2 mL). The mixture was irradiated with a 385-390 nm LED light for 24 h. Purification by flash chromatography on silica gel (EtOAc/hexane, 1 : 8 v/v) afford product **4v** (15.8 mg, 36%) as a transparent oil.

**<sup>1</sup>H NMR** (400 MHz, CDCl<sub>3</sub>) δ 7.24 – 7.13 (m, 3H), 6.80 (ddd, *J* = 7.7, 2.6, 1.4 Hz, 1H), 3.56 (s, 2H), 1.34 (s, 12H). **<sup>13</sup>C NMR** (101 MHz, CDCl<sub>3</sub>) δ 145.50, 128.73, 125.13, 121.23, 118.12, 83.70, 24.84. **<sup>11</sup>B NMR** (128 MHz, CDCl<sub>3</sub>) δ 30.83. **HRMS** (EI) Calcd. for C<sub>12</sub>H<sub>18</sub>O<sub>2</sub>NB [M]<sup>+</sup>: 219.1425. Found: 219.1427.

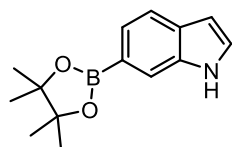


### 2-(3,5-dimethoxyphenyl)-4,4,5,5-tetramethyl-1,3,2-dioxaborolane (4w)

**From 1-fluoro-3,5-dimethoxybenzene:** The general procedure GP1 was followed with 1-fluoro-3,5-dimethoxybenzene (31.2 mg, 0.2 mmol), B<sub>2</sub>pin<sub>2</sub> (156 mg, 0.6 mmol, 3.0 equiv.), TMAF (56 mg, 0.6 mmol, 3.0 equiv.), Py<sub>2</sub>SNa (8.1 mg, 0.06 mmol, 0.3 equiv.) and CH<sub>3</sub>CN (2 mL). The mixture was irradiated with a 385-390 nm LED light for 24 h. Purification by flash chromatography on silica gel (EtOAc/hexane, 1 : 19 v/v) afford product **4w** (17.5 mg, 33%) as a white solid.

**<sup>1</sup>H NMR** (400 MHz, CDCl<sub>3</sub>) δ 6.95 (d, *J* = 2.4 Hz, 2H), 6.57 (t, *J* = 2.4 Hz, 1H), 3.81 (s, 6H), 1.34 (s, 12H). **<sup>13</sup>C NMR** (101 MHz, CDCl<sub>3</sub>) δ 160.39, 111.60, 104.51, 83.86, 77.32, 77.00, 76.68, 55.40, 24.83.

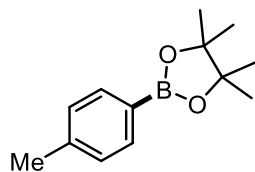
**<sup>11</sup>B NMR** (128 MHz, CDCl<sub>3</sub>) δ 29.89. **HRMS** (EI) Calcd. for C<sub>13</sub>H<sub>17</sub>O<sub>4</sub>B [M]<sup>+</sup>: 247.1251. Found: 247.1243.



### 6-(4,4,5,5-tetramethyl-1,3,2-dioxaborolan-2-yl)-1H-indole (4x)

**From 6-chloro-1H-indole:** The general procedure GP1 was followed with 6-chloro-1H-indole (30.2 mg, 0.2 mmol), B<sub>2</sub>pin<sub>2</sub> (156 mg, 0.6 mmol, 3.0 equiv.), TMAF (56 mg, 0.6 mmol, 3.0 equiv.), Py<sub>2</sub>SNa (8.1 mg, 0.06 mmol, 0.3 equiv.) and CH<sub>3</sub>CN (2 mL). The mixture was irradiated with a 385-390 nm LED light for 24 h. Purification by flash chromatography on silica gel (EtOAc/hexane, 1 : 8 v/v) afford product **4x** (27.7 mg, 57%) as a white solid and indole **4x'** (7 mg, 30%).

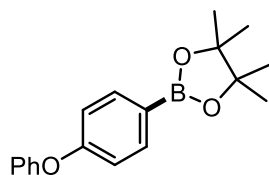
**<sup>1</sup>H NMR** (300 MHz, CDCl<sub>3</sub>) δ 8.26 (s, 1H), 7.92 (q, *J* = 1.0 Hz, 1H), 7.26 (dd, *J* = 3.2, 2.5 Hz, 1H), 6.56 (ddd, *J* = 3.1, 2.0, 1.0 Hz, 1H), 1.38 (s, 12H). **<sup>13</sup>C NMR** (75 MHz, CDCl<sub>3</sub>) δ 135.50, 130.34, 125.55, 120.02, 118.01, 102.67, 83.53, 24.87. **<sup>11</sup>B NMR** (128 MHz, CDCl<sub>3</sub>) δ 31.19. **HRMS** (EI) Calcd. for C<sub>14</sub>H<sub>18</sub>O<sub>2</sub>NB [M]<sup>+</sup>: 243.1425. Found: 243.1430.



#### 4,4,5,5-tetramethyl-2-(p-tolyl)-1,3,2-dioxaborolane (**4y**)

**From tert-butyl p-tolyl carbonate:** The general procedure GP2 was followed with 4-methyl tert-butyl phenyl carbonate (41.6 mg, 0.2 mmol), B<sub>2</sub>pin<sub>2</sub> (156 mg, 0.6 mmol, 3.0 equiv.), CsF (91.2 mg, 0.6 mmol, 3.0 equiv.), Py<sub>2</sub>SNa (10.8 mg, 0.08 mmol, 0.4 equiv.) and CH<sub>3</sub>CN (1.5 mL). The mixture was irradiated with a 385-390 nm LED light for 36 h. Purification by flash chromatography on silica gel (EtOAc/hexane, 1 : 49 v/v) afford product **4y** (21.9 mg, 50%) as a colorless oil.

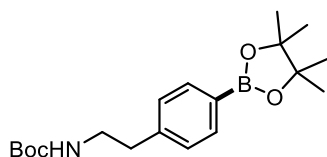
<sup>1</sup>H NMR (400 MHz, CDCl<sub>3</sub>) δ 7.76 – 7.67 (m, 2H), 7.22 – 7.16 (m, 2H), 2.37 (s, 3H), 1.34 (s, 12H). <sup>13</sup>C NMR (101 MHz, CDCl<sub>3</sub>) δ 141.37, 134.79, 128.50, 83.60, 24.84, 21.70. <sup>11</sup>B NMR (128 MHz, CDCl<sub>3</sub>) δ 31.00. HRMS (EI) Calcd. for C<sub>13</sub>H<sub>19</sub>O<sub>2</sub>B [M]<sup>+</sup>: 218.14726. Found: 218.14733.



#### 4,4,5,5-tetramethyl-2-(4-phenoxyphenyl)-1,3,2-dioxaborolane (**4z**)

**From tert-butyl (4-phenoxyphenyl) carbonate:** The general procedure GP2 was followed with tert-butyl (4-phenoxyphenyl) carbonate (57.2 mg, 0.2 mmol), B<sub>2</sub>pin<sub>2</sub> (156 mg, 0.6 mmol, 3.0 equiv.), CsF (91.2 mg, 0.6 mmol, 3.0 equiv.), Py<sub>2</sub>SNa (10.8 mg, 0.08 mmol, 0.4 equiv.) and CH<sub>3</sub>CN (1.5 mL). The mixture was irradiated with a 385-390 nm LED light for 36 h. Purification by flash chromatography on silica gel (EtOAc/hexane, 1 : 49 v/v) afford product **4z** (27.8 mg, 47%) as a colorless oil.

<sup>1</sup>H NMR (400 MHz, CDCl<sub>3</sub>) δ 7.81 – 7.75 (m, 2H), 7.39 – 7.31 (m, 2H), 7.17 – 7.09 (m, 1H), 7.06 – 7.00 (m, 2H), 7.00 – 6.95 (m, 2H), 1.34 (s, 12H). <sup>13</sup>C NMR (101 MHz, CDCl<sub>3</sub>) δ 160.18, 156.55, 136.61, 129.78, 123.64, 119.45, 117.66, 83.72, 24.85. <sup>11</sup>B NMR (128 MHz, CDCl<sub>3</sub>) δ 30.81. HRMS (EI) Calcd. for C<sub>18</sub>H<sub>21</sub>O<sub>3</sub>B [M]<sup>+</sup>: 296.1578. Found: 296.1592.

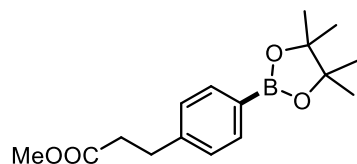


#### tert-butyl (4-(4,4,5,5-tetramethyl-1,3,2-dioxaborolan-2-yl)phenethyl)carbamate (**4aa**)

**From tert-butyl (4-((tert-butoxycarbonyl)oxy)phenethyl)carbamate:** The general procedure GP2 was followed with tert-butyl (4-((tert-butoxycarbonyl)oxy)phenethyl)carbamate (67.4 mg, 0.2 mmol), B<sub>2</sub>pin<sub>2</sub> (156 mg, 0.6 mmol, 3.0 equiv.), CsF (91.2 mg, 0.6 mmol, 3.0 equiv.), Py<sub>2</sub>SNa (10.8 mg, 0.08 mmol, 0.4 equiv.) and CH<sub>3</sub>CN (1.5 mL). The mixture was irradiated with a 385-390 nm LED light for 36 h. Purification by flash chromatography on silica gel (EtOAc/hexane, 1 : 7 v/v) afford product **4aa** (29.2 mg, 42%) as colorless oil.

<sup>1</sup>H NMR (400 MHz, CDCl<sub>3</sub>) δ 7.80 (d, *J* = 7.6 Hz, 2H), 7.25 (d, *J* = 7.5 Hz, 2H), 4.56 (s, 1H), 3.42 (q, *J* = 6.7 Hz, 2H), 2.86 (t, *J* = 7.0 Hz, 2H), 1.48 (s, 9H), 1.39 (s, 12H). <sup>13</sup>C NMR (101 MHz, CDCl<sub>3</sub>) δ 155.82, 142.34, 135.06, 128.25, 83.72, 41.62, 36.31, 28.38, 24.84. <sup>11</sup>B NMR (128 MHz, CDCl<sub>3</sub>) δ 29.67. HRMS (ESI) Calcd. for [M+Na]<sup>+</sup>: 370.2160. Found: 370.2167.

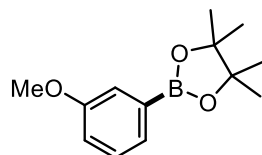




#### methyl 3-(4-(4,4,5,5-tetramethyl-1,3,2-dioxaborolan-2-yl)phenyl)propanoate (**4ab**)

**From methyl 3-(4-((tert-butoxycarbonyloxy)phenyl)propanoate:** The general procedure GP2 was followed with methyl 3-(4-((tert-butoxycarbonyloxy)phenyl)propanoate (56 mg, 0.2 mmol), B<sub>2</sub>pin<sub>2</sub> (156 mg, 0.6 mmol, 3.0 equiv.), CsF (91.2 mg, 0.6 mmol, 3.0 equiv.), Py<sub>2</sub>SNa (10.8 mg, 0.08 mmol, 0.4 equiv.) and CH<sub>3</sub>CN (1.5 mL). The mixture was irradiated with a 385–390 nm LED light for 24 h. Purification by flash chromatography on silica gel (EtOAc/hexane, 1 : 9 v/v) afford product **4ab** (22.1 mg, 38%) as a colorless oil. The product was contaminated with B<sub>2</sub>pin<sub>2</sub>, the yield has been calculated taking this into account.

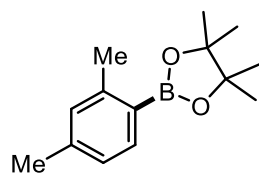
**<sup>1</sup>H NMR** (400 MHz, CDCl<sub>3</sub>) δ 7.80 – 7.67 (m, 2H), 7.21 (d, *J* = 7.8 Hz, 2H), 3.66 (s, 3H), 2.96 (t, *J* = 7.9 Hz, 2H), 2.63 (dd, *J* = 8.4, 7.2 Hz, 2H), 1.33 (s, 12H). **<sup>13</sup>C NMR** (101 MHz, CDCl<sub>3</sub>) δ 173.21, 143.81, 135.02, 127.69, 83.47, 51.60, 35.48, 24.82. **<sup>11</sup>B NMR** (128 MHz, CDCl<sub>3</sub>) δ 30.89. **HRMS** (EI) Calcd. for C<sub>16</sub>H<sub>23</sub>O<sub>4</sub>B [M]<sup>+</sup>: 290.1684. Found: 290.1689.



#### 2-(3-methoxyphenyl)-4,4,5,5-tetramethyl-1,3,2-dioxaborolane (**4ac**)

**From tert-butyl (3-methoxyphenyl) carbonate:** The general procedure GP2 was followed with tert-butyl (3-methylphenyl) carbonate (44.8 mg, 0.2 mmol), B<sub>2</sub>pin<sub>2</sub> (156 mg, 0.6 mmol, 3.0 equiv.), CsF (91.2 mg, 0.6 mmol, 3.0 equiv.), Py<sub>2</sub>SNa (10.8 mg, 0.08 mmol, 0.4 equiv.) and CH<sub>3</sub>CN (1.5 mL). The mixture was irradiated with a 385–390 nm LED light for 36 h. Purification by flash chromatography on silica gel (EtOAc/hexane, 1 : 49 v/v) afford product **4ac** (22.5 mg, 48%) as a colorless oil.

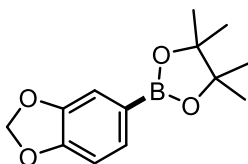
**<sup>1</sup>H NMR** (400 MHz, CDCl<sub>3</sub>) δ 7.44 (dt, *J* = 7.3, 1.1 Hz, 1H), 7.37 (d, *J* = 2.8 Hz, 1H), 7.32 (dd, *J* = 8.2, 7.2 Hz, 1H), 7.03 (ddd, *J* = 8.2, 2.8, 1.1 Hz, 1H), 3.85 (s, 3H), 1.37 (s, 12H). **<sup>13</sup>C NMR** (101 MHz, CDCl<sub>3</sub>) δ 158.98, 128.85, 127.10, 118.69, 117.77, 83.71, 55.10, 24.77. **<sup>11</sup>B NMR** (128 MHz, CDCl<sub>3</sub>) δ 30.41. **HRMS** (EI) Calcd. for C<sub>13</sub>H<sub>19</sub>O<sub>3</sub>B [M]<sup>+</sup>: 234.1422. Found: 234.1423.



#### 2-(2,4-dimethylphenyl)-4,4,5,5-tetramethyl-1,3,2-dioxaborolane (**4ad**)

**From tert-butyl (2,4-dimethylphenyl) carbonate:** The general procedure GP2 was followed with tert-butyl (2,4-dimethylphenyl) carbonate (44.4 mg, 0.2 mmol), B<sub>2</sub>pin<sub>2</sub> (156 mg, 0.6 mmol, 3.0 equiv.), CsF (91.2 mg, 0.6 mmol, 3.0 equiv.), Py<sub>2</sub>SNa (10.8 mg, 0.08 mmol, 0.4 equiv.) and CH<sub>3</sub>CN (1.5 mL). The mixture was irradiated with a 385–390 nm LED light for 36 h. Purification by flash chromatography on silica gel (EtOAc/hexane, 1 : 49 v/v) afford product **4ad** (26.5 mg, 57%) as a colorless oil.

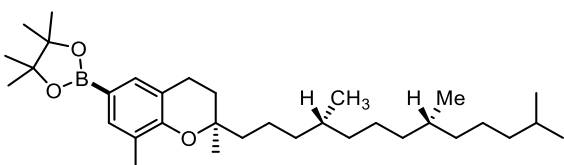
**<sup>1</sup>H NMR** (400 MHz, CDCl<sub>3</sub>) δ 7.69 – 7.63 (m, 1H), 6.99 (d, *J* = 7.4 Hz, 2H), 2.51 (s, 3H), 2.32 (s, 3H), 1.34 (s, 12H). **<sup>13</sup>C NMR** (101 MHz, CDCl<sub>3</sub>) δ 144.92, 140.84, 136.07, 130.70, 125.51, 83.21, 24.86, 22.09, 21.47. **<sup>11</sup>B NMR** (128 MHz, CDCl<sub>3</sub>) δ 30.78. **HRMS** (EI) Calcd. for C<sub>14</sub>H<sub>21</sub>O<sub>2</sub>B [M]<sup>+</sup>: 232.1629. Found: 232.1627.



#### 2-(benzo[d][1,3]dioxol-5-yl)-4,4,5,5-tetramethyl-1,3,2-dioxaborolane (4ae)

**From benzo[d][1,3]dioxol-5-yl tert-butyl carbonate:** The general procedure GP2 was followed with benzo[d][1,3]dioxol-5-yl tert-butyl carbonate (47.6 mg, 0.2 mmol), B<sub>2</sub>pin<sub>2</sub> (156 mg, 0.6 mmol, 3.0 equiv.), CsF (91.2 mg, 0.6 mmol, 3.0 equiv.), Py<sub>2</sub>SNa (10.8 mg, 0.08 mmol, 0.4 equiv.) and CH<sub>3</sub>CN (1.5 mL). The mixture was irradiated with a 385-390 nm LED light for 36 h. Purification by flash chromatography on silica gel (EtOAc/hexane, 1 : 49 v/v) afford product **4ae** (21.8 mg, 44%) as a colorless oil.

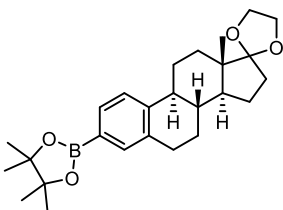
<sup>1</sup>H NMR (400 MHz, CDCl<sub>3</sub>) δ 7.36 (d, *J* = 7.7 Hz, 1H), 7.24 (s, 1H), 6.83 (dd, *J* = 7.7, 1.1 Hz, 1H), 5.95 (s, 2H), 1.32 (s, 12H). <sup>13</sup>C NMR (101 MHz, CDCl<sub>3</sub>) δ 150.14, 147.18, 129.70, 113.93, 108.26, 100.71, 83.69, 24.82. <sup>11</sup>B NMR (128 MHz, CDCl<sub>3</sub>) δ 30.35. HRMS (EI) Calcd. for C<sub>13</sub>H<sub>17</sub>O<sub>4</sub>B [M]<sup>+</sup>: 247.1251. Found: 247.1243.



#### 2-((R)-2,8-dimethyl-2-((4R,8R)-4,8,12-trimethyltridecyl)chroman-6-yl)-4,4,5,5-tetramethyl-1,3,2-dioxaborolane (4af)

**From (R)-2,8-dimethyl-2-((4R,8R)-4,8,12-trimethyltridecyl)chroman-6-yl dimethylsulfamate:** The general procedure GP2 was followed with (R)-2,8-dimethyl-2-((4R,8R)-4,8,12-trimethyltridecyl)chroman-6-yl dimethylsulfamate (101.8 mg, 0.2 mmol), B<sub>2</sub>pin<sub>2</sub> (156 mg, 0.6 mmol, 3.0 equiv.), TMAF (56.2 mg, 0.6 mmol, 3.0 equiv.), Py<sub>2</sub>SNa (10.8 mg, 0.08 mmol, 0.4 equiv.) and CH<sub>3</sub>CN (1.5 mL). The mixture was irradiated with a 385-390 nm LED light for 36 h. Purification by flash chromatography on silica gel (EtOAc/hexane, 1 : 30 v/v) afford product **4af** (66.6 mg, 65%) as a colorless oil.

<sup>1</sup>H NMR (400 MHz, CDCl<sub>3</sub>) δ 7.42 (s, 1H), 7.40 (s, 1H), 2.75 (t, *J* = 6.8 Hz, 2H), 2.16 (s, 3H), 1.85 – 1.71 (m, 2H), 1.60 – 1.49 (m, 3H), 1.49 – 1.34 (m, 4H), 1.33 (s, 12H), 1.29 – 1.19 (m, 10H), 1.18 – 1.00 (m, 7H), 0.88 – 0.82 (m, 12H). <sup>13</sup>C NMR (101 MHz, CDCl<sub>3</sub>) δ 155.22, 134.81, 134.10, 125.74, 119.94, 83.35, 76.51, 40.13, 39.36, 37.42, 37.27, 32.78, 32.66, 31.18, 27.97, 24.82, 24.79, 24.43, 24.33, 22.72, 22.62, 22.02, 20.95, 19.74, 19.63, 15.81. <sup>11</sup>B NMR (128 MHz, CDCl<sub>3</sub>) δ 30.90. HRMS (EI) Calcd. for C<sub>33</sub>H<sub>57</sub>O<sub>3</sub>B [M]<sup>+</sup>: 512.4395. Found: 512.4390.

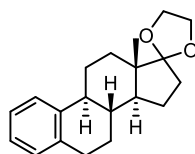


#### 4,4,5,5-tetramethyl-2-((8R,9S,13S,14S)-13-methyl-6,7,8,9,11,12,13,14,15,16-decahydrospiro[cyclopenta[a]phenanthrene-17,2'-[1,3]dioxolan]-3-yl)-1,3,2-dioxaborolane (4ag)

**From tert-butyl ((8R,9S,13S,14S)-13-methyl-6,7,8,9,11,12,13,14,15,16-decahydrospiro[cyclopenta[a]phenanthrene-17,2'-[1,3]dioxolan]-3-yl) carbonate:** The general procedure GP2 was followed with tert-butyl ((8R,9S,13S,14S)-13-methyl-6,7,8,9,11,12,13,14,15,16-decahydrospiro[cyclopenta[a]phenanthrene-

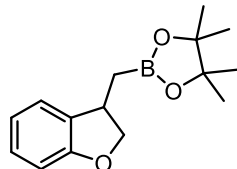
17,2'-[1,3]dioxolan]-3-yl) carbonate (82.8 mg, 0.2 mmol), B<sub>2</sub>pin<sub>2</sub> (156 mg, 0.6 mmol, 3.0 equiv.), CsF (91.2 mg, 0.6 mmol, 3.0 equiv.), Py<sub>2</sub>SNa (10.8 mg, 0.08 mmol, 0.4 equiv.) and CH<sub>3</sub>CN (1.5 mL). The mixture was irradiated with a 385-390 nm LED light for 36 h. Purification by flash chromatography on silica gel (EtOAc/hexane, 1 : 30 v/v) afford product **4ag** (38.2 mg, 44%) as a white solid and **4ag'** (9 mg, 15%).

**<sup>1</sup>H NMR** (400 MHz, CDCl<sub>3</sub>) δ 7.58 (dd, *J* = 7.8, 1.4 Hz, 1H), 7.55 (d, *J* = 1.4 Hz, 1H), 7.32 (d, *J* = 7.8 Hz, 1H), 3.99 – 3.86 (m, 4H), 2.93 – 2.83 (m, 2H), 2.44 – 2.23 (m, 2H), 2.07 – 1.99 (m, 1H), 1.95 – 1.73 (m, 4H), 1.70 – 1.36 (m, 6H), 1.34 (s, 12H), 0.88 (s, 3H). **<sup>13</sup>C NMR** (101 MHz, CDCl<sub>3</sub>) δ 143.87, 136.10, 135.54, 131.96, 124.78, 119.39, 83.58, 65.24, 64.56, 49.51, 46.08, 44.38, 38.68, 34.19, 30.71, 29.26, 26.89, 25.79, 24.81, 24.78, 22.35, 14.29. **<sup>11</sup>B NMR** (128 MHz, CDCl<sub>3</sub>) δ 31.37. **HRMS** (EI) Calcd. for C<sub>26</sub>H<sub>37</sub>O<sub>4</sub>B [M]<sup>+</sup>: 424.2779. Found: 424.1791.



**(8R,9S,13S,14S)-13-methyl-6,7,8,9,11,12,13,14,15,16-decahydrospiro[cyclopenta[a]phenanthrene-17,2'-[1,3]dioxolane] (4ag')**

**<sup>1</sup>H NMR** (400 MHz, CDCl<sub>3</sub>) δ 7.33 – 7.27 (m, 1H), 7.18 – 7.02 (m, 3H), 4.01 – 3.87 (m, 4H), 2.88 (dt, *J* = 8.3, 3.6 Hz, 2H), 2.40 – 2.25 (m, 2H), 2.08 – 2.01 (m, 1H), 1.97 – 1.72 (m, 4H), 1.69 – 1.62 (dm, 1H), 1.60 – 1.27 (m, 6H), 0.88 (s, 3H). **<sup>13</sup>C NMR** (101 MHz, CDCl<sub>3</sub>) δ 140.38, 136.75, 129.00, 125.54, 125.31, 119.42, 65.25, 64.58, 49.50, 46.13, 44.14, 38.77, 34.22, 30.75, 29.51, 26.93, 25.88, 22.36, 14.31. **HRMS** (EI) Calcd. for C<sub>20</sub>H<sub>26</sub>O<sub>2</sub> [M]<sup>+</sup>: 298.1927. Found: 298.1927.



**2-((2,3-dihydrobenzofuran-3-yl)methyl)-4,4,5,5-tetramethyl-1,3,2-dioxaborolane (4ae)**

**From 1-(allyloxy)-2-fluorobenzene:** The general procedure GP1 was followed with 1-(allyloxy)-2-fluorobenzene (30.4 mg, 0.2 mmol), B<sub>2</sub>pin<sub>2</sub> (156 mg, 0.6 mmol, 3.0 equiv.), TMAF (56 mg, 0.6 mmol, 3.0 equiv.), Py<sub>2</sub>SNa (8.1 mg, 0.06 mmol, 0.3 equiv.) and CH<sub>3</sub>CN (2 mL). The mixture was irradiated with a 385-390 nm LED light for 24 h. Purification by flash chromatography on silica gel (EtOAc/hexane, 1 : 8 v/v) afford product **4ae** (4.7 mg, 9%) as a transparent oil.

**<sup>1</sup>H NMR** (400 MHz, CDCl<sub>3</sub>) δ 7.20 (dd, *J* = 7.4, 1.3 Hz, 1H), 7.12 – 7.06 (m, 1H), 6.84 (td, *J* = 7.4, 1.0 Hz, 1H), 6.76 (d, *J* = 8.0 Hz, 1H), 4.70 (t, *J* = 8.9 Hz, 1H), 4.10 (dd, *J* = 8.7, 7.5 Hz, 1H), 3.68-3.60 (m, 1H), 1.37-1.30 (m, 1H), 1.26 (s, 6H), 1.24 (s, 6H), 1.13-1.07 (m, 1H). **<sup>13</sup>C NMR** (101 MHz, CDCl<sub>3</sub>) δ 159.69, 132.70, 127.82, 123.99, 120.29, 109.36, 83.41, 78.62, 37.68, 24.90, 24.74. **<sup>11</sup>B NMR** (128 MHz, CDCl<sub>3</sub>) δ 33.66. **HRMS** (EI) Calcd. for C<sub>15</sub>H<sub>21</sub>O<sub>3</sub>B [M]<sup>+</sup>: 260.1578. Found: 260.1581.

## 5.5 References

- [1] a) L. Marzo, S. K. Pagire, O. Reiser, B. König, *Angew. Chem. Int. Ed.* **2018**, *57*, 10034-10072; b) J. M. R. Narayanam, C. R. J. Stephenson, *Chem. Soc. Rev.* **2011**, *40*, 102-113; c) C. K. Prier, D. A. Rankic, D. W. C. MacMillan, *Chem. Rev.* **2013**, *113*, 5322-5363; d) N. A. Romero, D. A. Nicewicz, *Chem. Rev.* **2016**, *116*, 10075-10166; e) K. L. Skubi, T. R. Blum, T. P. Yoon, *Chem. Rev.* **2016**, *116*, 10035-10074; f) J. Xuan, W.-J. Xiao, *Angew. Chem. Int. Ed.* **2012**, *51*, 6828-6838.
- [2] F. Glaser, C. Kerzig, O. S. Wenger, *Angew. Chem. Int. Ed.* **2020**, *59*, 10266-10284.
- [3] a) I. Ghosh, L. Marzo, A. Das, R. Shaikh, B. König, *Acc. Chem. Res.* **2016**, *49*, 1566-1577; b) M. Majek, A. Jacobi von Wangelin, *Acc. Chem. Res.* **2016**, *49*, 2316-2327; c) I. Ghosh, *Phys. Sci. Rev.* **2019**, *4*.
- [4] a) I. Ghosh, T. Ghosh, J. I. Bardagi, B. König, *Science* **2014**, *346*, 725-728; b) M. Giedyk, R. Narobe, S. Weiß, D. Touraud, W. Kunz, B. König, *Nat. Catal.* **2020**, *3*, 40-47; c) I. Ghosh, B. König, *Angew. Chem. Int. Ed.* **2016**, *55*, 7676-7679.
- [5] a) N. G. W. Cowper, C. P. Chernowsky, O. P. Williams, Z. K. Wickens, *J. Am. Chem. Soc.* **2020**, *142*, 2093-2099; b) H. Kim, H. Kim, T. H. Lambert, S. Lin, *J. Am. Chem. Soc.* **2020**, *142*, 2087-2092.
- [6] I. A. MacKenzie, L. Wang, N. P. R. Onuska, O. F. Williams, K. Begam, A. M. Moran, B. D. Dunietz, D. A. Nicewicz, *Nature* **2020**, *580*, 76-80.
- [7] a) M. Schmalzbauer, M. Marcon, B. König, *Angew. Chem. Int. Ed.* **2021**, *60*, 6270-6292; b) W. Liu, J. Li, C.-Y. Huang, C.-J. Li, *Angew. Chem. Int. Ed.* **2020**, *59*, 1786-1796.
- [8] Boronic acids: preparation and applications in organic synthesis, medicine and materials, 2nd ed., Hall, D. G., Ed., Wiley-VCH: Weinheim, Germany, **2011**.
- [9] N. Miyaura, A. Suzuki, *Chem. Rev.* **1995**, *95*, 2457-2483.
- [10] a) T. Ishiyama, M. Murata, N. Miyaura, *J. Org. Chem.* **1995**, *60*, 7508-7510; b) E. C. Neeve, S. J. Geier, I. A. I. Mkhaliid, S. A. Westcott, T. B. Marder, *Chem. Rev.* **2016**, *116*, 9091-9161.
- [11] a) F. W. Friese, A. Studer, *Chem. Sci.* **2019**, *10*, 8503-8518; b) V. D. Nguyen, V. T. Nguyen, S. Jin, H. T. Dang, O. V. Larionov, *Tetrahedron* **2019**, *75*, 584-602; c) M. Wang, Z. Shi, *Chem. Rev.* **2020**, *120*, 7348-7398; d) G. Yan, D. Huang, X. Wu, *Adv. Synth. Catal.* **2018**, *360*, 1039-1039; e) Y.-M. Tian, X.-N. Guo, H. Braunschweig, U. Radius, T. B. Marder, *Chem. Rev.* **2021**, DOI: 10.1021/acs.chemrev.0c01236.
- [12] a) S. Ahammed, S. Nandi, D. Kundu, B. C. Ranu, *Tetrahedron Lett.* **2016**, *57*, 1551-1554; b) J. Yu, L. Zhang, G. Yan, *Adv. Synth. Catal.* **2012**, *354*, 2625-2628; c) T. Lei, S.-M. Wei, K. Feng, B. Chen, C.-H. Tung, L.-Z. Wu, *ChemSusChem* **2020**, *13*, 1715-1719.
- [13] a) A. M. Mfuh, J. D. Doyle, B. Chhetri, H. D. Arman, O. V. Larionov, *J. Am. Chem. Soc.* **2016**, *138*, 2985-2988; b) S. Jin, H. T. Dang, G. C. Haug, R. He, V. D. Nguyen, V. T. Nguyen, H. D. Arman, K. S. Schanze, O. V. Larionov, *J. Am. Chem. Soc.* **2020**, *142*, 1603-1613.
- [14] a) K. Chen, S. Zhang, P. He, P. Li, *Chem. Sci.* **2016**, *7*, 3676-3680; b) Y. Cheng, C. Mück-Lichtenfeld, A. Studer, *Angew. Chem. Int. Ed.* **2018**, *57*, 16832-16836; c) M. Jiang, H. Yang, H. Fu, *Org. Lett.* **2016**, *18*, 5248-5251; d) W. Liu, X. Yang, Y. Gao, C.-J. Li, *J. Am. Chem. Soc.* **2017**, *139*, 8621-8627; e) Y. Qiao, Q. Yang, E. J. Schelter, *Angew. Chem. Int. Ed.* **2018**, *57*, 10999-11003; f) Y.-M. Tian, X.-N. Guo, I. Krummenacher, Z. Wu, J. Nitsch, H. Braunschweig, U. Radius, T. B. Marder, *J. Am. Chem. Soc.* **2020**, *142*, 18231-18242; g) Y.-M. Tian, X.-N. Guo, M. W. Kuntze-Fechner, I. Krummenacher, H. Braunschweig, U. Radius, A. Steffen, T. B. Marder, *J. Am. Chem. Soc.* **2018**, *140*, 17612-17623; h) L. Zhang, L. Jiao, *J. Am. Chem. Soc.* **2019**, *141*, 9124-9128.
- [15] L. Candish, M. Teders, F. Glorius, *J. Am. Chem. Soc.* **2017**, *139*, 7440-7443.

- [16] a) M. Schmalzbauer, T. D. Svejstrup, F. Fricke, P. Brandt, M. J. Johansson, G. Bergonzini, B. König, *Chem* **2020**, *6*, 2658-2672; b) M. Schmalzbauer, I. Ghosh, B. König, *Faraday Discuss.* **2019**, *215*, 364-378.
- [17] S. Wang, N. Lokesh, J. Hioe, R. M. Gschwind, B. König, *Chem. Sci.* **2019**, *10*, 4580-4587.
- [18] a) E. de Pedro Beato, D. Mazzarella, M. Balletti, P. Melchiorre, *Chem. Sci.* **2020**, *11*, 6312-6324; b) H. Huang, J.-H. Ye, L. Zhu, C.-K. Ran, M. Miao, W. Wang, H. Chen, W.-J. Zhou, Y. Lan, B. Yu, D.-G. Yu, *CCS Chem.* **2020**, *2*, 1746-1756. c) G. Li, Q. Yan, Z. Gan, Q. Li, X. Dou, D. Yang, *Org. Lett.* **2019**, *21*, 7938-7942; d) H. Li, X. Tang, J. H. Pang, X. Wu, E. K. L. Yeow, J. Wu, S. Chiba, *J. Am. Chem. Soc.* **2021**, *143*, 481-487; e) K. Liang, N. Li, Y. Zhang, T. Li, C. Xia, *Chem. Sci.* **2019**, *10*, 3049-3053; f) B. Liu, C.-H. Lim, G. M. Miyake, *J. Am. Chem. Soc.* **2017**, *139*, 13616-13619; g) L. Marzo, S. Wang, B. König, *Org. Lett.* **2017**, *19*, 5976-5979; h) D. Mazzarella, G. Magagnano, B. Schweitzer-Chaput, P. Melchiorre, *ACS Catal.* **2019**, *9*, 5876-5880; i) B. Schweitzer-Chaput, M. A. Horwitz, E. de Pedro Beato, P. Melchiorre, *Nat. Chem.* **2019**, *11*, 129-135; j) D. Spinnato, B. Schweitzer-Chaput, G. Goti, M. Ošeka, P. Melchiorre, *Angew. Chem. Int. Ed.* **2020**, *59*, 9485-9490; k) M. Tobisu, T. Furukawa, N. Chatani, *Chemistry Letters* **2013**, *42*, 1203-1205; l) J. Wu, R. M. Bär, L. Guo, A. Noble, V. K. Aggarwal, *Angew. Chem. Int. Ed.* **2019**, *58*, 18830-18834; m) E. J. McClain, T. M. Monos, M. Mori, J. W. Beatty, C. R. J. Stephenson, *ACS Catal.* **2020**, *10*, 12636-12641.
- [19] K. Chen, M. S. Cheung, Z. Lin, P. Li, *Org. Chem. Front.* **2016**, *3*, 875-879.
- [20] a) H. Zeng, Z. Qiu, A. Domínguez-Huerta, Z. Hearne, Z. Chen, C.-J. Li, *ACS Catal.* **2017**, *7*, 510-519; b) Z. Qiu, C.-J. Li, *Chem. Rev.* **2020**, *120*, 10454-10515.
- [21] a) J. Gao, J. Feng, D. Du, *Chem. Asian J.* **2020**, *15*, 3637-3659; b) D. Kaiser, I. Klose, R. Oost, J. Neuhaus, N. Maulide, *Chem. Rev.* **2019**, *119*, 8701-8780; c) C. Huang, J. Feng, R. Ma, S. Fang, T. Lu, W. Tang, D. Du, J. Gao, *Org. Lett.* **2019**, *21*, 9688-9692.
- [22] Y. Maekawa, Z. T. Ariki, M. Nambo, C. M. Crudden, *Org. Biomol. Chem.* **2019**, *17*, 7300-7303.
- [23] C. Raviola, S. Protti, *Eur. J. Org. Chem.* **2020**, *2020*, 5292-5304.
- [24] a) G. E. M. Crisenza, D. Mazzarella, P. Melchiorre, *J. Am. Chem. Soc.* **2020**, *142*, 5461-5476; b) C. G. S. Lima, T. de M. Lima, M. Duarte, I. D. Jurberg, M. W. Paixão, *ACS Catal.* **2016**, *6*, 1389-1407.
- [25] a) W.-M. Cheng, R. Shang, B. Zhao, W.-L. Xing, Y. Fu, *Org. Lett.* **2017**, *19*, 4291-4294; b) P. Nguyen, C. Dai, N. J. Taylor, W. P. Power, T. B. Marder, N. L. Pickett, N. C. Norman, *Inorg. Chem.* **1995**, *34*, 4290-4291; c) Y. Katsuma, H. Asakawa, M. Yamashita, *Chem. Sci.* **2018**, *9*, 1301-1310.
- [26] a) S. Pietsch, E. C. Neeve, D. C. Apperley, R. Bertermann, F. Mo, D. Qiu, M. S. Cheung, L. Dang, J. Wang, U. Radius, Z. Lin, C. Kleeberg, T. B. Marder *Chem. Eur. J.* **2015**, *21*, 7082-7098; b) S. Pinet, V. Liautard, M. Debais, M. Pucheault, *Synthesis* **2017**, *49*, 4759-4768.
- [27] EDA complex is proposed to be formed by the [F--B<sub>2</sub>pin<sub>2</sub>]-activated sulfones with 1-AdSNa.
- [28] J. Lu, N. S. Khetrapal, J. A. Johnson, X. C. Zeng, J. Zhang, *J. Am. Chem. Soc.* **2016**, *138*, 15805-15808.
- [29] M. Niazi, H. R. Shahsavari, M. G. Haghighi, M. R. Halvagar, S. Hatami, B. Notash, *RSC Adv.* **2016**, *6*, 76463-76472.
- [30] J. Li, H. Wang, Z. Qiu, C.-Y. Huang, C.-J. Li, *J. Am. Chem. Soc.* **2020**, *142*, 13011-13020.
- [31] L. Pause, M. Robert, J.-M. Savéant, *J. Am. Chem. Soc.* **1999**, *121*, 7158-7159.
- [32] A. Jutand, A. Mosleh, *J. Org. Chem.* **1997**, *62*, 261-274.
- [33] J. Grimshaw, *Electrochemical reactions and mechanisms in organic chemistry*, Elsevier, **2000**.



## 6. Summary

This thesis presents photoredox catalytic carbonyl Umpolung methods for the generation of functionalized alkyl carbanions and photo-induced thiolate-catalyzed ipso-borylation of substituted arenes.

**Chapter 1** reviews different concepts for the catalytic generation of alkyl carbanion equivalents from carbonyls.

**Chapter 2** describes a photoredox catalysis for the generation of  $\alpha$ -boryl carbanions. This synthetically valuable intermediate can be generated from a photo-induced single-electron reduction of aldehydes and a subsequent radical borylation-deoxygenation reaction sequence. The resulting  $\alpha$ -boryl carbanion then reacts with another molecule of aldehyde to give alkenes as the final product, thus presenting a photo-McMurry type reaction. The key in realizing this transformation is the use of thiols as a catalyst to shuttle electrons from the diboron reagents to the photoredox catalytic cycle. The reaction mechanism was elucidated by radical inhibitors, deuterium labelling experiments, fluorescence spectroscopy, and cyclic voltammetry. Besides, key reaction intermediates are detected and characterized by NMR spectroscopy and DFT calculations.

The Wolff-Kishner reduction is one of the most efficient pathways to access alkyl carbanions from carbonyls. However classical WK reactions require harsh reaction conditions, and the carbanions in a WK process rarely react with electrophiles other than a proton. **Chapter 3** presents a photo-Wolff-Kishner reaction that uses N-tosyl hydrazone as a radical acceptor to produce  $\alpha$ -functionalized carbanions, which are then used for functionalization. With sulfur-centered radicals, the resulting carbanions can be readily trapped by electrophiles including  $\text{CO}_2$  and aldehydes, whereas  $\text{CF}_3$  radical addition furnishes a wide range of gem-difluoroalkenes through  $\beta$ -fluoride elimination of the generated  $\alpha$ - $\text{CF}_3$  carbanions.

In **chapter 4**, we give an overview of the recent advance in light-induced single electron transfer processes involving sulfur anions as catalysts. In particular, different activation modes of sulfur-based anionic species towards substrates under photochemical conditions are discussed.

In **chapter 5**, a novel photo-induced thiolate-catalyzed approach for the *ipso*-borylation of substituted arenes is reported. Thiolates were found to be good catalysts for photo-activation of substituted arenes to afford aryl radicals for borylation. A broad range of inert  $\text{C}_{\text{aryl}}$ -hetero bonds including  $\text{C}_{\text{aryl}}\text{-F}$ ,  $\text{C}_{\text{aryl}}\text{-Cl}$ ,  $\text{C}_{\text{aryl}}\text{-Br}$ ,  $\text{C}_{\text{aryl}}\text{-O}$ ,  $\text{C}_{\text{aryl}}\text{-N}$ , and  $\text{C}_{\text{aryl}}\text{-S}$  bonds were readily cleaved under the reaction conditions to construct synthetically versatile aryl boronates. Compared with typical photoredox catalysis, the reaction system exhibited a stronger reducing ability without comprising the functional group tolerance. A plausible charge transfer complex (CTC)-based mechanism was proposed for this reaction.

## 7. Zusammenfassung

Die vorliegende Arbeit behandelt photoredox-katalytische Methoden zur Carbonyl Umpolung. Diese wurden zum einen für die Erzeugung von funktionalisierten Alkylcarbanionen genutzt und zum anderen für die photoinduzierte Thiolat-katalysierte ipso-Borylierung von substituierten Aromaten.

**Kapitel 1** fasst verschiedene literaturbekannte Konzepte für die katalytische Erzeugung von Alkylcarbanionäquivalenten aus Carbonylen zusammen.

**Kapitel 2** beschreibt eine photoredox-katalytische Erzeugung von  $\alpha$ -Borylcarbanionen. Dieses synthetisch wertvolle Intermediat kann aus einer photoinduzierten Einelektronenreduktion eines Aldehyds und einer anschließenden radikalischen Borylierungs-Desoxygenierungs-Reaktionssequenz erzeugt werden. Das resultierende  $\alpha$ -Borylcarbanion reagiert dann mit einem anderen Aldehyd unter Bildung eines Alkens als Endprodukt. Als Ganzes betrachtet kann die Reaktion daher als photokatalytische Variante der McMurry Reaktion gesehen werden. Der Schlüssel zur Realisierung dieser Transformation ist die Verwendung eines Thiol Katalysators, welcher Elektronen vom Diboronreagenz hin zum Photoredox-Katalysezyklus transportiert. Der Reaktions-mechanismus wurde durch Radikalhemmungsreaktionen, Deuterium-markierungsexperimente, Fluoreszenzspektroskopie und Cyclovoltammetrie aufgeklärt. Darüber hinaus wurden entscheidende Reaktionszwischenprodukte durch NMR Spektroskopie und DFT-Berechnungen nachgewiesen und charakterisiert.

Die Wolff-Kishner-Reduktion ist einer der effizientesten Wege, um Alkylcarbanionen aus Carbonylgruppen zu Erzeugen. Die klassische WK-Reaktion erfordert jedoch harsche Reaktionsbedingungen. Zusätzlich reagieren die durch einen WK-Prozess geformten Carbanionen selten mit anderen Elektrophilen als einem Proton. **Kapitel 3** zeigt eine Photo-Wolff-Kishner-Reaktion, bei der N-Tosylhydrazon als Radikalakzeptor zur Herstellung von  $\alpha$ -funktionalisierten Carbanionen verwendet wird, die dann zur Funktionalisierung verwendet werden. Mit schwefelzentrierten Radikalen können die resultierenden Carbanionen leicht mit Elektrophilen, einschließlich  $\text{CO}_2$  und Aldehyden, reagieren. Durch die Verwendung von  $\text{CF}_3$ -Radikalen kann eine Reihe von gem-Difluoroalkenen hergestellt werden. Diese entstehen durch  $\beta$ -Fluorid-Eliminierung aus dem intermediär erzeugten  $\alpha$ - $\text{CF}_3$ -Carbanionen.

**Kapitel 4** liefert einen Überblick über die jüngsten Fortschritte bei den lichtinduzierten Einelektronentransferprozessen mit Schwefelanionen als Katalysator. Insbesondere werden verschiedene Aktivierungsmodi von anionischen Spezies auf Schwefelbasis inklusive ihrer Reaktivität gegenüber verschiedenen Substraten unter photochemischen Bedingungen diskutiert.

In **Kapitel 5** wird ein neuartiger photoinduzierter Thiolat-katalysierter Ansatz für die ipso-Borylierung substituierter Aromaten beschrieben. Es wurde festgestellt, dass Thiolate geeignete Katalysatoren für die Photoaktivierung substituierter Aromaten sind, um Arylradikale für die Borylierung zu erzeugen. Ein breites Spektrum inerter Caryl-Hetero-Bindungen, einschließlich  $\text{C}_{\text{aryl}}\text{-F-}$ ,  $\text{C}_{\text{aryl}}\text{-Cl-}$ ,  $\text{C}_{\text{aryl}}\text{-Br-}$ ,  $\text{C}_{\text{aryl}}\text{-O-}$ ,  $\text{C}_{\text{aryl}}\text{-N-}$  und  $\text{C}_{\text{aryl}}\text{-S-}$  Bindungen, wurde unter den Reaktionsbedingungen leicht gespalten, um synthetisch vielseitige Arylboronate zu erhalten. Im Vergleich zur typischen Photoredoxkatalyse wies



das Reaktionssystem eine stärkere Reduktionsfähigkeit auf, ohne die Toleranz gegenüber funktionellen Gruppen zu mindern. Für diese Reaktion wurde ein plausibler Mechanismus über die intermediäre Bildung von Charge Transfer Komplexen postuliert.

## 8. Abbreviations

°C	degrees Celsius
Φ	quantum yield
λ	wavelength
4CzIPN	2,4,5,6-tetra(carbazole-9-yl)isophthalonitrile
anhyd.	anhydrous
AIBN	azobisisobutyronitrile
Ar	arene
atm	atmosphere
B <sub>2</sub> cat <sub>2</sub>	bis(catecholato)diboron
B <sub>2</sub> pin <sub>2</sub>	bis(pinacolato)diboron
BDE	bond dissociation energy
BEt <sub>3</sub>	triethylborane
boc	<i>tert</i> -butyloxycarbonyl
bpy	2,2'-bipyridine
CDCl <sub>3</sub>	deuterated chloroform
CEST	chemical exchange saturation transfer
CF <sub>3</sub> SO <sub>2</sub> Na	sodium triflate
cm	centimeter
COD	1,5-cyclooctadiene
Cs <sub>2</sub> CO <sub>3</sub>	caesium carbonate
CsF	caesium fluoride
CTC	charge transfer complex
CV	cyclic voltammetry
DBU	1,8-Diazabicyclo[5.4.0]undec-7-ene
DCM	dichloromethane
DFT	density functional theory
DIPEA	<i>N,N</i> -diisopropylethylamine
DMA	dimethylacetamide
DMAP	4-dimethylaminopyridine
DMF	dimethylformamide
DMSO	dimethyl sulfoxide
DMPO	5,5-dimethyl-1-pyrroline N-oxide
DPZ	dicyanopyrazine
dtbpy/dtbbpy	di- <i>tert</i> -butyl-2,2'-bipyridine
E1cb	elimination unimolecular conjugated base
EA	ethyl acetate
EDA	electron donor acceptor
e.g.	for example (lat. <i>Exempli gratia</i> )
eq.	equivalent
EI	electron ionization
<i>E<sub>red</sub></i>	reduction potential
ESI	electrospray ionization
ET	electron transfer

EtOH	ethanol
Et <sub>2</sub> O	Diethyl ether
EWG	electron withdrawing group
EXSY	exchange spectroscopy
fc	ferrocene
FID	flame ionization detector
FT-IR	Fourier-transform infrared spectroscopy
g	gram
GC	gas chromatography
h	hour
HAT	hydrogen atom transfer
HE	Hantzsch ester
HRMS	high resolution mass spectrometry
HSQC	heteronuclear single quantum coherence
hν	incident photon energy
i.e.	that is (lat. Id est)
$I_0$	intensity of the incident light
iPr	isopropyl
IR	infrared
K	Kelvin
KI	potassium iodide
L	liter
LED	light emitting diode
LG	leaving group
M	molar (mol/L)
LiCl	lithium chloride
Me	methyl
MeCN	acetonitrile
MeOH	methanol
mg	milligram
MgCO <sub>3</sub>	magnesium carbonate
MgClO <sub>4</sub>	magnesium perchlorate
mL	milliliter
mM	millimolar (mmol/L)
mmol	millimole
MS	mass spectrometry
mW	Milliwatt
n-Bu	n-butyl
NHC	N-heterocyclic carbene
nm	nanometer
NMR	nuclear magnetic resonance
NMP	N-methyl-2-pyrrolidone
NOE	nuclear overhauser effect
OTf	trifluoromethanesulfonate group

PC	photocatalyst
PE	petroleum ether
PF <sub>6</sub>	hexafluorophosphate
Ph	phenyl group
ppm	parts per million
ppy	2-phenylpyridine
rt	room temperature
PTFE	polytetrafluoroethylene
s	second
SCE	saturated calomel electrode
SET	single electron transfer
SmI <sub>2</sub>	samarium (II) iodide
S <sub>N</sub> 2	bimolecular nucleophilic substitution
Sub	substrate(s)
<sup>t</sup> Bu	tert-butyl
TMAF	tetramethylammonium fluoride
TEA	triethylamine
TEMPO	(2,2,6,6-tetramethylpiperidin-1-yl)oxyl
Tf	trifluoromethanesulfonate
THF	tetrahydrofuran
TLC	thin layer chromatography
TMS	trimethylsilyl group
Ts	tosyl group
UV	ultra violet
Vis	visible light
vs.	against (lat. versus)
W	watt
WK	Wolff-Kishner

## 9. Acknowledgement

Firstly, I would like to express my deep respect and sincere gratitude to my research supervisor Prof. Dr. Burkhard König for giving me the opportunity to work in his research group. His patient supervision, constant encouragement and valuable discussions have inspired me throughout my research period. Moreover, his freedom to work and his problem-solving approach have helped me to explore different directions in research and have greatly helped me to work independently.

I am very much grateful to Prof. Dr. Alexander Breder and Prof. Dr. Patrick Nürnberger for being the doctoral committee members and examining my thesis. I am also thankful to Prof. Dr. Robert Wolf for being the chairperson in my Ph.D. defense.

I deeply acknowledge Prof. Li-Na Guo and Prof. Xin-Hua Duan (XJTU, China) for giving me the opportunity to carry out my first research in their laboratory during my M.Sc studies.

I would like to thank Dr. Rudolf Vasold and Simone Strauß for the GC and GC-MS measurements, Ernst Lautenschlager for all kinds of technical supports, Britta Badziura for ordering chemicals, Julia Zach for taking care of all the instruments, and Regina Hoheisel for CV measurements, Katharina and Barbara for administrative support.

My special thanks go to all my project partners for their excellent support, and fruitful discussions; especially Prof. Dr. Ruth Gschwind, Dr. Nanjundappa Lokesh, Dr. Leyre Marzo, Dr. Qing-Yuan Meng, and Dr. Hua Wang from whom I learned a lot. I also thank Beiyi Cheng and Matea Sršen for their contribution in this thesis. I would like to thank Dr. Qing-Yuan Meng, Dr. Kang Chen for their generous help and guidance all the time.

I thank Prof. Dr. Ruth Gschwind, Dr. Lokesh for the excellent cooperation and valuable ideas in the NMR studies. It was a great time working with you.

I convey my thanks to all past and present members of AK König for their generous help, ideas and support, especially Kang, Qing-Yuan, Hua, Karsten, Matthias, Tobi S, Beiyi, Leyre, Gerg, Indra, Saikat, Rok, Yi-Wen, Daniel P, Jerry, Alex, Andi G, Alessa, Uli and few others who made the last years so special for me during Ph.D. studies. The moments together in Ph.D parties, cake and coffee on birthdays, barbecue events, short group trips, winter seminars, Dult, dumpling making, hotpot parties, etc. will be in my lifelong memories.

I am very much grateful to China Scholarship Council (CSC) for the financial support during my doctoral research.

Finally, I would like to thank my family. The people who have supported me all my life and without whom I would not have come so far. Many thanks to my parents and my brother for their unconditional support and understanding. But the most important thing to me is my wife Hua and my daughter Suxi. I am infinitely grateful to have you by my side. Your happiness and smile are the meaning of my life. Thank you for your support and love, as well as the wonderful years we had and will have together.

## 10. Curriculum Vitae

Shun Wang  
Ph.D. Student  
Institute of Organic Chemistry  
University of Regensburg  
D-93053 Regensburg, Germany  
Email: [Shun.Wang@chemie.uni-regensburg.de](mailto:Shun.Wang@chemie.uni-regensburg.de)



### Personal Information

Nationality: China  
Date of Birth: 15.09.1992  
Marital status: Married

### Education

11/2016 - present	Ph. D. in Organic Chemistry with Prof. Burkhard König Institute of Organic Chemistry, University of Regensburg, Germany
09/2013 - 07/2016	M.Sc in Organic Chemistry with Prof. Li-Na Guo School of Science, Xi'an Jiaotong University, Xi'an, China
09/2009 - 07/2013	B.S. in Chemistry Sichuan Normal University, Chengdu, China

### Scholarships and Awards

- 2016 Chinese scholarship council (CSC) scholarship
- 2015 National scholarship for Master Student Award (China)
- 2015 Excellent postgraduate student award (Xi'an Jiaotong University)
- 2014 Excellent postgraduate student award (Xi'an Jiaotong University)

### Conference Contributions

- 26. Lecture Conference on Photochemistry, Munich, poster presentation (09/2018)
- 24th - 35<sup>th</sup> Seminar Days of the GRK 1626, oral contributions (2016 - 2019)
- The 9<sup>th</sup> Chinese Chemical Society (CCS), National Organic Chemistry Conference, Changchun, China (2015)

### List of Publications

1. **Shun Wang**, Bei-Yi Cheng, Matea Sršen, and Burkhard König\*. Umpolung Difunctionalization of Carbonyls via Visible-Light Photoredox Catalytic Radical-Carbanion Relay. *J. Am. Chem. Soc.* **2020**, *142*, 7524 - 7531.  
[Highlighted in *Synfacts* **2020**, *16*, 0811]
2. **Shun Wang**, N. Lokesh, Johnny Hioe, Ruth M. Gschwind\* and Burkhard König\*. Photoinitiated carbonyl-metathesis: deoxygenative reductive olefination of aromatic aldehydes

- via photoredox catalysis. *Chem. Sci.*, **2019**, *10*, 4580-4587.  
[Most popular 2018-2019 catalysis articles]  
[Selected for the “2019 Chemical Science HOT Article Collection”]  
[Highlighted in *Synfacts* **2019**, *15*, 0633]
3. **Shun Wang** and Burkhard König\*. Photo-Induced Thiolate Catalytic Activation of Inert Caryl-Hetero Bonds for Radical Borylation. *In preparation*.
  4. **Shun Wang**, Li-Na Guo, Hua Wang, and Xin-Hua Duan\*. Alkynylation of Tertiary Cycloalkanols via Radical C-C Bond Cleavage: A Route to Distal Alkynylated Ketones. *Org. Lett.* **2015**, *17*, 4798 - 4801.  
[Highlighted in Organic Chemistry Portal]
  5. Li-Na Guo\*, **Shun Wang**, Xin-Hua Duan and Shi-Liu Zhou. Iron-Catalyzed Tandem Cyclization of Olefinic Dicarboxyl Compounds with Benzylic Csp<sup>3</sup>-H Bonds for the Synthesis of Dihydrofurans. *Chem. Commun.* **2015**, *51*, 4803 - 4806.
  6. **Shun Wang**, Lin-Ye He, Li-Na Guo\*. Potassium Persulfate Mediated Oxidative Radical Cyclization of 1,3-Dicarbonyl Compounds with Styrenes for the Synthesis of Dihydrofurans. *Synthesis*. **2015**, *47*, 3191 - 3197.  
[Highlighted in *Synfacts* **2015**, *11*, 1257]
  7. Qing-Yuan Meng, **Shun Wang**, Gregory S. Huff, and Burkhard König\*. Ligand-Controlled Regioselective Hydrocarboxylation of Styrenes with CO<sub>2</sub> by Combining Visible Light and Nickel Catalysis. *J. Am. Chem. Soc.* **2018**, *140*, 3198 - 3201.
  8. Qing-Yuan Meng, **Shun Wang** and Burkhard König\*. Carboxylation of Aromatic and Aliphatic Bromides and Triflates with CO<sub>2</sub> by Dual Visible-Light–Nickel Catalysis. *Angew. Chem. Int. Ed.* **2017**, *56*, 13426 - 13430.
  9. Leyre Marzo, **Shun Wang**, and Burkhard König\*. Visible-Light-Mediated Radical Arylation of Anilines with Acceptor-Substituted (Hetero)aryl Halides. *Org. Lett.* **2017**, *19*, 5976 - 5979.
  10. Hua Wang, Li-Na Guo, **Shun Wang** and Xin-Hua Duan\*. Decarboxylative Alkynylation of  $\alpha$ -Keto Acids and Oxamic Acids in Aqueous Media. *Org. Lett.* **2015**, *17*, 3054 - 3057.
  11. Shi-Liu Zhou, Li-Na Guo, **Shun Wang** and Xin-Hua Duan\*. Copper-Catalyzed Tandem Oxidative Cyclization of Cinnamamides with Benzyl Hydrocarbons through Cross-Dehydrogenative Coupling. *Chem. Commun.* **2014**, *50*, 3589 - 3591.

## References

### **Prof. Burkhard König**

Email: [Burkhard.Koenig@chemie.uni-regensburg.de](mailto:Burkhard.Koenig@chemie.uni-regensburg.de)

Institute of Organic Chemistry, University of Regensburg, Regensburg D-93040, Germany

### **Prof. Li-Na Guo**

Email: [guoln81@mail.xjtu.edu.cn](mailto:guoln81@mail.xjtu.edu.cn)

Department of Chemistry, School of Science, Xi'an Jiaotong University, Xi'an 710049, China

## **Eidesstattliche Erklärung**

- (1) Ich erkläre hiermit an Eides statt, dass ich die vorliegende Arbeit ohne unzulässige Hilfe Dritter und ohne Benutzung anderer als der angegebenen Hilfsmittel angefertigt habe; die aus anderen Quellen direkt oder indirekt übernommenen Daten und Konzepte sind unter Angabe des Literaturzitats gekennzeichnet.
- (2) Bei der Auswahl und Auswertung folgenden Materials haben mir die nachstehend aufgeführten Personen in der jeweils beschriebenen Weise unentgeltlich geholfen:
  1. \_\_\_\_\_
  2. \_\_\_\_\_
  3. \_\_\_\_\_
- (3) Weitere Personen waren an der inhaltlich-materiellen Herstellung der vorliegenden Arbeit nicht beteiligt. Insbesondere habe ich hierfür nicht die entgeltliche Hilfe eines Promotionsberaters oder anderer Personen in Anspruch genommen. Niemand hat von mir weder unmittelbar noch mittelbar geldwerte Leistungen für Arbeiten erhalten, die im Zusammenhang mit dem Inhalt der vorgelegten Dissertation stehen.
- (4) Die Arbeit wurde bisher weder im In- noch im Ausland in gleicher oder ähnlicher Form einer anderen Prüfungsbehörde vorgelegt.

Regensburg, 12.04.2021